Durham E-Theses

Synthesis, characterisation and properties of amino acid terminated dendrimer wedges

Staples, Robert Mark

How to cite:

Use policy

SYNTHESIS, CHARACTERISATION AND PROPERTIES OF AMINO ACID TERMINATED DENDRIMER WEDGES

Robert M. Staples

A thesis submitted for the degree of Doctor of Philosophy at the
University of Durham.

October 1997

Abstract

Synthesis, Characterisation and Properties of Amino Acid Terminated Dendrimer Wedges.

Robert Mark Staples   PhD Thesis   October 1997

The rising demand for speciality polymers that possess novel properties has led to an interest in the tailored synthesis of dendritic polymers having highly controlled molecular architectures. Control over size, shape, molecular weight and functionality at the periphery of the molecule was used to design a series of dendrimer wedges with the ultimate aim of enhanced binding of a functional, property modifying unit to a cotton surface in water.

Poly(propyleneimine) dendrimer wedges with various foci were produced in a stepwise way *via* a repetitive reaction sequence using the divergent approach. Initially, long chain aliphatic amines were used as starting materials and optimisation of the reaction conditions produced wedges up to the third generation possessing eight primary amine end groups. Subsequently dendrimer wedges were synthesised from a siloxysilane core up to the second generation. End group modification with amino acid residues was performed at the periphery of the wedges and adsorption studies were carried out to ascertain if enhanced molecular recognition at a cotton surface occurred. Also an investigation of the modification of polar surfaces by amine terminated dendrimers with a siloxysilane unit at the focus was performed.

Acknowledgements

There are many people who helped me through the sudden transition from industry to academia and over the last three years which has culminated in the production of this thesis. Firstly, thanks to DuPont Nylon for the initial "encouragement" and making the decision all the more easier. Also to the final kick in the right direction, and Sim City, from a former Durham IRC inmate Robin Mac, you were right Robin.

I am eternally grateful to my supervisor, Professor Jim Feast for giving me the opportunity to study in Durham in such auspicious surroundings. His never-ending enthusiasm, encouragement, patience and understanding is a true inspiration to us all. If all else fails "I can always 'go boldly' and become a screenwriter for Captain Kirk". I am also grateful for a jolly to the ACS conference in Las Vegas, especially to see the so called 'major players' get one right where it hurts, Well done Lois! I would also like to thank my industrial supervisors, Ezat Khosdel, Jonathon Warr and Andy Hopkinson for their helpful discussions and contributions and everybody in Exploratory at Port Sunlight for the warm welcome I always received.

I am grateful to all the support staff in Durham particularly Julia Say in n.m.r for her expertise on the '400' and Alan Kenwright for his 'its a piece of paper' interpretations of spectra. Also to Dave 'what explosion' Hunter in the high pressure lab for his banter and calmness under fire. Thanks to Terry Harrison for being good at computers, but bad at the lottery.

Having been at DuPont, formally known as ICI, for seven years there are a number of people I have to thank who made '9 to 5' bearable. Johnathan, CJ, Russ, Ned, Andy, PB, and Gen (from day 1 at MSG) from Nylon Inters and Weby, Des and Derek for some memorable Friday nights out in the 'Boro and 'the back room'.

Life has been made all the more enjoyable within the IRC over the past three years by the many special characters passed and present that it has been my pleasure to know. Thanks to Townsey, Donney, Roach, Wee man, Pecky and Dave for a memorable Christmas shopping trip to York. Pecky for the 'gadge raid' tapes and some 'kicking' Grad Soc discos. The LFC contingent, Rich, (Boyzone), for being good at computer games and for keeping his side of the fumehood tidy (not) for 3 years and Foggy (oh my car has broken down again!) for his even more laid back attitude to life. Mike (Mad-Planet Derbyshire) for being the sanest person around. Robin (Jackpot) Harrison, my fellow executive coffee club member, we nearly drove home from Vegas in that BMW. Gav, the Jazz King, diamond geezer for his telephone manner 'Matron' and for some thrashing tennis games. Andy,(Cinders-up the Alex!) for taking me to Sainsburys and being the trivia 'master'. The lads from the card school, Andreas, Lian, etc, sorry for taking all your money. Thanks to all the 'girlies' for brightening up the office and Helen T (I work very hard, but I'm lazy!) for putting up with me for two years at 'the top of the hill'. To Susie (EBGB EBGB!) Campbell, 'my best friend' for so many special times I shall never forget.

To my parents, words cannot express how much I appreciate their never-ending love, support, and guidance, to my brother David, sister Janelle, and whatever big fluffy dog (Misty) we have at the time, this is for them.

Runner

Memorandum

The work in this thesis has been carried out at the Durham site of the Interdisciplinary Research Centre in Polymer Science and Technology between October 1994 and October 1997. This work has not been submitted for any other degree either in Durham or elsewhere and is the original work of the author except where acknowledged by means of appropriate reference.

Statement of Copyright

The copyright of this thesis rests with the author. No quotation from it should be published without the prior written consent and information derived from it should be acknowledged.

Financial Support

Nomenclature

To avoid the necessity of repetition in writing the full chemical formulae describing the various dendrimer architectures synthesised in this work a systematic shorthand nomenclature has been adopted. A key in the form of a bookmark has been constructed to assist the reader.

Hence a poly(propyleneimine) dendrimer wedge with a siloxysilane focus and a benzyloxycarbonyl (CBZ) N-protected phenylalanine residue at the periphery is described as Si-*wedge*-phe CBZ and the corresponding deprotected compound as Si-*wedge*-phe. A dendrimer wedge constructed from aliphatic amines at the focus, such as hexylamine, with eight nitrile end groups is described as Hex-*wedge*-(CN)$_8$; all of these structures are shown below.
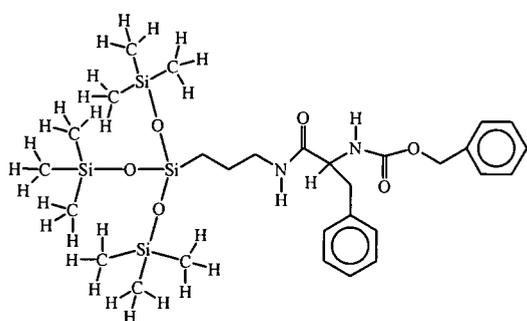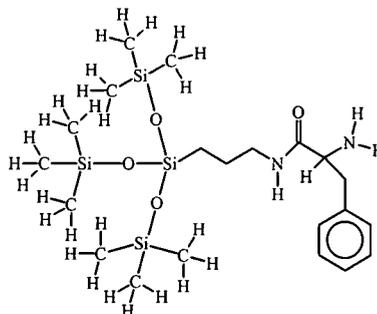
Si-*wedge*-phe CBZ   Si-*wedge*-phe
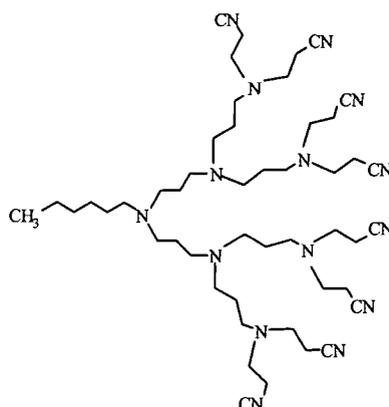
Hex-*wedge*-(CN)$_8$

Contents

page

"Invention my dear friends is

93% perspiration

6% electricity

4% evaporation and

2% butterscotch ripple!"

WW

CHAPTER 1

Introduction to Dendrimers and Hyperbranched Polymers

1.1 Introduction

The search for aesthetically attractive molecules is a concern going back to the origins of chemistry. The criteria for beauty have changed with time and are related to the power of the analytical and synthetic tools available. The ability of synthetic chemists to build more and more complicated structures has been developing spectacularly; recently highly sophisticated molecular architectures, such as catenanes and rotaxanes, have been achieved. The rising demand for speciality polymers with novel properties has led to an interest in the synthesis of polymers which have highly controlled molecular architectures and novel topologies or molecular geometries. [1]

As their name implies, dendritic macromolecules[1] have highly branched three-dimensional structures which in many ways mimic the structure of trees. From a central point the macromolecule branches outwards with the number of terminal groups increasing as the molecular weight increases, it is the number and nature of the branch points which gives rise to the three-dimensional structure. When the molecule has highly regular branching, it is termed a dendrimer,[2] in principle, when perfect, these materials are discrete molecules and are prepared via repetitive multi-step syntheses with purifications at each step. Successive cycles of synthesis yield a family of generations of monodisperse dendrimers with the same structural motif. De Gennes and Hervet[3] predicted that at a given number of generations the external surface of the dendrimer would become saturated because of dense packing. The point at which this occurs depends on the topology and the length of the segment added at each generation. If the synthesis

is continued beyond this point, defects start to appear and the dendrimer is no longer well defined.

In contrast to dendrimers, in a statistical AB_2 step-growth polymerisation hyperbranched macromolecules are produced with a distribution in both structure and molecular weight. Hybrid polymers, containing a combination of dendritic and linear segments have also been reported and, like hyperbranched polymers, are less precisely defined than dendrimers. These relatively new types of polymer have attracted interest since they may offer appealing development opportunities in specialised applications (see later).

1.2 Historical Background

Some of the key dates in the evolution of interest in the construction of tree-like molecular architectures are listed in Table 1 along with topics and authors. The origins of interest in molecular branching can be traced back to the network theory of Flory[4] and Stockmayer[5]. In 1944, Melville[6] delivered a paper to the Faraday Society in which he predicted "someone will discover a general method for inducing branching of the chains of atoms without allowing such chains to be linked up into a three-dimensional network". In 1952 Flory[7] discussed the theory of polymers derived from AB_x monomers (Figure 1), where only reactions between A and B functionalities were allowed. In this theory 'branch-on-branch' growth approach could be used to build up a new class of high molecular weight polymeric materials. Flory predicted the possibility of making *statistical hyperbranched polymers* of the kind suggested earlier by Melville but did not succeed in several attempts to prepare such polymers. These

structures represent the simplest form of dendritic architecture obtainable via polycondensation.

Date	Author	Event
1920	Staundiger	Macromolecular hypothesis
1941	Flory	Basic Theory for Networks
1944	Melville	First suggestion of tree-like molecules
1952	Flory	Non-linear polymerisation
1956	Erlander	Hyperbranched structure of amylopectin
1978	Vögtle	Concept of structure-perfect cascade molecules and their first synthetic examples
1982	Maciejewski	Concept of dense packing for cascade polymers
1983	Denkewalter	Reported synthesis of poly(lysine) molecular trees with asymmetrical branch junctions
1983	De Gennes and Hervet	Calculation of starburst, dense-packed generation limit for poly(amidoamine) dendrimers
1983	Tomalia	First successful synthesis of a symmetrical branched high molecular weight dendritic polymer
1985	Newkome	Synthesis of a 27-arborol
1989	Rebrov	First organo-Si dendrimers
1989	Kim and Webster	Synthesis of first hyperbranched polymers, poly(phenylenes)
1990	Frèchet	Convergent method for dendrimer synthesis
1990	Miller	Convergent method for dendrimer synthesis
1990	Tomalia	First comprehensive review on dendrimers
1991	Moore	First purely hydrocarbon dendrimer
1992	Balzani	Inorganic molecular trees
1992	Astruc	Organometallic molecular trees
1992	Dendritech™	Company for commercialisation of Starburst® (PAMAM) dendrimers.
1994	Majoral	Large neutral molecular trees based on phosphorus
1994	Meijer	Report of poly(propyleneimine) "dendritic box"
1997	DSM	Commercialisation of poly(propyleneimine) dendrimers as Astramol™.

Table 1. Dendrimers and hyperbranched polymers: historical background.
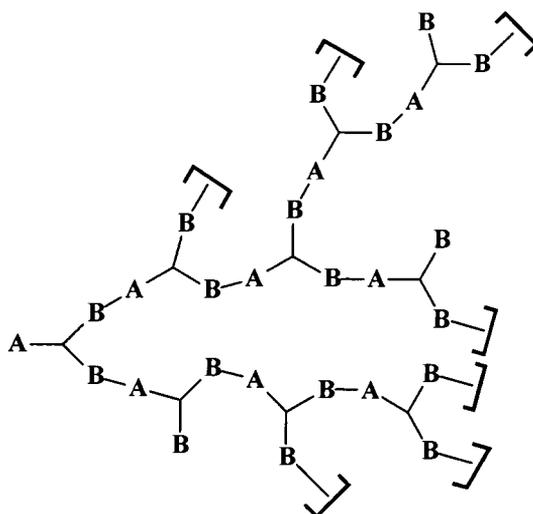
Figure 1. A fragment of Flory's proposed statistical hyperbranched polymer

architecture, formed via condensation of AB_2 monomers.

There were no well-characterised synthetic examples of such architectures,

although Meyer[8] had proposed a symmetrical, highly branched architecture for

amylopectin, subsequent work by Erlander and French,[9] and Burchard et al.,[10]

showed that amylopectin had a lightly branched structure with approximately 1

branch per 25 repeat units, as illustrated diagramatically in Figure 2.
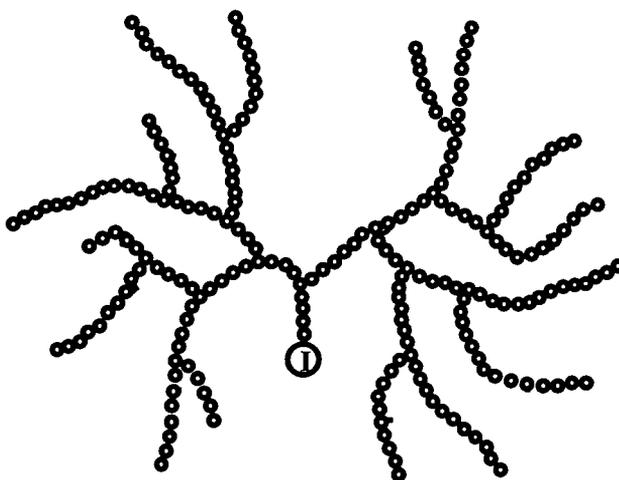
Figure 2. Dendritic branching topology of amylopectin, each circle represents a

glucose residue and (I) represents a cyclodextrin core.

The intense experimental interest in the synthesis of well defined macromolecular three-dimensional species with hyperbranched architectures only commenced in the mid-eighties with the work of Newkcome[11] and Tomalia[12]. The area also attracted theoretical studies leading to statistical treatment of cascade molecules and related networks[13,14,15]. In 1978 Vögtle[16] et al had reported the preparation of the 'cascade' structures, shown in Figure 3, this basic concept has been widely adopted and is used in the work reported in this thesis.
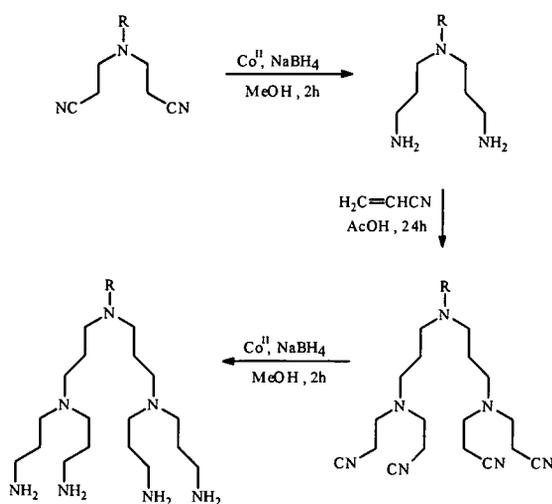
Figure 3. The original cascade synthesis of polyamines reported by Vögtle et al[16].

Vögtle reported an example of a protection/deprotection scheme which involved the double Michael addition of acrylonitrile to amines followed by reduction of the nitrile groups to amino groups. Due to the experimental difficulties and poor yields encountered during the reduction step the work was not persued; nevertheless, the idea of "cascade synthesis" was introduced to the literature by this work.

At around this time, Tomalia[17] described poly(amidoamines), well defined, three-dimensional, macromolecules with architectures and properties that were quite

different from classical polymers (see later) and coined the term 'starburst dendrimers'[TM]. Starburst materials are constructed by connecting molecular repeat units to a single 'nucleus' step by step, each cycle of the synthesis introducing branching. Tomalia called the branched units 'branch cells' and they accumulate according to a geometric progression to produce a symmetrical tree-like structure. This assembly of repeat units, branch cells and end groups resembles a single trunked tree attached to a root and is termed a 'dendron' (from the Greek word *dendritic* = treelike). Entities derived from several dendrons organised around the core are called **dendrimers**.

Denkewalter et al[18], using protection/deprotection methods of peptide chemistry produced a series of dendrimers based on lysine, possessing unsymmetrical branch lengths. These structures differed significantly from the starburst dendrimers in that they had a uniform density. Since 1985, Newcome and co-workers have reported syntheses of symmetrically branched molecules which they call "arborols". To date, examples of uni-[11], di-[19] tri-[11] and tetradirectional[20] arborols have been reported. In the period since these early observations there has been an enormous expansion of activity in this field, some aspects of which are reviewed in the following pages.

1.3 Synthesis of Dendrimers

1.3.1 Introduction

There are two distinct strategies for the preparation of dendrimers. The initial approach was established and developed independently by Tomalia for Starburst dendrimers[2] and Newkome for Cascade molecules[11] and is currently

known as the divergent growth approach. A more recent development is the convergent approach devised by Hawker and Fréchet[21]. The basic difference between these two synthetic strategies is in the direction of growth, see Figure 4.
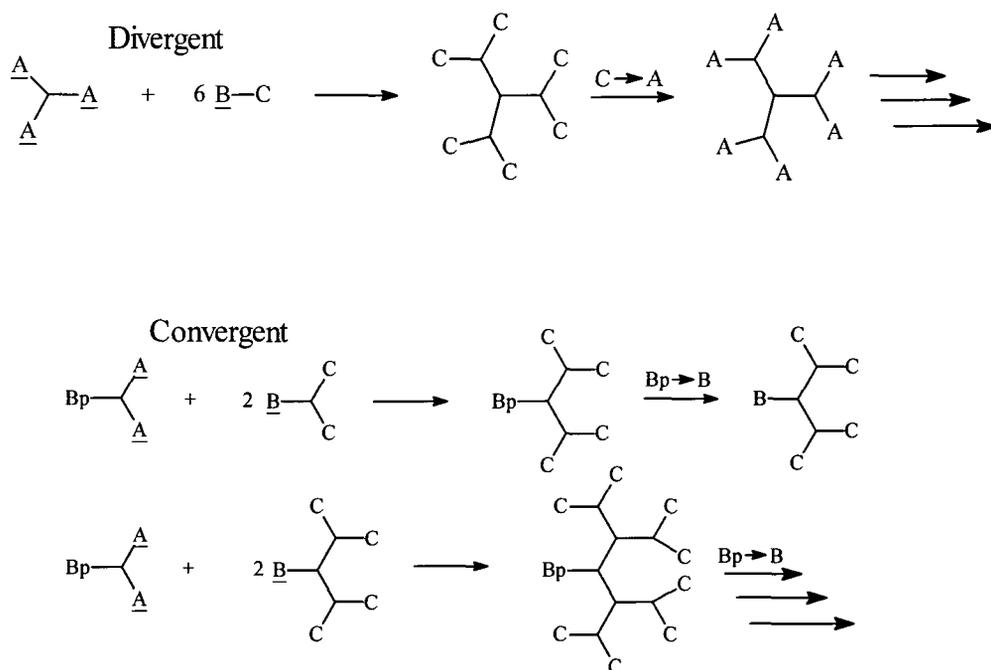
Figure 4. Schematic representations of dendritic growth.

The divergent approach initiates growth at a polyfunctional core (A_3), proceeding radially outwards with the stepwise addition of successive layers of monomer building blocks (BC). This leads to bigger and bigger dendritic structures with an ever increasing number of chain ends and reactive functional groups. In contrast, the convergent approach starts at what will be the chain ends and proceeds inwards by successive additions of the growing dendritic wedges (BC_n) to a mono-protected unit (BpA_2). Several of the dendron wedges produced in this manner can then be attached to a polyfunctional core (A_n) creating a dendritic structure.

1.3.2 Divergent Dendrimer Synthesis

The first dendrimers were synthesised using a 'divergent' strategy. In a typical example, see Figure 5, an initiator core attached to three repeat units gives a three armed entity to which further units can be added; this is generation zero. The next sequence adds branched cells with two arms to form generation one. Adding successively 12, then 24 and 48 repeat units and branch cells produces generations two, three and four respectively.

There is a certain 'limiting generation', normally around generation ten, which prevents further branches from being added in a regular way for a particular type of dendrimer. Irregular branching is due to the fact that the number of end groups on the surface of the dendrimer grows exponentially whereas the diameters of the dendrimers increase linearly thus crowding occurs which limits the number of generations possible. In 1983 de Gennes[3] predicted the number of ideally branched generations a particular dendrimer can have, and the existance of this 'starburst limiting generation' has been verified experimentally.

Tomalia[2,22] demonstrated many of the important features to be considered using a 'divergent' strategy in the synthesis of the polyamidoamine (PAMAM) dendrimers. Figure 6 shows the basic principles underlying their construction from an ammonia core.
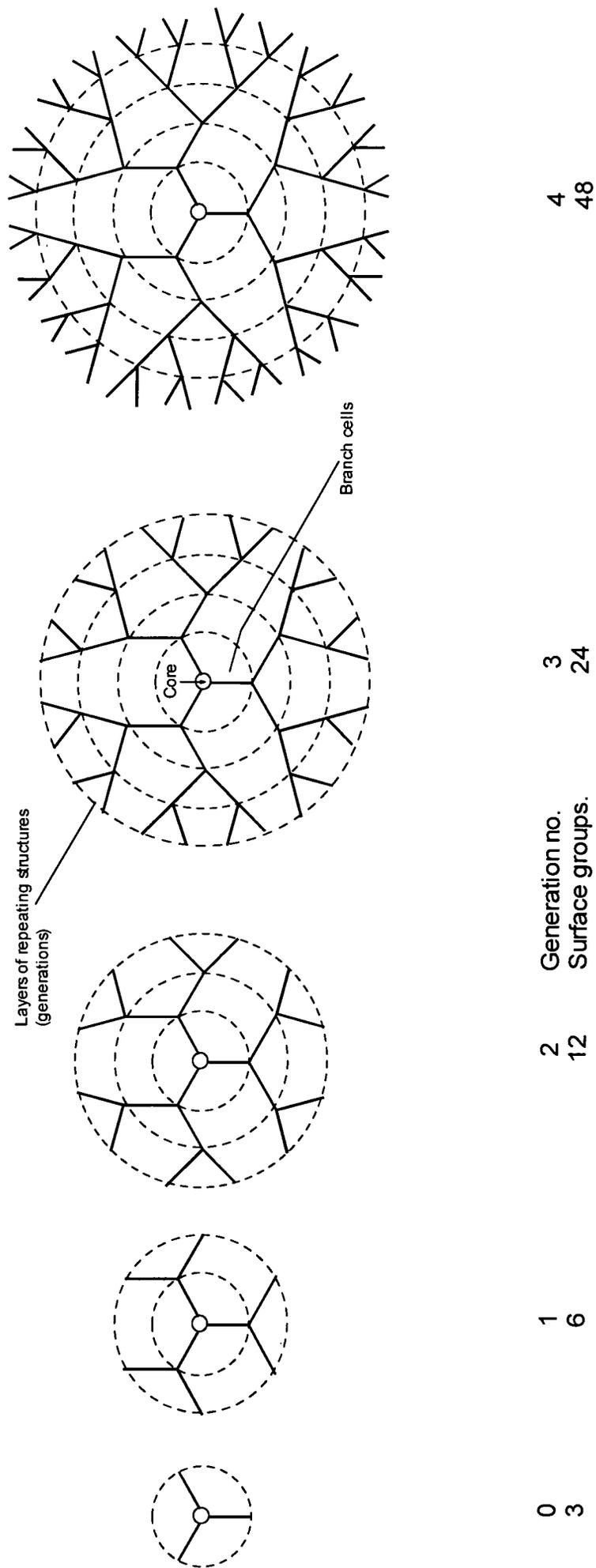
Figure 5. The divergent development of Starburst dendrimers from a trifunctional core and two armed branch.
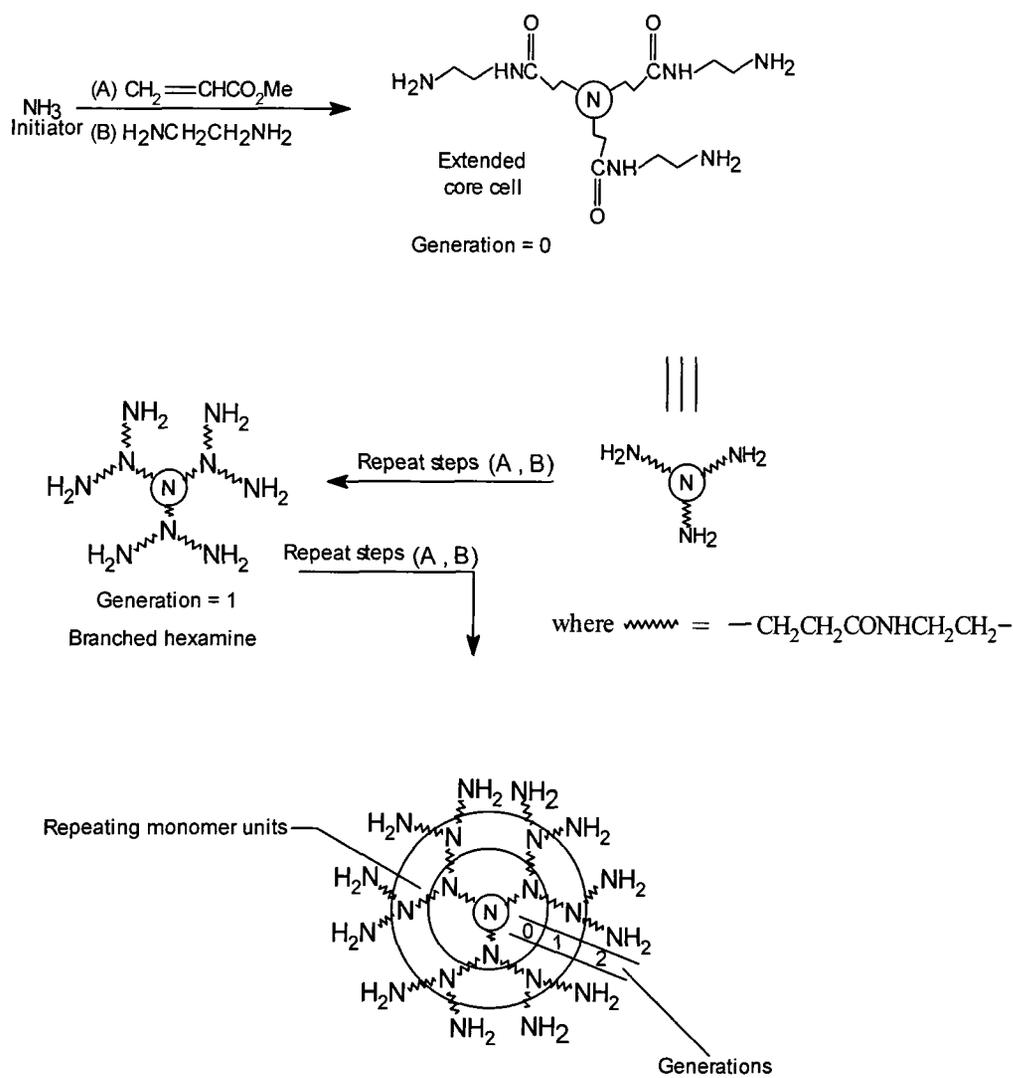
Figure 6. Synthetic scheme for the divergent synthesis of starburst PAMAM

dendrimers from an ammonia core.

The initial tridendron is formed by the Michael addition of ammonia to three

moles of methyl acrylate (A), followed by reaction with an excess of

ethylenediamine (B) to give three difunctional nucleophilic amine termini at

G=0. To repeat the reaction sequence, six moles of methyl acrylate are added to

give G=0.5 dendrimer, followed by further amidation to return to amine termini

and the first generation dendrimer, G=1. The reaction sequence is then repeated to give a second generation dendrimer with twice the number of terminal units with further concentric tiers being built up generation after generation, with purification procedures at each stage.

In Newkome's approach to the synthesis of water-soluble poly(ether amides) terminated by hydroxymethyl groups[11], growth was started from a trifunctional core and an AB_3 building block was employed, this gave an increase in branching density and speed of synthesis. Referring to Figure 7, reaction of (**1**) with chloroacetic acid followed by reduction and tosylation afforded the tritosylate (**2**). Reaction of (**2**) with the sodium anion of triethyl methanetricarboxylate gave the nonaester (**3**) which, on exhaustive amidation with tris(hydroxymethyl)aminomethane (**4**), produced the dendritic macromolecule (**5**) with 27 terminal hydroxy groups.

Divergent growth proved to be successful for dendrimer synthesis although some defects do occur, it is generally acknowledged that the presence of a few imperfections has little effect on the ultimate properties of the products.

Following Tomalia's and Newkome's early work, the divergent growth approach has been successfully exploited to prepare a large number of different dendritic macromolecules, a few of which are illustrated below.
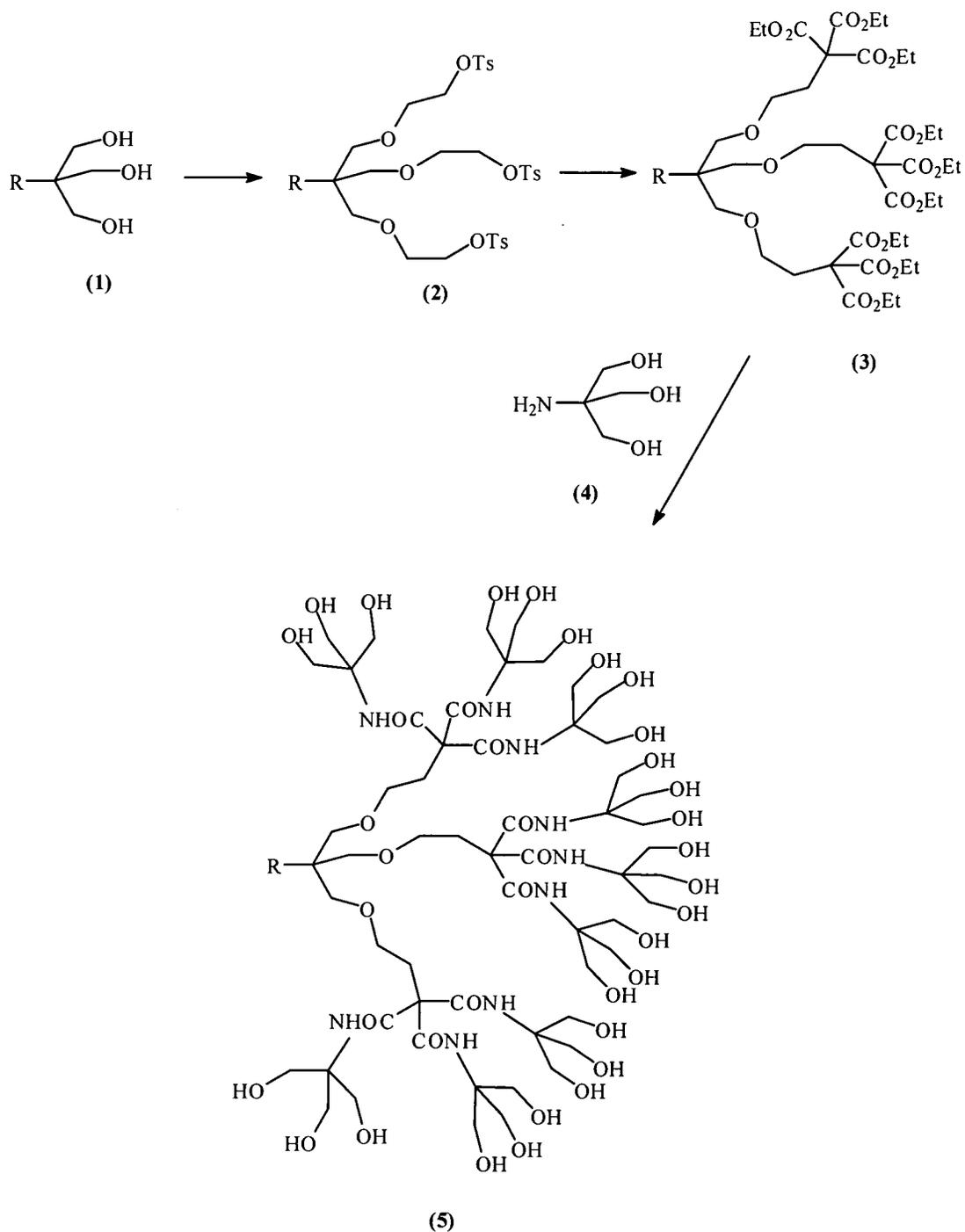
Figure 7. Newkome's divergent synthesis of a *one-directional* 'arborol'.

The lysine trees of Denkewalter[18] (Figure 8) represent one of the first examples

of well-defined, monodisperse dendritic polymers. The core is lysine

benzhydrylamide and the divergent construction proceeds via reaction with an activated ester of the di-t-BOC amino protected L-lysine as the branching agent, see Figure 8. Generation ten has 2048 terminal groups and its diameter reaches about 100Å.
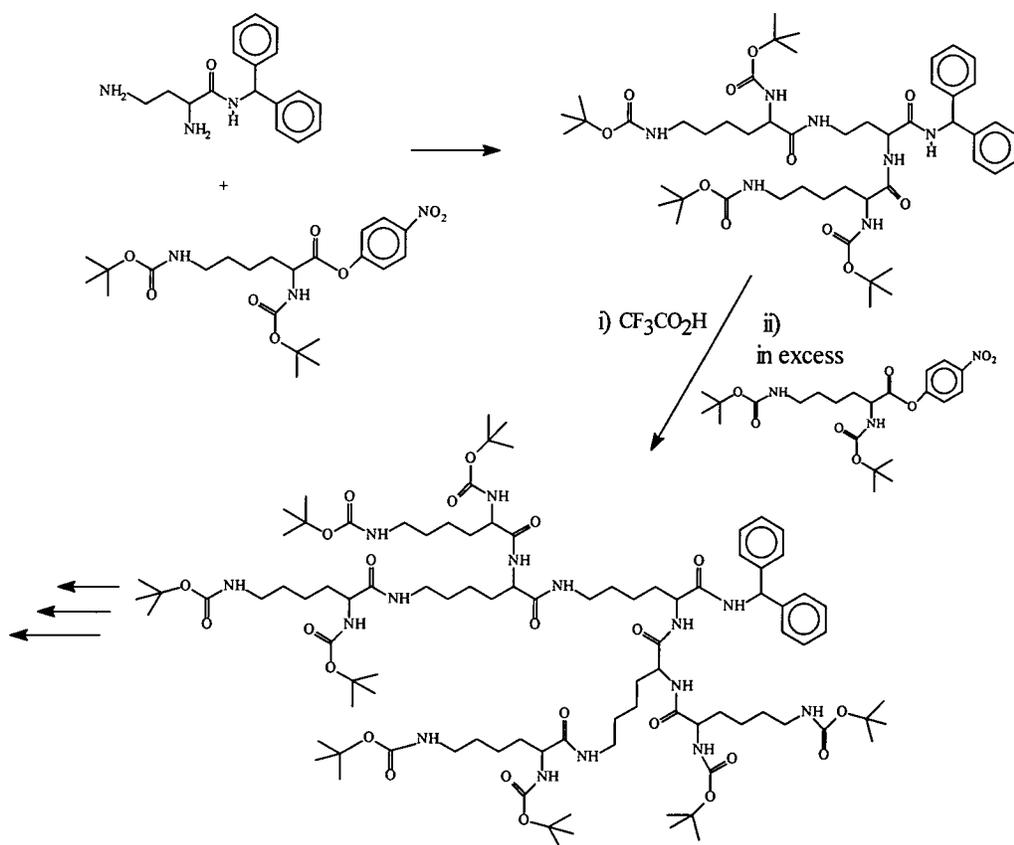
Figure 8. Synthesis of lysine-based dendrimers by Denkewalter et al.

The pioneering cascade molecules of Vögtle[16] utilised the Michael addition of acrylonitrile to amines. The groups of Meijer[23] and Mülhaupt[24] have improved the troublesome reduction step of the Vögtle method and Meijer has made poly(propyleneimine) dendrimers up to generation 5.5 with 64 terminal amine groups and a molecular weight of 7166 amu. DSM produce these materials on a large scale as Astramols™ for possible commercial applications.

Newkome[25,26,27] reported similar work relating to the use of the Michael addition of acrylonitrile or the related ester tert-butyl acrylate to nitromethane or polyols to build cores and branching units as shown in Figure 9. Aminotriesters such as $H_2NC(CH_2OCH_2CH_2CO_2Et)_3$, were reacted with 1,3,5-benzenetricarbonyl trichloride producing the *three-directional* nonaester cascade structure shown in Figure 10.
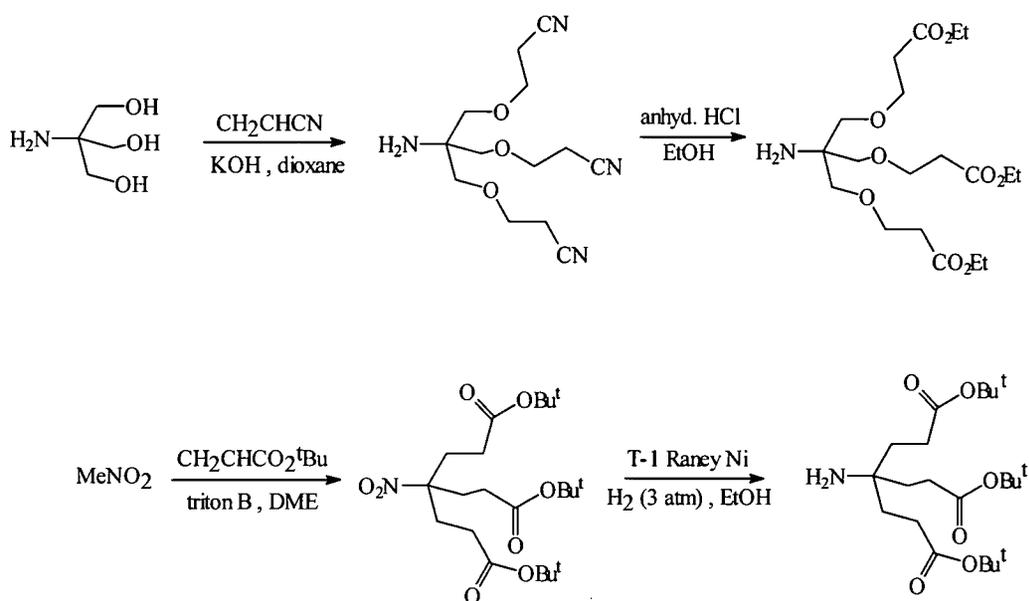
Figure 9. A variety of early cores and branching units reported by Newkome for arborol synthesis.
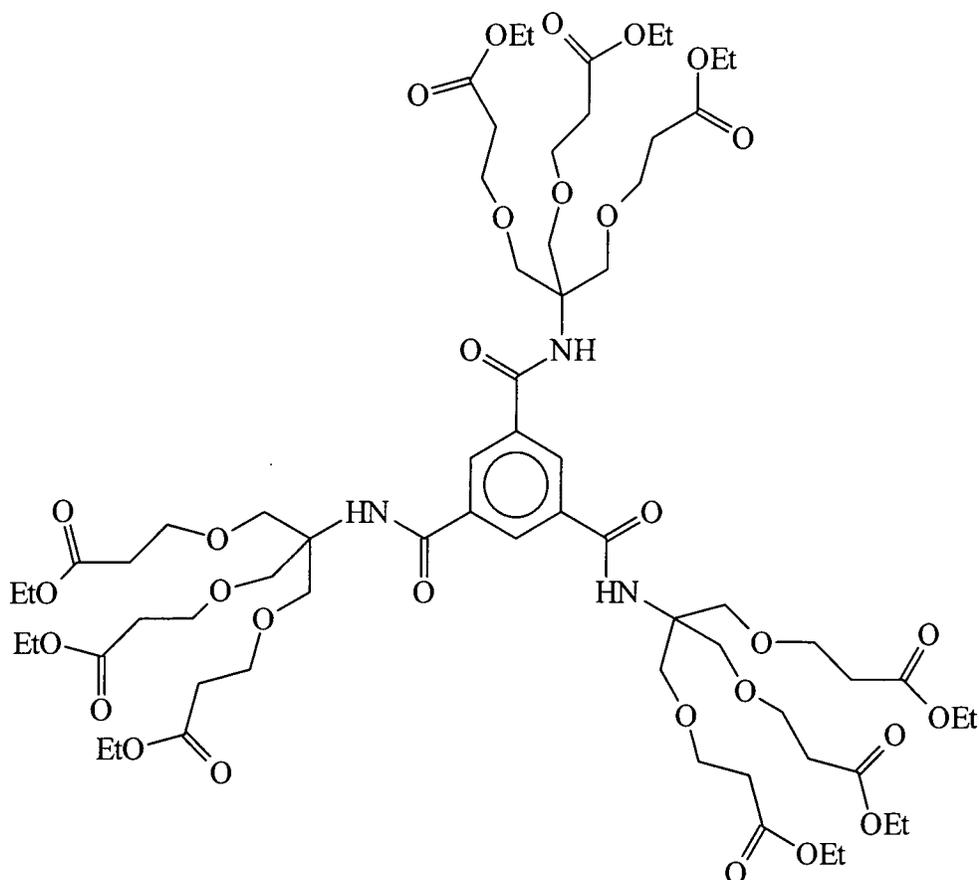
Figure 10. Newkomes *three-directional* nonaester "cascade" structure.

Roovers[28] synthesised a series of carbosilane dendrimers using tetravinylsilane as the core and dichloromethylsilane as the branching unit as shown in Figure 11. Repetitive platinum catalysed hydrosilylation of vinylsilane with dichloromethylsilane and nucleophilic replacement of silicon chloride by vinylmagnesium bromide produced dendrimers with up to 64 terminal groups and 6016 amu (4th generation).

Starting from tetraallylsilane (rather than the tetravinylsilane above), van der Made claimed the synthesis of a polysilane dendrimer with up to 972 end groups (73,912 amu, 5th generation) using repetitive alkenylation-hydrosilylation reactions[29,30].
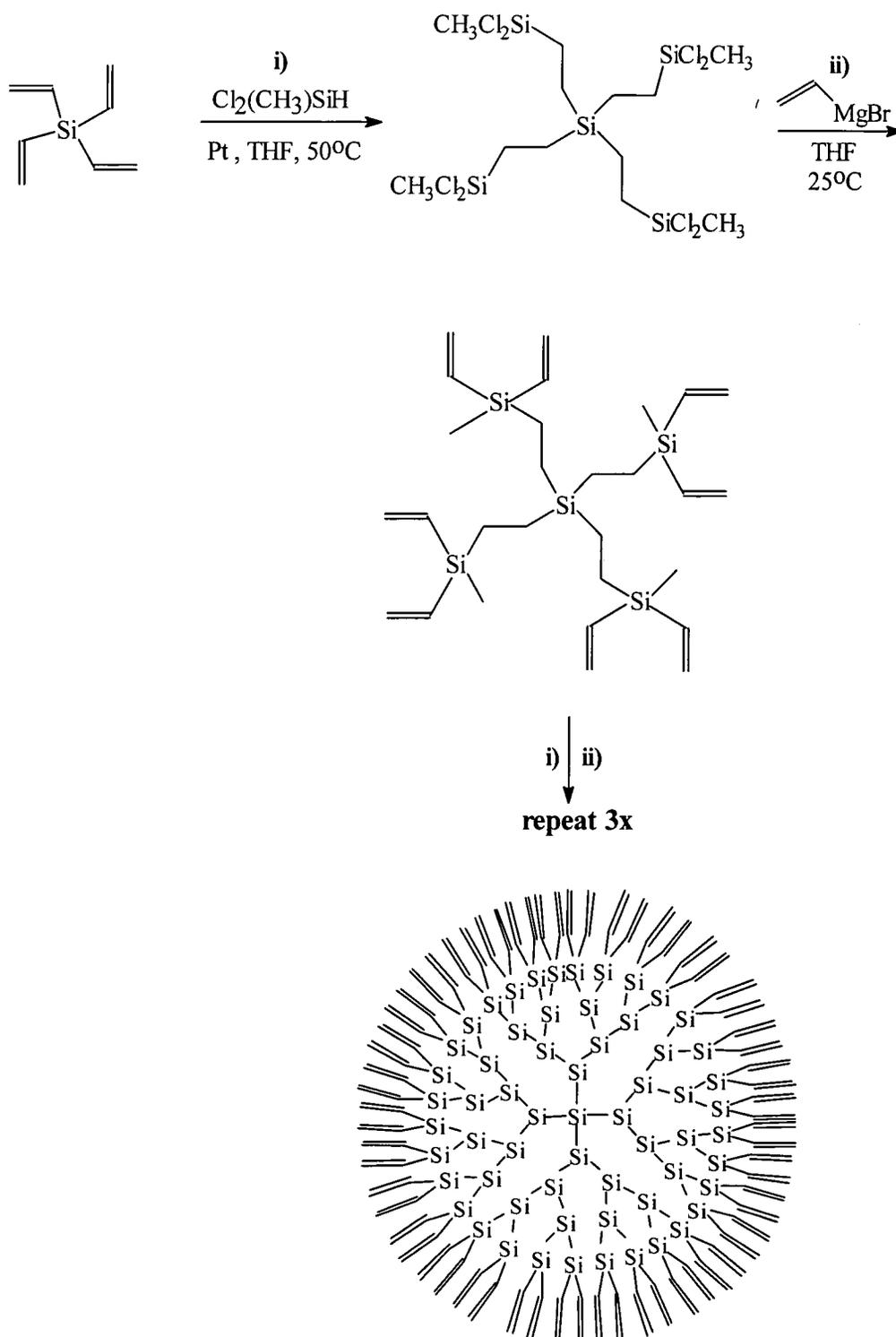
Figure 11. Roovers' synthesis of a four-directional silane cascade via Pt-

mediated hydrosilylation of alkenes; Si-Si links are $-CH_2CH_2-$, methyls on Si

omitted, surface groups are $-CH=CH_2$.

1.3.3 Convergent Dendrimer Synthesis

The divergent approach has certain limitations with regard to ideal dendrimer growth, particularly if accurate control over the placement of end groups at the periphery of the dendrimer is required. To overcome these limitations an alternative strategy was developed. This methodology, the convergent growth approach, was first reported by Fréchet[21,31] and Miller[32]. Disconnection of a dendrimer eventually leads to the chain ends and the core. In this approach it is the chain ends which are the starting point in the synthesis, which is exactly the reverse of the divergent growth approach where synthesis starts at the core. The convergent growth route is shown in Figure 12. Growth begins with the chain ends or terminal group, S, which carries a reactive group A for coupling to a monomer unit **3**, carrying two reactive groups B and a protected A group (P). Group A reacts specifically with B leading to the next generation dendron, **4**. Activation of the functionality, P, at the focal point of dendron (**4**), gives the reactive group A, which can again be coupled with the monomer unit to give the next generation dendron, **5**. Repetition leads to larger and larger reactive dendrons and, if desired, the final reaction step may involve attachment of several reactive dendrons to a polyfunctional core, to generate a dendritic macromolecule similar to that which might be obtained from a divergent strategy. Using the convergent strategy, Hawker and Fréchet[21,31] reported the synthesis of a series of dendritic polyether macromolecules as shown in Figure 13.

Figure 12. Convergent dendrimer growth.

Preparation proceeds by Williamson ether synthesis between benzyl bromide and 3,5-dihydroxybenzyl alcohol **6**, coupling proceeds in high yields under mild conditions with minimal side reactions. By design, alkylation of **6** occurs regioselectively at the more reactive phenolic hydroxy groups, leaving the hydroxymethyl group in **7** available for conversion to a bromomethyl group using carbon tetrabromide and triphenylphosphine to give the reactive dendron **8**. The two-step alkylation/bromination procedures are repeated to give monodisperse reactive dendrons, **9** and **10** that have a single functional group at their focal points available for further reaction with monomer **6**. Hawker et al. synthesised a sixth generation reactive dendron with 64 terminal groups possessing a molecular weight of 13,851 amu. Significant to the success of the overall synthesis is the choice of the monomer and end groups which make purification of the intermediate dendrons relatively easy.

For attachment to a polyfunctional core, three molecules of a fourth generation dendron **(10)**, are reacted with the trifunctional core 1,1,1-tris(4'-hydroxyphenyl)ethane affording the dendrimer **(11)** possessing no focal point reactivity and a molecular weight of 10,127. A series of monodisperse dendrimers with molecular weights ranging from 576 to 40,689 have been produced by this route.
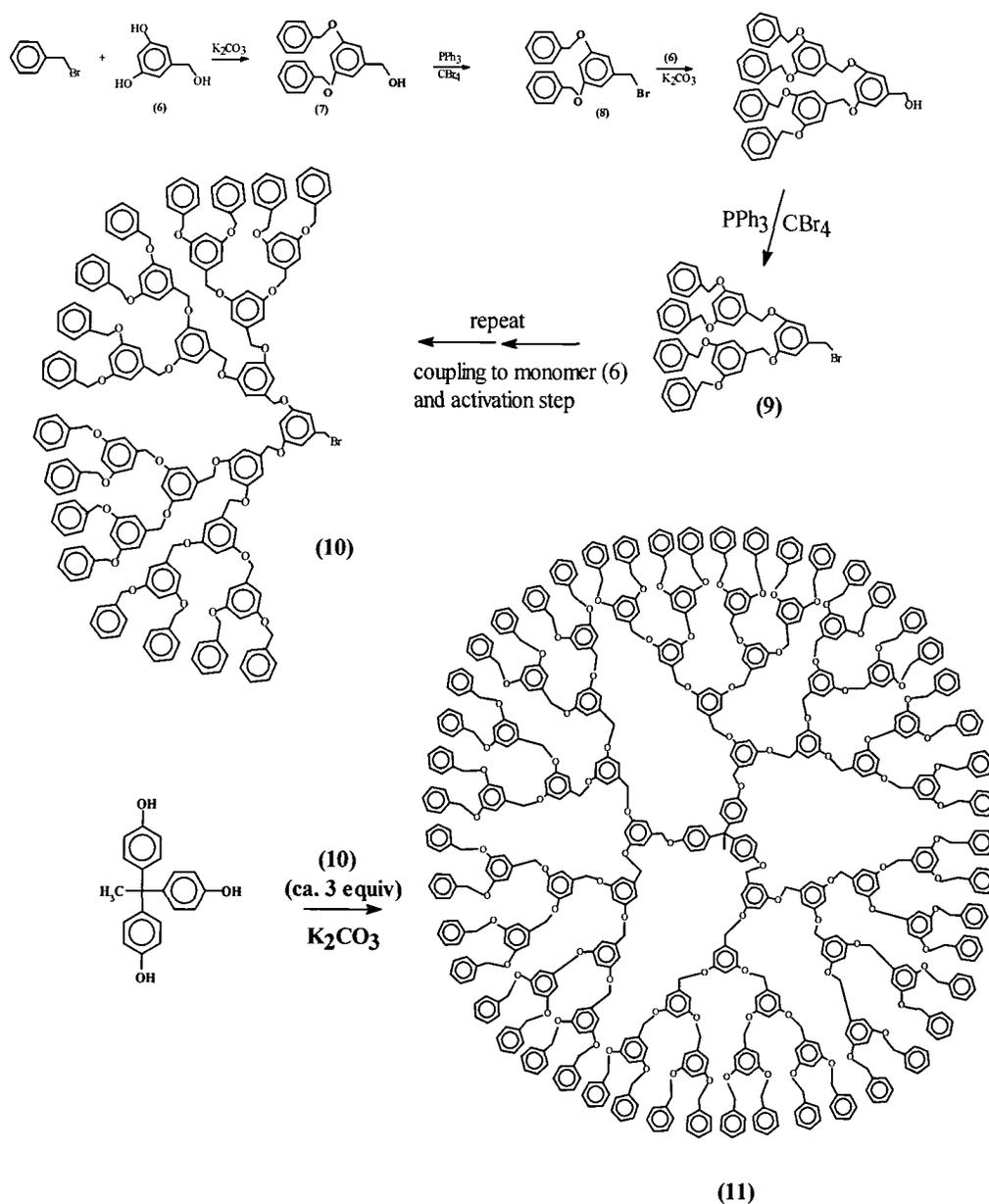
Figure 13. The convergent approach to poly(ether) dendrimers.

Fréchet reported the convergent synthesis of dendritic polyamides via coupling of a secondary amine to a N-t-BOC protected aminodicarboxylic acid. The polycondensation reaction with sequential coupling-deprotection steps afforded polyamides with molecular weights up to 5082 [33] as shown in Figure 14.
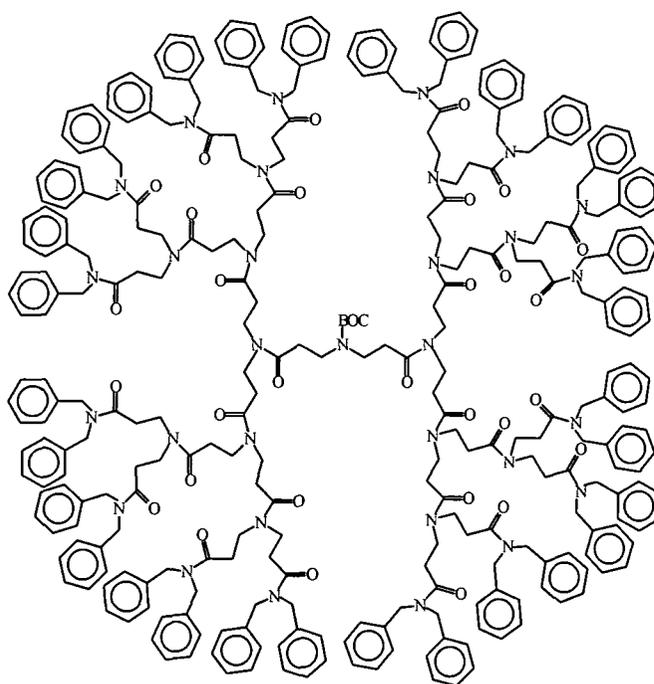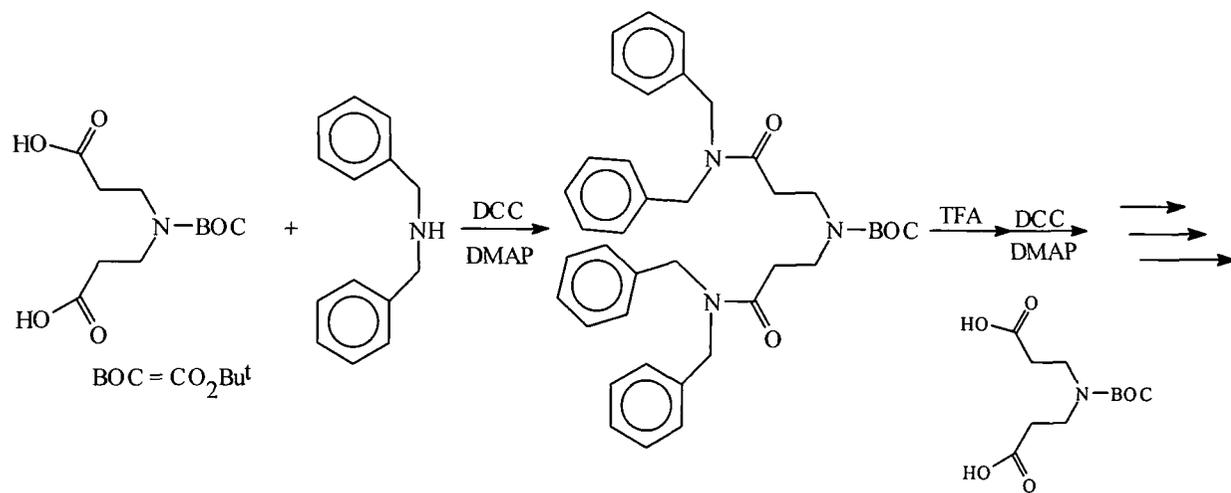
Figure 14. Fréchet's convergent construction of a polyamide cascade using peptide

coupling for monomer connectivity.

In 1990 Miller and Neenan[32] reported convergent syntheses based upon 1,3,5-

triaryl benzenes and 1,3,5-triarylamides, the former is illustrated in Figure 15.
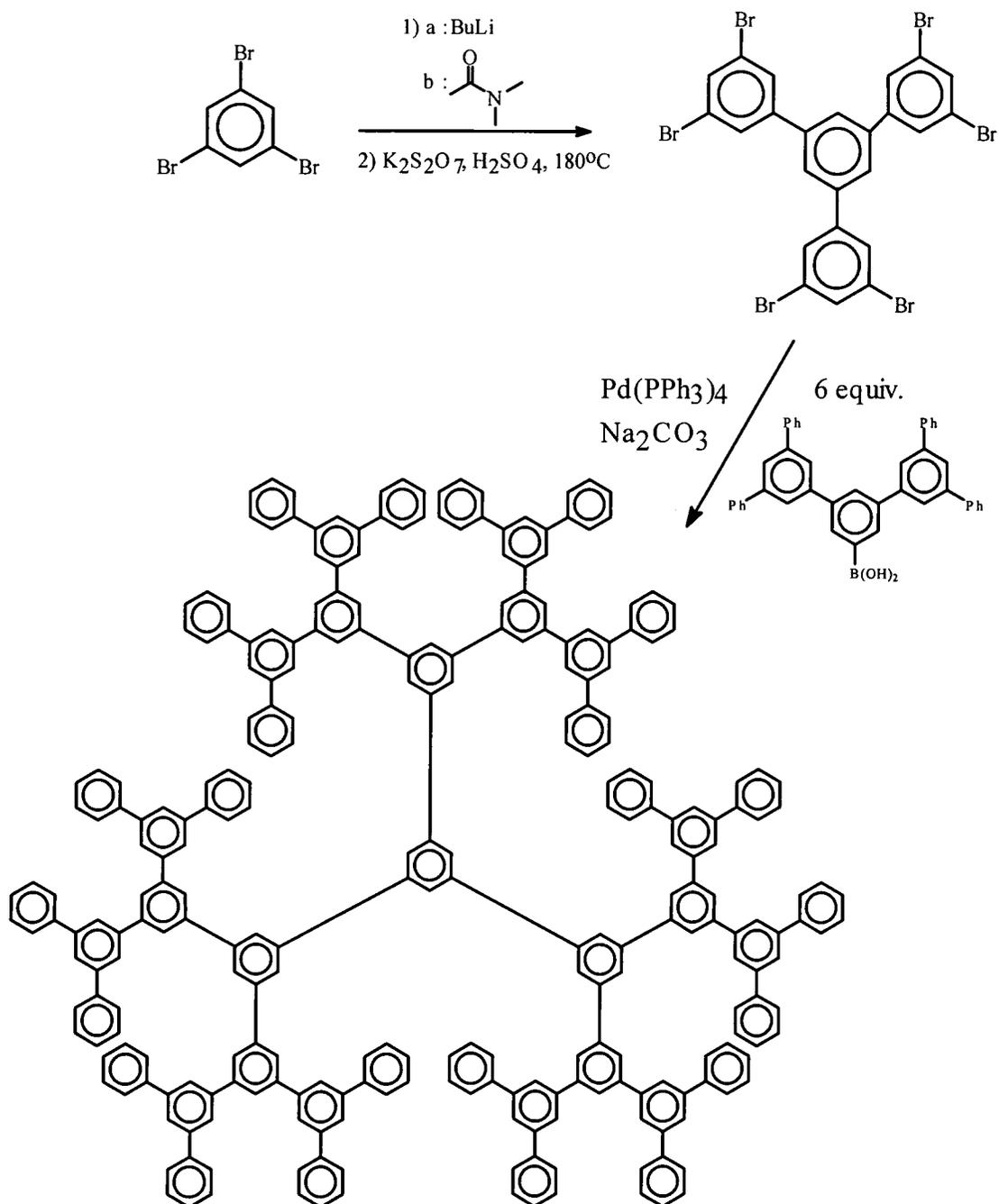
Figure 15. Strategy used to construct a four-tier, three-directional aromatic

hydrocarbon cascade using an extended hexabromide core.

Polypentafluorophenyl analogues were synthesised according to the same

scheme. Polyarylester dendrimers were also synthesised by Miller's group, the

largest having 46 chain end phenyl groups and a molecular weight of 5,483

amu[34], see Figure 16. These examples are illustrative of the very wide range of

dendrimer structures prepared during the last ten years.
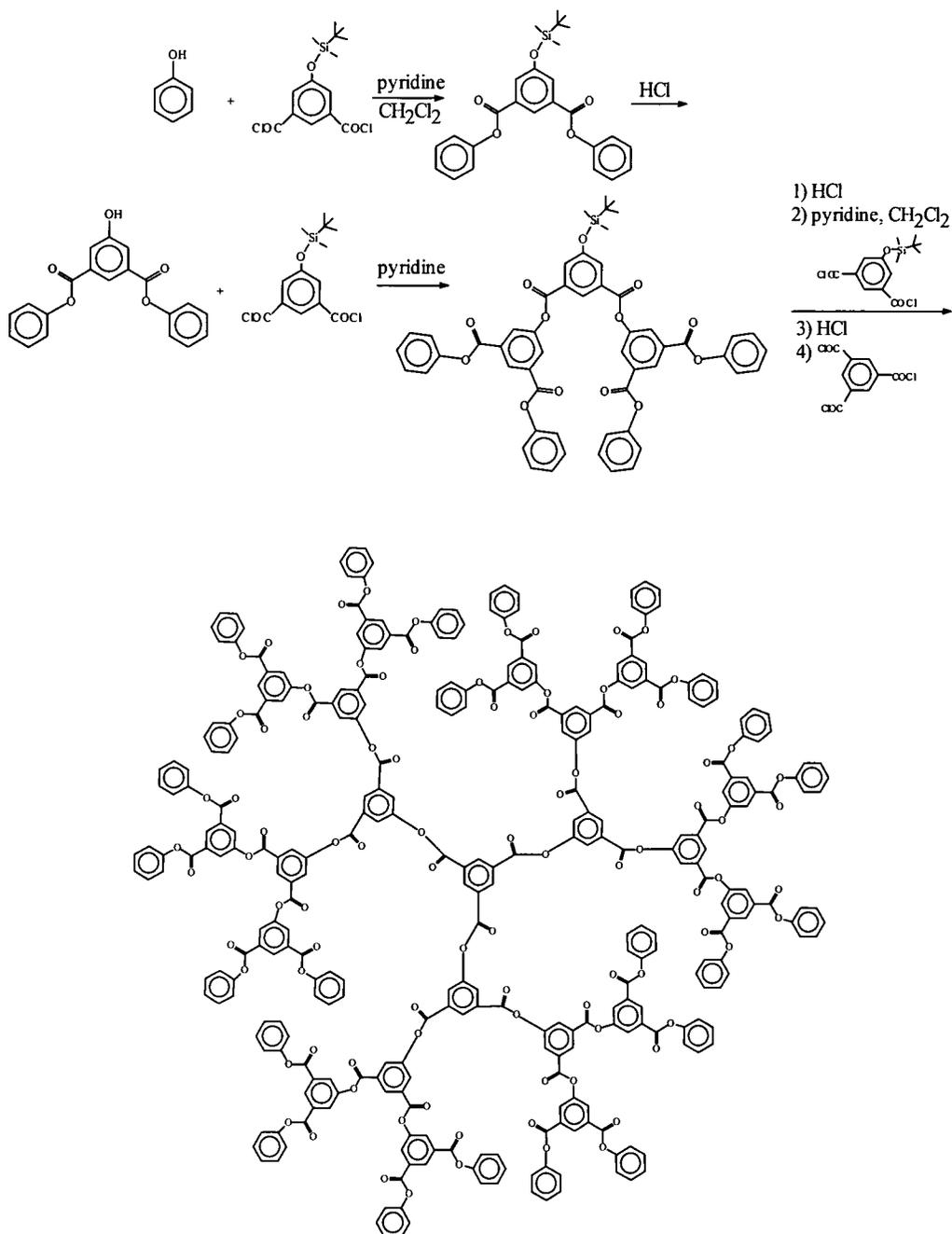
Figure 16. Preparation of a three-dimensional polyaryl ester dendrimer

1.3.4 A comparison of the divergent and convergent methods for dendrimer synthesis.

While both the convergent and divergent methodologies involve a step-wise growth approach and, depending on the choice of building blocks, can give the same dendritic structure there are some fundamental differences between the two approaches. These differences mean that careful examination of the desired dendrimer should be undertaken before planning any dendrimer synthesis, since one approach may be more appropriate than an other.

The more controlled nature of the convergent approach is better suited for the synthesis of very regular or precisely functionalised dendrimers where the number and nature of the chain ends, building blocks, and the focal point need to be controlled. Growth only requires coupling between the single reactive focal group and a small number of reactive sites on the monomer. Consequently, side reactions are minimal and, due to the significant differences in the sizes and polarity between the desired dendrimers and unreacted starting material, and unwanted side products, purification can be easily performed by standard techniques. In contrast, the divergent growth approach requires increasing numbers of both activation and coupling reactions for ideal growth to be achieved. The chances of defects increase rapidly as a function of the generation of the dendrimer and the small differences in the size and polarity between the perfect dendrimers and those with defects make their separation essentially impossible. Overall, the convergent synthesis provides easier access to "defect free" dendritic macromolecules. In contrast, for very large dendrimers (MW > 100,000) the divergent approach is the methodology of choice due to the ability

to use large excess of reagents and the minimisation of steric hindrance to reaction. Although the convergent growth approach maintains monodispersity, failure does occur when attempting to couple very large fragments to a core, or if purification of intermediate dendrons becomes impractical.

1.3.5 Inorganic and Organometallic Dendrimers

Dendrimers are not limited to those based on organic building blocks or even covalent bonds and consequently, as well as nitrogen, phosphorus and silicon, there have been a variety of creative synthetic strategies based on inorganic and organometallic compounds, a few of which are discussed below. The first neutral phosphorus containing dendrimer, in which the core and branch points are pentavalent phosphorus atoms was reported in 1994 by Majoral[35] see Figure 17. Starting from $SPCl_3$ or $OPCl_3$ cores, successive reaction with the sodium salt of 4-hydroxybenzaldehyde and $H_2NN(Me)P(S)Cl_2$, gave dendrimers up to the fourth generation with 48 terminal groups (15,000 amu). The only by-products of the reaction are NaCl and water. The terminal groups may be either aldehydes or phosphorus chlorine bonds allowing further reactions to produce dendrimers possessing a variety of end groups. Recent reports have described the grafting of 48 diphosphino ligands on the surface, the synthesis of the corresponding palladium, platinum and rhodium complexes, and their investigation as novel catalysts. The first inorganic transition-metal dendrimers with non-covalent bonding were designed by Balzani's group[36] and were based on a divergent approach via ruthenium 2,3-bis(2-pyridyl)1,4-pyrazine units and contained up to 22 ruthenium atoms. Puddephatt[37] used a similar strategy to

synthesise dendrimers containing up to 28 platinum atoms. The group of van der Made and van Koten[38] have reported the synthesis of arylnickel (II) complexes coupled to the chain ends of a silane dendrimer with up to 12 nickel atoms.
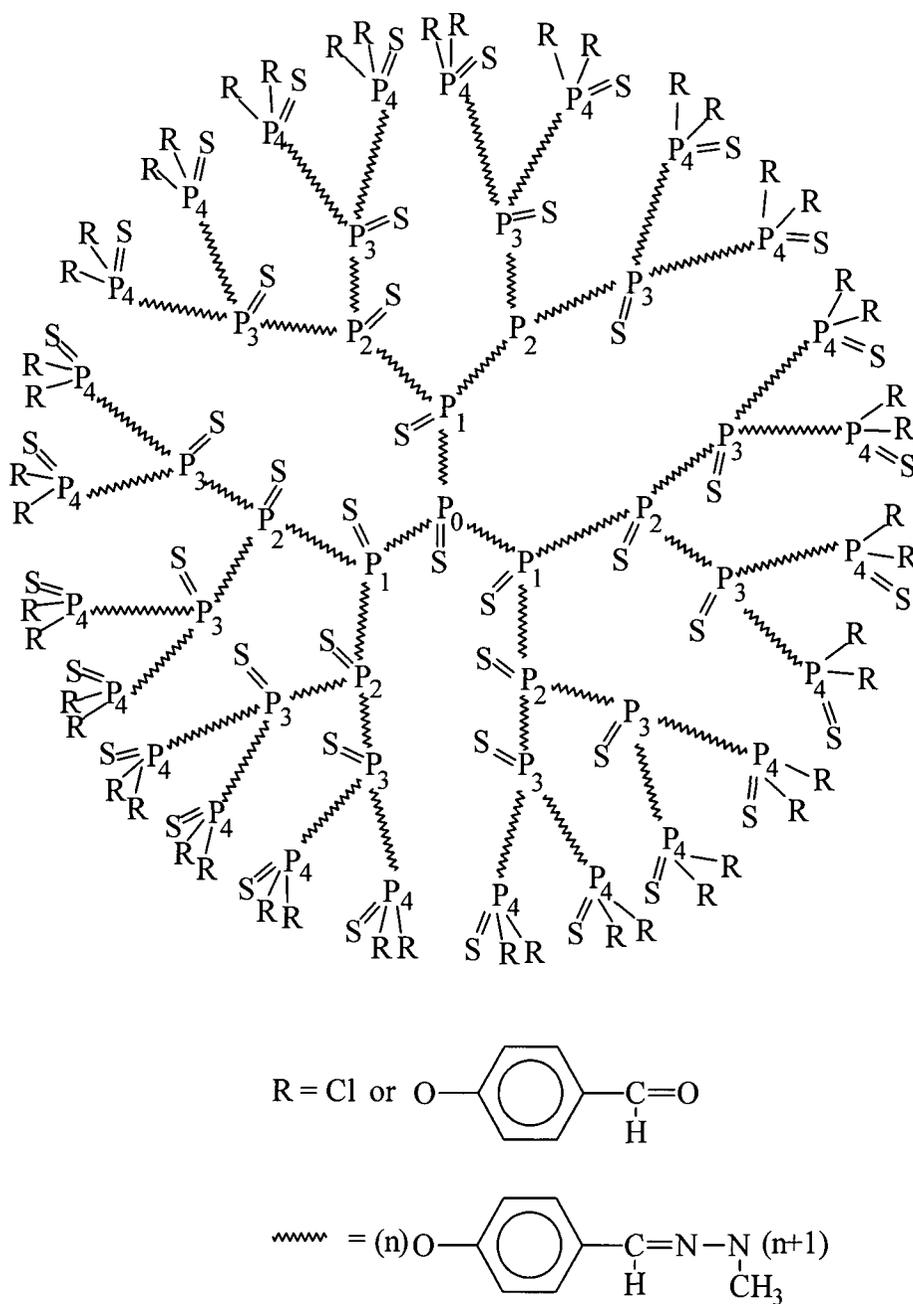
Figure 17. The first neutral phosphorus containing dendrimer synthesised by Majoral et al.

1.3.6 Charged, Chiral and Micellar Dendrimers

As early as 1985[39], the use of dendrimers as unimolecular micelles was proposed by Newkome and in 1991 he enhanced the water solubility of a 36-arborol, similar to (5) in Figure 7, by oxidation of the terminal primary hydroxy groups to carboxylic acids with $RuO_2/NaIO_4$, followed by generation of their corresponding ammonium and tetramethylammonium carboxylate salts in order to study the micellar properties by UV spectroscopy of non-polar guest molecules (pinacyanol chloride, phenol blue and naphthalene) in aqueous solution. The interactions of these water soluble cascade polymers with the guest molecules strongly suggested that the spherical polymers existed as single molecules (monodisperse) capable of molecular inclusion and therefore acting as unimolecular micelles. Recently, Meijer (1996)[40], reported the synthesis of *inverted* unimolecular dendritic micelles, by the modification of the end groups of hydrophilic poly(propylene imine) dendrimers (DAB-*dendr*-(NH$_2$)$_4$) to (DAB-*dendr*-(NH$_2$)$_{64}$), with hydrophobic alkyl chains. Evidence for an inverted micellar structure of the alkyl amide-modified dendrimers was obtained by their capability to act as host systems for guest molecules like Rose Bengal, a polar dye, in organic media. Fréchet has reported unimolecular micelles based on the convergent synthesis of dendritic polyether dendrimers with 3,5-dihydroxybenzyl alcohol building blocks[41]. The chain ends were modified with carboxylate groups and their ability to solvate hydrophobic molecules in water was investigated by UV-VIS spectroscopy.

Polyphosphonium[42] and polyammonium[43] dendrimers made by Engel and Rengan are shown in Figure 18. The polyphosphonium dendrimers were

synthesised by reacting tri-[(methoxymethyl)phenyl]phosphine with an alkyl halide or bromo-4-(methoxymethyl)benzene and $NiBr_2$ giving three or four directional cores respectively. The structures shown in Figure 18 result from four directional cores. Transformation of the benzyl ether groups to benzyl iodides using Me_3SiI followed by the addition of four equivalents of tri-[(4-methoxymethyl)phenyl]phosphine and repetition of the sequence produced a 36 branch dendrimer insoluble in water, but soluble in acetonitrile and alcohols. The polyammonium dendrimer shown in Figure 18 was synthesised in a similar manner by reaction of triethanolamine with 2-chloroethanol to give a four directional core. The polyol was then tosylated in pyridine and treated with excess triethanolamine, repetition of the sequence gave the 36-branch dendrimer. The first report of an organic chiral dendrimer was published by Newkome[44], who modified an amine-terminated dendrimer with enantiomerically pure tryptophan. Since that time many groups have prepared dendrimers based on or capped by amino acids[45,46]. Meijer has investigated the properties of chiral dendrimers based on the attachment of four different wedges to a pentaerythritol core[47] and also chiral structures based on poly(propylene imine) dendrimers terminated with chiral amino acid derivatives[48]. The latter systems, known as "dendritic boxes", can encapsulate and physically lock guest molecules within the internal cavities of the dendrimer structure and possess peculiar chiroptical properties in that they have low or vanishing optical activity despite the surface coating of chiral units.

17 I⁻

R = CH₂OCH₃

17 Cl⁻
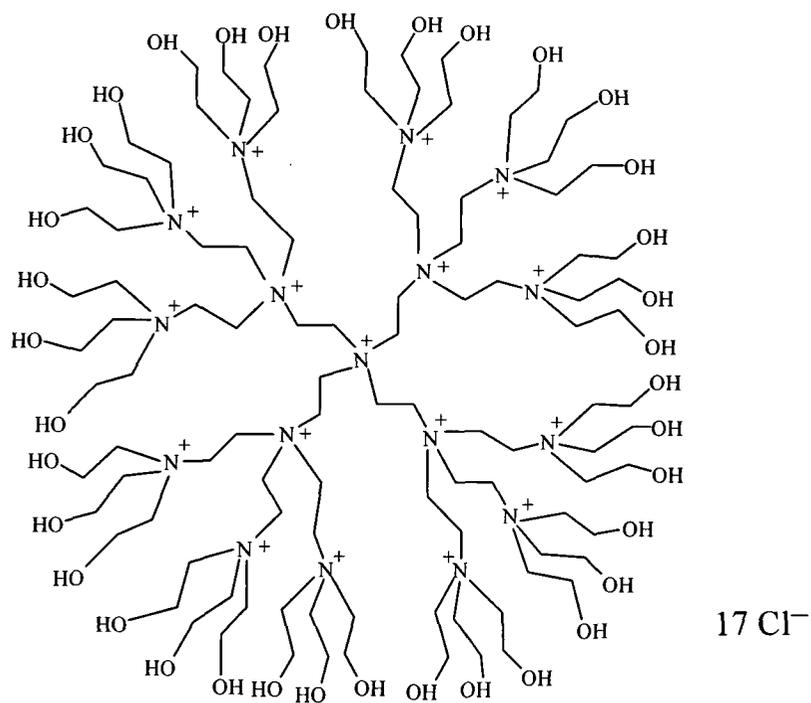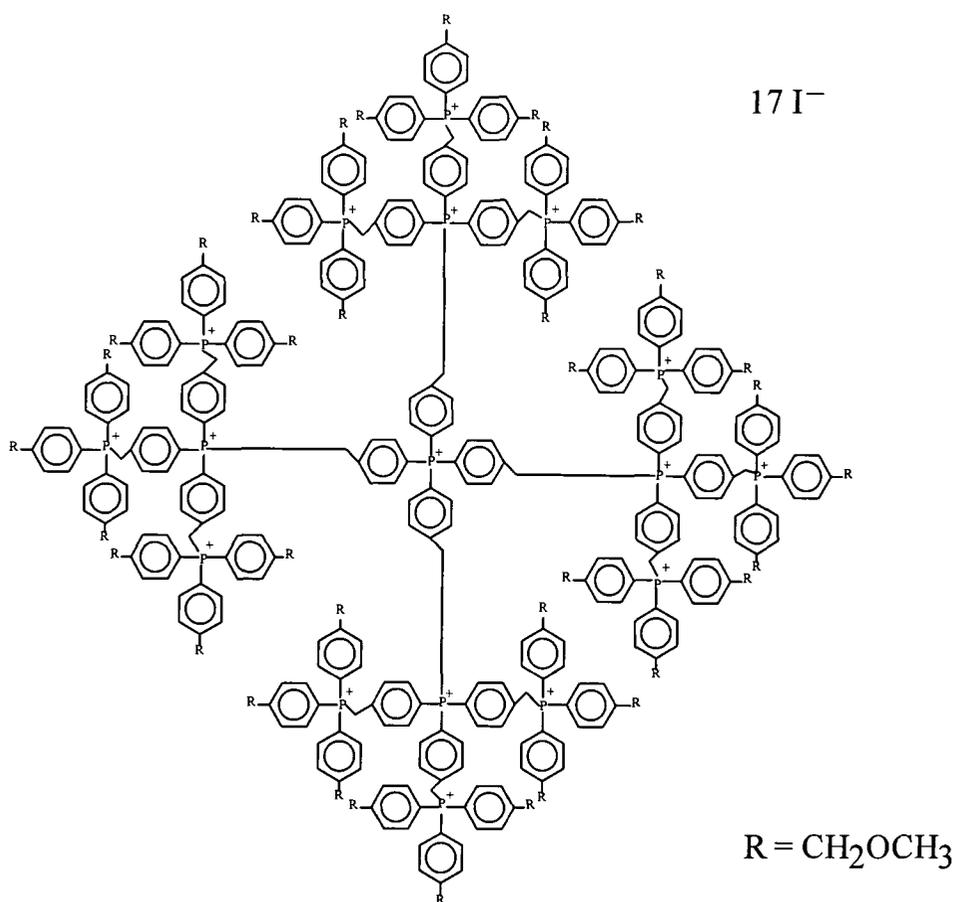
Figure 18. Polyionic dendrimers using phosphonium and ammonium moieties as branching centres.

1.4 Characterisation of Dendrimers

Unlike conventional synthetic polymers which are polydisperse in molecular size and frequently polydisperse in structure also, dendrimers are truly monodisperse and, when perfect, are unique molecules. The precision with which dendrimers can be characterised results from their high symmetry and monodispersity. Analytical and spectroscopic techniques useful for the characterisation of dendrimers are the same as used in conventional organic chemistry; namely, elemental analysis, infrared and NMR spectroscopy (especially ^{13}C and 2D-HETCOR and COSY). Gel permeation chromatography (GPC) is a useful tool for monitoring dendritic growth by the convergent approach since the hydrodynamic volumes of substrates and products change dramatically with each step. Incomplete reactions result in multimodal distributions and purified dendrons give single narrow peaks. The GPC traces for dendritic macromolecules have appreciably narrower peak widths than conventional polystyrene calibration standards.

Recent developments in soft ionisation techniques for mass spectrometry have also contributed to establishing the molecular weights of dendrimers. The ionization techniques used for dendrimers include fast atom bombardment (FAB), laser desorption and electrospray. Matrix assisted laser desorption/ionisation time of flight mass spectroscopy (MALDI - TOF), has been used to confirm the very low polydispersity of dendrimers[49].

The structure and purity of dendrimers can be confirmed by NMR spectroscopy since the highly ordered and symmetrical branching sequence allows small changes in the focal group, terminal groups, and interior building block

structures to be observed. ^{13}C NMR and electrospray mass spectroscopy are considered to be the best techniques to investigate branch defects. Structurally 'perfect' dendrimers are monodisperse whereas dendrimers with defects are polydisperse. For example, the PAMAM dendrimers of Tomalia have been found to have a polydispersity of 1.08 for generation 10 which is similar to the polydispersities found for linear polymers produced by living chain growth techniques.

1.5 Synthesis of Hyperbranched Polymers.

Hyperbranched macromolecules are prepared by a one-step synthetic strategy involving the polymerisation of an AB_x type monomer unit. The reactive groups, A and B, react only with each other. This one-step synthetic strategy results in significant structural differences between dendrimers and hyperbranched polymers. In most cases the one-step polymerisation of an AB_2 monomer unit generates uncontrolled growth and leads to a complex polydisperse hyperbranched product (13), shown in Figure 19. Such polymers contain structural features that resemble both dendrimers and linear polymers.

Three different sub-units have been identified and these are known as dendritic, linear and terminal and differ in the number of B functionalities that have undergone reactions to form polymeric linkages, C. Dendritic units are obtained by reaction of both B functionalities and resemble the internal building blocks present in dendrimers. If only one of the two B functionalities react, a linear unit, analogous to that which would be found in a true linear polymer, is obtained. It is

these "defects" which create the main structural differences between hyperbranched polymers and dendrimers.
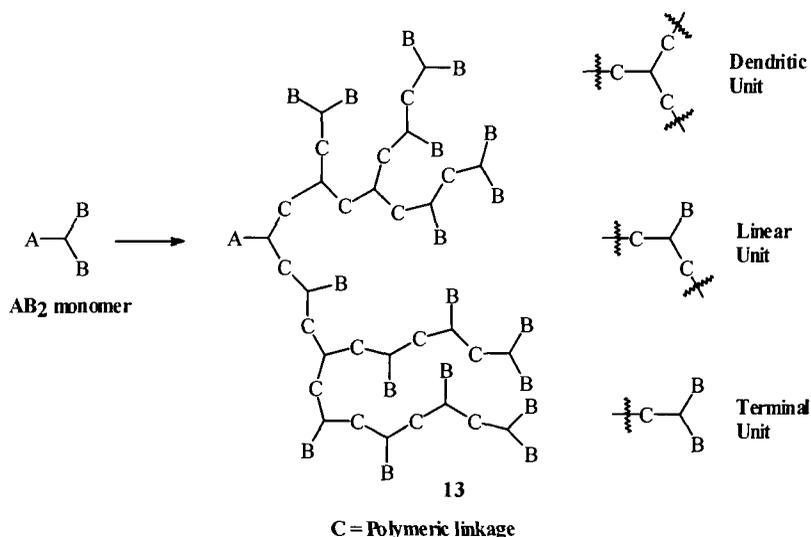
Figure 19. Hyperbranched polymer architectures.

A terminal unit is obtained when neither of the B functionalities react and is comparable to an outer layer, or chain end unit of a dendrimer. Hence, the structure of hyperbranched polymers are intermediate between those of "perfect" dendrimers and linear polymers.

Kim and Webster[50] reported the preparation of hyperbranched polyphenylenes in 1989. They made them from the AB_2 monomers, 3,5-dibromophenyl boronic acid or 3,5-dibromophenyl magnesium bromide (Figure 20).
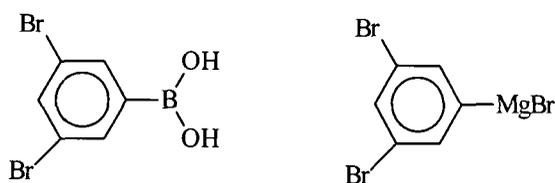
Figure 20. Building blocks for the synthesis of polyphenylenes.

Like dendrimers, the synthesis of hyperbranched polymers has progresssed rapidly and numerous hyperbranched *systems* have been described. Hyperbranched polyesters[51], poly(etherketones)[52] , poly(ethers)[53] , poly(urethanes)[54] , poly (siloxanes)[55] , *etc.*, have all been prepared using classical step growth chemistry.

1.6 Properties of Dendrimers and Hyperbranched Polymers.

One of the driving forces in the study of highly branched macromolecules is the belief that these materials will have fundamentally different properties when compared to traditional linear polymers with only two chain ends. The contributions from these chain ends is negligible at high molecular weights and physical properties are dominated by chain entanglements and the presence, or absence, of functionalities attached to the polymer backbone. In contrast, both dendrimers and hyperbranched polymers are expected to adopt a globular structure, both in solution and in the solid state, and the influence of chain entanglements and intermolecular interactions are minor factors in determining their physical properties. A fundamental feature of hyperbranched polymers and dendrimers is the presence of large numbers of chain ends and these chain ends are thought to play a major role in determining the physical properties observed.

Thermal characteristics, such as glass transition temperatures, and thermal decomposition temperatures of dendrimers and hyperbranched polymers are both similar to those displayed by their linear analogues.[56] The solubility of dendrimers, due to the highly branched, globular structure, is significantly improved when compared to their linear analogues, indeed Miller and Neean have

reported solubility enhancements of 10^5 for dendritic poly(phenylenes) when compared to linear poly(phenylenes)[32]. Plots of log[intrinsic viscosity] vs log[molecular weight] have been reported to produce different curves for all three architectures[57] (Figure 21). For dendrimers a bell shaped relationship is observed instead of the linear relationship expected from the Mark-Houwink equation which describes the behaviour of linear polymers. In contrast to dendrimers, hyperbranched polymers are reported to follow the Mark-Houwink relationship, ($[\eta]$=K M$^\alpha$), albeit with fairly low values of α when compared to linear polymers. The area of investigation is still in its early stages and although the generalisations reported above have been published they are based on a limited set of examples and may be subject to modification. Thus, for example, Hobson has recently described a synthesis of core-terminated hyperbranched analogues of the Tomalia PAMAM dendrimers in which branching is perfect and which display the peak in the log(intrinsic viscosity) vs log(molecular weight) plot which is normally associated with dendrimers[58]. Also the commercial data published for DSM's dendrimers indicate a probable plateau in the curve rather than a peak,[59] although in recent lectures Meijer has indicated that higher members of this series do show decreasing intrinsic viscosity. Clearly these matters need further study before the picture becomes entirely clear. Similarly, melt viscosity[60] studies on dendrimers (Figure 22), do not show the dramatic increase in viscosity with increasing molecular weight like linear polymers, instead a linear relationship between viscosity and molecular weight is observed up to molecular weights of 100,000 amu in the systems studied so far. Hyperbranched polymers show low melt viscosities when compared to linear polymers. This viscosity behaviour is thought

to be a consequence either of geometrical considerations assuming that dendrimers have a spherical shape, or a significant reduction of entanglements for dendrimers and hyperbranched polymers as compared to their linear analogues.
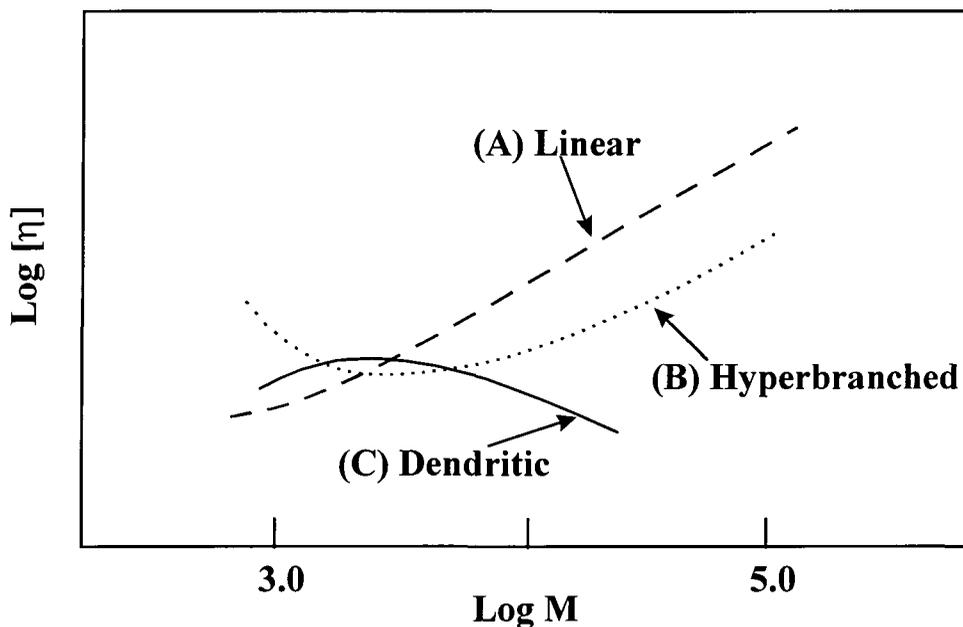
Figure 21. Schematic plot of log(intrinsic viscosity) versus log (molecular weight) for linear (A), hyperbranched (B), and dendritic (C) polymers[57].
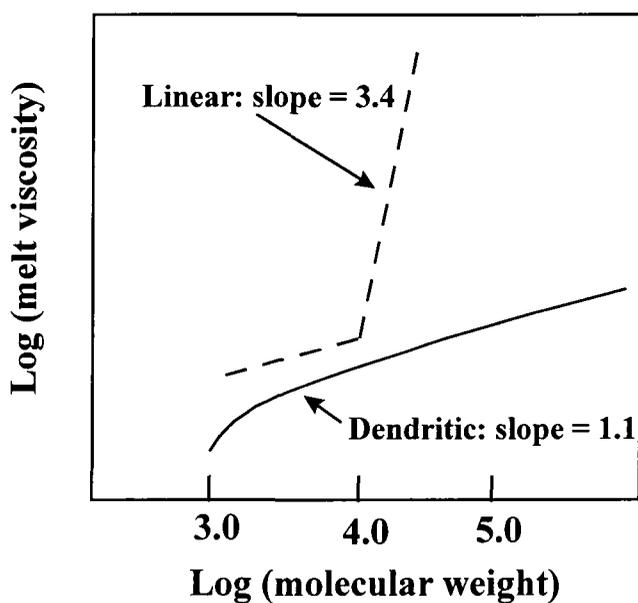
Figure 22. Schematic plot of log (melt viscosity) versus log (molecular weight) for linear and dendritic polymers[60].

For linear polymers the chains can coil and entangle and the onset of these entanglements leads to the dramatic increase in viscosity observed at a specific molecular weight. In contrast, the globular and highly branched architecture of dendrimers effectively prevents entanglements at all molecular weights, therefore the individual molecules do not entangle and no dramatic increase in melt viscosity is observed.

In conclusion, at this early stage in the study of these systems it appears that some physical properties such as glass transition temperature and thermal degradation are independent of architecture but are dependent on the number and nature of the chain ends. Other physical properties such as solubility, chemical reactivity, viscosity, etc. are dependent on macromolecular architecture and definite differences are observed between linear, dendritic and hyperbranched polymers based on the same building block.

1.7 Novel Linear - Dendritic Block Copolymers.

AB or ABA block copolymers can be synthesised by attachment of a single linear polymer chain to the focal point of a dendrimer in which the dendrimer and the linear polymer are the A and B blocks, respectively. Recently, hybrid structures have been reported based on attachment of linear polymers (PEO,PEG), by the Williamson reaction, to the focal point of a reactive benzylic dendritic polyether dendron obtained by the convergent growth approach[61]. Several novel copolymers were also prepared by copolymerisation of a hyperbranched polyether macromonomer, (having a polymerisable group attached at the focal point), with styrene under standard free-radical conditions[62].

Recently, Meijer et al. has synthesised an amphiphilic macromolecule by creating

well-defined diblock copolymers of polystyrene with poly(propylene imine)

dendrimers[63], see Figure 23. The polystyrene precursor had a primary amine chain

end and was prepared by a three-step modification procedure of acid-

functionalised polystyrene. Dendrimers up to the 5th generation with 32 end

groups were grown from the polystyrene in high yields. Generation-dependent

amphiphilic behaviour was observed using conductivity measurements and

monolayer pressure-area isotherm determinations. These amphiphiles show a

similarity to traditional block copolymers with regard to size and stability, and are

like surfactants with respect to tuning of the shape. There is a practical limit to the

polystyrene chain length which can be used in the synthesis of these novel

amphiphiles which is below the entanglement length of polystyrene[64].
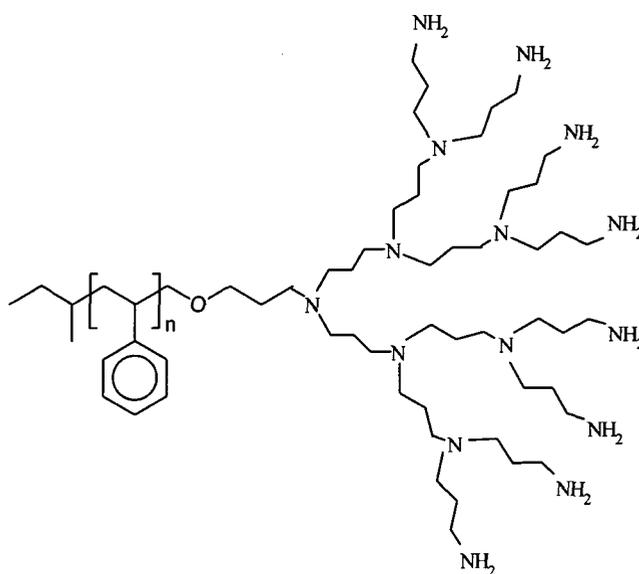
Figure 23. An amphiphilic diblock copolymer consisting of a 3rd generation

poly(propylene imine) dendrimer wedge grown from a linear polystyrene core.

1.8 SUMMARY - Novel Functionalised Dendritic Architectures - Application orientated macromolecules.

The rapid development of research in the field of dendrimer synthesis over the past decade has seen a near exponential increase in the number of publications produced. To date the synthesis of high molecular weight dendrimers such as poly(amidoamines) (PAMAM)[2], poly(propylene imines)[23,24], and silicon dendrimers[29,30] to high generations has been established. The polyacetylene dendrimer prepared by Moore et al[65] formula C_{1398} H_{1278} and mass 18,079 gmol^{-1}, is the biggest pure hydrocarbon dendrimer reported. Recently the emphasis has changed and an indication of new trends was seen by the report in 1992 by Shinkai et al describing a "crowned arborol" dendrimer possessing crown ether end groups[66], and in 1993, Vögtle et al's reversibly photoswitchable dendrimer with azobenzene at the periphery of the molecule[67]. Therefore synthetic strategies are being developed allowing properties to be modified by the incorporation of specific functional components into these relatively new macromolecular architectures. Not the dendrimer itself but the multiplication of functionalities attached to the dendritic framework appears to be the more important factor, and new materials with specific properties are anticipated.

Generally, the functional units are located on the dendrimer surface but Vögtle has synthesised a dendrimer with a complexing inner core (hexacyclen = hexaaza[18]crown-6) via a convergent approach[68], shown in Figure 24.
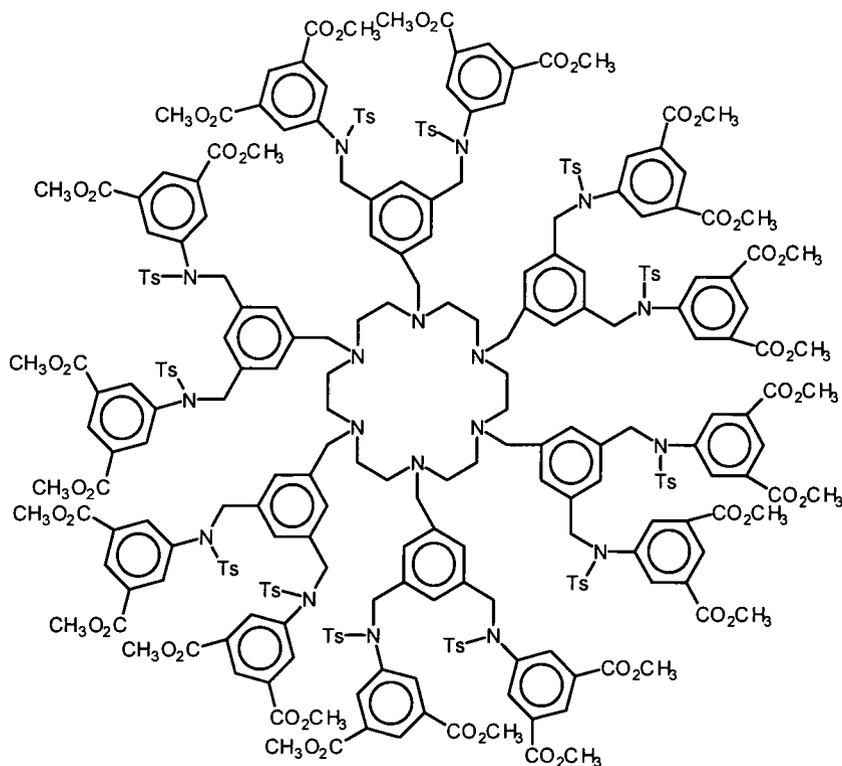
Figure 24. Dendrimer possessing a hexacyclen complexing inner core obtained by a convergent strategy.

This structure contains a nucleus capable of performing special functions (e.g. complexation of luminescent metal ions) which are influenced to some extent (sterically or electronically) by the periphery.

Using a convergent approach Inoue et al have prepared a dendrimer with a sterically shielded photoactive metal porphyrin at its centre[69]. Using Newkome's divergent synthesis Diederich et al prepared a third generation dendrimer with a molecular weight of 19000 amu containing a zinc porphyrin at its centre[70].

Newkome et al prepared a dendrimer framework containing triple bonds, which could be complexed by dicobalthexacarbonyl units and when treated with decaborane ($B_{10}H_{14}$) produces a dendritic "boron supercluster" with up to twelve

covalently bound borane clusters at defined sites inside the dendrimer[71,72] , see

Figure 25. This is not simple complexation but reaction with the dendrimer to

give a polycarborane[72].
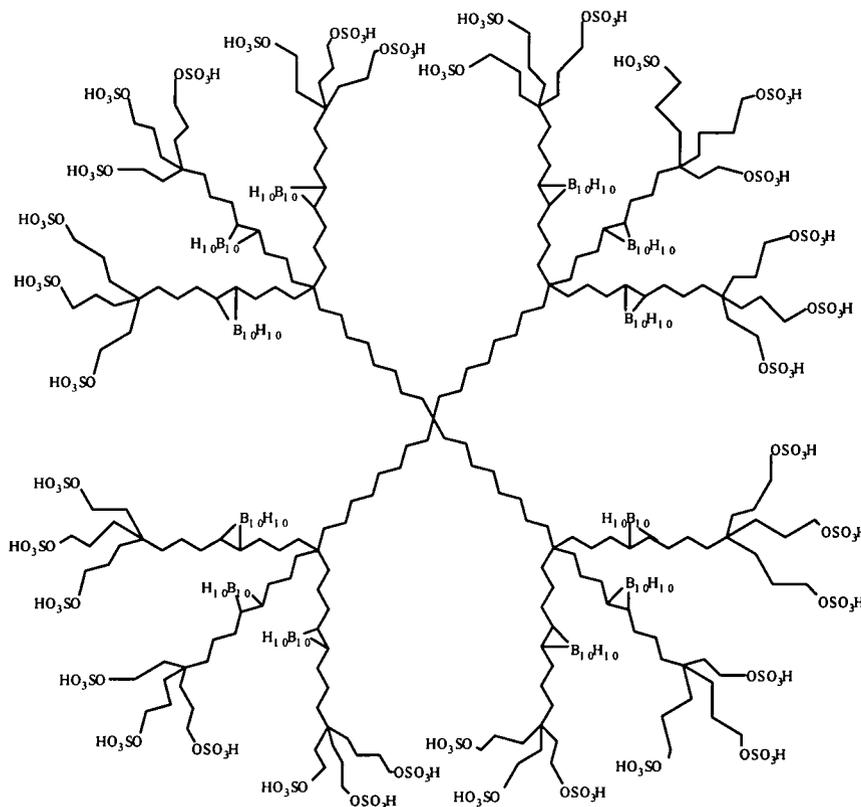
Figure 25. Functionalised dendrimer with 12 borane clusters on the interior of the

dendritic structure.

It was suggested that when functionalised at the periphery with sulphonate groups

to give water solubility, these materials may find application in catalysis[71,73] or

boron-neutron-capture therapy in cancer treatment[74]. Redox-active dendrimers

have been prepared by a number of groups[75] and may be useful as organic

conductors or for the investigation of charge-transfer interactions.[76]

Biochemically active dendrimers via the connection of natural products or drugs to a dendritic skeleton is also reported to be very promising[77,78] Analogues of nucleic acids and peptides have been synthesised in a dendritic manner by Hudson and Damha[46] and Rao and Tam[79] respectively. Recent advances in the synthesis of dendrimers from inorganic building blocks and the preparation of chiral structures and dendrimers containing cavities has been discussed previously (Section **1.3.6**). Of particular interest are dendrimers that have been prepared which release guests on changes of pH and have potential for the targeted application of pharmaceuticals. The synthesis of liquid crystalline dendrimers may have potential for possible industrial applications. Due to the round, flattened shape of many dendritic structures, particularly lower generations, they should be able to form discotic phases. Dendrimers with liquid crystalline properties have been reported by a number of research groups already.[80,81] "Willowlike" thermotropic liquid crystalline hyperbranched polyethers have been prepared by Percec and Kawasumu, one example is shown in Figure 26.[82] Due to the conformational flexibility of this molecule, the asymmetric three-dimensional compound is mesogenic. The polymer was obtained from a monomer consisting of a diphenol carrying an alkyl bromide using phase-transfer catalysis (Bu_4NHSO_4, 10M NaOH, o-dichlorobenzene) followed by alkylation of the terminal groups. Transitions between the nematic and isotropic states were found to occur between 20 and 50°C (R = *n*-octyl, *n*-hexyl), a range interesting for potential applications. Moore et al.[83] recently reported the design and fabrication of LED's using new luminescent phenylacetylene dendrimers as the organic layer. These authors suggest that a modular approach to the design and construction of electroluminescent materials

may provide a systematic approach to altering the active layer of organic LED's; however, the efficiency of the dendrimer segment needs to be improved.

80°C

1) TBAH/ o-dichlorobenzene/ 10M aqueous NaOH

2) X-Br or X-Cl / o-dichlorobenzene

Solution or Isotropic state

$R=$ $-(CH_2)_7-CH_3$
$-(CH_2)_5-CH_3$
$-(CH_2)_3-CH_3$
$-CH_2-$

Nematic state
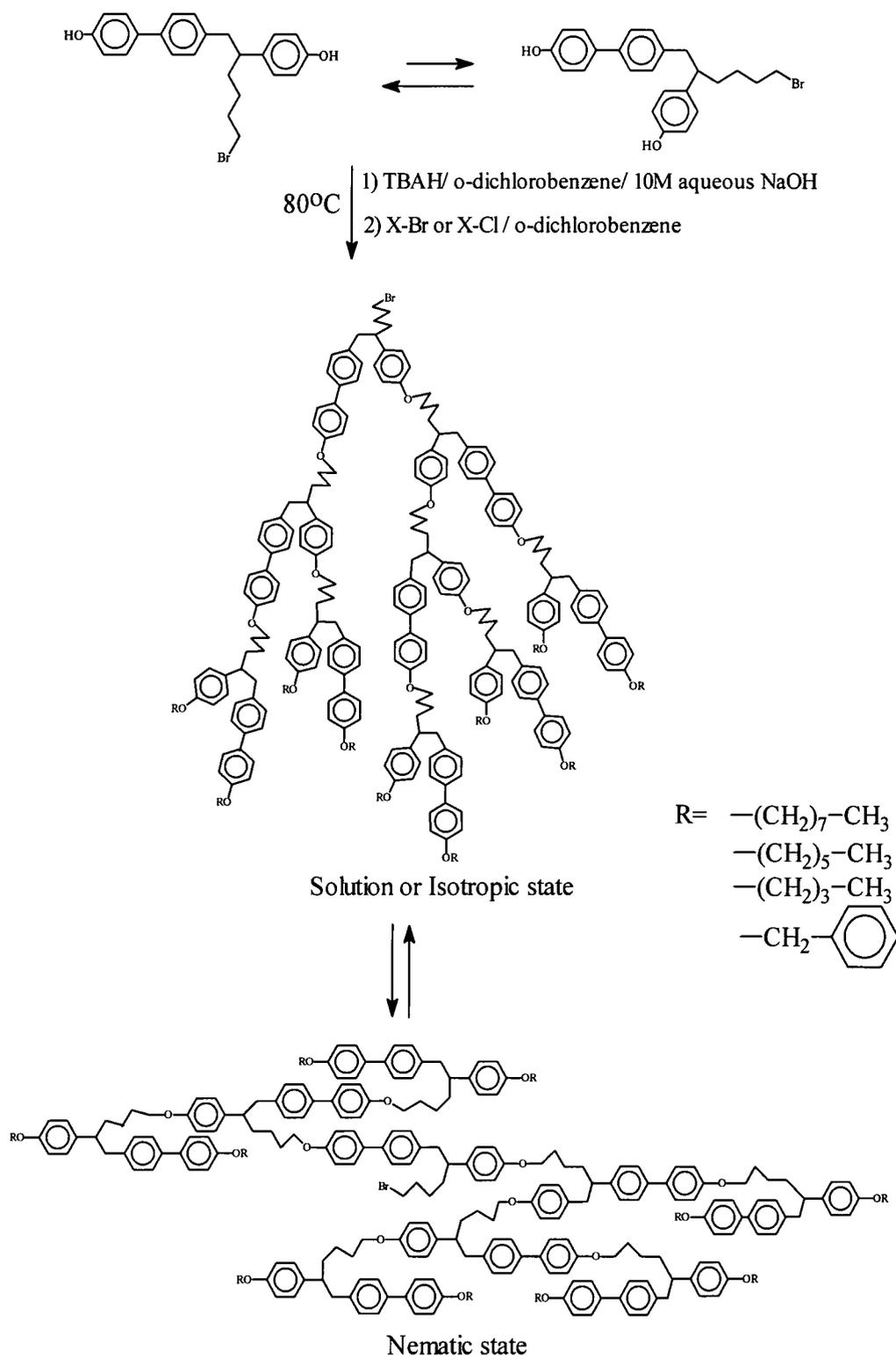
Figure 26. A liquid crystalline hyperbranched polyether.

The enthusiastic activity in the field of dendritic and hyperbranched polymers has made many unusual structures available and provided substantial knowledge of dendrimer properties and dendrimer reactions. There is now commercial interest and industry is investigating possible applications for these macromolecules. This is illustrated by the PAMAM Starbursts[2,29] which are sold by Dendritech Inc. mainly to the pharmaceutical industry for investigation as carrier molecules in medical diagnostics and therapy. Similarly, DSM produce poly(propylene imine) dendrimers on a multi-kilogram scale[34] and these materials are available as Astramol[TM]. Dendritic structures and their hyperbranched analogues may find applications as sealants or adhesives, in coatings or as rheology and mechanical property modifiers in the not to distant future.

1.9 Background to this project.

This work was sponsored by Unilever and formed part of a larger programme of work in the IRC in Polymer Science and Technology investigating fundamental and applied aspects of dendrimer science and technology. One potential application which was explored in this study was the use of such materials as possible additives in detergents designed to carry an expensive functional component more cost-effectively to a specific surface.

For example, optical brighteners and fouling release agents are added to detergents to give improved fabric effects. However, most of these expensive additives are washed down the drain during the wash cycle and not recovered. If a dendritic structure could be attached to the brightener and functionalised with specific surface recognition groups so as to provide a bigger "footprint" for

increased recognition of a cotton surface, less additive would be needed to exhibit the same effect, producing cost and environmental benefits. Due to the ease of incorporating a variety of different end groups at the periphery of the dendritic wedge a huge number of possible applications are now beginning to be investigated in many industrial and academic laboratories[84].

1.10 Basic concept and aim of the project.

In this project the possibility of using particular surface recognition groups to bind specific functions to a cotton surface in an aqueous environment was investigated. Poly(propyleneimine) dendritic wedges are potentially attractive for this purpose in that the focus (R in Figure 27, see below) could have a specific active property such as a fluorescence brightener, or passive property such as surface modifying behaviour via silylation or fluorination to produce low surface energy effects. The periphery of the wedge structure possessing a large number of end groups could be modified with a specific moiety capable of recognising elements of the cotton surface structure and if the hydrophobe/hydrophile balance of the molecule, its solubility in water and the number and strength of surface interactions, the "footprint", could be optimised it might prove possible to obtain specific segregation of the molecule to a surface in an aqueous environment. A schematical representation of the basic concept is presented in Figure 27 below.

The dendritic wedges used were synthesised in a step-wise way via a repetitive reaction sequence. The syntheses which form the bulk of the experimental work reported here use a divergent route in which the branching is obtained by a

double Michael addition of the surface modifying primary amine to acrylonitrile[22,23], followed by a small scale homogeneously catalysed hydrogenation[85] (DIBAL-H) or a large scale heterogeneous high pressure hydrogenation (Raney Nickel) of the nitrile groups regenerating the amine functionality resulting in a doubling of the number of primary amine groups at each successive generation. The surface modifying group is the unit (R) and the cellulose recognition is achieved by terminal amino acid residues (X).
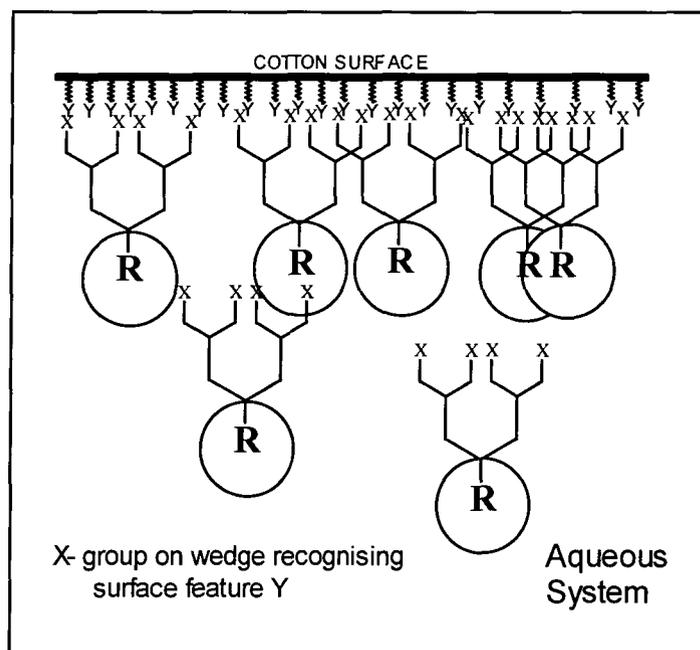
Figure 27. Basic concept of specific surface recognition in water.

In the next chapter study of the dendrimer wedge synthesis and preparation of such wedges from aliphatic and siloxysilane primary amines is described. Chapter 3 reports the end group functionalisation of the dendrimer wedges with L-tryptophan, L-tyrosine and L-phenylalanine amino acids and Chapter 4

discusses the physico-chemical study of the absorption of some of these materials onto cotton in methanol and water/methanol solutions. The thesis concludes with a brief overview of the achievements, suggestions for further work and several appendices of data.

1.11 References

[1] Fréchet, J.M.J., *Science*, 263, (**1994**), 1710.

[2] Tomalia, D.A., Baker, H., Dewald, J., Hall, M., Kallos, G., Martin, S., Roeck, J., Ryder, J., and Smith P., *Polym. J.*, 17, (**1985**), 117.

[3] De Gennes, P.G., and Hervet, H.J., *J. Phys. Lett.* (Paris) 44, (**1983**), 351.

[4] Flory, P.J., *J. Am. Chem. Soc.* 63, (**1941**), 3083;3091;3096.

[5] Stockmayer, W.H., *J. Chem. Phys.* 11, (**1943**), 45; 12, (**1944**), 125.

[6] Melville, H.W., *Trans Faraday Soc.*, 40, (**1944**), 217

[7] Flory, P.J., *Ann. New York Acad. Sci.*, 57, (**1953**), 327

Flory, P.J., *J. Am. Chem. Soc.* 74, (**1952**), 2718

[8] Beckman, C.O., *Ann. N.Y. Acad. Sci.* 57, (**1953**), 384.

[9] Erlander, S., and French, D., *J Polym. Sci.*, 20, (**1956**), 7

[10] Burchard, W., *Macromolecules*, 5, (**1972**), 604.

[11] Newcome, G.R., Yao, Z., Baker, G.R., and Gupta, V.K., *J.Org.Chem.* 50, (**1981**), 2003.

[12] Tomalia, D.A., Baker, H., Dewald, J., Hall, M., Kallos, G., Martin, S., Roeck, J., Ryder, J., and Smith, P., *Polym.J.* (Tokyo) 17, (**1985**), 117.

[13] Graessley W.W., *Macromolecules*, 8, (**1975**), 185; 865.

[14] Gordon M., and Dobson G.R, *J. Chem. Phys.* 43, (**1975**), 35

[15] Good I, *.J., Proc. R. Soc.* (London), A263, (**1963**), 54.

[16] Buhleier, E., Wehner, W., and Vögtle, F., *Synthesis* (**1978**), 155.

[17] Tomalia, DA., and Dewald, RJ., US Patent 4 507 466 (**1985**).

[18] Denkewalter, RG., Kolc, JF., Lukasavage, WJ, US Pat. 4 410 688 (**1983**); Chem Abstr. (**1984**) 100, 103907.

[19] Newcome, G.R., Yao, Z., Baker, G.R., Gupta, V.K., Russo, P.S., Saunders, M.J., Miller, J.E., and Bouillion, K., *J.Chem.Soc.,Chem.Commun.* (**1986**), 752.

[20] Newcome, G.R., and Lin, X., *Macromolecules* 24, (**1991**), 1443.

[21] Hawker, C.J., and Fréchet, J.M.J., *J Am. Chem. Soc.*, 112, (**1990**), 7638.

[22] Tomalia, D.A., Naylor, AM., and Goddard, III WA., *Angew. Chem. Int. Ed. Engl.*, 29, (**1990**), 138.

[23] Brabander van den Berg, E.M.M., and Meijer, EW., *Angew.Chem.Int.Ed.Engl.* 32, (**1993**), 1308.

[24] Wörner, C., and Mülhaupt, R., *Angew.Chem.Int.Ed.*Engl. 32, (**1993**), 1306.

[25] Newcome, G.R., Yao, Z., Baker, G.R., Gupta, V.K., Russo, P.S., and Saunders, M.J., *J.Am.Chem.Soc.* 108, (**1986**), 849.

[26] Newkome, G.R., Moorfield, C.N., and Theriot, K.J., *J. Org. Chem.* 53, (**1988**), 5552.

[27] Newkome, G.R., Moorfield, C.N., Nayak, A., Behera, R.K., and Baker, G.R., *J. Org. Chem.* 57, (**1992**), 358.

[28] Roovers, J., Toporowski, P.M., and Zhou, L.L., *Polymer Preprints* 33, (**1992**), 182.

[29] van der Made, A.W., and van Leeuwen, P.W.N.M., *J. Chem. Soc. Chem. Commun.* (**1992**), 1400.

[30] van der Made, A.W., van Leeuwen, P.W.N.M., de Wilde, J.C., and Brandes R.A.C., *Adv. Mat.* 5, (**1993**), 446.

[31] Hawker, C.J., and Fréchet, J.M.J., *J. Chem. Soc. Chem. Commun.*, (**1990**), 1010.

[32] Miller, T.M. and Neenan, T.X., *Chem Mat.* 2, (**1990**), 346.

[33] Uhrich, K.E., Fréchet, J.M.J., *J. Chem. Soc., Perkin. Trans. I.*, (**1992**), 1623.

[34] Kwock, E.W., Neenan, T.X., and Miller, T.M., *Chem. Mat.*, 3, (**1991**), 775.

[35] Launay, N., Caminade, A.M., Lahana, R., Majoral, J.P., *Angew.Chem.Int.Ed.Engl.*, 33, (**1994**), 1589.

[36] Serroni, S., Denti, G., Campagna, s., Juris, A., Ciano, M., and Balzani, V., *Angew.Chem.Int.Ed.Engl.,* 31, (**1992**), 1493.

[37] Achar, S., and Puddephatt, R.J., *Angew.Chem.Int.Ed.Engl.,* 33, (**1994**), 847; Achar S., and Puddephatt RJ., *J. Chem. Soc. Chem. Commun.* (**1994**), 1895.

[38] Knapen, J.W.J., van der Made, A.W., de Wilde, J.C., van Leeuwen, P.W.N.M., Wijkens, P., Groove, D.M., and van Koten, G., *Nature ,* 372, (**1994**), 659.

[39] Newkome

[40] Stevelmans, S., van Hest, J.C.M., Jansen, J.F.G.A., van Boxtel, D.A.F.J., de Brabander-van den Berg, E.M.M., and Meijer, EW., *J. Am. Chem. Soc.,* 118, (**1996**), 7398.

[41] Hawker, C.J., Wooley, K.L., and Fréchet, J.M.J., *J. Chem. Soc., Perkin. Trans. I.,* (**1993**), 1287.

[42] Rengan, K., and Engel, R., *J. Chem. Soc., Perkin. Trans. I.,* (**1991**), 987.

[43] Rengan, K., and Engel, R., *J. Chem. Soc. Chem. Commun.,* (**1992**), 757.

[44] Newkome, G.R., Lin, X., and Weis, C.D., *Tetrahedron Assymetry,* 2, (**1991**), 957

[45] Chow, H.F., Fok, C.C., and Mak, C.C., *Tetrahedron Lett.,* 35, (**1994**), 3547. Chow, H.F., and Mak, C.C., *J. Chem. Soc., Perkin. Trans. I.,* (**1994**), 2223.

[46] Hudson, RHE., and Dahma, M.J., *J. Am. Chem. Soc.,* 115, (**1993**), 2119.

[47] Kremers, JA., and Meijer, EW., *J. Org. Chem.,* 59, (**1994**), 4262.

[48] Jansen, J.F.G.A., and Meijer, EW., *J. Am. Chem. Soc.,* 117, (**1995**), 4417.

[49] Xu, ZF., Kahr, MS., Walker, KL., Wilkins, CL., and Moore, JS., *J. Am. Chem. Soc.,* 116, (**1994**), 4537.
Xu, Z., Kahr, MS., Walker, KL., Wilkins, CL., and Moore, JS., *J. Am. Soc. Mass Spectrom.,* 5, (**1994**), 731.

[50] Kim, Y.H., and Webster, O.W., *J. Am. Chem. Soc.,* 112, (**1990**), 4592.

[51] Johansson, M., Malmstrom, E., and Hutt, A. *J. Polym. Sci., Polym. Chem.,* 31, (**1993**), 619.

[52] Chu, F., and Hawker, C.J., *Poly Bull.* 30, (**1993**), 265.

[53] Ulrich, KE., Hawker, C.J., Fréchet, J.M.J., and Turner, S.R., *Macromolecules* 25, (**1992**), 4583.

[54] Spindler, R., and Fréchet, J.M.J., *Macromolecules* 26, (**1993**), 4809.

[55] Mathias, L.J., and Carothers, T.W., *J. Am. Chem. Soc.,* 113, (**1991**), 4043.

[56] Wooley, K.L., Hawker C.J., and Fréchet J.M.J., *Polymer*, 35, (**1994**), 4489.

[57] Mourney, T.H., Turner, S.R., Rubenstein, M., Hawker, C.J., Fréchet, J.M.J., Wooley, K.L., *Macromolecules* 25, (**1992**), 2401.

[58] Hobson, L.J., Kenwright, A.M., Feast, W.J., *J.Chem Soc.Chem.Commun.*, 19, (**1997**), 1877.

[59] DSM technical publication.

[60] Hawker, C.J., Farrington, P., Mackay, M., Wooley, K.L., and Fréchet J.M.J., *J. Am. Chem. Soc.*, 117, (**1995**), 6123.

[61] Gitsov, I., Wooley, K.L., Hawker, C.J., Ivanova, J.M., and Fréchet J.M.J., *Macromolecules* 26, (**1993**), 5621.

[62] Hawker, C.J., and Fréchet, J.M.J., Polymer 33 (1992), 1507.

[63] van Hest, J.C.M., Delnoye, D.A.P., Baars, M.W.P.L., Elissen-Román, C., van Genderen, M.H.P., and Meijer, E.W., *J. Chem. Eur.* 12, (**1996**), 1616.

[64] Feast, W.J. and Richards, R.W., private communication of the results of an undergraduate project; confirmed by Meijer, E.W. in discussion with Feast.

[65] Xu, Z., and Moore, J.S., *Angew. Chem. Int. Ed. Engl.*, 32, (**1993**), 246

[66] Nagasaki, T., Ukon, M., Arimori, S., and Shinkai, S., *J. Chem. Soc. Chem. Commun.*, (**1992**), 608.
Nagasaki, T., Ukon, M., Arimori, S., Kimira, O., Hamachi, I., and Shinkai, S., *J. Chem. Soc. Perkin. Trans. I.* (**1994**), 75.

[67] Mekelburger, H.B., Rissanen, K., and Vögtle, F., *Chem. Ber.* 126, (**1993**), 1161.

[68] Kadei, K., Moors, R., and Vögtle, F., *Chem. Ber.* 127, (**1994**), 897.

[69] Jin, RH., Aida, T., and Inove, S., *J. Chem. Soc. Chem. Commun.*, (**1993**), 1260.

[70] Dandliker, P.J., Diederich, F., Gross, M., Knobler, CB., Lovati, A., and Sandford, EM., *Angew. Chem. Int. Ed. Engl.*, 33, (**1994**), 1739.

[71] Newkome, G.R., Moorefield, C.N., Keith, J.M., Baker, G.R., and Escamilla, G.H., *Angew. Chem. Int. Ed. Engl.*, 37, (**1994**), 666.

[72] Newkome, G.R., and Moorefield, C.N., *Macromol. Symp.*,77, (**1994**), 1.

[73] Plesek, J., *Chem. Rev.*, 92, (**1992**), 69.

[74] Hawthorne, M.F., *Angew. Chem. Int. Ed. Engl.*, 32, (**1993**), 950.

[75] Bryce, MR., Devonport, W., and Moore, AJ., *Angew. Chem. Int. Ed. Engl.,* 33, (**1994**), 1761.

[76] Moulines, F., Djakovith, L., Boese, R., Gloaguen, B., Thiel, W., Fillant, JL., Delville, MH., and Astruc, D., *Angew. Chem. Int. Ed. Engl.,* 32, (**1993**), 1075.

[77] Roy, R., Zanini, D., Meunier, SJ., and Romanowska, A., *J. Chem. Soc. Chem. Commun.,* (**1993**), 1869.

[78] Daly, W.D., Poche, D., Russo, P.S., and Negulesco, I., *Polym. Preprints. Am. Chem. Soc. Div. Polym. Chem.,* 33, (**1992**), 188.

[79] Rao, C., and Tam., JP., *J. Am. Chem. Soc.* 116, (**1994**), 6975.

[80] Kim, YH., *J. Am. Chem. Soc.* 114, (**1992**), 4947.

[81] Lorenz, K., Hölter, D., Stühn, B., Mulhaupt, R., and Holger, F., *Adv. Mater.,* 8, (**1996**), 414.

[82] a) Percec, V., Chu, P., and Kawasumi, M., *Polym. Macromolecules* 27, (**1994**), 4441.

[83] Wang, P.W., Liu, Y.J., Devadoss, C., Bharathi, P., and Moore, JS., *Adv. Mater.,* 8, (**1996**), 237.

[84] Proceedings of ACS Symposia, Sept. 8-11, Las Vegas, Nevada, *PMSE Prepr.* (Am. Chem. Soc. PMSE-Div.) 77, (**1997**).

[85] Moors, R., and Vögtle, F., *Chem. Ber.* 126, (**1993**), 2133.

CHAPTER 2

Synthesis and Characterisation of Dendrimer Wedges

2.1 Introduction

This chapter describes the synthesis and characterisation of dendrimer wedges derived from aliphatic amines and aminopropyltris(trimethylsiloxy)silane (APTTMSS). Poly(propyleneimine) dendrimer wedges up to the 3rd generation with eight primary amine end groups have been produced by using the repetitive reaction sequences of cyanoethylation and hydrogenation. A brief introduction to the general synthetic strategy is given with particular emphasis on the nature and choice of the catalysts used for the hydrogenation step.

2.2 Synthetic strategy for poly(propyleneimine) wedge syntheses.

2.2.1 The reactions of the repetitive reaction sequence

2.2.1.1 The Cyanoethylation Step

A special example of the Michael condensation occurs when addition takes place, not to an α,β-unsaturated carbonyl compound, but to the closely related acrylonitrile. The cyano group, by virtue of the polarisation of the carbon-nitrogen bond, has a similar effect to that of a carbonyl group and permits the attack of a nucleophilic reagent at the methylene end of the conjugated system. An amine addition to the conjugated system can occur by attack of the nucleophilic nitrogen atom at the methylene of acrylonitrile with subsequent protonation. The N-cyanoethyl amine formed from a primary amine still has one active α-hydrogen atom and can undergo a second cyanoethylation at elevated temperature to form the first generation of the wedge structure (STEP 1, Scheme 2.2).

2.2.1.2 Homogeneous and heterogeneous hydrogenations of nitriles.

a) Small scale homogeneous hydrogenation for conversion of nitriles into primary amines using **DIisoButylAluminium Hydride (DIBAL-H)**[1].

Treatment of nitriles with lithium aluminium hydride gives primary amines in high yields. The reaction occurs by nucleophilic addition of hydride ion to the polar C≡N bond, yielding an imine anion, which (presumably after picking up a proton) undergoes further addition of a second equivalent of hydride to give the final product on protonation. However, if the less powerful but more convenient reducing agent DIBAL-H is used at -78°C in toluene, the second addition of hydride does not occur, and the iminium intermediate can be hydrolysed to yield an aldehyde. Modification of the reaction conditions using a more polar solvent and an increase in temperature, facilitates the formation of the desired primary amine product in high yields (90%) with little or no purification required, see scheme 2.1.
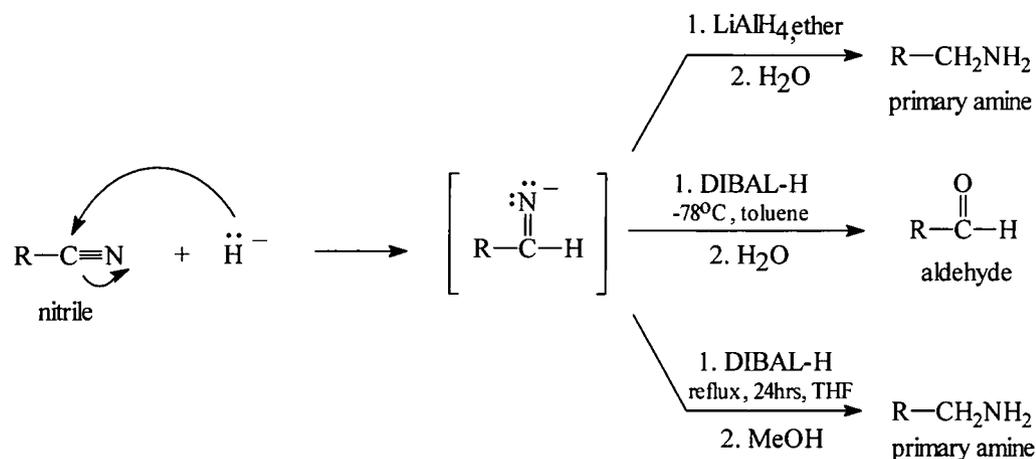
Scheme 2.1 Conditions for homogeneous nitrile hydrogenation using DIBAL-H.

STEP 1
Cyanoethylation

STEP 2
Homogeneous/Heterogeneous
Hydrogenation

R-NH$_2$ $\xrightarrow[\text{Michael Addition}]{\text{CH}_2\text{=CHCN}}$

$\xrightarrow[\text{Reduction}]{\text{Raney nickel or DIBAL-H}}$

STEP 1

STEP 2
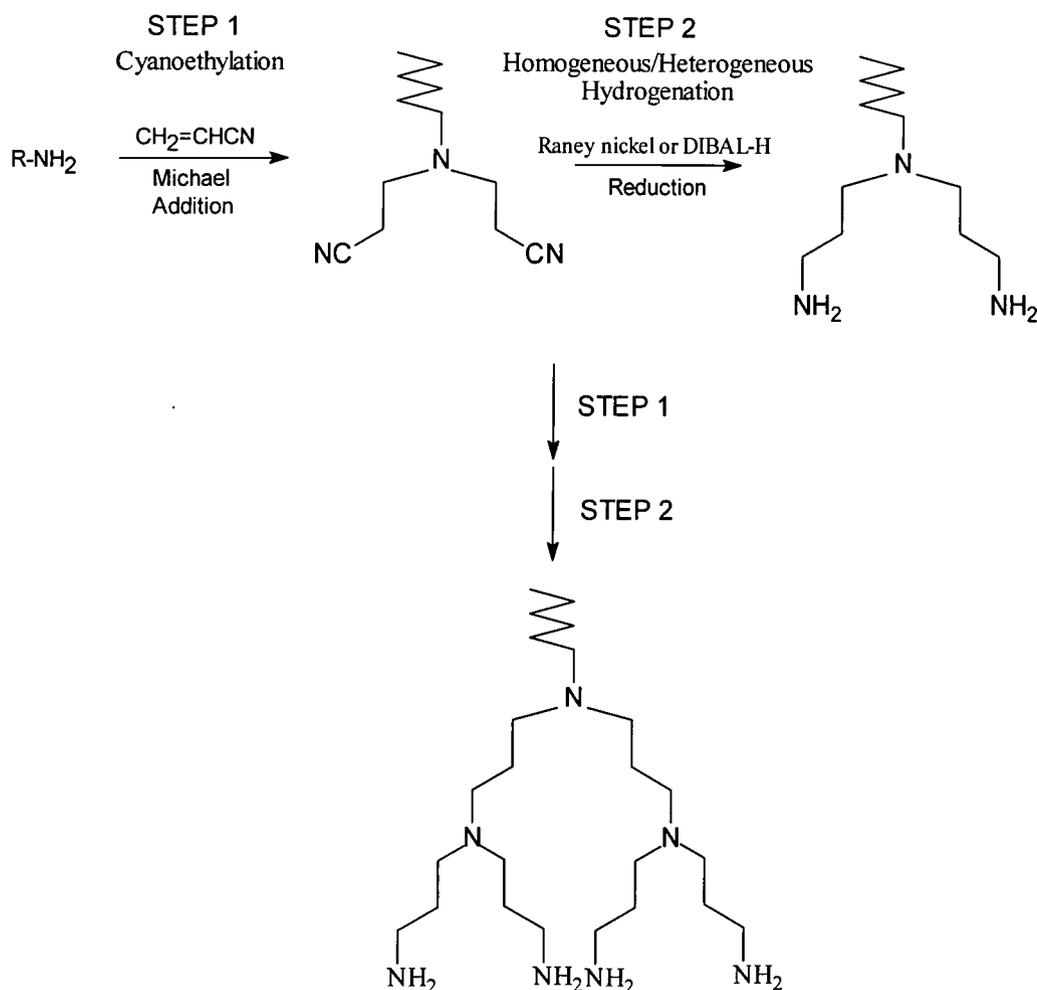
Scheme 2.2 General synthetic pathway for poly(propyleneimine) dendrimer

wedge formation.

b) Large scale Heterogeneous Catalytic Hydrogenation using Raney Nickel.

1) Activity and Selectivity

A number of catalyst systems used for hydrogenation reactions are specific in application but the majority are useful for a variety of different reactions. Choice of a particular catalyst is governed by two factors; namely the activity and the selectivity required. The activity is a measure of the ease with which it catalyses a given reaction, and selectivity by its ability to promote the hydrogenation of one functional group in preference to any other. Selectivity is a

property of the metal itself and is closely related to the activity, in that the more active the catalyst the less selective the hydrogenation. For reactions where selectivity is of prime importance, it is advisable to use an inactive form of the catalyst. If selectivity is not required, it is advantageous to use the most active catalyst system available for the reaction.

The activity of a catalyst system is governed by many factors among which are the nature of the catalyst itself, the method used for its preparation, and the presence of any added materials in the reaction medium. Some knowledge of these factors and other variables involved can prove to be quite useful but they will not be discussed at length here.

2) The catalyst system

Nickel has been used extensively as a hydrogenation catalyst and is associated with high temperature and high pressure reactions, the most popular is Raney nickel[2]. The catalyst contains from 25 to 150ml. of adsorbed hydrogen per gram of nickel with the exact amount dependent on the procedure used to prepare the catalyst[3,4]. The more adsorbed hydrogen present, the more active the catalyst[2,5] and there are a number of different types available differing in their activity. The Raney nickel catalyst used for all high pressure hydrogenations in this work was purchased from Aldrich Chemical Co. supplied as a 50% slurry in water and specified in the catalogue as "analogous to Raney 28 or W-2"[6].

3) Hydrogenation of nitrile to primary amine.

The formation of a primary amine from a nitrile requires high temperatures and pressures in a methanol solution saturated with ammonia[7]. In the absence of ammonia the yield is drastically reduced and large amounts of

secondary and tertiary amines are formed. This is due to the addition of the primary amine product to the imine formed in the initial step of the nitrile hydrogenation and is discussed later.

When the presence of ammonia or other base in the reaction system is undesirable, quantitative and selective primary amine formation can be effected by the use of a Raney cobalt catalyst in water under similar conditions used for the Raney nickel hydrogenations[8]. DSM workers report that Raney cobalt is a superior catalyst for this reaction but it was only available from a supplier in the U.S.A. and air freight transport was prohibitively expensive so the less effective Raney nickel was used in this work.

2.3 Synthesis and characterisation of aliphatic dendritic wedges.

2.3.1 General Introduction

This section describes initial studies of the syntheses of poly(propyleneimine) dendritic wedges starting from C-6 to C-8 aliphatic amines. Using hexylamine as the focus, dendrimer wedges up to the 3rd generation with eight primary amine end groups have been synthesised using water or methanol as solvent. The sparingly water soluble hexylamine becomes increasingly more water soluble at each successive generation. Similarly, dendrimer wedges up to the 2nd generation were synthesised starting from heptylamine, octylamine, and tert-octylamine.

2.3.2 Synthesis and characterisation of hexylamine poly(propyleneimine) dendrimer wedges.

2.3.2.1 Introduction

The repetitive reaction sequence of the double Michael addition of acrylonitrile to aliphatic primary amines, followed by the heterogeneously catalysed hydrogenation of the nitrile groups was originally carried out in water using 1,4-diaminobutane as the dendrimer core by DSM workers[9]. In this study, in order to acquire understanding and familiarity with this chemistry and the general method for the synthesis of wedges, initial studies were carried out using hexylamine. Hexylamine was chosen as our starting material because it is one of the longest chain aliphatic primary amines showing any solubility in water.

2.3.2.2 The cyanoethylation reaction

The reaction sequence described here is shown in scheme 2.3 and is based on a combination of the DSM methodology[9,10] for the synthesis of poly(propyleneimine) dendrimers, and the Wörner and Mülhaupt synthesis of poly(trimethyleneimine) dendrimers[11].

All Michael additions were performed in a similar way; acrylonitrile, 2.5 to 4 equivalents per primary amine was used at a concentration of 0.1mol/L in aqueous media. The acrylonitrile was added dropwise over a period of 30 minutes (to control the exotherm produced) at room temperature. Hexylamine is only sparingly soluble in water and consequently the mixture was vigorously stirred throughout the acrylonitrile addition. The first equivalent of acrylonitrile was added at room temperature, then the solution was heated to 80⁰C and the

excess added. The reaction time required to achieve complete conversion increased as a function of the generation, from stirring overnight for the 1st generation (Hex-*wedge*-(CN)$_2$),(**2**) to 3 days for the 3rd generation (Hex-*wedge*-(CN)$_8$),(**6**).
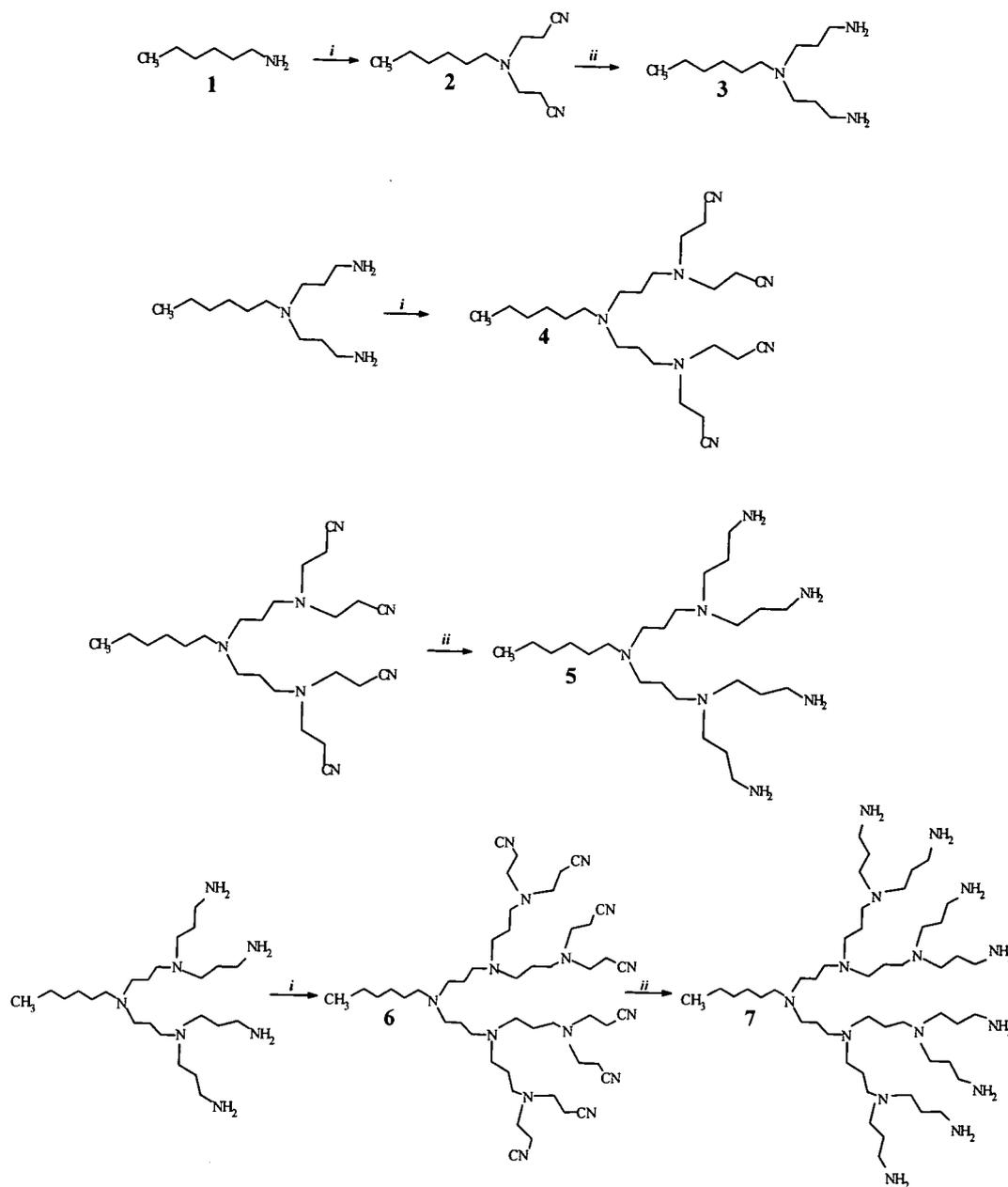
Scheme 2.3 Synthetic route toward Hex-wedge-(NH$_2$)$_8$. i) Cyanoethylation with acrylonitrile in water; ii) hydrogenation at 45 bar H$_2$ pressure, 70^{0}C, with Raney nickel as catalyst.

After the reaction was complete the excess of acrylonitrile was removed as a water azeotrope by vacuum distillation (12mmHg at 40^0C), leaving a two-phase system. The water layer was decanted to give the crude product as an orange oil. Methanol can be used as a solvent for the cyanoethylation reaction following Wörner and Mülhaupt's synthesis of poly(trimethyleneimine) dendrimers[11]. They reported that in the presence of methanol the cyanoethylation occurs without formation of monosubstituted side products and, since acrylonitrile, methanol and cyanoethylated methanol are readily removed under vacuum, no special purification processes were necessary. The cyanoethylation reactions starting from hexylamine were carried out in water, methanol was used for the formation of small wedges starting from the non-water soluble hydrophobic amines, i.e. heptylamine, octylamine and tert-octylamine.

2.3.2.3 Heterogeneous hydrogenations.

The DSM hydrogenation method[9,10] uses H_2 and Raney cobalt catalyst in water at 70°C and pressures higher than 30bar. The reaction time for hydrogenation increases with substrate molecular weight but is complete and selective for the formation of primary amine terminated dendrimers. The amine terminated dendrimers are isolated by evaporating water from the filtered reaction mixture. However, the process window for a complete hydrogenation is small and side reactions occur readily. The three major side reactions in the dendrimer synthesis leading to imperfect dendrimers are shown in scheme 2.4. They are:-

1) incomplete cyanoethylation in the Michael addition resulting in dendrimers that miss one ethyl cyanide side chain compared to the perfect structures,

2) the retro-Michael addition during the hydrogenation yielding secondary amines and,

3) ammonia elimination during the hydrogenation step leading to intramolecular cyclisation or intermolecular condensation reactions.
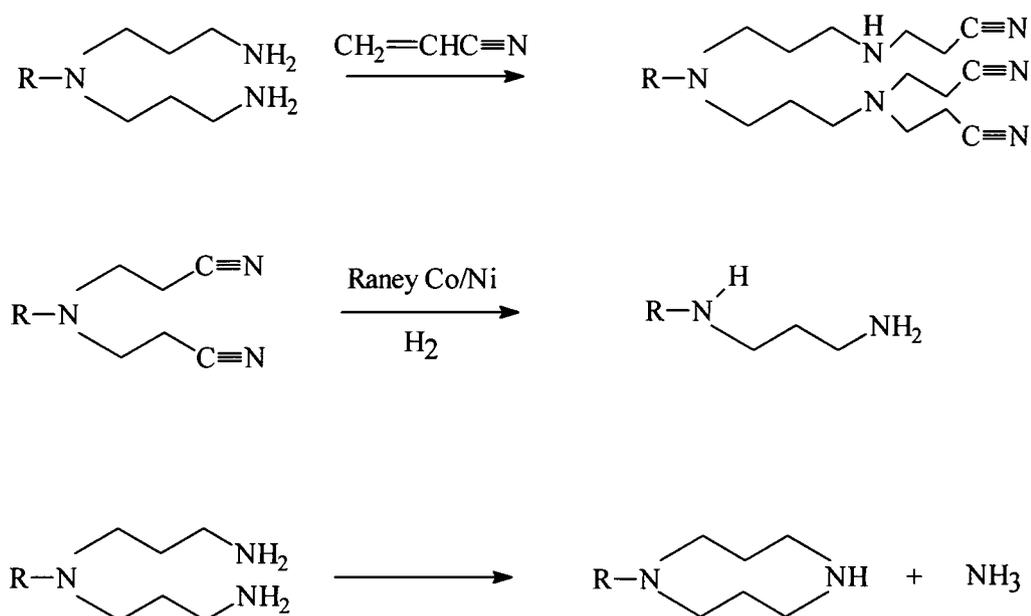
Scheme 2.4. Possible side reactions during dendrimer synthesis.

Under optimised conditions the side-products are not detectable. All hexylamine large scale hydrogenations undertaken in this study used the reaction conditions of DSM except Raney nickel replaced Raney cobalt. Although Raney nickel is not as selective towards hydrogenation of a nitrile to an amine, it has the advantage of being readily available and cheap and high yields were achieved under optimised conditions. Wörner and Mülhaupt used Raney nickel in their

heterogeneous hydrogenation step, the nitrile group being completely hydrogenated at room temperature (25^0C) and 8 bar hydrogen pressure when small amounts of sodium hydroxide were added to an ethanol solvent[12]. Sodium hydroxide was reported to play an active role in the reduction process and was not just for activation of the catalyst. Without any added base as cocatalyst the yield of amine was significantly reduced and the reaction was not as clean.

Raney nickel was required in small quantities and could be reused at least twice with little loss of activity. The ratio of nitrile to Raney nickel (w/w) could be varied from 5:1 to 7:1 with higher ratios requiring longer reaction times for complete reduction, as expected. The concentration of sodium hydroxide could be varied from 1 to 5 molar in 95% ethanol or methanol with equal success. The reaction was best performed on a moderate scale as yields were poor on a small scale, possibly due to adsorption of reactant or product on the catalyst. Also, the strongly alkaline reduction medium placed specific restrictions on the types of functional groups which could be used. The advantages of this reduction method is that the catalyst is available commercially, requires no pre-treatment and can be used several times which makes it very cost effective. Also, the procedure works well for moderate scale reactions, allowing access to larger quantities of amine terminated dendrimer wedges and ease of purification. Using a combination of these two techniques and optimisation of the reaction conditions, yields of the hydrogenation reactions carried out in the course of this work were 90% for the smaller wedges. However, yields steadily decreased at the higher generations even with the addition of an ammonia solution. This could be due to increased adsorption of dendrimer wedge onto the catalyst surface and the

increased solubility of the wedge in an aqueous solution causing problems with extraction into an organic solvent.

The role of ammonia during hydrogenation is crucial and fairly well-known[13]. One of the major side reactions that can occur during dendrimer wedge synthesis is the intramolecular bridging reaction between an imine and a primary amine, with the release of ammonia (scheme 2.5). Ammonia is thought to compete with the primary amines in attack on the intermediate imine. The attack of ammonia leads to the formation of the desired amine via the mechanism outlined in scheme 2.5.
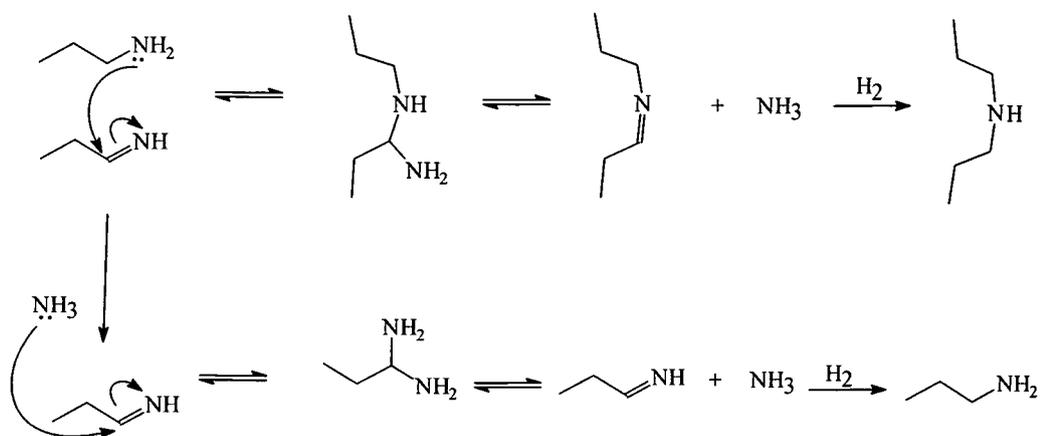
Scheme 2.5 The mechanism of intramolecular bridging and the role of ammonia.

2.3.2.4 Purification Techniques.

Purification of nitrile terminated wedges involved washing with water to remove water soluble by-products e.g. $HOCH_2CH_2CN$ (adduct of H_2O to acrylonitrile) or incompletely cyanoethylated products. Further purification has been carried out by using the method of Vögtle et al for the purification of their nitrile terminated dendrimers, which involved chromatography on neutral

alumina eluting first with a 30:1 dichloromethane:methanol mixture, then 50:1 dichloromethane:methanol, the purified product is collected as a light yellow or clear oil. The hydrogenation step was the most difficult to control in the reaction sequence and gave rise to by-products readily. These by-products could not be separated from the desired product using column chromatography because of the similar polarity of both materials. In the multi-step divergent dendrimer wedge synthesis it is therefore very difficult, almost impossible, to completely prevent formation of side products or to isolate totally pure product. The number of impurities present at higher generations is compounded due to the cumulative effect of the impurities produced during each repetitive reaction step. It was however possible to purify the lower generation amine terminated wedges by Kulgelruhr distillation. Apart from the first generation (**3**) which is a white crystalline solid, all the other generations are colourless or light yellow oils, which are readily soluble. Hex-*wedge*-(NH$_2$)$_n$ products dissolves in water and methanol and the Hex-*wedge*-(CN)$_n$ compounds in common organic solvents.

2.3.2.5 Characterisation of Hex-*wedge*-(NH$_2$)$_n$ with n = 2, 4 and 8 and Hex-*wedge*-(CN)$_n$ with n = 2, 4 and 8.

The structures proposed for the individual generations in Scheme 2.3 were confirmed by elemental analysis, ^{1}H and ^{13}C NMR, IR spectroscopy, conventional mass spectrometry, and Matrix Assisted Laser Desorption-Ionisation Time of Flight Mass Spectrometry (MALDI-TOF MS).

IR and NMR spectroscopy are the most useful techniques for following the successful completion of the various steps, providing positive structural

identification and indicating the presence of defects in the dendrimer wedge structure. The hydrogenation step could be followed by IR spectroscopy with the disappearance of the CN stretching vibration around 2245cm^{-1} and the appearance of amine peaks at approximately 3200 and 3300cm^{-1} as a good indication for the completion of the reaction. The IR spectra of the various generations with identical end groups are very similar.

The structure assigned to the 2nd generation nitrile terminated hexylamine wedge was consistent with the chemical shifts and integrated intensities recorded in Figure 2.1 and Table 2.1. Thus the shape and integrated intensity of the triplet at δ = 2.85 ppm due to the N*CH$_2$*CH$_2$CN methylene groups (h), is a characteristic indicator for the monodispersity of the outer layer, whilst the ratio of the integrals for the CH$_3$CH$_2$CH$_2$CH$_2$*CH$_2$*CH$_2$N protons (c) at δ = 1.4 ppm and the NCH$_2$*CH$_2$*CH$_2$N protons (f) at δ = 1.6 ppm is only consistent with the structure assigned.

In the ^{13}C nmr spectrum for the same wedge, (Figure 2.2 and Table 2.2), all of the major signals can be positively assigned on the basis of relative intensities and chemical shifts taken from standard literature tabulations. It is possible to discern between the different dendritic layers of the molecules, as is clear from the shifts and relative intensities of the resonances of the carbons alpha to tertiary amines (around δ = 50) and the carbons beta to tertiary amines (around δ = 25). Single carbons due to the hexylamine backbone are also clearly visible as assigned in Table 2.2 (C1 to C6). All ^{13}C nmr spectra for the various generations can be assigned in a similar manner and the details are recorded in the Experimental section 2.5.1 and the spectra in Appendix 1.3.
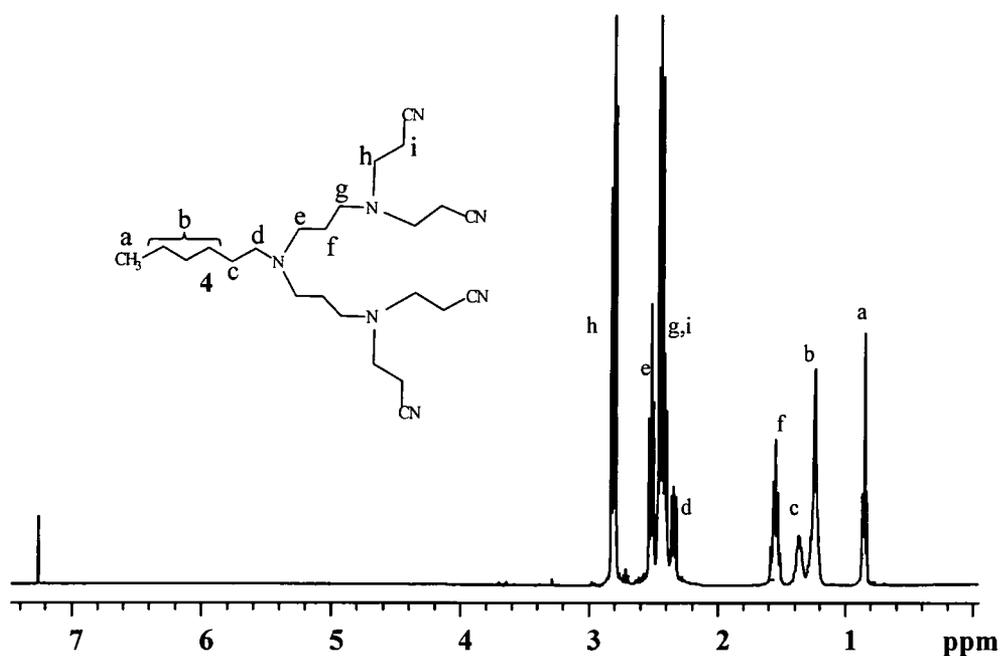
Figure 2.1. ^{1}H nmr (400 MHZ) of Hex-*wedge*-(CN)$_4$ in CDCl$_3$

chemical shift (ppm)	multiplicity	H integration	H assignment
0.89	t	3	a
1.3	m	6	b
1.4	m	2	c
1.6	m	4	f
2.35	t	2	d
2.4	t	4	g
2.45	t	8	i
2.53	t	4	e
2.85	t	8	h

Table 2.1 Summary of ^{1}H nmr assignment of Hex-*wedge*-(CN)$_4$.

As has been discussed previously, the repetitive reaction steps cannot be optimised to the point of producing a perfect material with no side products or

impurities, especially in the case of large scale hydrogenations for synthesising bigger wedges using Raney nickel. This has been extensively studied by Meijer who has shown that additional peaks in the ^{1}H-decoupled ^{13}C nmr spectra can be used to identify incompletely cyanoethylated wedges, thus signals at δ =49.1 (NHCH_2CH$_2$CN) and 16.7 (NHCH$_2$$CH_2$CN) are indicative of this type of defect and, when present, can be seen as very small signals in the spectrum[14]. Similarly, the occurrence of retro-Michael additions during hydrogenation is evident if peaks are present at 48.7 ppm, 47.8 ppm, 39.4 ppm, 33.8 ppm, and 27.2 ppm in the spectra of the amine-terminated wedges. There is some evidence in Figures 2.1 and 2.2 and the spectra recorded in Appendix 1.3 for the presence of such structural defects although they are present at very low concentrations.

Figure 2.2 ^{13}C nmr (100 MHZ) of Hex-*wedge*-(CN)$_4$ in CDCl$_3$.

chemical shift (ppm)	C assignment
13.8	1
16.6	11
22.4	2
24.7	8
26.6	3
27.0	4
31.5	5
49.3	10
51.1,51.3	7,9
53.7	6
118.6	12

Table 2.2 Summary of ^{13}C nmr assignment of Hex-*wedge*-$(CN)_4$.

2.3.2.6 Matrix-Assisted Laser Desorption/Ionisation Time Of Flight (MALDI - TOF) Mass Spectrometry.

Molecular weight and molecular weight distribution determinations have been carried out using MALDI-TOF mass spectrometry for a wide variety of materials. Although MALDI is a powerful technique for the analysis of the monodisperse samples, it is a quite complex characterisation method, still under development and there are many uncertainties concerning its application[15]. Sample preparation and the choice of matrix especially need meticulous optimisation in order to obtain satisfactory spectra. For the dendrimer wedges prepared in this study, a single monodisperse peak was recorded using 2,5-dihydroxybenzoic acid (2,5-DHB) as the matrix. The spectra are recorded in Appendix 1.5.

2.3.3 Synthesis and characterisation of heptylamine, octylamine and tert-octylamine dendrimer wedges.

Hexylamine dendrimer wedges were synthesised up to the third generation in water, yields were satisfactory and the defect level was low (see above). Other workers have described a similar method for dendrimer formation[11] using methanol as the solvent system and, starting from ammonia as the core molecule, dendrimers up to generation five were synthesised. Using methanol as the solvent for the cyanoethyation step, and the same conditions for the heterogeneous hydrogenation step as described earlier for hexylamine derivatives, hydrophobic linear and branched chain aliphatic amines were used as starting materials for wedge formation. The aliphatic starting materials used in this study were; heptylamine, octylamine and tert-octylamine. Wedges were synthesised up to the second generation, i.e. having four primary amine end groups. At each successive generation the materials exhibited an increased solubility in water as previously observed for hexylamine wedges; this qualitative observation was not quantified.

Structurally, tert-octylamine derived wedges are dissimilar to the rest due to the steric hindrance caused by the two methyl groups alpha to the primary amine, consequently only a mono-cyanoethylated adduct was produced in the first step. Numerous attempts to obtain the di-substituted product failed. The aliphatic dendritic wedges produced are shown in Figure 2.3.

Hep-*wedge*-(NH2)4

Oct-*wedge*-(NH2)4

mono-tert-Oct-*wedge*-(NH2)4

Figure 2.3 Water soluble dendrimer wedges derived from hydrophobic foci.

The ^{1}H and ^{13}C nmr spectra of octylamine and heptylamine are very similar to hexylamine except for the presence of extra backbone CH_2 signals. Confirmation of the structure of the mono-cyanoethylated tert-octylamine was provided by its IR and nmr spectra, Figures 2.4 and 2.5 In the IR spectrum (Figure 2.4), the

presence of a secondary amine functionality is clearly seen from the single sharp

peak at 3317.7cm⁻¹ (N-H stretch), and the sharp signal at 2247.1cm⁻¹ is indicative

of a CN stretch. All the peaks in the ¹H nmr spectrum in figure 2.5 are readily

assigned (Table 2.3) and are consistent with the assigned structure.

Small scale homogeneous hydrogenation utilising DIBAL-H generates a primary

amine functionality at the end of the spacer unit, from which normal wedge

growth can proceed in the usual manner.

Figure 2.4. FTIR spectrum of mono-tert-Oct-*wedge*-CN.

Figure 2.5. ^{1}H nmr spectrum of mono-tert-Oct-*wedge*-CN.

chemical shift (ppm)	multiplicity	H integration	H assignment
0.93	s	9	a
1.11	s	6	c
1.27	s	2	b
2.34	t	2	e
2.71	t	2	d

Table 2.3 Summary of ^{1}H nmr assignment of mono-tert-Oct-*wedge*-CN.

2.4 Synthesis and characterisation of dendrimer wedges with 3-aminopropyltris(trimethylsiloxy)silane (APTTMSS) at the foci.

2.4.1 Introduction

The synthesis of poly(propyleneimine) dendrimer wedges derived from C-6 to C-8 linear and branched chain aliphatic amines provided the author with practical experience and an understanding of the general synthetic strategy and various methods of characterisation. It was observed that the molecules become increasingly water soluble with each successive attachment of a hydrophilic amine terminated wedge generation. The experience gained using the repetitive reaction sequences on relatively cheap amines were applied to the synthesis of siloxysilane derived wedges, incorporating 3-aminopropyltris(trimethylsiloxy)silane (APTTMSS), at the focus. APTTMSS was selected as a suitable starting material because of the bulk and surface active properties expected from such a focal unit. In order to test the basic concept of molecular recognition in an aqueous solution we need to synthesise a molecule that has a specific property which can be measured to give some indication of recognition at a specific surface. Siloxanes have a low surface free energy and consequently lower the surface free energy of any interface to which they are attached. This is a property which, in principle can be measured in aqueous solution via contact angle measurements (see Chapter 4). Siloxysilane dendrimer wedges with amine end groups up to the second generation have been synthesised and fully characterised.

2.4.2 Synthesis and characterisation of the APTTMSS focus.

2.4.2.1 Synthesis of APTTMSS

APTTMSS is not commercially available and was synthesised following

the method reported by Harvey[16].

$$H_2N(CH_2)_3Si(OEt)_3 + (CH_3)_3SiNHSi(CH_3)_3 \longrightarrow H_2N(CH_2)_3Si(OSiMe_3)_3 + (CH_3)_3SiOSi(CH_3)_3$$

Aminopropyltriethoxysilane was mixed with six equivalents of

hexamethyldisilazane in distilled water. The mixture was then stirred under

reflux for two days. Two phases separated and the lower, aqueous phase was

discarded. The organic phase was diluted with dichloromethane and dried over

molecular sieves (3A). After filtration, the solvent and the side product

hexamethyldisiloxane were removed by evaporation under vacuum and the

residual clear fluid was purified by vacuum distillation.

2.4.2.2 Characterisation of APTTMSS.

The structure of the product was confirmed by a combination of mass

spectroscopy, elemental analysis, FTIR, ^{1}H and ^{13}C NMR spectroscopy.

The presence of peaks in the FTIR spectrum (Appendix 1.1.6) at approximately

$1055cm^{-1}$ and $841cm^{-1}$ correspond to the Si-O-Si and Si-Me$_3$ stretches. Two

sharp peaks at $3300cm^{-1}$ and $3378cm^{-1}$ for N-H stretches provide verification of

the presence of a primary amine. In the ^{1}H nmr spectrum, Figure 2.6 and Table

2.4, all the peaks are readily assigned. The large peak at 0.05ppm corresponds to

the methyl hydrogens of the siloxysilane which integrates to 27 hydrogens. The

signals for the methylene groups are seen at 0.42, 1.45 and 2.6ppm. The peak at

approximately 1.2ppm is due to the primary amine hydrogens, confirmed by a

D$_2$O exchange experiment. From the ^{13}C nmr spectrum in Figure 2.7 and Table

2.5, the methyl carbons of the siloxysilane are readily observed as the large peak

at 1.8ppm with the three methylene carbons of the aminopropyl group at 11.5,

27.8 and 45.2ppm.

Figure 2.6 ^{1}H nmr (400MHZ) of 3-aminopropyltris(trimethylsiloxy)silane

(APTTMSS) in CDCl$_3$.

chemical shift (ppm)	multiplicity	H integration	H assignment
0.05	s	27	a
0.42	t	2	b
1.15	s	2	e
1.45	m	2	c
2.6	t	2	d

Table 2.4 Summary of ^{1}H nmr assignment of APTTMSS.

Figure 2.7 ^{13}C nmr (100MHZ) of 3-aminopropyltris(trimethylsiloxy)silane

(APTTMSS) in CDCl$_3$.

chemical shift (ppm)	C assignment
1.8	1
11.5	2
27.8	3
45.2	4

Table 2.5 Summary of ^{13}C nmr assignment of APTTMSS.

2.4.3 Synthetic pathway

2.4.3.1 The Cyanoethylation Step

The Michael addition to APTTMSS was performed in a similar manner to that established for the aliphatic amines. Acrylonitrile, 2 to 4 equivalents, was added slowly to a solution of the amine in methanol and the mixture, after being heated to 80^{0}C for an hour, was left to stir at 65^{0}C overnight to complete the reaction. Again, the time required to complete the cyanoethylation reaction increased for successive generations. Due to the increased solubility of the higher generation wedges it was possible to perform the Michael addition in water. The desired product was produced in high yield requiring minimal purification.

2.4.3.2 Small Scale Homogeneous Hydrogenation using DIBAL-H.

The conditions used for the large scale hydrogenations using Raney nickel and sodium hydroxide turned out to be too harsh for the siloxysilane focus. The integrity of the molecule was compromised due to the susceptibility

to nucleophilic attack of the siloxysilane bonds, especially in the presence of strong base. Therefore, following the method of Wörner and Mülhaupt, homogeneous hydrogenations were performed in anhydrous tetrahydrofuran (THF), using DIBAL-H as the hydrogenation agent. DIBAL-H was added slowly to a solution of the nitrile terminated wedge dissolved in dry THF and the resulting solution was refluxed for 24 hours. The solution was allowed to cool to room temperature and methanol added to quench the reaction. Filtration of the methoxy-addition product and evaporation *in vacuo* gave the desired product in high yield.

2.4.3.3 Purification Techniques.

The nitrile terminated wedges are all clear yellow or orange oils and required minimal purification. During the synthesis of higher generation wedges the methanol adduct of acrylonitrile, $MeOCH_2CH_2CN$, was formed in increased amounts but was easily removed by distilling under vacuum using a Kulgelruhr apparatus. The amine terminated wedges were dried under vacuum for a few hours and did not require any further purification. The APTTMSS focus is a colourless transparent oil and is not water soluble. The higher generation Si-*wedge*-$(NH_2)_2$ (yellow oil) (3) and Si-*wedge*-$(NH_2)_4$ (gel) (5), showed ready solubility in water. The Si-*wedge*-$(CN)_x$ wedges (2 and 4) were soluble in common organic solvents.

Scheme 2.6. Synthetic route for Si-wedge-(NH$_2$)$_4$ (**5**). i) Cyanoethylation with acrylonitrile in methanol; ii) homogeneous hydrogenation using DIBAL-H.

2.4.3.4 Characterisation of Si-*wedge*-(NH$_2$)$_n$ with n= 2 and 4 and Si-*wedge*-(CN)$_n$ with n= 2 and 4.

The structures proposed for the individual generations in Scheme 2.6 were confirmed by elemental analysis, ^{1}H and ^{13}C nmr, FTIR spectroscopy, and mass spectrometry.

IR and NMR spectroscopy are the most useful techniques for following the successful completion of the reaction steps and an indication of the presence of structural defects. The disappearance of the CN stretching vibration at 2248cm^{-1} (Appendix 1.1.7 and 1.1.9), and the appearance of two amine stretches at approximately 3288cm^{-1} and 3360cm^{-1} (Appendix 1.1.8 and 1.1.10) in the FTIR spectra provides evidence for a successful hydrogenation. FTIR provides information on degradation of the siloxane focus due to breakage of the siloxy bond by the absence of peaks in the FTIR spectra at approximately 1058cm^{-1} and 841cm^{-1} which correspond to Si-O-Si and Si-Me$_3$ stretches, their presence verifies that the focus is intact. As a representative example of the spectroscopic characterisation the structure assigned to Si-*wedge*-(CN)$_4$ from the chemical shifts and integrated intensities recorded in Figure 2.8 and Table 2.6 is discussed here. The signals of the APTTMSS focus are clearly seen due to the presence of the large peak at 0.07ppm (a) for Si-**Me$_3$** hydrogens (27H), and the presence of signals at 0.36 (b), 1.38 (c), and 2.35 (d) for the propyl methylene groups. It is possible to distinguish between distinct generations of the growing wedge structure from the integrated ratio of focus (c) to branch signals (f and h). The uniformity of the outer layer was confirmed from the shape and integrated intensity of the triplet at 2.85ppm (h) due to N*CH$_2$*CH$_2$CN proton signals.

Figure 2.8 ^{1}H nmr (400MHZ) spectrum of Si-*wedge*-(CN)$_4$ in CDCl$_3$.

chemical shift (ppm)	multiplicity	H integration	H assignment
0.07	s	27	a
0.36	t	2	b
1.38	m	2	c
1.60	m	4	f
2.35	t	2	d
2.48	m	12	g,i
2.55	t	4	e
2.85	t	8	h

Table 2.6 Summary of ^{1}H nmr assignment of Si-*wedge*-(CN)$_4$.

In the ^{13}C nmr for the same wedge structure shown in figure 2.9, all the peaks are readily assigned (Table 2.7) confirming the identity and purity of the product. Carbons of the APTTMSS focus have been assigned to the peaks at 1.76, 12.03, 20.64, and 57.05 on the basis of relative intensities, standard literature chemical shifts and previous assignments. It is possible to discern between the different dendritic layers of the molecules, as is clear from the shifts and relative intensities of the resonances of the carbons alpha to tertiary amines (around δ =

50) and the carbons beta to tertiary amines (around $\delta = 25$). All ^{13}C nmr spectra

for the various generations can be assigned in a similar manner and the details

are recorded in the Experimental section 2.5.2 and the spectra in Appendix 1.3.

Figure 2.9 ^{13}C nmr (100MHZ) spectrum of Si-*wedge*-(CN)$_4$ in CDCl$_3$.

chemical shift (ppm)	C assignment
1.76	1
12.03	2
16.90	9
20.64	3
25.10	6
49.59	8
51.40,51.63	5,7
57.05	4
118.64	10

Table 2.7 Summary of the ^{13}C nmr assignment of Si-*wedge*-(CN)$_4$.

2.5 EXPERIMENTAL

All organic and inorganic reagents were purchased from Aldrich Chemical Co. and were used without further purification. IR spectra were recorded using a Perkin-Elmer 1600 series FTIR. ^{1}H and ^{13}C nmr spectra were recorded using a Varian 400MHz spectrometer and were referenced to internal Me$_4$Si. Molecular weight determinations were recorded on a Kratos Kompact MALDI IV time of flight mass spectrometer utilising 2,5-dihydroxybenzoic acid (DHB) as the matrix. Chemical and Electron impact ionisation mass spectra were recorded using a VG Analytical Model 7070E mass spectrometer. Elemental analyses were performed using a Carlo-Elba-466 elemental analyser produced by Exeter Analytical Inc.

2.5.1 Hexylamine derived dendrimer wedges

2.5.1.1 Synthesis of Hex-*wedge*-(CN)$_2$ (2)

Acrylonitrile (78.65g , 1.48 moles) was added to a solution of hexylamine (50g, 0.49 moles) in demineralised water (200 mls). Hexylamine is only sparingly soluble in water and therefore the mixture was vigorously stirred throughout the acrylonitrile addition. Acrylonitrile was added over a period of 30 minutes producing an exotherm leading to a maximum temperature of 45°C. The mixture

was left to stir overnight to allow the reaction to go to completion. The excess

acrylonitrile was removed as a water azeotrope (22.5g) by vacuum distillation

(16mbar) at pot and still head temperatures of 40^0C and 24^0C respectively. The

two phase mixture remaining in the pot was transferred to a separation funnel and

the lower aqueous layer was removed. The product was then washed with

demineralised water (2 x 75 mls) to remove water soluble by-products. After

separation, the product was dried (Na_2SO_4) and filtered to give crude Hex-*wedge*-

$(CN)_2$ as a light yellow oil which was purified by vacuum distillation (0.35mbar,

128°C) to give Hex-*wedge*-$(CN)_2$, *N-hexyl-3-aza pentane-1,5-dinitrile*, (68.72g,

67.8%) as a colourless oil. Found: C,69.54, H,10.14, N,20.27 MS M+1=208

determined by EI mass spectrometry, $C_{12}H_{21}N_3$ requires C,69.56,H,10.14,N,20.28

%, M 207.32; ^1H nmr. ($CDCl_3$, 400MHZ) $\partial 0.89$ (3H, CH_3CH_2), 1.3 (6H,

$CH_3CH_2CH_2CH_2CH_2CH_2N$), 1.4 (2H, $CH_3CH_2CH_2CH_2CH_2CH_2N$), 2.4 (4H,

NCH_2CH_2CN), 2.43 (2H, CH_2N) 2.85 (4H, NCH_2CH_2CN); ^{13}C nmr. ($CDCl_3$,

100MHZ) ∂ 13.8 (CH_3-), 16.7 (NCH_2CH_2CN) 22.4 (CH_3CH_2-), 24.7

(NCH_2CH_2CN) 26.5/27.1 ($CH_3CH_2CH_2CH_2$), 31.4 ($CH_3CH_2CH_2CH_2CH_2CH_2N$),

49.3 (NCH_2CH_2CN), 51.1/51.3 ($NCH_2CH_2CH_2N$), 53.2

($CH_3CH_2CH_2CH_2CH_2CH_2N$), 118.6 (CN); FTIR. ($v_{max}$/$cm^{-1}$): 2247.5, 1626.8.

2.5.1.2 Synthesis of Hex-*wedge*-(NH$_2$)$_2$ **(3)**

The hydrogenation was carried out in a Parr 2L stainless steel autoclave.

Hex-*wedge*-(CN)$_2$ (35.76g, 0.178moles) was added to 100mls of a 1.4M solution

of NaOH in methanol/water (95:5). Raney nickel (15g) (slurry in water, Aldrich)

was added under a nitrogen blanket to the mixture, the total volume was brought

to approximately 800mls with a 95:5 solution of methanol/water and purged with

N$_2$ for 15 minutes. The reaction mixture was mechanically stirred for 15 hrs at

75°C under 45 bar (600psi) H$_2$ pressure. The hydrogenation could be followed

by the decrease of the CN stretching vibration in the IR spectrum. After the

reaction mixture had been cooled and the pressure released, the catalyst was

removed by filtration on a sinter funnel over a layer of diatomaceous earth.

Methanol was removed by rotary evaporation and the residue extracted several

times with CH$_2$Cl$_2$. The combined organic extracts were dried (NaSO4) and the

solvent evaporated in vacuo affording crude Hex-*wedge*-(NH$_2$)$_2$ as a colourless

oil. (27g, 73%). Purification was carried out by Kulgelrohr distillation (125°C ,

0.1 mbar) to give Hex-*wedge*-(NH$_2$)$_2$, *N-hexyl-4-aza heptane-1,7-diamine* . The

purity was confirmed by IR, ^{1}H, and ^{13}C nmr.

Found: C,66.96, H,13.45, N,19.43 MS M+1=216 determined by EI mass

spectrometry, MALDI-TOF-MS-single peak at 214.45 (factory calibration)

$C_{12}H_{29}N_3$ requires C,66.97,H,13.48,N,19.53 %, M, 215 ; ^1H nmr (CDCl$_3$,

400MHZ) : ∂ 0.89 (3H, CH$_3$CH$_2$), 1.3 (6H, CH$_3$CH$_2$CH$_2$CH$_2$CH$_2$CH$_2$N), 1.4 (2H,

CH$_3$CH$_2$CH$_2$CH$_2$CH$_2$CH$_2$N), 1.6 (4H, NCH$_2$CH$_2$CH$_2$NH$_2$), 2.38 (2H,

CH$_3$CH$_2$CH$_2$CH$_2$CH$_2$CH$_2$N), 2.5 (4H, NCH$_2$CH$_2$CH$_2$NH$_2$), 2.7 (4H,

NCH$_2$CH$_2$CH$_2$NH$_2$); ^{13}C nmr (CDCl$_3$, 100MHZ): ∂ 13.8 (CH$_3$-), 22.4 (CH$_3$CH$_2$-),

26.7,27.0 (CH$_3$CH$_2$CH$_2$CH$_2$), 30.8 (NCH$_2$CH$_2$CH$_2$NH$_2$), 31.6

(CH$_3$CH$_2$CH$_2$CH$_2$CH$_2$CH$_2$N), 40.5 (NCH$_2$CH$_2$CH$_2$NH$_2$), 51.7

(NCH$_2$CH$_2$CH$_2$NH$_2$), 53.9 (CH$_3$CH$_2$CH$_2$CH$_2$CH$_2$CH$_2$N); FTIR (v_{max}/cm^{-1}):

3284.2, 3363.4.

2.5.1.3 Synthesis of Hex-*wedge*-(CN)$_4$ (4)

Acrylonitrile (16 mol equiv, 36mls, 0.1M w.r.t H$_2$O) was added dropwise over 30

minutes to a solution of diamine **3** (7.29g, 0.03moles) in distilled water (80mls).

The mixture was heated under reflux for 48 hours. The product was purified by

chromatography on neutral alumina eluting with 3% MeOH in CH$_2$Cl$_2$ to give

pure tetranitrile **4**, Hex-*wedge*-(CN)$_4$, *N-hexyl-4-aza-heptane-1,7-*

di(biscyanoethylamine), (11.40g, 79%). Found C,66.96, H,9.77, N,22.43 MS

M+1=428 determined by EI mass spectrometry, C$_{24}$H$_{41}$N$_7$ requires C,67.35,

H,9.59, N,22.92 %, M, 427; ^1H nmr (CDCl$_3$, 400MHZ) : ∂ 0.89 (3H, CH$_3$CH$_2$),

1.3 (6H, CH$_3$CH$_2$CH$_2$CH$_2$CH$_2$CH$_2$N), 1.4 (2H, CH$_3$CH$_2$CH$_2$CH$_2$CH$_2$CH$_2$N), 1.6

(4H, NCH$_2$CH$_2$CH$_2$N), 2.35 (2H, CH$_3$CH$_2$CH$_2$CH$_2$CH$_2$CH$_2$N), 2.4 (4H,

NCH$_2$CH$_2$CH$_2$N), 2.45 (8H, NCH$_2$CH$_2$CN), 2.53 (4H, NCH$_2$CH$_2$CH$_2$N); 2.85

(8H, NCH$_2$CH$_2$CN); ^{13}C nmr (CDCl$_3$, 100MHZ): ∂ 13.8 (CH$_3$-), 16.6

(CH$_2$CH$_2$CN) 22.4 (CH$_3$CH$_2$-), 24.7 (NCH$_2$CH$_2$CN) 26.6/27.0

(CH$_3$CH$_2$CH$_2$CH$_2$), 31.5 (CH$_3$CH$_2$CH$_2$CH$_2$CH$_2$CH$_2$N), 49.3 (NCH$_2$CH$_2$CN),

51.1/51.3 (NCH$_2$CH$_2$CH$_2$N), 53.7 (CH$_3$CH$_2$CH$_2$CH$_2$CH$_2$CH$_2$N), 118.6 (CN).

FTIR (v$_{max}$/cm^{-1}): 2929.6, 2855.2, 2246.1.

2.5.1.4 Synthesis of Hex-*wedge*-(NH$_2$)$_4$ (5)

Tetranitrile **4** (17.67g, 0.04moles) was hydrogenated for 24hrs according to the

procedure described for the synthesis of **3** in 2.5.1.2. 13g of catalyst and 13g of

NH$_3$ were used. After extraction with CH$_2$Cl$_2$, tetraamine **5**, Hex-*wedge*-(NH$_2$)$_4$,

N-hexyl-4-aza-heptane-1,7-di(bisaminopropylamine) (10g, 55%) was obtained as

a viscous yellow oil. The structure was confirmed by IR, ^{1}H and ^{13}C nmr. Found:

C,64.83, H,12.76, N,21.92 MS M+1= 445 determined by EI mass spectrometry,

MALDI-TOF-MS major peak at 441.31 (factory calibration) C$_{24}$H$_{57}$N$_{17}$ requires

C,64.89, H,12.84, N,22.08 %, M, 443; ^{1}Hnmr (CDCl$_3$,400MHZ) : ∂ 0.8 (3H,

CH$_3$CH$_2$), 1.2 (6H, CH$_3$CH$_2$CH$_2$CH$_2$CH$_2$CH$_2$N), 1.3 (2H,

$CH_3CH_2CH_2CH_2CH_2CH_2N$), 1.5 (12H, $NCH_2CH_2CH_2N$ + $NCH_2CH_2CH_2NH_2$),

2.2-2.38 (6H, $CH_3CH_2CH_2CH_2CH_2CH_2N$ + $NCH_2CH_2CH_2N$), 2.4 (8H,

$NCH_2CH_2CH_2NH_2$), 2.7 (8H, $NCH_2CH_2CH_2NH_2$); ^{13}Cnmr (CDCl$_3$,100MHZ): ∂

13.9 (CH$_3$-), 22.4 (CH$_3$CH$_2$-),24.4 (NCH$_2$CH$_2$CH$_2$N), 26.8,27.1

($CH_3CH_2CH_2CH_2$), 30.8 ($NCH_2CH_2CH_2NH_2$), 31.6 ($CH_3CH_2CH_2CH_2CH_2CH_2N$),

40.6 ($NCH_2CH_2CH_2NH_2$), 51.6 ($NCH_2CH_2CH_2NH_2$), 52.1 ($NCH_2CH_2CH_2N$),

53.9 ($CH_3CH_2CH_2CH_2CH_2CH_2N$); FTIR ($v_{max}$/cm^{-1}): 3271.8, 3354.1

2.5.1.5 Synthesis of Hex-*wedge*-(CN)$_8$ (6)

Acrylonitrile, (20 mol equiv, 15mls, 0.1M w.r.t H$_2$O) was added dropwise over

30 minutes to a solution of tetraamine **5** (5.0g, 0.01moles) in distilled water

(40mls). The mixture was heated under reflux for 72 hours. After work up

impurities were detected in the ^{1}H nmr and ^{13}C nmr spectra. The product was

purified by chromatography on neutral alumina. Elution with 3% MeOH in

CH$_2$Cl$_2$ followed by 2% MeOH in CH$_2$Cl$_2$ gave the desired octanitrile **6**, Hex-

wedge-(CN)$_8$,N-hexyl-4-aza-heptyl-1,7-di[bis-(N',N'-dicyanoethyl)propylamine],

(7.40g, 75%) as a colourless viscous oil. Found: C,66.18, H,9.25, N,23.93 MS

M+1= 869 determined by EI mass spectrometry, $C_{48}H_{81}N_{15}$ requires C,66.43,

H,9.34, N,24.22 %, M, 868; ^{1}H nmr (CDCl$_3$, 400MHZ) : ∂ 0.85 (3H, CH_3CH_2-),

1.2 (6H, $CH_3CH_2CH_2CH_2CH_2CH_2N$), 1.39 (2H, $CH_3CH_2CH_2CH_2CH_2CH_2N$),

1.55 (12H, $NCH_2CH_2CH_2N$), 2.37-2.4 (14H, $CH_3CH_2CH_2CH_2CH_2CH_2N$ +

$NCH_2CH_2CH_2N$), 2.43 (16H, NCH_2CH_2CN), 2.48 (12H, $NCH_2CH_2CH_2N$); 2.80

(16H, NCH_2CH_2CN); ^{13}C nmr (CDCl$_3$, 100MHZ): ∂ 13.99 (CH_3-), 16.78

(CH_2CH_2CN), 22.55 ($NCH_2CH_2CH_2N$), 24.33 (CH_3CH_2-), 24.88

($NCH_2CH_2CH_2N$), 226.80/27.18 ($CH_3CH_2CH_2CH_2$), 31.74

($CH_3CH_2CH_2CH_2CH_2CH_2N$), 49.4 ($NCH_2CH_2CN$), 51.2/53.4 ($NCH_2CH_2CH_2N$),

52.0/52.2 ($NCH_2CH_2CH_2N$), 53.9 ($CH_3CH_2CH_2CH_2CH_2CH_2N$), 118.7 (8C, CN).

FTIR (v_{max}/cm^{-1}): 2950.2, 2853.7, 2246.6.

2.5.1.6 Synthesis of Hex-*wedge*-(NH₂)₈ (7)

Octanitrile **6** (11.5g, 0.01moles) was hydrogenated for 30hrs according to the procedure described for the synthesis of **3**, see 2.5.1.2. 13g of catalyst and 16g of NH_3 were used. Octaamine **7**, Hex-*wedge*-(NH₂)₈, *N-hexyl-4-aza-heptyl-1,7-di[bis-(N',N'-diaminopropyl)propylamine]*, (3.0g, 25%) was obtained after extraction with CH_2Cl_2. The structure was confirmed by IR, ^1H NMR and ^{13}C NMR. ^1H nmr (CDCl₃ , 400MHZ) : ∂ 0.8 (3H, CH₃CH₂), 1.2 (6H, CH₃CH₂CH₂CH₂CH₂CH₂N), 1.4 (2H, CH₃CH₂CH₂CH₂CH₂CH₂N), 1.5-1.71 (28H, NCH₂CH₂CH₂N + NCH₂CH₂CH₂NH₂), 2.34-2.40 (26H, CH₃CH₂CH₂CH₂CH₂CH₂N + NCH₂CH₂CH₂N), 2.43 (16H, NCH₂CH₂CH₂NH₂), 2.69 (16H, NCH₂CH₂CH₂NH₂); ^{13}C nmr (CDCl₃ , 100MHZ): ∂ 14.0 (CH₃-), 22.6 (CH₃CH₂-), 24.5 (NCH₂CH₂CH₂N), 27.2 (CH₃CH₂CH₂CH₂), 30.8 (NCH₂CH₂CH₂NH₂), 31.8 (CH₃CH₂CH₂CH₂CH₂CH₂N), 40.7 (NCH₂CH₂CH₂NH₂), 51.8 (NCH₂CH₂CH₂NH₂), 52.2 (NCH₂CH₂CH₂N), 54.1 (CH₃CH₂CH₂CH₂CH₂CH₂N). FTIR (ν_{max}/cm⁻¹): 3271.8, 3354.1.

2.5.2 Siloxysilane derived dendrimer wedges.

2.5.2.1 Synthesis of 3-aminopropyltris(trimethylsiloxy)silane (APTTMSS).

$$H_2N(CH_2)_3Si(OEt)_3 + (CH_3)_3SiNHSi(CH_3)_3 \longrightarrow H_2N(CH_2)_3Si(OSiMe_3)_3$$

Aminopropyltriethoxysilane (4.03g, 0.018 moles) and hexamethyldisilazane (17.63g, 0.11 moles) were added to distilled water (50 mls). Two layers separated, an upper organic layer and a lower aqueous layer. The mixture was stirred and refluxed for two days. After the two days at reflux, two phases separated on cooling. The mixture was put into a separation funnel and the lower aqueous phase was discarded. A water white, clear fluid (18.37g) was recovered. The material was purified by vacuum distillation through a Vigreux column (152°-153°C at 47mmHg lit.[15] 92°C at 1mmHg) to give the required product, 3-aminopropyltris(trimethylsiloxy)silane, as a clear transparent oil (1.67g, 33%). Found: C,39.89, H,9.84, N,3.85 MS M+1 =354 determined by E.I. mass spectrometry, calculated for $C_{12}H_{35}N$ requires C40.79, H9.91, N3.96%, M, 353

^{1}H nmr (CDCl$_3$, 400MHZ): δ 0.05 (s, 27, OSiCH_3), 0.42 (t, 2, CH_2Si), 1.15 (s, 2, NH_2), 1.45 (m, 2, CH$_2$CH_2CH$_2$), 2.6 (t, 2, H$_2$NCH_2); ^{13}C nmr (CDCl$_3$, 100MHZ): 1.8 (OSiCH$_3$), 11.5 (CH$_2$Si), 27.8 (CH$_2$$CH_2CH_2$), 45.2 (H$_2NCH_2$). FTIR (ν$_{max}$/cm^{-1}): 3374.7, 3295.4, 2957.9, 2928.3, 1054, 841.2.
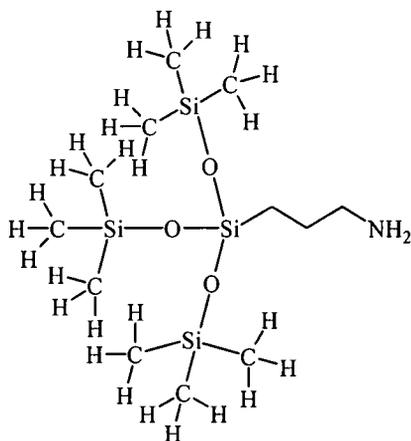
2.5.2.2 Synthesis of Si-*wedge*-(CN)$_2$.
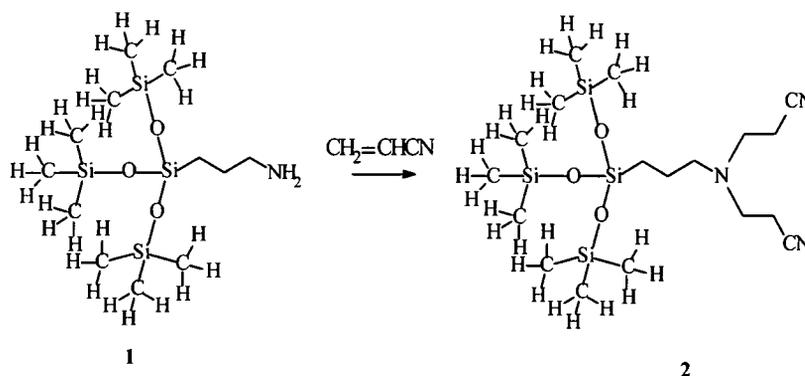
Acrylonitrile (16g, 0.3 mols) was added to a solution of APTTMSS (10.21g, 29 mmols), in methanol (70mls). The addition of the acrylonitrile took 20 minutes. The temperature of the mixture was taken up to 80^{0}C for 1 hour and then maintained at 65^{0}C for 24 hours to complete the reaction. The solvent and excess acrylonitrile were removed under vacuum generating the crude product (Si-*wedge*-(CN)$_2$) as a clear yellow transparent oil (13.62g). Purification of the crude product was carried out by Kulgelrohr distillation, removing the addition product of acrylonitrile with methanol to give Si-*wedge*-(CN)$_2$, *tris(trimethylsiloxy)silyl propyl-3-aza-pentane-1,5-dinitrile* as a clear oil (12.5 g, 94%). Found: C,46.96, H,9.08, N,8.86, MS M+1= 460 determined by E.I. mass spectrometry, C$_{18}$H$_{41}$N$_3$ requires C,47.05, H,8.93, N,9.15%, M, 459 ; ^{1}H nmr (CDCl$_3$, 400MHZ): δ 2.85 (t, 4H, NCH_2), 2.5 (t, 2H, CH_2N), 2.45 (t, 4H, CH_2CN), 1.46 (m, 2H, CH$_2$CH_2CH$_2$), 0.42 (t, 2H, CH_2Si), 0.1 (s, 27H, OSiCH_3)

^{13}C nmr (CDCl$_3$, 100MHZ): δ 1.68 (OSiCH$_3$), 11.52 (CH$_2$-Si), 16.9 (CH$_2$CN),

21.1 (CH$_2$$CH_2CH_2$), 49.7 (H$_2NCH_2$); 56.2 (H$_2NCH_2CH_2$)$_1$: 118.4 (4C, CN).

F.T.I.R. ν$_{max}$/cm^{-1}: 3179.8, 2957.3, 2899.1, 1057.9, 843.

2.5.2.3 Synthesis of Si-*wedge*-(NH$_2$)$_2$.

2   3

Diisobutylaluminiumhydride (DIBAL-H), (100mls in hexane solution, 0.49

mols), was added to a solution of Si-*wedge*-(CN)$_2$ (**2**) (3.00g, 6.54mmol), in dry

tetrahydrofuran (100mls). The dropwise addition of the DIBAL-H took 30

minutes. The solution was refluxed for 24 hours, and then cooled to room

temperature. Methanol (30 mls), was added to the clear solution producing a

white solid precipitate. After filtration the clear organic layer was removed under

vacuum affording the crude product as a white gel or clear yellow oil, the

physical form of the product varied from preparation to preparation but the

spectra were identical. (3.85g) Purification of the crude product was carried out

by Kulgelrohr distillation giving Si-*wedge*-(NH$_2$)$_2$, *tris(trimethylsiloxy)silyl*

propyl-4-aza-heptane-1,7-diamine as a clear yellow oil. (2.72g, 89%). Found:

C,45.89, H,10.25, N,8.68, MS M+1 = 468 determined by E.I. mass spectrometry,

C$_{18}$H$_{49}$N$_3$ requires C,46.25, H,10.49, N,8.99%, M, 467

^{1}H nmr (CDCl$_3$, 400MHZ): δ 0.05 (s, 27H, SiMe$_3$); 0.29 (t, 2H, CH$_2$Si); 1.36 (m, 2H, Si-CH$_2$C*H$_2$*CH$_2$); 1.5 (m, 4H, N CH$_2$C*H$_2$*CH$_2$N); 2.28 (t, 2H,C*H$_2$*N CH$_2$); 2.36 (t, 4H, C*H$_2$*NH$_2$).); 2.62 (t, 4H, CH$_2$NC*H$_2$*); ^{13}C nmr (CDCl$_3$, 100MHZ) 1.75 (Si*C*H$_3$); 12.05 (Si*C*H$_2$); 20.73 (SiCH$_2$*C*H$_2$CH$_2$); 31.13 (NCH$_2$*C*H$_2$CH$_2$N); 40.81 (*C*H$_2$NH$_2$); 51.92 (CH$_2$N*C*H$_2$); 57.29 (*C*H$_2$NCH$_2$).

FTIR (v$_{max}$/cm^{-1}): 3368.3, 3288.4, 2955.6, 1057.8, 842.1.

2.5.2.4 Synthesis of Si-*wedge*-(CN)$_4$.

Acrylonitrile (15mls, 0.23mol) was added to a cloudy solution of APTTMSS1GA (1.6g, 3.43 mmol) in distilled water (50mls). The addition of the acrylonitrile took 20 minutes. The temperature was taken up to 80^{0}C and left to stir overnight and then maintained at 65^{0}C for 8 hours. The solution was allowed to cool was left to stir at room temperature overnight to complete the reaction. The solvent and excess acrylonitrile were removed under vacuum and the solution extracted with dichloromethane (2 x 100mls). The organic layers were combined and removed under vacuum affording the crude Si-*wedge*-(CN)$_4$ as a cloudy yellow oil. Purification of the crude product by Kulgelrohr distillation generated Si-*wedge*-(CN)$_4$, *tris(trimethylsiloxy)silyl propyl-4-aza-heptane-1,7-*

di(biscyanoethylamine), as a clear yellow oil. (1.91g, 82%). Found: C,52.83, H,9.04, N,14.16, MS M+1= 680 determined by E.I. mass spectrometry, $C_{30}H_{61}N_7$ requires C,53.02, H,8.98, N,14.43%, M, 680 ; ^{1}H nmr (DMSO$_{d6}$, 400MHZ) δ0.07 (s, 27H, SiMe$_3$), 0.36 (t, 2H, CH$_2$Si), δ1.38 (m, 2H, Si-CH$_2$CH$_2$CH$_2$), 1.60 (m, 4H, N CH$_2$CH$_2$CH$_2$N), 2.35 (t, 2H Si CH$_2$CH$_2$CH$_2$N CH$_2$), 2.48 (m, 12H, NCH$_2$CH$_2$CH$_2$N + CH$_2$CH$_2$CN), 2.55 (t, 4H, NCH$_2$CH$_2$CH$_2$N), 2.85 (t, 8H, NCH$_2$CH$_2$CN); ^{13}C nmr (DMSO$_{d6}$, 100MHZ) δ 1.76 (SiCH$_3$), 12.03 (SiCH$_2$), 16.90 (CH$_2$CN), 20.64 (SiCH$_2$CH$_2$CH$_2$), 25.10 (NCH$_2$CH$_2$CH$_2$N), 49.59 (NCH$_2$CH$_2$CN), 51.40 (NCH$_2$CH$_2$CH$_2$N), 51.63 (NCH$_2$CH$_2$CH$_2$N), 57.05 (SiCH$_2$CH$_2$CH$_2$N), 118.64 (4C, CN).

FTIR (v_{max}/cm^{-1}): 2955.7, 2247.3, 1058, 843.3.

2.5.2.5 Synthesis of Si-*wedge*-(NH$_2$)$_4$.

Diisobutylaluminiumhydride (DIBAL-H), (100mls, 0.49 mols), was added to a solution of Si-*wedge*-(CN)$_4$ (1.66g, 2.44mmol), in dry tetrahydrofuran (100mls). The dropwise addition of the DIBAL-H took 30 minutes. The solution was refluxed for 24 hours and then cooled to room temperature. Methanol (30 mls), was added to the clear solution until a white solid was produced. After filtration

the clear organic layer was removed under vacuum affording the crude Si-*wedge*-

$(NH_2)_4$, as a yellow gel. Purification of the crude product was carried out by

Kulgelrohr distillation giving Si-*wedge*-$(NH_2)_4$, *tris(trimethylsiloxy)silyl propyl-*

4-aza-heptane-1,7-di(bisaminopropylamine), as a clear yellow gel. (1.47g, 86%)

^{1}H nmr (CD$_3$OD, 400MHZ) δ 0.12 (s, 27H, Si**Me**$_3$); 0.42 (t, 2H, C**H**$_2$Si); 1.55

(m, 2H, Si-CH$_2$C**H**$_2$CH$_2$); 1.64 (m, 12H, NCH$_2$C**H**$_2$CH$_2$N); 2.2-2.38 (6H,

SiC**H**$_2$CH$_2$CH$_2$N + NCH$_2$CH$_2$C**H**$_2$N), 2.4 (8H, NCH$_2$CH$_2$C**H**$_2$NH$_2$), 2.7 (8H,

NC**H**$_2$CH$_2$CH$_2$NH$_2$); ^{13}C nmr (CD$_3$OD, 100MHZ): δ 2.01 (Si**C**H$_3$), 13.24

(Si**C**H$_2$), 21.71 (SiCH$_2$**C**H$_2$CH$_2$), 24.73 (NCH$_2$**C**H$_2$CH$_2$N), 30.57

(NCH$_2$**C**H$_2$CH$_2$NH$_2$), 41.08 (**C**H$_2$NH$_2$), 52.80 (N**C**H$_2$CH$_2$CH$_2$NH$_2$), 53.30

(N**C**H$_2$CH$_2$CH$_2$N + NCH$_2$CH$_2$**C**H$_2$N), 53.30 (SiCH$_2$CH$_2$**C**H$_2$N).

FTIR (ν$_{max}$/cm^{-1}): 3355.1, 3287.7, 2955.2, 1057.9, 843.7.

2.6 References

[1] Moors, R., and Vögtle, F., Chem. Ber. 126, (**1993**), 2133.

[2] Schrötter, R., *Newer Methods of Preparative Organic Chemistry*, Interscience, New York, (**1948**), 61.

[3] Smith, H.A., Chadwell, A.J., Kirslis, S.S., *J. Phys. Chem.*, 59, (**1955**), 820.

[4] Kokes, R.J., Emmett, P.H., *J. Am. Chem. Soc.*, 81, (**1959**), 5032.

[5] Kokes, R.J., Emmett, P.H., *J. Am. Chem. Soc.*, 82, (**1960**), 4497.

[6] Mozingo, R., *Org. Synthesis, Coll. Vol 3*, (**1955**), 181.

[7] Winans, C.F., Adkins, H., *J. Am. Chem. Soc.*, 54, (**1932**), 306.

[8] Reeve, W., Christian, J., *J. Am. Chem. Soc.*, 78, (**1956**), 860.

[9] de Brabander-van den Berg, E.M.M., Nijenhuis, A., Mure, M., Keulen, J., Reintjens, R., Vandenbooren, F., Bosman, B., de Raat, R., Frijns, T., v.d. Wal, S., Castelijns, M., Put, J., and Meijer, E.W., *Macromol. Symp.* 11, (**1994**), 51.

[10] de Brabander-van den Berg, E.M.M., and Meijer, E.W., *Angew. Chem. Int. Ed. Engl.* 32, (**1993**), 1308.

[11] Wörner, C., and Mülhaupt, R., *Angew. Chem. Int. Ed. Engl.* 32, (**1993**), 1306.

[12] Bergeron, R.J., and Garlich, J.R., *Synthesis* (**1984**), 782.

[13] Freifelder, M., *Catalytic Hydrogenation in Organic Synthesis, Procedures and Commentary*, Wiley, New York (**1978**), 43.

[14] van Hest, J.C.M., Delnoye, D.A.P., Baars, M.W.P.L., Elissen-Román, van Genderen, M.H.P., and Meijer, E.W., Chem. Eur. J. 12, (**1996**), 1616

[15] Hamilton, L.M., Rannard, S., and Feast, W.J., *Polymer Bulletin* 39, (**1997**), 347.

[16] Harvey III, T.B., U.S. Patent, 4711943, (**1987**).

CHAPTER 3

Modification of Dendrimer Wedges

3.1 Introduction

This chapter describes the synthesis and characterisation of various amino acid terminated dendrimer wedges. The bulk of the experimental work is concerned with the activation and coupling of N-benzyloxycarbonyl (CBZ) protected L-tyrosine, tryptophan and phenylalanine amino acids to various amine terminated generations of hexylamine and aminopropyltris(trimethylsiloxy)silane dendrimer wedges. The tactics and strategies for peptide bond formation are discussed with particular reference to the choice of the amino protecting group and the importance of this choice in relation to the final deprotection step. The investigation of the use of the modified dendrimer wedges for cellulose surface recognition is described and discussed in Chapter 4.

3.2 Chemical Activation and Coupling

Common procedures for formation of peptide bonds involve the generation and aminolysis of reactive carboxy derivatives.

Scheme 3.1 Mechanism of peptide bond formation

Activation is achieved by attachment of a leaving group to the acyl carbon of the carboxy component enabling attack by the amine group of the amino component.

This is necessary because ordinary carboxylic acids simply form salts with amines at ambient temperatures. Formation of an amide bond between two amino acids is an endothermic reaction. Carboxylic acids react with amines to give amides at elevated temperature but this is not a suitable method for synthesis of complex peptides. Usually, peptide synthesis is performed at or below room temperature and coupling methods which involve heating are not generally useful. In order to form a peptide bond one of the groups, either the carboxyl or amine group, has to be activated.

At present, activation of the carboxyl group is the underlying principle for all coupling methods and 'X', in scheme 3.1, is an electron-withdrawing atom (e.g. Cl) or group (such as an activated ester) which renders the carbon atom of the carboxyl sufficiently electrophilic to facilitate the nucleophilic attack by the amino group. The tetrahedral intermediate thus formed is stabilised by the elimination of X^-, which is usually a good leaving group;

There are generally three different ways of coupling along the lines of scheme 3.1;

a) those in which a reactive acylating agent is formed from the carboxy component in a separate step or steps, followed by immediate treatment with the amino component;

b) those in which an isolable acylating agent is formed separately, and may even be purified before aminolysis; and

c) those in which the acylating intermediate is generated in the presence of the amino component, by the addition of an activating agent to a mixture of the two components.

The activation in (a), (b) and (c) is usually achieved by reaction of the carboxy component with an electrophilic reagent, either by addition or substitution.

3.3 The Coupling method

3.3.1 Activated Esters

Active esters can be prepared by dicyclohexylcarbodiimide (DCCI) mediated coupling or mixed anhydride methods, and a variety of specialised reagents are available[1]. Active esters are generally crystalline, stable materials; because they are at a relatively low level of activation, side reactions during coupling, including racemisation, are generally less of a problem than with most peptide bond forming procedures. Examples of activated esters are shown below, Figure 3.1.

$RCO-O-\bigcirc-NO_2$, RCO_2Np
1)
Para-nitrophenyl esters

$RCO-O-\bigcirc-Cl$, RCO_2Tcp
2)
Trichlorphenyl esters

$RCO-O-\bigcirc-F$, RCO_2Pfp
3)
Pentafluorophenyl esters

$RCO-O-N$, RCO_2Su
4)
Hydroxysuccinimide esters

Figure 3.1 Structures of active esters and commonly used abbreviations.

The reactivities of the various active esters correlate broadly with the acidities of the ester moieties, after due allowance for steric and special effects. In practice

choice is dictated by a combination of reactivity and ease of co-product removal. Thus, for a water-insoluble protected peptide, a succinimido ester coupling is convenient, because N-hydroxysuccinimide is very water-soluble. By contrast, for a water-soluble product, a halophenyl ester may be best, because halophenols are ether soluble.

3.3.2 Coupling Reagents and Auxiliary Nucleophiles.

Dicyclohexylcarbodiimide (DCC or DCCI) has been the single most important reagent for activating carboxy groups for peptide synthesis since Sheehan and Hess reported their results in 1955[2]. DCCI may be used to generate activated carboxy derivatives such as active esters or as a direct coupling reagent. In all these cases, the primary activating agent is formed by addition of the acid hydroxyl to the carbodiimide to give an *O*-acylisourea, which is a potent acylating agent. Direct peptide coupling with DCCI involves mere mixing of the amino and carboxy components with DCCI in equimolar amounts in an organic solvent, at ambient temperature or a little below. *O*-Acylisourea formation is rapid, leading to peptide either by immediate aminolysis or via a symmetrical anhydride, with the accompanying formation of dicyclohexylurea, as shown in scheme 3.2. The urea is only sparingly soluble in most solvents and so its separation from the desired product is straightforward. There are, however, some disadvantages with the DCCI coupling procedure. Side reactions readily occur due to the high reactivity of the intermediates and extensive racemisation takes place with susceptible carboxy components. Futhermore, the collapse of the *O*-acylisourea by intramolecular acyl transfer sometimes competes significantly

with the desired attack by external nucleophiles. The much less reactive *N*-acylurea formed consequently reduces the yield and gives rise to purification problems.

$$R-COOH \quad + \quad DCCI$$

$$R-C=O$$

HOBt

HOBt

$$R-C=O \\ O \\ R-C=O$$

$$R-\overset{O}{\overset{\|}{C}}-O-N$$

$$H_2N-R'$$

$$H_2N-R'$$

$$H_2N-R'$$

$$R-CO-NH-R'$$

$$R-CO-NH-R' \\ + HOBt$$

$$R-CO-NH-R'$$
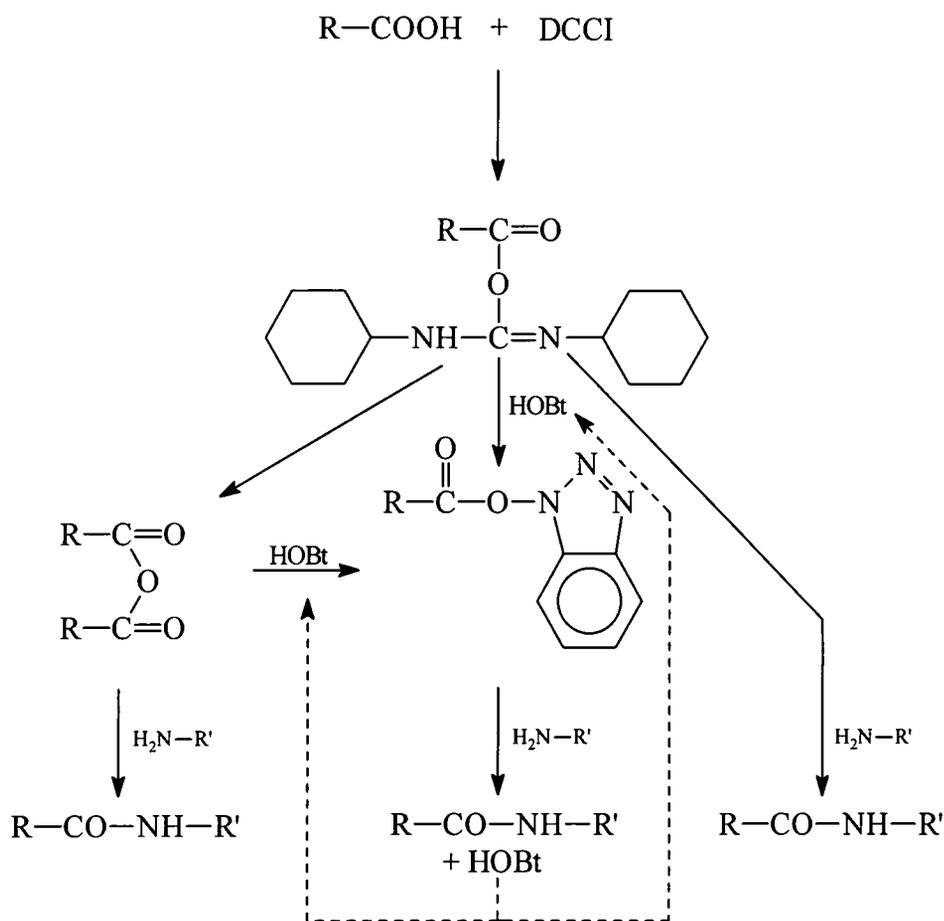
Scheme 3.2 Multiple pathways in DCCI coupling in the presence of auxillary nucleophiles. (see discussion)

These problems and the danger of racemisation can be greatly reduced by performing the coupling in the presence of an additive, often designated an auxiliary nucleophile. This reacts rapidly with the *O*-acylisourea before side reactions can intervene. An acylating agent of lower potency is formed, which is still reactive with respect to aminolysis, but which is more discriminating and does not lead to racemisation or other side reactions.

(HOBt)   (HOSu)   (HOOBt)
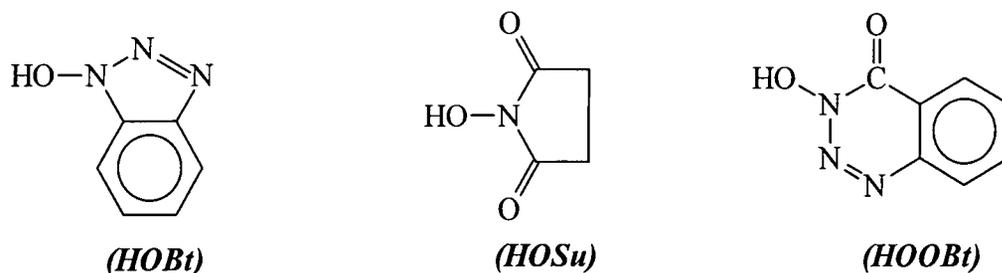
Figure 3.2 Auxiliary nucleophiles.

Numerous additives, which in effect generate an active ester *in situ,* have been investigated. Of these, 1-hydroxybenzotriazole (HOBt)[3] is probably the most commonly applied, although N-hydroxysuccinimide (HOSu)[4] and 3-hydroxy-3,4-dihydro-1,2,3-benzotriazin-4-one (HOOBt)[10] are also important. The ability of additives to provide multiple pathways to the same product is shown in Scheme 3.2. In the work reported below HOBt was used in trial experiments but made no difference to recovered yields.

3.4 Tactics and Strategies for Peptide Bond Formation

3.4.1 Choice of the amino protecting group and activated ester.

Since amino acids are di-functional molecules, directed coupling of the carboxyl group of the amino acid with the amino group of the wedge can be achieved only by protecting all the functional groups not involved in the coupling. This is accomplished by temporary attachment of blocking groups that mask the reactivity of the functions to be protected. Blocking groups that are readily introduced and readily and selectively removed without side reactions must be employed. After these protecting groups are introduced, one of the components of the peptide-bond-to-be, usually that providing the carboxyl side,

is converted to a reactive form. The activated carboxyl component and the amino component are then allowed to react to form the peptide bond and, finally, the blocking groups are removed.

The most useful and widely available amine protecting groups are the C-alkoxycarbonyls (urethanes) of which the benzyloxycarbonyl (Z or CBZ) group has been preferred for N-protection in this work. The CBZ group is based on *benzyl esters* of carbamoic acids which allow the cleavage of the ester bond by catalytic hydrogenation, a simple procedure which can be performed without special equipment and in high yields. Most importantly, removal of the CBZ protection by catalytic reduction does not affect the peptide bond or the sensitive siloxysilane bonds and the by-products of the deprotection reaction, toluene and carbon dioxide, are readily removed from the reaction mixture. A further advantage of the CBZ group lies in the fact that over and above the protection it provides against undesired acylation, it also avoids the racemisation of the amino acid to which it is attached.

The CBZ protected active esters of p-nitrophenyl and hydroxysuccinimide were chosen as the most suitable reagents for modification of dendrimer wedge amine termini because of the ease of removal of the nitrophenol and hydroxysuccinimide by-products liberated during the reaction and the reasonable speed at which the aminolysis reaction proceeds. Even at room temperature and without a catalyst yields exceed 80%. A particular advantage of using nitrophenol activated esters is that they can be purchased readily from commercial sources and stored in their stable crystalline form for several months without any significant loss of activation. N-CBZ amino acids activated with

hydroxysuccinimide esters could not be purchased and were synthesised using DCCI mediated coupling.

3.4.2 Protection and Final Deprotection

Coupling of the various protected amino acids to the dendrimer wedge has been executed using the activated ester method leaving the amino group of the amino acid protected with the CBZ group. For tyrosine residues, o-*benzyl* protective groups are also present. The final step requires removal of the protecting groups to reform the functionality at the periphery of the wedge. As already stated, the deprotection procedure must not interfere with the peptide bond formed or any other part of the molecule as a whole. Therefore the deprotection method has to remove all the protecting groups quickly and efficiently and in high yield.

The classic cleavage conditions for removal of the CBZ group are acidolysis e.g. HBr in acetic acid[5,6] or catalytic hydrogenolysis[7,8]. HBr in acetic acid was inappropriate for the final deprotection step for a number of reasons. Firstly, HBr/AcOH is a highly corrosive system and it was considered to be too harsh an environment for the survival of the siloxysilane bonds. Also, the generation of electrophilic species such as benzyl cations could attack the susceptible electron-rich side chains of tryptophan and tyrosine. Although the addition of additives like anisole and ethanedithiol diminish difficulties by acting as 'scavengers' for such species, they can act as nucleophiles which may attack the siloxysilane bonds. For the simultaneous removal of benzyl ethers, benzyl esters and the CBZ group the mildest and the most attractive method involves a specific form

of catalytic hydrogenolysis known as Catalytic Transfer Hydrogenation (CTH)[9,10,11]. Transfer hydrogenation is a simple and convenient method for removal of all protecting groups that are normally removed by catalytic hydrogenation. Using 5 or 10% palladium on charcoal or palladium black catalysts and 1,4-cyclohexadiene as the hydrogen source reduction takes a few hours. The rapid disproportionation of 1,4-cyclohexadiene makes it highly effective as a hydrogen donor, with optimum deprotection occurring with a 5-10% excess per protecting group. The oxidation potential for 1,4-cyclohexadiene is low and the optimum temperature for reaction is ~20^{0}C. Most of the solvents employed for catalytic hydrogenolysis of peptides are also useful for the CTH process, but there is a substantial difference in rate. Reduction is fastest in glacial acetic acid but this leaves the deprotected molecule as the acetate. The reaction rate is slower in ethanol (1.5hrs), methanol (3.5hrs), and dimethylformamide (5hrs) but generates the deprotected amino acid as the free amine. CTH proceeds at the rate described above when the concentrations of the substrate are in the range of 0.05-0.25mmol/ml.

3.4.3 Residue-specific considerations

Every amino acid has unique problems and points of interests that need careful consideration when attempting to form a peptide bond.

Tyrosine

Hydroxy groups, especially phenolic hydroxy groups, react with acylating agents, and are therefore usually protected in peptide synthesis. In tyrosine, the reactivity of the side chain phenolic hydroxyl group very much depends upon the

conditions which prevail in the reaction mixture during coupling. In the presence of bases deprotonation of the hydroxyl group occurs and a potent nucleophile is generated; the formerly inert phenol changes into a reactive phenolate. Standard blocking of the phenolic hydroxyl group of the tyrosine residue is in the form of benzyl ether protection which, again, is cleaved by CTH. The only major problem arises from the susceptibility of the phenolic ring to attack by electrophiles. This is a problem with cleavage of *O*-benzyltyrosine protection with HF or HBr/TFA leading to the formation of 3-benzyltyrosine residues, which can be diminished by using HBr/AcOH with thioanisole. This potential problem is circumvented by the use of CTH as the deprotection method.

Tryptophan

The indole ring of trytophan does not interfere with peptide bond formation, but captures electrophiles with great ease at several positions, and even under relatively mild acidic deprotection conditions competitive scavengers are essential. The deprotection method of CTH should not cause any problems and it is not considered necessary to protect the indole nitrogen in tryptophan.

Phenylalanine

Phenylalanine has no side-chain functionality and the only consideration that needs to be taken into account is that it may suffer reduction to cyclohexylalanine if extended catalytic hydrogenolysis reaction times cannot be avoided.

3.5 **Synthesis and characterisation of amino acid terminated dendrimer wedges.**

3.5.1 Introduction

In this section representative examples of the synthesis and characterisation of the intermediates and final functionalised dendritic wedges are discussed in detail. The details for each compound prepared are recorded in the experimental section (3.6) and Appendix 2. Reaction schemes for each stage in the synthesis of the amino acid terminated dendrimer wedges are presented at the appropriate points in the experimental section.

3.5.2 Formation of amino acid N-hydroxysuccinimide esters.

N-Hydroxysuccinimide esters of t-BOC and CBZ protected amino acids are well known[12] and are stable, crystalline materials. Unlike t-BOC amino acid esters, the N-CBZ-hydroxysuccinimide esters of tyrosine, tryptophan and phenylalanine are not commercially available. However, they can be readily synthesised by modification of the method outlined by Bodansky[13], and described in Section 3.6.1 (page 124). Utilising DCCI mediated coupling in anhydrous 1,2-dimethoxyethane at 0°C and recrystallisation from isopropanol twice afforded the required material as a white crystalline solid in high yields (70-90%).

The activated esters were characterised by ^{1}H and ^{13}C nmr spectroscopy. The ^{1}H and ^{13}C nmr spectra of benzyloxycarbonyl-L-phenylalanine-N-hydroxysuccinimide ester in CDCl$_3$ are shown in Figures 3.3 and 3.4 respectively. The ^{1}H nmr spectrum (Figure 3.3) shows a singlet at 2.79ppm due

to the CH_2 hydrogens (a) of the hydroxysuccinimide assigned by comparison with starting material. The ABX pattern of the phenylalanine residue is seen at approximately 3.25ppm for the non-equivalent CH_2 geminal hydrogens (AB) (b), whilst the OCH hydrogen (X) component (c) appears at 5.03ppm (dd) and is partially overlapped by the major multiplet at 5.08ppm which is assigned to the OCH_2 hydrogens (d) of the CBZ protecting group. The doublet at 5.28ppm is assigned to the amide NH hydrogen (e), whilst the broad multiplet at 7.2-7.3 corresponds to aromatic CH signals (f). The above assignments were confirmed from COSY, DEPT and Hetcor 2D spectra, see Appendices 2.3 and 2.4.
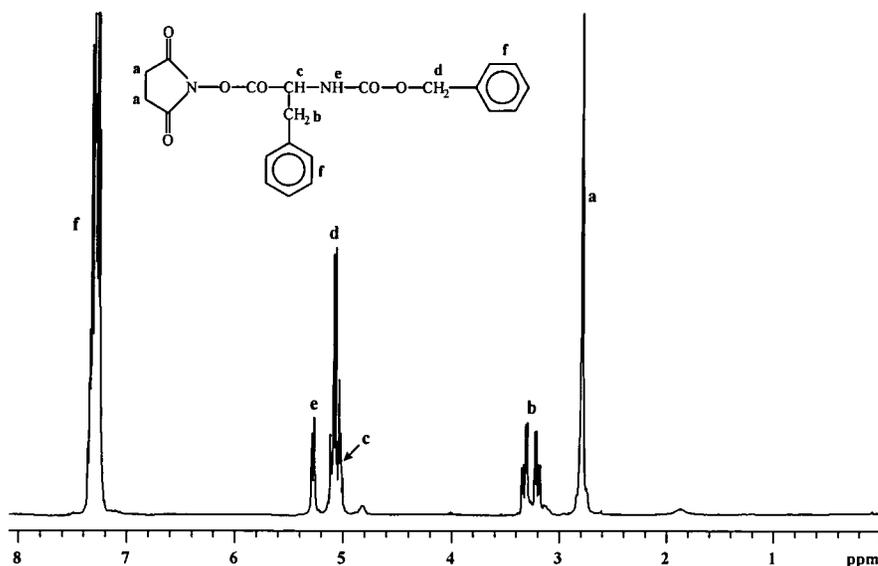
Figure 3.3. ^{1}H nmr spectra of CBZ-L-phenylalanine N-hydroxysuccinimide ester in $CDCl_3$.

The ^{13}C nmr spectrum (Figure 3.4) was assigned by analogy with the starting material and from DEPT and Hetcor analysis. The signal at 25.45ppm is due to

the CH_2 of the hydroxysuccinimide (1), whilst the signal at 37.81ppm corresponds to the CH_2 of the amino acid residue (2), which was confirmed from the Hetcor spectrum since this signal has two non-equivalent hydrogens attached.
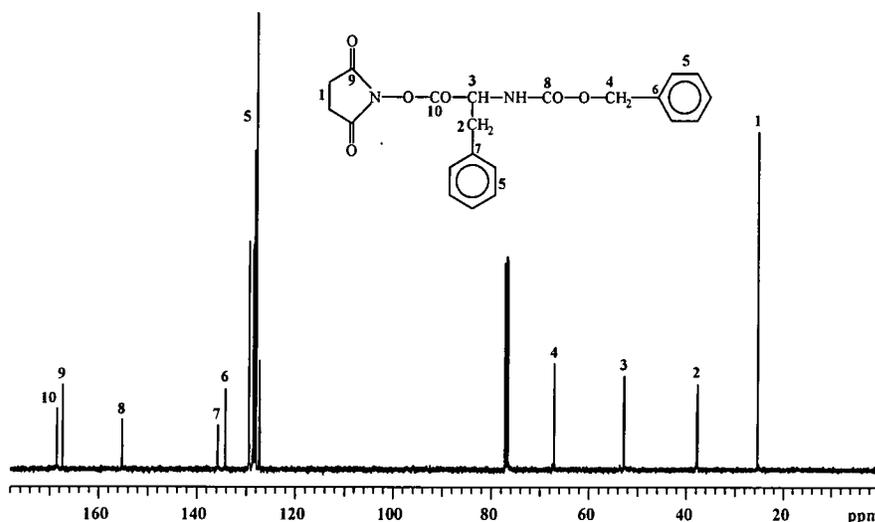
Figure 3.4 ^{13}C nmr spectra of CBZ-L-phenylalanine N-hydroxysuccinimide ester in $CDCl_3$.

The signal at 52.87ppm corresponds to a CH signal as shown from the DEPT spectra and can therefore be unambiguously assigned to the CH of the amino acid residue (3), whilst the signal at 67.15ppm arises from the OCH2 of the benzyl ester protecting group (4). Aromatic CH signals are observed at 127.34,128.05,128.14,128.41,128.63 and 129.51ppm (5). The signals at 134.31ppm (6) (protecting group) and 135.84ppm (7) (amino acid) are due to ipso-aromatic carbons. The signal at 155.26ppm is due to the protecting group carbonyl (8), whilst the signals at 167.41ppm and 168.61ppm correspond to the hydroxysuccinimide carbonyls (9) and the protected carbonyl of the amino acid carboxylic acid (10), respectively.

Interestingly, the ^{1}H nmr spectrum of this ester in DMSOd$_6$, (Figure 3.5) shows a different splitting pattern for the geminal **CH$_2$** hydrogens of the amino acid residue. Instead of the double doublet of doublets in CDCl$_3$ observed for a normal ABX system, a triplet at 3.02ppm and a doublet of doublets at 3.23ppm is observed. The presence of water in the polar DMSOd$_6$ solvent allows hydrogen bonding to occur and locks the molecule in a fixed conformation. As a consequence, there is restricted rotation about the CH$_2$ carbon atom and so the two geminal hydrogens (AB) are diastereotopic and couple to the CH hydrogen (X) of the amino acid residue with different coupling constants, one large and one small.
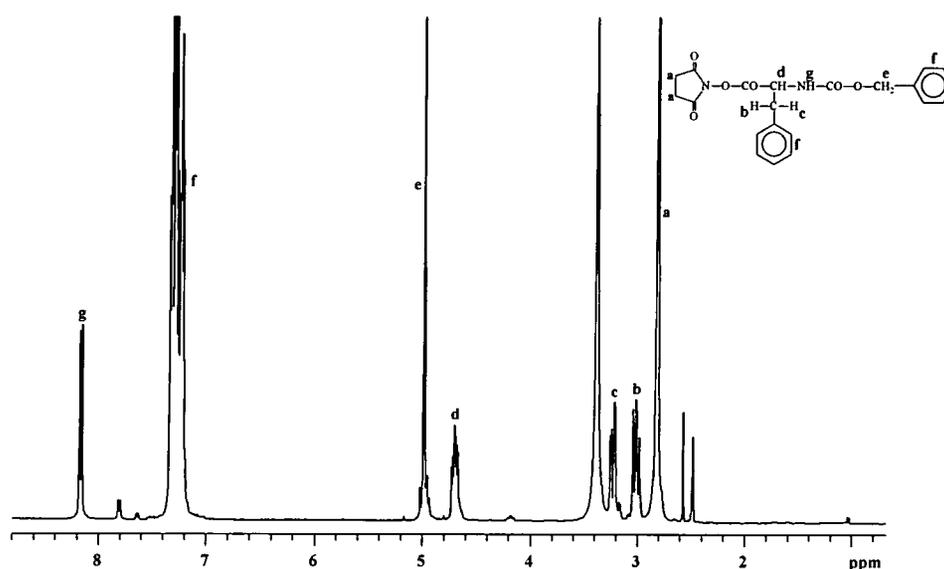
Figure 3.5 ^{1}H nmr spectra of CBZ-L-phenylalanine N-hydroxysuccinimide ester in DMSOd$_6$.

Figure 3.6 shows an expansion of the ^{1}H nmr spectrum of CBZ-L-phenylalanine N-hydroxysuccinimide ester in DMSOd$_6$ and CDCl$_3$.
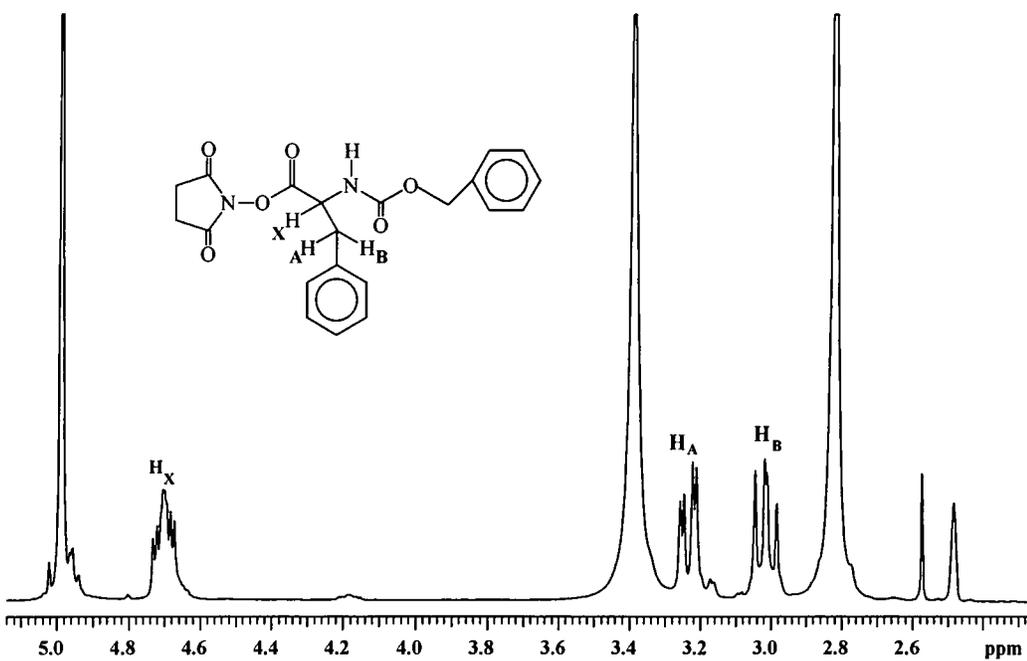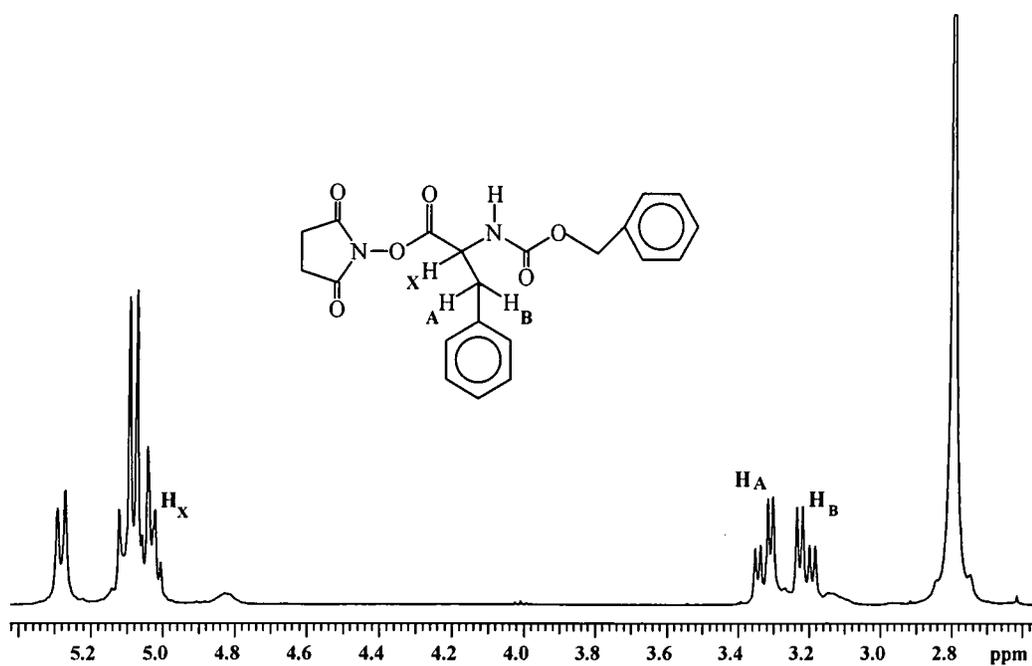
Figure 3.6. Expansion of the ¹H nmr spectrum of CBZ-L-phenylalanine N-hydroxysuccinimide ester in CDCl₃ (*top*) and DMSOd₆ (*bottom*).

The geminal hydrogen with the smaller coupling constant (A) which is closer in chemical shift to the X hydrogen is split into a doublet of doublets, whilst the geminal hydrogen furthest away from the X hydrogen with the largest coupling constant (B) is split into four signals of similar intensity observed in fine structure as an overlapping doublet of doublets (pseudo triplet). The signal at 8.17ppm (Figure 3.5) is due to the NH amide hydrogen (g) which has shifted from 5.28ppm when observed in $CDCl_3$.

3.5.3 Coupling of the amino acid N-hydroxysuccinimide activated esters to hexylamine and siloxysilane dendrimer wedges.

Acylation with N-hydroxysuccinimide esters[14] is well known and has been successfully achieved by following the method outlined by Meijer et al for the synthesis of their "dendritic box" structure.[15] The synthesis of the rigid chiral shell was performed through a critical end group modification of amine terminated poly(propyleneimine) dendrimers with the N-hydroxysuccinimide ester of a tert-butoxycarbonyl (t-BOC) protected amino acid in a dichloromethane triethylamine solution. The ^{1}H and ^{13}C nmr spectra of Si-*wedge*-phe-CBZ in $DMSOd_6$ are shown in Figures 3.7 and 3.8, the assignment of signals and structure has been confirmed by DEPT and Hetcor analysis. The sharp singlet at 2.79ppm in the ^{1}H spectrum (Figure 3.7) due to the CH_2 hydrogens of the hydroxysuccinimide group and the corresponding signals in the ^{13}C nmr spectra at 167.41ppm (hydroxysuccinimide C=O) and 25.45ppm (hydroxysuccinimide CH_2 hydrogens) are totally absent giving a good indication that a successful coupling reaction has occurred and that the eliminated

hydroxysuccinimide had been totally removed during work up. In the ^{1}H nmr

spectrum the large sharp singlet at 0.06ppm is due to the CH_3 hydrogens of the

siloxysilane core (1) and the signals at 0.37ppm (2), 1.36ppm (3), and the doublet

of multiplets at 2.95ppm and 3.06ppm (4), correspond to the three methylene

CH_2 groups of the propyl unit of the silane core. The geminal CH_2 hydrogens of

the amino acid residue (12) are seen at 2.73ppm and 2.90ppm and the methine

CH (6) at 4.19ppm. The singlet at 4.91ppm is due to the OCH_2 hydrogens of the

benzyl ester. Aromatic CH hydrogens are observed at 7.21ppm to 7.3ppm and

the doublet signal at 7.45ppm (7) and the triplet at 7.98ppm (5) have been

assigned as amide NH hydrogens.
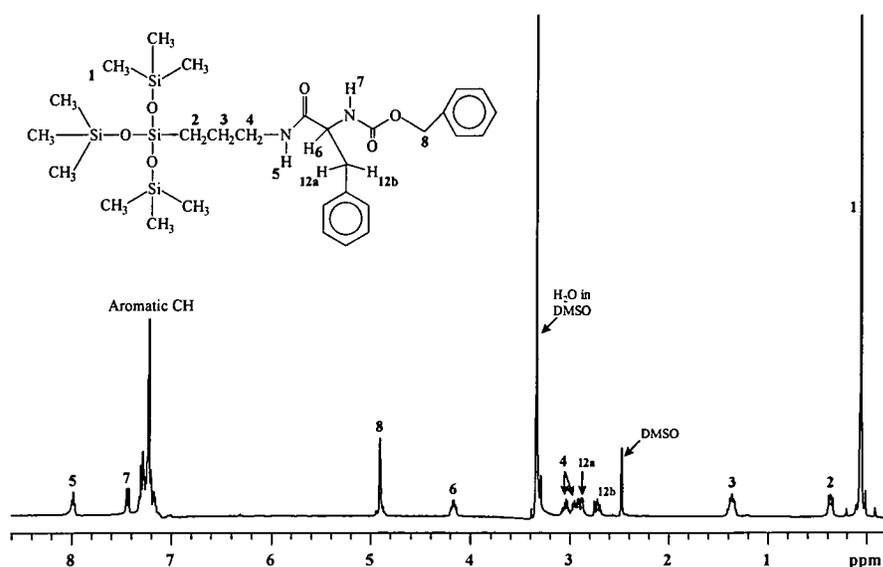
Figure 3.7. ^{1}H and nmr spectra of Si-*wedge*-phe-CBZ in DMSOd$_6$.
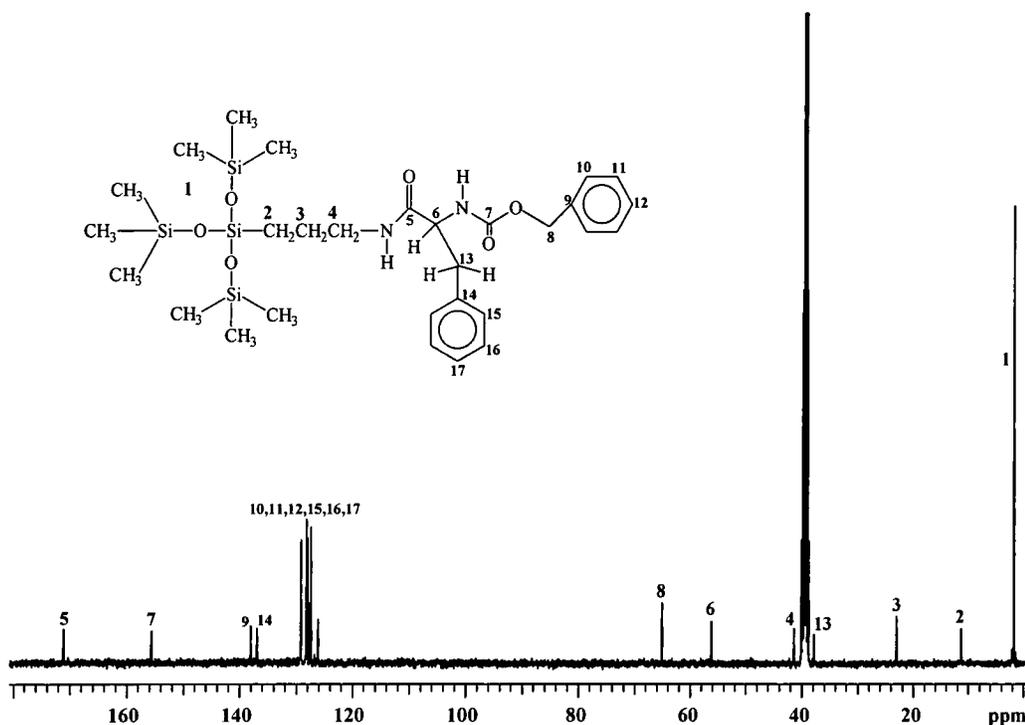
Figure 3.8 ^{13}C nmr spectra of Si-*wedge*-phe-CBZ in DMSOd$_6$.

The ^{13}C nmr (Figure 3.8) has been assigned with the aid of Hetcor and DEPT

analysis (see Appendices 2.3 and 2.4). The signal at 1.76ppm (1) (CH$_3$) and the

signals at 11.34ppm (2), 23.11ppm (3), and 41.42ppm (4) (CH$_2$) are observed in

the expected region and are assigned to the siloxysilane core and propyl residue.

The methylene (13) and methine (6) carbons of the amino acid residue are

observed at 37.89 and 56.25ppm, confirmed from DEPT and Hetcor analysis,

whilst the methylene carbon of the benzyl ester (8) is found at 65.14ppm.

Aromatic ortho, meta and para carbon signals are observed in the expected region

(126-129ppm) and the signals at 137.04 and 138.09ppm have been assigned to

ipso-aromatic carbons of the phenylalanine ring (14) and the benzyl ester (9)

respectively. The signal at 155.75ppm is due to the carbonyl carbon of the

benzyl ester (7), whilst the signal at 171.18ppm has been assigned to the carbonyl of the peptide bond (5).

3.5.4 Deprotection of the amino acid residue by Catalytic Transfer Hydrogenation (CTH).[9,10,11]

The characterisation of the fully deprotected amino acid modified dendrimer wedges is discussed in detail since these molecules are to be the probes for cellulose recognition (Chapter 4) which is the basis of the investigation in this thesis. Successful removal of the benzyloxycarbonyl group can be readily observed from the resultant ^{1}H and ^{13}C nmr spectra as shown for Si-*wedge*-phe in Figure 3.9. In the ^{1}H nmr spectra the singlet at 4.91ppm corresponding to the benzyl ester CH_2 hydrogens (Figure 3.7) is absent and a new broad peak at 1.92ppm (f) is observed due to the deprotected primary amine hydrogens of the amino acid. Complete loss of the protecting group can be further validated by integration of the aromatic CH signals (5H), confirming the presence of only one phenyl ring system, corresponding to the phenylalanine ring (i). All the other peaks are observed in the expected positions and are totally consistent with the assigned structure.
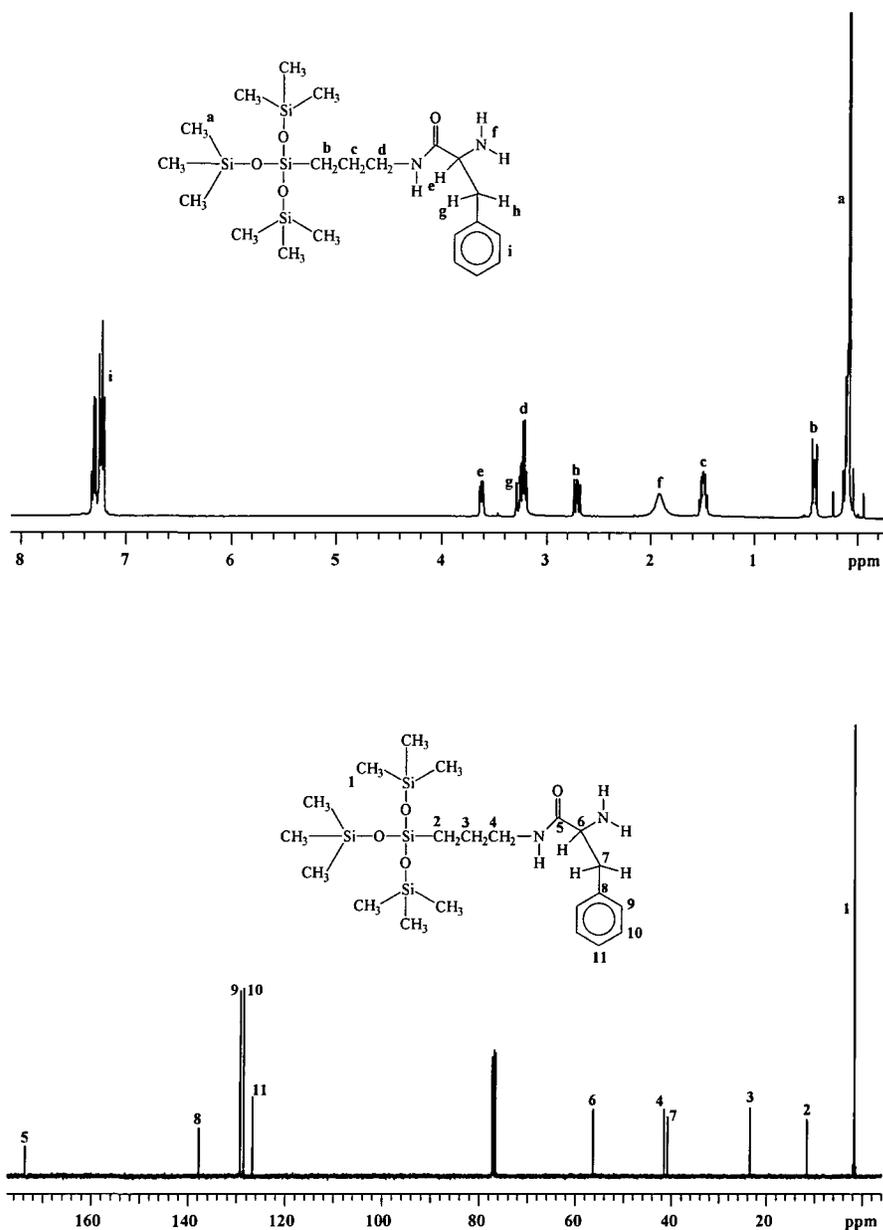
Figure 3.9 ^{1}H and ^{13}C nmr spectra of Si-*wedge*-phe in DMSOd$_6$.

In the ^{13}C nmr spectra deprotection is confirmed by the absence of the signals at

65.14ppm (benzyl ester CH$_2$), and the carbonyl signal at 155.75ppm (benzyl ester

C=O), whilst the presence of four aromatic signals confirms the presence of one

mono-substituted aromatic ring system. The signal at 40.95ppm (CDCl$_3$) or

41.16ppm (DMSOd$_6$) is shifted downfield from the expected region and has been

assigned to the CH_2 carbon of the amino acid (7), which has been confirmed from Hetcor and DEPT analysis. The remainder of the signals are observed in the expected region and totally consistent with the assigned structure.

The ^1H and ^{13}C nmr spectra of the amino acid terminated dendrimer wedges utilising hexylamine as the starting molecule exhibit certain similarities to the siloxysilane core amino acid dendrimer wedge described above. The major difference in the ^1H nmr spectra is in the upfield region from 0 to 4ppm. The ^1H and ^{13}C nmr spectra of Hex-*wedge*-phe$_2$ in DMSOd$_6$ is shown in Figure 3.10, assignment of signals to structure was confirmed with the aid of DEPT and Hetcor analysis. The triplet at 0.82ppm is due to the methyl hydrogens of hexylamine (a), whilst the broad singlet at 1.21ppm integrating to 6H (b,c,d) and the small overlapping broad singlet at 1.31ppm integrating to 2H (e), are due to the hexyl CH_2 hydrogens assigned by comparison with starting material. The multiplet centred at 1.41ppm (4H) was assigned to CH_2 hydrogens of the dendrimer wedge structure (h), whilst the multiplet at 2.24ppm (6H) is due to the CH_2 hydrogens next to the tertiary amine (g,f). The methylene and methine hydrogens of the amino acid residue are observed at 2.6, 2.86ppm (m) and 3.33ppm (k) respectively, as in analogous structures discussed above. The broad multiplet at 3.03ppm was assigned to dendrimer wedge CH_2 hydrogens adjacent to the secondary amine of the peptide bond (i). Aromatic (7.2ppm) (n,o,p) and amide peaks (7.8ppm) (j) are observed in the expected regions.
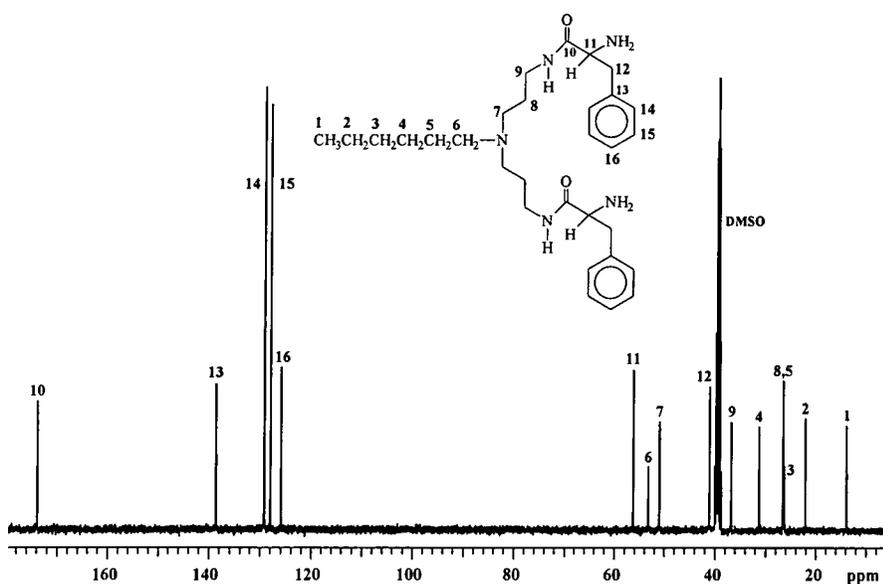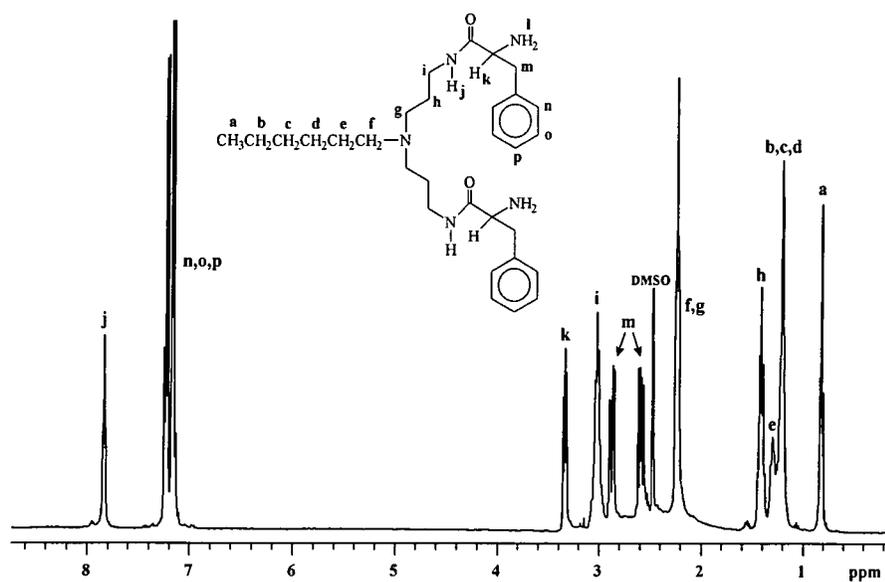
Figure 3.10. ^{1}H and ^{13}C nmr spectra of Hex-*wedge*-phe$_2$ in DMSOd$_6$.

The ^{13}C spectra was assigned by analogy with the related structures discussed above and with the help of Hetcor and DEPT analysis. The signal at 13.96ppm is due to the methyl carbon of hexylamine (1), whilst the signals at 22.17 (2), 26.42

(3), 31.30 (4), and 53.34ppm (6), due to hexyl CH_2 carbons, are observed in the expected region and have been assigned by comparison to starting material. The methylene signals of the dendrimer wedge structure (8) and the CH_2 carbon at position 5 of the hexyl group could only be assigned unambiguously from the corresponding Hetcor spectrum and overlap at 26.64ppm. The signal at 36.87ppm corresponds to the CH_2 carbons of the methylene groups next to secondary amine (9), whilst the signal at 51.05ppm is due to the CH_2 carbons adjacent to the tertiary amine (7). The methine CH (11) and methylene CH_2 (12) carbons of the phenylalanine residue are observed in the expected region with signals at 56.24 and 41.18ppm respectively. The aromatic region exibits signals with the correct chemical shift (126.05,128.03,129.25,138.67ppm) and the required number of carbon resonances for a mono-substituted phenyl ring as previously observed for the siloxysilane phenylalanine terminated structure. The signal at 173.92ppm has been assigned to the amide C=O of the peptide bond as observed in previous assignments of analogous structures.

The deprotected amino acid dendrimer wedges show characteristic signals in the aromatic regions of their ^{1}H and ^{13}C nmr spectra, possessing specific chemical shifts which are directly related to the type of terminal amino acid functionality present at the periphery of the wedge structure. Figure 3.11 shows an expansion of the aromatic region of the ^{1}H and ^{13}C nmr spectra corresponding to phenylalanine, tyrosine, and tryptophan modified dendrimer wedges. The splitting pattern for the phenylalanine ring is complicated due to 2nd order coupling effects.
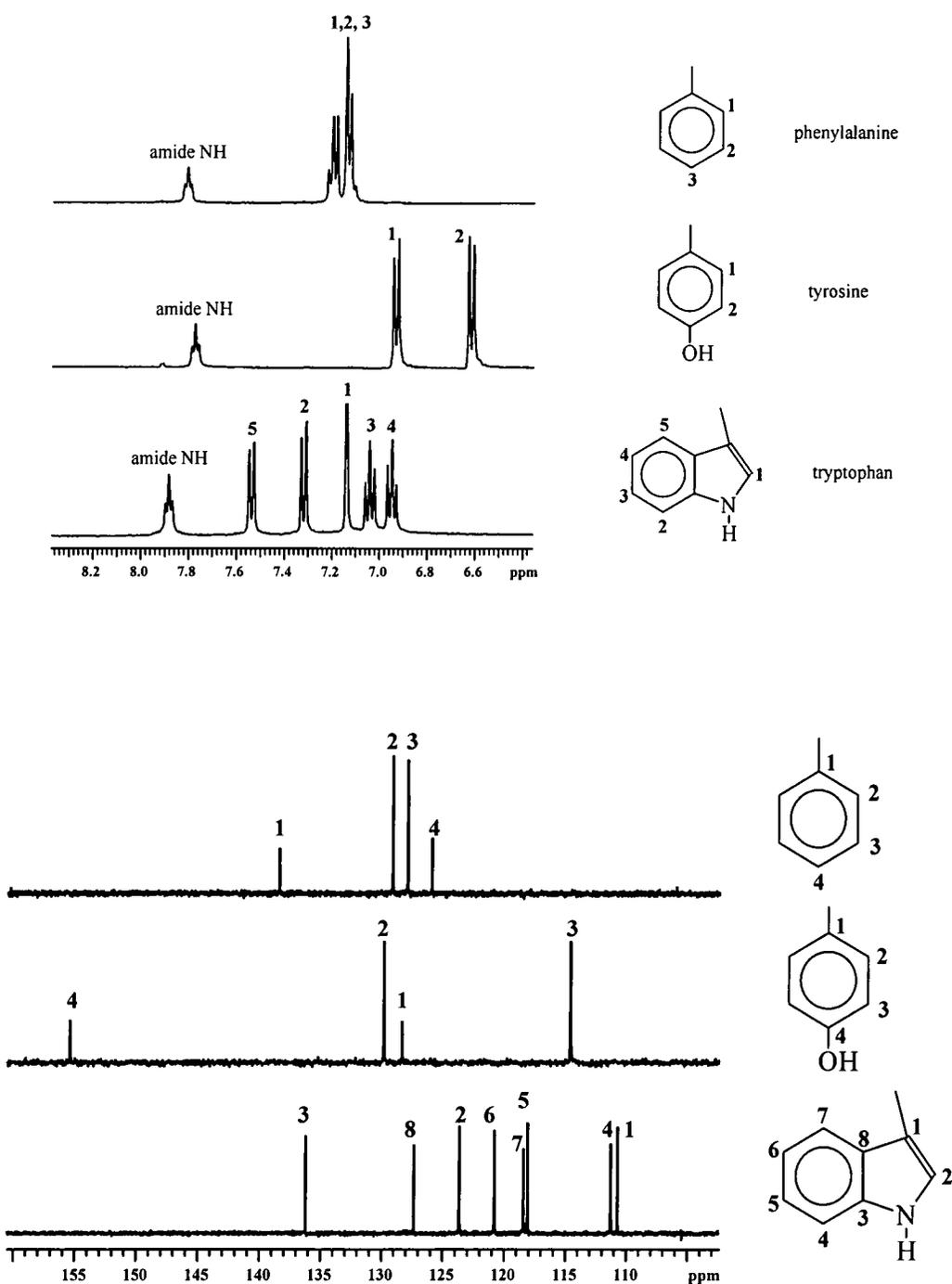
Figure 3.11. Expansion of the ^{1}H (*top*) and the ^{13}C (*bottom*) nmr spectra of the aromatic region of amino acid terminated dendrimer wedges.

As can be seen from the spectra reproduced in the above discussions and Appendix 2 the intermediates and the final amino acid terminated dendritic

wedges designed to be used as probes for cellulose surface recognition were produced in well characterised clean forms. It proved difficult to obtain good elemental analyses for several of the products possibly due to absorption of traces of water or solvent despite prolonged drying under vacuum. All the deprotected compounds produced gave single peaks in their MALDI-TOF mass spectra which corresponded to the expected molecular formulae.

3.6 Experimental

All organic reagents were purchased from Aldrich Chemical Co., except the benzyloxycarbonyl (CBZ) protected amino acids which were obtained from SIGMA, and were used without further purification. IR spectra were recorded using a Perkin-Elmer 1600 series FTIR. ^{1}H and ^{13}C nmr spectra were recorded using a Varian 400MHz spectrometer and were referenced to internal Me$_4$Si. Molecular weight determinations were recorded on a Kratos Kompact MALDI IV time of flight mass spectrometer using 2,5-dihydroxybenzoic acid (DHB) as the matrix. Chemical and Electron impact ionisation mass spectra were recorded using a VG Analytical Model 7070E mass spectrometer. Elemental analyses were performed using a Carlo-Elba-466 elemental analyser produced by Exeter Analytical Inc.

3.6.1 General Procedure for the synthesis of *N*-hydroxysuccinimide activated esters.
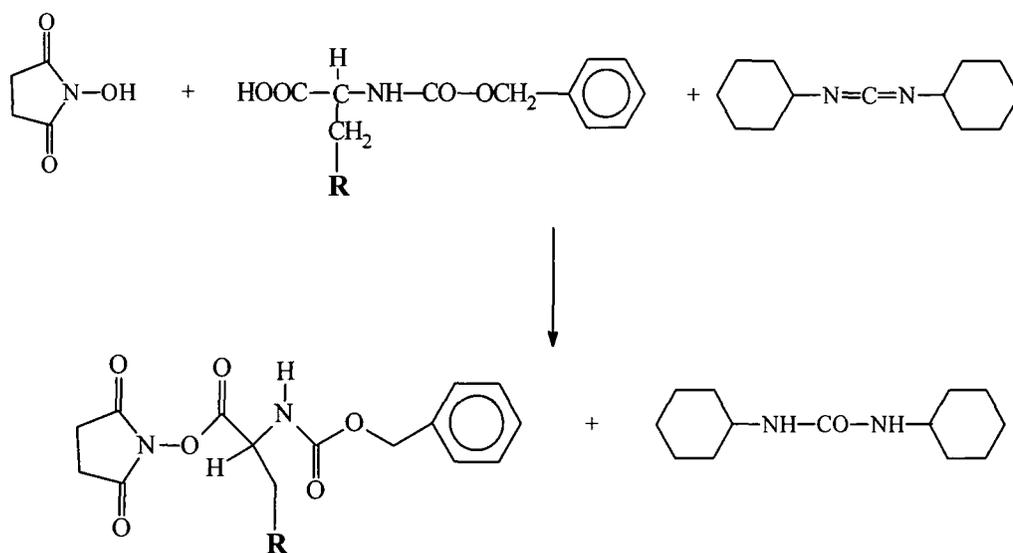
Reaction scheme.

Dicyclohexylcarbodiimide (DCCI) was added to a stirred solution of benzyloxycarbonyl-L-amino acid (2.00g) and N-hydroxysuccinimide (HOSu), (1:1:1 molar ratio DCCI:HOSu:amino acid) in dry 1,2-dimethoxymethane (35mls) in an ice-water cooling bath. The mixture was kept in the refrigerator (between 0°C and +5°C) overnight. The N,N'-dicyclohexylurea which precipitated was removed by filtration and the solvent evaporated *in vacuo*. The crude product was recrystallised twice from isopropanol affording the pure benzyloxycarbonyl-L-amino acid N-hydroxysuccinimide ester as a white crystalline solid. The products were all known products and their yields and characterisation details are recorded below, the spectra (Appendix 2) indicated that the products were obtained in a purity which was satisfactory for use in the next step.

3.6.1.1 Benzyloxycarbonyl-L-phenylalanine N-hydroxysuccinimide ester.
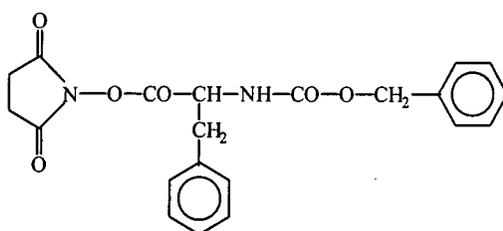
White crystalline solid (2.00g, 75%) m. pt. 133-135°C (lit.[16] 136-137.5); ^{1}H NMR (CDCl$_3$, 400 MHZ) : δ 2.79 (s, 4H, CH$_2$CON), 3.23,3.30 (dd, 2H, CH$_2$Ph) 5.04 (m, 1H, COCHNH), 5.09 (m, 2H, OCH$_2$Ph), 5.27 (d, 1H, amide N-**H**), 7.27-7.34 (10**H** aromatics); ^{13}C NMR (CDCl$_3$, 100MHZ) : 25.45 (**C**H$_2$CON), 37.81 (**C**H$_2$Ph), 52.87 (CO**C**HNH), 67.15 (O**C**H$_2$Ph), 127.34, 128.05, 128.14, 128.41, 128.63, 129.51 (aromatic **C**-H), 134.31, 135.84 (aromatic **C**), 155.26 (NH**C**OOCH$_2$), 167.41 (CH$_2$**C**ONO), 168.61 (**C**OCHNH).

3.6.1.2 Benzyloxycarbonyl-L-Tryptophan N-hydroxysuccinimide ester.
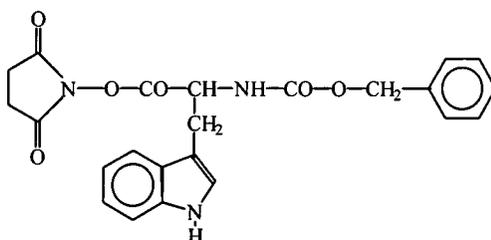
White crystalline solid (2.10g, 81%); ^{1}H NMR (CDCl$_3$, 400 MHZ) : δ 2.64 (s, 4H, CH$_2$CON), 3.40,3.49 (dd, 2H, CH$_2$Ph) 5.05 (m, 1H, COCHNH), 5.10 (m, 2H, OCH$_2$Ph), 5.44 (d, 1H, amide N-**H**), 7.08-7.56 (10**H** aromatics), 8.43 (s,1H, N-**H** indole ring) ; ^{13}C NMR (CDCl$_3$, 100MHZ) : 25.38 (**C**H$_2$CON), 27.60 (**C**H$_2$-indole), 53.39 (CO**C**HNH), 67.11 (O**C**H$_2$Ph), 128.09,128.12, 128.41 (aromatic **C**-H), 135.92 (aromatic **C**), 155.54 (NH**C**OOCH$_2$), 167.72 (CH$_2$**C**ONO), 168.92 (**C**OCHNH).
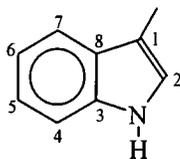
indole ring *C*-H: 2 (124.24), 4 (111.30), 5 (118.24), 6 (122.01), 7 (119.69)

indole ring aromatic: 1 (108.01), 3 (135.96), 8 (127.70).

3.6.1.3 *Benzyloxycarbonyl*-L-Tyrosine -σ-*benzyl* N-hydroxysuccinimide ester.
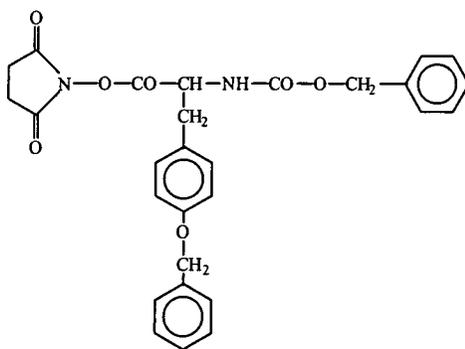
White crystalline solid (1.089g, 88%); ^{1}H NMR (DMSO$_{d6}$, 400 MHZ) : δ 2.79 (s, 4H, CH_2CON), 3.23,3.30 (dd, 2H, CH_2Ph) 5.04 (m, 1H, COCHNH), 5.09 (m, 2H, OCH_2Ph), 5.27 (d, 1H, amide N-H), 7.27-7.34 (10H aromatics) ; ^{13}C NMR (DMSO$_{d6}$, 100MHZ) : 25.51 (CH$_2$CON), 35.52 (CH$_2$Ph), 53.95 (COCHNH), 65.15 (OCH$_2$Ph), 69.14 (PhOCH$_2$Ph), 114.55,127.53, 127.68, 127.81, 128.33, 128.43, 128.50 (aromatic *C*-H), 130.38, 136.69, 137.14 (aromatic *C*), 155.30 (aromatic *C*-O), 157.28 (NH*C*OOCH$_2$), 168.18 (CH$_2$*C*ONO), 169.98 (*C*OCHNH).

3.6.2 General procedures for coupling amino acid N-hydroxysuccinimide (i) and

p-nitrophenyl activated esters (ii) to various generations of amino terminated

dendrimer wedges derived from hexylamine and siloxysilane.
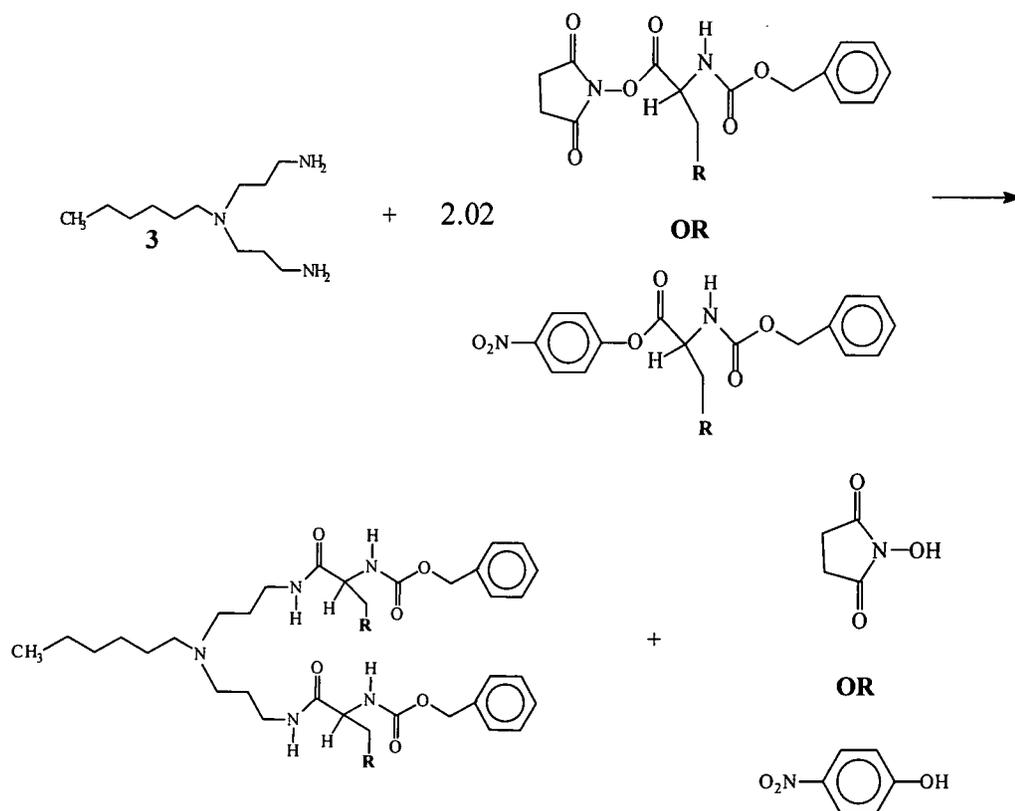
Reaction scheme.

i)   The N-hydroxysuccinimide activated ester (1.01equiv. per amine end

group)   was added to a solution of the dendrimer wedge (200mg) and

triethylamine (100mg) in dichloromethane (25mls) in a 100ml round bottomed

flask. The solution was stirred overnight at room temperature using a magnetic

stirrer bar. The solution was diluted with dichloromethane (50mls) and washed

with distilled water (3 x 30mls), and then a saturated solution of sodium

carbonate (3 x 30mls). The organic layer was dried over sodium sulphate,

filtered and the solvent removed under vacuum affording the required product without further purification.

ii) The *p*-nitrophenol active ester (1.1equiv. per amine end group) was added to a solution of the dendrimer wedge (250mg) in anhydrous chloroform (20mls). The clear yellow solution was allowed to stand at room temperature overnight. After removal of the solvent *in vacuo,* ethyl acetate (40mls) and water (10mls) were added to the residue. The organic layer was then washed with water (10mls), N NH$_4$OH (10mls), water (10mls), N HCl (10mls) and water again (10mls). The required pure product was recovered after drying the solution over sodium sulphate and removal of the solvent under vacuum.

All the derivatives prepared by the routes described above are new compounds and their structures, trivial names, yields and spectroscopic characterisation details are recorded below. The spectra (Appendix 2) showed that the products were sufficiently pure for use in the next step (N-deprotection) and the final deprotected species were fully characterised (C,H,N, molecular weight and spectroscopy), see later.

3.6.2.1 Hexylamine benzyloxycarbonyl-L-phenylalanine terminated wedges.

3.6.2.1.1 Hex-*wedge*-Phe$_2$ (CBZ)$_2$.
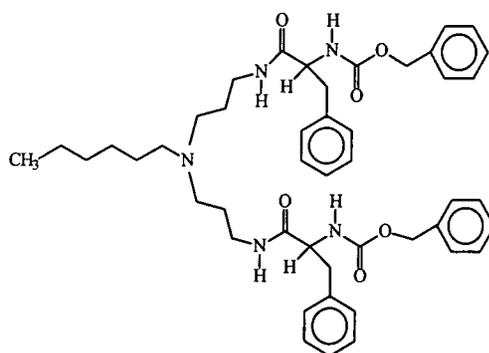
Sticky white solid (0.51g, 94%); ^{1}H nmr (DMSOd$_6$, 400 MHZ): δ 0.80 (t, 3H, methyl), 1.21 (s, 6H, CH$_3$CH$_2$CH$_2$CH$_2$CH$_2$CH$_2$N) 1.32 (b, 2H, CH$_3$CH$_2$CH$_2$CH$_2$CH$_2$CH$_2$N), 1.45 (m, 4H, NCH$_2$CH$_2$CH$_2$N), 2.28 (b, 6H, CH$_2$NCH$_2$), 2.77+2.91 (t,dd, 2H+2H, CH$_2$Ph) 3.02 (b, 4H, NCH$_2$CH$_2$CH$_2$N), 4.20 (b, 2H, COCHCH$_2$), 4.93 (s, 4H, OCH$_2$Ph), 7.16-7.32 (m, 20H, aromatic C-H), 7.47 (d, 2H, CHNHCOOPh), 7.97 (b, 2H, CH2NHCO) ; ^{13}C NMR (DMSOd$_6$,100MHZ): 14.27 (methyl), 22.51 (CH$_3$CH2), 26.79 (CH$_3$CH$_2$CH$_2$CH$_2$CH$_2$CH$_2$N), 26.91 (CH$_3$CH$_2$CH$_2$CH$_2$CH$_2$CH$_2$N), 27.00 (NCH$_2$CH$_2$CH$_2$N) 31.63 (CH$_3$CH$_2$CH$_2$CH$_2$CH$_2$CH$_2$N), 37.41 (NCH$_2$CH$_2$CH$_2$N), 38.09 (CHCH2Ph), 51.33 (NCH$_2$CH$_2$CH$_2$N), 53.72 (CH$_2$N), 56.60 (COCHNH), 65.48 (OCH2Ph), 126.53,127.73,127.97,128.33,128.58,129.49, (aromatic C-H), 137.34,138.41 (ipso-aromatic), 156.10 (NHCOOCH$_2$Ph), 171.47 (NHCOCHCH$_2$Ph).

3.6.2.1.2 Hex-*wedge*-Phe₄ (CBZ)₄.
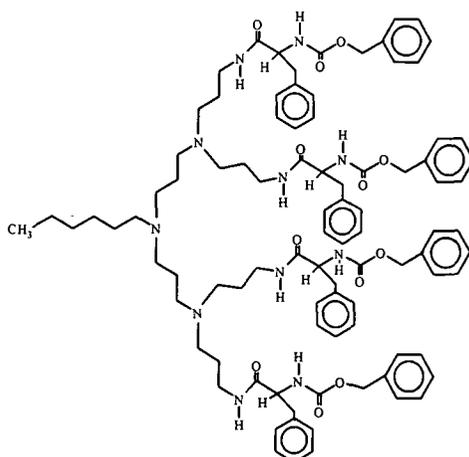
White crystalline solid (0.36g, 68%); MS M+ ion= 1557.82 determined by

MALDI TOF mass spectrometry, M, 1568.6, ^{1}H nmr (DMSOd₆, 400 MHZ): δ

0.79 (t, 3H, methyl), 1.17 (s, 6H, $CH_3CH_2CH_2CH_2CH_2CH_2N$) 1.32 (b, 2H,

$CH_3CH_2CH_2CH_2CH_2CH_2N$), 1.44 (b, 12H, $NCH_2CH_2CH_2N$), 2.28 (b, 18

CH_2NCH_2), 2.74+2.91 (t,dd, 4H+4H, CH_2Ph) 3.02 (b, 8H, $NCH_2CH_2CH_2N$),

4.19 (b, 4H, $COCHCH_2$), 4.92 (s, 8H, OCH_2Ph), 7.17-7.29 (m, 40H, aromatic C-

H), 7.47 (d, 4H, CHNHCOOPh), 7.97 (b, 4H, CH_2NHCO);

^{13}C nmr (DMSOd₆,100MHZ): 13.95 (methyl), 22.17 (CH_3CH2), 26.56

($CH_3CH_2CH_2CH_2CH_2CH_2N$), 26.65

($CH_3CH_2CH_2CH_2CH_2CH_2N+NCH_2CH_2CH_2N$), 31.27

($CH_3CH_2CH_2CH_2CH_2CH_2N$), 37.13 ($NCH_2CH_2CH_2N$), 37.81 ($CHCH2Ph$), 51.00

($NCH_2CH_2CH_2N$), 51.65 (CH_2N), 56.30 ($COCHNH$), 65.20 ($OCH2Ph$),

126.24,127.43,127.68,127.79,128.28,129.19, (aromatic C-H), 137.03,138.08

(ipso-aromatics), 155.80 ($NHCOOCH_2Ph$), 171.18 ($NHCOCHCH_2Ph$).

3.6.2.1.3 Hex-*wedge*-Phe$_8$ (CBZ)$_8$.
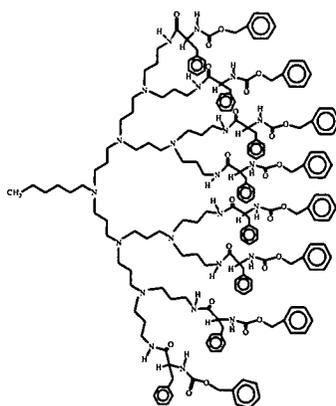
White crystalline solid (0.36g, 69%); ^{1}H NMR (DMSOd$_6$, 400 MHZ): δ 0.79 (t,

3H, methyl), 1.18 (b, 6H, CH$_3$CH$_2$CH$_2$CH$_2$CH$_2$CH$_2$N) 1.32 (b, 2H,

CH$_3$CH$_2$CH$_2$CH$_2$CH$_2$CH$_2$N), 1.43 (b, 28H, NCH$_2$CH$_2$CH$_2$N), 2.27 (b, 42H

CH$_2$NCH$_2$), 2.74+2.91 (t,dd, 8H+8H, CH$_2$Ph) 3.02 (b, 16H, NCH$_2$CH$_2$CH$_2$N),

4.19 (b, 8H, COCHCH$_2$), 4.92 (s, 16H, OCH$_2$Ph), 7.12-7.27 (m, 80H, aromatic

C-H), 7.47 (d, 8H, CHNHCOOPh), 7.97 (b, 8H, CH2NHCO);

^{13}C NMR (DMSOd$_6$,100MHZ): 14.26 (methyl), 22.48 (CH$_3$CH2), 26.89

(CH$_3$CH$_2$CH$_2$CH$_2$CH$_2$CH$_2$N+CH$_3$CH$_2$CH$_2$CH$_2$CH$_2$CH$_2$N+NCH$_2$CH$_2$CH$_2$N) 31.60

(CH$_3$CH$_2$CH$_2$CH$_2$CH$_2$CH$_2$N), 37.43 (NCH$_2$CH$_2$CH$_2$N), 38.12 (CHCH2Ph), 51.35

(NCH$_2$CH$_2$CH$_2$N), 51.99 (CH$_2$N), 56.59 (COCHNH), 65.49 (OCH2Ph),

126.53,127.72,127.96,128.32,128.57,129.48, (aromatic C-H), 137.32,138.37

(ipso-aromatics), 156.09 (NHCOOCH$_2$Ph), 171.46 (NHCOCHCH$_2$Ph).

3.6.2.2 Hexylamine benzyloxycarbonyl-L-tryptophan terminated wedges.

3.6.2.2.1 Hex-*wedge*-trp$_2$ (CBZ)$_2$.
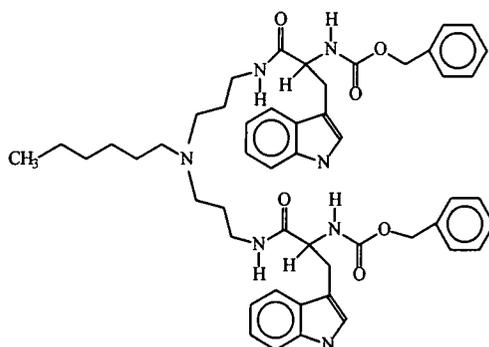
White crystalline solid (0.40g, 68%); ^{1}H NMR (DMSO$_{d6}$, 400 MHZ): δ 0.83 (t, 3H, methyl), 1.22 (b, 6H, CH$_3$CH$_2$CH$_2$CH$_2$CH$_2$CH$_2$N) 1.30 (b, 2H, CH$_3$CH$_2$CH$_2$CH$_2$CH$_2$CH$_2$N), 1.44 (m, 4H, NCH$_2$CH$_2$CH$_2$N), 2.25 (b, 6H, CH$_3$CH$_2$CH$_2$CH$_2$CH$_2$CH$_2$NCH$_2$), 2.85+3.10 (t+m, 2H+2H, CH$_2$-indole) 3.10 (b, 4H, NCH$_2$CH$_2$CH$_2$N), 4.21 (m, 2H, COCHCH$_2$-indole), 4.95 (s, 4H, COCHCH$_2$Ph), 7.2-7.4 (m, 10H + 2H, aromatic C-**H** + indole C-**H** (3),) 7.97 (t, 2H, NCH$_2$CH$_2$CH$_2$N**H**),

indole ring C-**H**, 1 (s, 2H, 7.14), 4 (t, 2H, 6.95), 5 (t, 2H, 7.05), 6 (d, 2H, 7.56).

indole ring N-**H**, 2 (s, 2H, 10.82).

^{13}C NMR (DMSO$_{d6}$, 100MHZ) : 13.96 (methyl), 22.20 (CH$_3$CH2), 26.47 (CH$_3$CH$_2$CH$_2$CH$_2$CH$_2$CH$_2$N), 26.54 (CH$_3$CH$_2$CH$_2$CH$_2$CH$_2$CH$_2$N), 26.70 (NCH$_2$CH$_2$CH$_2$N), 31.30 (CH$_3$CH$_2$CH$_2$CH$_2$CH$_2$CH$_2$N+CH$_2$-indole), 37.17 (NCH$_2$CH$_2$CH$_2$N), 51.02 (NCH$_2$CH$_2$CH$_2$N), 53.40 (CH$_3$CH$_2$CH$_2$CH$_2$CH$_2$CH$_2$N),

55.40 (CO*C*HCH$_2$-indole), 65.20 (CO*C*H$_2$Ph), 127.25,127.46,128.29 (aromatic

C-H), 137.01 (ipso-aromatic), 155.43 (NH*C*OOCH$_2$Ph), 171.55 (NH*C*OCHCH$_2$-

indole).
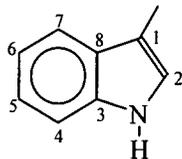
indole ring *C*-H, 2 (123.74), 4 (111.28), 5 (118.16), 6 (120.83), 7 (118.49).

indole ring aromatic, 1 (110.21), 3 (136.07), 8 (127.67).

3.6.2.2 Hex-*wedge*-trp$_4$ (CBZ)$_4$.
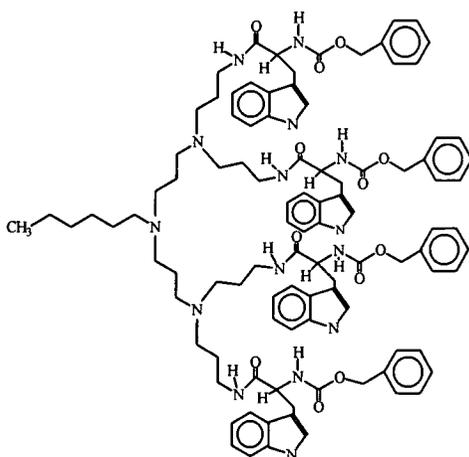
White crystalline solid (0.36g, 62%); ^{1}H NMR (DMSO$_{d6}$, 400 MHZ): δ 0.83 (t,

3H, methyl), 1.22 (b, 6H, CH$_3$CH$_2$CH$_2$CH$_2$CH$_2$CH$_2$N) 1.30 (b, 2H,

CH$_3$CH$_2$CH$_2$CH$_2$CH$_2$CH$_2$N), 1.44 (m, 4H, NCH$_2$CH$_2$CH$_2$N), 2.25 (b, 6H,

CH$_3$CH$_2$CH$_2$CH$_2$CH$_2$CH$_2$NCH$_2$), 2.85+3.10 (t+m, 2H+2H, CH$_2$-indole) 3.10 (b,

4H, NCH$_2$CH$_2$CH$_2$N), 4.21 (m, 2H, COCHCH$_2$-indole), 4.95 (s, 4H,

COCHCH$_2$Ph), 7.2-7.4 (m, 10H + 2H, aromatic C-**H** + indole C-**H** (3),) 7.97 (t,

2H, NCH$_2$CH$_2$CH$_2$N**H**),

indole ring C-**H**, 1 (s, 2H, 7.14), 4 (t, 2H, 6.95), 5 (t, 2H, 7.05), 6 (d, 2H, 7.56).

indole ring N-**H**, 2 (s, 2H, 10.82).

^{13}C NMR (DMSO$_{d6}$, 100MHZ) : 13.93 (methyl), 22.14 (CH$_3$*C*H2), 26.51

(CH$_3$CH$_2$*C*H$_2$CH$_2$CH$_2$CH$_2$N),26.63(CH$_3$CH$_2$CH$_2$CH$_2$*C*H$_2$CH$_2$N+N*C*H$_2$CH$_2$CH$_2$N)

, 31.24 (CH$_3$CH$_2$CH$_2$*C*H$_2$CH$_2$CH$_2$N+CH$_2$-indole), 37.19 (NCH$_2$CH$_2$*C*H$_2$N), 50.98

(N*C*H$_2$CH$_2$CH$_2$N), 51.64 (CH$_3$CH$_2$CH$_2$CH$_2$CH$_2$*C*H$_2$N), 55.61 (CO*C*HCH$_2$-

indole), 65.21 (CO*C*H$_2$Ph), 127.25,127.46,128.29 (aromatic C-H), 136.98 (ipso-

aromatic), 155.77 (NH*C*OOCH$_2$Ph), 171.60 (NH*C*OCHCH$_2$-indole).
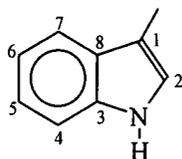
indole ring *C*-H, 2 (123.73), 4 (111.27), 5 (118.15), 6 (120.81), 7 (118.49).

indole ring aromatic, 1 (110.21), 3 (136.06), 8 (127.65).

3.6.2.3 Hexylamine benzyloxycarbonyl-*o-benzyl*-L-tyrosine terminated wedges.

3.6.2.3.1 Hex-*wedge*-tyr₂ *(o-benzyl)*₂(CBZ)₂.
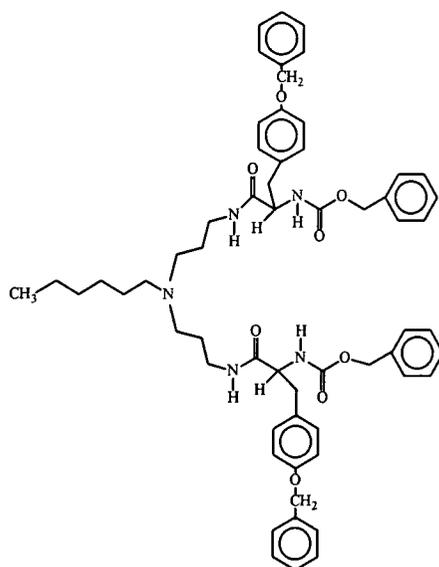
White crystalline solid (0.62g, 71%); ¹H NMR (DMSO$_{d6}$, 400 MHZ) : δ 0.82 (t, 3H, methyl), 1.25 (b, 6H, CH₃CH₂CH₂CH₂CH₂CH₂N) 1.57 (m, 2H, CH₃CH₂CH₂CH₂CH₂CH₂N), 1.76 (m, 4H, NCH₂CH₂CH₂N), 2.65+2.78 (m, 2H+2H, CH₂Ph), 2.90 (b, 6H, CH₂NCH₂), 3.15 (m, 4H, NCH₂CH₂CH₂N), 4.12 (m, 2H, COCHCH₂), 4.94 (m, 4H+4H, OOCH₂Ph+OCH₂Ph) 6.66-8.15 (28H, aromatic C-**H**) 8.25 (s, 2H, NCH₂CH₂CH₂N**H**); ¹³C NMR (DMSO$_{d6}$, 100MHZ) : 13.84 (methyl), 21.97 (CH₃**C**H2), 25.79 (CH₃CH₂**C**H₂CH₂CH₂CH₂N) 30.77 (CH₃CH₂CH₂CH₂**C**H₂CH₂N+NCH₂**C**H₂CH₂N+CH₃CH₂CH₂**C**H₂CH₂CH₂N), 35.78 (NCH₂CH₂**C**H₂N), 36.78 (**C**H2Ph), 49.64 (N**C**H₂CH₂CH₂N), 52.36 (CH₃CH₂**C**H₂CH₂CH₂**C**H₂N), 56.82 (CO**C**HCH₂), 65.18 (OO**C**H₂Ph+O**C**H₂Ph), 114.89,127.43,127.63,128.29,130.09, (aromatic C-H), 128.33,137.01,155.81, (aromatic), 155.87 (**C**OOCH2Ph), 171.88 (NH**C**OCHNH).

3.6.2.4 Siloxysilane benzyloxycarbonyl-L-phenylalanine terminated wedges.

3.6.2.4.1 Si-*wedge*-phe-(CBZ).
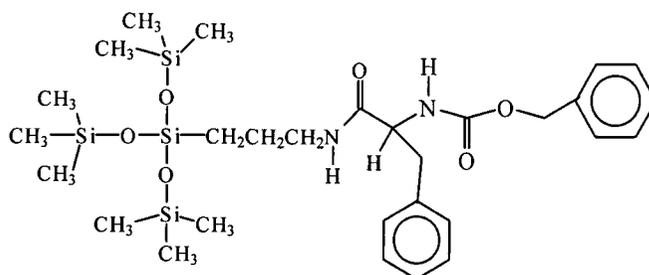
Clear oil (0.486g, 90%); ^{1}H NMR (DMSOd$_6$, 400 MHZ) : δ 0.06 (s, 27H,

CH$_3$Si), 0.37 (t, 2H, Si-CH$_2$) 1.36 (m, 2H, Si-CH$_2$CH$_2$CH$_2$N), 2.73+2.90 (m,

1H+1H CH$_2$Ph), 2.95,3.06 (m, 1H+1H Si-CH$_2$CH$_2$CH$_2$N) 4.19 (m, 1H,

CHCH$_2$Ph), 4.91 (OCH$_2$Ph), 7.20-7.30 (m, 10H, aromatic C-**H**), 7.45 (d, 1H,

CHNHCO) 7.98 (t, 1H, NCH$_2$CH$_2$CH$_2$NH) ; ^{13}C NMR (DMSOd$_6$, 100MHZ) :

1.76 (*C*H$_3$Si), 11.34 (Si-*C*H$_2$), 23.11 (Si-CH$_2$*C*H$_2$CH$_2$N), 37.89 (*C*H$_2$Ph), 41.42

(Si-CH$_2$CH$_2$*C*H$_2$N), 56.25 (*C*HCH$_2$Ph), 65.14 (CO*C*H$_2$Ph),

126.22,127.43,127.66,128.01,128.28,129.16 (aromatic C-H), 137.04,138.09

(aromatic), 155.75 (*C*OOCH$_2$Ph), 171.18 (NH*C*OCHCH$_2$Ph).

3.6.2.4.2 Si-*wedge*-phe₂ (CBZ)₂.
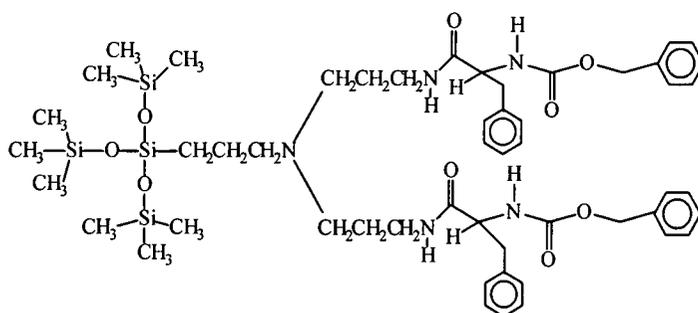
Off white waxy solid (0.36g, 82%); ^{1}H NMR (DMSOd$_6$, 400 MHZ) : δ 0.06 (s, 27H, CH$_3$Si), 0.37 (t, 2H, Si-CH$_2$) 1.36 (m, 2H, Si-CH$_2$CH$_2$CH$_2$N), 1.45 (b, 4H, NCH$_2$CH$_2$CH$_2$N), 2.28 (b, 6H, CH$_2$NCH$_2$), 2.75+2.92 (m, 2H+2H CH$_2$Ph), 2.95,3.06 (m, 2H+2H Si-CH$_2$CH$_2$CH$_2$N) 4.19 (m, 2H, CHCH$_2$Ph), 4.93 (OCH$_2$Ph), 7.20-7.30 (m, 20H, aromatic C-H), 7.45 (d, 2H, CHNHCO) 7.98 (b, 2H, NCH$_2$CH$_2$CH$_2$NH); ^{13}C NMR (DMSOd$_6$, 100MHZ) : 1.76 (CH$_3$Si), 11.48 (Si-CH$_2$), 20.18 (Si-CH$_2$CH$_2$CH$_2$N), 26.74 (NCH$_2$CH$_2$CH$_2$N), 37.12 (NCH$_2$CH$_2$CH$_2$N), 37.82 (CH$_2$Ph), 51.06 (CH$_2$NCH$_2$), 56.28 (CHCH$_2$Ph), 65.19 (COCH$_2$Ph), 126.22,127.43,127.66,128.01,128.28,129.20 (aromatic C-H), 137.04,138.08 (aromatic), 155.79 (COOCH$_2$Ph), 171.14 (NHCOCHCH$_2$Ph).

### 3.6.2.4.3 Si-*wedge*-phe₄ (CBZ)₄.
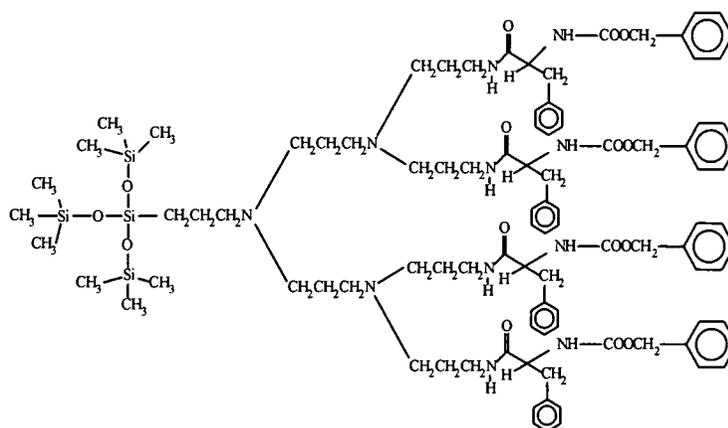
Off white waxy solid (0.40g, 76%); ¹H NMR (DMSOd₆, 400 MHZ) : δ 0.05 (s, 27H, CH₃Si), 0.34 (t, 2H, Si-CH₂) 1.43 (b, 2H, Si-CH₂CH₂CH₂N + 12H, NCH₂CH₂CH₂N), 2.28 (b, 18H, CH₂NCH₂), 2.74+2.92 (t+dd, 4H+4H CH₂Ph), 3.00-3.05 (m, 4H+4H NCH₂CH₂CH₂N) 4.19 (m, 4H, CHCH₂Ph), 4.92 (t, 8H, OCH₂Ph), 7.21-7.31 (m, 40H, aromatic C-H), 7.47 (d, 4H, CHNHCO) 7.97 (b, 4H, NCH₂CH₂CH₂NH); ¹³C NMR (DMSOd₆, 100MHZ) : 1.77 (*C*H₃Si), 11.48 (Si-*C*H₂), 20.18 (Si-CH₂*C*H₂CH₂N), 26.59 (NCH₂*C*H₂CH₂N), 30.72 (NCH₂*C*H₂CH₂NH) 37.12 (NCH₂CH₂*C*H₂NH), 37.82 (*C*H₂Ph), 51.01 (N*C*H₂CH₂CH₂NH), 51.95 (*C*H₂N*C*H₂ *C*H₂CH₂N), 56.28 (*C*HCH₂Ph), 65.18 (CO*C*H₂Ph), 126.22,127.43,127.66,128.02,128.27,129.19 (aromatic C-H), 137.04,138.09 (aromatic), 155.79 (*C*OOCH₂Ph), 171.16 (NH*C*OCHCH₂Ph).

3.6.2.5 Siloxysilane benzyloxycarbonyl-L-tryptophan terminated wedges.

3.6.2.5.1 Si-*wedge*-trp (CBZ).
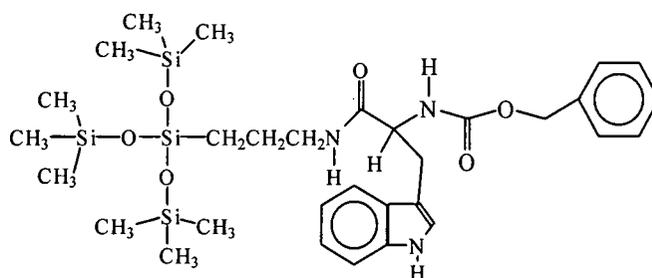
Clear oil (0.45g, 79%); ^{1}H NMR (DMSO$_{d6}$, 400 MHZ) : δ 0.08 (s, 27H, CH$_3$Si),

0.41 (t, 2H, Si-CH$_2$) 1.42 (m, 2H, Si-CH$_2$CH$_2$CH$_2$N), 2.92+3.02 (m, 1H+1H

CH$_2$-indole), 3.06 (m, 2H Si-CH$_2$CH$_2$CH$_2$N) 3.31 (b, 1H, CHCH$_2$-indole), 4.92

(s, 2H, OCH$_2$Ph), 6.94-7.62 (5H, indole C-**H**), 8.04 (t, 1H, amide N-**H**); ^{13}C

NMR (DMSO$_{d6}$, 100MHZ) : 1.71 (*C*H$_3$Si), 11.33 (Si-*C*H$_2$), 23.13 (Si-

CH$_2$*C*H$_2$CH$_2$N), 28.09 (*C*H$_2$-indole), 41.17 (Si-CH$_2$CH$_2$*C*H$_2$N), 55.52

(CO*C*HCH2), 65.12 (O*C*H$_2$Ph), 127.41,127.62,128.25 (aromatic C-H), 137.01

(ipso-aromatic), 155.74 (*C*OOCH2Ph) 171.69 (COCHCH$_2$-indole).
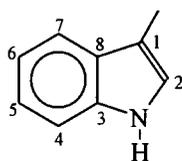

indole ring *C*-H, 2 (123.71), 4 (111.26), 5 (118.10), 6 (120.79), 7 (118.48).

indole ring aromatic, 1 (110.28), 3 (136.04), 8 (127.20).

3.6.2.6 Siloxysilane benzyloxycarbonyl-*o-benzyl*-L-tyrosine terminated wedges.

3.6.2.6.1 Si-*wedge*-tyr-*o-benzyl*-(CBZ).
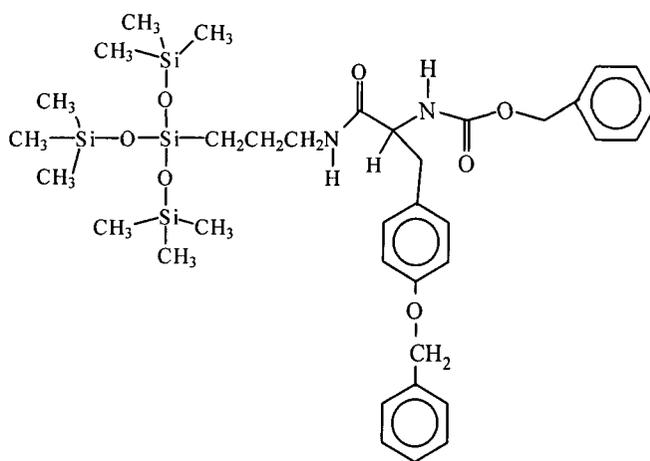
Off white waxy solid (0.46g, 88%); ^{1}H NMR (DMSOd$_6$, 400 MHZ) : δ 0.07 (s, 27H, CH$_3$Si), 0.44 (t, 2H, Si-CH$_2$) 1.42 (m, 2H, Si-CH$_2$CH$_2$CH$_2$N), 2.67+2.85 (t+dd, 1H+1H CH$_2$Ph), 3.00,3.01 (m, 1H+1H Si-CH$_2$CH$_2$CH$_2$N) 4.17 (m, 1H, CHCH$_2$Ph), 4.98 (s, 2H, COOCH$_2$Ph), 5.03 (s, 2H, PhOCH$_2$Ph), 6.88-7.41 (14H, aromatic C-H), 8.02 (s, 1H, Si- CH$_2$CH$_2$CH$_2$NH); ^{13}C NMR (DMSOd$_6$, 100MHZ): 2.05 (CH$_3$Si), 11.66 (Si-CH$_2$), 23.46 (Si-CH$_2$CH$_2$CH$_2$N), 37.37 (CH$_2$Ph), 41.72 (Si-CH$_2$CH$_2$CH$_2$N), 56.80 (CHCH2Ph), 65.42 (COOCH$_2$Ph), 69.43(PhOCH$_2$Ph),114.59,127.73,127.94,128.07,128.55,128.71,130.49,137.38,1 37.51 (aromatic), 156.07 (aromatic C-O), 157.22 (COOCH$_2$Ph), 171.61 (NHCOCHNH).

3.6.3 General procedure for deprotection of CBZ-amino acids by Catalytic Transfer Hydrogenation (CTH).
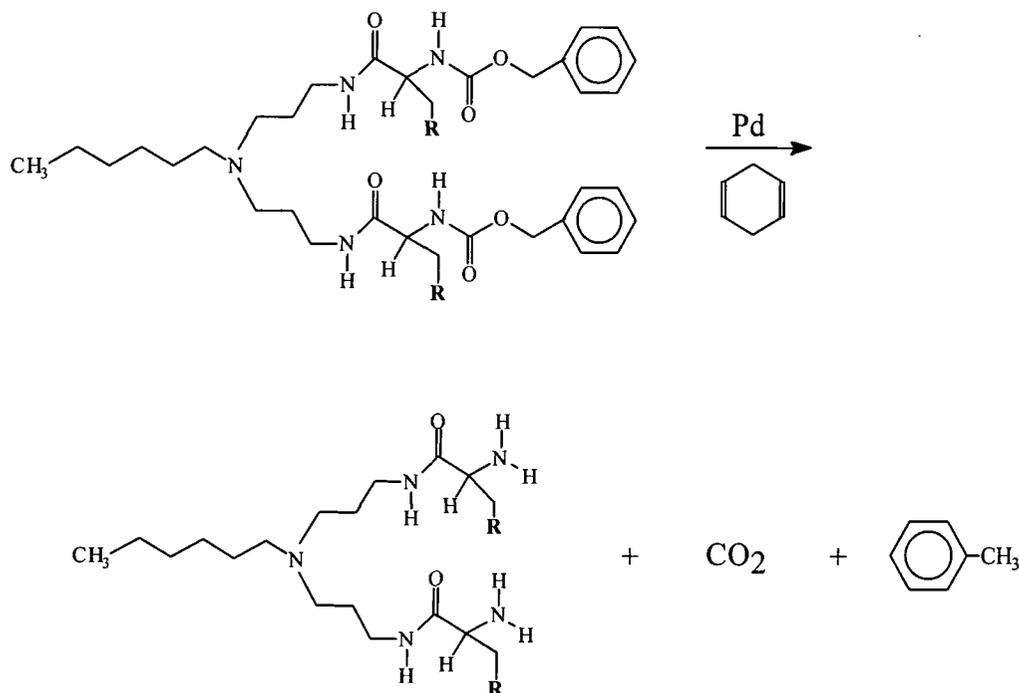

Reaction scheme.

The CBZ-protected amino acid terminated wedge (1g) was dissolved in either absolute ethanol or DMF (0.05-0.25mmoles/ml of protected amino acid wedge) and the solution was placed in a 50ml round bottomed flask provided with a magnetic stirrer, gas inlet and outlet tubes and surrounded by a water bath at 25°C. A slow stream of nitrogen was introduced above the surface of the solution and a suspension of 5 or 10% palladium-on-charcoal (0.5g palladium metal per protecting group) or palladium black catalyst (10% of the substrate for each protecting group) was added with vigorous stirring, followed by 1,4-cyclohexadiene (5 to 10 equiv. per protecting group), the mixture was stirred

under nitrogen for 3 hours per protecting group. On completion of the hydrogenolysis (TLC), the catalyst was removed by filtration (celite), and the solvent removed by evaporation under reduced pressure. The residue, the fully deprotected amino acid dendrimer wedge derivative was then dried under vacuum, this gave the deprotected material in a form suitable for use. Characterisation details for all these new compounds are presented below. The spectra are recorded in Appendix 2. The elemental analysis were not particularly good although all compounds were single spots on TLC and gave the correct molecular ion and appropriate spectra indicative of pure compounds. The materials appeared to be somewhat hygroscopic.

3.6.3.1 Hexylamine-L-phenylalanine terminated wedges.

3.6.3.1.1 The di-N,N'-phenylalanine amide of 4-hexyl-4-aza-heptane-1,7-diamine, Hex-*wedge*-phe$_2$
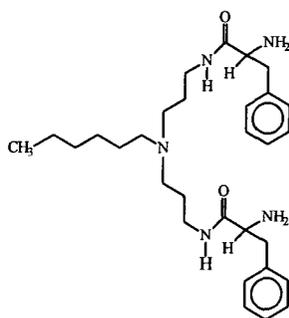
White crystalline solid (0.5g, 82%) m. pt. 82.0-84.0^{0}C; Found: C,69.18, H,9.22, N,13.50 , MS M+1 ion = 508.89 determined by MALDI TOF mass spectrometry, C$_{30}$H$_{47}$N$_5$ requires C,70.7, H,9.23, N,13.75% , M, 509, ^{1}H NMR (CDCl$_3$, 400 MHZ) : δ 0.80 (t, 3H, methyl), 1.18 (m, 6H, CH$_3$CH$_2$CH$_2$CH$_2$CH$_2$CH$_2$N) 1.32 (m, 2H, CH$_3$CH$_2$CH$_2$CH$_2$CH$_2$CH$_2$N), 1.54 (m, 4H, NCH$_2$CH$_2$CH$_2$N), 2.27 (t, 2H,

CH$_3$CH$_2$CH$_2$CH$_2$CH$_2$CH$_2$N), 2.32 (t, 4H, NCH$_2$CH$_2$CH$_2$N), 2.60+3.19 (m, 2H+2H, CH$_2$Ph) 3.22 (m, 4H, NCH$_2$CH$_2$CH$_2$N), 3.49 (m, 2H, COCHCH$_2$), 7.12-7.22 (m, 10H, aromatic), 7.63 (s, 2H, amide N-**H**) ; ^{13}C NMR (CDCl$_3$, 100MHZ): 13.99 (methyl), 22.58 (CH$_3$**C**H2), 26.53 (CH$_3$CH$_2$CH$_2$CH$_2$**C**H$_2$CH$_2$N +NCH$_2$**C**H$_2$CH$_2$N), 27.14 (CH$_3$CH$_2$**C**H$_2$CH$_2$CH$_2$CH$_2$N), 31.74 (CH$_3$CH$_2$CH$_2$**C**H$_2$CH$_2$CH$_2$N), 37.73 (NCH$_2$CH$_2$**C**H$_2$N), 41.14 (**C**H2Ph), 51.70 (N**C**H$_2$CH$_2$CH$_2$N), 53.90 (**C**H$_2$N), 56.50 (CO**C**HCH$_2$), 126.62 (*p*-aromatic), 128.52 (*m*-aromatic), 129.19 (*o*-aromatic), 137.94 (ipso-aromatic), 174.18 (amide **C**=O).

3.6.3.1.2 *The di(bis-N,N'-phenylalanine amide) of 4-hexyl-4-aza-heptane-1,7-di(bisaminopropylamine)*, Hex-*wedge*-phe$_4$.
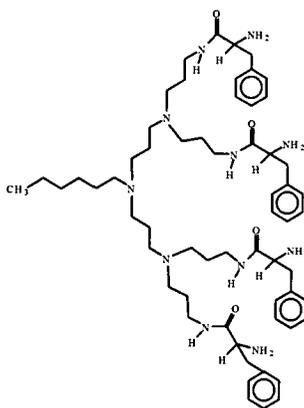
White crystalline solid (0.354g, 80%); MS M+1 ion = 1030.81 determined by MALDI TOF mass spectrometry, M, 1032, ^{1}H NMR (CDCl$_3$, 400 MHZ) : δ 0.82 (m, 3H, methyl), 1.20 (m, 6H, CH$_3$CH$_2$CH$_2$CH$_2$CH$_2$CH$_2$N) 1.26 (m, 2H, CH$_3$CH$_2$CH$_2$CH$_2$CH$_2$CH$_2$N), 1.42 (m, 12H, NCH$_2$CH$_2$CH$_2$N), 2.25 (t, 18H, CH$_2$NCH$_2$), 2.58+2.89 (m, 4H+4H, CH$_2$Ph) 3.03 (m, 8H, NCH$_2$CH$_2$CH$_2$N), 3.33

(m, 2H, COCHCH$_2$), 7.15-7.25 (m, 20H, aromatic C-**H**), 7.83 (s, 4H, amide N-**H**) ; ^{13}C NMR (CDCl$_3$, 100MHZ) : 13.99 (methyl), 22.58 (CH$_3$$C$H2), 26.53 (CH$_3CH_2$$CH_2CH_2CH_2CH_2$N+CH$_3CH_2CH_2CH_2$$CH_2CH_2$N+N$CH_2$$CH_2CH_2$N), 31.74 (CH$_3CH_2CH_2$$CH_2CH_2CH_2$N), 37.73 (NCH$_2CH_2$$CH_2$N), 41.14 ($C$H2Ph), 51.70,51.90 ($CH_2$ NCH$_2$), 56.50 (COCHCH$_2$), 126.62 (p-aromatic), 128.52 (m-aromatic), 129.19 (σ-aromatic), 138.94 (ipso-aromatic), 174.18 (amide C=O).

3.6.3.2 Hexylamine-L-tryptophan terminated wedges.

3.6.3.2.1 *The di-N,N'-tryptophan amide of 4-hexyl-4-aza-heptane-1,7-diamine, Hex-wedge-trp$_2$.*
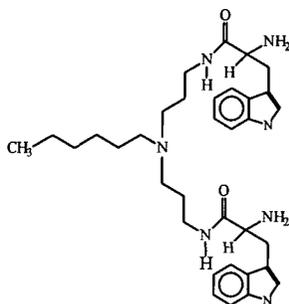
Off white crystalline solid (0.655g, 83%) m. pt. 70.0-72.0°C; Found: C,68.71, H,8.48, N,16.21 MS M+1 ion = 587.79 determined by MALDI TOF mass spectrometry, C$_{34}$H$_{49}$N$_7$ requires C,69.5, H,8.34, N,16.70% , M, 588, ^{1}H NMR (DMSO$_{d6}$, 400 MHZ): δ 0.83 (t, 3H, methyl), 1.21 (m, 6H, CH$_3$CH$_2$CH$_2$CH$_2$CH$_2$CH$_2$N) 1.32 (m, 2H, CH$_3$CH$_2$CH$_2$CH$_2$CH$_2$CH$_2$N), 1.43 (m, 4H, NCH$_2$CH$_2$CH$_2$N), 2.24 (t, 6H, CH$_3$CH$_2$CH$_2$CH$_2$CH$_2$CH$_2$NCH$_2$), 2.78+3.04

(m, 2H+2H, C**H**$_2$Ph) 3.07 (m, 4H, NC**H**$_2$CH$_2$C**H**$_2$N), 3.49 (m, 2H, COC**H**CH$_2$),

7.89 (s, 2H, amide N-**H**),
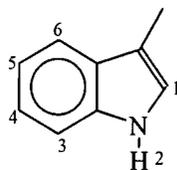
indole ring C-**H**, 1 (s, 2H, 7.14), 3 (d, 2H, 7.32), 4 (m, 2H, 6.95), 5 (m, 2H, 7.05),

6 (d, 2H, 7.56).

indole ring N-**H**, 2 (s, 2H, 10.86).

^{13}C NMR (DMSO$_{d6}$, 100MHZ) : 13.97 (methyl), 22.19 (CH$_3$**C**H2), 26.44

(CH$_3$CH$_2$**C**H$_2$CH$_2$CH$_2$CH$_2$N), 26.56 (CH$_3$CH$_2$CH$_2$CH$_2$**C**H$_2$CH$_2$N), 26.65

(NCH$_2$**C**H$_2$CH$_2$N), 31.14 (CH$_3$CH$_2$CH$_2$**C**H$_2$CH$_2$CH$_2$N), 31.31 (**C**H$_2$-indole), 36.95

(NCH$_2$CH$_2$**C**H$_2$N), 51.02 (N**C**H$_2$CH$_2$CH$_2$N), 53.34 (CH$_3$CH$_2$CH$_2$**C**H$_2$CH$_2$**C**H$_2$N),

55.35 (CO**C**HCH$_2$), 174.35 (amide **C**=O).
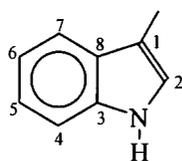
indole ring **C**-H, 2 (123.73), 4 (111.30), 5 (118.16), 6 (120.84), 7 (118.49).

indole ring aromatic, 1 (110.58), 3 (136.23), 8 (127.41).

3.6.3.2.2 The di(bis-N,N'-tryptophan amide) of 4-hexyl-4-aza-heptane-1,7-di(bisaminopropylamine), Hex-*wedge*-trp₄.
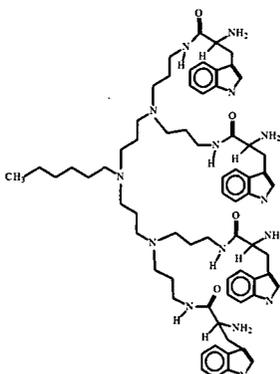
Off white waxy solid (0.622g, 94%) m. pt. 102.0-104.0⁰C; Found: C,67.93, H,8.10, N,16.89 MS M+1 ion= 1192.04 determined by MALDI TOF mass spectrometry, $C_{68}H_{97}N_{15}$ requires C,68.74, H,8.17, N,17.69%, M, 1189, ¹H NMR (DMSO$_{d6}$, 400 MHZ): δ 0.83 (t, 3H, methyl), 1.21 (m, 6H, $CH_3CH_2CH_2CH_2CH_2CH_2N$) 1.32 (m, 2H, $CH_3CH_2CH_2CH_2CH_2CH_2N$), 1.43 (m, 12H, $NCH_2CH_2CH_2N$), 2.24 (m, 18H, CH_2NCH_2), 2.78+3.04 (m, 4H+4H, CH_2-indole) 3.07 (m, 12H, $NCH_2CH_2CH_2N$), 3.45 (m, 4H, $COCHCH_2$), 7.89 (s, 4H, amide N-**H**),
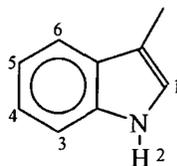
indole ring C-**H**, 1 (s, 4H, 7.13), 3 (d, 4H, 7.33), 4 (m, 4H, 6.94), 5 (m, 4H, 7.04), 6 (d, 4H, 7.55), indole ring N-**H**, 2 (s, 4H, 10.86).

¹³C NMR (DMSO$_{d6}$, 100MHZ) : 13.95 (methyl), 22.16 (CH_3**C**H_2), 26.57 (CH_3CH_2**C**$H_2CH_2CH_2CH_2N$+$CH_3CH_2CH_2CH_2$**C**H_2CH_2N),26.66 (NCH_2**C**H_2CH_2N), 31.26 ($CH_3CH_2CH_2$**C**$H_2CH_2CH_2N$+CH_2-indole), 36.97

(NCH$_2$CH$_2$CH$_2$N), 51.07 (NCH$_2$CH$_2$CH$_2$N), 51.09 (CH$_3$CH$_2$CH$_2$CH$_2$CH$_2$CH$_2$N),

55.44 (COCHCH$_2$), 174.56 (amide C=O).
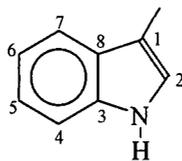
indole ring *C*-H, 2 (123.69), 4 (111.30), 5 (118.14), 6 (120.82), 7 (118.47).

indole ring aromatic, 1 (110.70), 3 (136.23), 8 (127.41).

3.6.3.3 Hexylamine-L-tyrosine terminated wedges.

3.6.3.3.1 The di-N,N'-tyrosine amide of 4-hexyl-4-aza-heptane-1,7-diamine, Hex-
wedge-tyr$_2$.
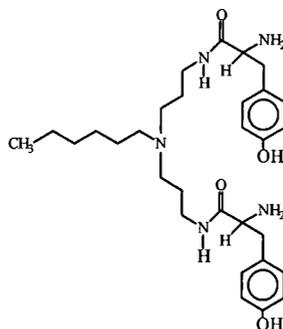
Clear oil (0.25g, 74%); ^{1}H NMR (DMSO$_{d6}$, 400 MHZ) : δ 0.82 (t, 3H, methyl),

1.22 (m, 6H, CH$_3$CH$_2$CH$_2$CH$_2$CH$_2$CH$_2$N) 1.32 (m, 2H,

CH$_3$CH$_2$CH$_2$CH$_2$CH$_2$CH$_2$N), 1.43 (m, 4H, NCH$_2$CH$_2$CH$_2$N), 2.25 (m, 6H,

CH$_2$NCH$_2$), 2.48+2.78 (m, 2H+2H, CH$_2$Ph) 3.02 (m, 4H, NCH$_2$CH$_2$CH$_2$N), 3.25

(m, 2H, COCHCH$_2$), 6.64 (d, 4H, *m*-aromatic C-H) 6.95 (d, 4H, *σ*-aromatic C-

H), 7.79 (t, 2H, amide N-H), 9.20 (broad, 2H, OH). ; ^{13}C NMR (DMSO$_{d6}$,

100MHZ) : 13.98 (methyl), 22.17 (CH$_3$*C*H2), 26.46 (CH$_3$CH$_2$*C*H$_2$CH$_2$CH$_2$CH$_2$N)

26.65(CH$_3$CH$_2$CH$_2$CH$_2$CH$_2$CH$_2$N+NCH$_2$CH$_2$CH$_2$N),31.31

(CH$_3$CH$_2$CH$_2$CH$_2$CH$_2$CH$_2$N), 36.88 (NCH$_2$CH$_2$CH$_2$N), 40.10 (CH2Ph), 51.09

(NCH$_2$CH$_2$CH$_2$N), 53.36 (CH$_3$CH$_2$CH$_2$CH$_2$CH$_2$CH$_2$N), 56.49 (COCHCH$_2$),

114.89 (*m*-aromatic), 128.62 (ipso-aromatic), 130.10 (*o*-aromatic), 155.68 (*p*-aromatic), 174.21 (amide **C**=O).

3.6.3.4 Siloxysilane-L-phenylalanine terminated wedges.

3.6.3.4.1 *The N-phenylalanine amide of 3-aminopropyltris(trimethylsiloxy)silane*, Si-*wedge*-phe.
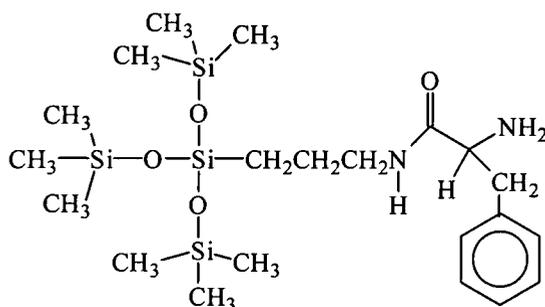
Clear light yellow oil (0.50g, 68%); Found: C,48.99, H,8.54, N,5.31 MS M+1 ion = 497.59 determined by MALDI TOF mass spectrometry, C$_{21}$H$_{44}$N$_2$ requires C,50.40, H,8.80, N,5.60%, M, 500; ^{1}H NMR (CDCl$_3$, 400 MHZ) : δ 0.10 (s, 27H, CH$_3$Si), 0.42 (t, 2H, Si-CH$_2$) 1.5 (m, 2H, Si-CH$_2$CH$_2$CH$_2$N), 1.92 (broad, 2H, NH$_2$), 2.70+3.26 (m, 1H+1H CH$_2$Ph), 3.23 (m, 2H Si-CH$_2$CH$_2$CH$_2$N) 3.63 (dd, 1H, CHCH$_2$Ph), 7.20-7.30 (m, 5H, aromatic C-**H**); ^{13}C NMR (CDCl$_3$, 100MHZ) : 1.73 (CH$_3$Si), 11.61 (Si-CH$_2$), 23.55 (Si-CH$_2$CH$_2$CH$_2$N), 40.95 (CH$_2$Ph), 41.64 (Si-CH$_2$CH$_2$CH$_2$N), 56.43 (CHCH2Ph), 126.76 (*p*-aromatic C-H), 128.65, 129.26 (*o, m*,-aromatic C-H), 137.89 (ipso-aromatic C-R), 173.73 (amide C=O).

3.6.3.4.2 The di-N,N'-phenylalanine amide of tris(trimethylsiloxy)silyl propyl-4-aza-heptane-1,7-diamine, Si-wedge-phe$_2$.
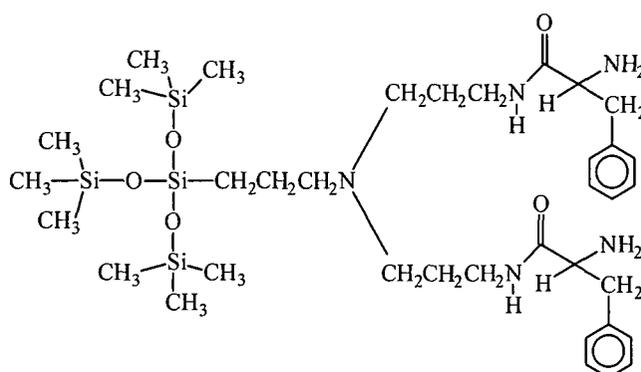
Clear yellow oil (0.436g, 58%); Found: C,56.07, H,8.51, N,8.83 MS M+1ion = 1023.63 determined by MALDI TOF mass spectrometry, C$_{36}$H$_{67}$N$_5$ requires C,56.76, H,8.80, N,9.2%, M, 1029; ^{1}H NMR (DMSOd$_6$, 400 MHZ) : δ 0.06 (s, 27H, CH_3Si), 0.37 (t, 2H, Si-CH_2) 1.36 (m, 2H, Si-CH$_2$CH_2CH$_2$N), 1.42 (b, 4H, NCH$_2$CH_2CH$_2$N), 2.25 (b, 6H, CH_2NCH_2), 2.62+2.88 (m, 2H+2H CH_2Ph), 3.03 (b, 4H Si-CH$_2$CH$_2$CH_2N) 3.36 (t, 2H, CHCH2Ph), 7.15-7.26 (m, 10H, aromatic C-H), 7.98 (b, 2H, NCH$_2$CH$_2$CH$_2$NH); ^{13}C NMR (DMSOd$_6$, 100MHZ): 1.73 (CH_3Si), 11.45 (Si-CH_2), 20.15 (Si-CH$_2$CH_2CH$_2$N), 26.72 (NCH$_2$CH_2CH$_2$N), 36.86 (NCH$_2$CH$_2$CH_2N), 41.00 (CH_2Ph), 51.07 (CH_2NCH_2), 56.21 (CHCH$_2$Ph), 126.05,128.02,129.25 (aromatic C-H), 138.52 (aromatic), 171.14 (NHCOCHCH$_2$Ph).

3.6.3.5 Siloxysilane L-tryptophan terminated wedges.

3.6.3.5.1 *The N-tryptophan amide of 3-aminopropyltris(trimethylsiloxy)silane,* Si-*wedge*-trp.
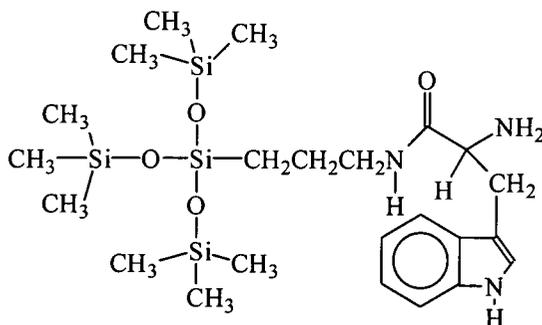
Clear oil (0.93g, 95%); Found: C,50.37, H,8.54, N,7.54 MS M+Na ion = 561.66 determined by MALDI TOF mass spectrometry, $C_{23}H_{45}N_3$ requires C,51.20, H,8.30, N,7.79%, M, 539, ^{1}H NMR (DMSO$_{d6}$, 400 MHZ) : δ 0.08 (s, 27H, CH_3Si), 0.41 (t, 2H, Si-CH_2) 1.41 (m, 2H, Si-$CH_2CH_2CH_2N$), 1.92 (broad, 2H, NH_2), 2.69+3.07 (m, 1H+1H CH_2-indole), 3.04 (m, 2H Si-$CH_2CH_2CH_2N$) 3.42 (dd, 1H, CHCH_2-indole),
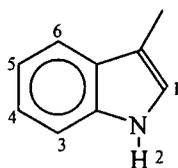
indole ring C-**H**, 1 (s, 7.14), 3 (d, 7.33), 4 (m, 6.94), 5 (m, 7.04), 6 (d, 7.55).

indole ring N-**H**, 2 (s, 10.84).

^{13}C NMR (DMSO$_{d6}$, 100MHZ) : 1.71 (CH_3Si), 11.32 (Si-CH_2), 23.19 (Si-$CH_2CH_2CH_2N$), 31.34 (CH_2-indole), 41.17 (Si-$CH_2CH_2CH_2N$), 55.35 (COCHCH2), 174.43 (amide C=O).
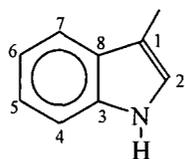
indole ring *C*-H, 2 (123.67), 4 (111.30), 5 (118.12), 6 (120.82), 7 (118.42).

indole ring *C* aromatic, 1 (110.74), 3 (136.24), 8 (127.35).

3.6.3.5.2 Si-*wedge*-trp-NH$_2$-**CBZ**.
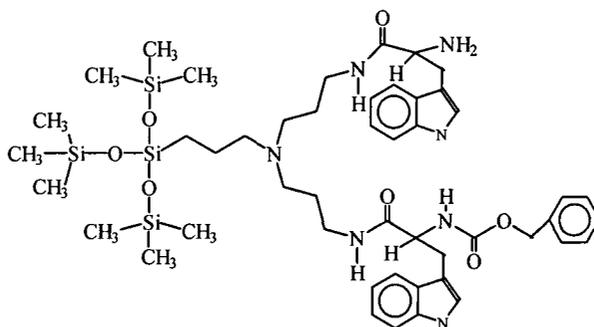
Yellow oil (0.85g, 84%); ^{1}H NMR (DMSO$_{d6}$, 400 MHZ) : δ 0.06 (s, 27H, CH$_3$Si), 0.35 (t, 2H, Si-CH$_2$) 1.42 (m, 2H, Si-CH$_2$CH$_2$CH$_2$N), 2.26 (b, 6H, CH$_2$NCH$_2$) 2.69+2.93 (m, 2H+2H CH$_2$-indole), 3.03 (m, 4H, NCH$_2$CH$_2$CH$_2$NH), 4.22 (b, 2H, COCHCH$_2$-indole), 4.92 (s, 2H, COOCH$_2$Ph), 7.25-7.29 (m, 5H + 2H, aromatic C-**H** + indole C-**H** (3),) 7.96,7.89 (d, 2H, NCH$_2$CH$_2$CH$_2$NH),
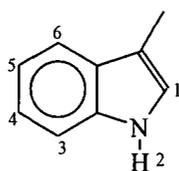
indole ring C-**H**, 1 (s, 2H, 7.11), 4 (t, 2H, 6.93), 5 (t, 2H, 7.02), 6 (d, 2H, 7.52,7.58).

indole ring N-**H**, 2 (d, 2H, 10.83,10.79); ^{13}C NMR (DMSO$_{d6}$, 100MHZ): 1.76

(*C*H$_3$Si), 11.45 (Si-*C*H$_2$), 21.05 (Si-CH$_2$*C*H$_2$CH$_2$N), 26.67 (NCH$_2$*C*H$_2$CH$_2$N),

30.96 (*C*H$_2$-indole), 34.39 (Si-CH$_2$CH$_2$*C*H$_2$N+ NCH$_2$CH$_2$*C*H$_2$N), 51.05

(N*C*H$_2$CH$_2$CH$_2$N), 55.24,55.61 (CO*C*HCH$_2$-indole), 65.20 (CO*C*H$_2$Ph),

127.25,127.45,128.27 (aromatic C-H), 137.01 (ipso-aromatic), 151.48

(NH*C*OOCH$_2$Ph).
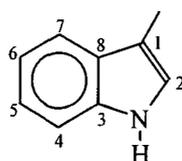
indole ring *C*-H, 2 (123.77), 4 (111.30), 5 (118.16), 6 (120.85), 7 (118.48).

indole ring aromatic, 1 (110.20,110.44), 3 (136.07,136.24), 8 (127.65).

3.6.3.6 Siloxysilane-L-tyrosine terminated wedges.

3.6.3.6.1 *The N-tyrosine amide of 3-aminopropyltris(trimethylsiloxy)silane,*
Si-*wedge*-tyr.
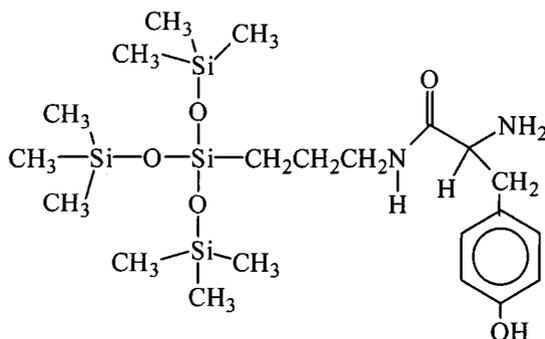
Yellow oil (0.60g, 93%); MS M+Na ion = 538.23 determined by MALDI TOF

mass spectrometry, M, 516, ^{1}H NMR (CDCl$_3$, 400 MHZ) : δ 0.10 (s, 27H,

CH$_3$Si), 0.44 (t, 2H, Si-CH$_2$) 1.52 (m, 2H, Si-CH$_2$CH$_2$CH$_2$N), 2.57+3.20 (m,

1H+1H CH$_2$Ph), 3.25 (m, 2H Si-CH$_2$CH$_2$CH$_2$N) 3.60 (dd, 1H, CHCH$_2$Ph), 6.82

(d, 2H, σ-aromatic C-**H**), 7.02 (d, 2H, *m*-aromatic C-**H**), 7.36 (amide N-**H**); ^{13}C

NMR (CDCl$_3$, 100MHZ): 1.63 (C**H**$_3$Si), 11.50 (Si-C**H**$_2$), 23.40 (Si-

CH$_2$C**H**$_2$CH$_2$N), 40.10 (C**H**$_2$Ph), 41.68 (Si-CH$_2$CH$_2$C**H**$_2$N), 56.45 (C**H**CH2Ph),

115.63 (*m*-aromatic *C*-H), 128.74 (ipso-aromatic C-R), 130.18 (σ,-aromatic *C*-

H),), 155.87 (*p*,-aromatic *C*-H), 174.73 (amide *C*=O).

3.7 References

[1] Bodansky, M., Bodansky, A., *The Practice of Peptide Synthesis*, (1984), 113.

[2] Sheehan, J.C., Hess, G.P., *J. Am. Chem. Soc.* 77, (**1955**), 1067.

[3] König, W., Geiger, R., *Chem. Ber.* 103, (**1970**), 788, 2024.

[4] Wünsch, E., Drees, F., *Chem. Ber.* 99, (**1966**), 110.

[5] Harding, K.E., Marman, T.H., Nam, D.H., *Tetrahedron Lett.*, 29 (**1988**), 1627.

[6] Bodansky, M., du Vigneaud, V., *J. Am. Chem. Soc.* 81, (**1959**), 5688.

[7] Evans, D.A., Ellman, J., *J. Am. Chem. Soc.* 111, (**1989**), 1063.

[8] Heffner, R.J., Jiang, J., Joullié, M.M., *J. Am. Chem. Soc.* 114, (**1992**), 10181.

[9] Felix, A.M., Heimer, E.P., Lambros, T.J., Tzougraki, C., Meienhofer, J., *J. Org. Chem.* 43, (**1978**), 4194.

[10] Bodansky, M., Bodansky, A., *The Practice of Peptide Synthesis*, (1984), 158.

[11] Anwer, M.K., Spatola, A.F., *Synthesis*, (**1980**), 929.

[12] Anderson, G.W., Zimmerman, J.E., Callahan, F.M., *J. Am. Chem. Soc.* 85, (**1963**), 3039.
Anderson, G.W., Zimmerman, J.E., Callahan, F.M., *J. Am. Chem. Soc.* 86, (**1964**), 1839.

[13] Bodansky, A., Bodansky, M., The Practice of Peptide Chemistry, (1984), 125.

[14] Bodansky, A., Bodansky, M., The Practice of Peptide Chemistry, (1984), 133.

[15] Brabander-van-den Berg, E.M.M., Jansen, J.F.G.A., Meijer, E.W., *Science* 266 (**1994**), 1226.

[16] Mukaiyama et al, *Tetrahedron Lett.*, 29 (**1970**), 5293.

CHAPTER 4

Molecular Recognition Studies

4. Cellulose Recognition

The bulk of the experimental work reported in this thesis is concerned with making and characterising well defined probe molecules with potential for recognising cellulose surfaces in water. In this chapter work designed to test the hypothesis is described and discussed.

4.1 Introduction

Cellulose is a polymeric material made up of repeating β-1,4-linked glucopyranose residues, Figure 4.1. It is the most abundant macromolecule produced by living organisms and occurs in several crystalline phases and morphologies resulting from the disruption of the non-covalent forces that normally bind the individual carbohydrate strands together within the crystal lattice.
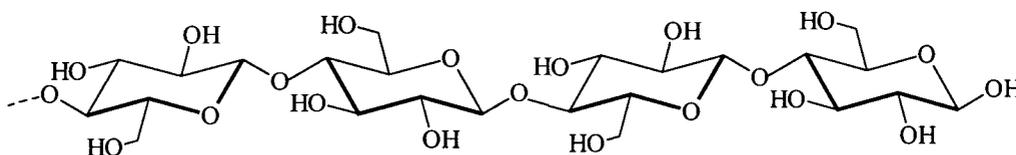
Figure 4.1 Cellulose polymer of *β*-1,4-linked glucopyranose units.

Structural cellulose is highly crystalline but regions of cellulose that are highly disrupted can be so low in crystallinity that they are referred to as amorphous cellulose[1]. Amorphous cellulose can be generated experimentally by swelling with phosphoric acid. In nature cellulose recognition has evolved and different organisms have acquired the capacity to recognise different forms of the carbohydrate. Cellulolytic bacteria and fungi produce a wide variety of

cellulases to efficiently degrade cellulose[1,2] and a common feature is their modular design in which the enzyme/substrate binding is mediated by a cellulose binding domain (CBD), while hydrolysis is carried out by a distinct catalytic domain. For the purpose of this work the author has accepted the hypothesis that structural features of the CBDs can be adopted for cellulose recognition units[3]. Over 100 different CBD's have been identified and grouped into ten families based primarily on their amino acid sequence similarities[4]. It is difficult to ascribe a precise role to CBDs due to the limited understanding of the mechanism of binding, conflicting reports on the properties of the CBDs and incomplete characterisation of the biological function. It is thought that CBDs play at least two roles in cellulose degradation. The most obvious of these is to concentrate the enzyme near the surface of cellulose. However, the CBDs may have a more active function in disrupting the cellulose surface, thereby making the individual polysaccharide chains more accessible for hydrolysis[5]. Either mechanism could involve targeting of enzymes to distinct regions of the substrate by CBDs with different specificities.

Most CBDs bind both crystalline and amorphous cellulose albeit with different affinities[6]. Others, are more specific and bind only crystalline[7] or amorphous[8] cellulose or have affinities for related structural carbohydrates often found in conjunction with cellulose, such as xylan[6] or the amino carbohydrate chitin[5, 9]. Currently, there are two published structures of CBDs: those of *Trichoderma reesi* cellobiohydrolase I (CBD$_{CBH1}$)[10] and *Cellulomonas fimi* xylanase-glucanase Cex (CBD$_{Cex}$)[11].
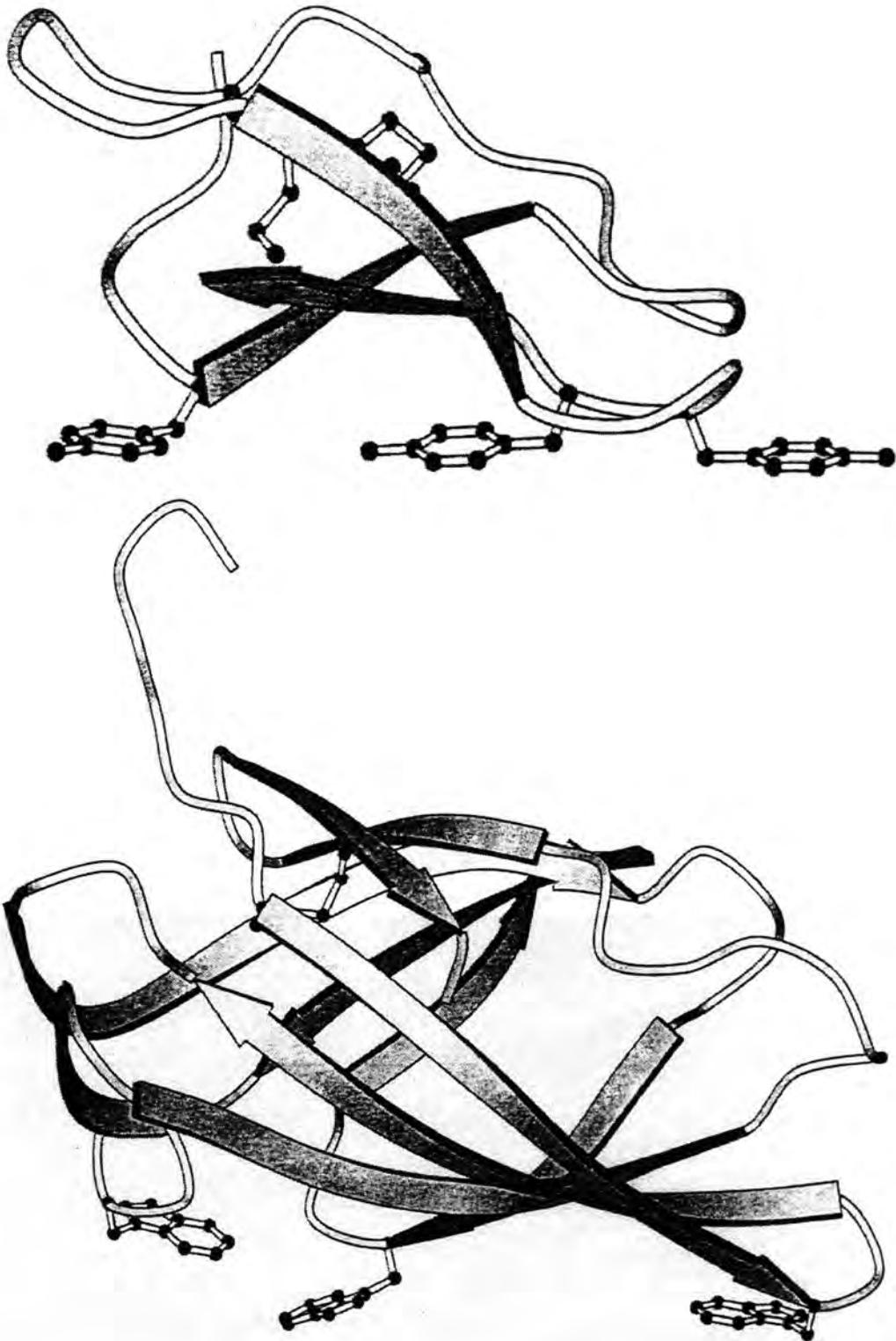
Figure 4.2 Ribbon diagrams of the solution structures of the family I CBD from *T.reesei* CBH I (top)[9] and the sub-family IIa CBD from *C.fimi* Cex (bottom)[10]. β- sheets are represented as arrows. Aromatic residues implicated in binding to cellulose and disulphide bonds are shown in "ball and stick" form.

As shown in Figure 4.2, in both of these CBDs, the postulated cellulose-binding face is a flat surface highlighted by three conspicuously exposed aromatic side chains. The three tyrosine residues on the surface of CBD_{CBHI}, Figure 4.2 (top), are important for the ability of the protein to bind crystalline cellulose[12] . Similarly, a recent chemical modification study by Bray et al, has demonstrated that the three surface tryptophans of CBD_{Cex}, Figure 4.2 (bottom) are necessary for its binding activity. Mutational analyses of CBDs in a previous study in the same family as CBD_{Cex} also support the conclusion that the exposed tryptophan side chains are involved in cellulose recognition[13]. These CBDs lack a carbohydrate binding groove or cleft. Despite the large body of structural and functional information available, only the mechanism of interaction of CBD_{Cex} with crystalline cellulose is reasonably well characterised. Microcalorimetric analysis has provided data which has been interpreted on the basis that the aromatic tyrosine or tryptophan rings provide a hydrophobic driving force for binding which is accompanied by a relatively large increase in entropy resulting from displacement of water molecules associated with the binding site and also from van der Waals interactions, especially stacking type van der Waals forces. The sugar and aromatic amino acid residues in the binding pocket are thought to stack directly against the pyranose rings of crystalline cellulose[14], conferring both stability and specificity to the protein-sugar complex[15]. However, the precise structural details of the protein-sugar interactions, such as the orientation of the CBDs along or across the cellulose chains on the face or edge of the crystalline lattice, still remains to be elucidated.

The foregoing discussion relates to a binding site on cellulose suitable for interaction with the aromatic side chain of an amino acid residue. This may not be the only kind of recognition and binding site; indeed at the same time that this study was in progress another student in the IRC was investigating the use of fragments of the cellulose structure as cellulose recognition units[16].

A relatively large number of tryptophan and tyrosine residues are usually present in the binding sites of sugar-binding and polysaccharide-degrading proteins. In this study the author has used probe molecules containing potential cellulose recognition and binding units formed by functionalisation of poly(propyleneimine) dendrimer wedges with various aromatic amino acids (see Chapter 3 and below) to test the idea of using synthetic cellulose recognition units to carry surface modifying groups to cotton fabrics in water.

4.2 Adsorption Studies on amino acid terminated dendrimer wedges.

4.2.1 Introduction

This section deals with the adsorption behaviour of various amino acid functionalised dendrimer wedges from a dilute solution onto a cotton surface. First and second generation tryptophan terminated hexylamine wedges have been tested from dilute methanol and water/methanol solutions and characteristic adsorption isotherms have been produced by utilising the technique of u.v. depletion.

4.2.2 The Adsorption Isotherm

In adsorption from solution at the solid/liquid interface the change in concentration of the solution consequent upon adsorption is what is experimentally measured. The characteristic adsorption isotherm is generated from a plot of the amount of solute adsorbed (Q) against the concentration in the external phase (C) at constant temperature and generally under equilibrium conditions. The isotherm is complete when the solute concentration reaches equilibrium. Initial classification of the isotherm shape produced is necessary because this is largely determined by the adsorption mechanism and can therefore be used to diagnose the nature of the adsorption process occuring.

4.2.3 Mechanism of Adsorption

The interaction between the surface and adsorbed species can be either chemical or physical. The process of adsorption can involve several types of bonding and these can be classified as follows:

- i) Chemical adsorption (chemisorption),
- ii) Hydrogen bonding,
- iii) Hydrophobic bonding, and
- iv) van der Waals forces.

The overall interaction of a solute molecule with a specific surface may involve more than one type of bonding and is directly related to the chemical structure of both constituents.

Recording of the adsorption isotherm, Figure 4.3, is the general method for establishing the type of adsorption mechanism involved. The important features

are: a) the rate of adsorption; b) the shape of the isotherm; c) the significance of

the plateau found in many isotherms; d) the extent of solvent adsorption; e)

whether the adsorption is monomolecular or extends over several layers; f) the

orientation of the adsorbed molecules; g) the effect of temperature; and h) the

nature of the interaction between adsorbate and adsorbant. A variety of isotherm

shapes for adsorption from dilute solutions have been reported from extensive

experimental studies and these have been classified by Giles et al[17]. More

recently a theoretical rationalisation has been proposed for the experimental

classification adopted, [18] the various isotherm shapes are shown in Figure 4.3.

The analysis is similar to that used by Langmuir for gas adsorption.
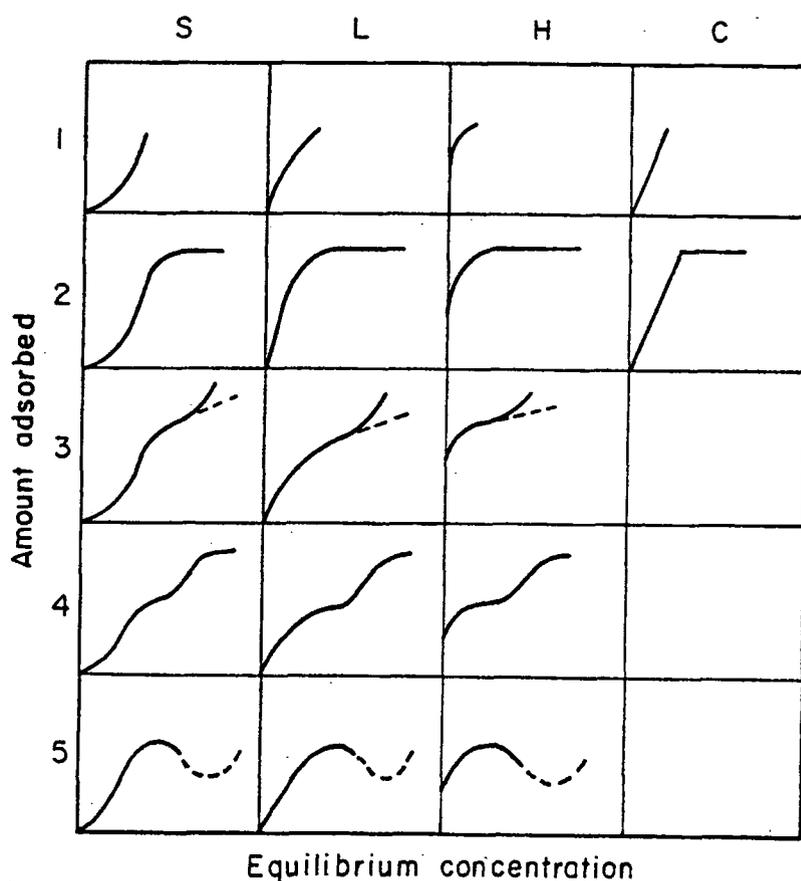
Figure 4.3 Classification of isotherm shapes.

Four characteristic classes are identified which are based on the slope of the initial part of the isotherm. These characteristic classes are further divided into several subgroups related to the behaviour at higher concentrations. The classes are the S (S shaped), L (Langmuir), H (high affinity), and C (constant partition) and subgroups, 1,2 3, etc., see Figure 4.3. The L (Langmuir) class is the most common and is characterised by an initial region that is concave to the concentration axis. For the S class the initial slope is convex to the concentration axis, and this is frequently followed by a point of inflection leading to an S-shaped isotherm; the H (high affinity) class results from extremely strong adsorption at very low concentrations; the C (constant partition) class has an initial linear portion which indicates constant partition of the solute between solution and absorbant, and occurs with microporous adsorbants.

The initial slope of the isotherm depends on the rate of change of site availability with increase in solute adsorbed. As increasing amounts of solute are adsorbed , there is usually progressively less chance that a solute molecule arriving at the surface will find a suitable site on which it can be adsorbed. If the interaction between adsorbed molecules is negligible, the activation energy for adsorption will be independent of coverage, and this leads to an L or H isotherm. When the force of interaction between adsorbed molecules is significant relative to that between solute and adsorbant, the activation energy will be higher, and cooperative adsorption occurs and S isotherms result. In this case the solute molecules tend to be packed in rows or clusters on the surface, and this situation is encouraged when the solvent is strongly adsorbed and the solute is monofunctional. Parallel orientation (i.e. the absorbing molecules are parallel

with their long axis perpendicular to the surface), of solute molecules gives L type isotherms. Some dyes form aggregates in solution, and these are adsorbed giving the S shaped isotherm. The H curves are associated with chemisorption or other strong interactions.

The C curve is found with microporous adsorbents, and is consistent with conditions in which the number of adsorption sites remains constant throughout the concentration range. As sites are covered new sites appear, and the surface available expands proportionately with the amount of solute adsorbed. Cases of C type linear adsorption have been found after an initial portion of L or H type. The inflections in subgroup 3 and the second plateau in subgroup 4 may reflect a change in orientation of the adsorbed solute or the formation of a second layer.

4.2.4 Langmuir adsorption theory.

Langmuir adsorption is based on the assumption that every adsorption site is equivalent[19], and that the ability of an adsorbing species to bind to a surface is independent of whether or not nearby sites are occupied. There is no interaction between individual molecules, only with an unoccupied site, and adsorption is limited to a monolayer.

The adsorption process can be summarised by the equilibrium equation:-

A (solute in solution) + B (adsorbed solvent) = A (adsorbed solute) + B (solvent in solution)
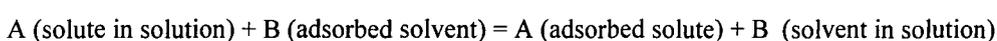
-where A and B represent concentrations and there are corresponding rate constants k_a for adsorption and k_d for desorption.

The rate of adsorption, r_a, is directly related to the concentration of the solution and number of freely available sites by Equation 1:-

$$r_a = k_a \times C \times N\left(1 - \frac{Q}{N}\right) \tag{1}$$

where Q is the quantity of solute (moles) adsorbed per gram of adsorbent, C is the equilibrium concentration of solute in presence of the absorbing surface, and N is the total number of sites (moles) per gram of adsorbant. The corresponding rate of desorption, r_d, is directly related to the quantity of solute adsorbed, hence,

$$r_d = k_d \times Q \tag{2}$$

At equilibrium the rate of adsorption is equivalent to the rate of desorption, i.e. $r_a = r_d$ and making this equivalence and rearranging gives:

$$\frac{C}{Q} = \frac{1}{K_L N} + \frac{C}{N} \tag{3}$$

Where $K_L = \dfrac{k_a}{k_d}$

Therefore a plot of $\dfrac{C}{Q}$ vs. C will give a straight line with gradient $\dfrac{1}{N}$, and intercept $\dfrac{1}{K_L N}$, where N has units (mol. per gram of substrate) and K_L, M^{-1}.

4.3 Investigation to ascertain the classification of the adsorption isotherm for tryptophan terminated dendrimer wedges on cellulose.

4.3.1 Determination of the extinction coefficients for Hex-*wedge*-trp$_2$, and Hex-*wedge*-trp$_4$.

The wavelength of maximum absorbance (λ_{max}) for each dendrimer wedge in an Analar methanol solution was found to be 282nm (Appendix 3), which is in good agreement with actual values for the indole ring of the

tryptophan residue. A series of solutions of Hex-*wedge*-(trp)$_2$, and Hex-*wedge*-(trp)$_4$ at various concentrations were prepared in Analar methanol and their absorbance at 282nm, referenced to a point on the baseline at 500nm, were recorded at room temperature (20°C).

The Beer-Lambert law[20] states that:

$$A = \varepsilon c l$$

where A is absorbance or optical density, ε the extinction coefficient ($M^{-1}cm^{-1}$), c the concentrtion (μM), and l the path length (cm). Standard calibration curves for the various dendrimers can therefore be produced by plotting the absorbance at λ_{max}, A, versus the concentration, c, yielding a straight line with a slope equal to εl (Figures 4.4, 4.5).
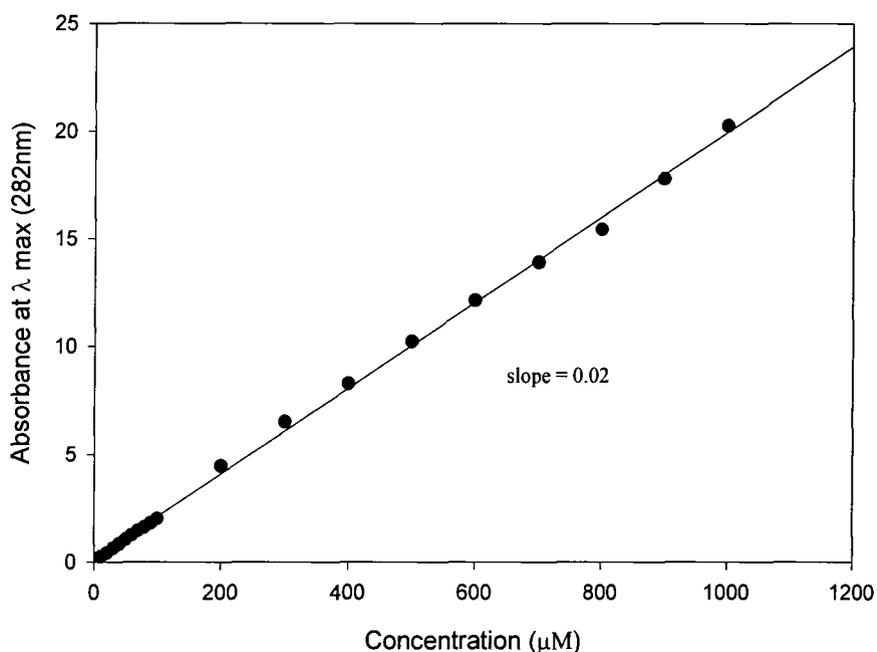
Figure 4.4 Calibration curve for Hex-*wedge*-(trp)$_4$
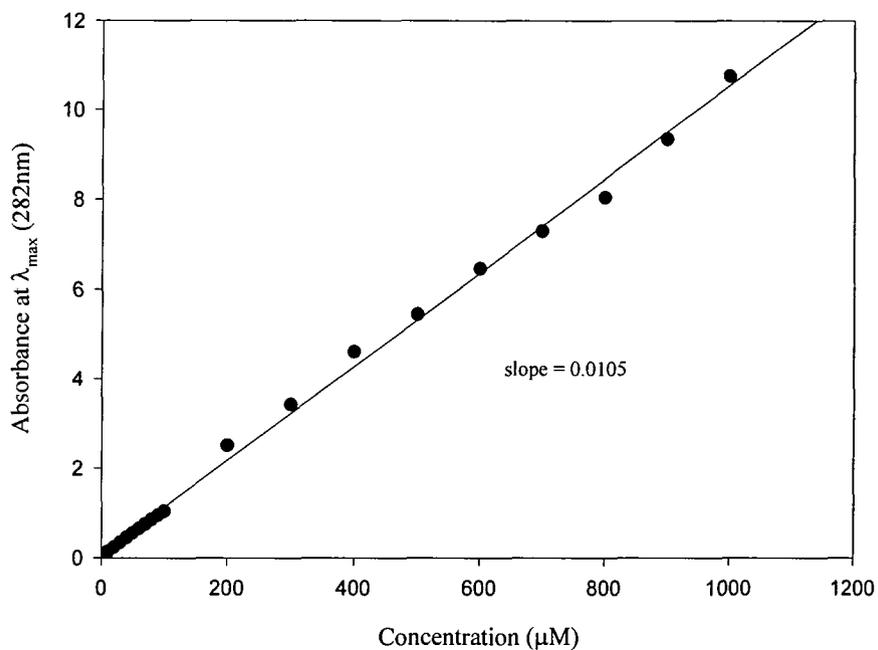
Figure 4.5. Calibration curve for Hex-*wedge*-(trp)$_2$

Therefore, since the path length of the cell used was 1cm, the slope of the calibration curve is equivalent to the extinction coefficient for the corresponding dendrimer wedge.

From a linear regression fit of the calibration curves, it was found that the extinction coefficient for Hex-*wedge*-(trp)$_4$ = 2.00x10^4 M^{-1}cm^{-1}, see Figure 4.4 and Hex-*wedge*-(trp)$_2$ = 1.05x10^4 M^{-1}cm^{-1} , see Figure 4.5.

4.3.2 Experimental Procedure

Experiments were performed to ascertain the shape of the corresponding adsorption isotherm for each dendrimer wedge adsorbing onto a cotton surface from an organic solution. The cotton used was woven, unbleached, not dyed, and

desized[*] which had been supplied and previously pre-treated at Unilever Research Port Sunlight laboratory.

A series of solutions of known concentration for each dendrimer wedge tested were made up in Analar methanol and their initial absorbance at 282nm (λmax) was measured, referenced to a point on the baseline (500nm). To 4ml of each dendrimer wedge solution was added a pre-cut piece of cotton (0.5g) in a sample vial. The vials were then placed on a Denley Spiramix DS507 which rotates at 50 rev/min with a pitch of 10mm until the solution concentration had reached equilibrium at room temperature (20^0C). Determination of the time required for the solution to reach equilibrium was performed by monitoring the concentration of the solution with time. From Figure 4.6, for Hex-*wedge*-trp$_2$, it can be seen that 4 hours is a sufficient length of time for the solution to reach equilibrium.

After 4 hours, the absorbance of the solutions was measured referenced to a methanol solution that had undergone the same experimental process. Dendrimer solutions without any cotton added were subjected to the same procedure and there was found to be no change in their absorbance.

---

[*] Desizing involves washing the cotton at 95^0C in Synperonic A7 (4g/l), a linear alcoholethoxylate non-ionic surfactant, and sodium carbonate (4g/l), and then rinsing in demineralised water at 95^0C.
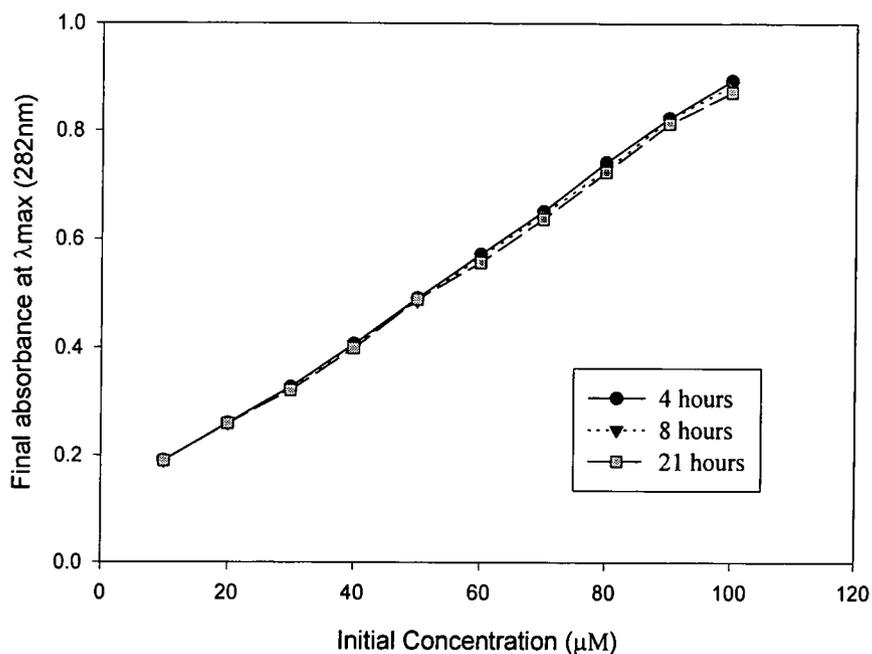
Figure 4.6. Determination of the time for the adsorbing solution to reach

equilibrium with the cotton surface.

4.3.3 Results

From the final absorbance, the equilibrium (final) concentration (C) can

be calculated using the Beer-Lambert equation (section 4.3.1). The amount

adsorbed per gram of substrate (Q) can be calculated from equation 5:

$$Q = \frac{dA}{\varepsilon l} \times \frac{\text{volume of dendrimer solution}}{\text{mass of cotton}} \tag{5}$$

where dA is the change in adsorption of the solution during the experiment. The

results are shown in Tables 4.1 and 4.2.

Initial Absorbance at λmax (282nm)	Final Absorbance at λmax (282nm)	C (μM)	Q (μmol./gram of cotton)
0.13	0.19	18.1	-0.05
0.23	0.26	24.8	-0.03
0.34	0.33	31.4	0.008
0.45	0.41	39.0	0.03
0.55	0.49	46.7	0.05
0.66	0.57	54.3	0.07
0.75	0.65	61.9	0.08
0.85	0.74	70.5	0.08
0.96	0.82	78.1	0.11
1.04	0.89	84.8	0.11
2.50	2.32	220.9	0.14
3.42	3.12	297.1	0.23
4.60	4.02	382.8	0.44
5.44	5.11	486.7	0.25
6.46	6.26	596.2	0.15
7.29	6.91	658.1	0.29
8.04	7.78	740.9	0.20
9.33	8.79	837.1	0.41
10.74	9.85	938.1	0.68

Table 4.1 Adsorption data for Hex-*wedge*-trp$_2$.

Initial Absorbance at λmax (282nm)	Final Absorbance at λmax (282nm)	C (μM)	Q (μmol./gram of cotton)
0.25	0.19	9.5	0.024
0.42	0.25	12.5	0.068
0.64	0.31	15.5	0.13
0.84	0.43	21.5	0.16
1.05	0.56	28.0	0.20
1.25	0.71	35.5	0.22
1.46	0.84	42.0	0.25
1.62	0.92	46.0	0.28
1.82	1.13	56.5	0.28
2.02	1.24	62.0	0.31
4.46	3.94	197.0	0.21
6.51	5.50	275.0	0.41
8.28	6.60	330.0	0.67
10.22	8.47	423.5	0.70
12.13	9.66	483.0	0.99
13.90	11.40	570.0	1.00
15.42	12.60	630.0	1.13
17.77	14.45	722.5	1.33
20.26	17.60	880.0	1.06
34.85	29.85	1492.5	2.00
102.5	93.4	4670.0	3.64

Table 4.2 Adsorption data for Hex-*wedge*-trp$_4$.

4.3.4 Adsorption isotherms for Hex-*wedge*-trp$_2$ and Hex-*wedge*-trp$_4$ from a methanol solution .

Adsorption isotherms were produced for each dendrimer wedge from a plot of the amount of dendrimer wedge adsorbed per gram of cotton (*Q*) versus the equilibrium concentration of the solution (*C*). Both Hex-*wedge*-trp$_2$ and Hex-*wedge*-trp$_4$ produce characteristic L2 (Figure 4.3) shaped isotherms indicative of Langmuir adsorption, see Figures 4.7 and 4.8. The curves are well defined at low concentration but the errors in measurement and consequent scatter of data points increase with increasing solute concentration as is common in this kind of work[21].
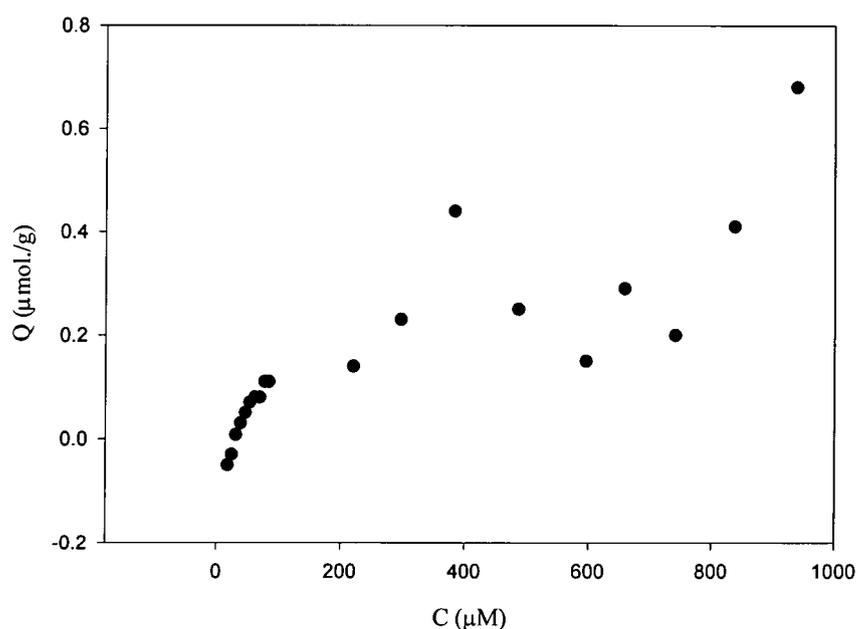
Figure 4.7. Adsorption isotherm for Hex-*wedge*-trp$_2$.
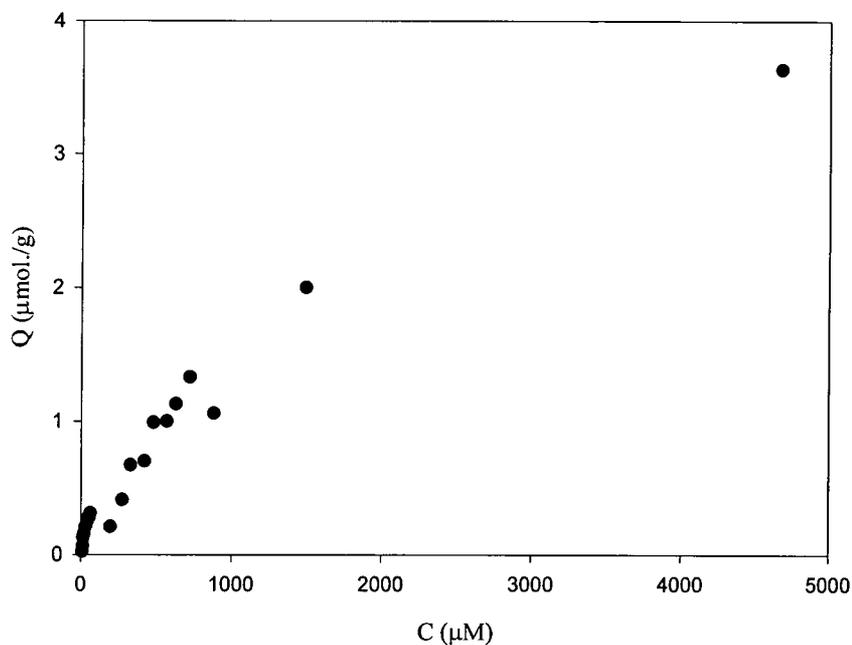
Figure 4.8 Adsorption isotherm for Hex-*wedge*-trp$_4$.

From a comparison of the two isotherms, it can be observed that Hex-*wedge*-trp$_4$ (Figure 4.9) is much more adsorbed onto the cotton surface than Hex-*wedge*-trp$_2$ particularly at low concentrations (Figure 4.10). A possible explanation of this is that it could be due to the increased number and perhaps more effective orientation of the tryptophan amino acid residues on the cotton surface from the "footprint" of the Hex-*wedge*-trp$_4$ probe. Unfortunately, although Hex-*wedge*-trp$_4$ shows an increased recognition of the cotton surface, only low levels of the probe molecules are adsorbed in either case. A possible explanation is that the molecule was so highly soluble in methanol that the adsorption process was not favoured.
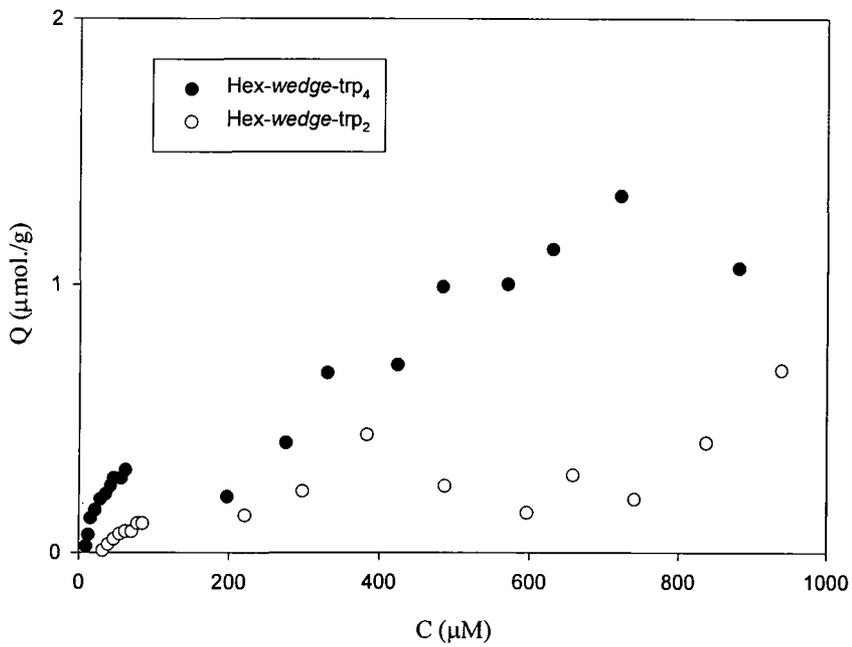
Figure 4.9 A comparison of the adsorption isotherms of Hex-*wedge*-trp$_2$ and
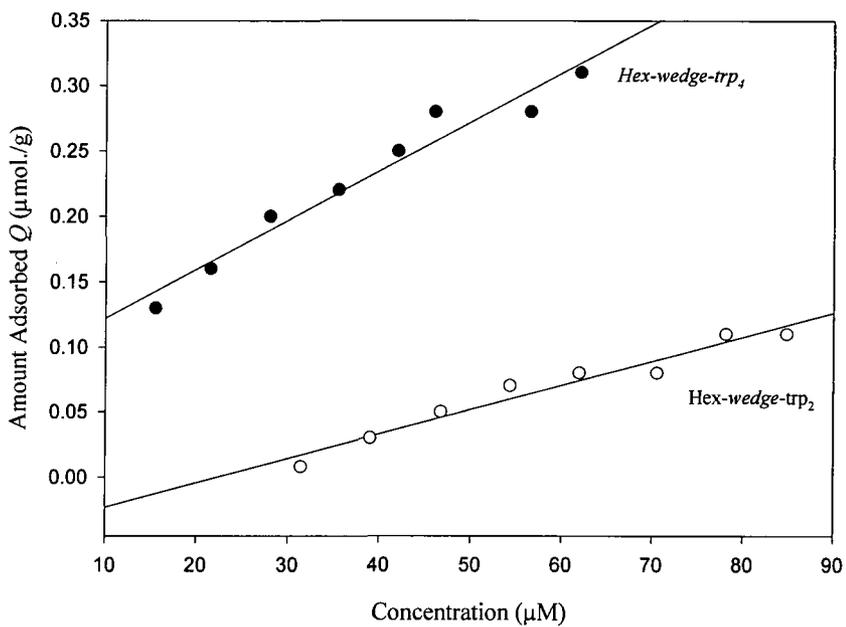
Hex-*wedge*-trp$_4$.

Figure 4.10 Comparison of Hex-*wedge*-trp$_2$ and Hex-*wedge*-trp$_4$ at low

concentrations.

4.3.5 Analysis of adsorption isotherms

The initial slope and the overall shape of the upper part of the curves for the isotherms produced for Hex-*wedge*-trp$_n$ adsorbing onto a cotton surface from a methanol solution are characteristic of Langmuir type isotherms. The L curves are the best known examples of isotherms produced by adsorption from dilute solution with the L2 curve seen in this study occurring in the majority of cases, see Figures 4.7 and 4.8. In the case of the L2 curves observed, the initial curvature of the isotherms show that as more sites on the cotton surface are filled it becomes increasingly difficult for a dendrimer wedge molecule arriving at the surface to find an available vacant site. The types of systems which give rise to L curves have certain characteristics, as discussed previously in Section 4.2.3, and some of these conditions are fulfilled in this case and can be used to explain the isotherms observed.
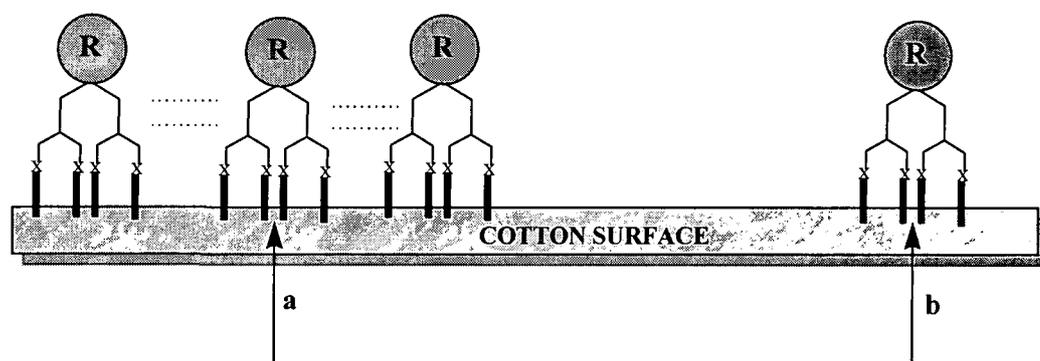
Figure 4.11 A schematic representation of conditions favouring the production of L isotherms.

The dendrimer molecules are likely to be adsorbed flat on the surface with the amino acid tryptophan residues aligned along the backbone of the cellulose molecule suffering little competition for adsorption sites from solvent

(methanol) molecules. Figure 4.11 shows an illustration of the conditions necessary for the formation of L isotherms. There are relatively strong attractive forces (illustrated by thick black lines) between dendrimer recognition units (x) and the cotton surface, but very weak forces (illustrated by dotted lines) between the dendrimer molecules themselves. Consequently, a dendrimer molecule is equally stable when adsorbed at **a** as at **b** and this situation results in L isotherms. Langmuir adsorption theory can be applied over the full concentration range of plots of C/Q versus C which give straight line relationships (Figures, 4.12, 4.13 and 4.14) with gradient $1/N$ and intercept on the y-axis, $1/K_LN$.

Langmuir adsorption theory has been used to fit the data ($r^2=0.70$) over the full concentration range for Hex-*wedge*-trp$_2$, (Figure 4.14). The data for Hex-*wedge*-trp$_4$ gave a better fit ($r^2=0.87$) at low concentration (Figure 4.12) than at higher concentrations ($r^2=0.63$), Figure 4.13.
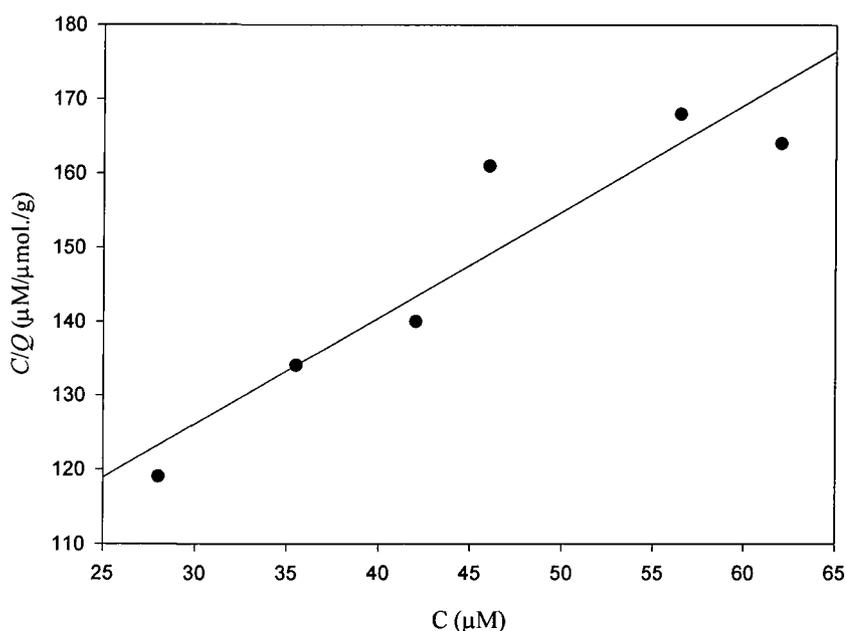
Figure 4.12 Langmuir adsorption analysis on Hex-*wedge*-trp$_4$ at low concentration.
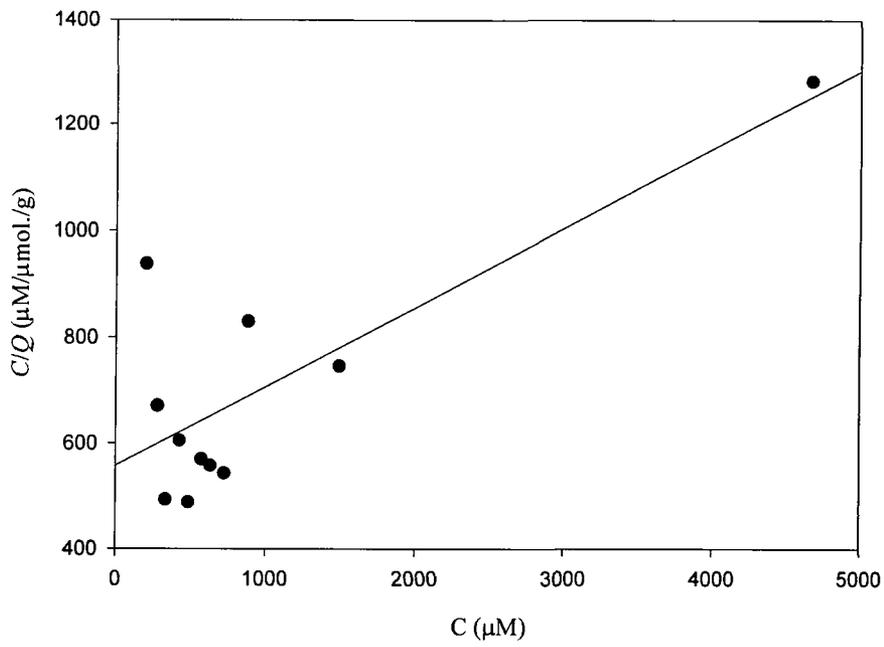
Figure 4.13 Langmuir adsorption analysis on Hex-*wedge*-trp$_4$ at high

concentration.
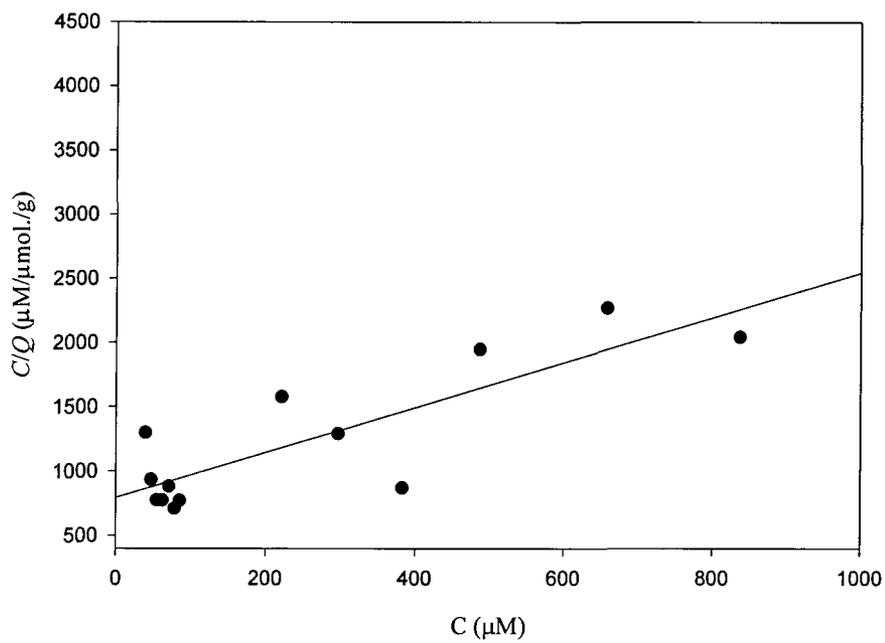
Figure 4.14. Langmuir adsorption analysis on Hex-*wedge*-trp$_2$.

The values of K_L and N obtained for each dendrimer using the theory of Langmuir adsorption, described previously in Section 4.2.4, are recorded in Table 4.4.

Dendrimer	Langmuir Adsorption Theory		
	$K_L N$ (lg^{-1})	N $(mol.g^{-1})$	K_L (M^{-1})
Hex-*wedge*-trp$_2$	1.25×10^{-3}	5.71×10^{-7}	2.2×10^{3}
Hex-*wedge*-trp$_4$	1.2×10^{-2}	6.94×10^{-7}	1.73×10^{4}

Table 4.4 K_L and N values for Hex-*wedge*-trp$_2$ and Hex-*wedge*-trp$_4$ at 293K.

From the values of K_L the value of $\Delta G^{\ominus}$ can be calculated from the equation

$$\Delta G^{\ominus} = -RT \ln K_L$$

This gives values of $\Delta G^{\ominus}$ for Hex-*wedge*-trp$_2$ and Hex-*wedge*-trp$_4$ as -19kJmol^{-1} and -24kJmol^{-1} respectively, where T = 293K and R = 8.315JK^{-1}mol^{-1}.

These results are of the appropriate orders of magnitude for adsorption onto cellulose,[16] but it is difficult to know how much weight can be attached to them. Hex-*wedge*-trp$_4$ has been found to adsorb significantly more effectively onto the cotton surface (Figure 4.10), and this has been further confirmed from N and K_L values calculated by Langmuir adsorption theory (Table 4.4). Qualitatively, the N values indicate there are slightly fewer sites per gram of cotton which can accommodate Hex-*wedge*-trp$_2$ than Hex-*wedge*-trp$_4$, and the K_L values imply that there are considerably more of the available sites for Hex-*wedge*-trp$_4$ being

occupied. This is in good agreement with calculated ΔG° values which suggest that the free energy of adsorption for Hex-*wedge*-trp$_4$ is more favourable than Hex-*wedge*-trp$_2$.

4.3.6 Adsorption isotherms for Hex-*wedge*-trp$_4$ from a 80/20 methanol/water solvent system .

4.3.6.1 Introduction

Networks of interconnecting channels do not exist in substantial amounts in typical dry cellulose fibres but these channels and pores are opened up on exposure to a suitable solvent, acting as an inter- and intra-fibrillar swelling agent. The relative penetrating ability of the solvent is a function of its hydrogen bonding capacity and decreases in the order water > acetic acid > methanol > less polar organic solvents. The opening up of channels and pores in cellulose fibres depends upon the penetration of the solvent into the cellulose surface which depends upon the solvent's ability to disrupt less-ordered and ordered hydroxylic hydrogen bonds between and within elementary cellulose fibres. The relatively large internal surfaces that are developed in the cotton fibre are evident from surface area measurements for the cotton fibre in a saturated vapour environment as compared to the dry fibre. Areas of 0.6-0.7m^2/g , 137m^2/g, and 20.1m^2/g are found for dry fibres, water and methanol environments respectively[22].

Hex-*wedge*-trp$_4$ is not water soluble but is soluble in a 80:20 methanol/water mixture, the lowest solvent ratio mixture that can support a stable solution. Therefore, adsorption studies were repeated for Hex-*wedge*-trp$_4$ using a 80:20

methanol/water solvent mixture to see if there was any significant change in the adsorption characteristics for this probe as a function of solvent composition.

4.3.6.2 Results

The wavelength of maximum absorbance (λ_{max}) was found at 282nm as for the previous system for the pure methanol solvent system (see 4.3.1). The calibration graph produced is shown in Figure 4.15, and the corresponding extinction coefficient for this system is 1.86×10^4 M^{-1} cm^{-1} (see 4.3.1). The results of the adsorption measurements are shown in table 4.5 and the adsorption isotherm in Figure 4.16.
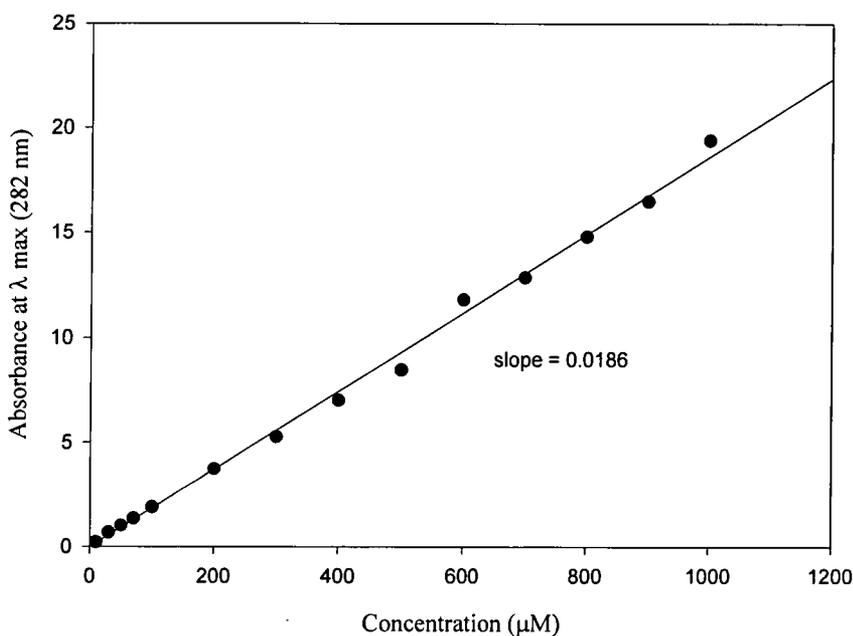
Figure 4.15 Calibration curve for Hex-*wedge*-(trp)$_4$ from a 80:20 methanol/water solvent system.

Langmuir adsorption is again observed and the experimental data is in good agreement with conventional analysis over the whole concentration range (Figure 4.17); however, adsorption is still occurring at relatively low levels.

Initial Absorbance at λmax (282nm)	Final Absorbance at λmax (282nm)	C (μM)	Q (μmol./gram of cotton)
0.212	0.152	8.17	0.026
0.683	0.279	15	0.174
1.019	0.407	21.9	0.263
1.353	0.775	41.7	0.249
1.905	1.14	61.3	0.329
3.74	2.57	138.2	0.503
5.27	4.11	221	0.499
7.01	6.03	324	0.42
8.46	7.79	419	0.29
11.8	9.43	507	1.02
12.85	11.27	606	0.68
14.78	13.05	701.6	0.74
16.47	15.01	807	0.63
19.4	17.63	947.8	0.76

Table 4.5 Adsorption data for Hex-*wedge*-trp$_4$ in a 80/20 water/methanol solvent system.

Interestingly, the L2 characteristic shape seen previously for Hex-*wedge*-trp$_4$ in the pure methanol solvent system (Figure 4.8) has changed to the characteristic shape of an L4 or L5 curve (Figure 4.3) for the mixed solvent system as seen from Figure 4.16. The shapes of the isotherms for these sub-groups (L4 and L5)

are attributed to the development of a fresh surface on which adsorption can occur. This fresh surface may be due to a) parts of the surface layer already present becoming exposed and accessible to the probe, b) new, probably more crystalline regions of the substrate structure into which the solute begins to penetrate, or c) parts of the original surface which are exposed by solvent penetration. Thus, for c), a proportion of the original surface may be uncovered by re-orientation of the molecules already adsorbed and this is consistent with the postulated adsorption mechanism. Hex-*wedge*-trp$_4$ molecules which completely cover the surface in a flat orientation at the first plateau, may adsorb in a different orientation in the second layer.
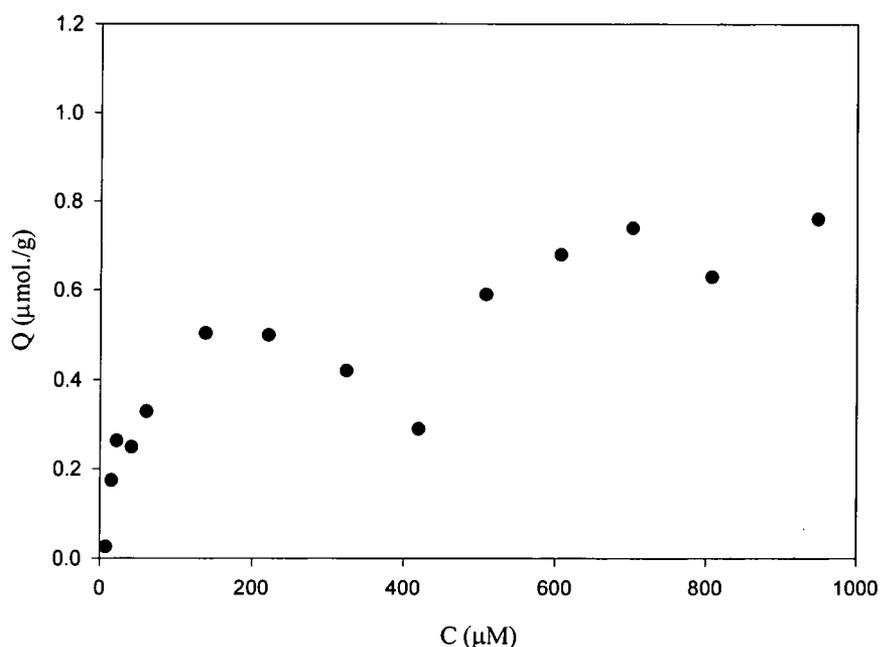
Figure 4.16 Adsorption isotherm for Hex-*wedge*-trp$_4$ in a 80/20 water/methanol solvent system.

Alternatively, the second plateau observed may represent simply the formation of a second monolayer on top of the first without any special reorganisation. For

L5 curves, the isotherm has a maximum due to association of the solute in solution, i.e., with increase in concentration the solute-solute attraction begins to increase more rapidly than the substrate-solute attraction. Known examples have a maximum occurring at solution concentrations a little higher than the critical micelle concentration. It is reported that often there is a minimum after the first plateau, and that with increasing solute concentration the adsorption curve rises again. This behaviour agrees well with the isotherm observed in this case, see Figure 4.16.

Langmuir analysis has been performed over the whole concentration range (r^2=0.95), see Figure 4.17. The values of K_L and N calculated from the theory of Langmuir adsorption for Hex-*wedge*-trp$_4$ in a 80/20 water/methanol solvent system compared to Hex-*wedge*-trp$_4$ in pure methanol are recorded in Table 4.6.
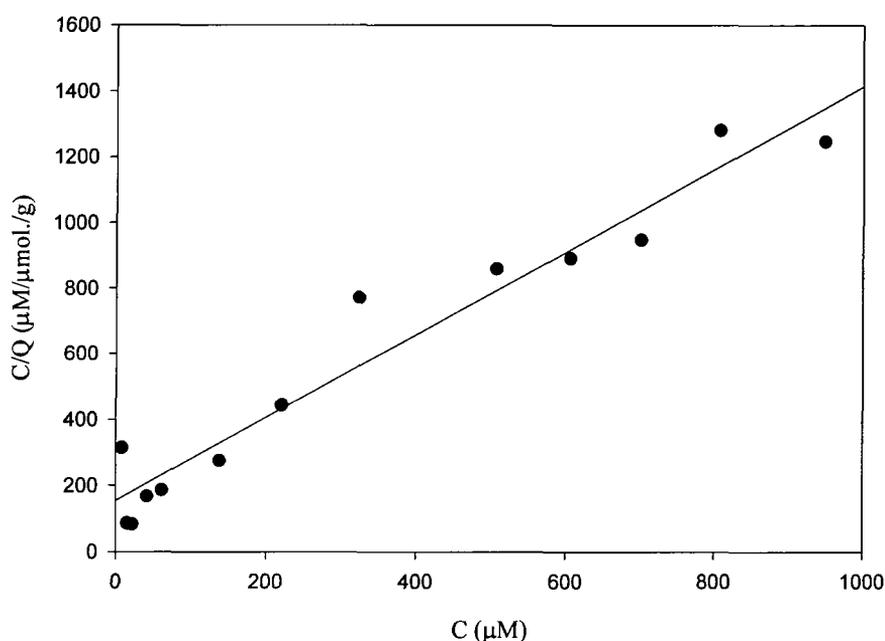
Figure 4.17. Langmuir adsorption analysis on Hex-*wedge*-trp$_4$ in a 80/20 water/methanol solvent system.

Dendrimer	Langmuir Adsorption Theory		
	$K_L N$ (lg^{-1})	N (mol.g^{-1})	K_L (M^{-1})
1) Hex-*wedge*-trp$_4$, 80/20 methanol/water	6.51x10^{-3}	7.94x10^{-7}	8.2x10^3
2) Hex-*wedge*-trp$_4$, pure methanol system	1.2x10^{-2}	6.94x10^{-7}	1.73x10^4

Table 4.6 K_L and N values for Hex-*wedge*-trp$_4$ in 1) 80/20 methanol/water and 2) pure methanol solvent systems at 293K.

From the values of K_L the value of ΔG° can be calculated from the equation

$$\Delta G^\circ = -RT \ln K_L$$

This gives the value of ΔG° for Hex-*wedge*-trp$_4$ in the 80/20 methanol/water solvent system as -21kJmol^{-1}, where T = 293K and R = 8.315JK^{-1}mol^{-1}.

As can be seen in Figure 4.18, compared to Hex-*wedge*-trp$_4$ in the pure methanol system, there has not been a significant increase in the amount of Hex-*wedge*-trp$_4$ adsorbed onto the cotton surface in the mixed solvent system. Interestingly, the N values indicate that there are more sites per gram of cotton which can accommodate Hex-*wedge*-trp$_4$ present in the mixed solvent system. This is consistent with the assumption that parts of the original surface have been exposed by solvent (water) penetration. Although there are more sites available, the K_L value implies that there are relatively fewer sites available for Hex-

wedge-trp$_4$ in the mixed solvent system being occupied compared to Hex-*wedge*-trp$_4$ in the pure methanol solvent system. This suggests that although water is able to penetrate into the cotton surface exposing new parts of the original surface, uncovering new unoccupied sites available for adsorption by probe molecules, there is strong competition for the occupancy of these new sites from solvent (water) molecules. These observations are consistent with the formation of multi-layers in this case. The $\Delta G^\ominus$ values calculated for Hex-*wedge*-trp$_4$ in the two solvent systems suggest that the free energy of adsorption is marginally more favourable in pure methanol (-24kJmol^{-1}) than in the mixed methanol/water solvent system (-21kJmol^{-1}).
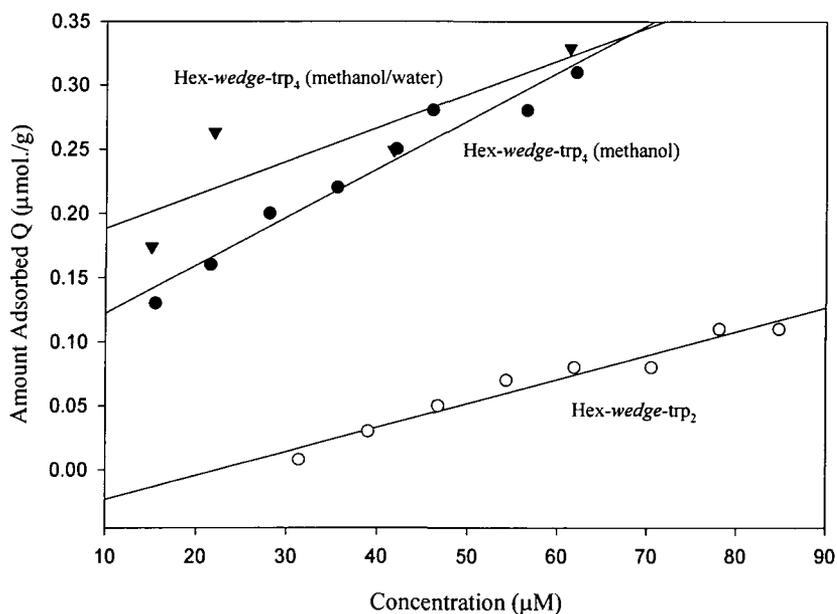
Figure 4.18 Comparison of the amount of probe molecule adsorbed at low concentration for Hex-*wedge*-trp$_2$ and Hex-*wedge*-trp$_4$ in pure methanol and Hex-*wedge*-trp$_4$ in 80/20 methanol/water .

Thus, in summary, these results lead to the conclusion that both Hex-*wedge*-trp$_2$ and Hex-*wedge*-trp$_4$ adsorb from methanol solution onto a cotton surface in a typical Langmuir fashion. That is to say that the probe adsorbs at a free site independent of whether the adjacent site is occupied or not. Hex-*wedge*-trp$_4$ is more effectively adsorbed than Hex-*wedge*-trp$_2$ but neither probe is strongly adsorbed. Changing the solvent from methanol to methanol/water (80/20) makes little or no difference. The one positive conclusion which can be drawn from this work is that probe design (Hex-*wedge*-trp$_4$ is better than Hex-*wedge*-trp$_2$) has an influence on adsorption efficiency. Unfortunately, since both molecules are insoluble in water, the hydrophile/hydrophobe balance in the probe molecule falls too heavily on the hydrophobe side to make this system capable of yielding more interesting results. The primary purpose of this work was to design, make, characterise and test possible probe molecules based on dendrimer wedges terminated with amino acids carrying potential cellulose surface recognition residues. These results were obtained with tryptophan terminated wedges, time did not allow investigation of the other probe molecules prepared but these molecules have been passed on to the sponsors for further study. The results obtained provide a partial validation of the concept on which the work reported in this thesis is based.

4.4 In Vitro Anti-Stain Studies

4.4.1 Introduction

In this study various generations of unfunctionalised dendrimer wedges with a siloxysilane group at the focus, (Si-*wedge*-$(NH_2)_n$), and primary amine end groups were tested as possible stain inhibitors for polar surfaces; for example, for potential use as additives in toothpaste formulations. This is a different test of the concept on which the work described in this thesis is based.

4.4.2 Experimental

All experimental procedures were carried out in the Dental Section of Unilever Exploratory Division, Port Sunlight laboratories. All materials and organic reagents were supplied by Unilever and used without further purification. Lightness values were recorded on a Minolta CR-300 series Colorimeter.

4.4.3 General procedure for Anti-Stain Assay.

The anti-stain assays were carried out on hydroxyapatite discs that were initially 'roughened' on a piece of P600 wet-dry sandpaper to achieve baseline whiteness. The discs were incubated at 37^0C in sterile saliva for a 24 hour period and then treated with approximately $200\mu l$ of a 3% dendrimer wedge solution in ethanol or left untreated to act as the control. After rinsing with water and blotting gently with tissue the discs were allowed to air dry and their initial L*, a*, and b* lightness values (see later) were measured on a chromameter CR-300. The discs were then submersed into a 1% tea / 1% coffee / 0.2% ferrous

ammonium sulphate aqueous solution. The discs were removed from the stain broth at set times, rinsed with water, and, after blotting gently with tissue, allowed to air dry and their corresponding L*, a*, and b* values measured.

4.4.4 L*a*b* Colour Space

Colour space is a method for expressing the colour of an object or a light source using a numerical notation. The L*a*b* colour space is presently one of the most popular colour spaces for measuring object colour and is widely used in virtually all fields associated with personal products. It is one of the uniform colour spaces defined by the Commission Internationale de l'Eclairage (CIE) in 1976, for expressing the colour of an object numerically to provide clear definitions of colour differences in relation to visual differences.
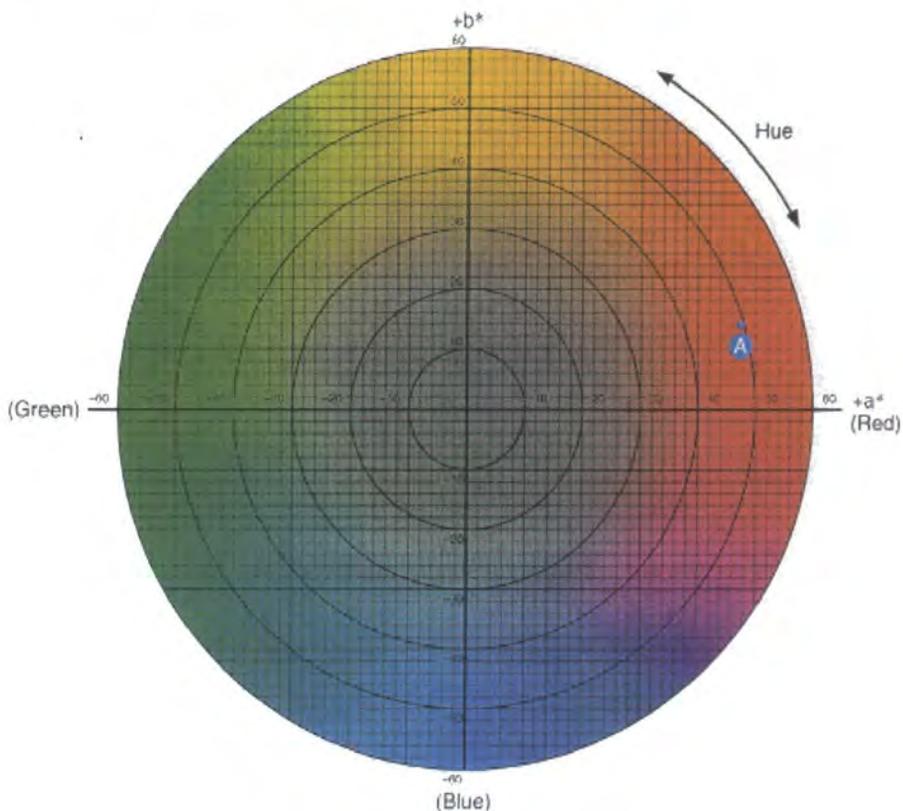
Figure 4.19 a*,b* chromaticity diagram.

In this colour space, L* indicates lightness and a* and b* are the chromaticity coordinates. Figure 4.19 shows the a*, b* chromaticity diagram. In this diagram the a* and b* indicate colour directions: +a* is the red direction, -a* is the green direction, +b* is the yellow direction, and -b* is the blue direction. The centre is achromatic; as the a* and b* values increase and the point moves out from the centre, the saturation of the colour increases. Figure 4.21 is a representation of the colour solid for the L*a*b* colour space. Figure 4.19 is a view of this solid cut horizontally at a constant L* value. For instance, if a "red apple" is measured using the L*a*b* colour space, specific numerical values are produced (L=43.31, a= +47.63, b= +14.12) and to see what colour these values represent the a* and b* values found are plotted on the a*,b* chromaticity diagram in Figure 4.19 to obtain point A, which shows the chromaticity of the apple. Consequently, if the colour solid of Figure 4.21 is cut vertically through point A and the centre, a view of chromaticity versus lightness is obtained, part of which is shown in Figure 4.20 below.
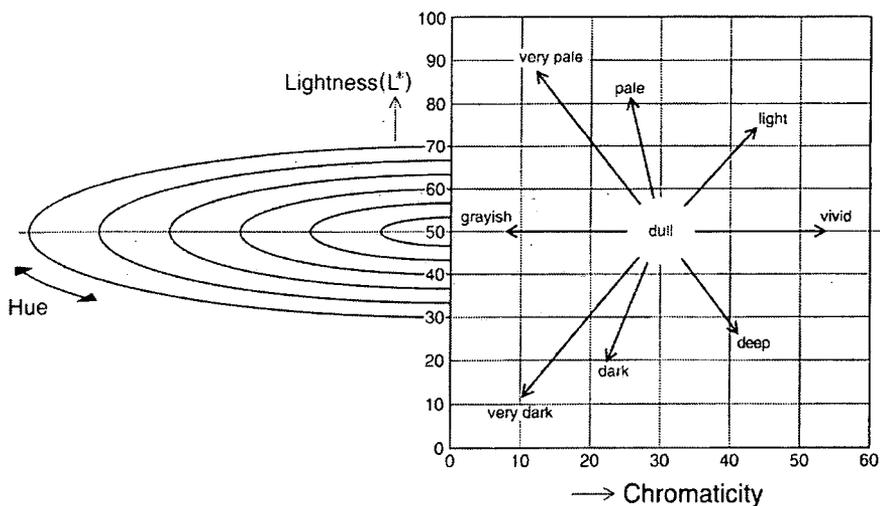
Figure 4.20 Relationship between chromaticity and lightness.
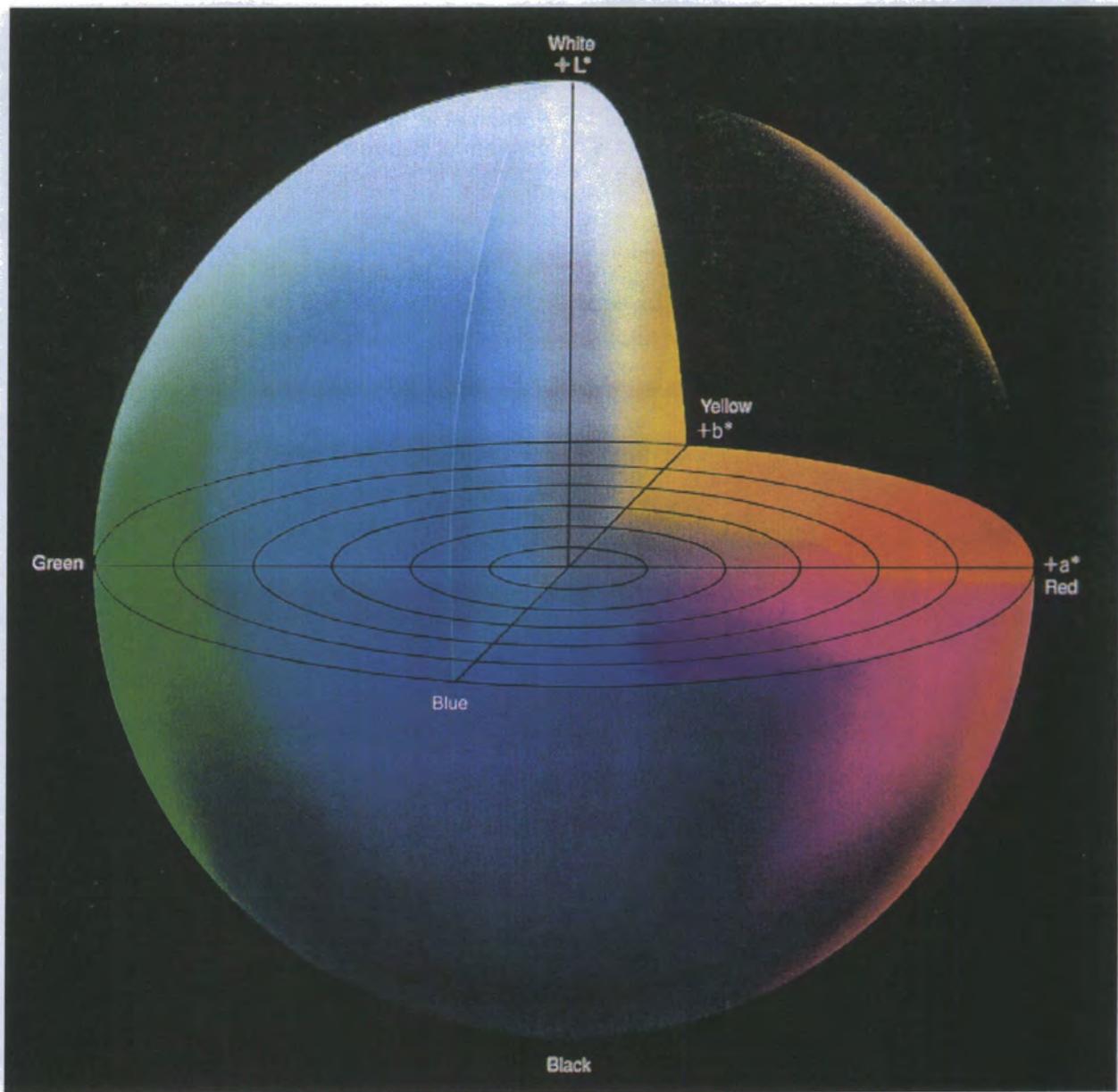
Figure 4.21 Representation of the colour solid for L*a*b* colour space.

4.4.5 Results

Control discs			Si-*wedge*-$(NH_2)_2$			Si-*wedge*-$(NH_2)_4$		
$\overline{L}_0^*$	a_0^*	b_0^*	$\overline{L}_0^*$	a_0^*	b_0^*	$\overline{L}_0^*$	a_0^*	b_0^*
93.34	+0.26	+2.85	93.90	+0.23	+2.42	94.69	+0.22	+1.63
94.21	+0.30	+2.16	93.44	+0.29	+2.60	93.89	+0.33	+2.15
94.00	+0.33	+2.16	93.42	+0.21	+2.86	94.28	+0.39	+1.98
94.03	+0.35	+1.74	94.18	+0.35	+1.93	94.82	+0.25	+0.25
94.15	+0.22	+2.14	93.96	+0.37	+2.31	95.32	+0.34	+1.13
93.82	+0.27	+2.63	93.84	+0.23	+2.29	95.44	+0.25	+2.19
93.90	+0.31	+2.27	94.25	+0.37	+1.81	94.15	+0.28	+1.69

Table 4.7. Initial L*a*b* lightness values (Day 0) for hydroxyapetite discs prior to treatment with dendrimer wedge solution and submersion in synthetic stain solution.

Control discs			Si-*wedge*-$(NH_2)_2$			Si-*wedge*-$(NH_2)_4$		
$\overline{L}_1^*$	a_1^*	b_1^*	$\overline{L}_1^*$	a_1^*	b_1^*	$\overline{L}_1^*$	a_1^*	b_1^*
53.74	+2.41	+17.93	23.85	+1.00	+4.46	66.67	-0.03	+9.37
56.80	+2.16	+17.57	30.76	+0.95	+7.61	65.02	+0.03	+10.08
55.96	+2.18	+17.58	18.62	+0.31	+0.63	62.12	-0.17	+9.69
59.41	+2.09	+17.46	19.22	+0.85	+3.45	66.67	+0.05	+9.78
56.04	+2.20	+18.03	29.52	+0.62	+5.93	64.76	-0.20	+8.96
54.18	+2.34	+17.97	38.20	+2.19	+8.78	67.90	+0.07	+9.47
54.15	+2.29	+17.80	19.40	+0.61	+3.28	62.49	-0.10	+9.71

Table 4.8. L*a*b* lightness values (Day 1) for hydroxyapetite discs with no dendrimer wedge surface layer (control) and discs treated with Si-*wedge*-$(NH_2)_n$ after 23 hours in synthetic stain solution.

Control discs			Si-*wedge*-$(NH_2)_2$			Si-*wedge*-$(NH_2)_4$		
$\overline{L}_2{}^*$	$a_2{}^*$	$b_2{}^*$	$\overline{L}_2{}^*$	$a_2{}^*$	$b_2{}^*$	$\overline{L}_2{}^*$	$a_2{}^*$	$b_2{}^*$
48.88	+3.45	+18.45	19.02	+1.24	+5.57	60.18	+0.74	+10.92
52.02	+3.28	+18.55	28.75	+0.97	+7.85	58.98	+0.77	+11.29
51.23	+3.29	+18.33	16.20	+0.52	+2.09	58.53	+0.57	+10.81
54.55	+3.12	+18.48	21.34	+0.90	+5.19	60.64	+0.66	+10.81
50.93	+3.33	+18.74	19.70	+0.58	+3.30	61.61	+0.37	+10.01
49.55	+3.43	+18.53	29.08	+1.18	+7.01	60.84	+0.72	+11.22
50.25	+3.11	+18.07	31.01	+0.93	+7.70	59.09	+0.49	+10.67

Table 4.9. L*a*b* lightness values (Day 2) for hydroxyapetite discs with no dendrimer wedge surface layer (control) and discs treated with Si-*wedge*-$(NH_2)_n$ after 51 hours in synthetic stain solution

Control discs			Si-*wedge*-$(NH_2)_2$			Si-*wedge*-$(NH_2)_4$		
$\overline{L}_3{}^*$	$a_3{}^*$	$b_3{}^*$	$\overline{L}_3{}^*$	$a_3{}^*$	$b_3{}^*$	$\overline{L}_3{}^*$	$a_3{}^*$	$b_3{}^*$
47.30	+3.74	+18.37	30.70	+0.66	+7.72	58.41	+1.00	+12.07
49.92	+3.54	+18.45	32.59	+0.94	+8.76	57.93	+1.03	+12.21
49.47	+3.64	+18.54	29.87	+0.58	+6.82	57.08	+0.88	+11.90
53.41	+3.36	+18.72	27.46	+0.72	+6.79	59.00	+1.02	+12.21
49.32	+3.68	+18.95	37.90	+1.01	+9.08	60.26	+0.68	+11.06
47.90	+3.75	+18.49	30.33	+1.14	+8.27	58.77	+1.03	+12.18
48.26	+3.57	+18.32	31.28	+1.20	+8.92	57.77	+0.74	+11.85

Table 4.10 L*a*b* lightness values (Day 3) for hydroxyapetite discs with no dendrimer wedge surface layer (control) and discs treated with Si-*wedge*-$(NH_2)_n$ after 74 hours in synthetic stain solution.

The ΔL^* values for each day are then calculated from equation 1 and from these values the mean change in L^* for each day is calculated and plotted against the corresponding day, see Figure 4.21.

$$\Delta L^* = \overline{L_0}^* - \overline{L_t}^* \quad \text{equation (1)} \quad \text{where } t = \text{time in days.}$$

Control discs	Si-*wedge*-$(NH_2)_2$	Si-*wedge*-$(NH_2)_4$
ΔL_1^*	ΔL_1^*	ΔL_1^*
39.59	70.05	28.02
37.40	62.68	28.87
38.04	74.79	32.16
34.62	74.96	28.15
38.11	64.44	30.56
39.63	55.64	27.54
39.75	74.85	31.66
SD 1.82	7.52	1.87

Table 4.11. Day 1: Change in lightness values (ΔL^*) for hydroxyapatite discs after 23 hours in synthetic stain solution compared to values taken on day 0.

Control discs	Si-*wedge*-$(NH_2)_2$	Si-*wedge*-$(NH_2)_4$
ΔL_2^*	ΔL_2^*	ΔL_2^*
44.45	74.88	34.51
42.19	64.69	34.90
42.76	77.22	35.75
39.47	72.84	28.15
43.22	74.25	33.71
44.27	64.75	34.60
43.65	63.24	35.06
SD 1.69	5.82	2.57

Table 4.12. Day 2. Change in lightness values (ΔL^*) for hydroxyapatite discs after 51 hours in synthetic stain solution compared to values taken on day 0.

Control discs	Si-*wedge*-$(NH_2)_2$	Si-*wedge*-$(NH_2)_4$
ΔL_3^*	ΔL_3^*	ΔL_3^*
46.03	63.20	36.28
44.29	60.85	35.96
44.53	63.54	37.20
40.61	66.72	35.82
44.82	56.05	35.05
45.92	63.50	36.67
45.64	62.97	36.38
SD 1.87	3.29	0.68

Table 4.13. Day 3. Change in lightness values (ΔL^*) for hydroxyapatite discs

after 74 hours in synthetic stain solution compared to values taken on day 0.

	CONTROL	Si-*wedge*-$(NH_2)_2$	Si-*wedge*-$(NH_2)_4$
	$\Delta \bar{L}^*$	$\Delta \bar{L}^*$	$\Delta \bar{L}^*$
DAY 1	38.17	68.20	29.57
DAY 2	42.86	70.27	33.81
DAY 3	44.55	62.41	36.20
$\bar{X}$	41.86	66.96	33.19

Table 4.14. Summary of mean lightness change, $\Delta \bar{L}^*$, on hydroxyapatite discs

for each day.
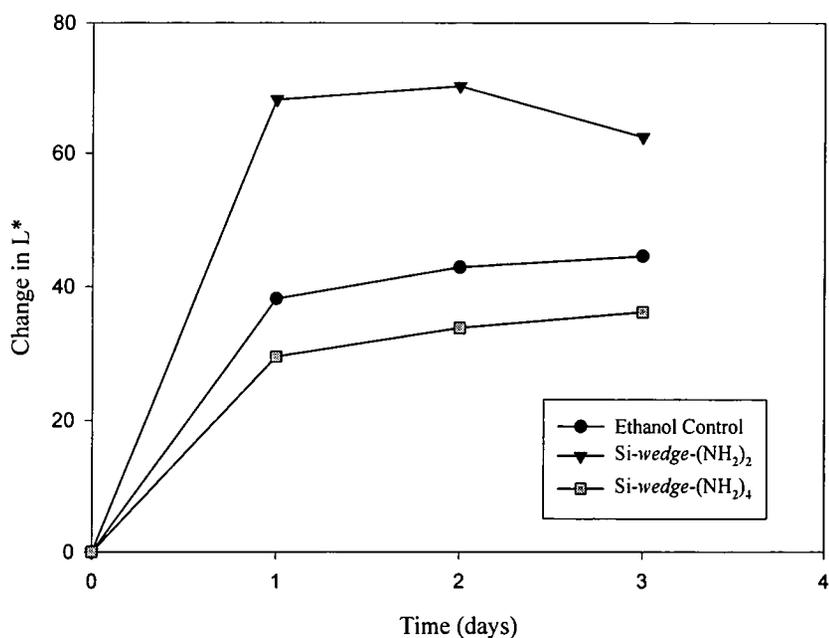
Figure 4.21. Mean lightness change as a function of time for Si-*wedge*-$(NH_2)_2$

and Si-*wedge*-$(NH_2)_4$ dendrimer wedges on hydroxyapatite discs.

A second study was carried out using the starting material for wedge formation, 3-aminopropyltris(trimethylsiloxy)silane (APTTMSS) possessing a single amine end group, and comparing this to Si-*wedge*-$(NH_2)_2$ and Si-*wedge*-$(NH_2)_4$ dendrimer wedges possessing two and four amine end groups respectively. Using fresh discs and following the same procedures as outlined previously the results are summarised in Figure 4.22 (Experimental data can be found in Appendix 3). At the end of the assay, day three, the discs were brushed with Signal 5s toothpaste and their corresponding lightness values compared.
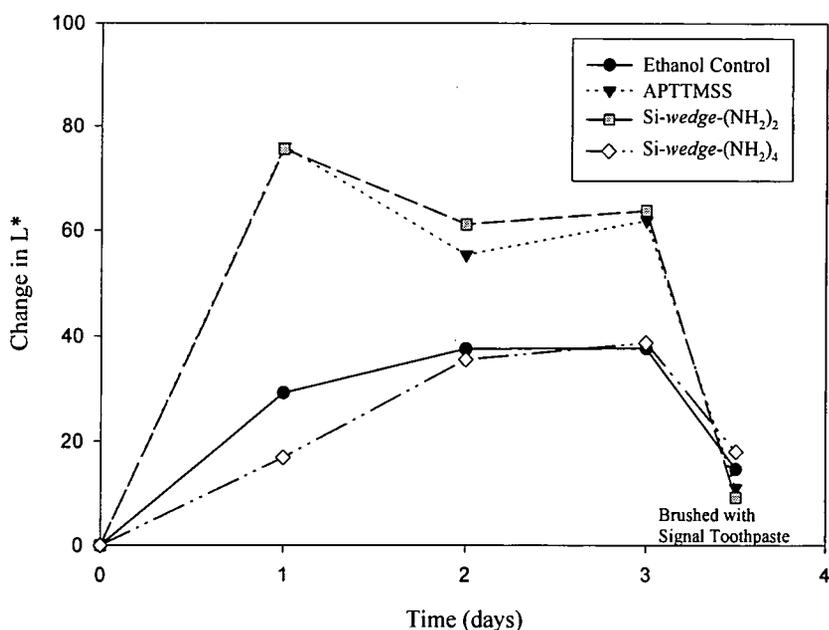
Figure 4.22. Mean lightness change as a function of time for APTTMSS, Si-*wedge*-(NH$_2$)$_2$ and Si-*wedge*-(NH$_2$)$_4$; the discs were brushed on day 3 with Signal 5S Toothpaste.

4.4.6 Interpretation of results.

From a comparison of the two graphs a number of trends can be observed which are related to the specific generation (number of end groups) of the two dendrimer wedges tested, and which may be related to the possible molecular orientation of the molecules on the surface.

APTTMSS and the smaller first generation dendritic wedge, having one and two amine end groups respectively, behave similarly in both experiments, attracting stain molecules. This suggests that the polar staining materials are being attracted to a surface which is more polar than that of the untreated hydroxyapatite disc. This may be explained in terms of the hydrophobic/hydrophilic balance of the adsorbed layer. In these small molecule examples the hydrophobic

195

tris(trimethyl)siloxysilane is roughly the same size as the hydrophilic end groups of the wedge. Represented schematically in Figure 4.23, the molecules are adsorbed with the hydrophobic siloxysilyl group down onto the surface with the hydrophilic amine groups pointing away from the surface thus attracting stain molecules.
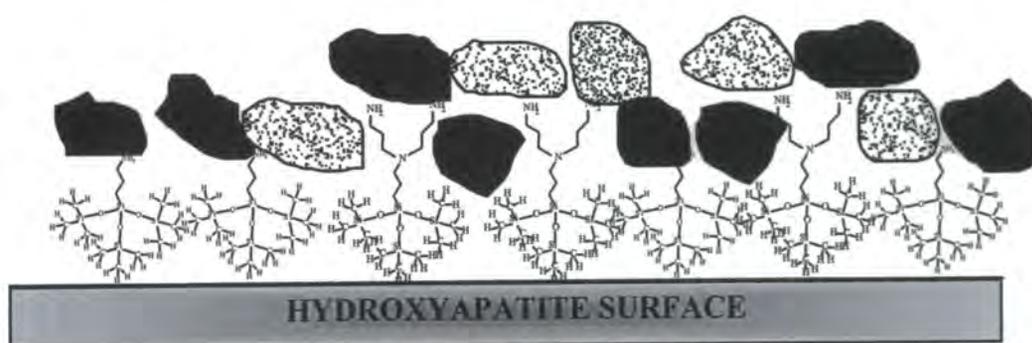
Figure 4.23. Schematic representation of the orientation of APTTMSS and Si-*wedge*-(NH$_2$)$_2$ at the hydroxyapatite surface.

The 2nd generation Si-*wedge*-(NH$_2$)$_4$ with four amine end groups seems to be the size at which the number and strength of surface interactions is sufficient to orient the molecule with the bulky hydrophobic group pointing away from the surface consequently blocking bombarding stain molecules from reaching the surface. Therefore, when the discs are removed from the stain broth and rinsed with water, the polar stain molecules are washed off resulting in a lighter, cleaner, disc surface as compared to the discs treated with the smaller generation

dendrimer wedges and the untreated discs (control) which have a covering of stain molecules, see Figure 4.25. However, the discs with a layer of Si-*wedge*-$(NH_2)_4$ on the surface did show a change in lightness value corresponding to the attraction of a small amount of stain molecules. This is due to the fact that not all of the dendrimer molecules will be orientated in the same way, a few will have the hydrophobic group adsorbed down onto the surface with their hydrophilic, and hence stain attracting, parts pointing away from the surface, as shown schematically in Figure 4.24. The results of the second study from Figure 4.22, after day one, showed that Si-*wedge*-$(NH_2)_4$ had little effect behaving similarly to the control. This could be possibly due to the dendrimer wedge being rinsed off the disc on work up prior to analysis.
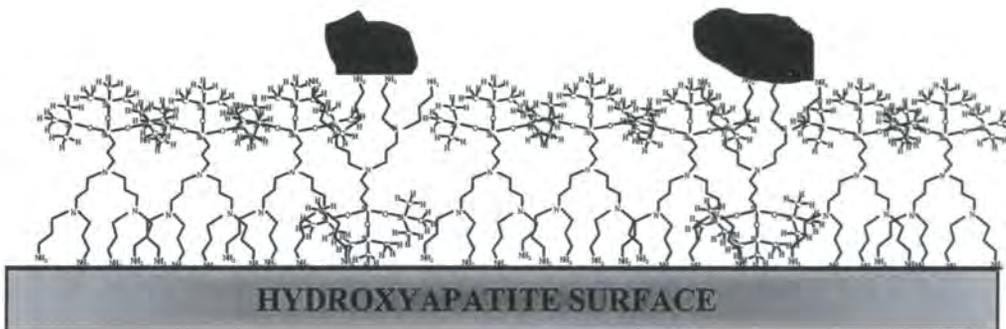
Figure 4.24 Schematic representation of the orientation of Si-*wedge*-$(NH_2)_4$ at the hydroxyapatite surface.

On brushing with Signal toothpaste all discs showed considerable improvement in lightness values, particularly the smaller generations, the flaky black stain deposits were easy to remove giving the cleanest discs after brushing, see Figure 4.22.
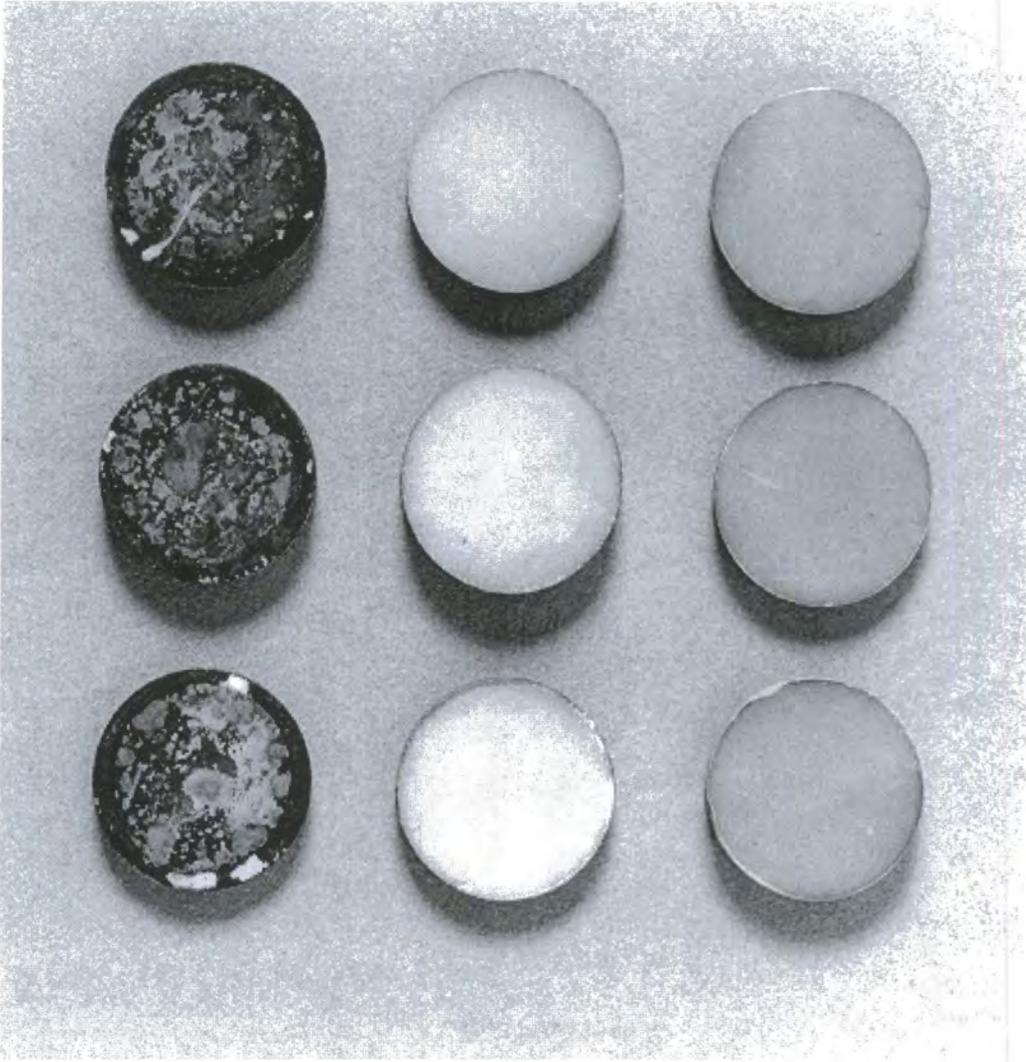
Figure 4.25. Hydroxyapatite discs after 3 days in synthetic stain solution.

Left to right;

1. 1st Generation : Si-wedge-$(NH_2)_2$

2. 2nd Generation : Si-wedge-$(NH_2)_4$

3. Ethanol Control

Thus, in summary, these results lead to the conclusion that both the starting material, APTTMSS, and the first generation siloxysilane dendrimer, Si-*wedge-*

$(NH_2)_2$, modify a hydroxyapatite surface in a way that creates a more polar surface due to the observation seen by an increased attraction of polar staining molecules. This is apparent from the appearance of the surface of hydroxyapatite discs treated with these materials which are highly stained and covered in a thick flakey layer of stain deposits compared to the untreated control discs which are considerably lighter. In comparison, Si-*wedge*-$(NH_2)_4$ with four amine end groups, show the opposite effect to Si-*wedge*-$(NH_2)_2$ and APTTMSS apparently blocking the majority of stain molecules from reaching the surface evident from the lighter appearance of corresponding hydroxyapatite discs treated and having a surface layer of Si-*wedge*-$(NH_2)_4$, see Figure 4.25. This could be explained in terms of the number and strength of surface interactions of the various siloxysilane molecules tested in relation to their specific orientation on the hydroxyapatite surface. APTTMSS and Si-*wedge*-$(NH_2)_2$, have one and two amine end groups respectively and the attraction between these hydrophilic polar end groups with the hydroxyapatite polar surface by electrostatic or hydrogen bonding was not sufficient to overcome adsorbtion by the bulky hydrophobic siloxysilyl group onto the surface. Consequently, APTTMSS and Si-*wedge*-$(NH_2)_2$, are orientated with their hydrophilic polar end groups pointing away from the surface therefore attracting polar stain molecules. In contrast, Si-*wedge*-$(NH_2)_4$ possesses the number and strength of surface interactions to orient the molecule with the bulky hydrophobic siloxysiyl group pointing away from the surface with its hydrophilic amine end groups attracted to the polar hydroxyapatite surface. This was due to the hydrophilic/hydrophobic balance of Si-*wedge*-$(NH_2)_4$ in favour of hydrophilicity due to the increased number of polar

amine end groups and larger size of the hydrophilic "footprint" producing stronger electrostatic and hydrogen bonding capabilities with the surface groups on the hydroxyapatite surface.

4.5 References

[1] Tomme, P., Warren, R.A.J., Gilkes, N.R. *Adv. Microb. Physiol.* (**1995a**), 1

[2] Henrissat, B., *Cellulose 1*, (**1994**), 169

[3] Khosdel, E., Warr, J., and Hopkinson, A., Unilever Research Port Sunlight workers, personal communication.

[4] Tomme, P., Warren, R.A.J., Miller, R. C., Jr., Kilburn, D.G., Gilkes, N.R. *in Enzymatic Degradation of Insoluble Polysaccharides* (**1995b**) 142

[5] Teeri, T., Reinikainen, T., Ruohonen, L., Jones, T.A., Knowles, J.K.C. *J. Biotechnol.* 24 (**1992**), 169

[6] Ong, E., Gilkes, N.R., Miller, R.C., Jr., Warren, R.A.J., Kilburn, D.G., *Biotechnol. Bioeng.* 42 (**1993**) 401

[7] Millward-Sadler, S.J., Poole, D.M., Henrissat, B., Hazlewood, G.P., Clarke, J.H., Gilbert, H.J., *Mol. Microbiol.* 11 (**1994**) 375

[8] Johnson, P.E., Tomme, P., Joshi, M.D., McIntosh, L.P., *Biochemistry* 35 (**1996**) 13895

[9] Tomme, P., Gilkes, N.R., Miller, R. C., Jr., Warren, R.A.J., Kilburn, D.G., *Protein Eng.* 7 (**1994**) 117

[10] Kraulis, P.J., Clore, G.M., Nilges, M., Jones, T. A., Petterson, G., Knowles, J., Gronenborn, A.M., *Biochemistry* 28 (**1989**) 7241

[11] Xu, G.Y., Ong, E., Gilkes, N.R., Kilburn, D.G., Muhandiram, D.R., Harris-Brandts, M., Carver, J.P., Kay, L.E., Harvey, T.S., *Biochemistry* 34 (**1995**) 6993

[12] Linder, M., Mattinen, M.L., Kontteli, M., Lindberg, G., Ståhlberg, J., Drakenberg, T., Reinikainen, T., Pettersson, G., Annila, A., *Protein Sci.*, 4 (**1995**) 1056

[13] Din, N., Forsythe, I.J., Burtnick, L.D., Gilkes, N.R., Miller, R.C.J., Warren, R.A.J., Kilburn, D.G., *Mol. Microbiol.* 11 (**1994**) 747

[14] Creagh, A.L., Ong, E., Jervis, E., Kilburn, D.G., Haynes, C.A. *Proc. Natl. Acad. Sci. U.S.A,* 93 (**1996**) 12229

[15] Vyas, N.K., *Curr. Opin. Struct. Biol.* 1 (**1991**) 732

[16] Ainsworth, R.L., PhD Thesis, Durham University, 1997.

[17] Giles, C.H., MacEwan, T.H., Nakhwa, S.N., Smith, D., *J. Chem. Soc.* (**1960**) 3973

[18] Giles, C.H., Smith, D., Huitson, A., *J. Colloid Interface Sci.* 47 (**1974a**) 755

[19] Adamson, A.W., "Physical Chemistry of Surfaces", 4th Edn., (**1982**) Chapter 11, Wiley Interscience.

[20] Atkins, P.W., "Physical Chemistry," 4th Edn., (**1990**) Chapter 17, Oxford University Press

[21] Hopkinson, A., Unilever Research worker - personal communication.

[22] Klenkova, N.I., Ivaskin, G.P., *J. Appl. Chem., USSR* 36, (**1963**), 378.

Chapter 5

Overall Conclusions and Proposals for Future Work

.

5.1 Overall Conclusions

The divergent synthesis and characterisation of poly(propyleneimine) dendrimer wedges starting from hexylamine, heptylamine, octylamine, tert-octylamine and 3-aminopropyltris(trimethylsiloxy)silane (APTTMSS) has been successfully achieved. It was found that the hydrophobic foci became increasingly soluble in water with the attachment of successive amine terminated dendrimer wedge generations. Repetitive reaction sequences for dendrimer wedge formation employed successive cyanoethylation and reduction steps. Large scale heterogeneous reduction of nitrile to primary amine end groups using Raney nickel was performed. Optimisation of the reaction conditions produced high yields at lower generations but by-products were evident in increasing amounts in the synthesis of the higher generations resulting in low yields even in the presence of an ammonia solution. Small scale homogeneous hydrogenations utilising diisobutylaluminiumhydride (DIBAL-H) gave wedges in high yields with minimal side reactions.

End group modification of hexylamine and APTTMSS amine terminated dendrimer wedges was performed by coupling L-tyrosine, L-tryptophan and L-phenylalanine benzyloxycarbonyl (CBZ) N-protected amino acid residues at the amine termini. Standard conditions for peptide bond formation were employed and coupling proceeded efficiently via the hydroxysuccinimide or p-nitrophenol activated ester of the N-CBZ-L amino acid. Successful deprotection of the N-CBZ protecting group was achieved using the technique of Catalytic Transfer Hydrogenation (CTH) reforming the primary amine end group at the periphery of the wedge structure. Amino acid functionalised dendrimer wedges were fully

characterised and pure materials were produced in high yields as confirmed by the single peaks observed in their corresponding MALDI-TOF mass spectra. They were however hygroscopic which, in most cases, inhibited obtaining good elemental analysis results. Unfortunately, it was found that the hydrophobic/hydrophilic balance of **all** the amino acid dendrimer wedges carrying aliphatic or APTTMSS units at the focus was not sufficiently weighted in favour of hydrophilicity for the molecules to be water soluble. Therefore the surface active properties of the APTTMSS probe and hence the quantitative measurement of molecular recognition at a cotton surface in an aqueous media could not be tested via submersion contact angle measurements, which was the technique originally envisaged. As an alternative, due to the U.V. active properties of the amino acid residues it was possible to test the basic concept of cotton recognition for hexylamine tryptophan wedges in organic and a mixed organic/aqueous solvent system from U.V. depletion studies.

Tryptophan terminated wedges were found to have a wavelength of maximum absorbance (λ_{max}) at 282nm in pure methanol and 80:20 methanol/water solutions and extinction coefficients suitable for surface adsorption studies to be performed. Experiments were carried out on a pre-treated cotton surface and corresponding adsorption isotherms were produced. Hex-*wedge*-trp$_2$ and Hex-*wedge*-trp$_4$ show characteristic L2 shaped isotherms in pure methanol solution indicative of Langmuir adsorption. Hex-*wedge*-trp$_4$ is significantly more effectively adsorbed onto the cotton surface possibly due to the increased number and perhaps more appropriate orientation of the four tryptophan amino acid residues, the "footprint", on the cotton surface, however, the adsorption observed

was at relatively low levels in both cases. Interestingly, Hex-*wedge*-trp$_4$ in the methanol/water solvent system has an adsorption isotherm characteristic of L4 or L5 Langmuir isotherms. This can be explained due to parts of the original cotton surface being exposed by solvent (water) penetration. Strong competition for the occupancy of new and existing sites from water molecules is consistent with multi-layer formation as observed.

Each isotherm obeyed Langmuir adsorption theory, especially at low concentration, and the equilibrium constant for the adsorption process and hence the free energy of adsorption was calculated. This showed that the adsorption process (ΔG°) for Hex-*wedge*-trp$_4$ (-24kJmol^{-1}) was more favourable than Hex-*wedge*-trp$_2$ (-19kJmol^{-1}) in methanol, and marginally better than Hex-*wedge*-trp$_4$ (-21kJmol^{-1}) in the methanol/water solvent solution.

An investigation into the modification of polar surfaces by Si-*wedge*-(NH$_2$)$_n$ dendrimer wedge molecules was performed to establish their possible use as anti-staining agents in toothpaste formulations. It was found that Si-*wedge*-(NH$_2$)$_4$ possessed the required number and strength of surface interactions to orient the molecule with the bulky hydrophobic siloxysilyl group pointing away from the hydroxyapatite surface hence blocking incoming stain molecules from reaching the modified surface whereas APTTMSS and Si-*wedge*-(NH$_2$)$_2$ showed opposite orientations at the surface attracting stain molecules.

In conclusion, preliminary studies have established the synthetic pathway for the successful syntheses of amino acid terminated dendrimer wedges derived from various foci but in their present form the materials are not water soluble. U.V. depletion studies have provided preliminary indications of the likely optimum

number of tryptophan amino acid residues, the "footprint", for recognition on a cotton surface. Due to the time constraints on the duration of experimental work during the course of this study, not all the potential probe molecules produced have been investigated for their surface recognition behaviour; however, the samples have been passed onto Unilever Research for further studies.

5.2 Proposals for future work

It may prove possible to alter the hydrophobic/hydrophilic balance of the functionalised wedges for solubility in water by initiating further iterative steps for dendrimer wedge synthesis starting from the free primary amine group of the terminal amino acid residue. It would then be interesting to establish if there was any increased recognition of such species in water onto a cotton surface compared to those discussed in this work.

The use of Raney cobalt as the reduction catalyst might be beneficial for the synthesis of high generation dendrimer wedges with the possibility of achieving higher yields and hence ease of purification of the amine terminated wedges. It should also be possible to synthesise Si-*wedge*-$(NH_2)_n$ wedges on a large scale using Raney cobalt due to the omission of strong base from the reaction medium.

The tyrosine and phenylalanine modified wedges synthesised in this work should be assessed for any cotton recognition for a comparison with the tryptophan wedges tested in this study. Initial studies were carried out during the course of this work (not reported in detail here) on the attachment of L-aspartic acid and phosphoserine to hexylamine wedges. A synthetic strategy was

established and indeed, after deprotection, aspartic acid possessing two primary amine and two carboxylic acid end groups was successfully attached to Hex-*wedge*-$(NH_2)_2$. Although it was not comprehensively characterised it was submitted for initial testing at the Unilever research laboratories. These types of molecules might prove interesting due to their possible novel crystal habit modification of calcium carbonate for use industrially as possible anti-scale or anti-fouling agents.

Unsuccessful attempts were made to synthesise APTTMSS via the hydrosilylation of tris(trimethylsiloxy)silane with allylamine using hexachloroplatinic acid and a synthesised Rhodium oligomeric catalyst, ([Rh(μ - PPh$_2$)(COD)]$_2$). If the reaction conditions can be optimised it may prove possible to use these conditions for the synthesis of the tristris analogue, tris[tris(trimethylsiloxy)]silane propylamine as a starting material for dendrimer wedge formation. Such a molecule might be interesting for the modification of polar surfaces, although it might prove necessary to go to high generations before the hydrophobe/hydrophile balance was in favour of water solubility.
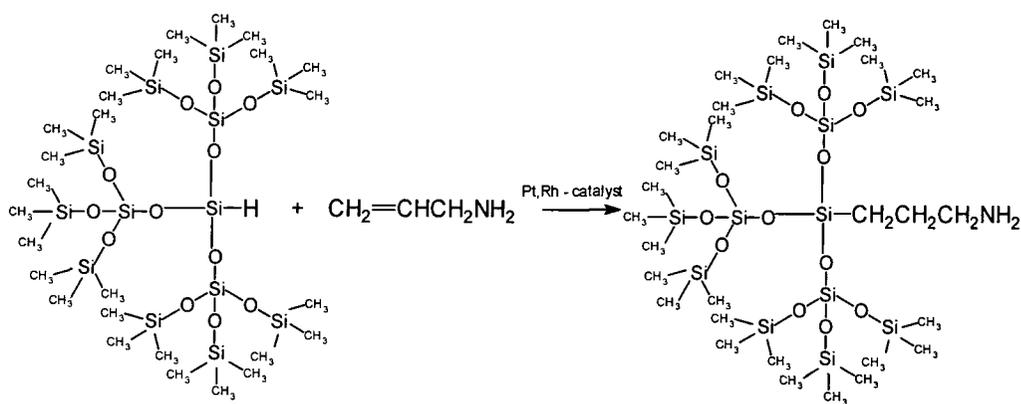
Figure 5.1 Postulated synthetic pathway for the synthesis of tris[tris(trimethylsiloxy)]silane propylamine.

Appendix 1

Analytical Data for Chapter 2

Appendix 1.1 FTIR spectra

Appendix 1.2 ^{1}H nmr spectra

Appendix 1.3 ^{13}C nmr spectra

Appendix 1.4 DEPT nmr spectra

Appendix 1.5 MALDI-TOF mass spectra

Appendix 1.1.1 FTIR spectrum of Hex-*wedge*-(CN)$_2$.

Peaks: 726.4, 1029.8, 1099.5, 1138.0, 1377.1, 1420.9, 1465.9, 2247.1, 2856.0, 2854.5

%T axis: 67.59 to 121.57
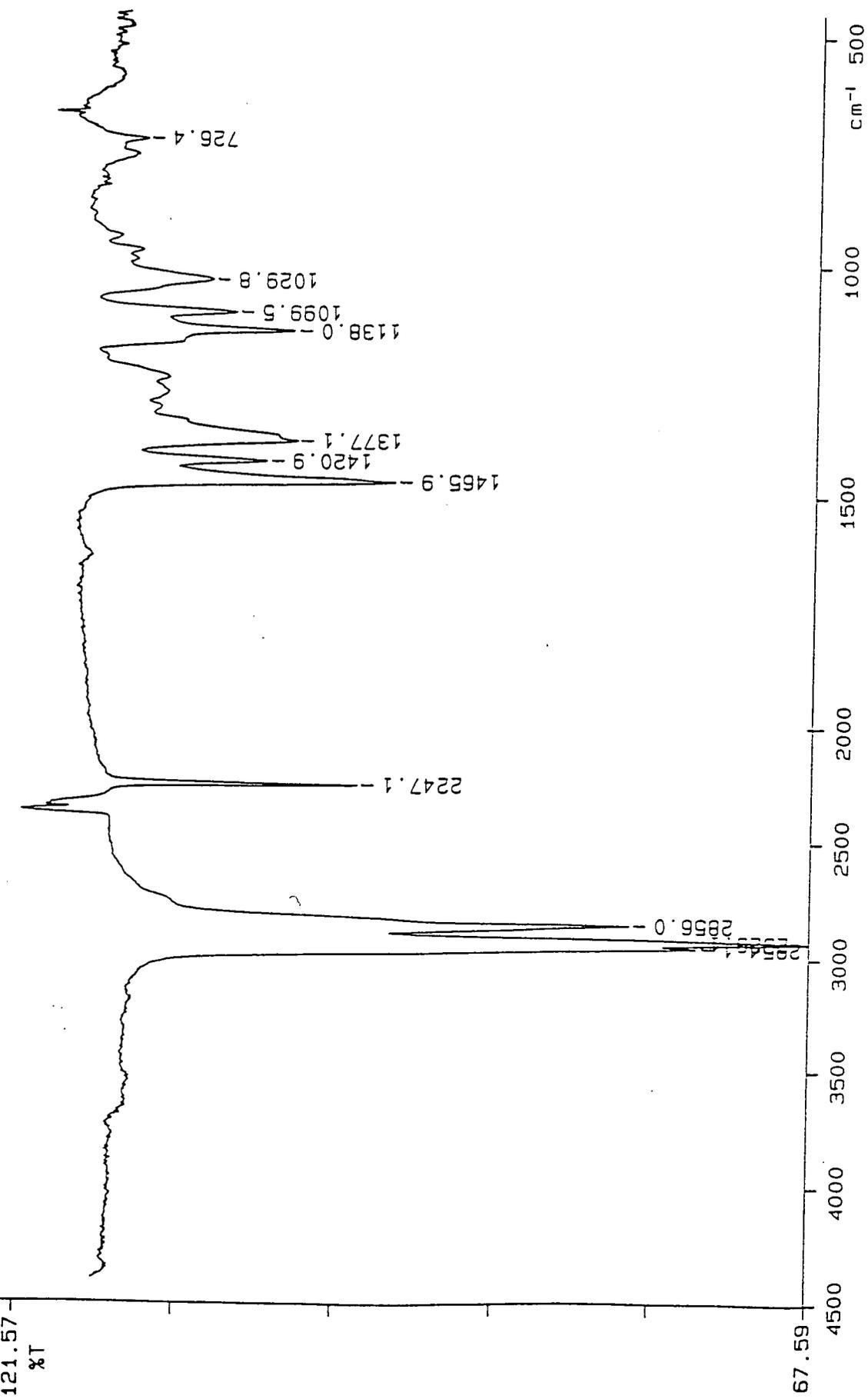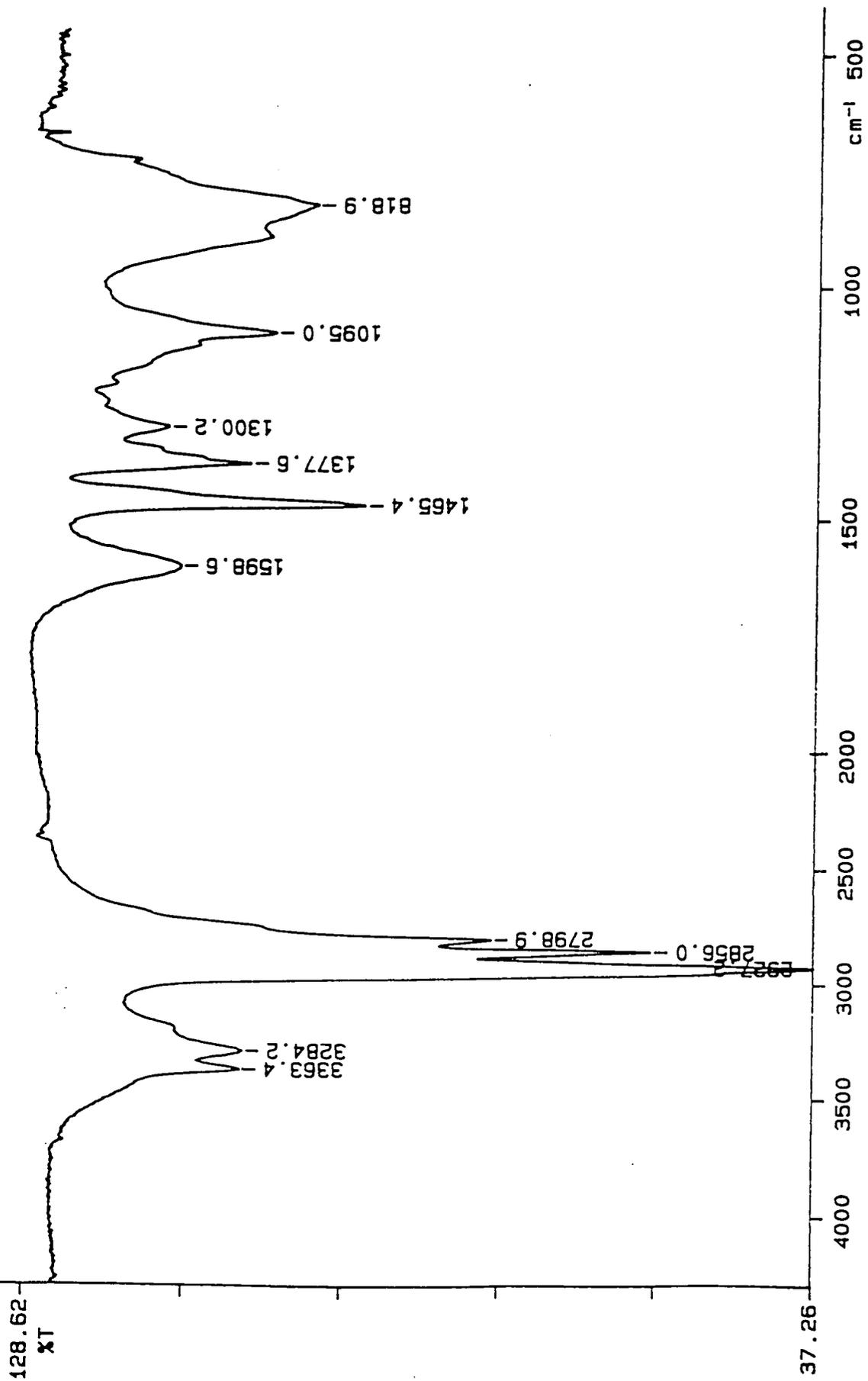
Appendix 1.1.2 FTIR spectrum of Hex-*wedge*-(NH$_2$)$_2$.

818.9
1095.0
1300.2
1377.6
1465.4
1598.6
2798.9
2856.0
2937
3284.2
3363.4

128.62
%T

37.26

cm^{-1}

500
1000
1500
2000
2500
3000
3500
4000
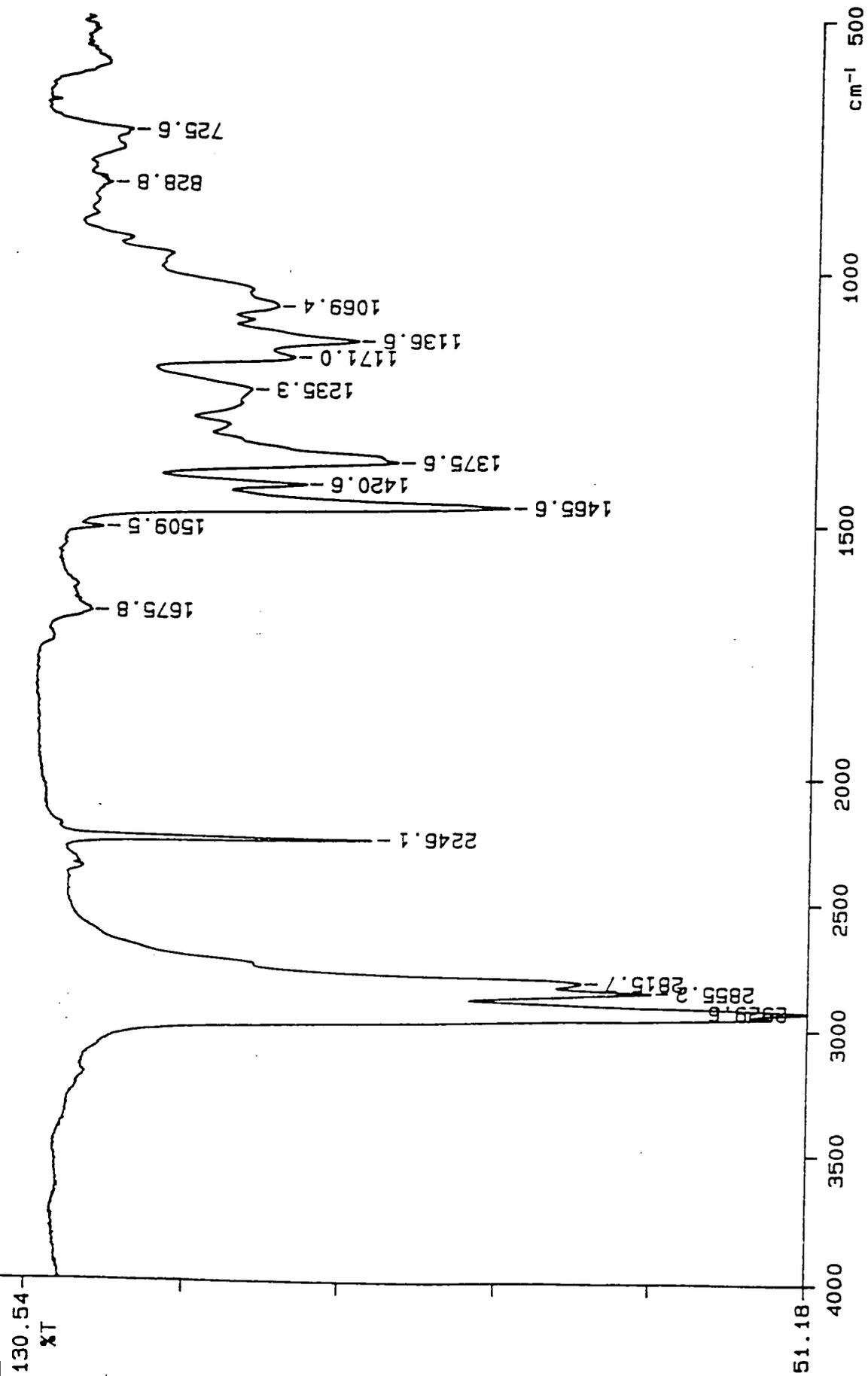
Appendix 1.1.3 FTIR spectrum of Hex-*wedge*-(CN)$_4$.
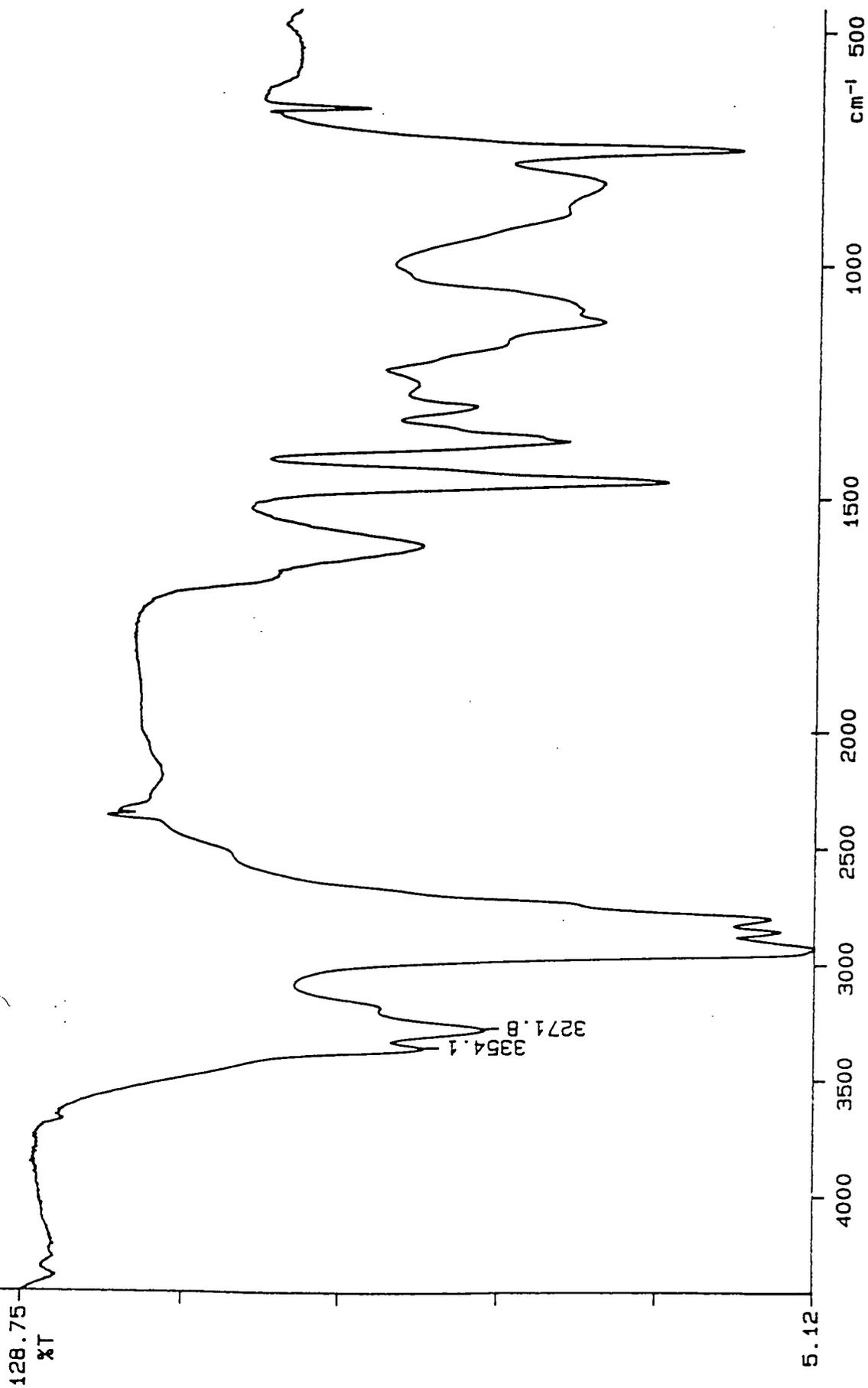
Appendix 1.1.4 FTIR spectrum of Hex-*wedge*-(NH)$_4$.
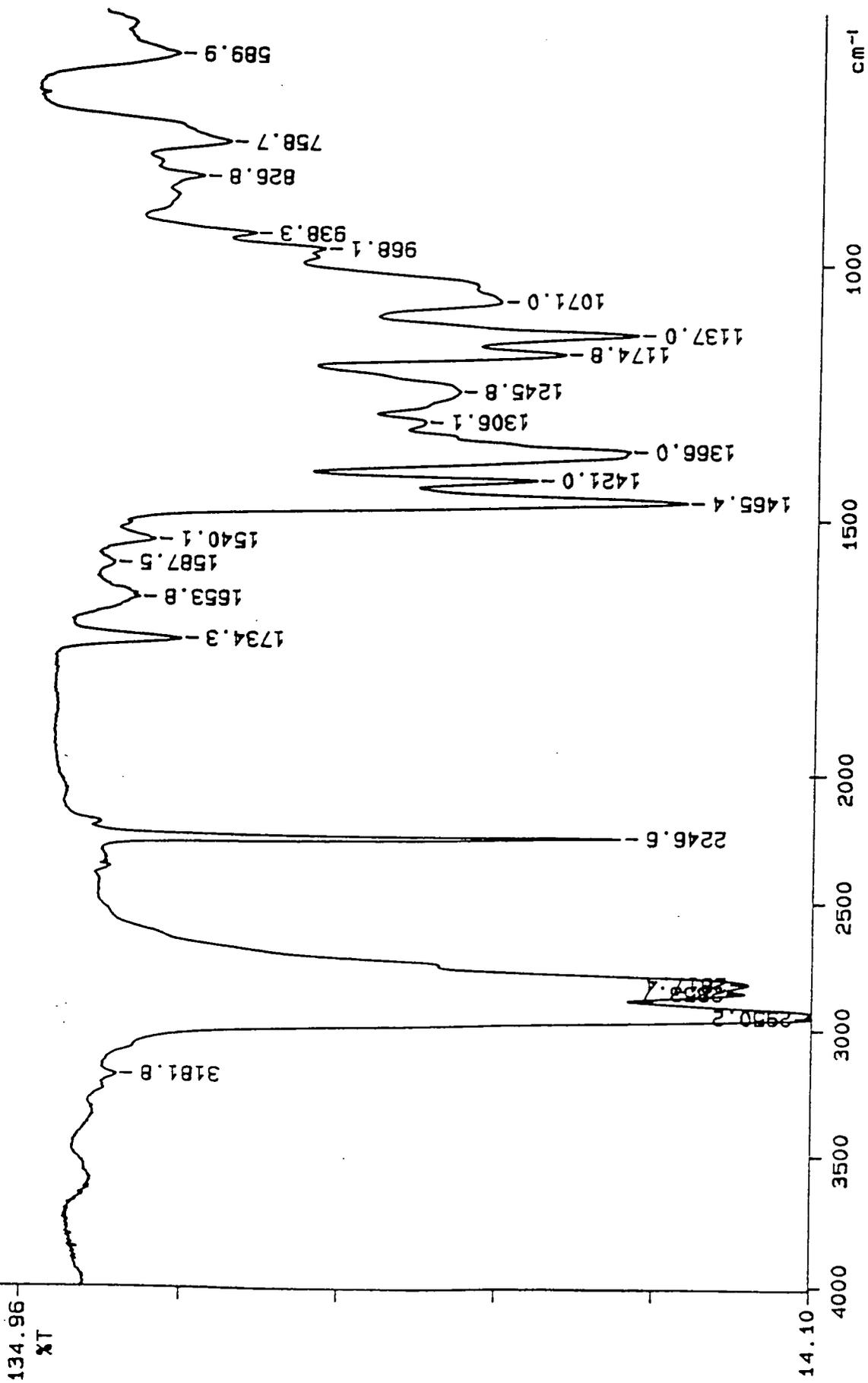
Appendix 1.1.5 FTIR spectrum of Hex-*wedge*-(CN)$_8$.
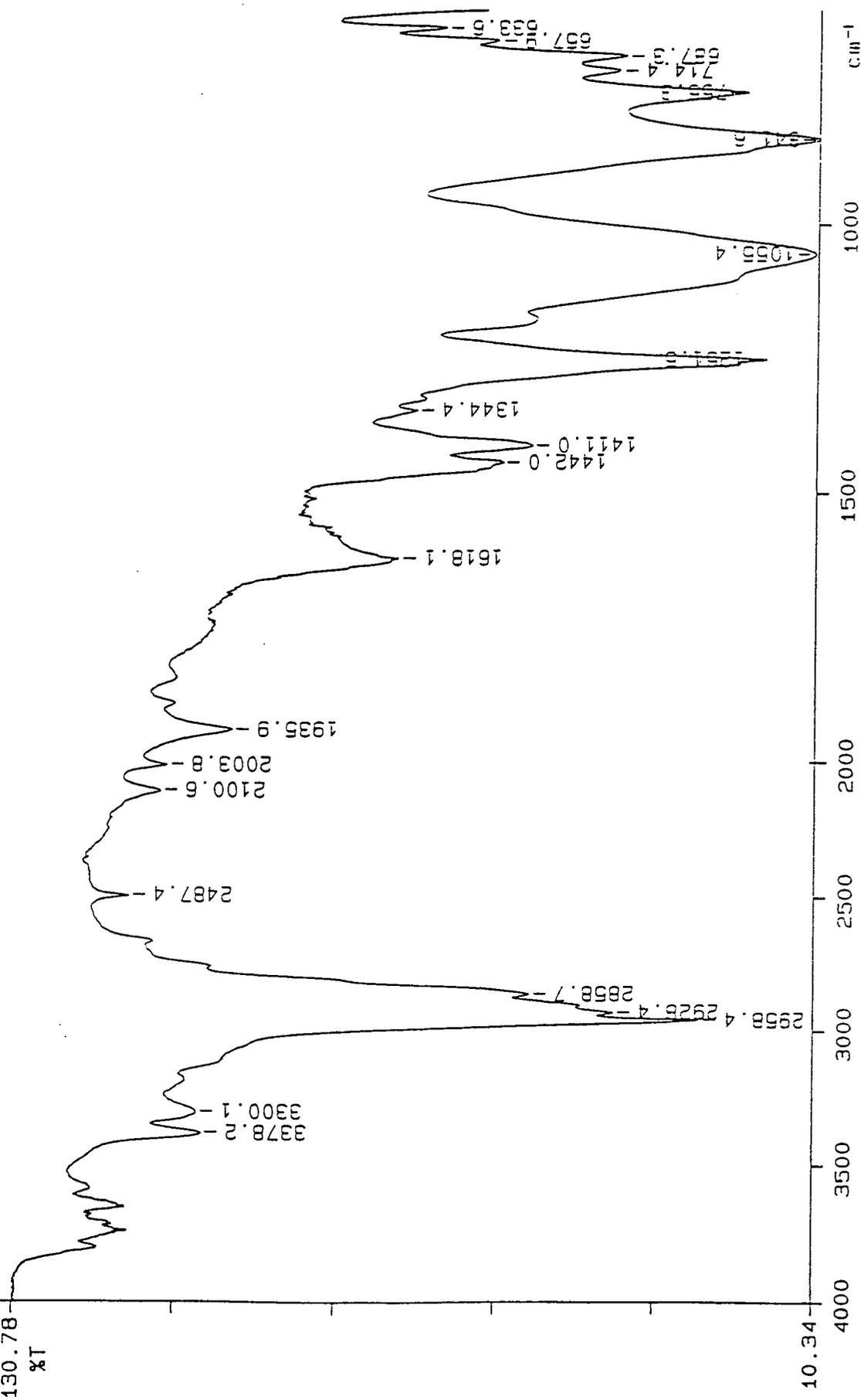
Appendix 1.1.6 FTIR spectrum of 3-aminopropyltris(trimethylsiloxy)silane (APTTMSS).

Peaks: 3378.2, 3300.1, 2958.4, 2928.4, 2858.7, 2487.4, 2100.6, 2003.8, 1935.9, 1618.1, 1442.0, 1411.0, 1344.4, 1055.4, 714.4, 687.3, 657, 653.5
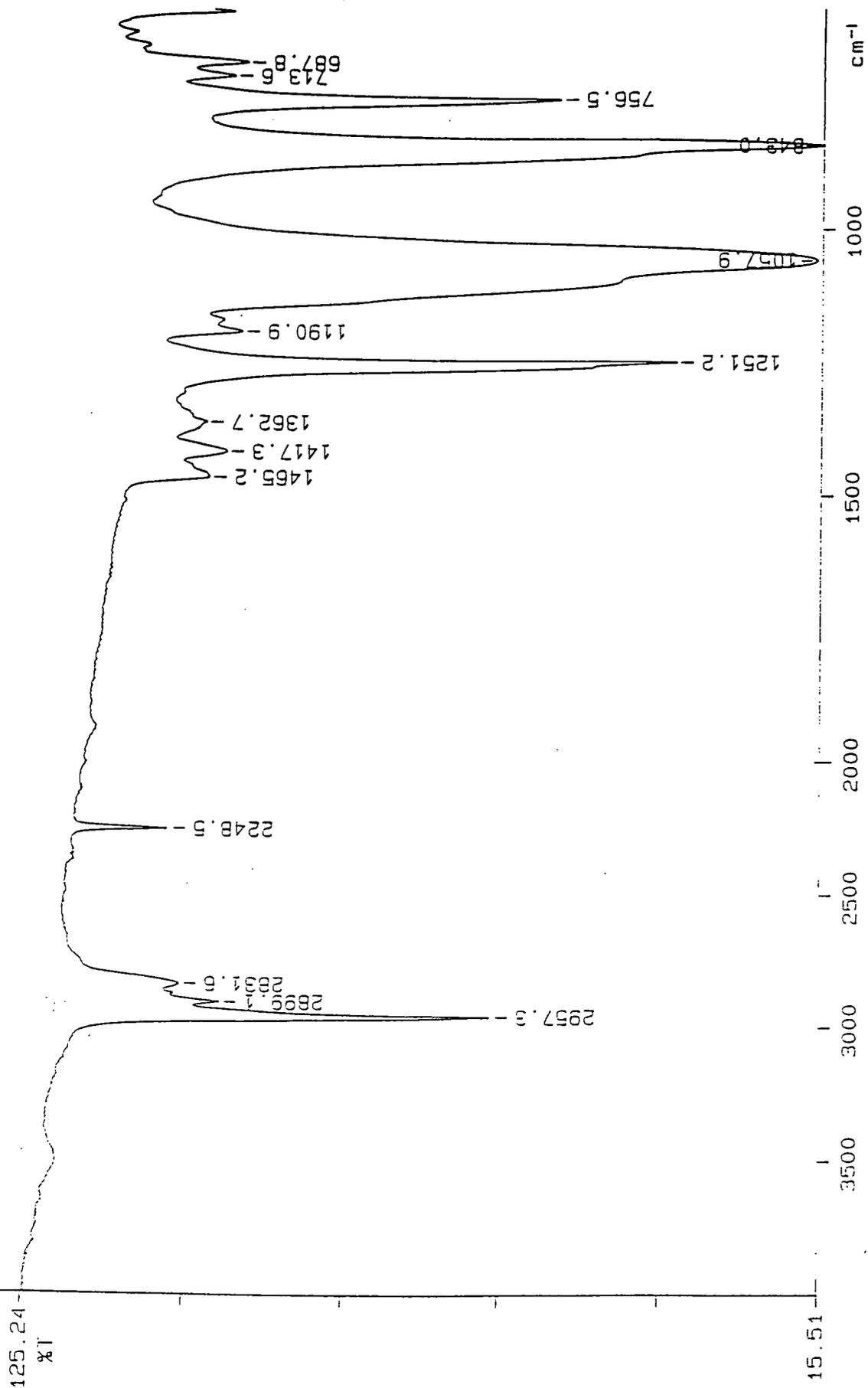
Appendix 1.1.7 FTIR spectrum of Si-*wedge*-(CN)$_2$.
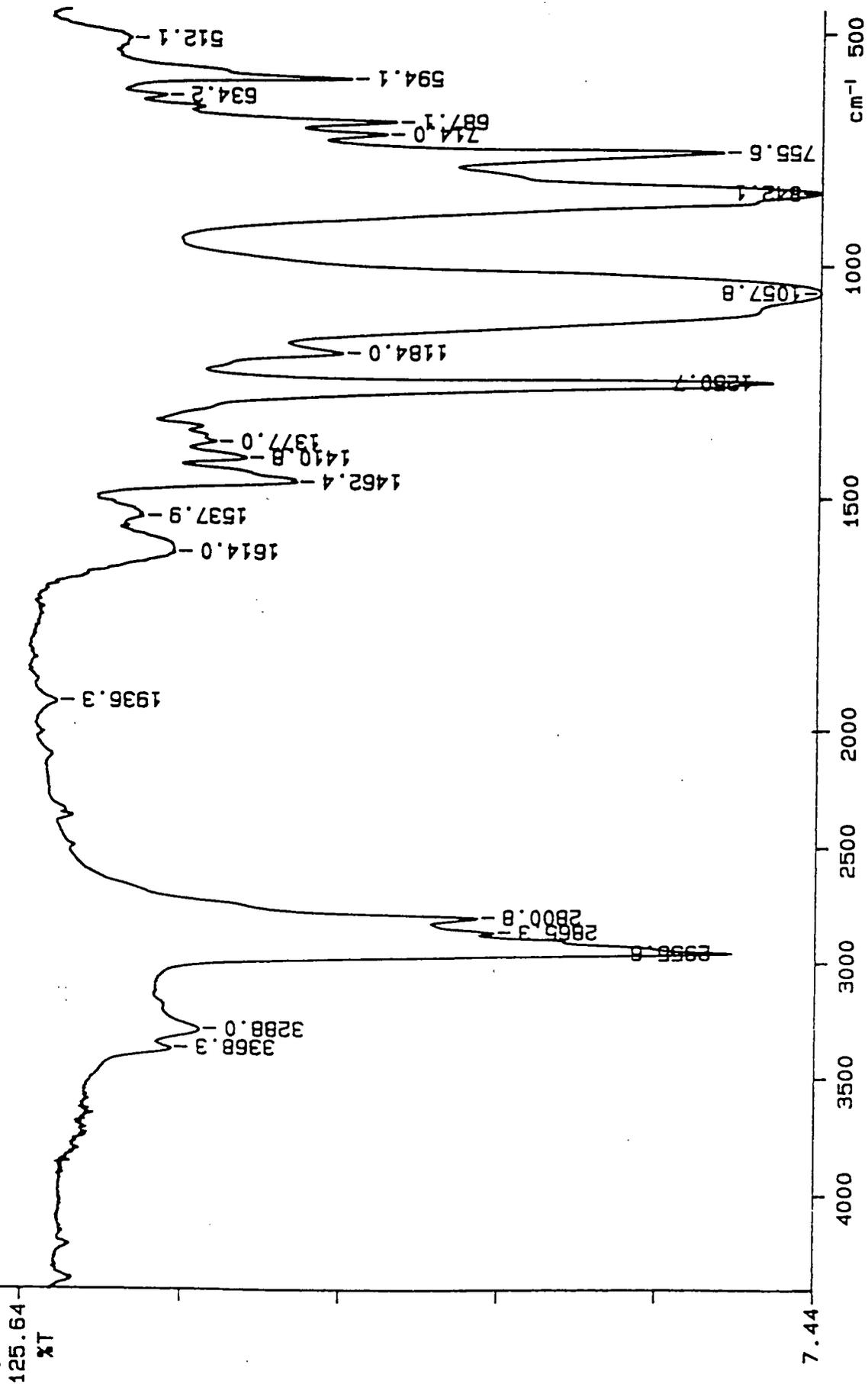
Appendix 1.1.8 FTIR spectrum of Si-*wedge*-(NH$_2$)$_2$.
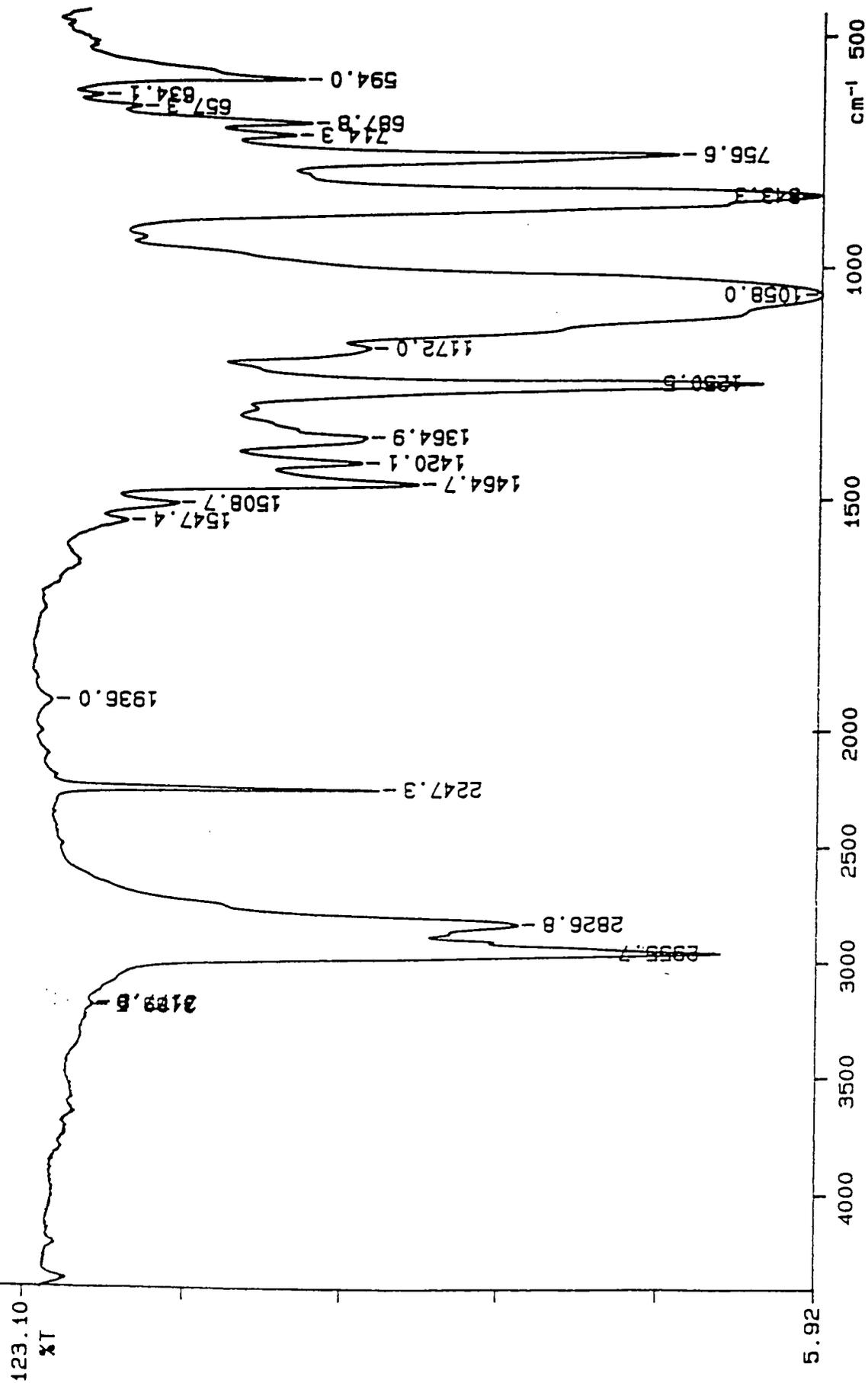
Appendix 1.1.9 FTIR spectrum of Si-*wedge*-(CN)$_4$.
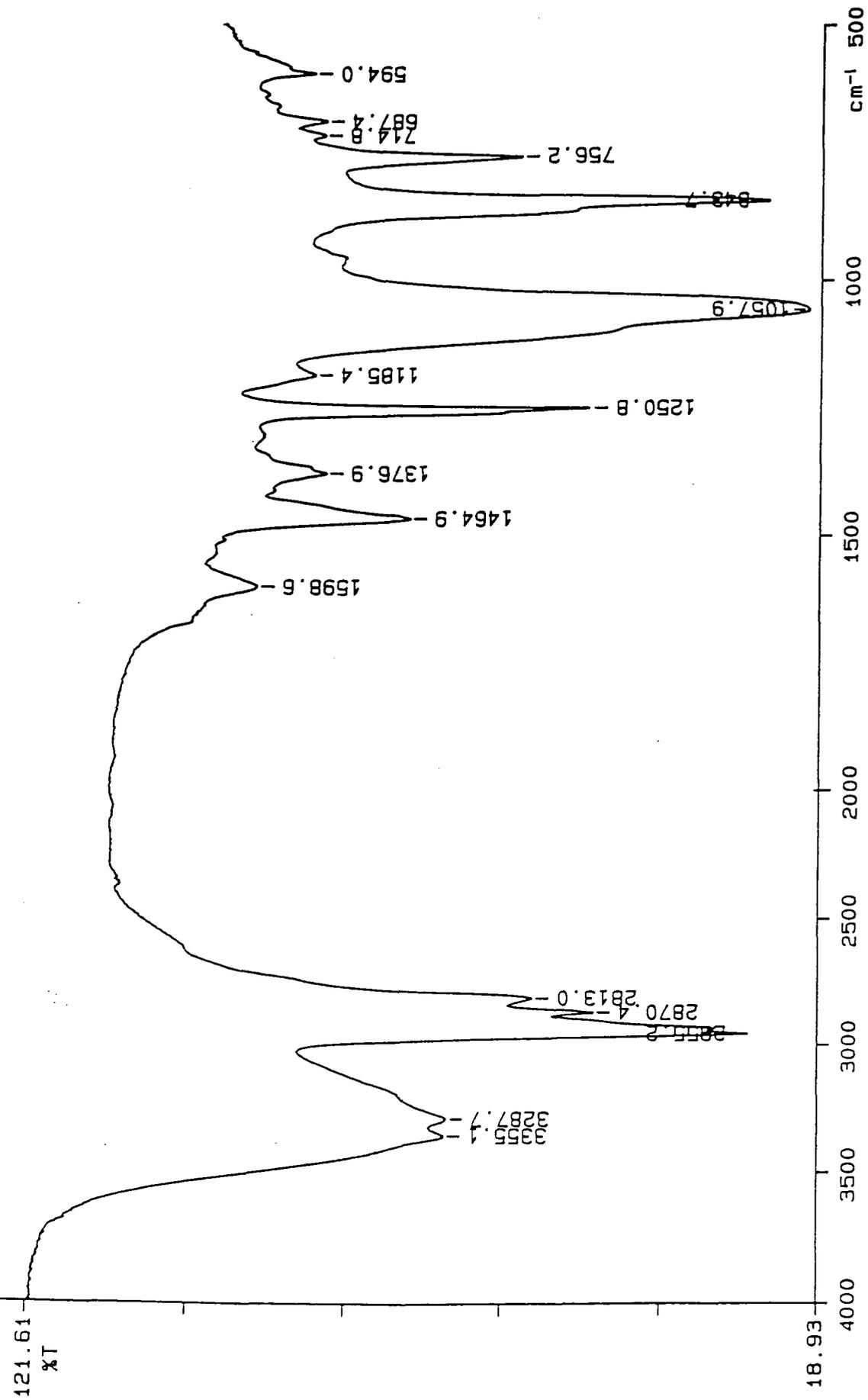
Appendix 1.1.10 FTIR spectrum of Si-*wedge*-$(NH_2)_4$.
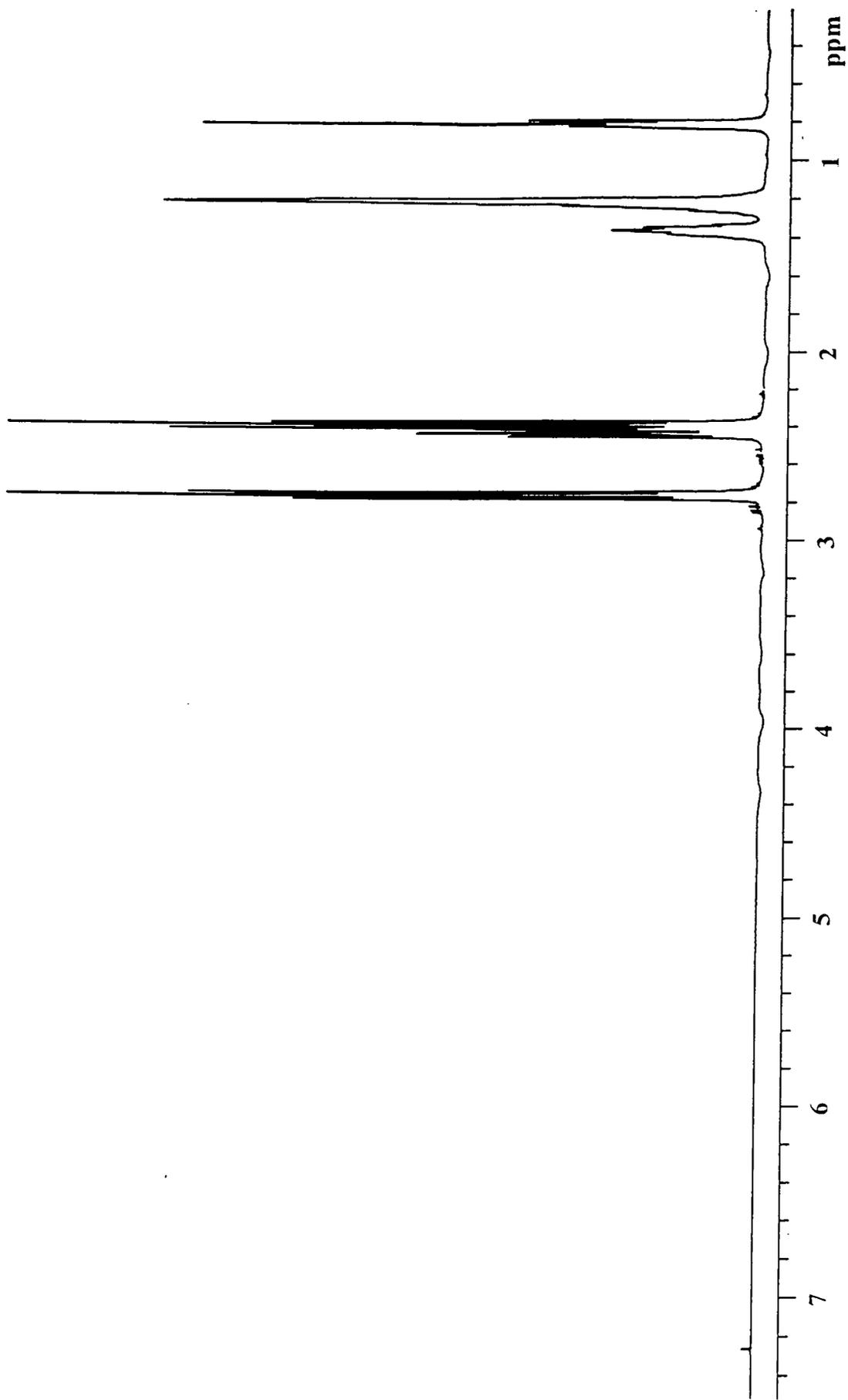
Appendix 1.2.1 ^{1}H nmr spectrum of Hex-*wedge*-(CN)$_2$ in CDCl$_3$.
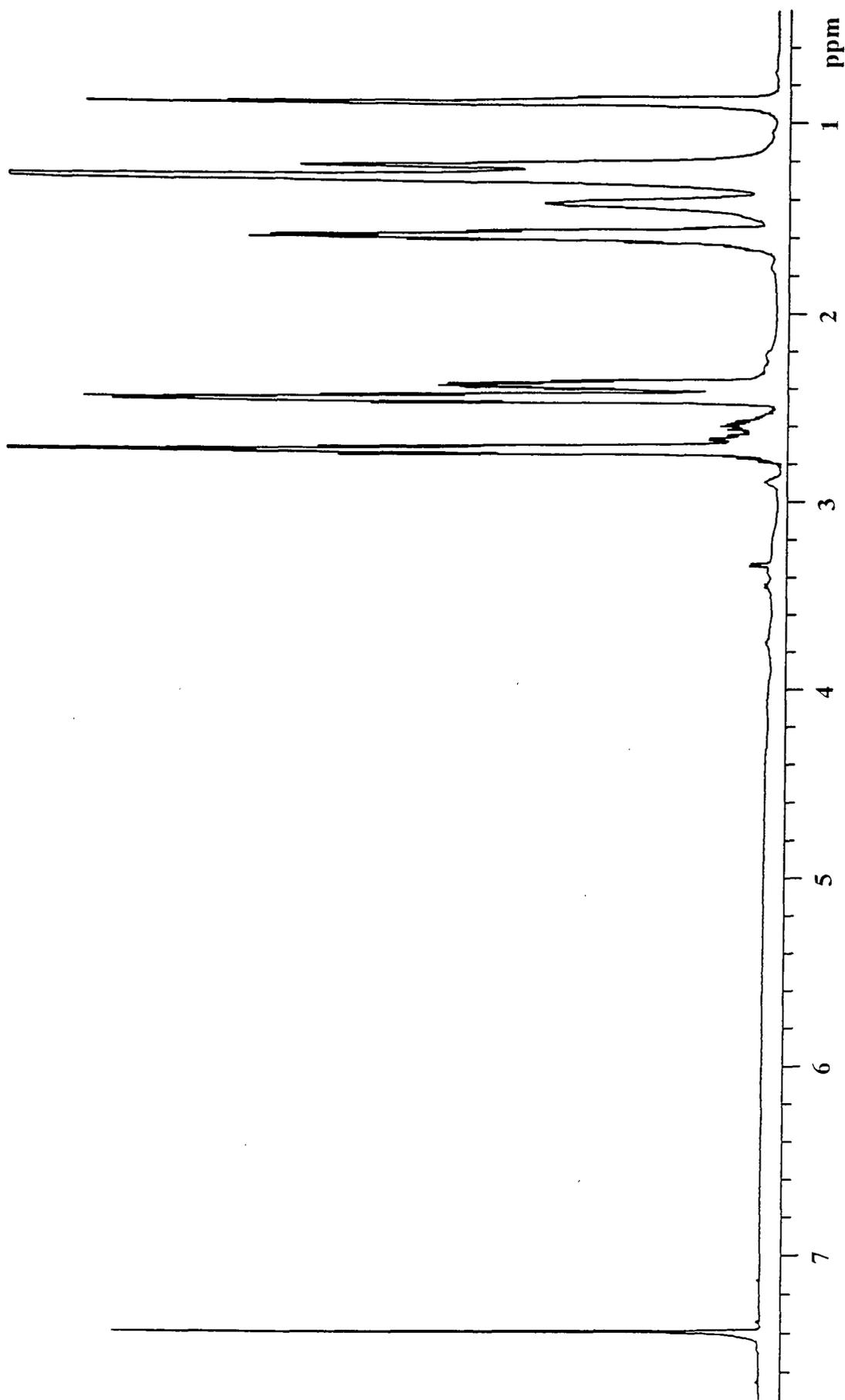
Appendix 1.2.2 ^{1}H nmr spectrum of Hex-*wedge*-(NH$_2$)$_2$ in CDCl$_3$.
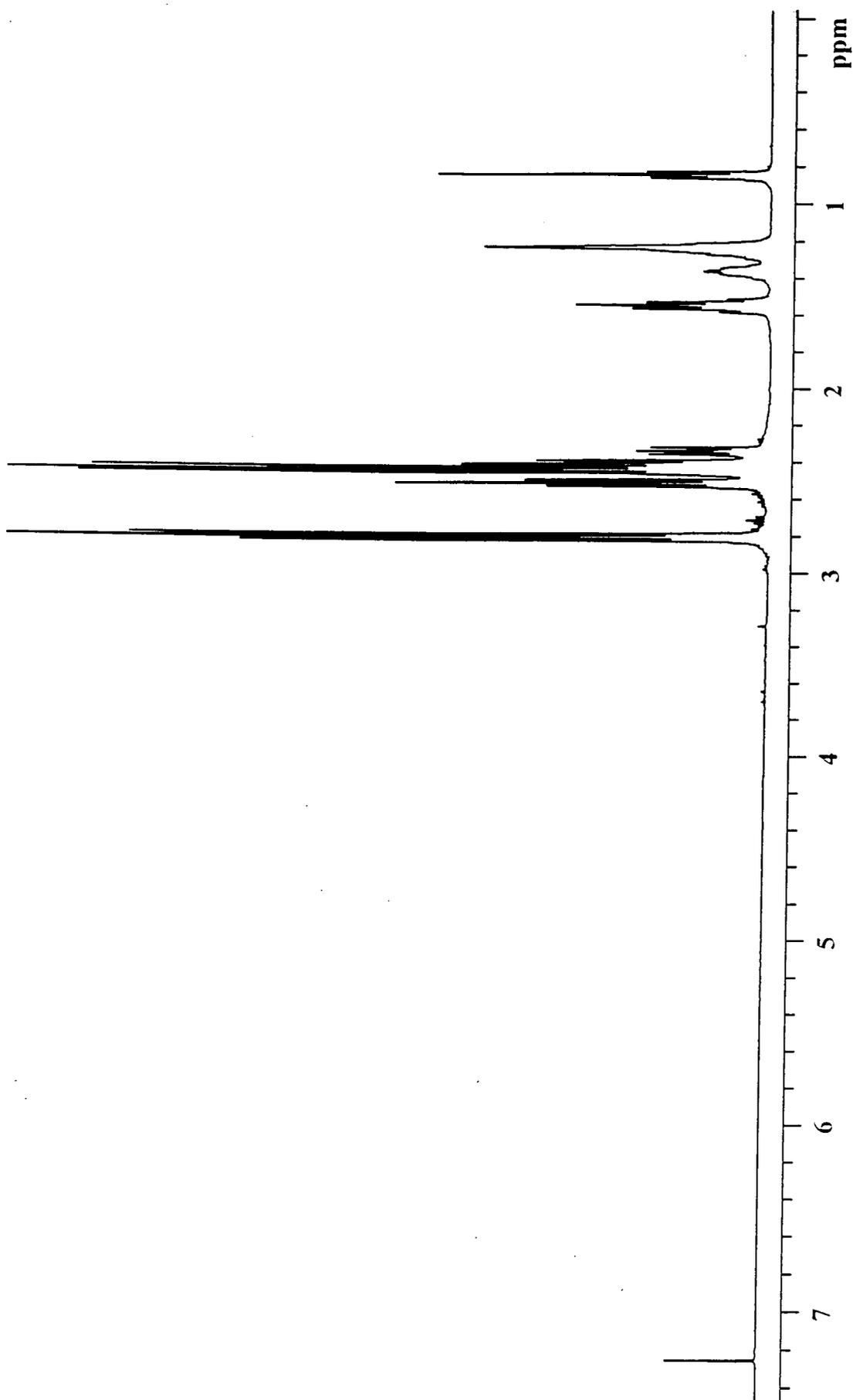
Appendix 1.2.3 ^{1}H nmr spectrum of Hex-*wedge*-$(CN)_4$ in $CDCl_3$
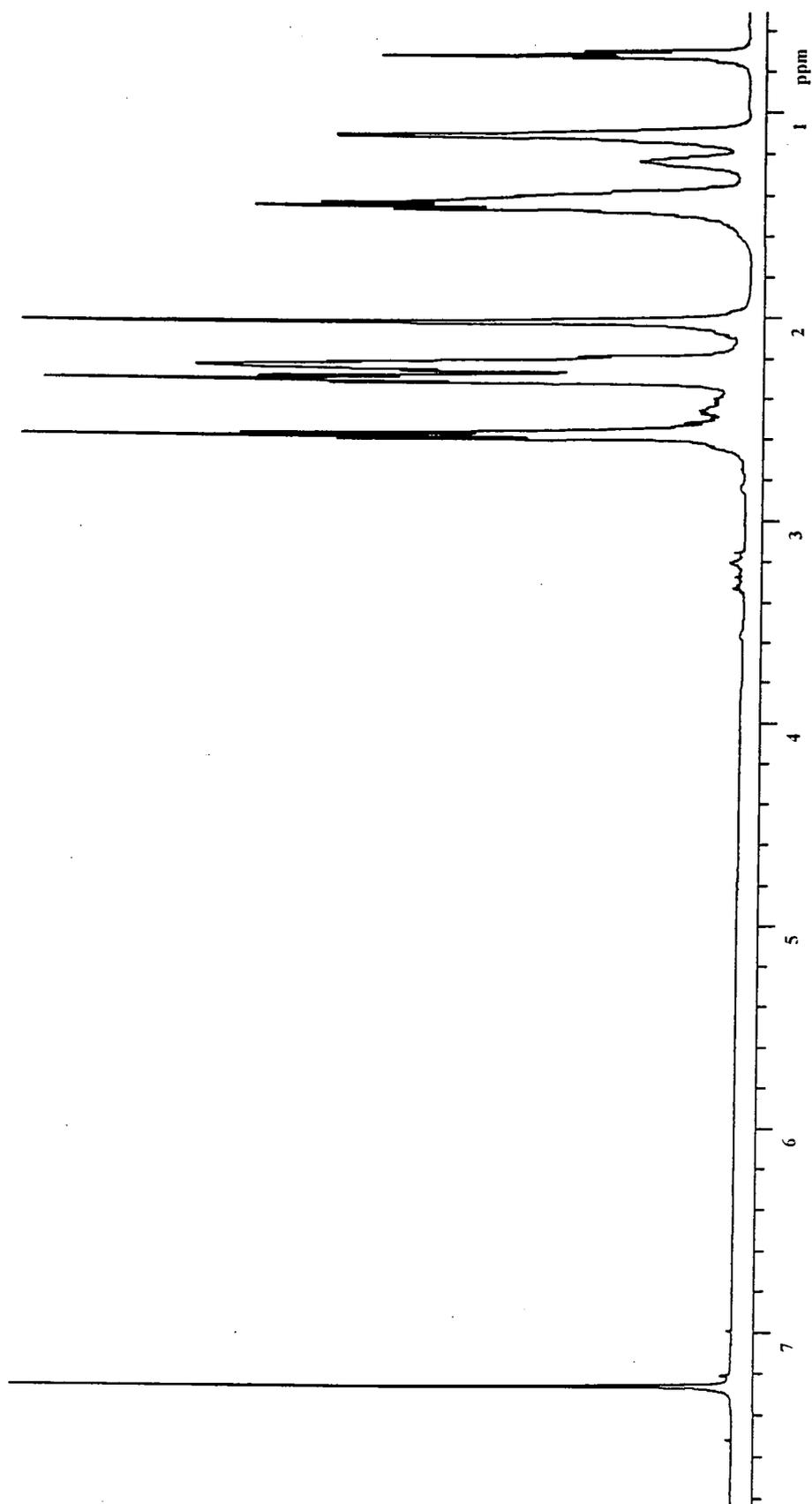
Appendix 1.2.4 ^{1}H nmr spectrum of Hex-*wedge*-$(NH_2)_4$ in $CDCl_3$.
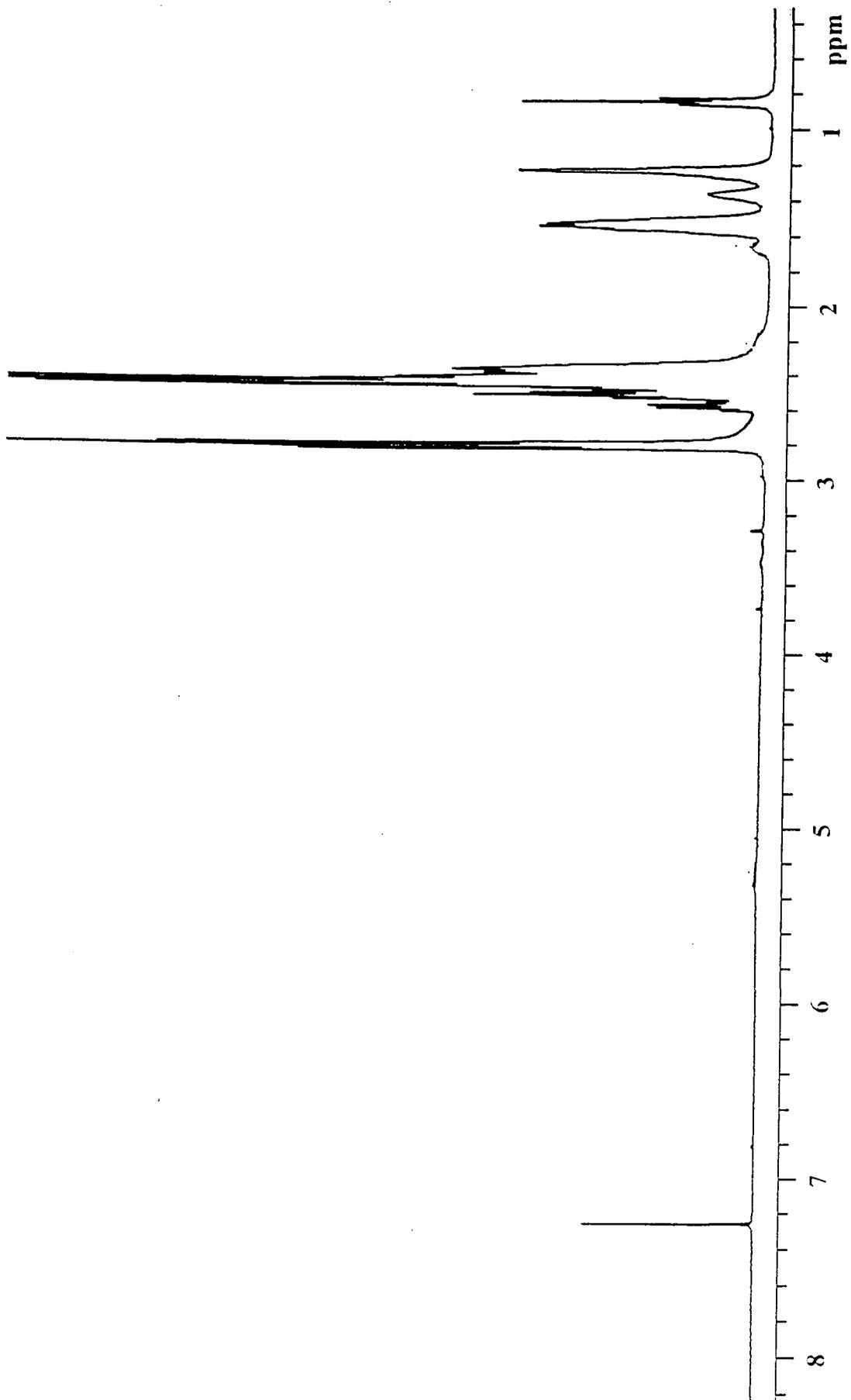
Appendix 1.2.5 [^1]H nmr spectrum of Hex-*wedge*-(CN)$_8$ in CDCl$_3$.
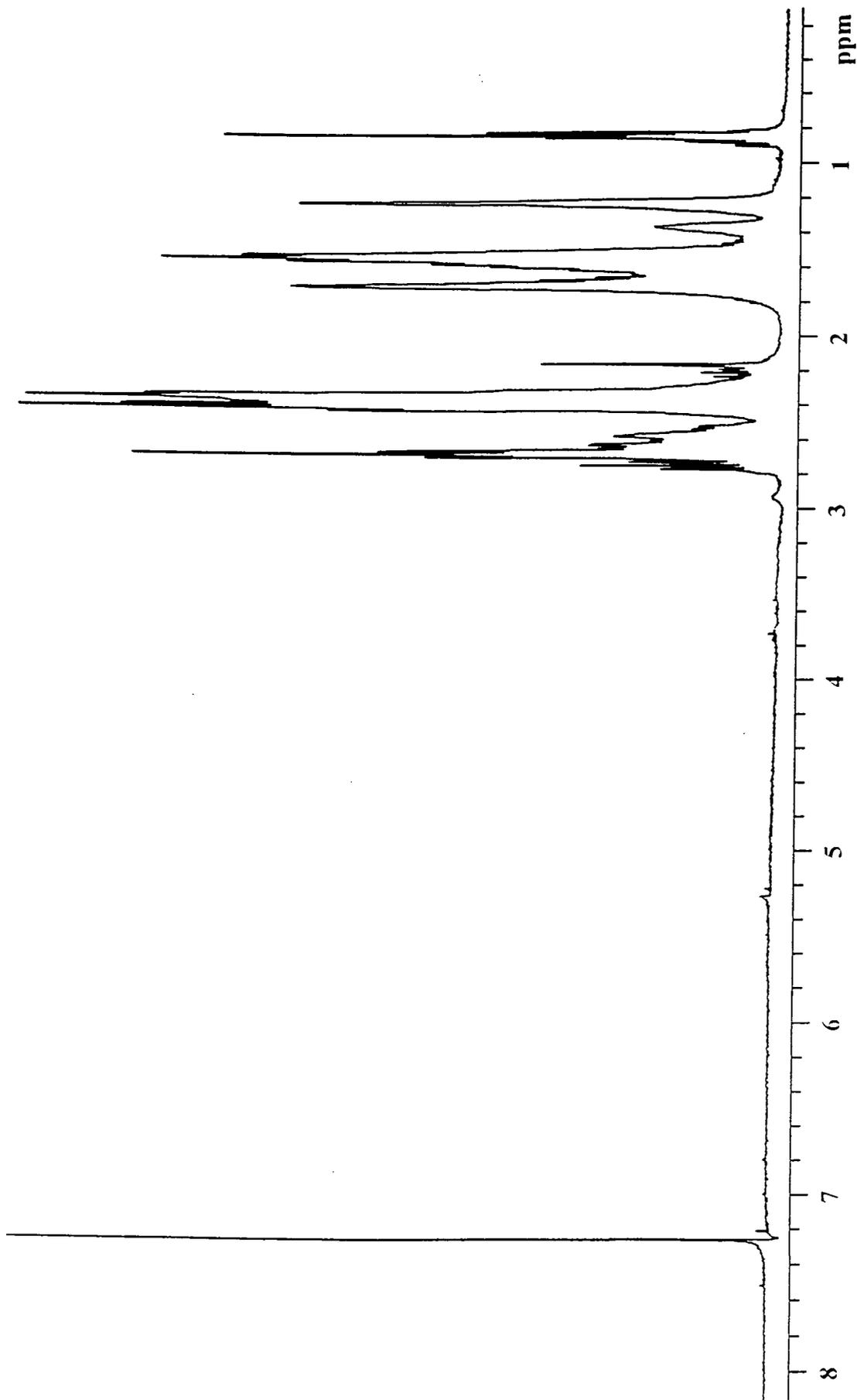
Appendix 1.2.6 ^{1}H nmr spectrum of Hex-*wedge*-$(NH_2)_8$ in $CDCl_3$.
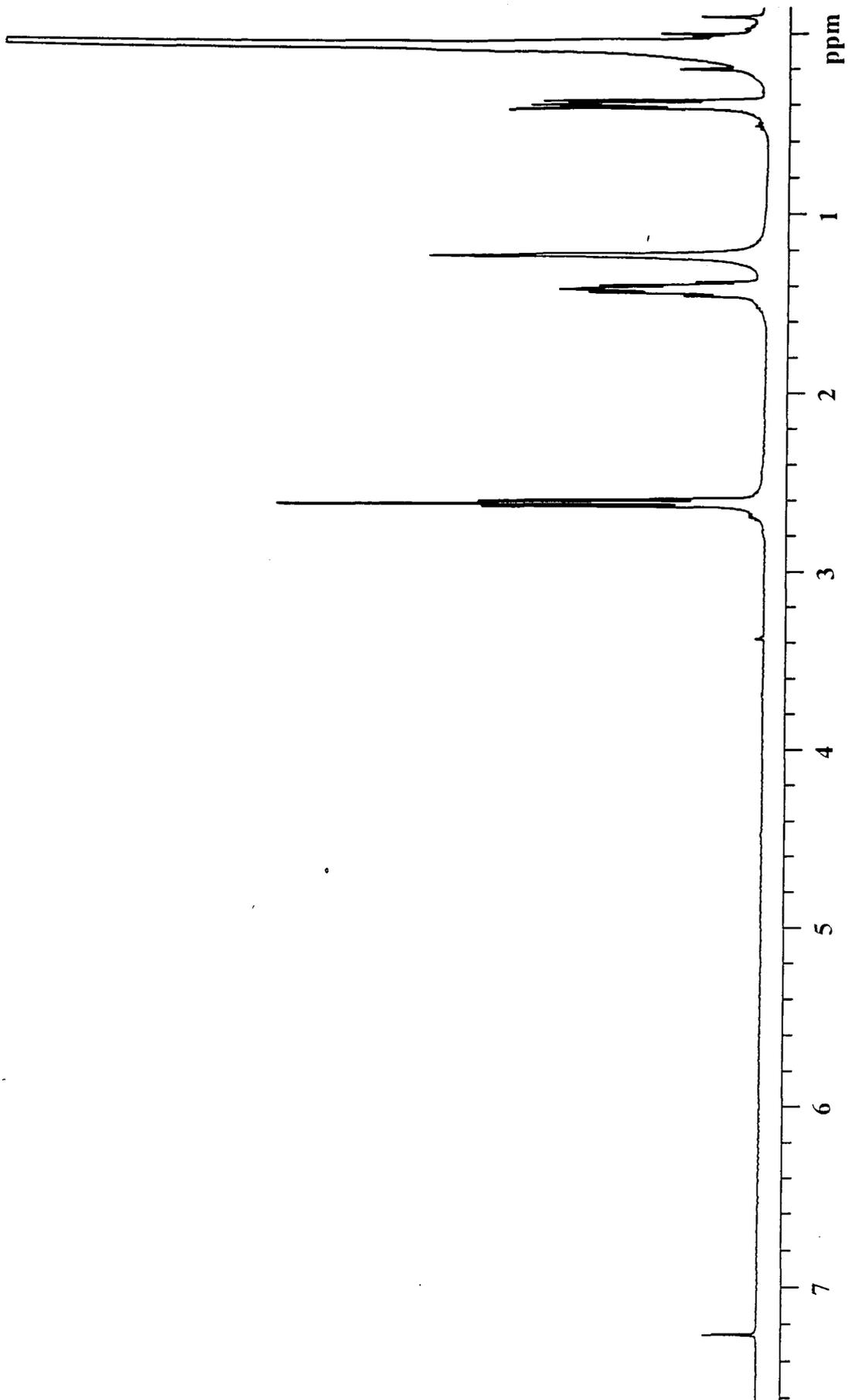
Appendix 1.2.7 ^{1}H nmr spectrum of 3-aminopropyltris(trimethylsiloxy)silane (APTTMSS) in CDCl$_3$.
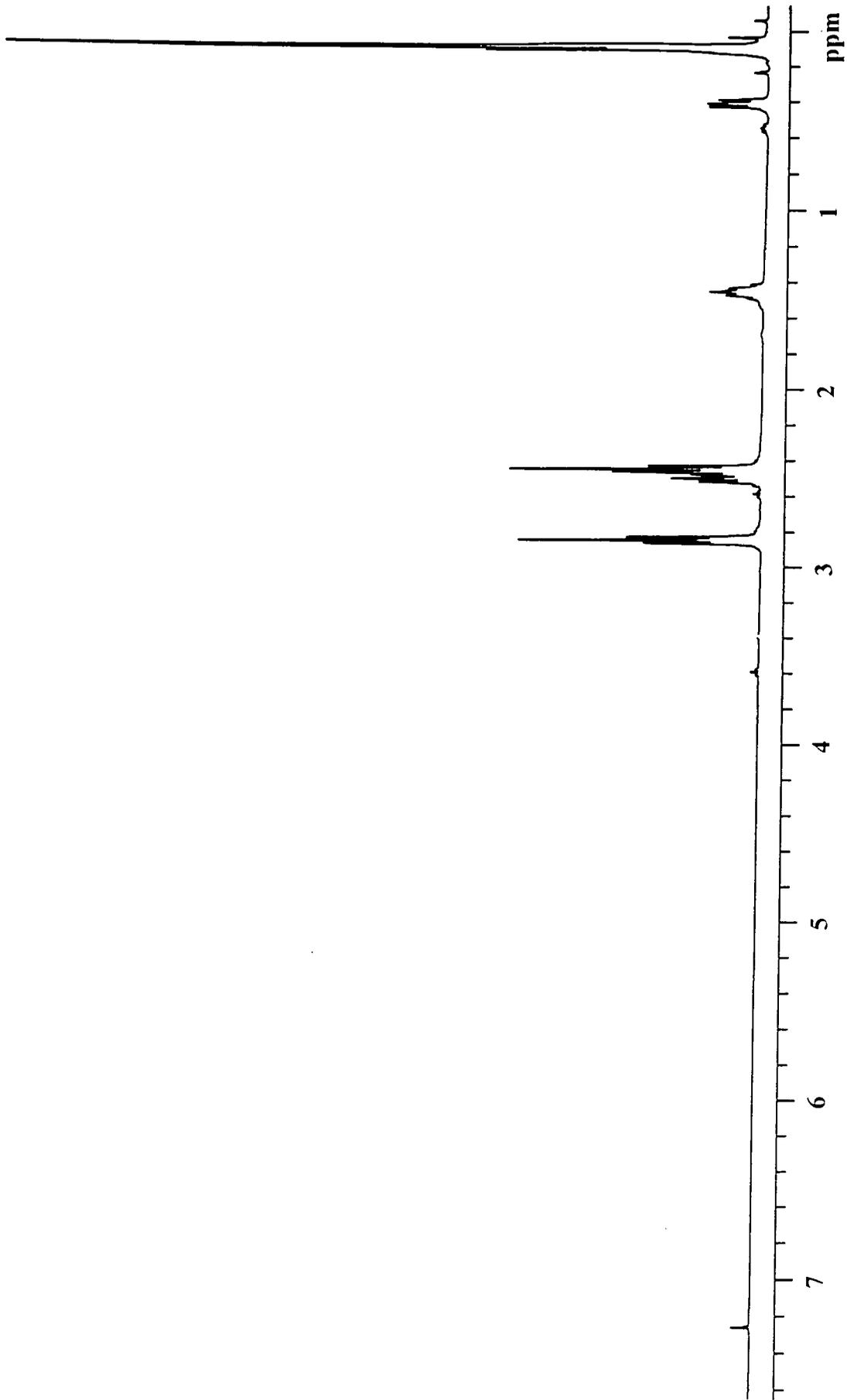
Appendix 1.2.8 ^{1}H nmr spectrum of Si-*wedge*-(CN)$_2$ in CDCl$_3$.
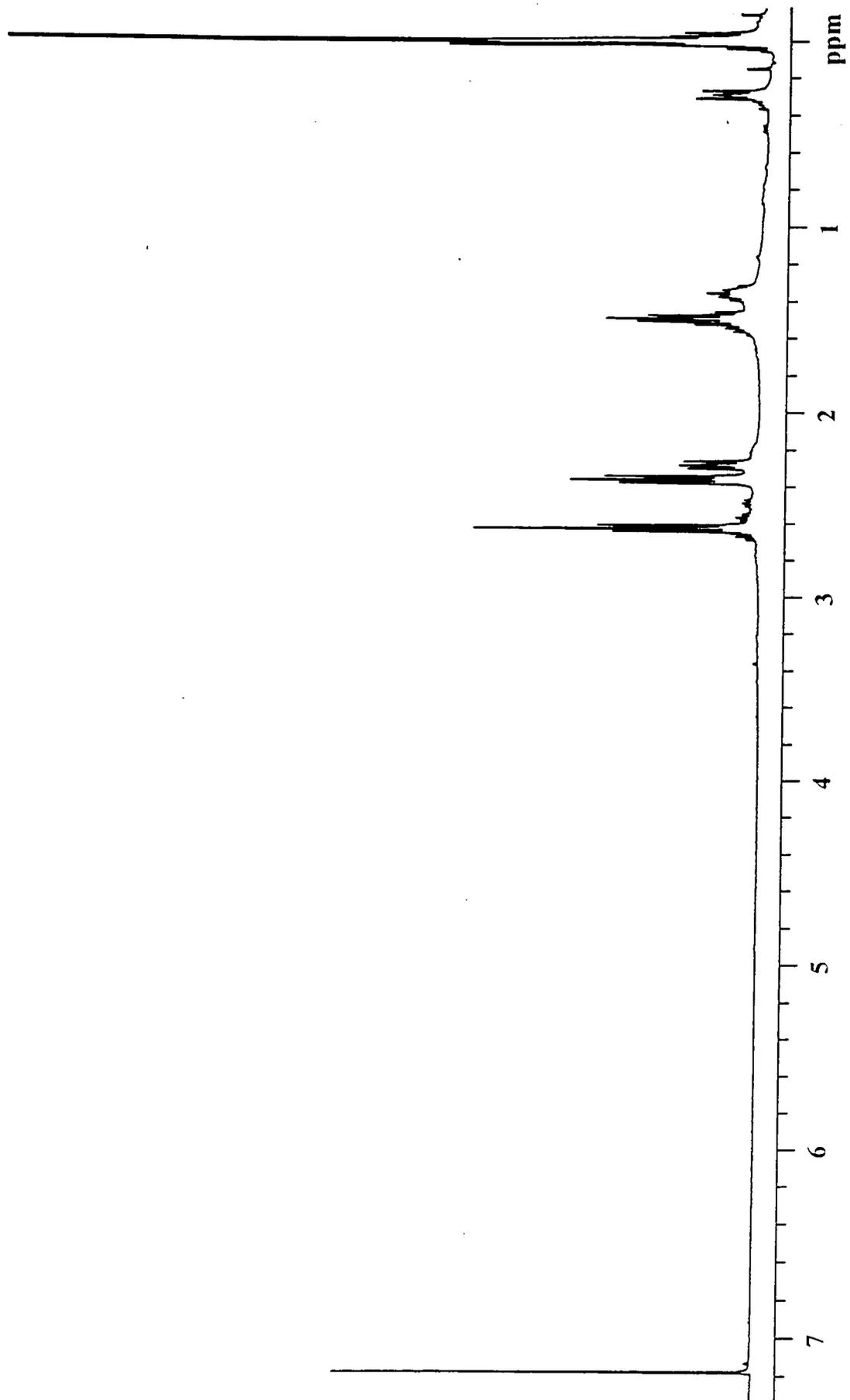
Appendix 1.2.9 ^{1}H nmr spectrum of Si-*wedge*-$(NH_2)_2$ in CDCl$_3$.
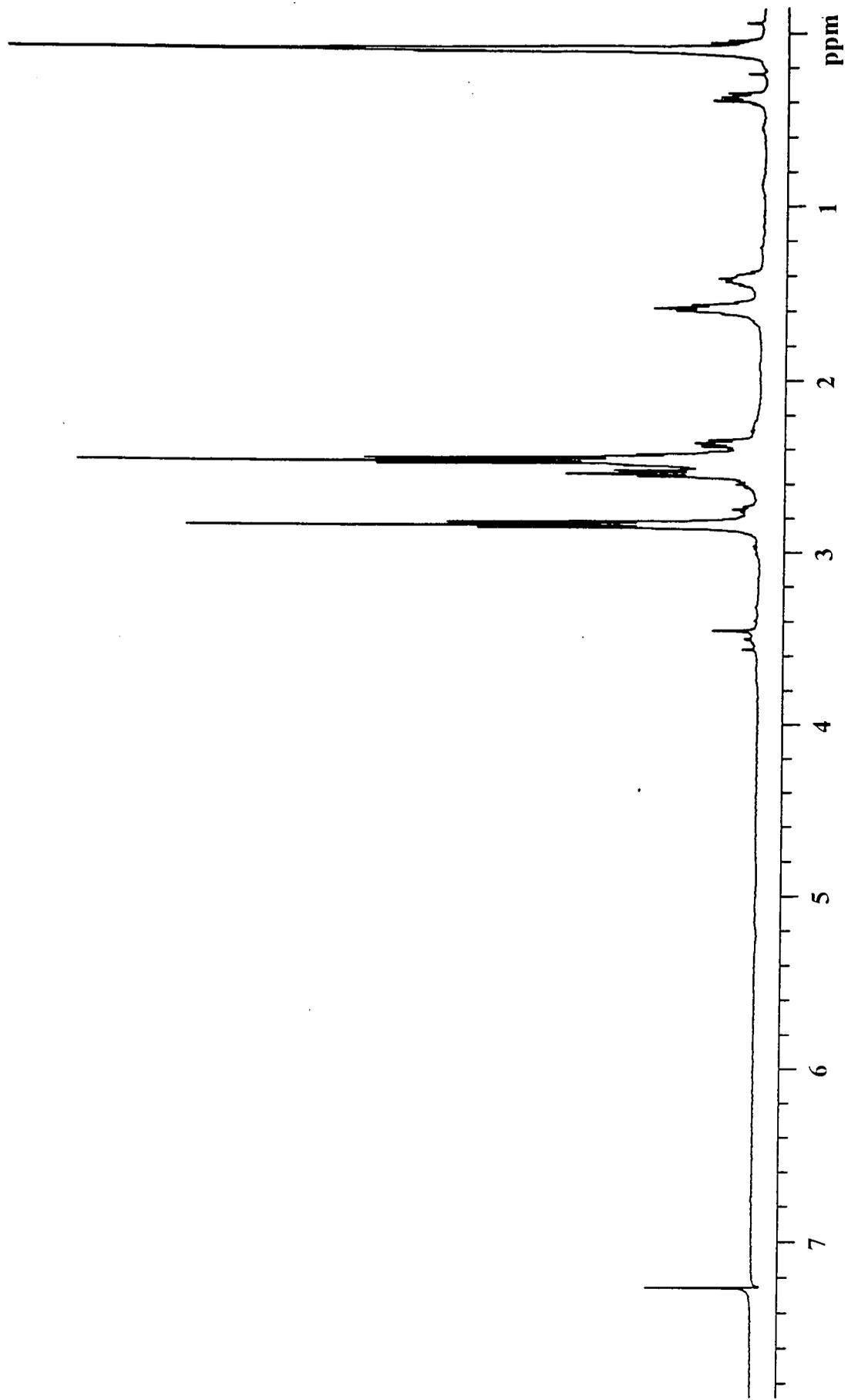
Appendix 1.2.10 ^{1}H nmr spectrum of Si-*wedge*-(CN)$_4$ in CDCl$_3$.
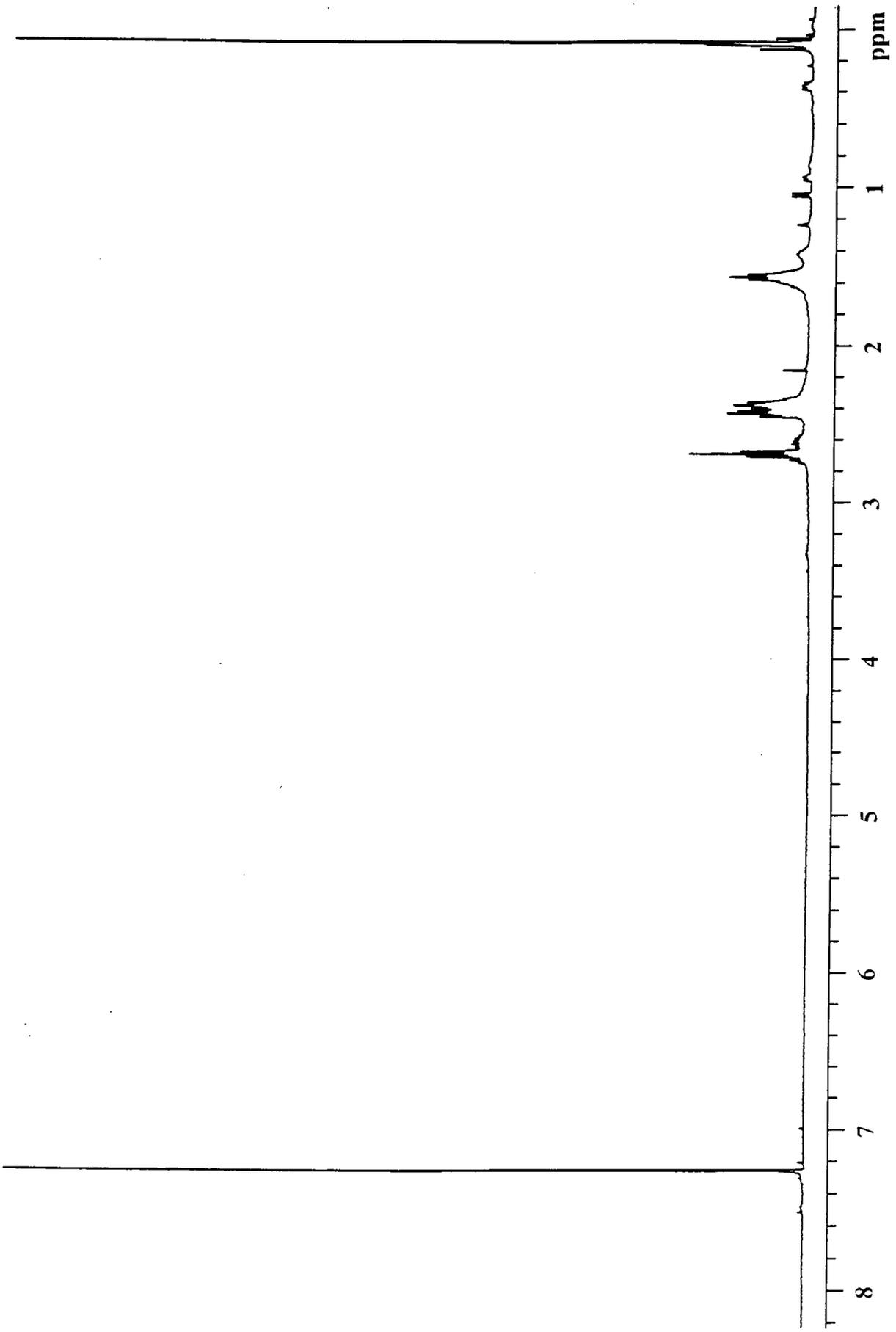
Appendix 1.2.11 ^{1}H nmr spectrum of Si-*wedge*-$(NH_2)_4$ in $CDCl_3$.
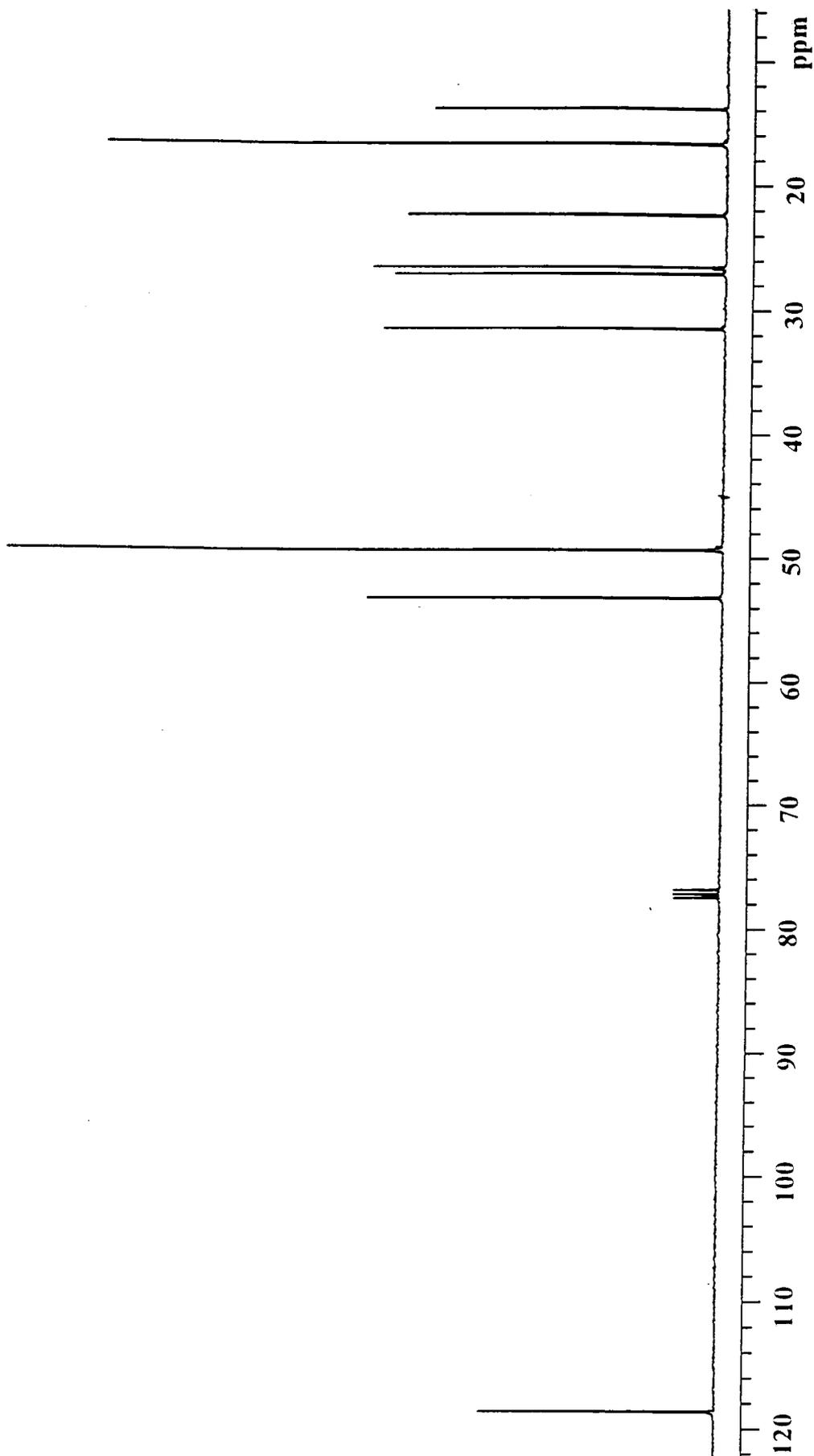
Appendix 1.3.1 ^{13}C nmr spectrum of Hex-*wedge*-(CN)$_2$ in CDCl$_3$.
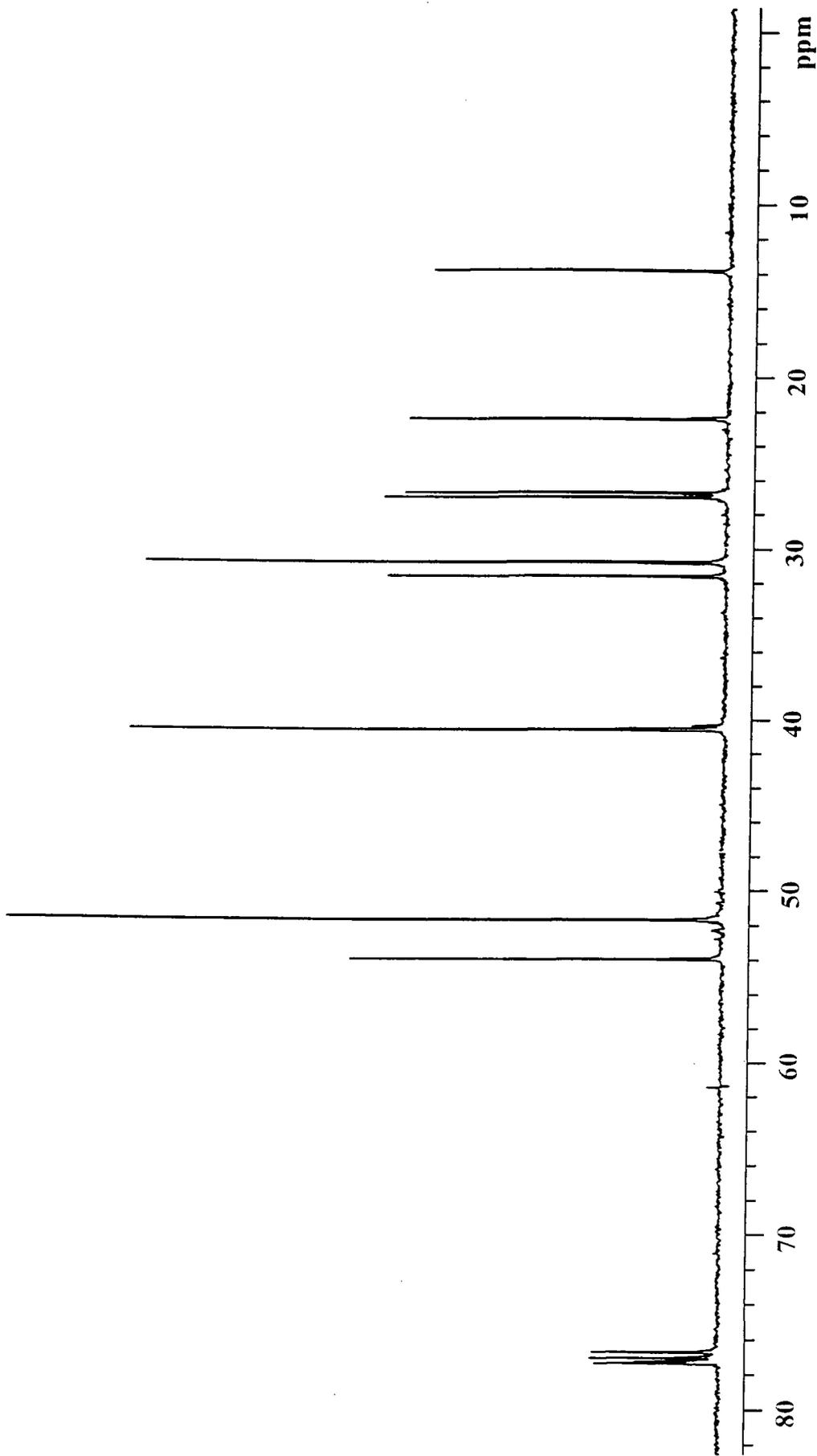
Appendix 1.3.2 ^{13}C nmr spectrum of Hex-*wedge*-NH$_2$ in CDCl$_3$.
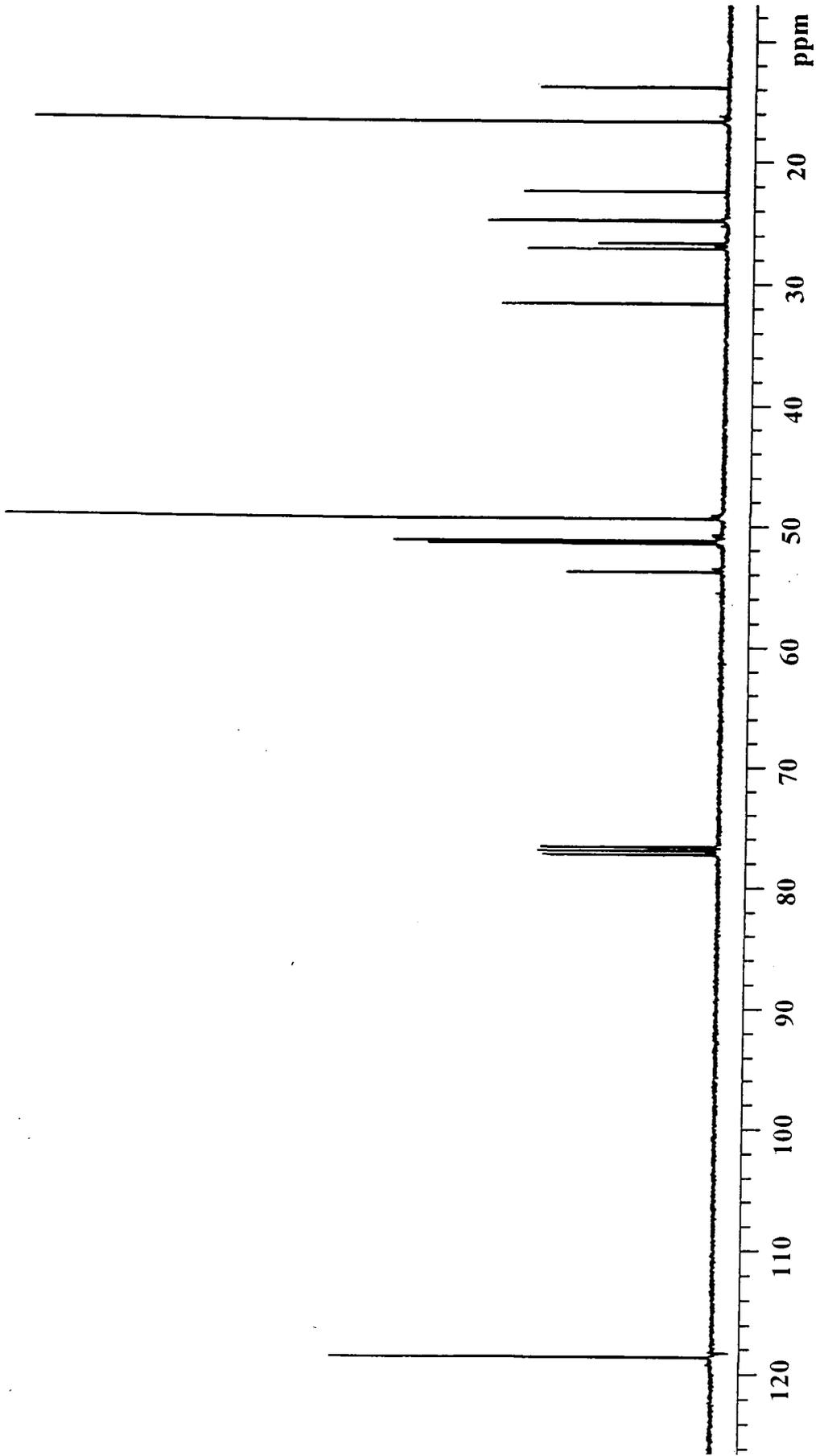
Appendix 1.3.3 ^{13}C nmr spectrum of Hex-*wedge*-$(CN)_4$ in $CDCl_3$.
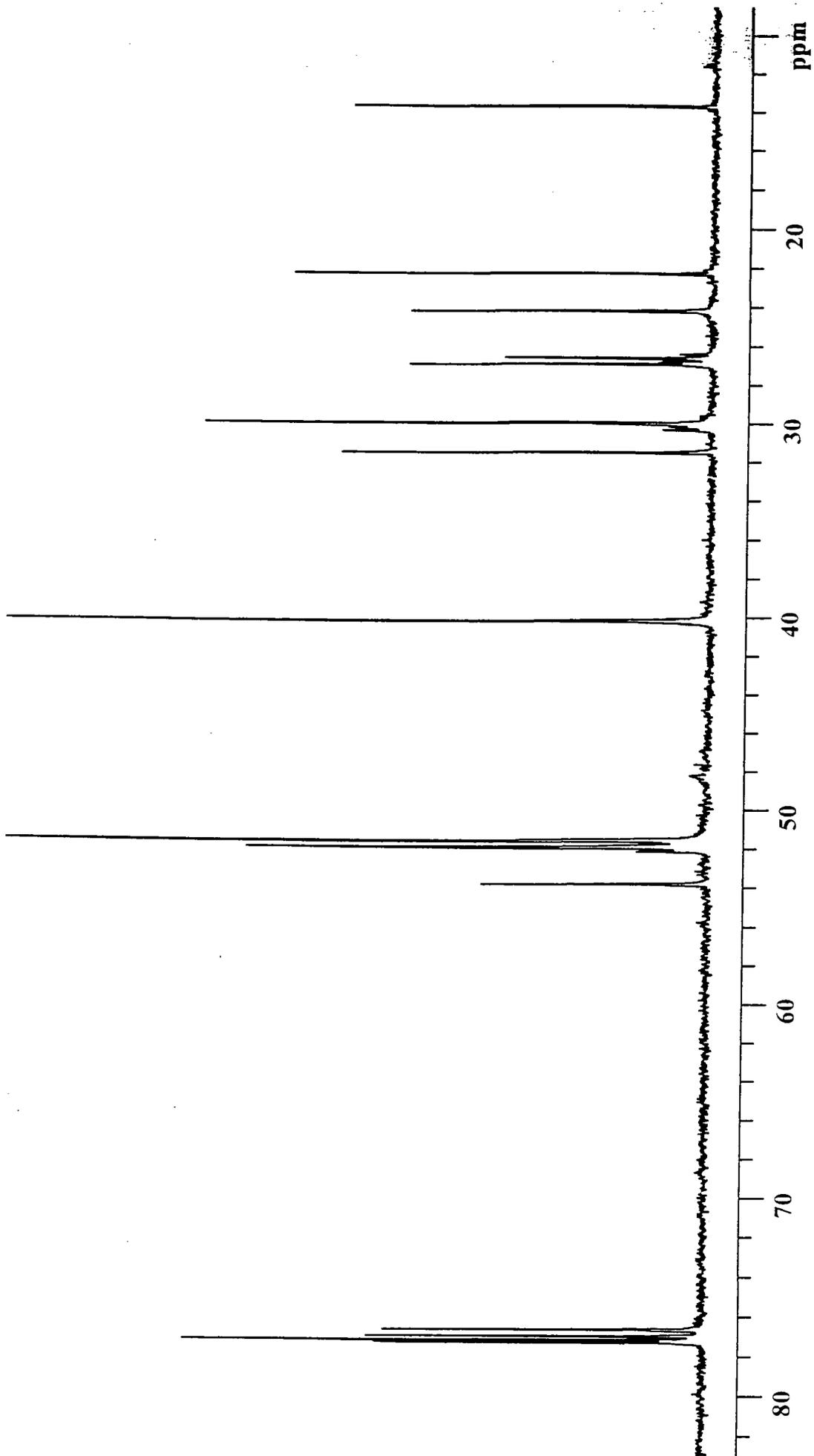
Appendix 1.3.4 ^{13}C nmr spectrum of Hex-*wedge*-(NH$_2$)$_4$ in CDCl$_3$.
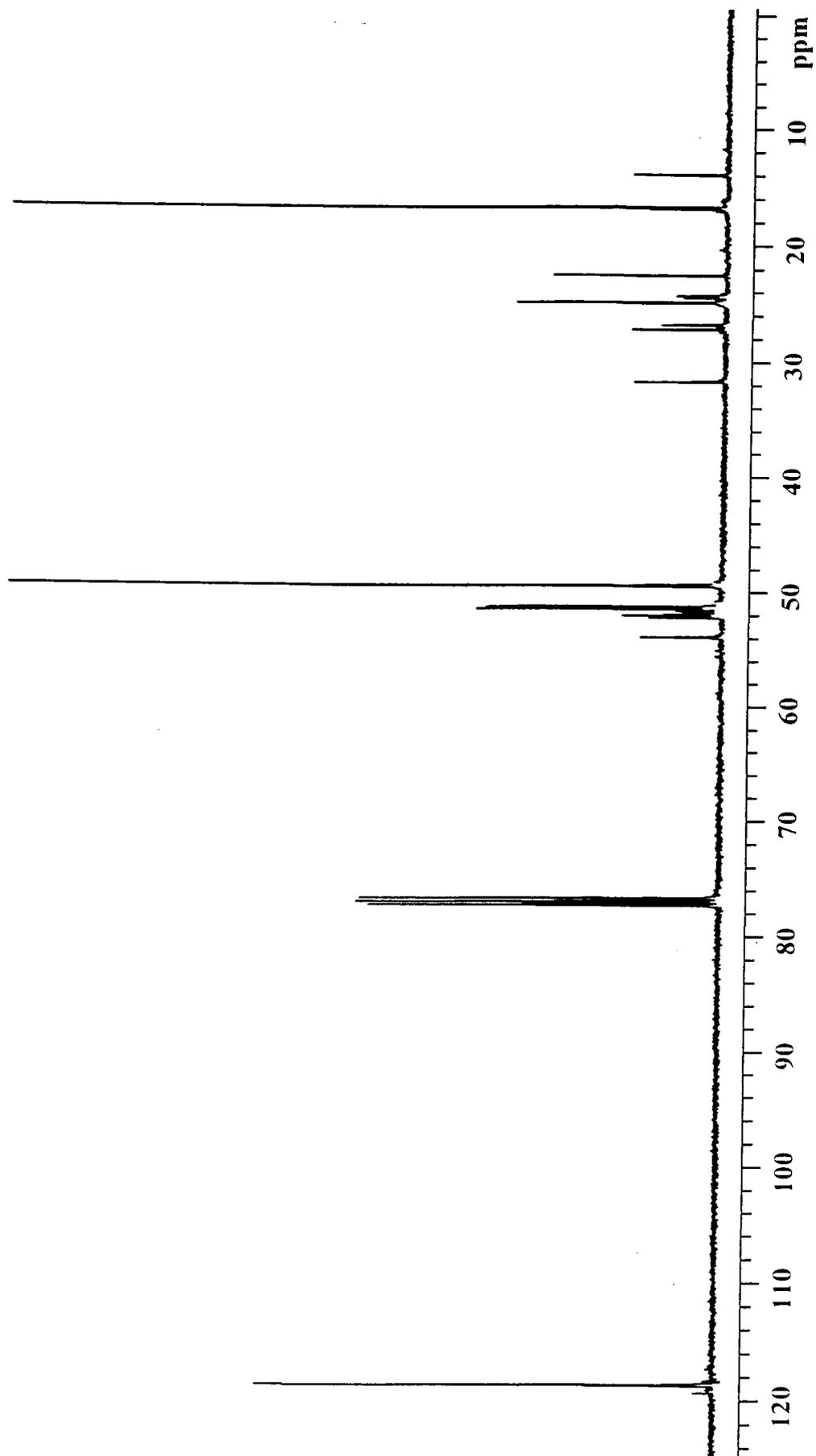
Appendix 1.3.5 ^{13}C nmr spectrum of Hex-*wedge*-(CN)$_8$ in CDCl$_3$.
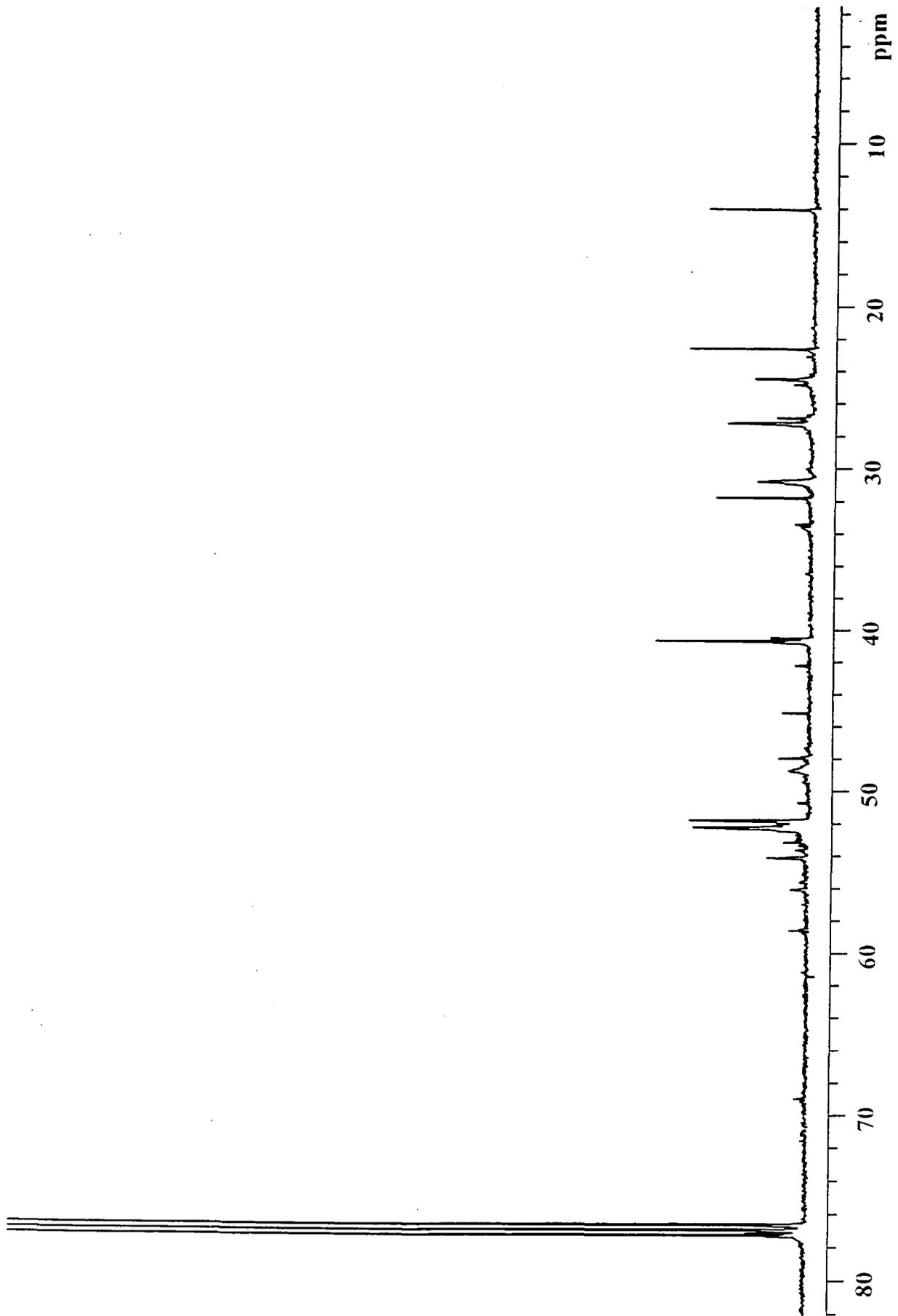
Appendix 1.3.6 ^{13}C nmr spectrum of Hex-*wedge*-$(NH_2)_8$ in $CDCl_3$.
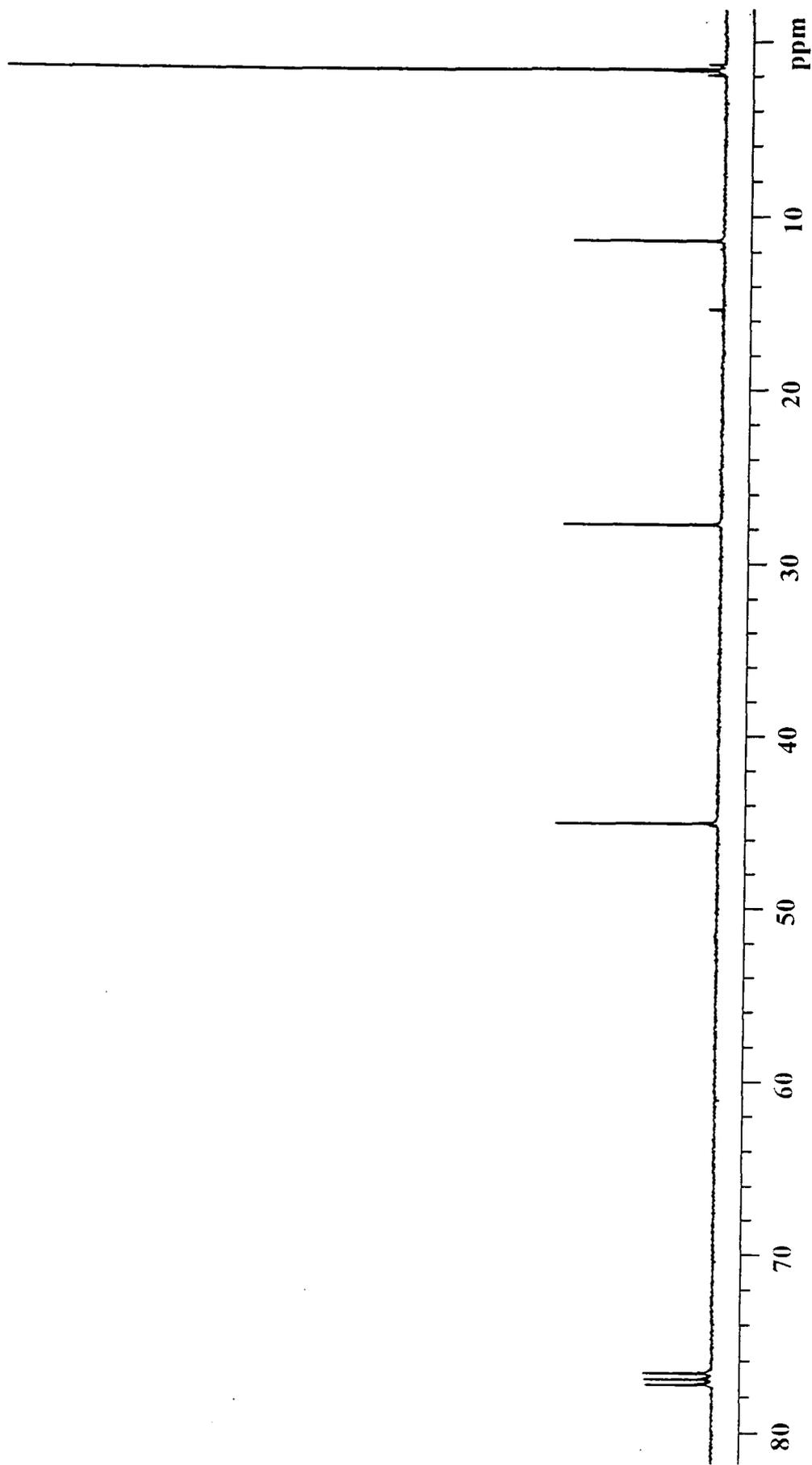
Appendix 1.3.7 ¹³C nmr spectrum of 3-aminopropyltris(trimethylsiloxy)silane (APTTMSS) in CDCl$_3$.
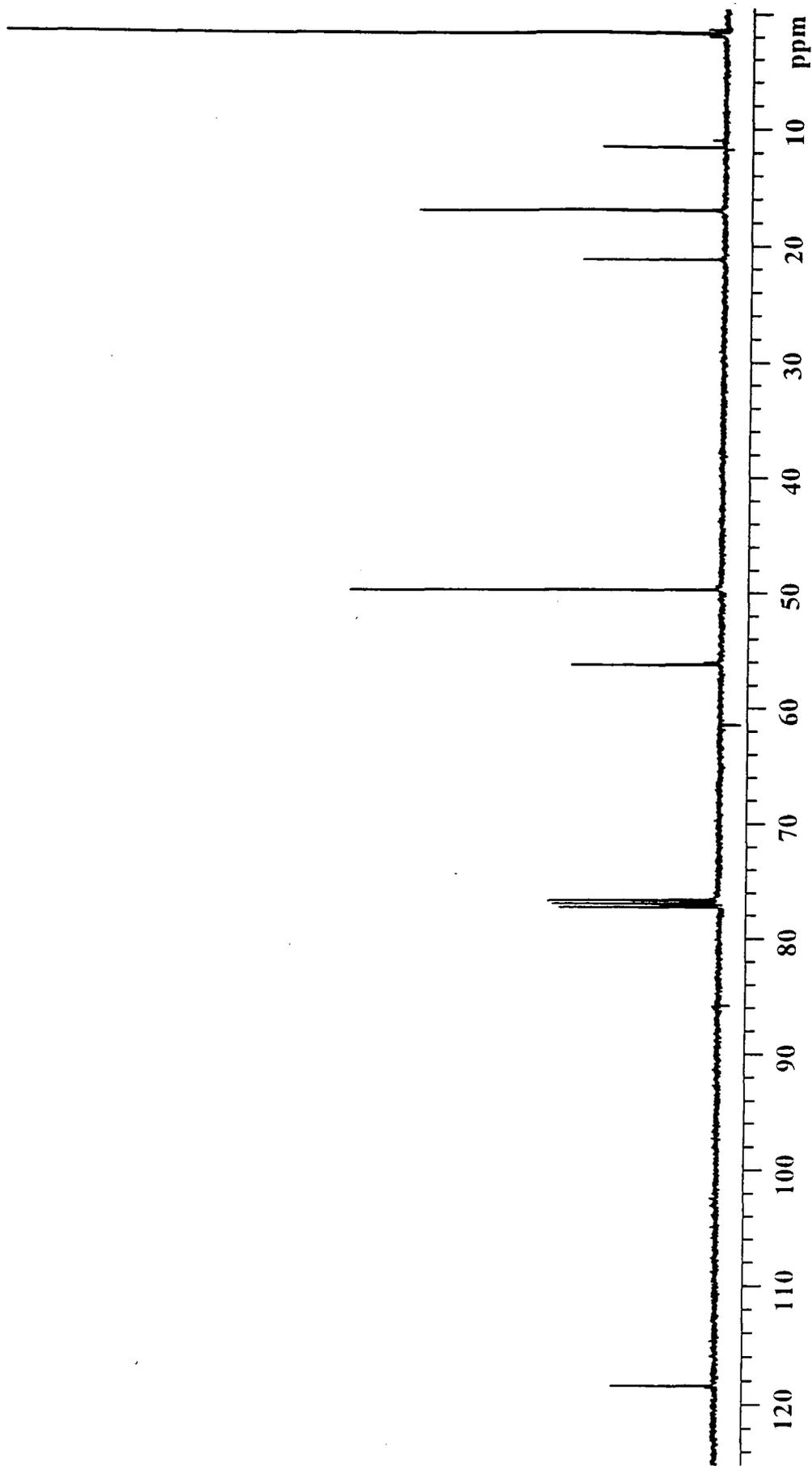
Appendix 1.3.8 ^{13}C nmr spectrum of Si-*wedge*-(CN)$_2$ in CDCl$_3$.
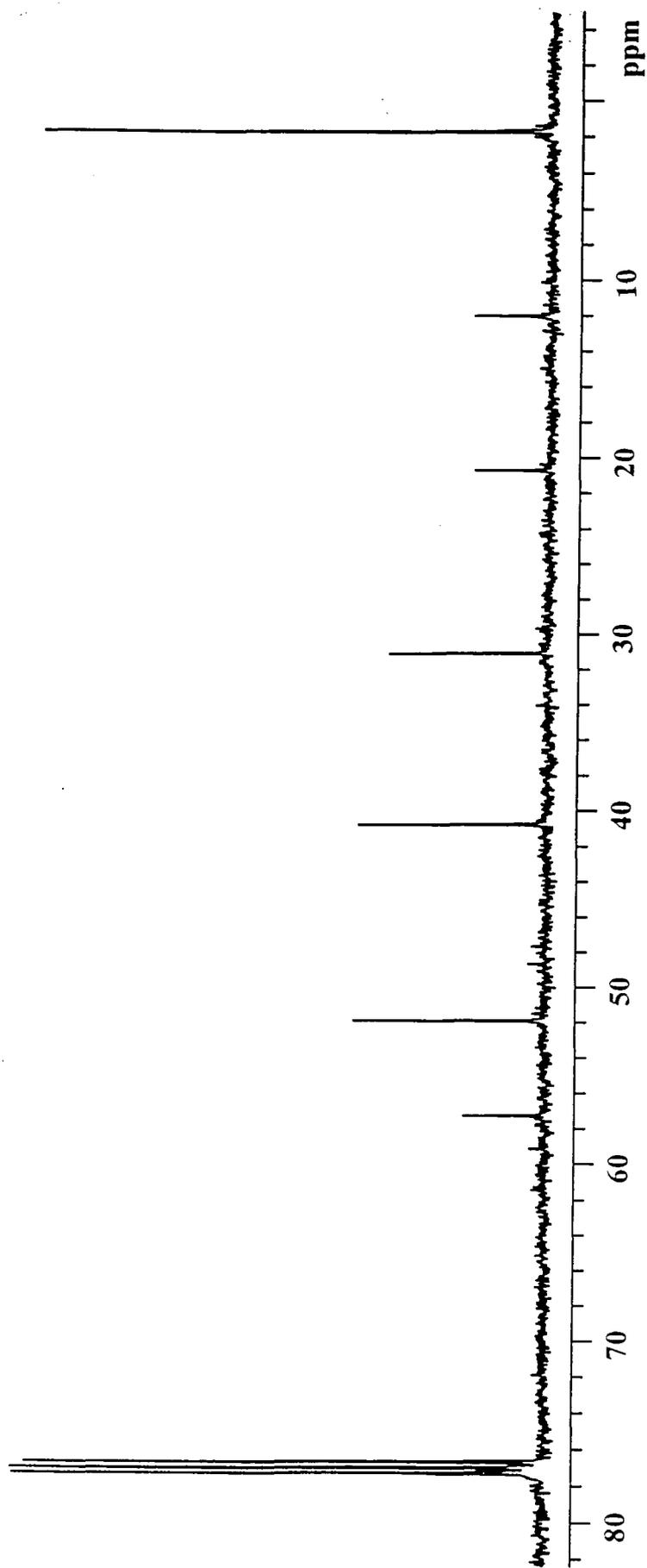
Appendix 1.3.9 ^{13}C nmr spectrum of Si-*wedge*-$(NH_2)_2$ in $CDCl_3$.
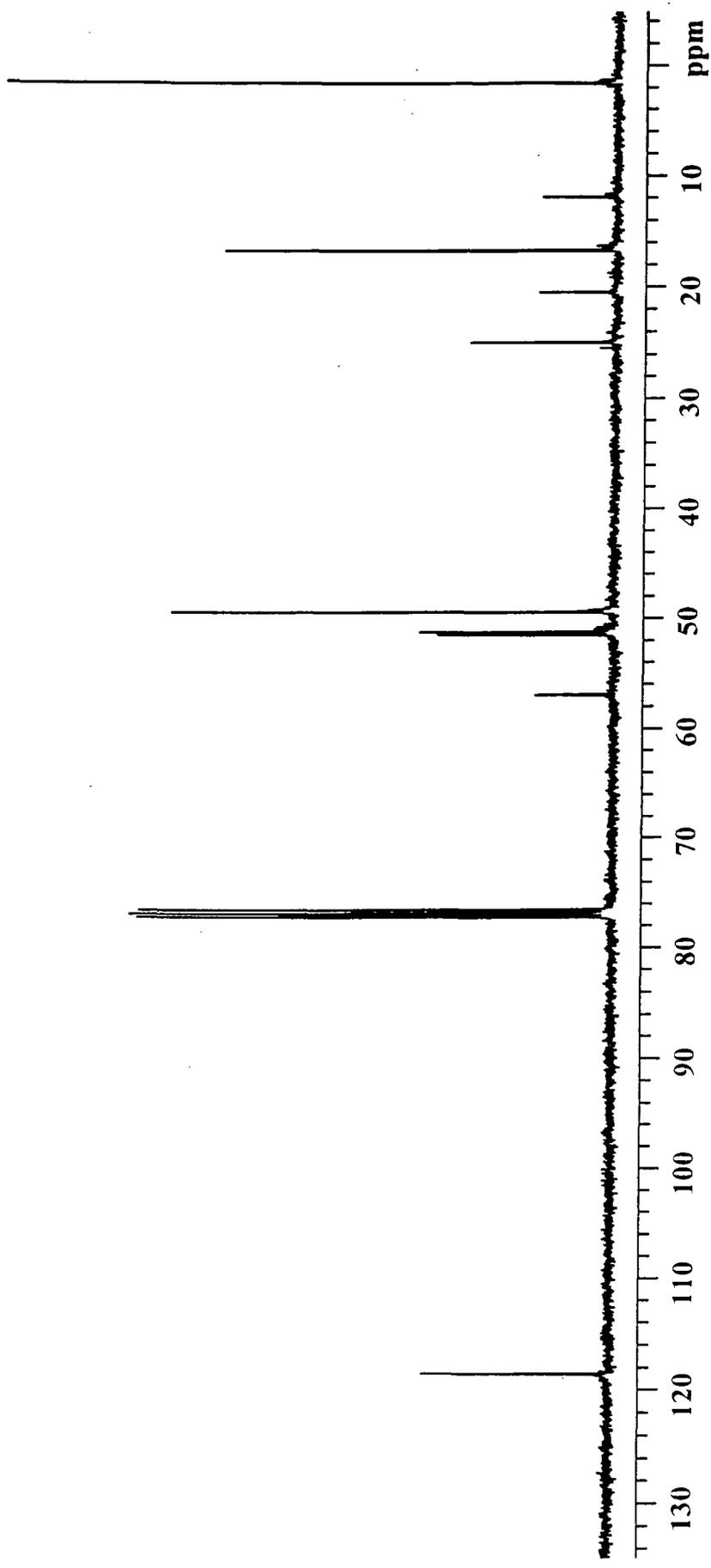
Appendix 1.3.10 ^{13}C NMR Spectrum of Si-*wedge*-$(CN)_4$ in $CDCl_3$.
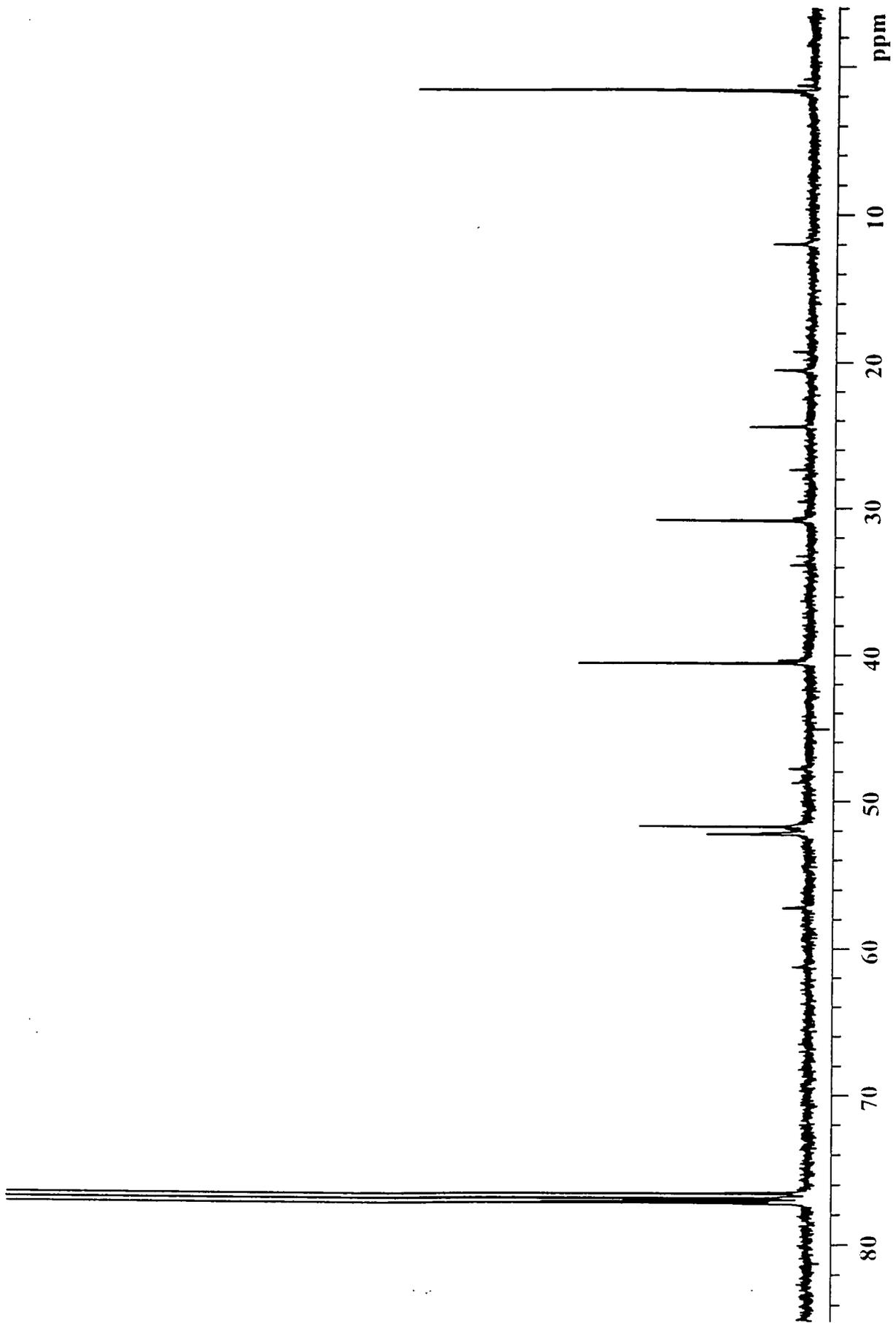
Appendix 1.3.11 ^{13}C nmr spectrum of Si-*wedge*-$(NH_2)_4$ in $CDCl_3$.
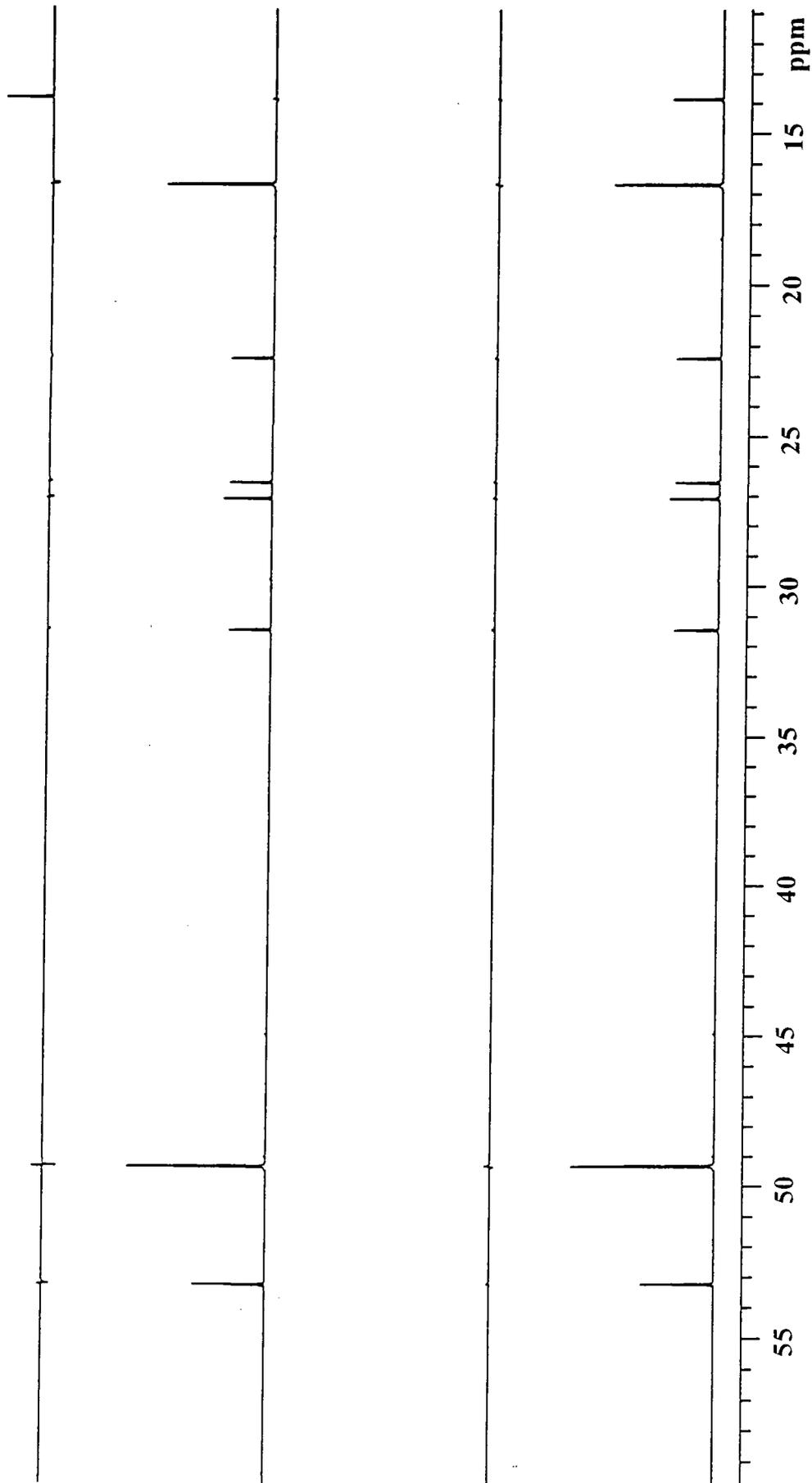
Appendix 1.4.1 DEPT nmr spectrum of Hex-*wedge*-(CN)$_2$ in CDCl$_3$.
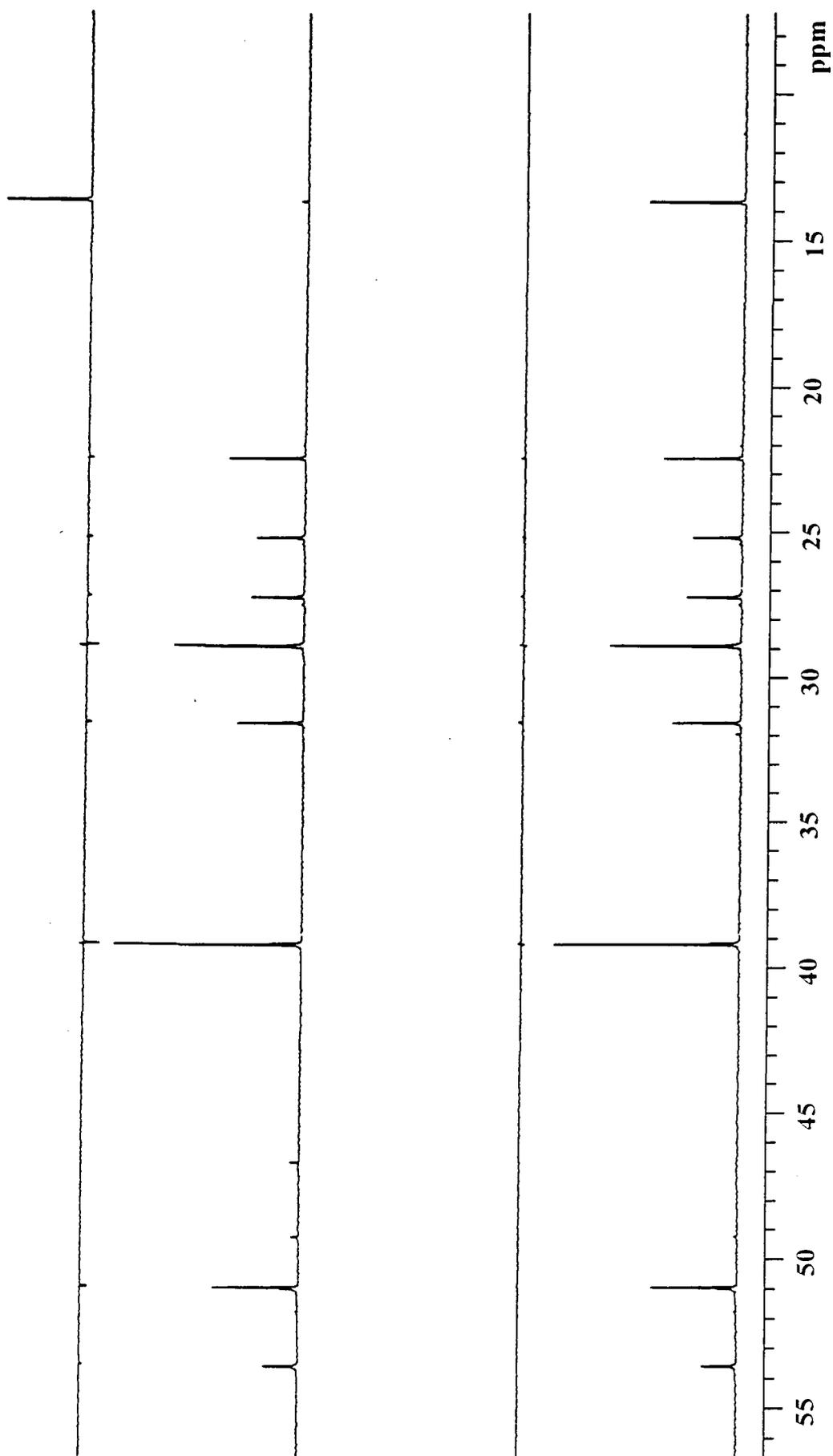
Appendix 1.4.2 DEPT nmr spectrum of Hex-*wedge*-(NH$_2$)$_2$ in CDCl$_3$.
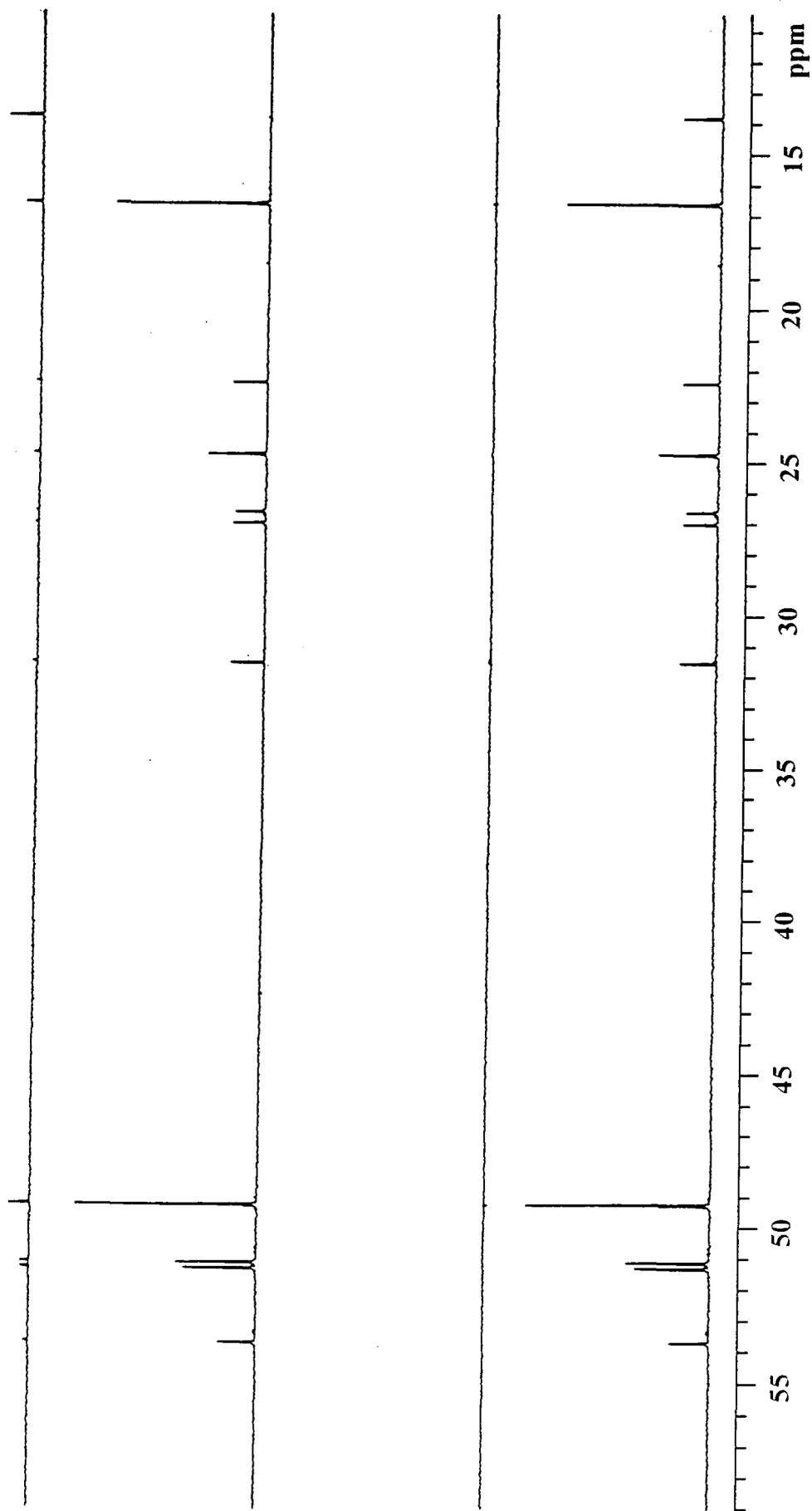
Appendix 1.4.3 DEPT nmr spectrum of Hex-*wedge*-(CN)$_4$ in CDCl$_3$.
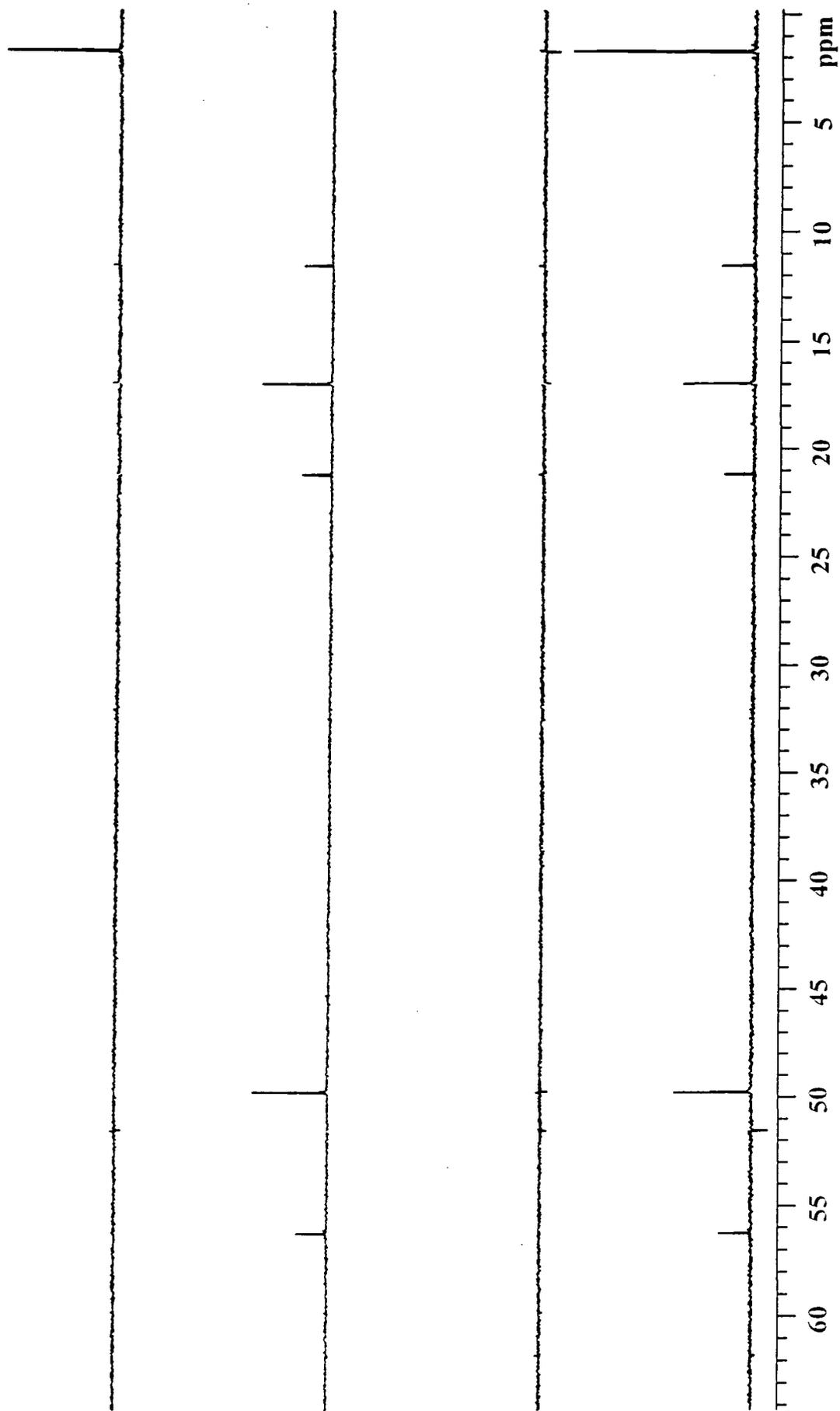
Appendix 1.4.4 DEPT nmr spectrum of Si-*wedge*-(CN)$_2$ in CDCl$_3$.
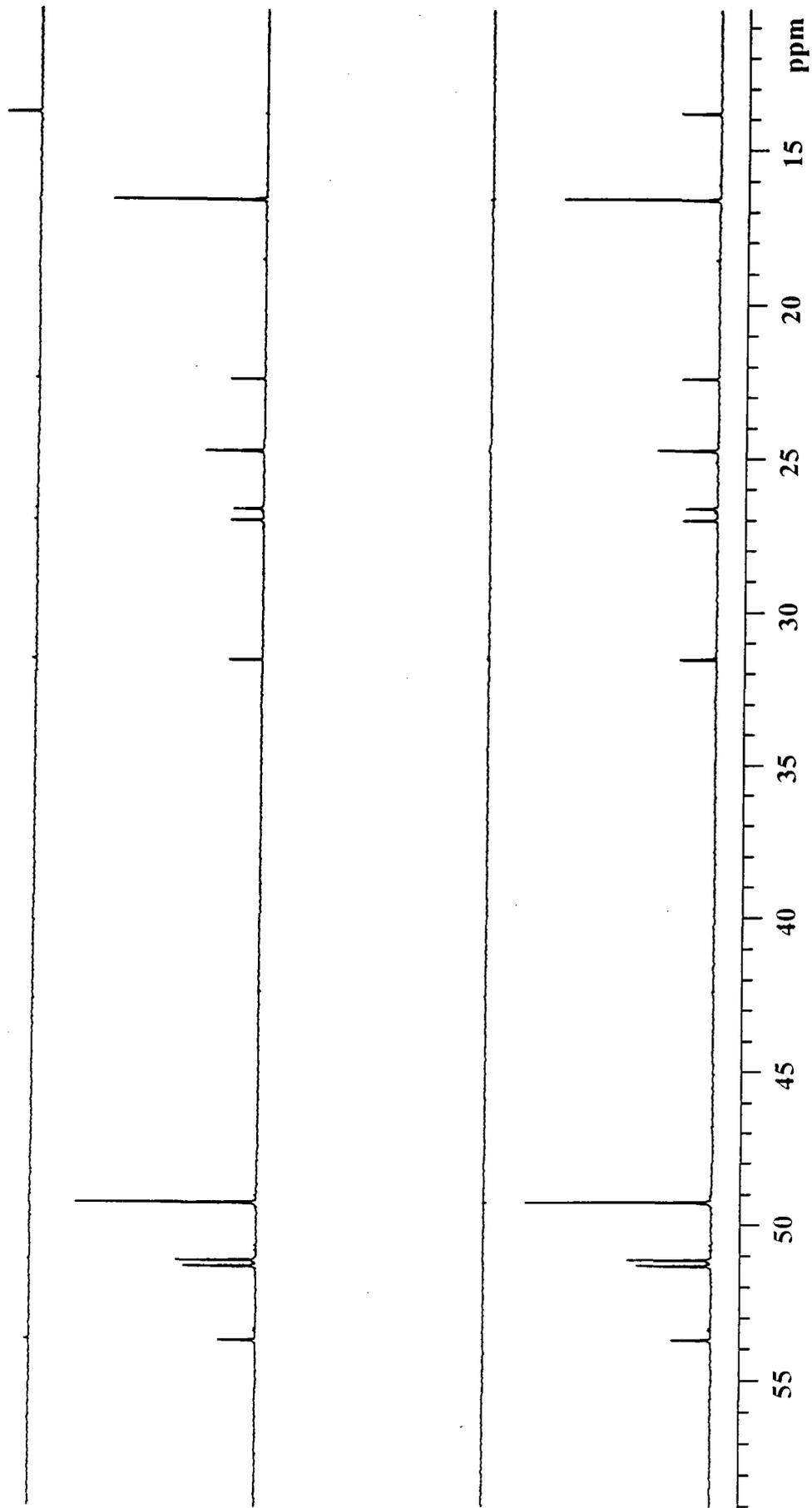
Appendix 1.4.5 DEPT nmr spectrum of Si-*wedge*-(CN)$_4$ in CDCl$_3$.
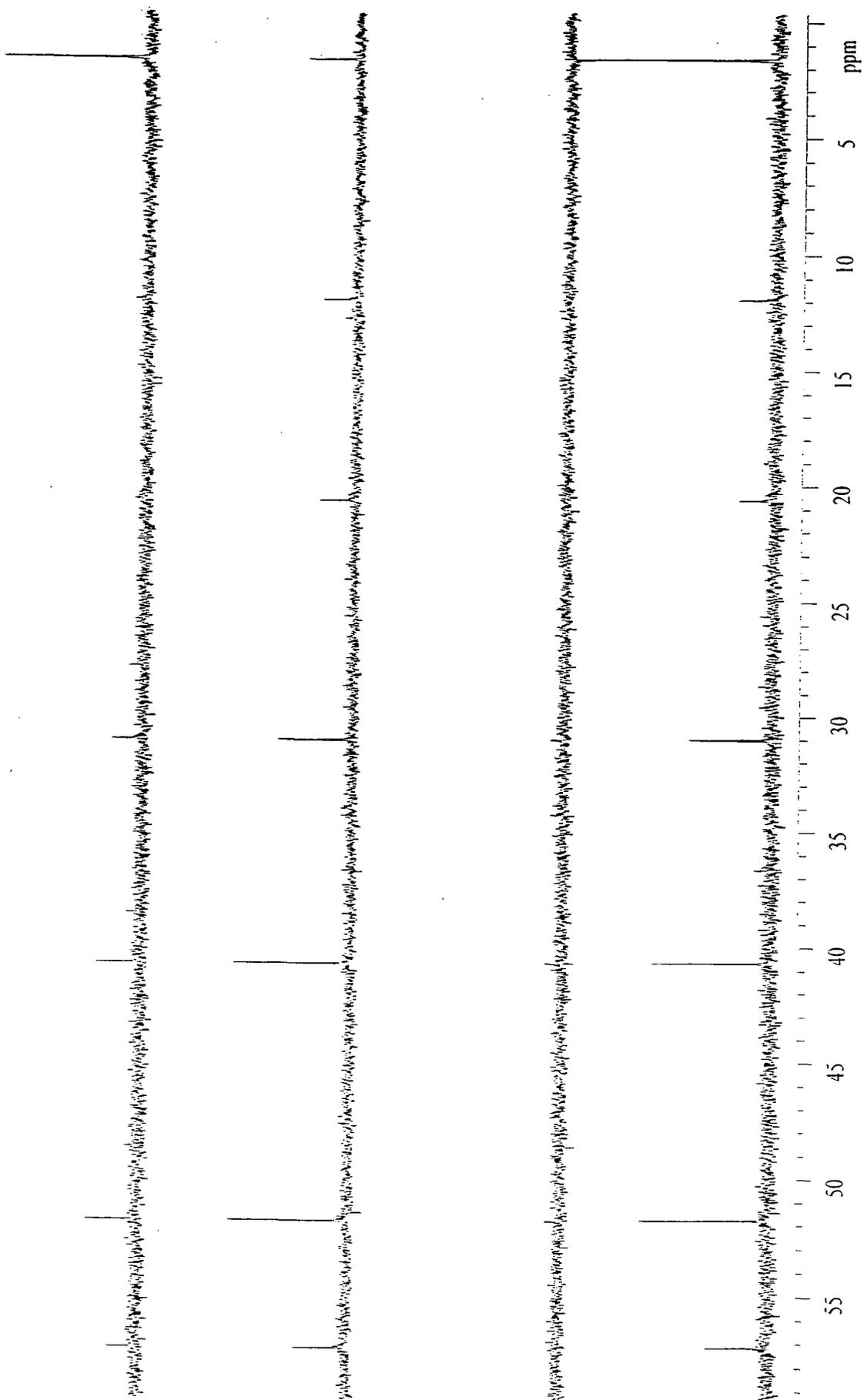
Appendix 1.4.6 DEPT nmr spectrum of Si-*wedge*-(NH$_2$)$_2$ in CDCl$_3$.
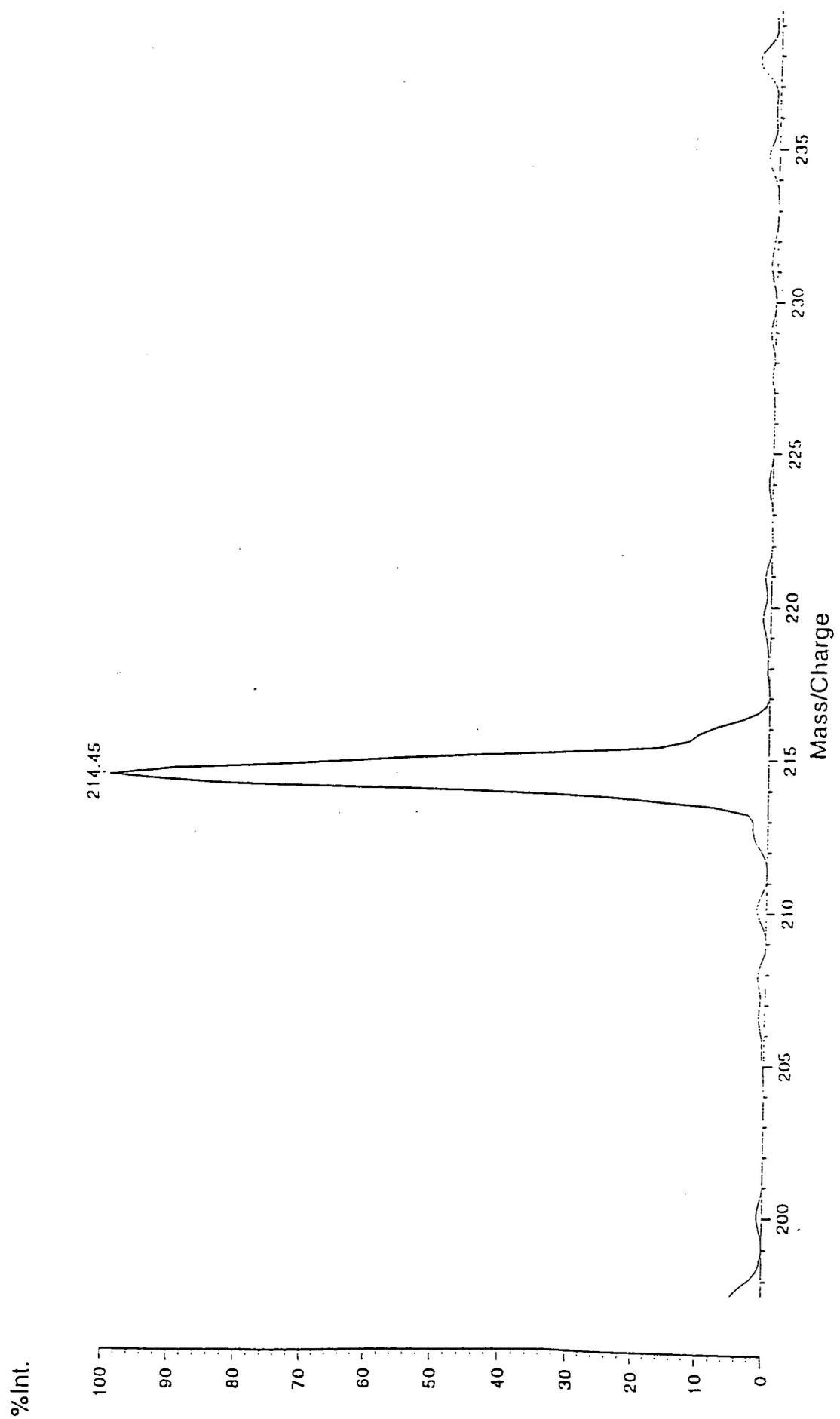
Appendix 1.5.1 MALDI-TOF-MS spectrum of Hex-*wedge*-(NH$_2$)$_2$.
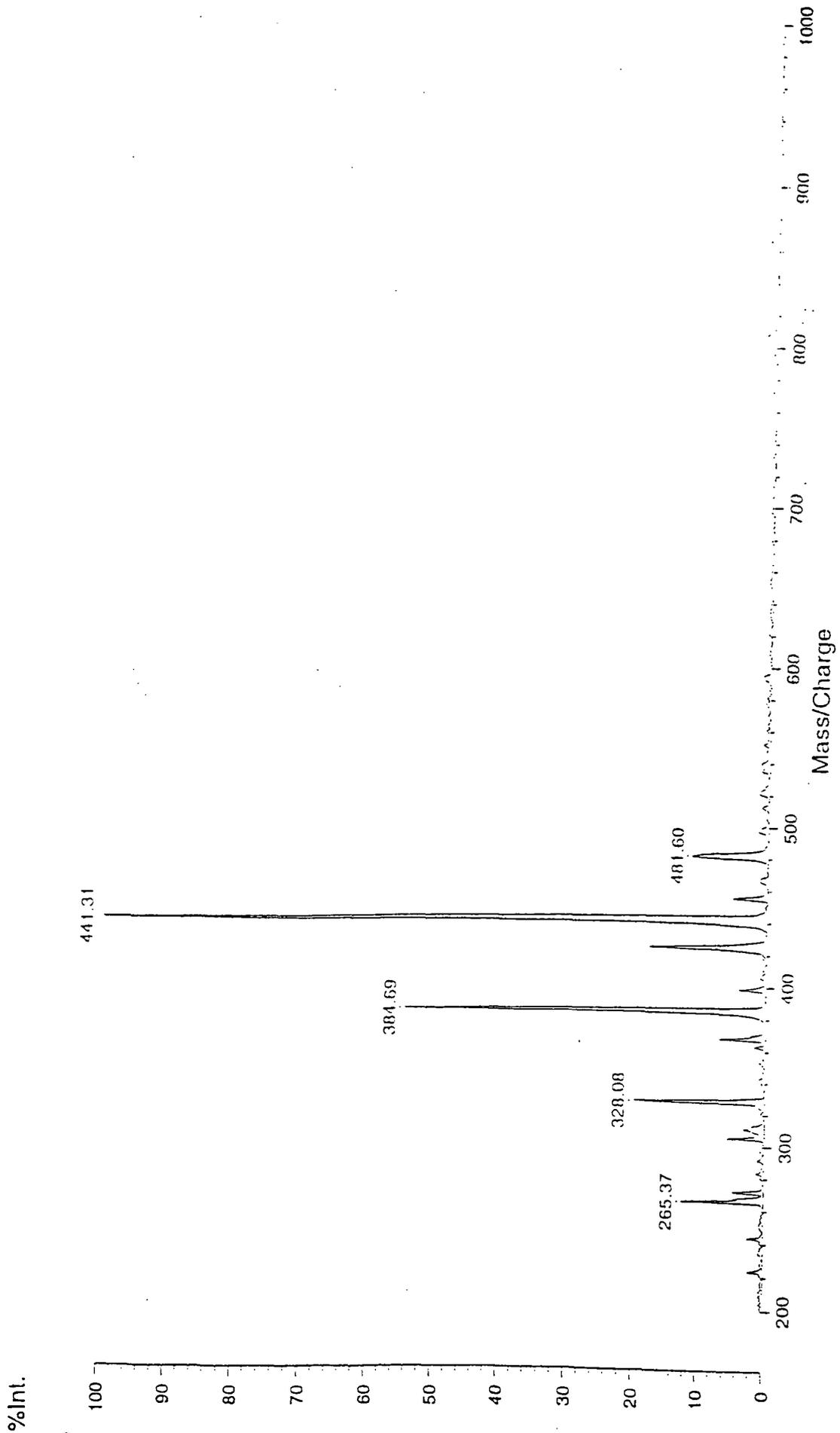
Appendix 1.5.2 MALDI-TOF-MS spectrum of Hex-*wedge*-(NH$_2$)$_4$.

Appendix 2

Analytical Data for Chapter 3

Appendix 2.1 ^{1}H nmr spectra

Appendix 2.2 ^{13}C nmr spectra

Appendix 2.3 DEPT nmr spectra

Appendix 2.4 HETCOR and COSY nmr spectra

Appendix 2.5 MALDI-TOF mass spectra

Appendix 2.1.1 ^{1}H nmr spectrum of NCBZ-phe-hydroxysuccinimide ester in CDCl$_3$.

Appendix 2.1.2 ^{1}H nmr spectrum of NCBZ-trp-hydroxysuccinimide ester in CDCl$_3$.
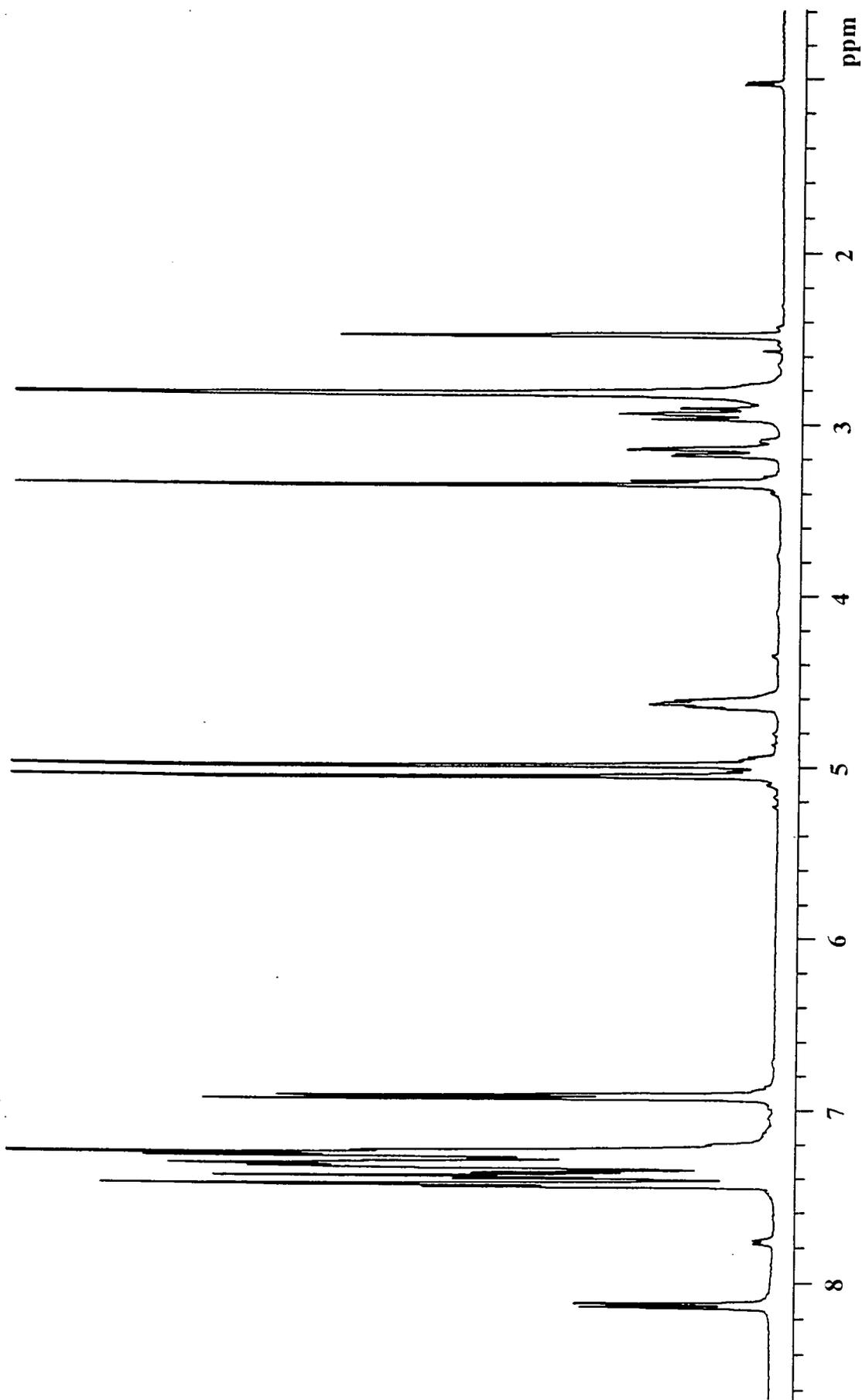
Appendix 2.1.3 ¹H nmr spectrum of NCBZ-tyr-hydroxysuccinimide ester in DMSOd₆.
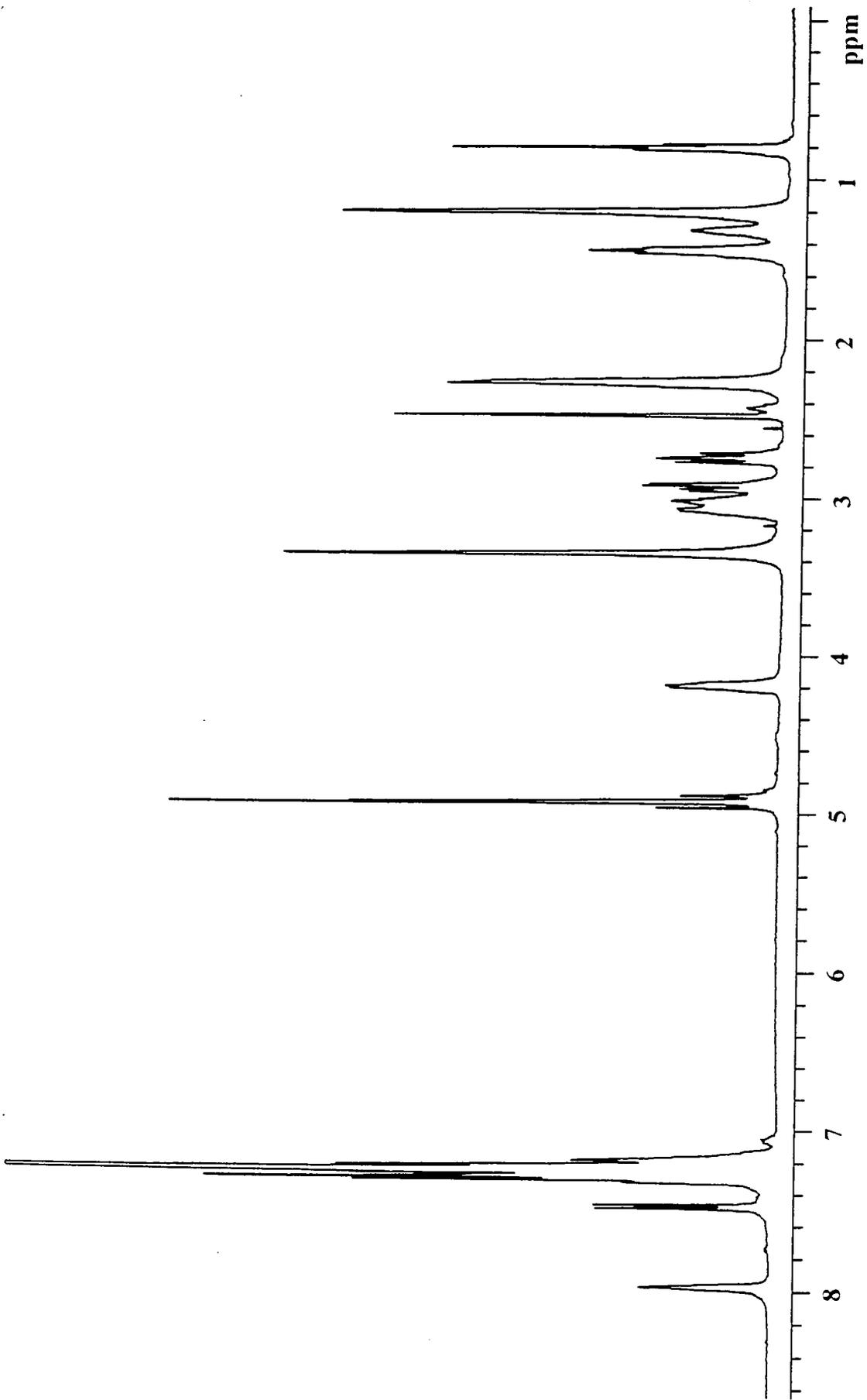
Appendix 2.1.4 ^{1}H nmr spectrum of Hex-*wedge*-phe$_2$CBZ$_2$ in DMSOd$_6$.
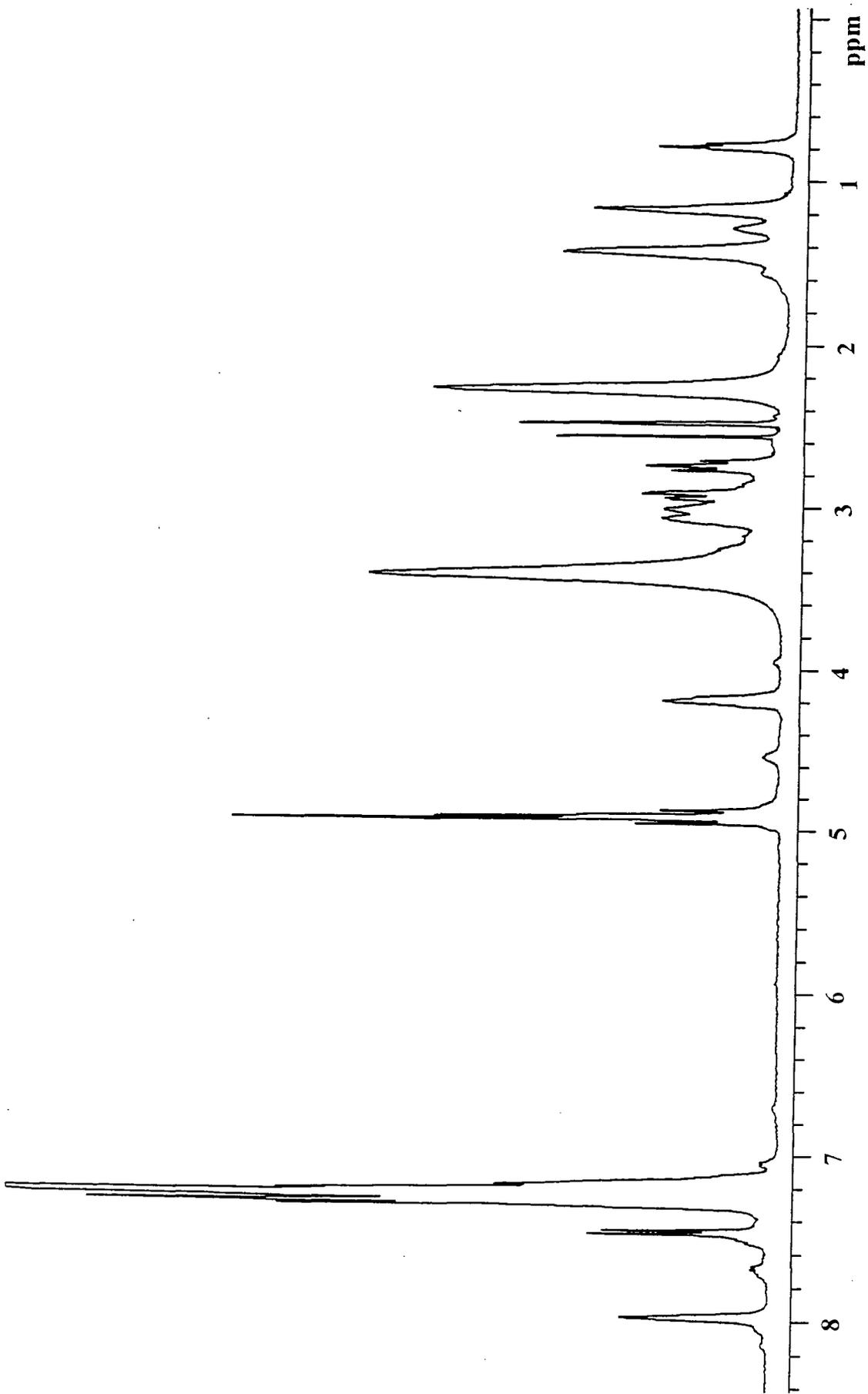
Appendix 2.1.5 ^{1}H nmr spectrum of Hex-*wedge*-phe$_4$CBZ$_4$ in DMSOd$_6$.
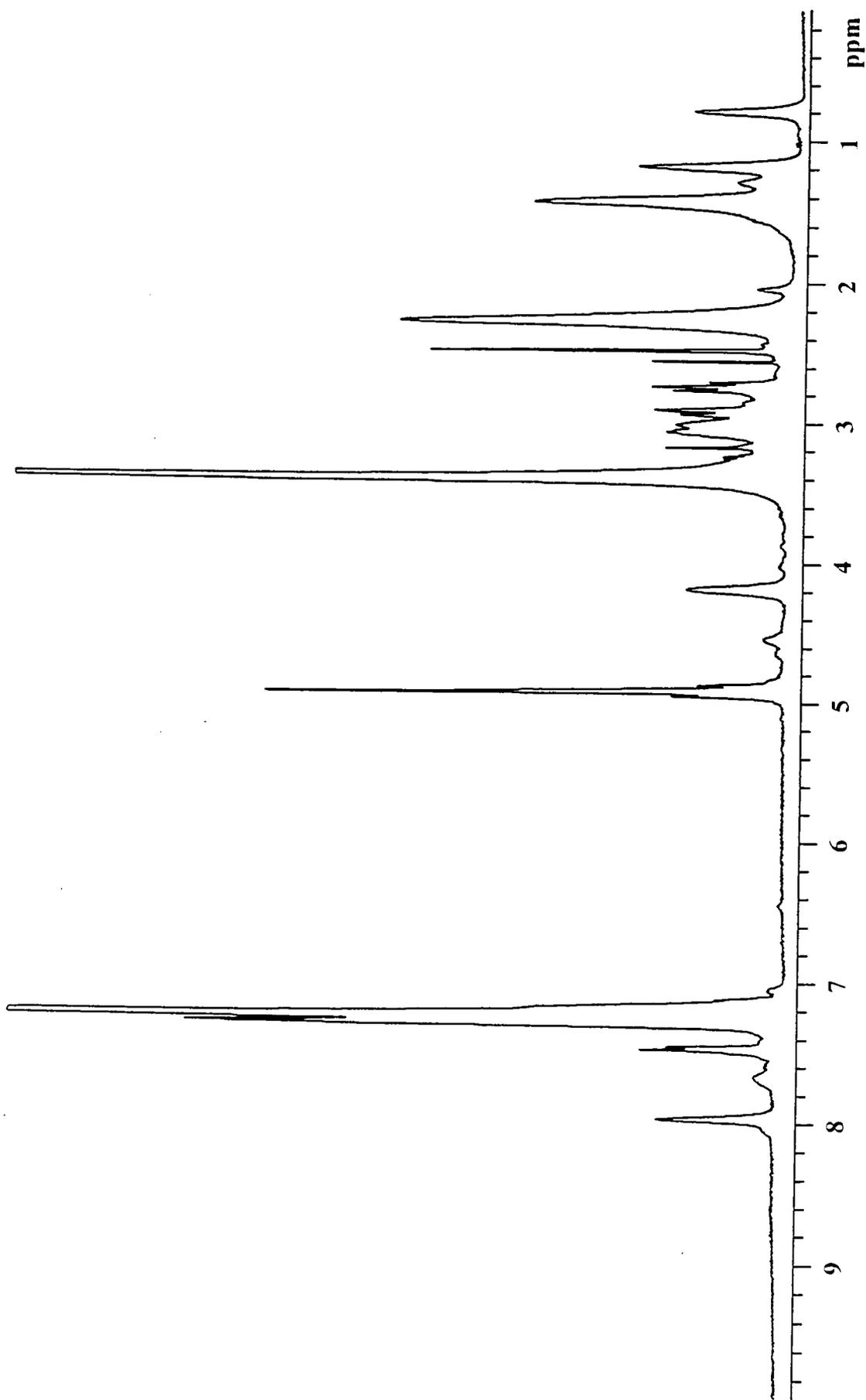
Appendix 2.1.6 ^{1}H nmr spectrum of Hex-*wedge*-phe$_8$CBZ$_8$ in DMSOd$_6$.
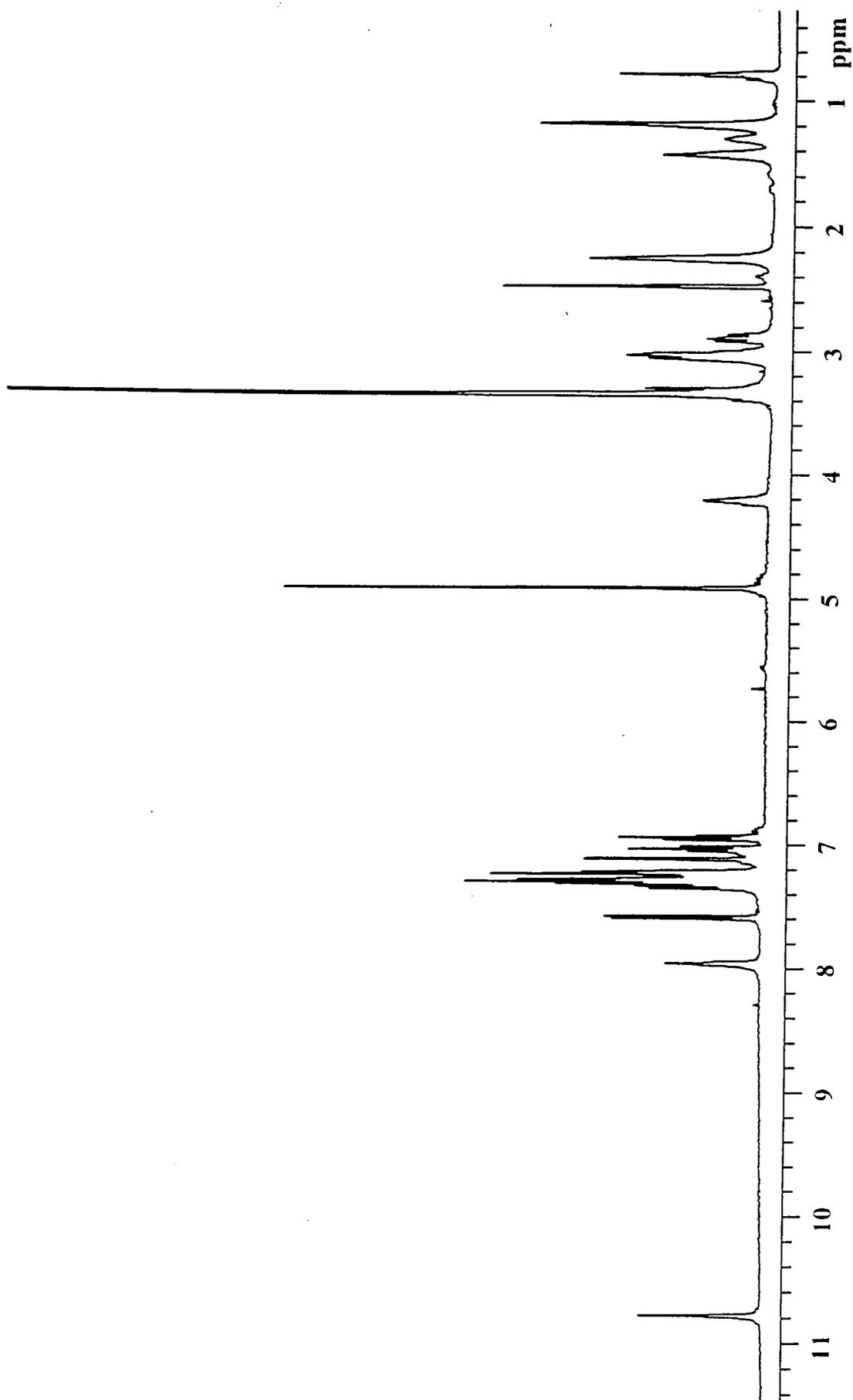
Appendix 2.1.7 ^{1}H nmr spectrum of Hex-*wedge*-trp$_2$-CBZ$_2$ in DMSOd$_6$.
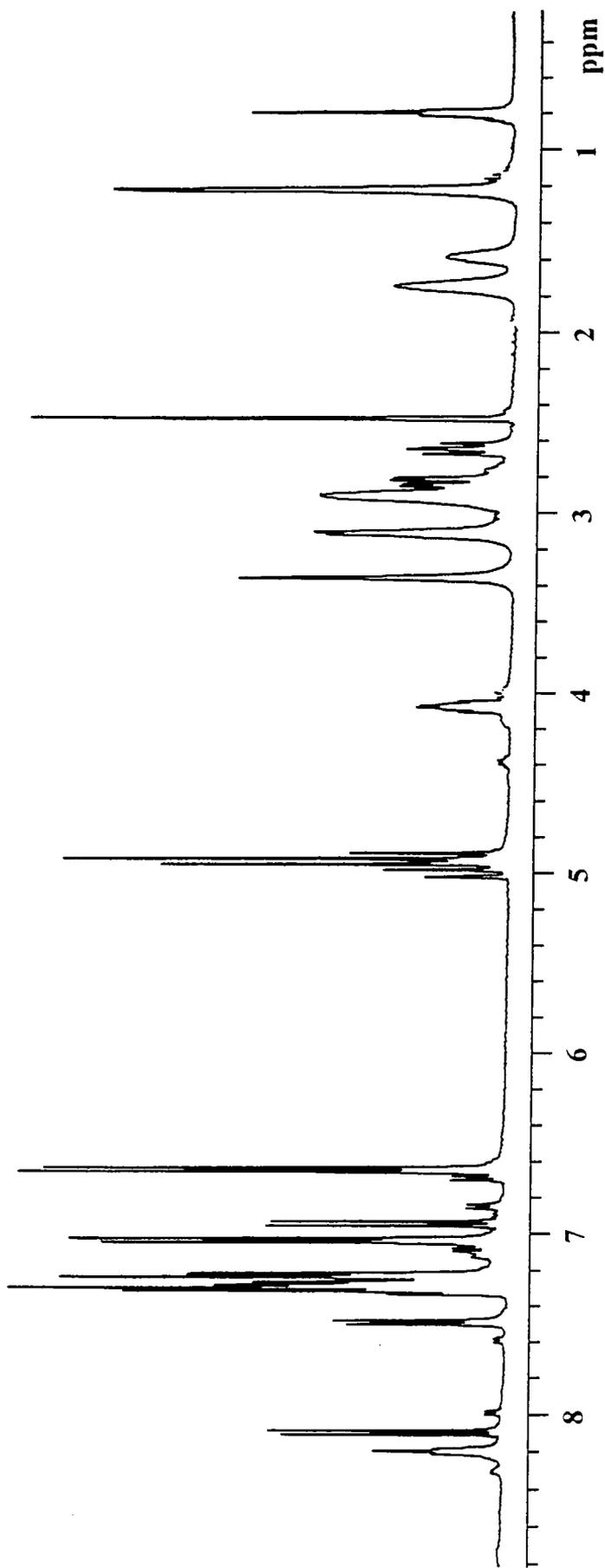
Appendix 2.1.8 ^{1}H nmr spectrum of Hex-*wedge-o-benzyl*-tyr$_2$-CBZ$_2$ in DMSOd$_6$.

Appendix 2.1.9 ^{1}H nmr spectrum of Hex-*wedge*-phe$_2$ in DMSOd_6.
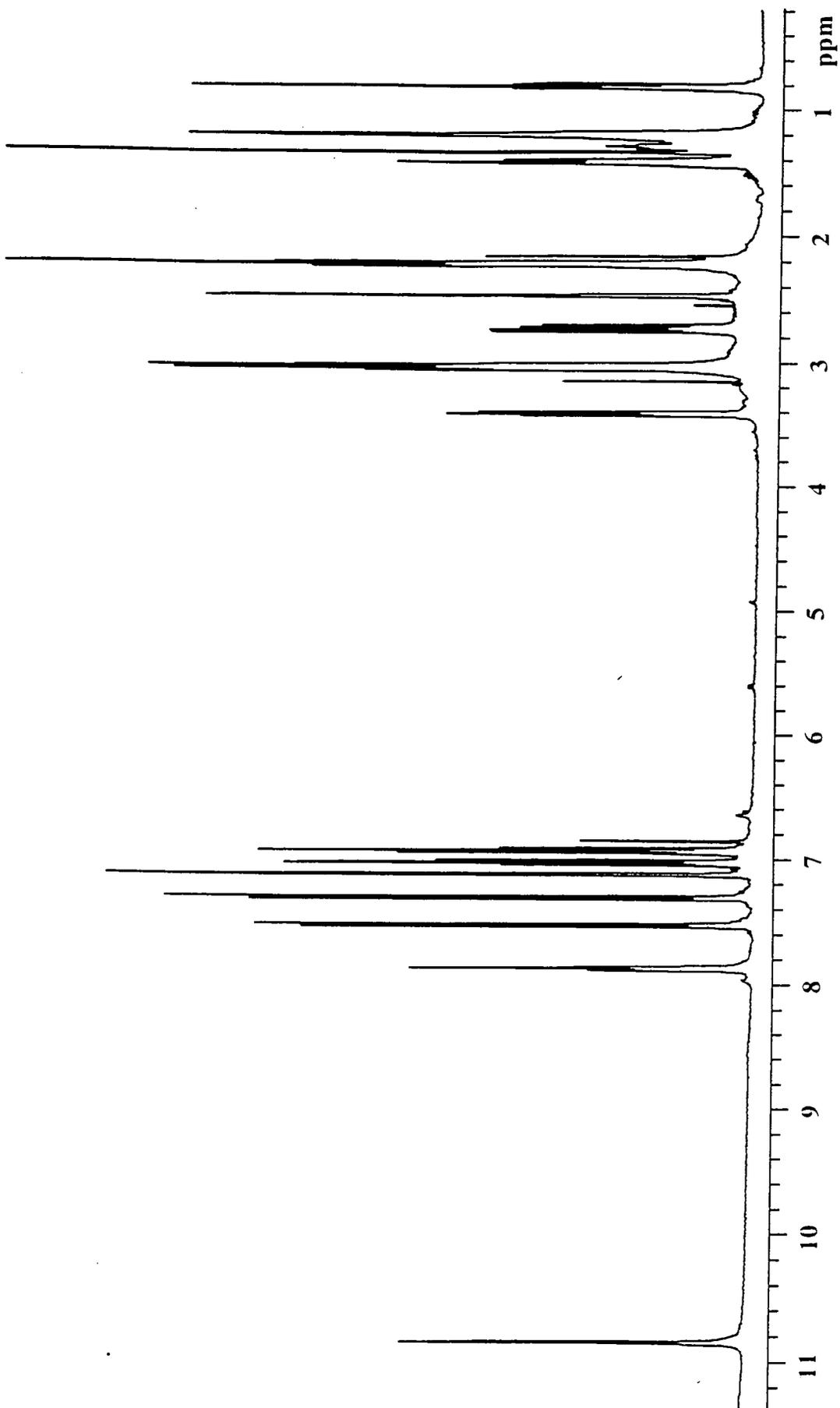
Appendix 2.1.10 ^{1}H nmr spectrum of Hex-*wedge*-trp$_2$ in DMSOd$_6$.
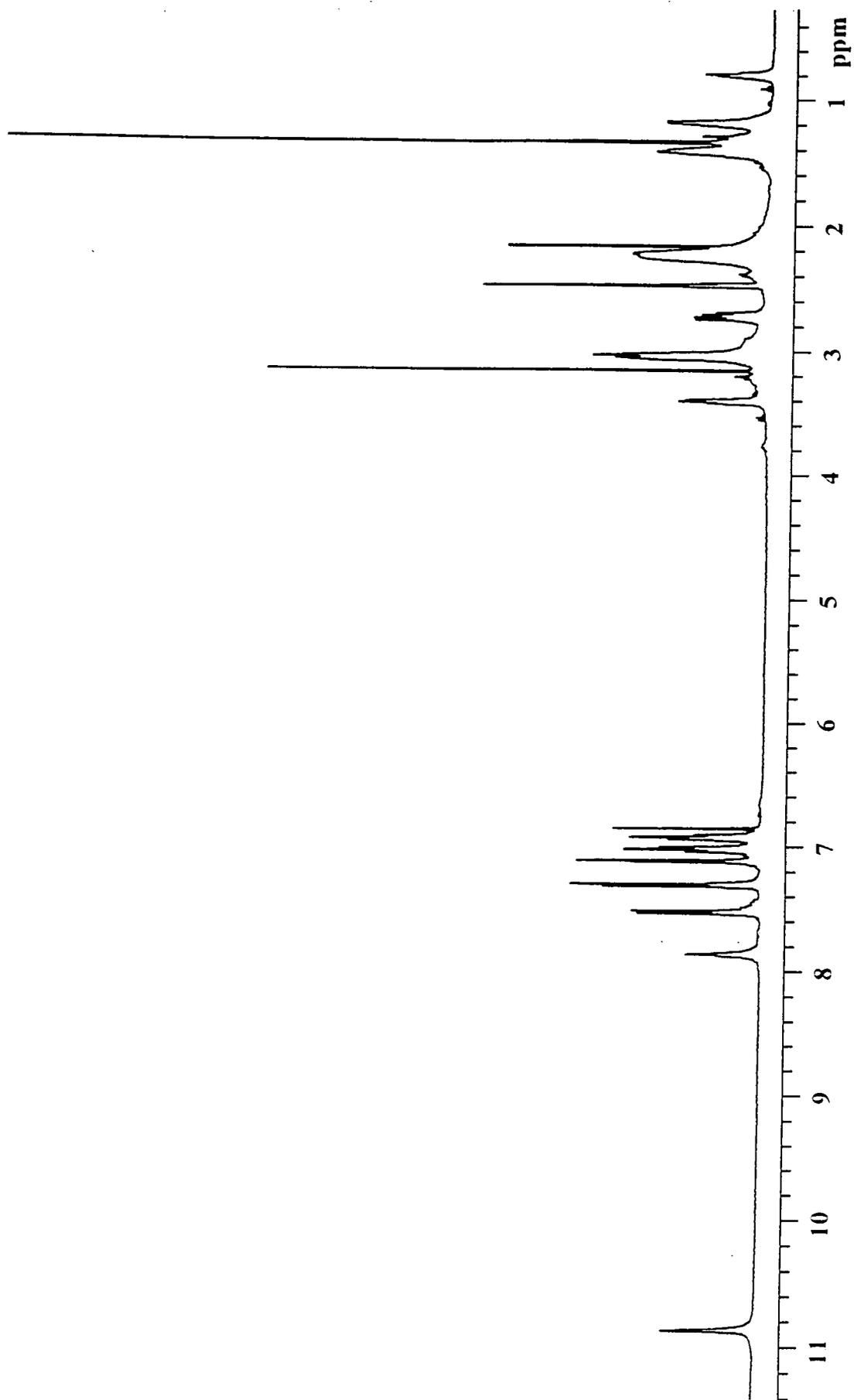
Appendix 2.1.11 [^1]H nmr spectrum of Hex-*wedge*-trp$_4$ in DMSOd$_6$.
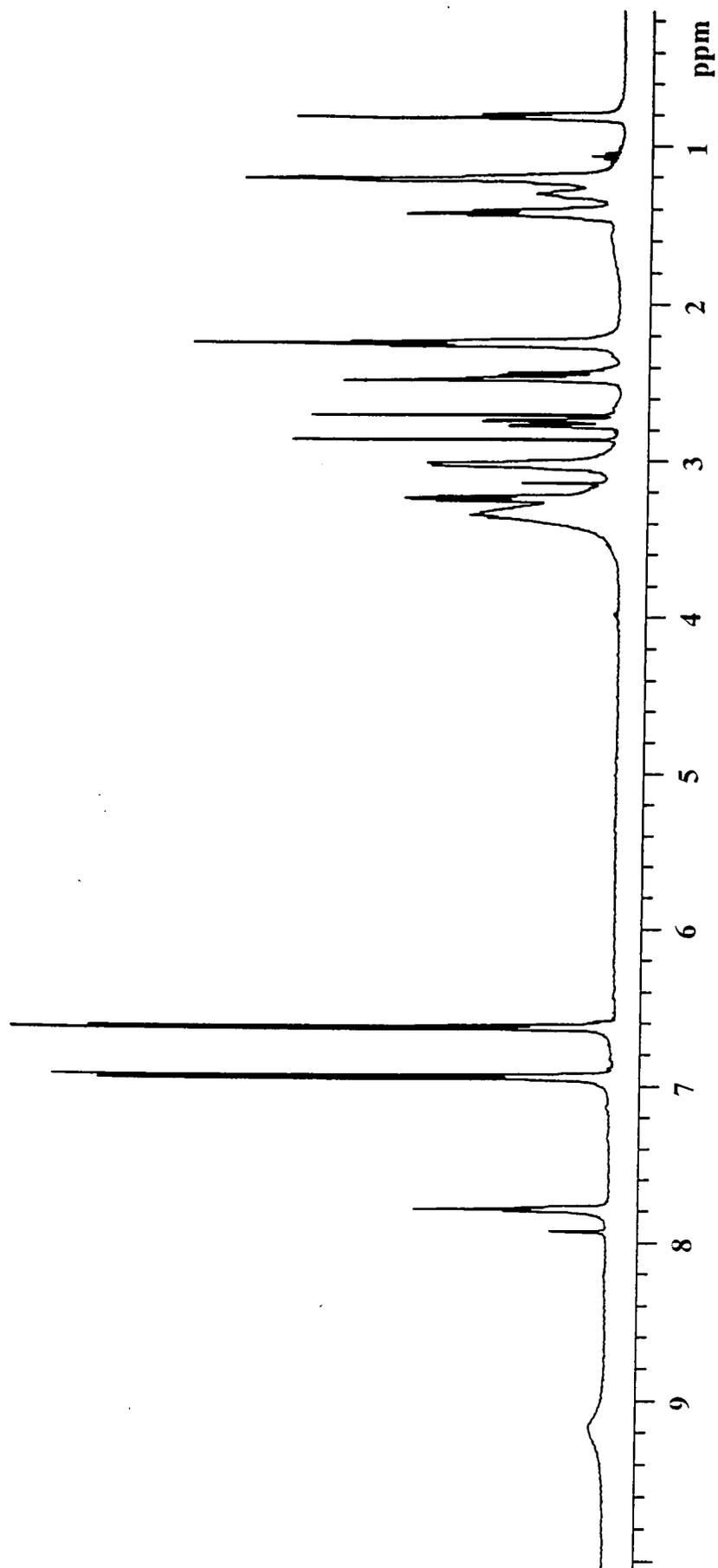
Appendix 2.1.12 ^{1}H nmr spectrum of Hex-*wedge*-tyr$_2$ in DMSOd$_6$.
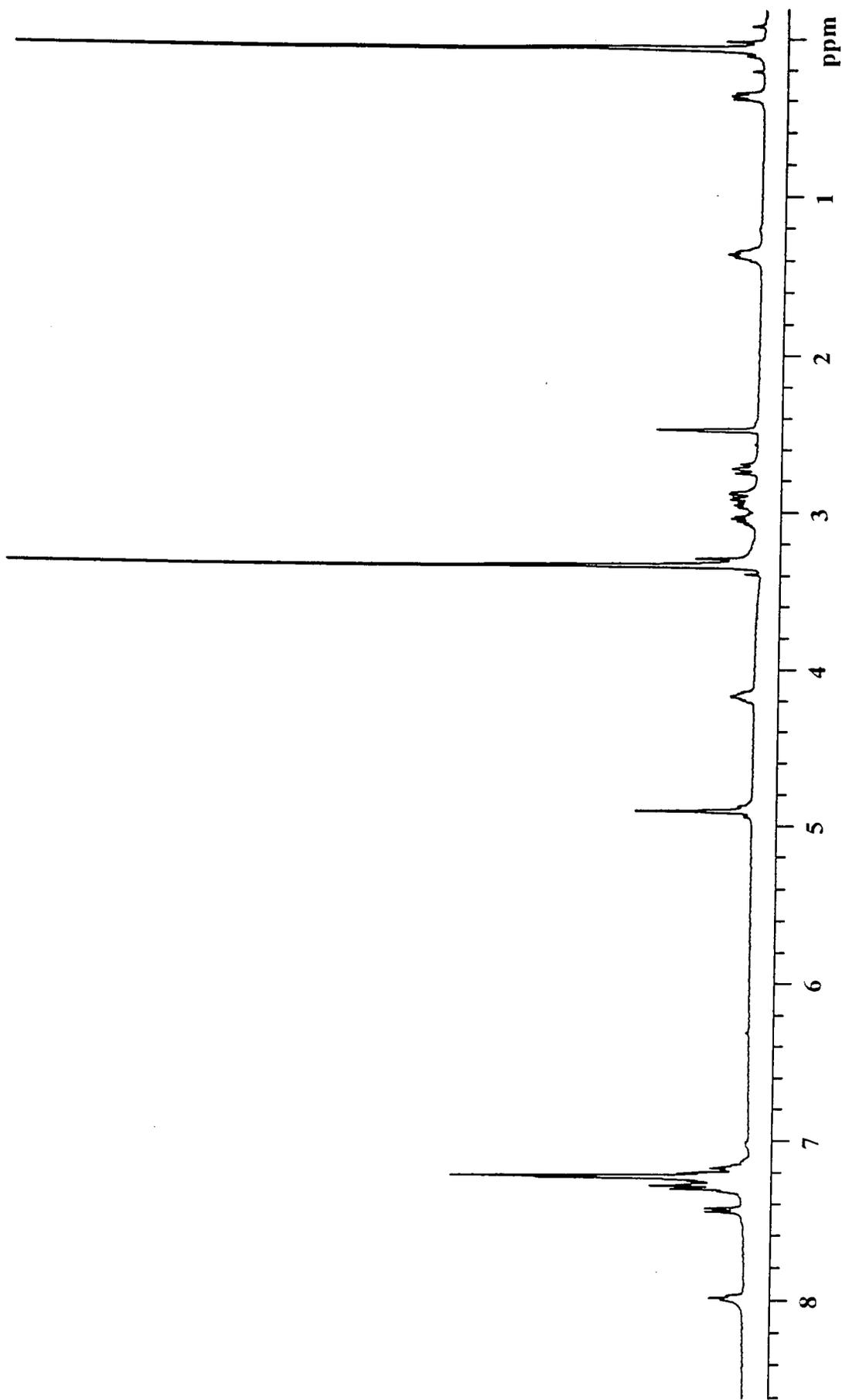
Appendix 2.1.13 ^{1}H nmr spectrum of Si-*wedge*-phe-CBZ in DMSOd$_6$.
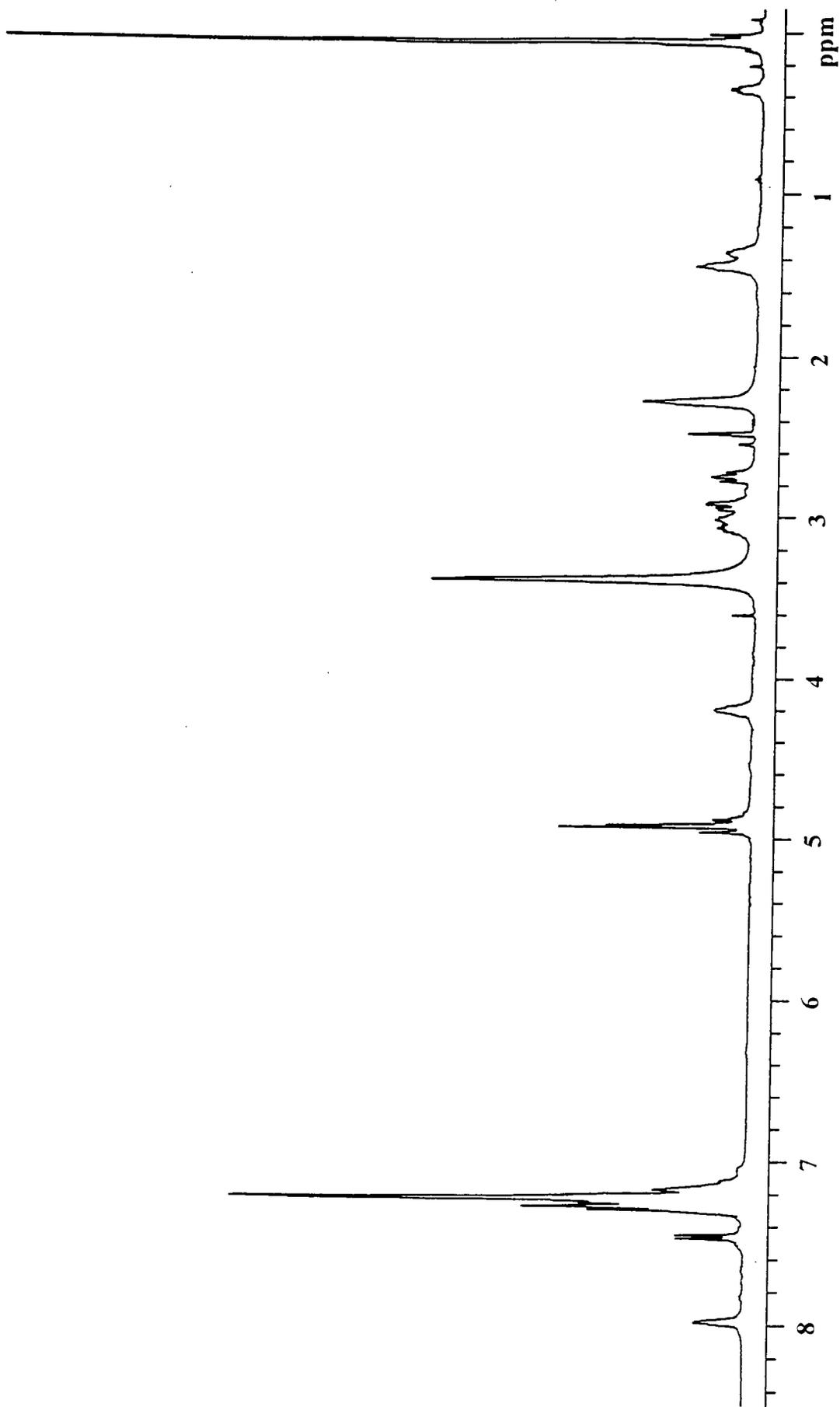
Appendix 2.1.14 ^{1}H nmr spectrum of Si-*wedge*-phe$_2$-CBZ$_2$ in DMSOd$_6$.
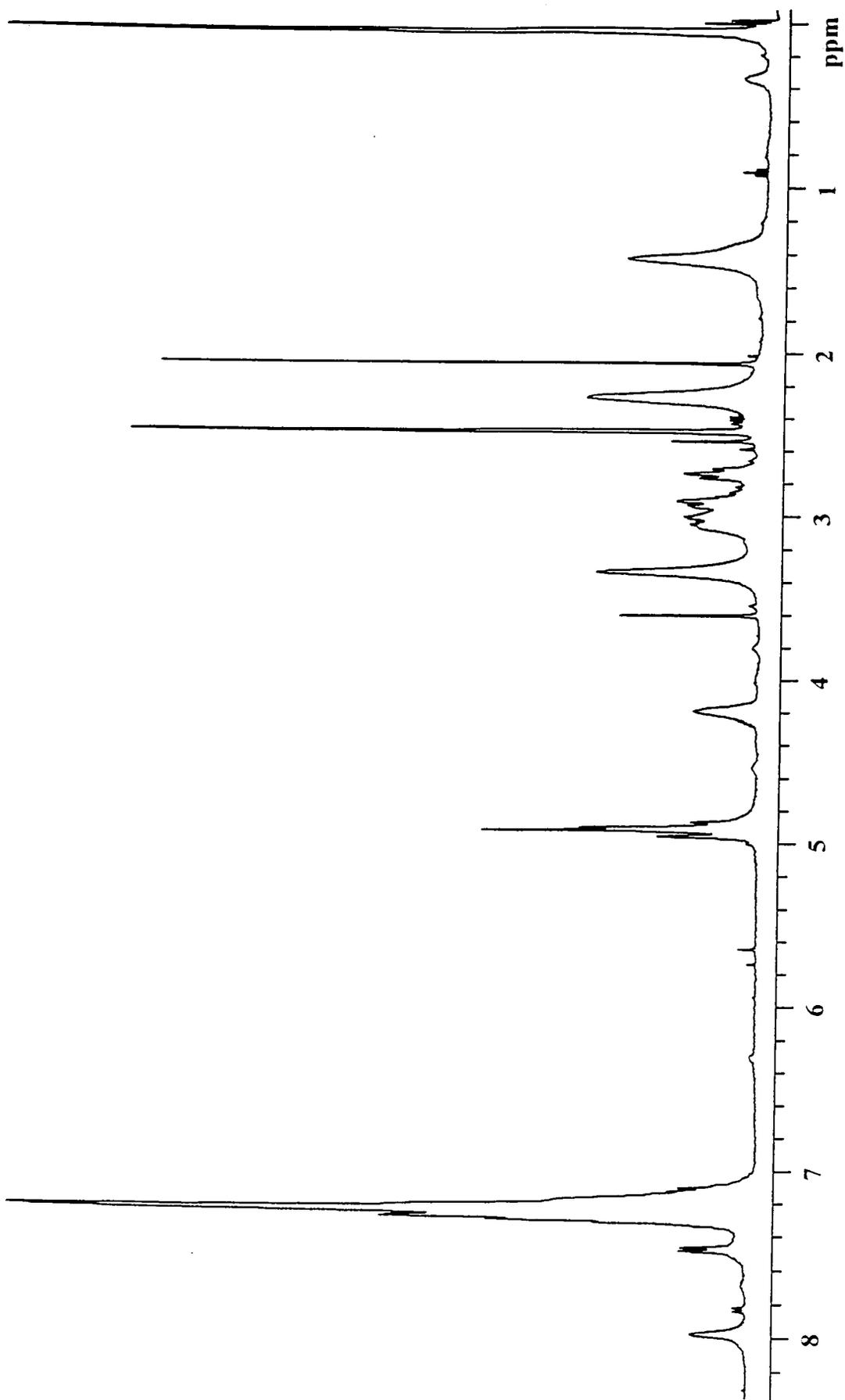
Appendix 2.1.15 ^{1}H nmr spectrum of Si-*wedge*-phe$_4$-CBZ$_4$ in DMSOd$_6$.
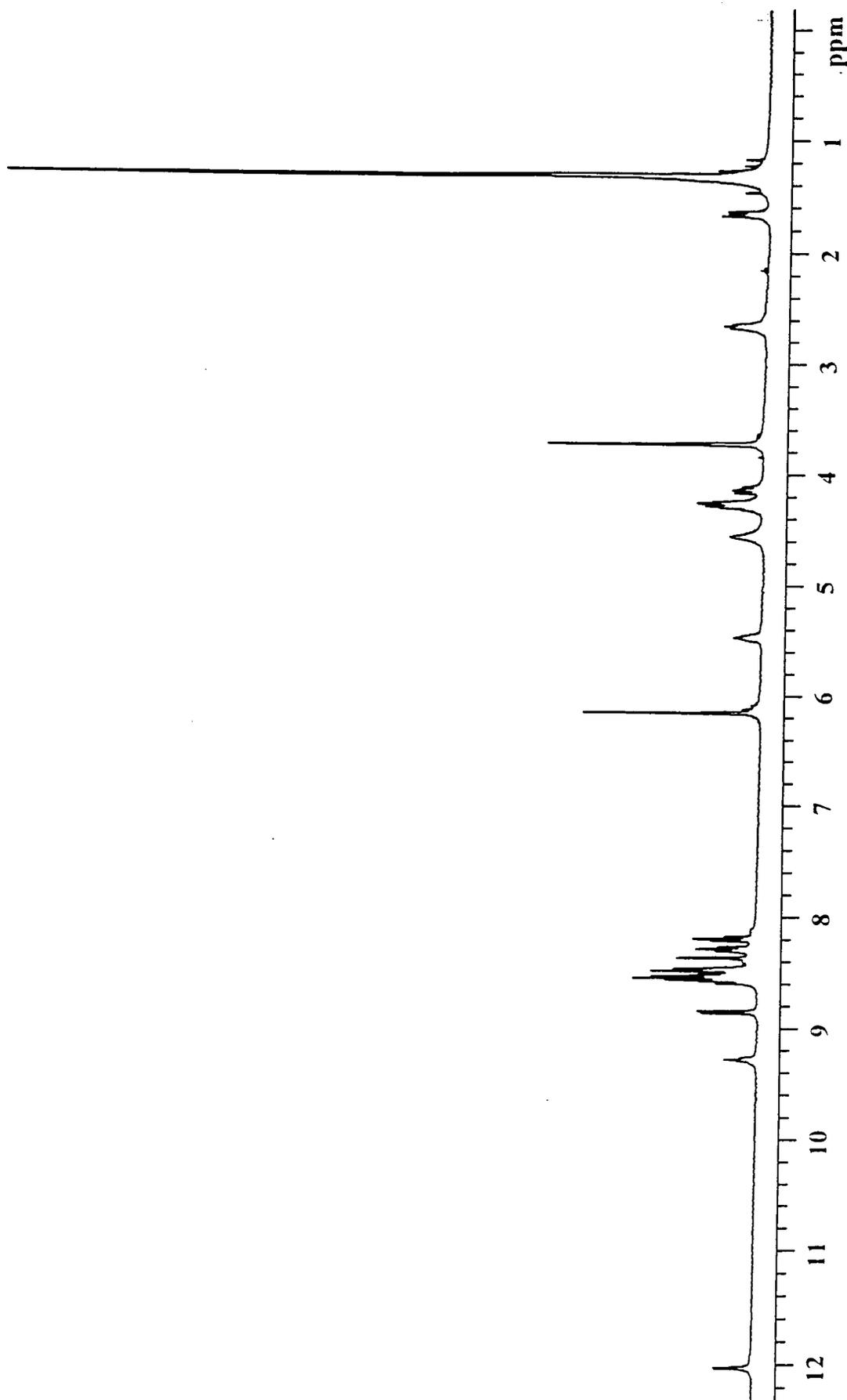
Appendix 2.1.16 ^{1}H nmr spectrum of Si-*wedge*-trp-CBZ in DMSOd$_6$.
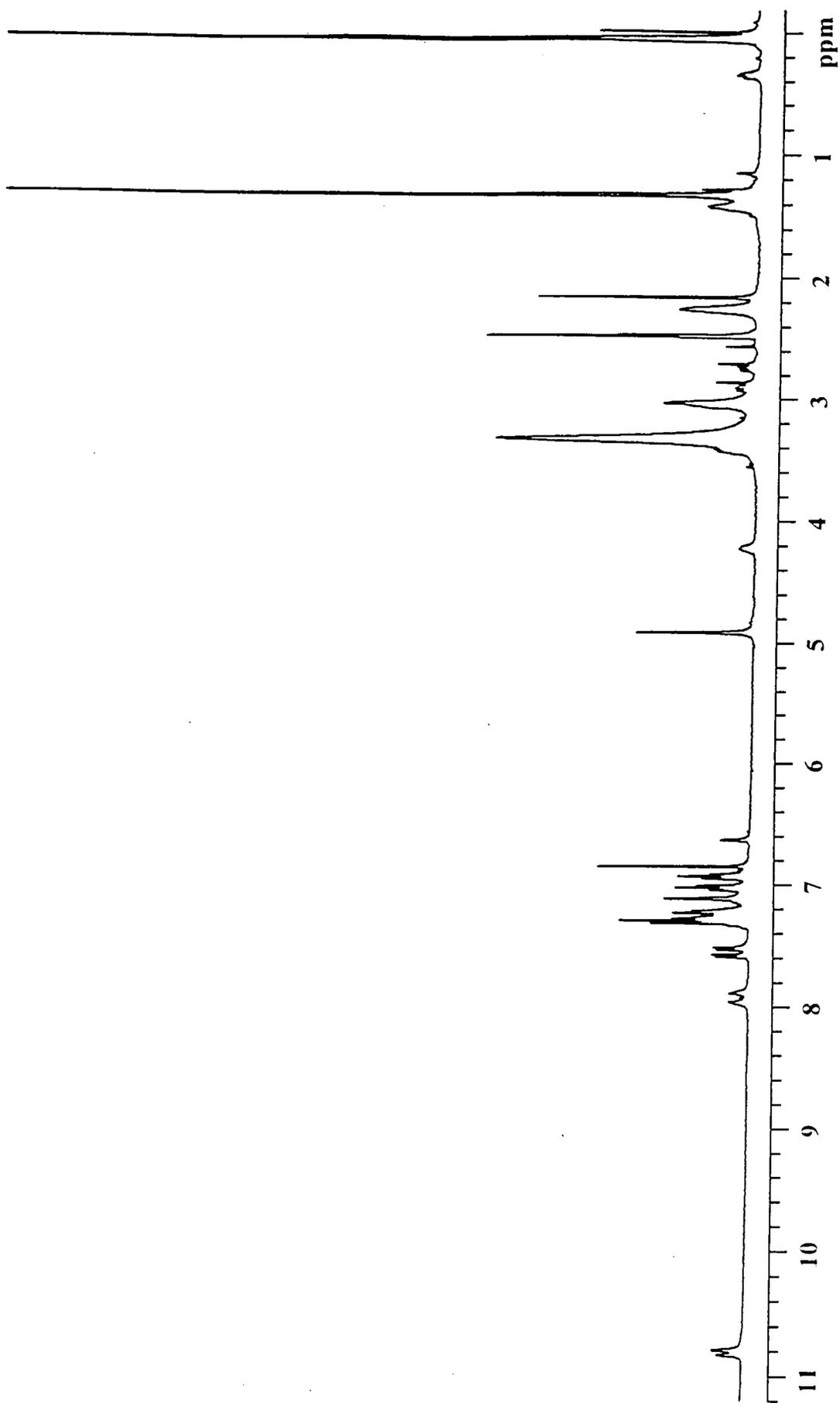
Appendix 2.1.17 ^{1}H nmr spectrum of Si-*wedge*-trp-NH$_2$-CBZ in DMSOd$_6$.
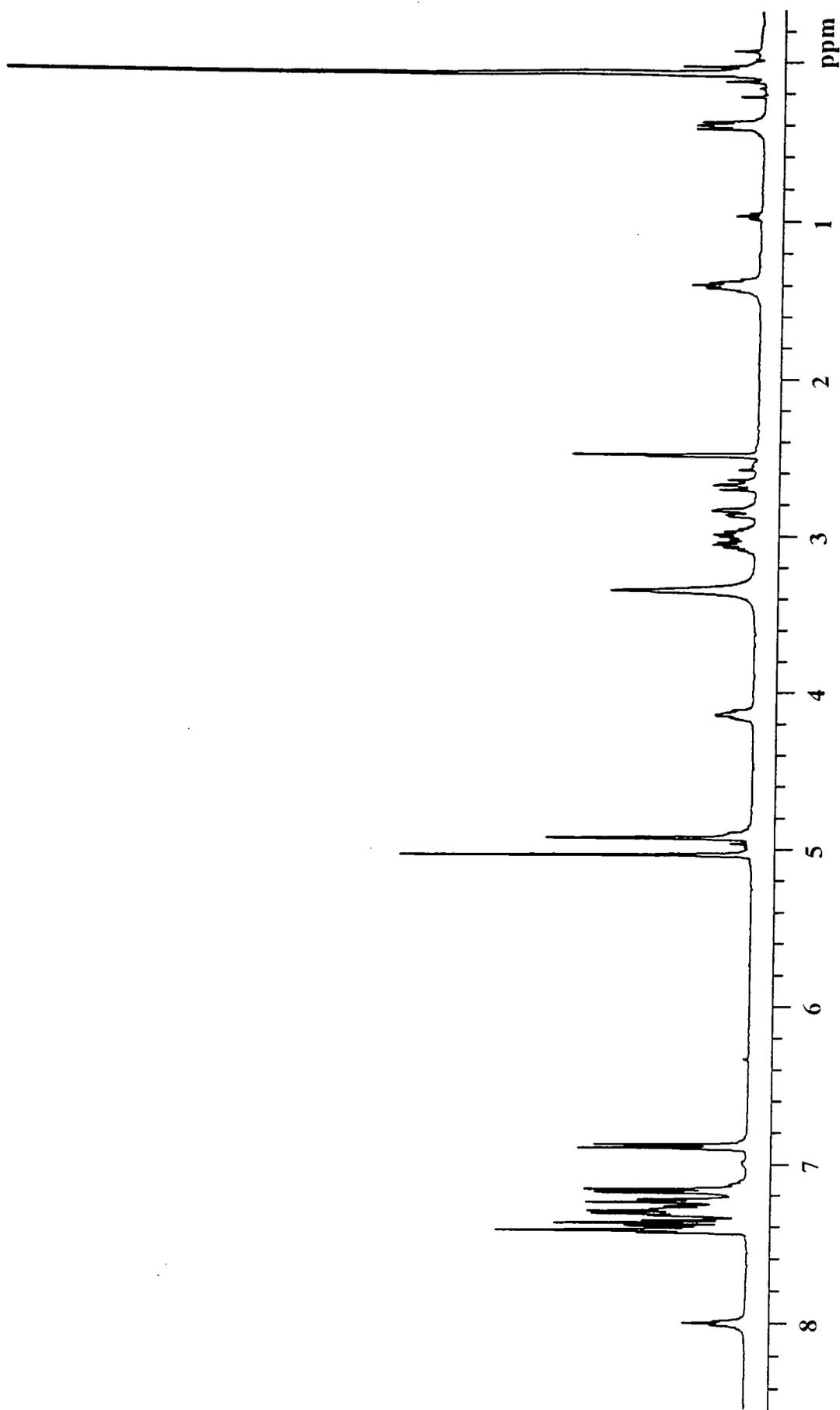
Appendix 2.1.18 ^{1}H nmr spectrum of Si-*wedge-o-benzyl*-tyr-CBZ in DMSOd$_6$.
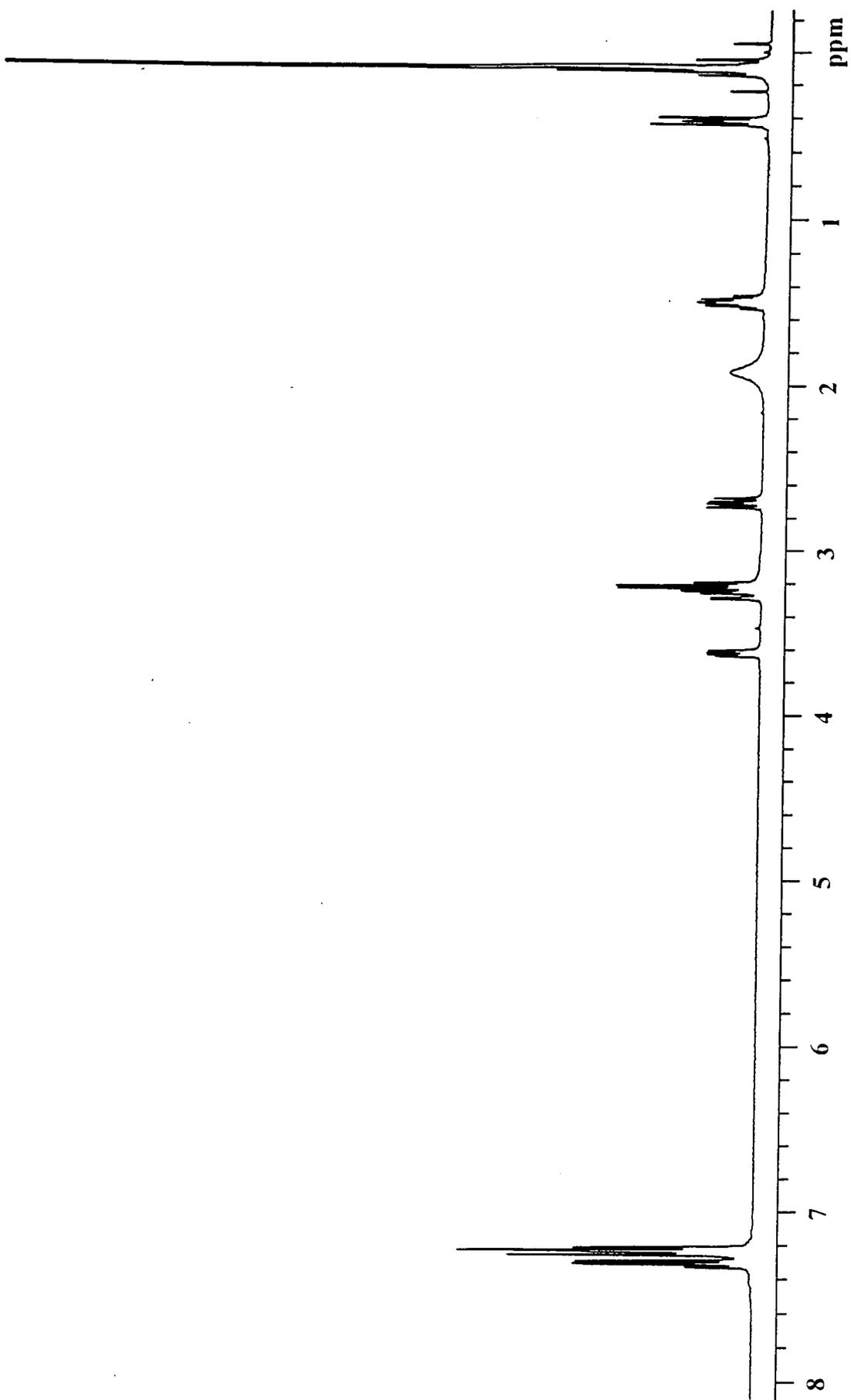
Appendix 2.1.19 ^{1}H nmr spectrum of Si-*wedge*-phe in CDCl[3].
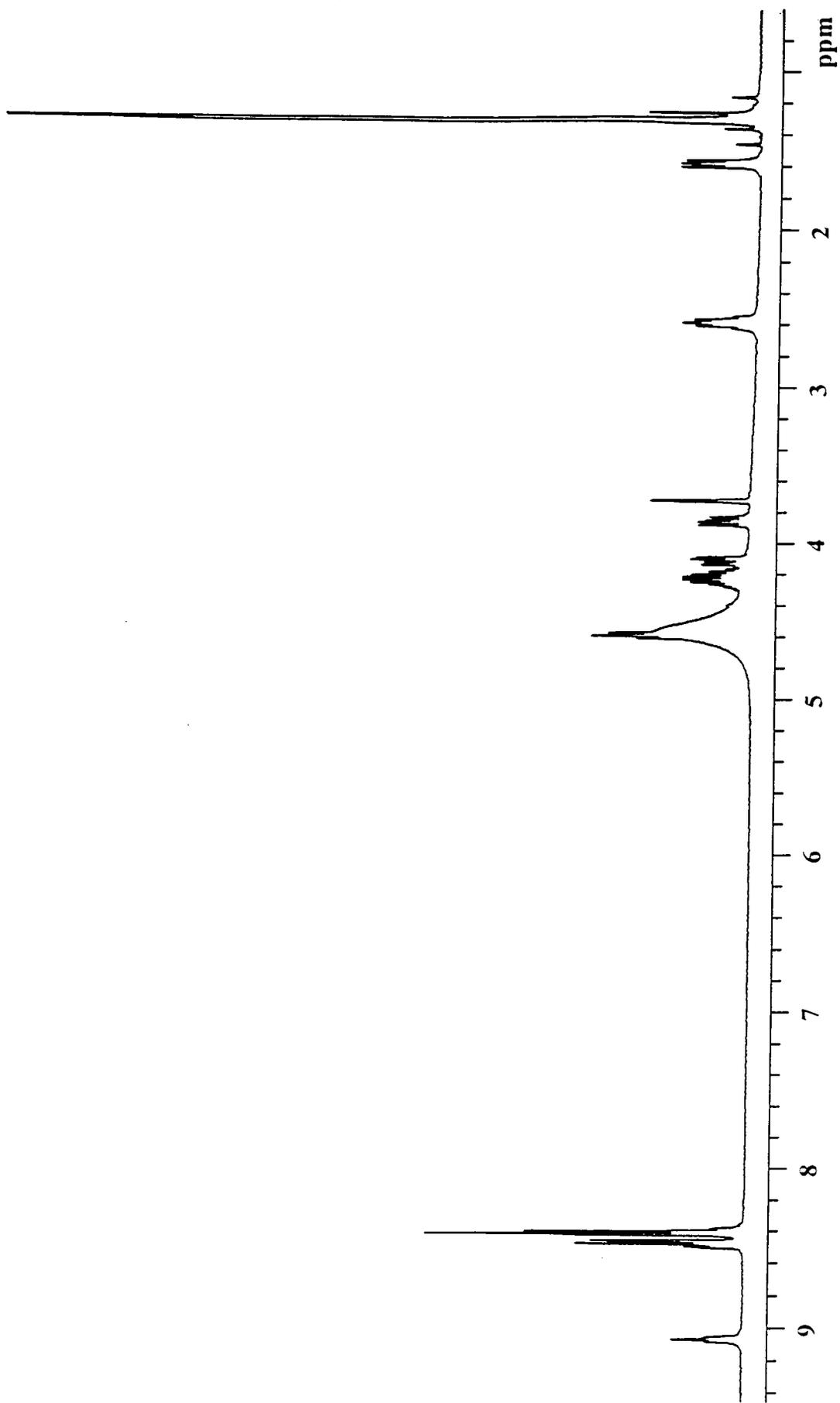
Appendix 2.1.20 ^{1}H nmr spectrum of Si-*wedge*-phe in DMSOd6.
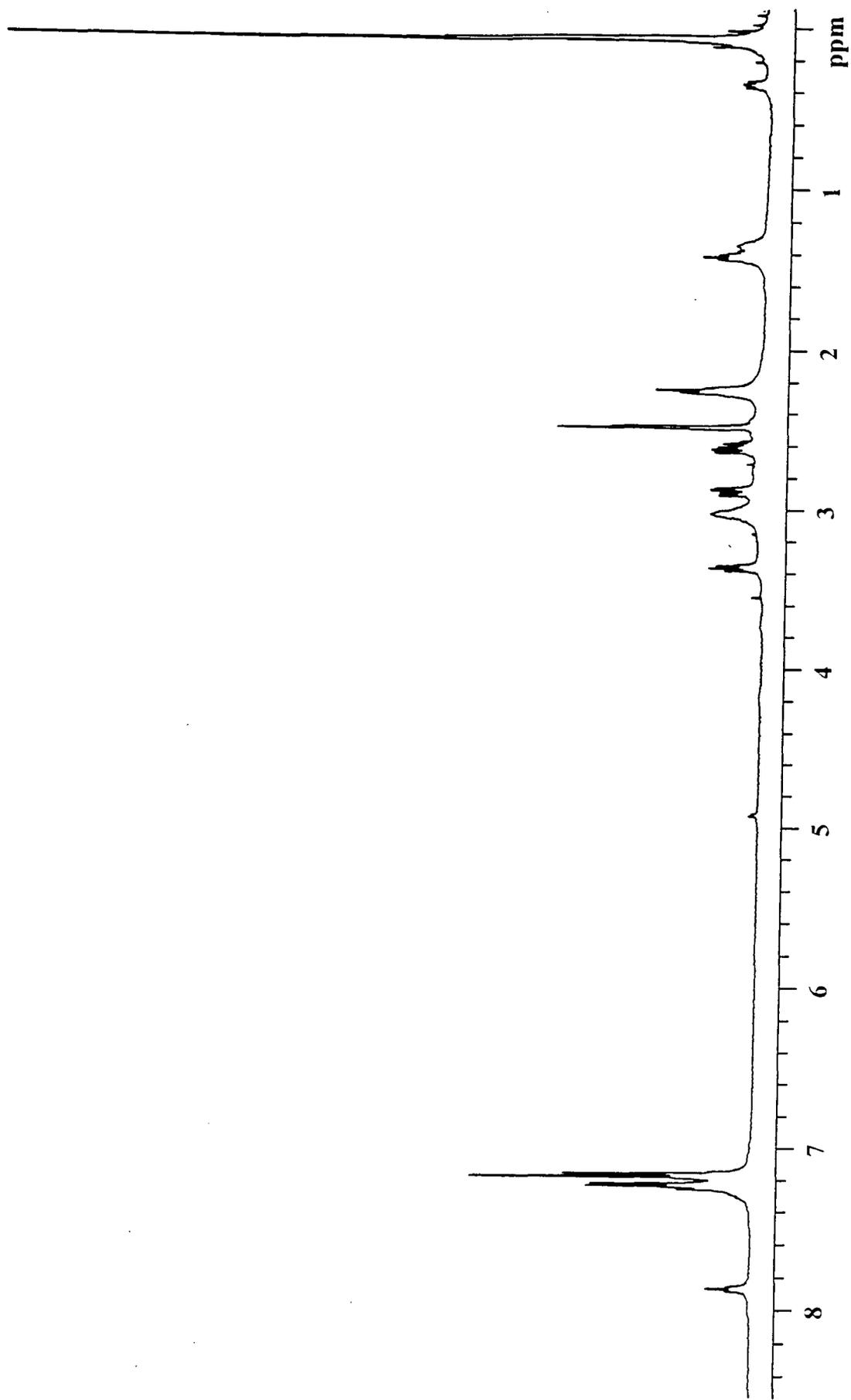
Appendix 2.1.21 ^{1}H nmr spectrum of Si-*wedge*-phe$_2$ in DMSOd$_6$.
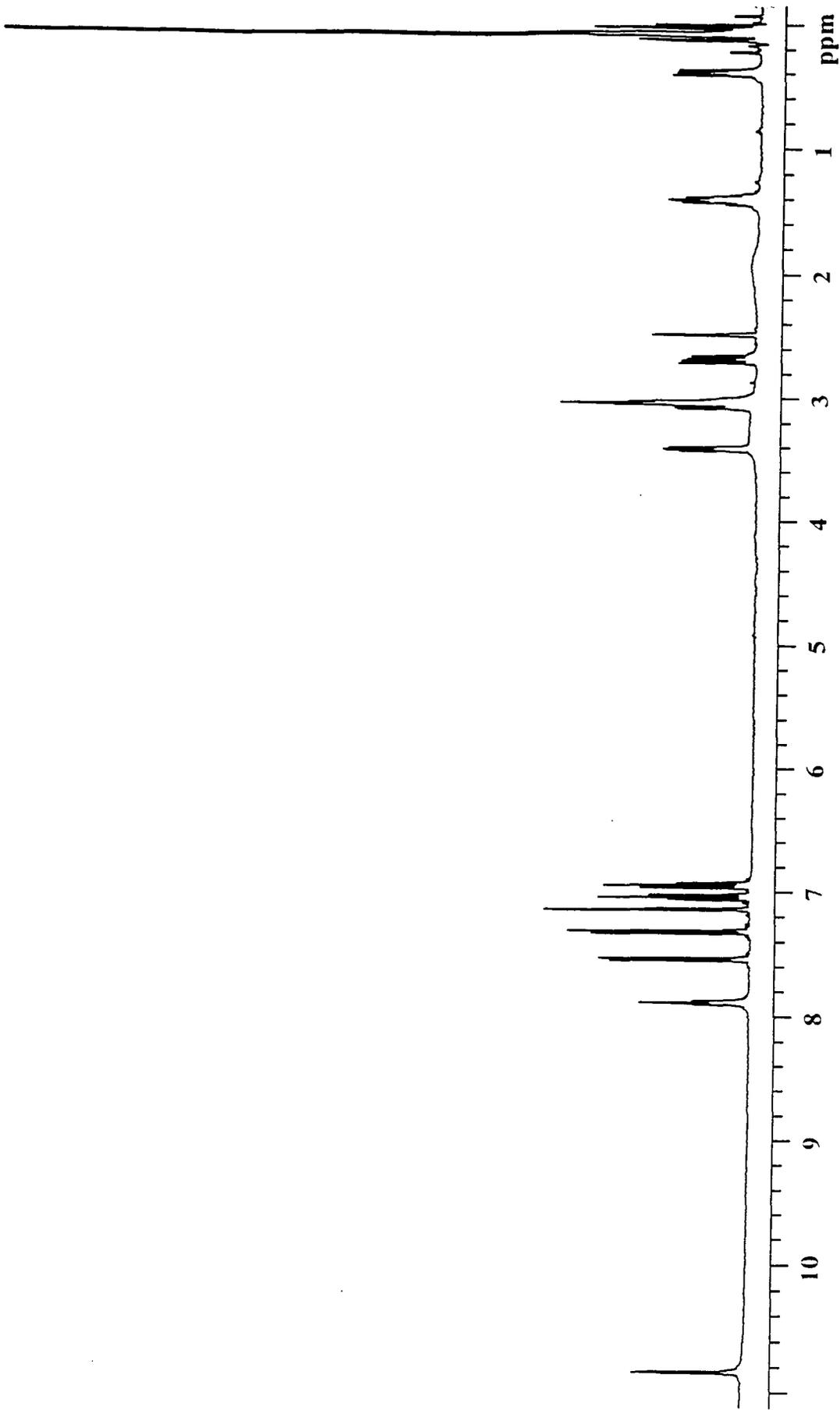
Appendix 2.1.22 ^{1}H nmr spectrum of Si-*wedge*-trp in DMSOd$_6$.
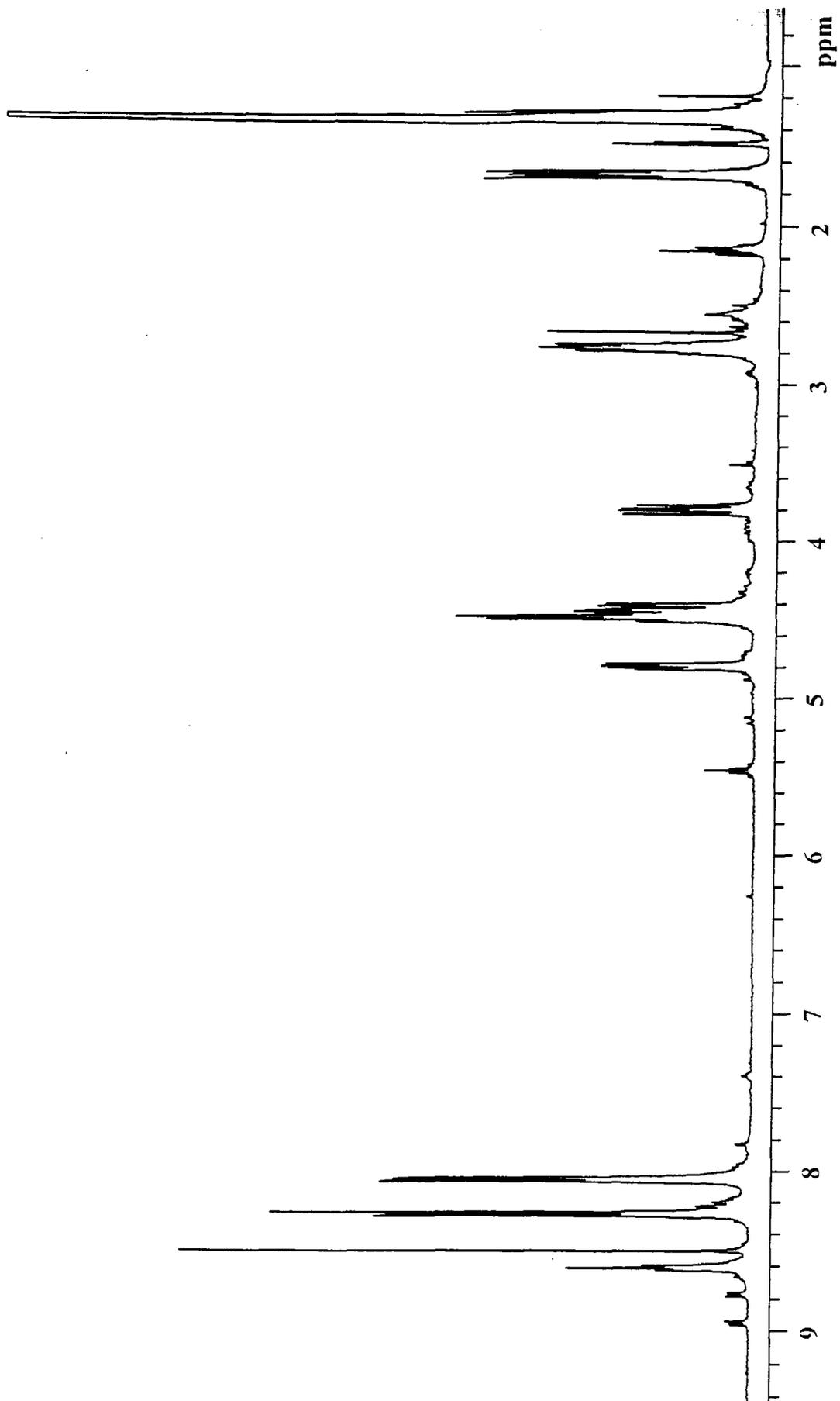
Appendix 2.1.23 ^{1}H nmr spectrum of Si-*wedge*-tyr in CDCl$_3$.
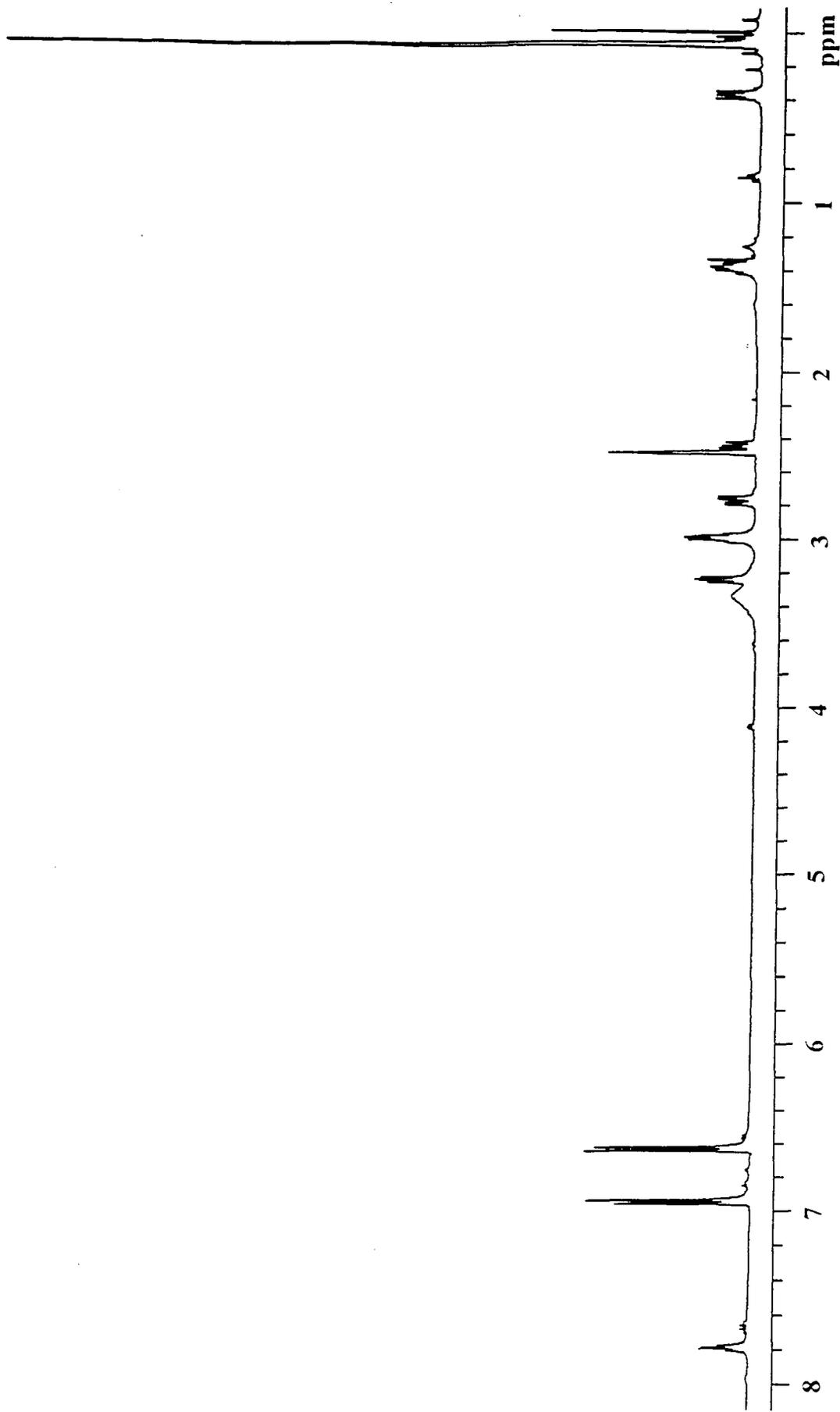
Appendix 2.1.24 [^1]H nmr spectrum of Si-*wedge*-tyr in DMSOd[6].
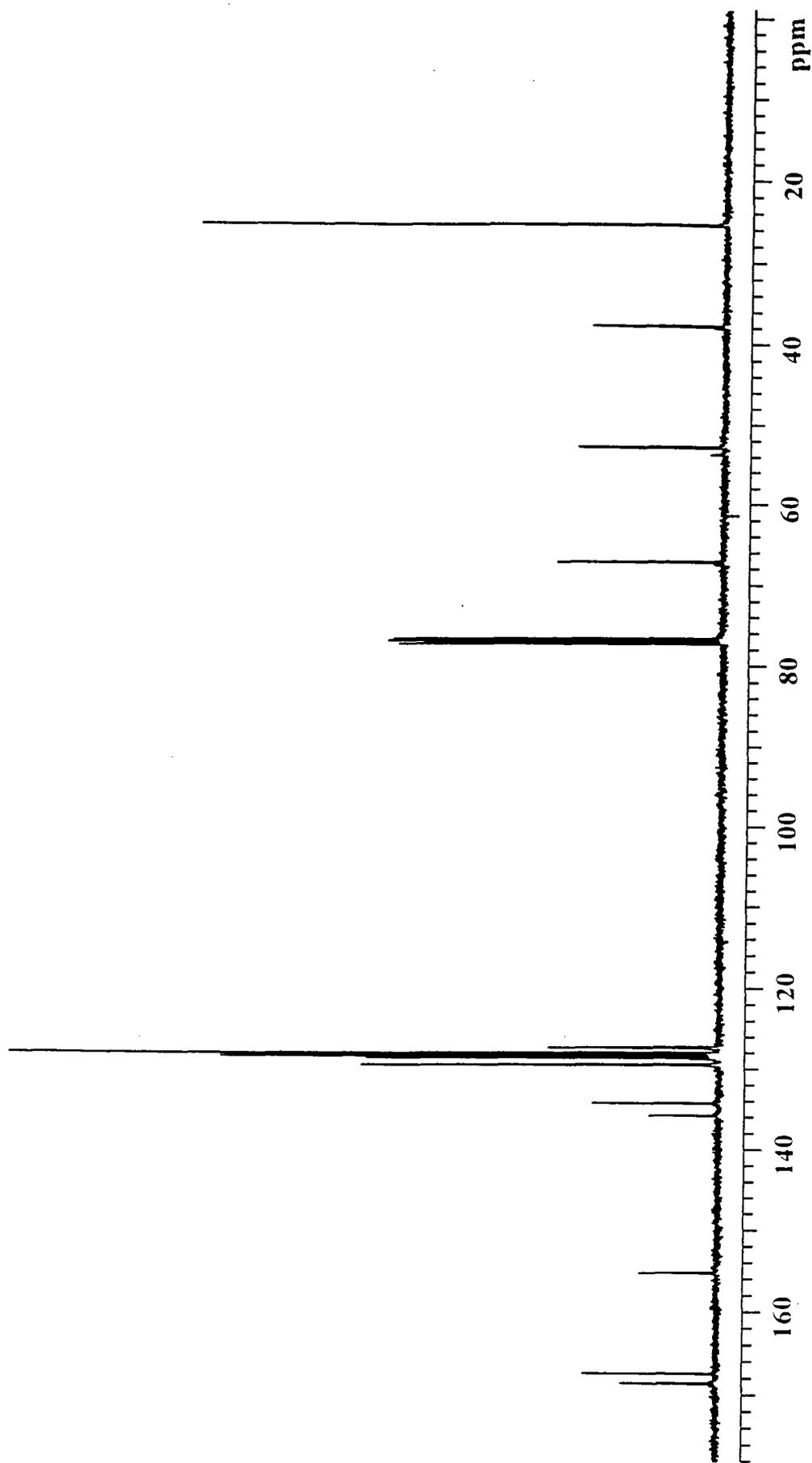
Appendix 2.2.1 ^{13}C nmr spectrum of NCBZ-phe-hydroxysuccinimide ester in CDCl$_3$.
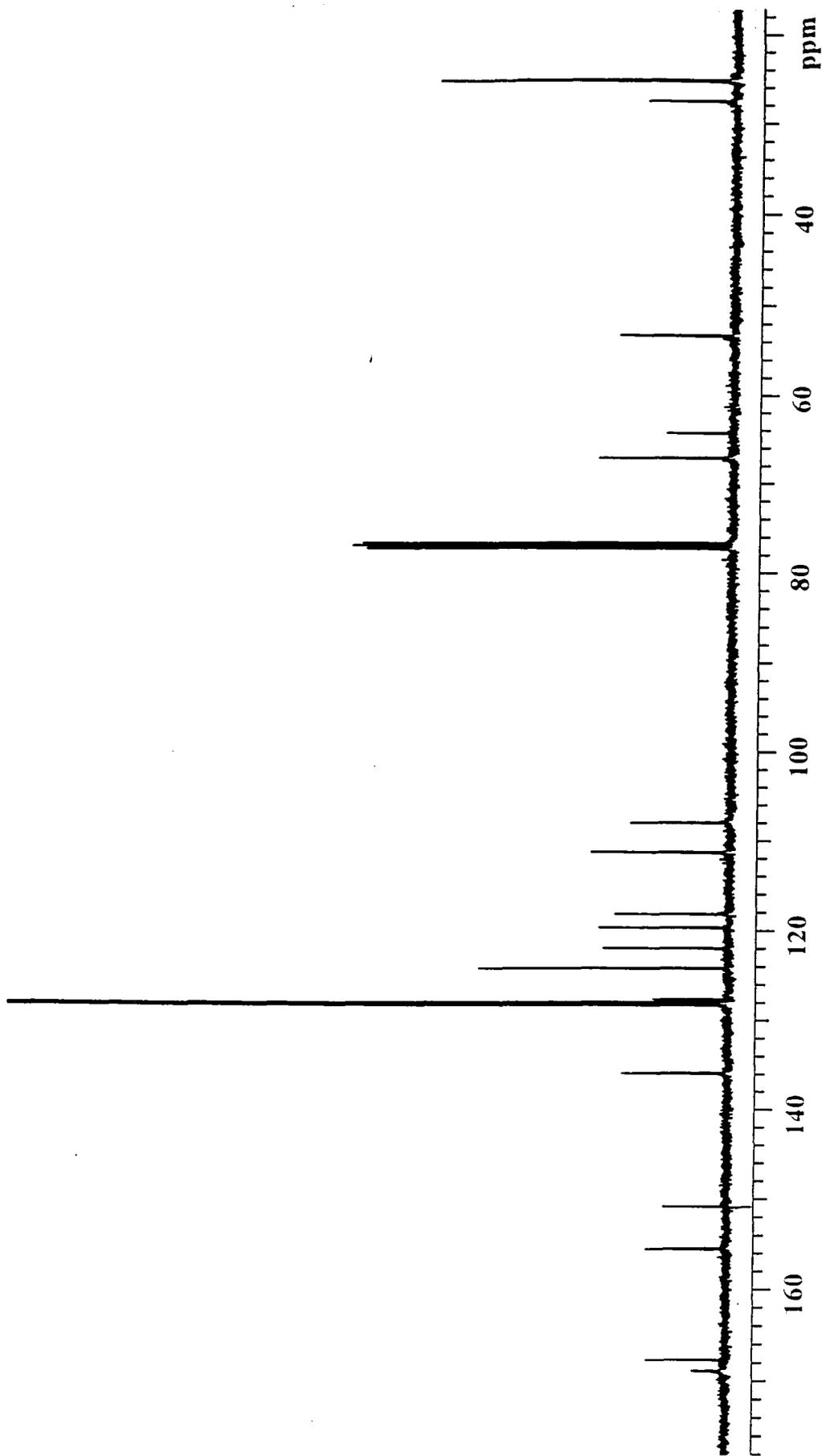
Appendix 2.2.2 ^{13}C nmr spectrum of NCBZ-trp-hydroxysuccinimide ester in $CDCl_3$.
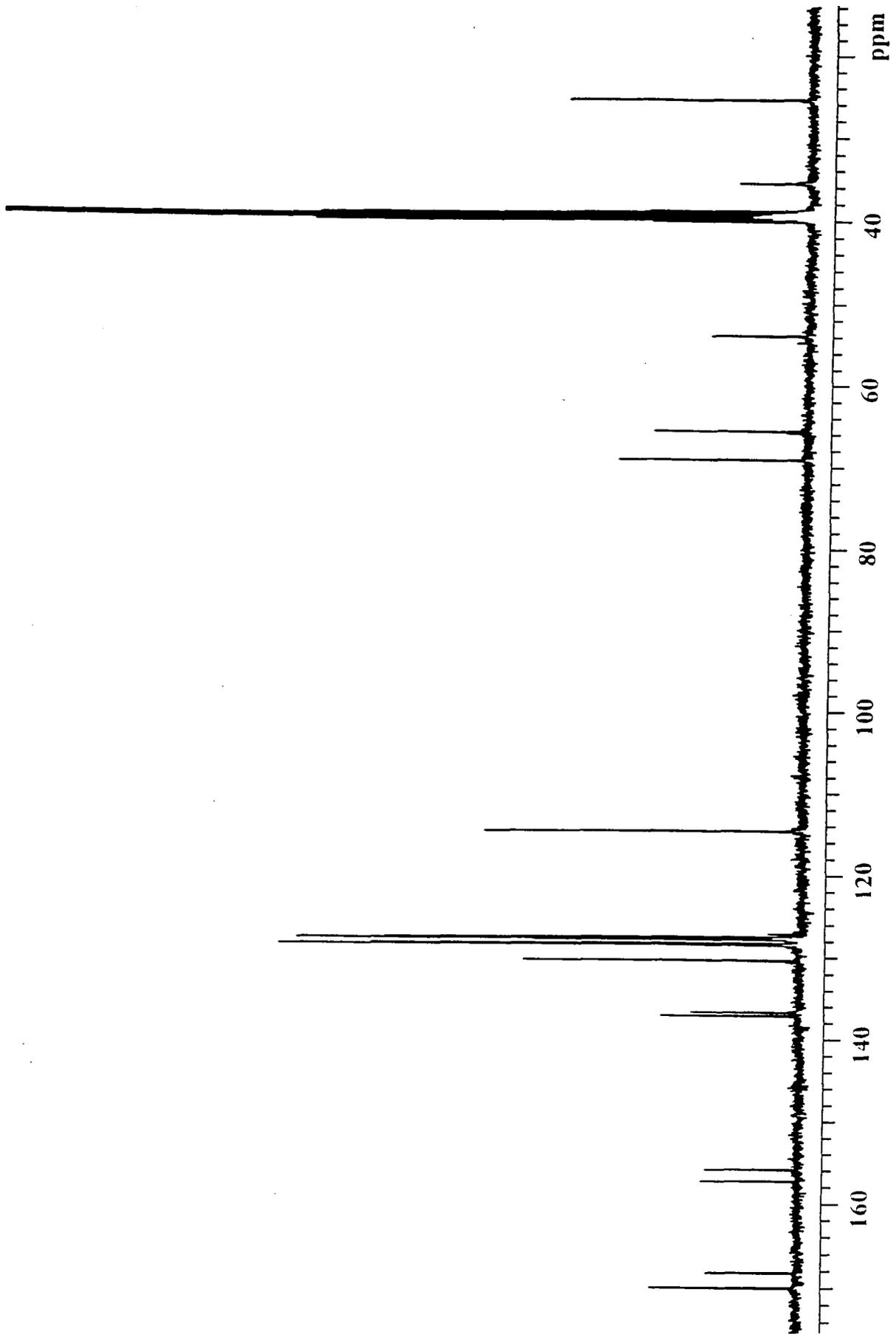
Appendix 2.2.3 ^{13}C nmr spectrum of NCBZ-tyr-hydroxysuccinimide ester in DMSOd[6].
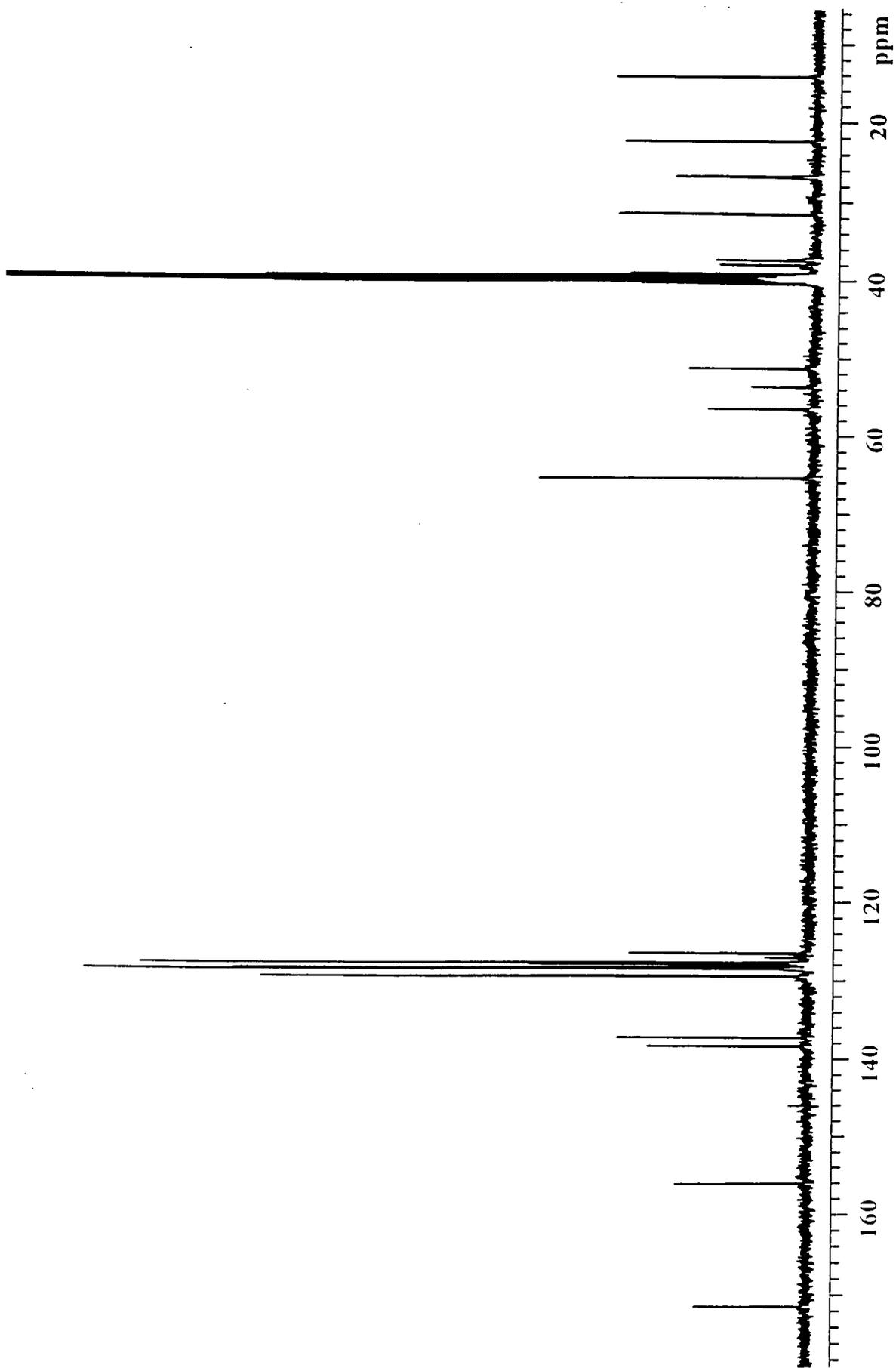
Appendix 2.2.4 ^{13}C nmr spectrum of Hex-*wedge*-phe$_2$-CBZ$_2$ in DMSOd$_6$.

Appendix 2.2.5 ^{13}C nmr spectrum of Hex-*wedge*-phe$_4$-CBZ$_4$ in DMSOd$_6$.
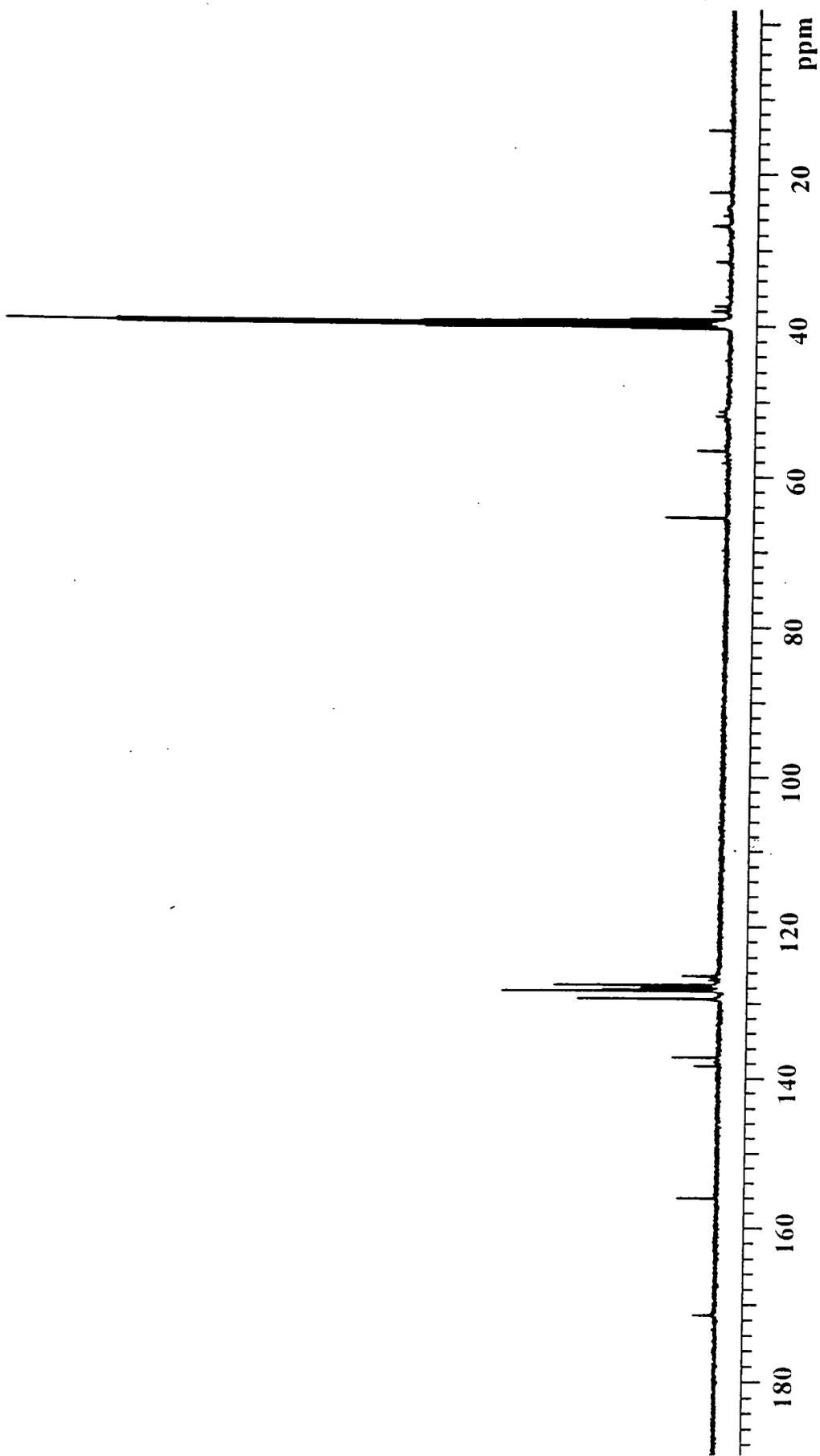
Appendix 2.2.6 ^{13}C nmr spectrum of Hex-*wedge*-phe$_8$-CBZ$_8$ in DMSOd$_6$.
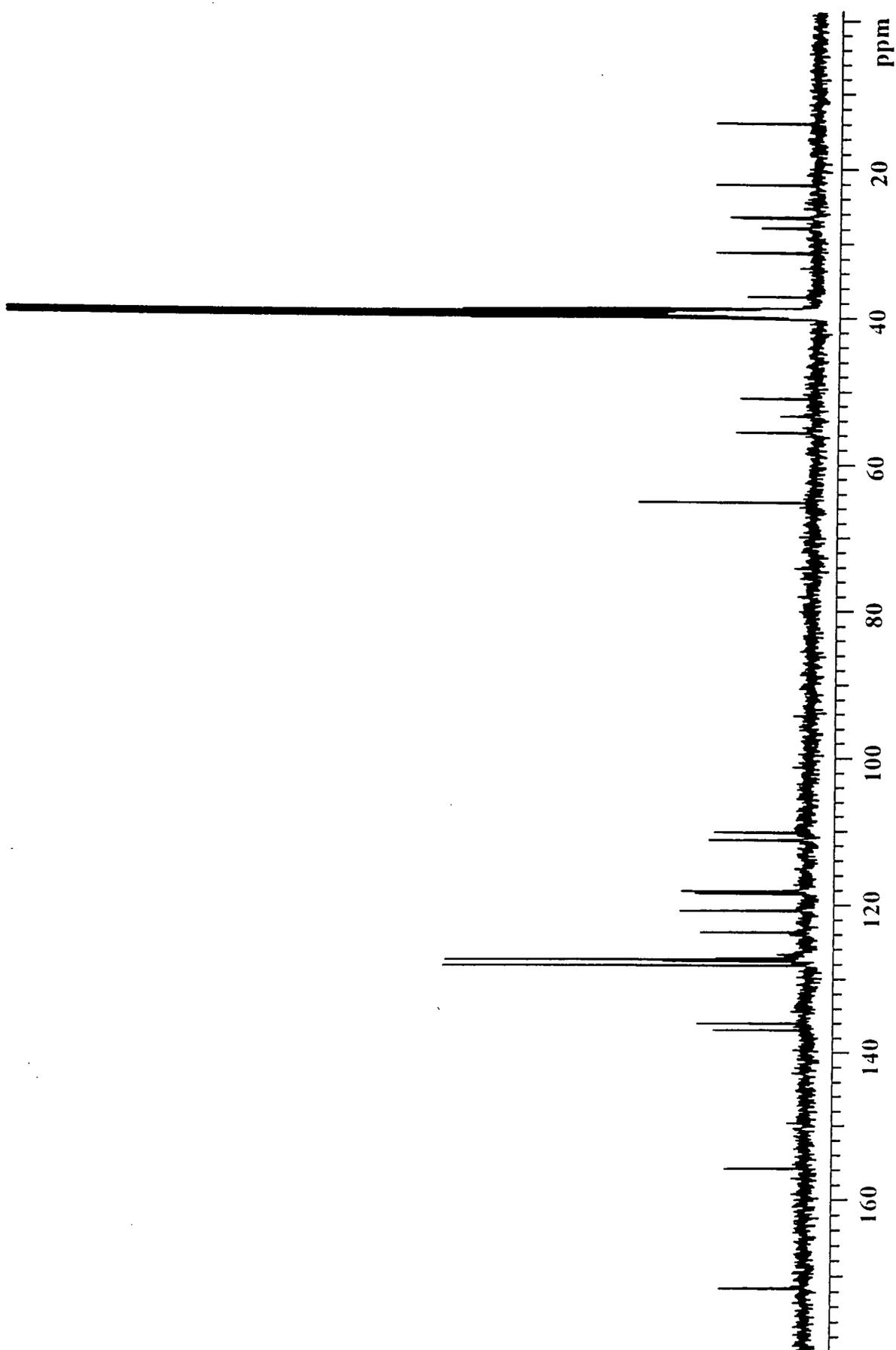
Appendix 2.2.7 ^{13}C nmr spectrum of Hex-*wedge*-trp$_2$-CBZ$_2$ in DMSOd$_6$.
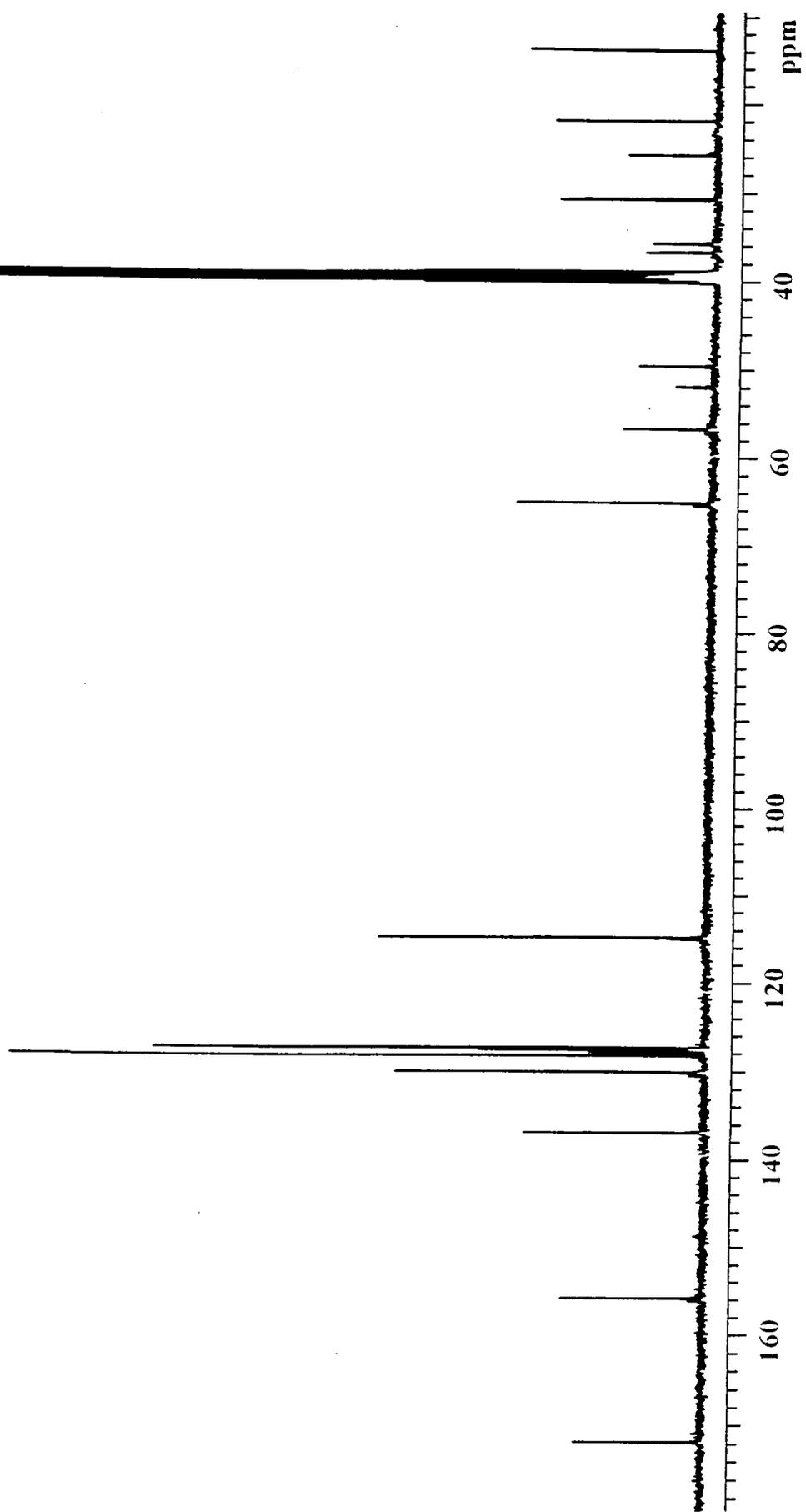
Appendix 2.2.8 ^{13}C nmr spectrum of Hex-*wedge*-tyr$_2$-CBZ$_2$ in DMSOd$_6$.
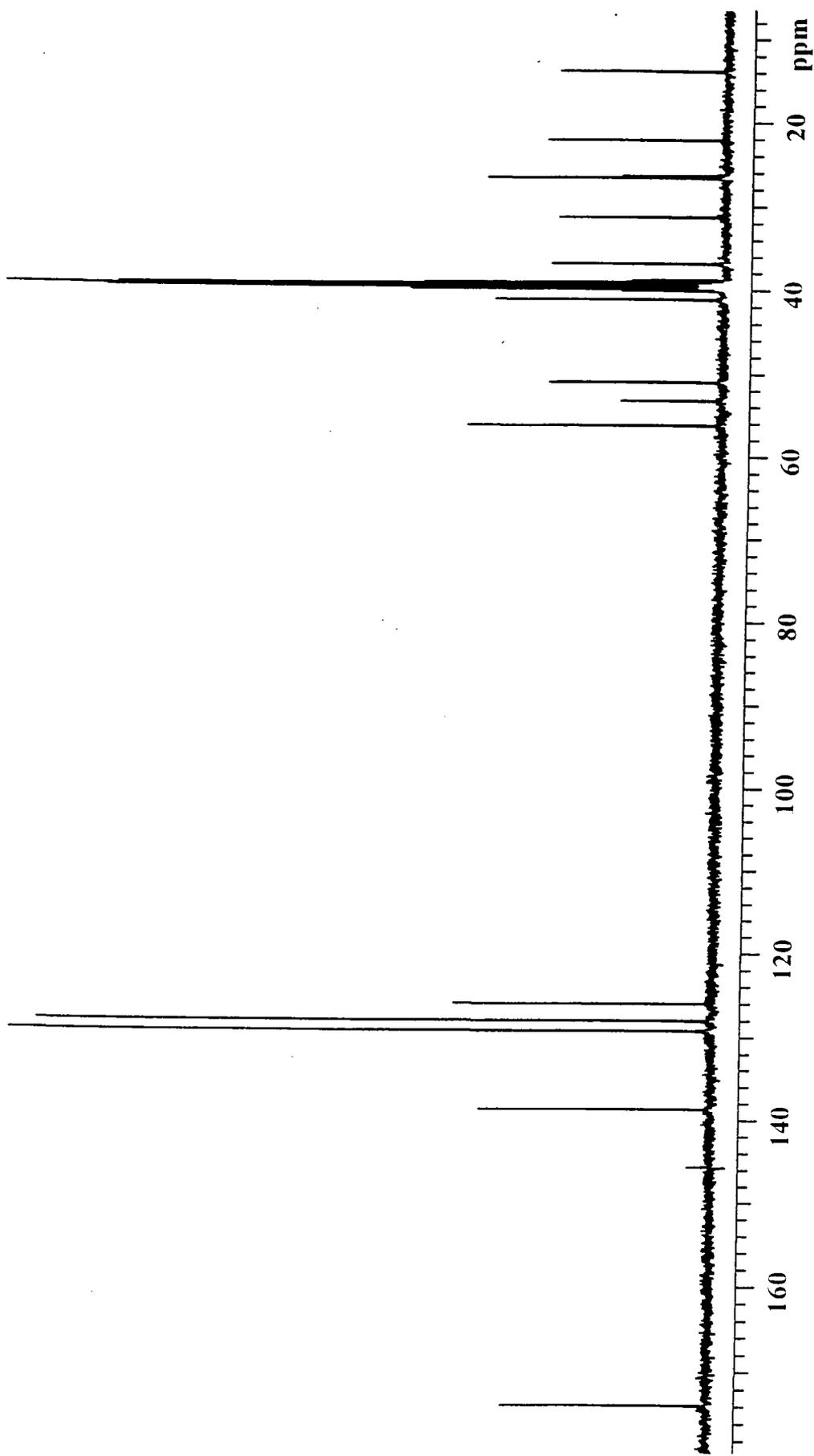
Appendix 2.2.9 ^{13}C nmr spectrum of Hex-*wedge*-phe$_2$ in DMSOd$_6$.
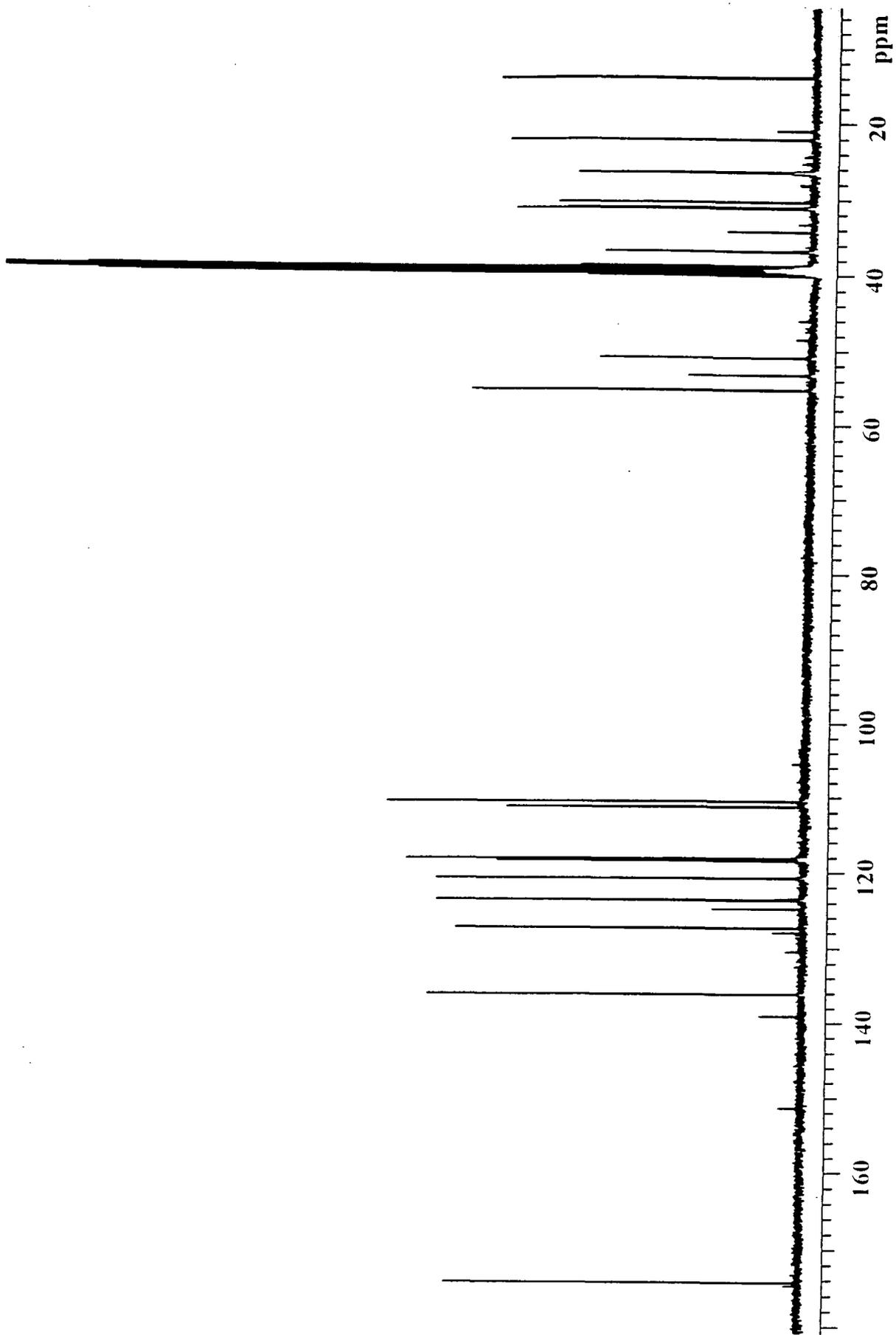
Appendix 2.2.10 ^{13}C nmr of spectrum Hex-*wedge*-trp$_2$ in DMSOd$_6$.
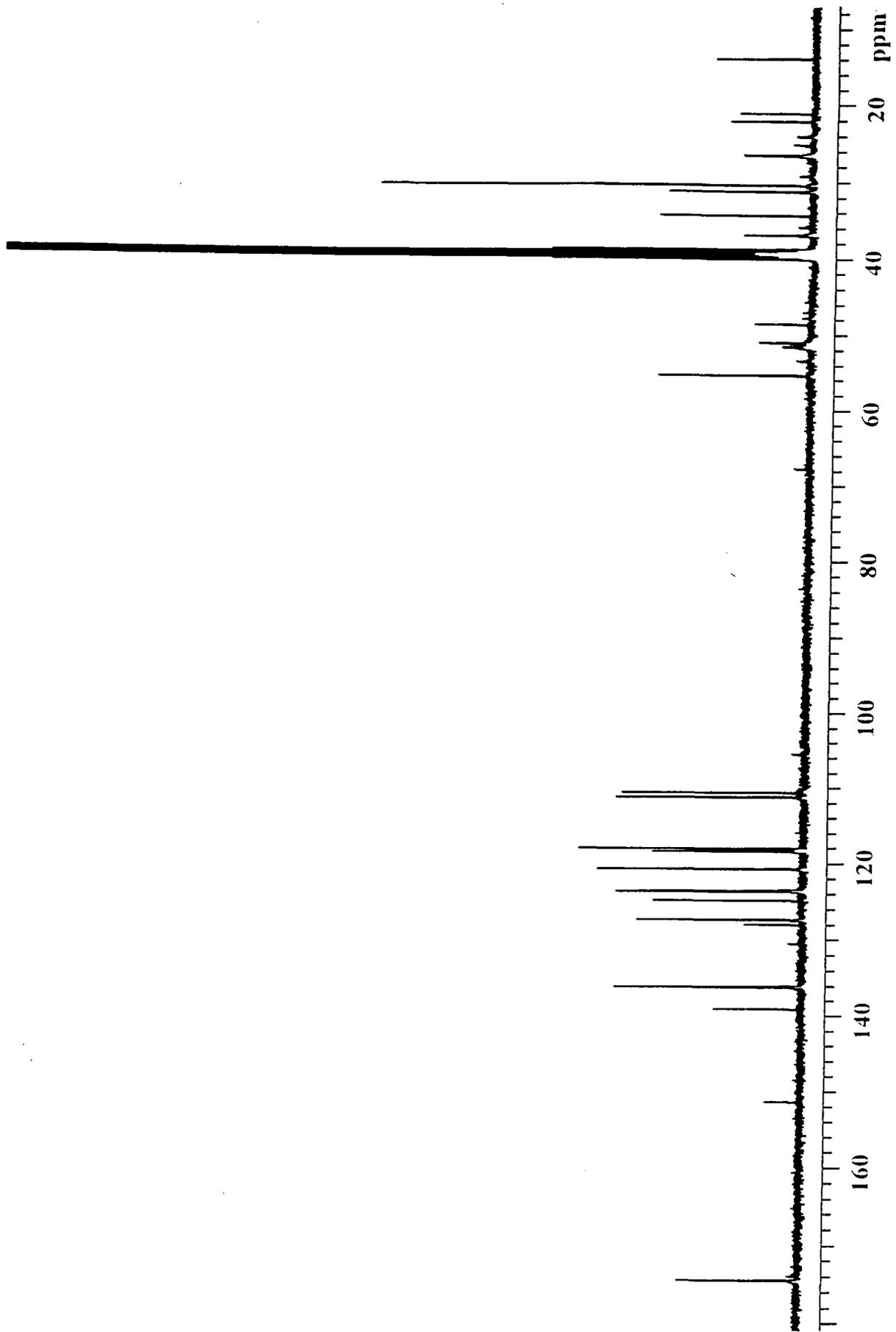
Appendix 2.2.11 [^13]C nmr spectrum of Hex-*welge*-trp$_4$ in DMSOd$_6$

Appendix 2.2.12 ^{13}C nmr spectrum of Hex-*wedge*-tyr$_2$ in DMSOd$_6$.
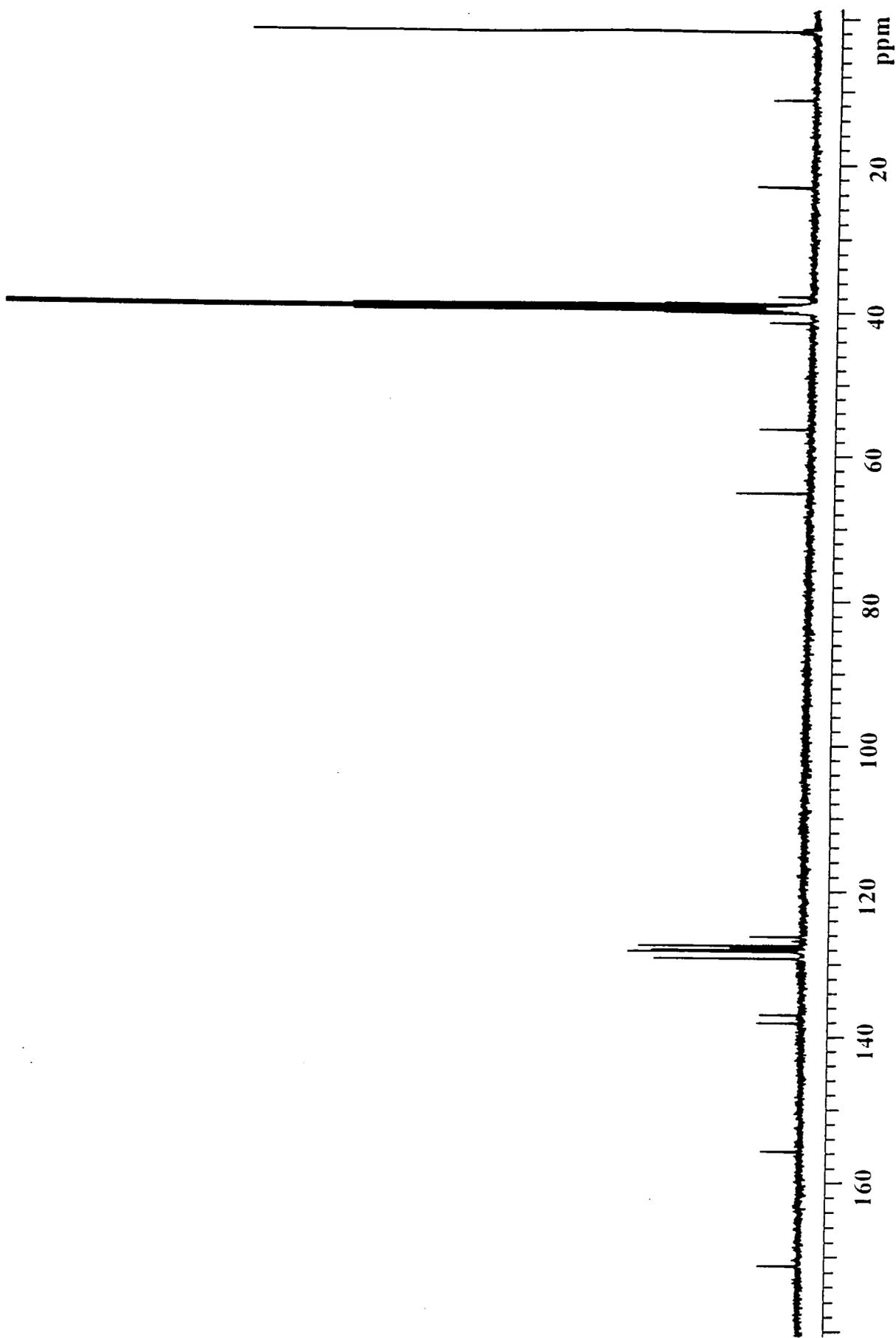
Appendix 2.2.13 ^{13}C nmr spectrum of Si-*wedge*-phe-CBZ in DMSOd$_6$.
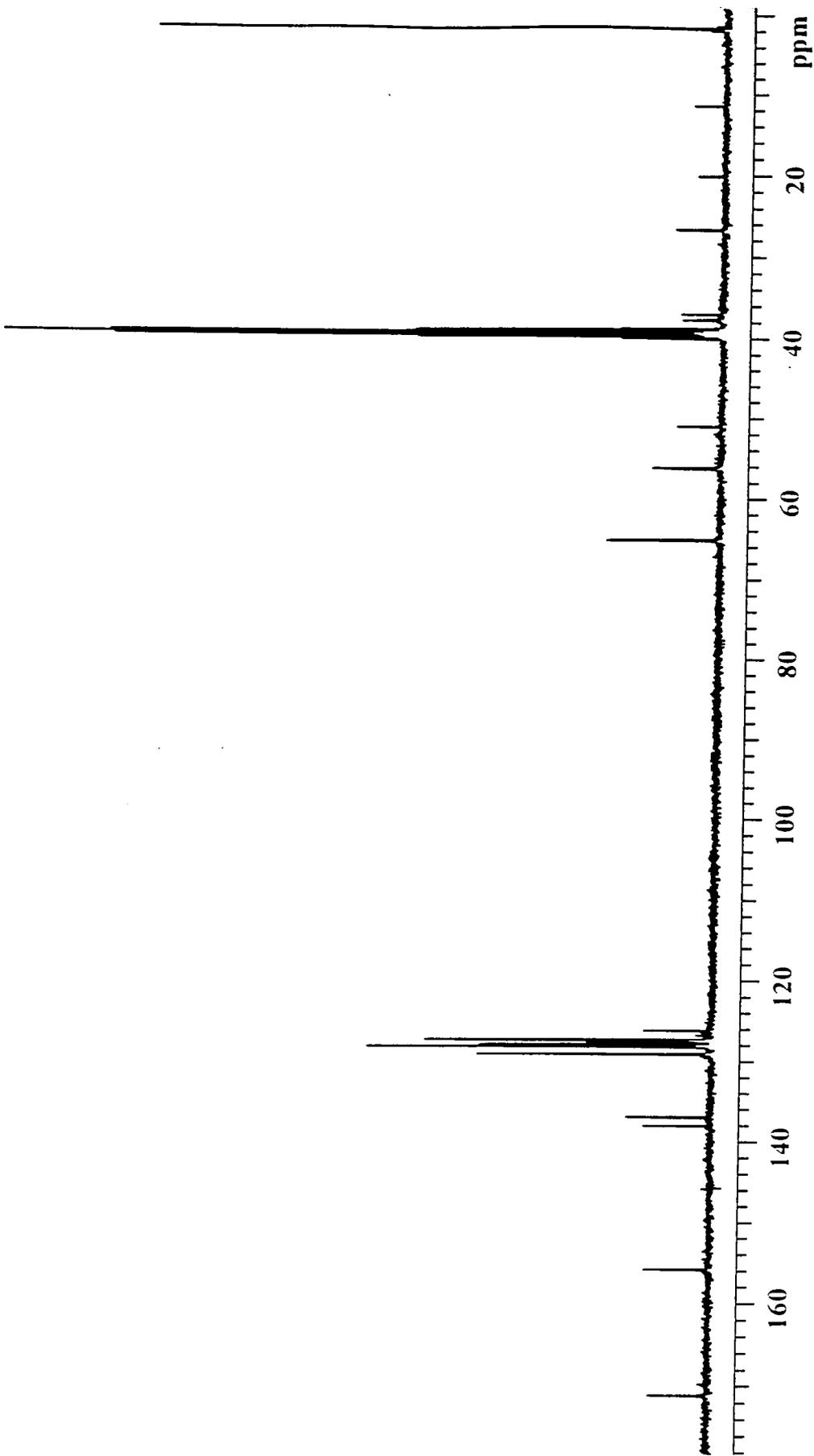
Appendix 2.2.14 ^{13}C nmr spectrum of Si-*wedge*-phe$_2$-CBZ$_2$ in DMSOd$_6$.
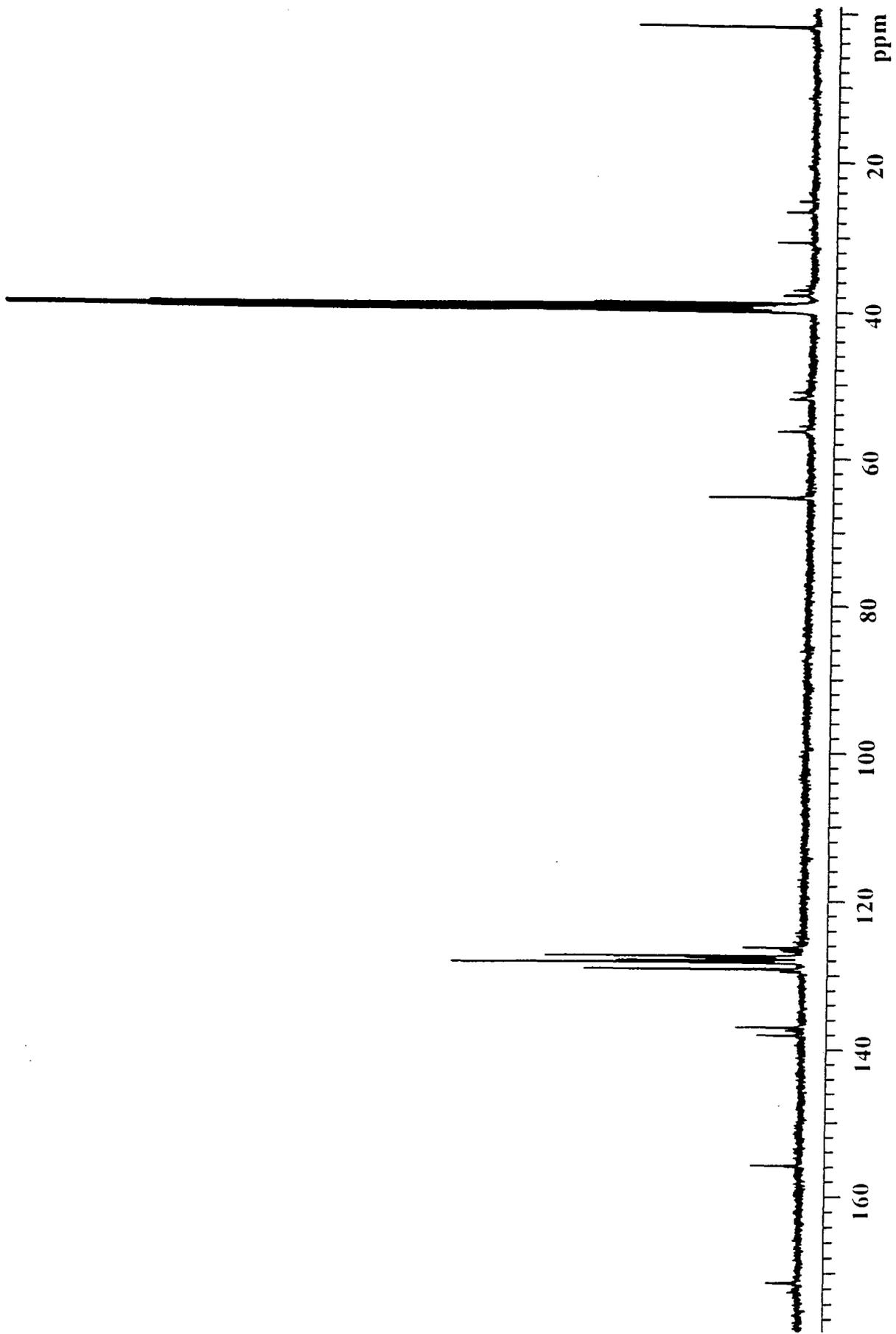
Appendix 2.2.15 ^{13}C nmr spectrum of Si-*wedge*-phe$_4$-CBZ$_4$ in DMSOd$_6$.
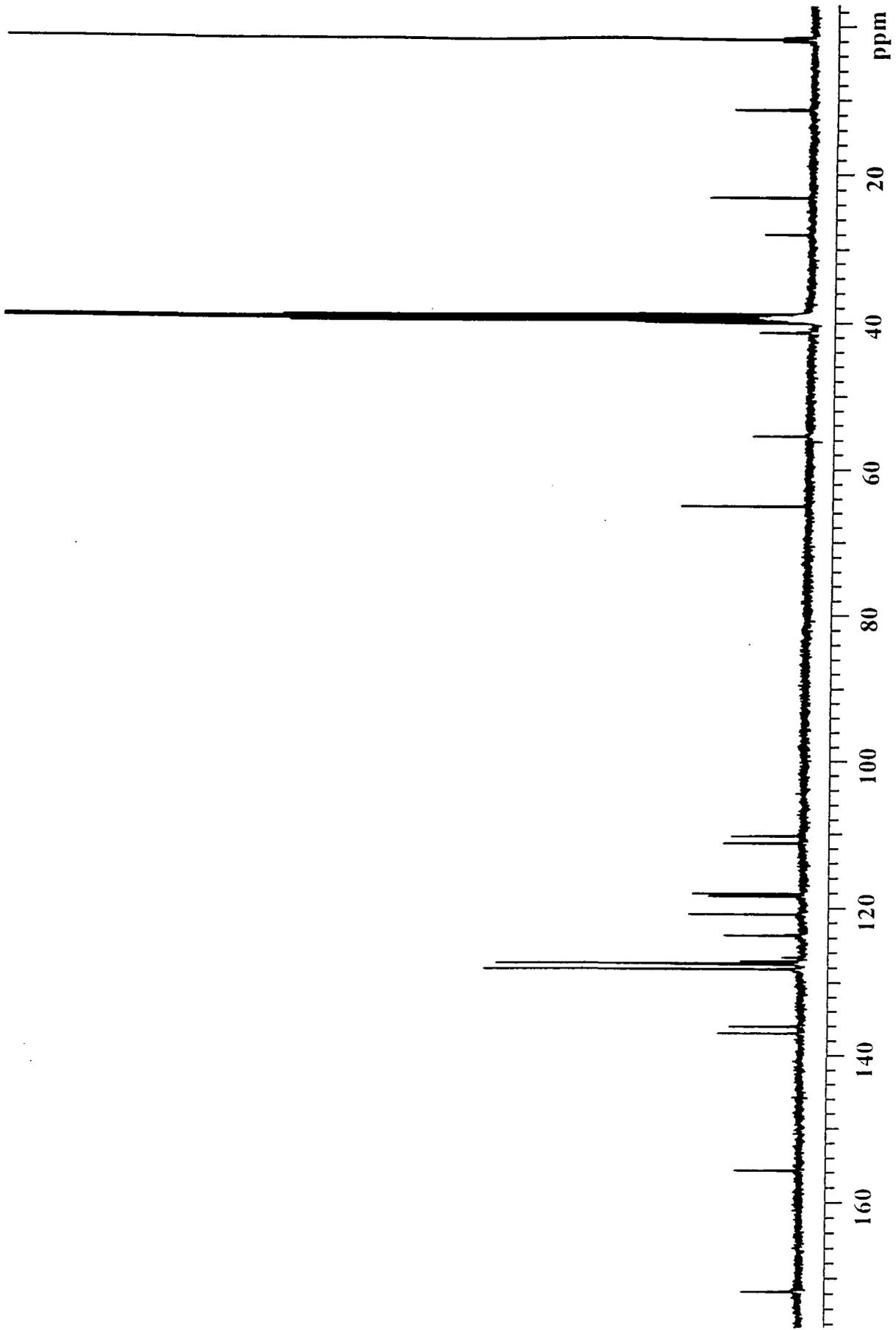
Appendix 2.2.16 ^{13}C nmr spectrum of Si-*wedge*-trp-CBZ in DMSOd$_6$.
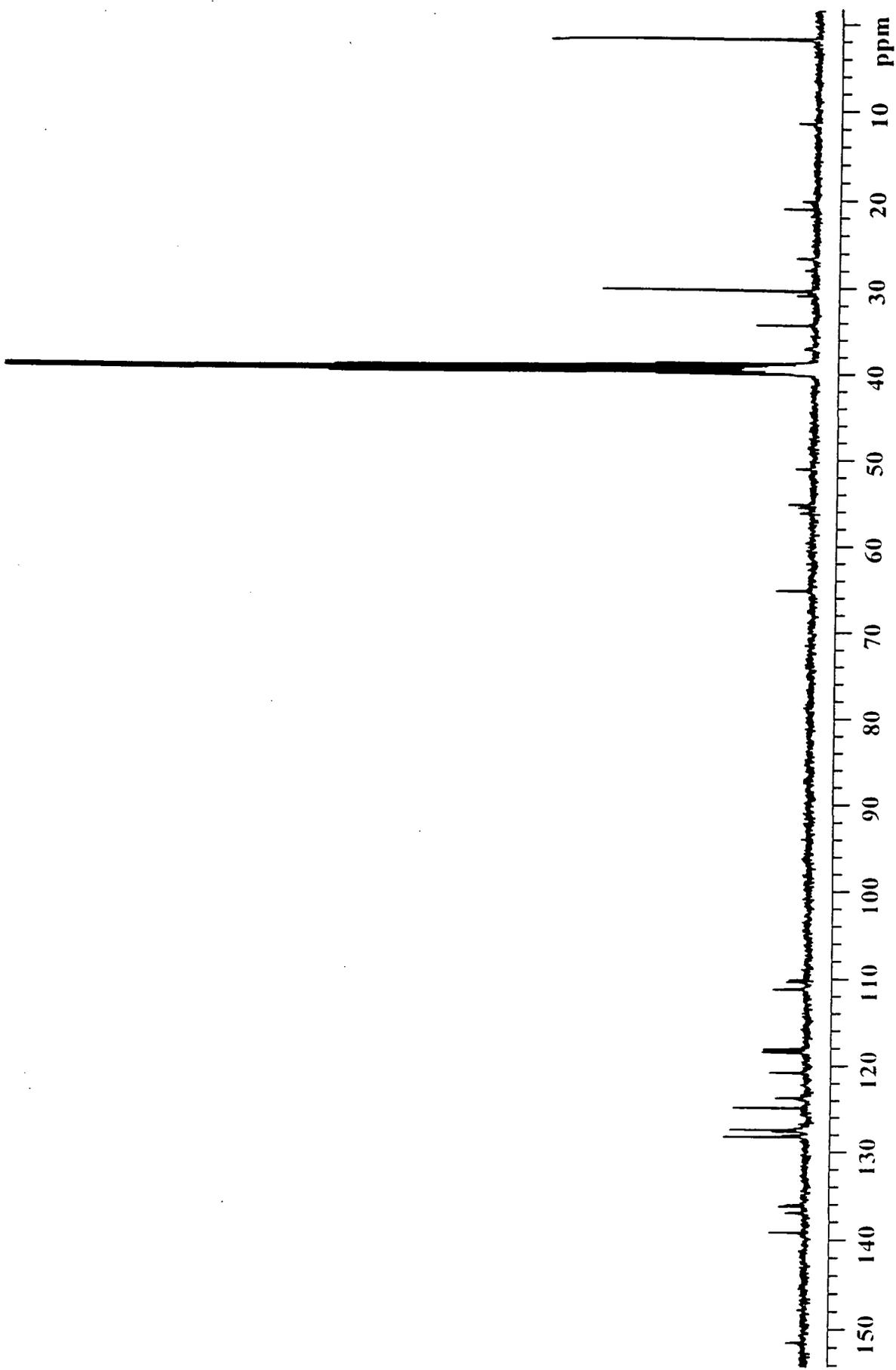
Appendix 2.2.17 ¹³C nmr spectrum of Si-*wedge*-trp-NH₂-CBZ in DMSOd₆.
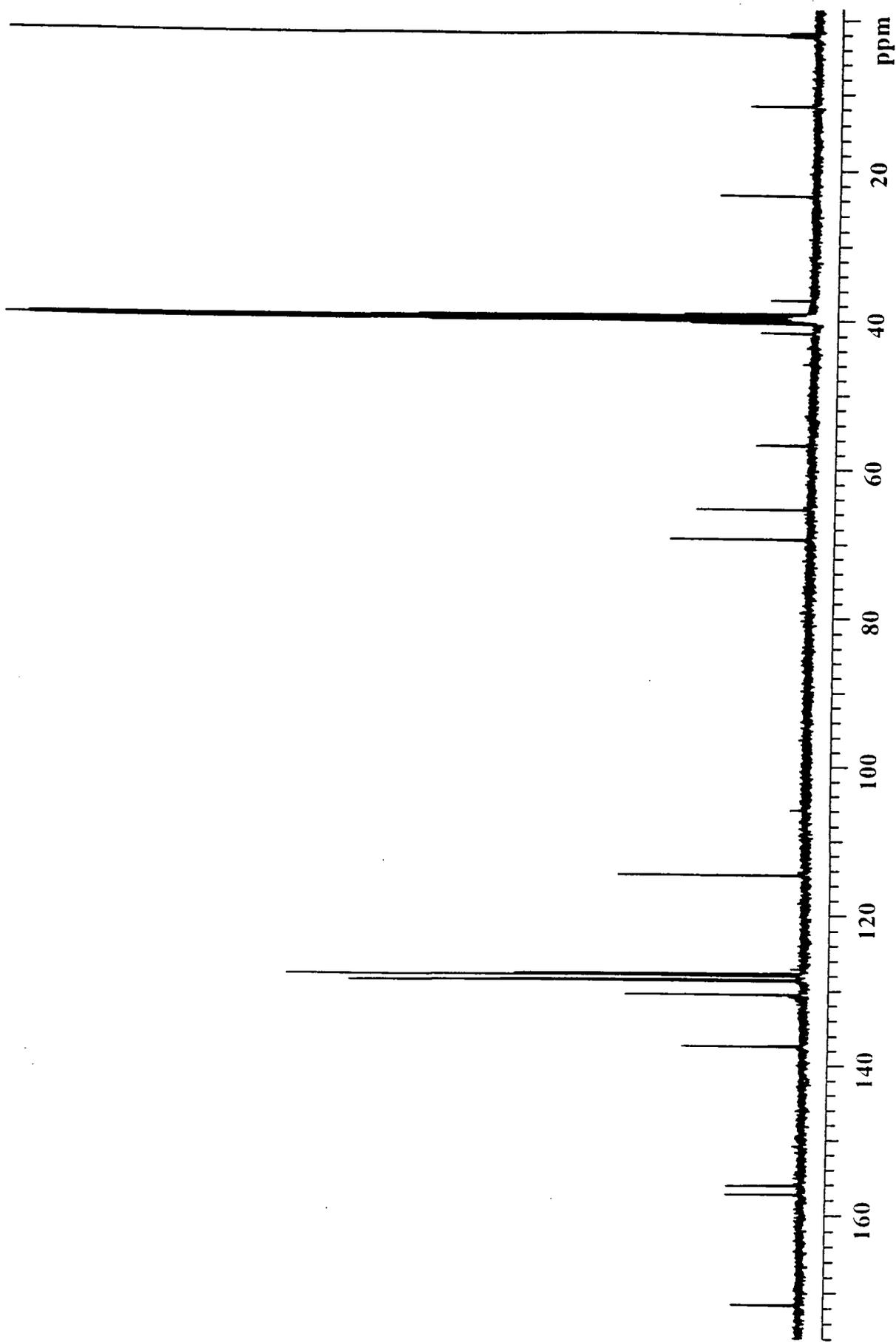
Appendix 2.2.18 ^{13}C nmr spectrum of Si-*wedge-o-benzyl*-tyr-CBZ in DMSOd$_6$.
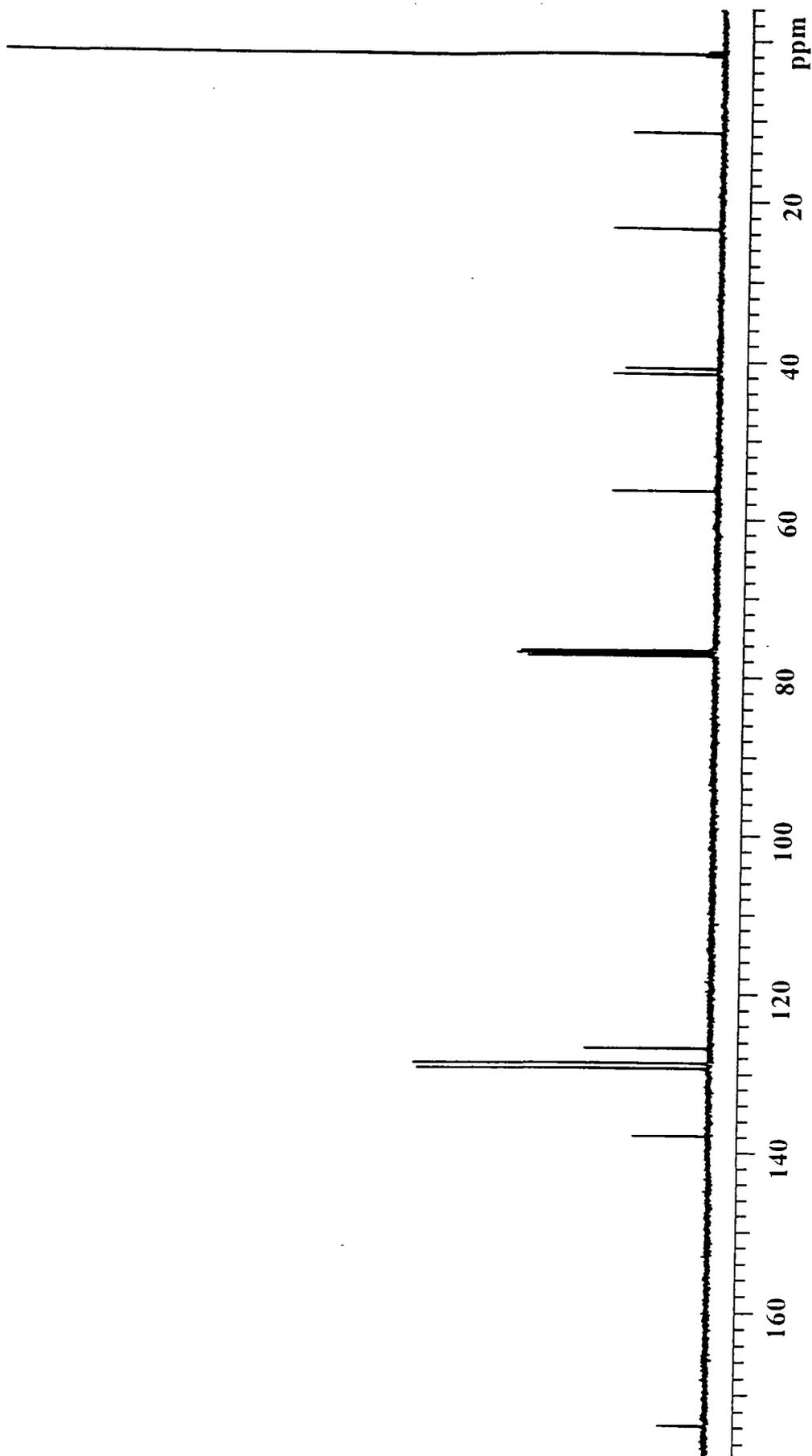
Appendix 2.2.19 ¹³C nmr spectrum of Si-*wedge*-phe in CDCl₃.
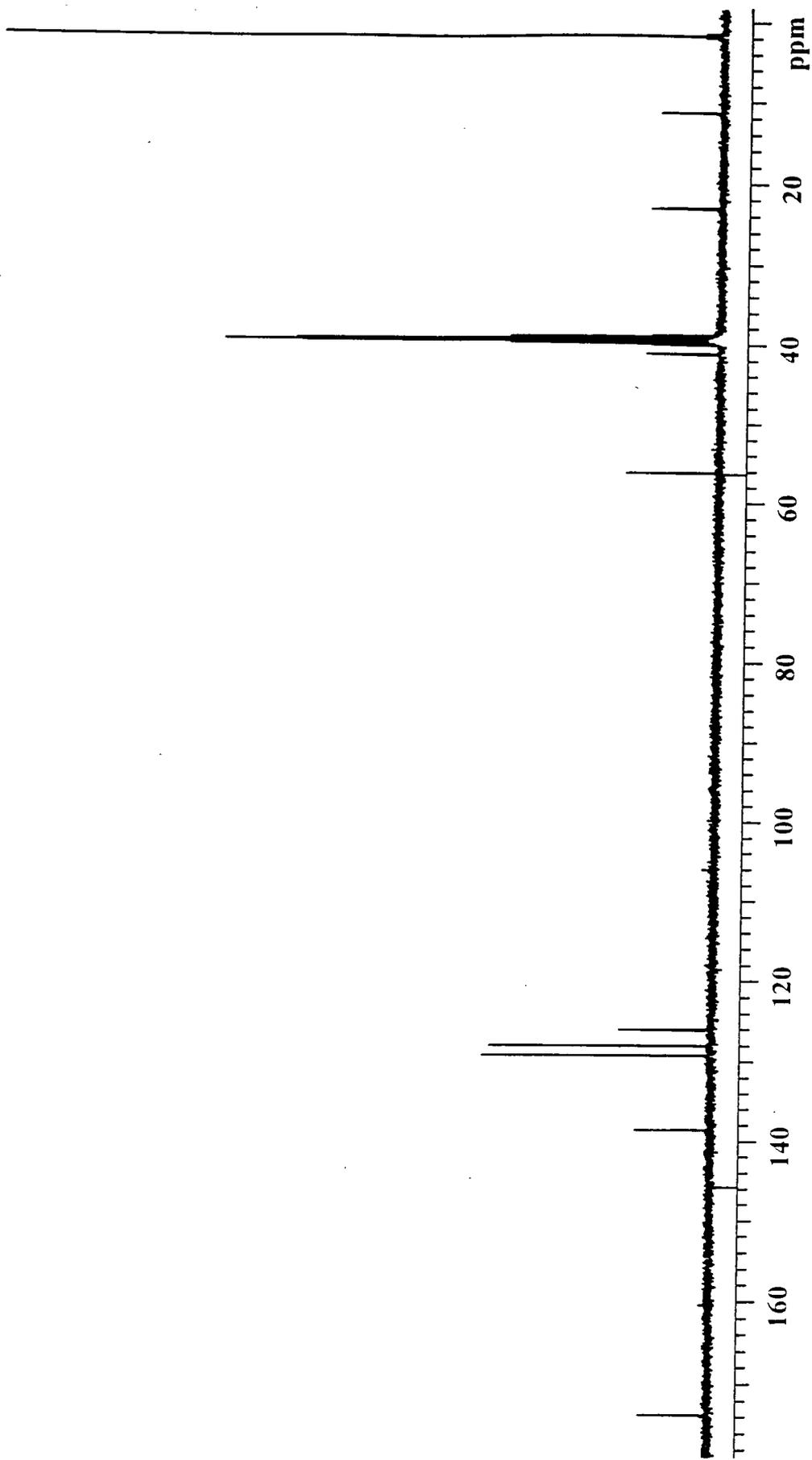
Appendix 2

Appendix 2.2.20 ^{13}C nmr spectrum of Si-*wedge*-phe in DMSOd$_6$.
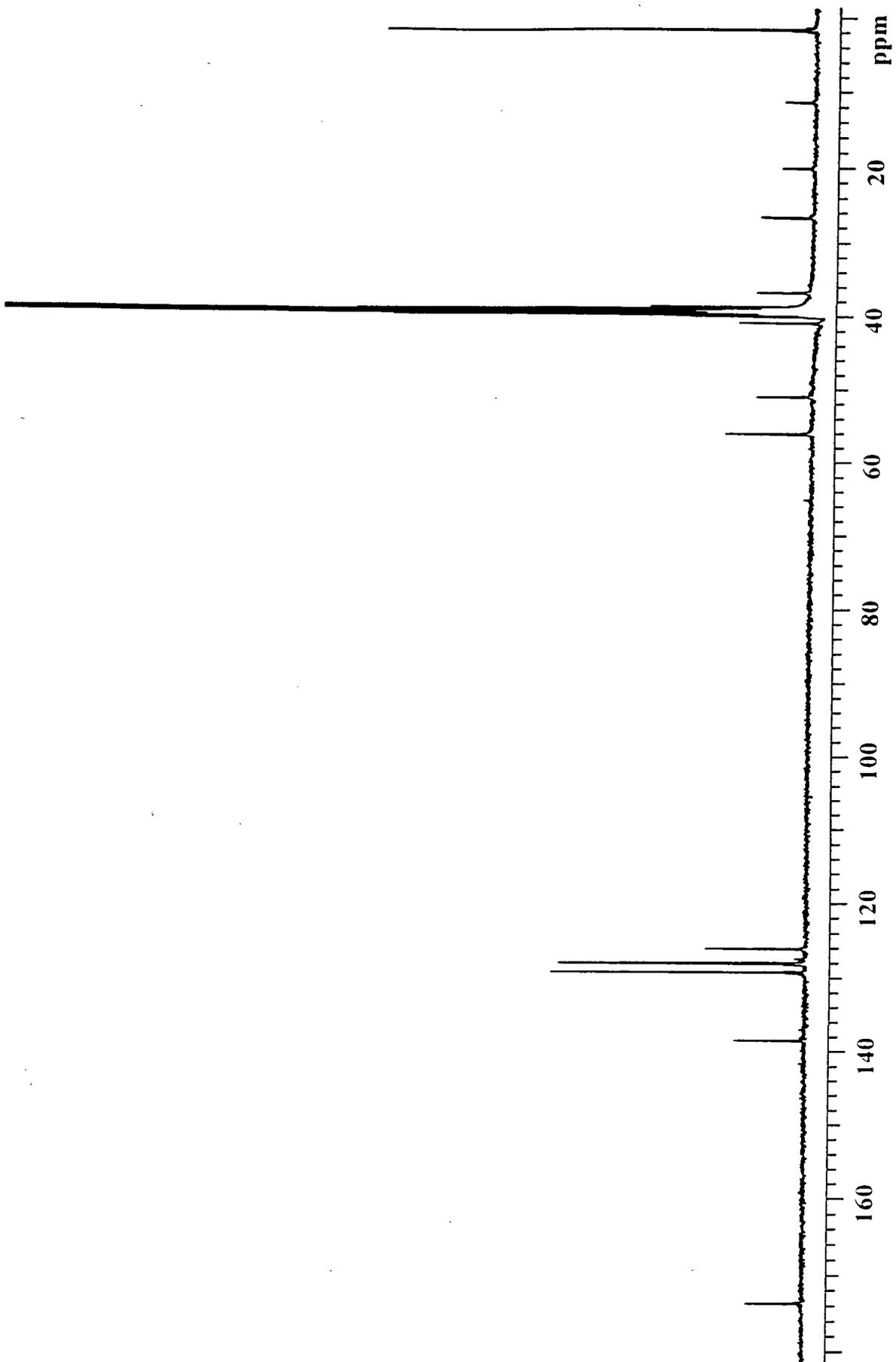
Appendix 2.2.21 ^{13}C nmr spectrum of Si-*wedge*-phe$_2$ in DMSOd$_6$.
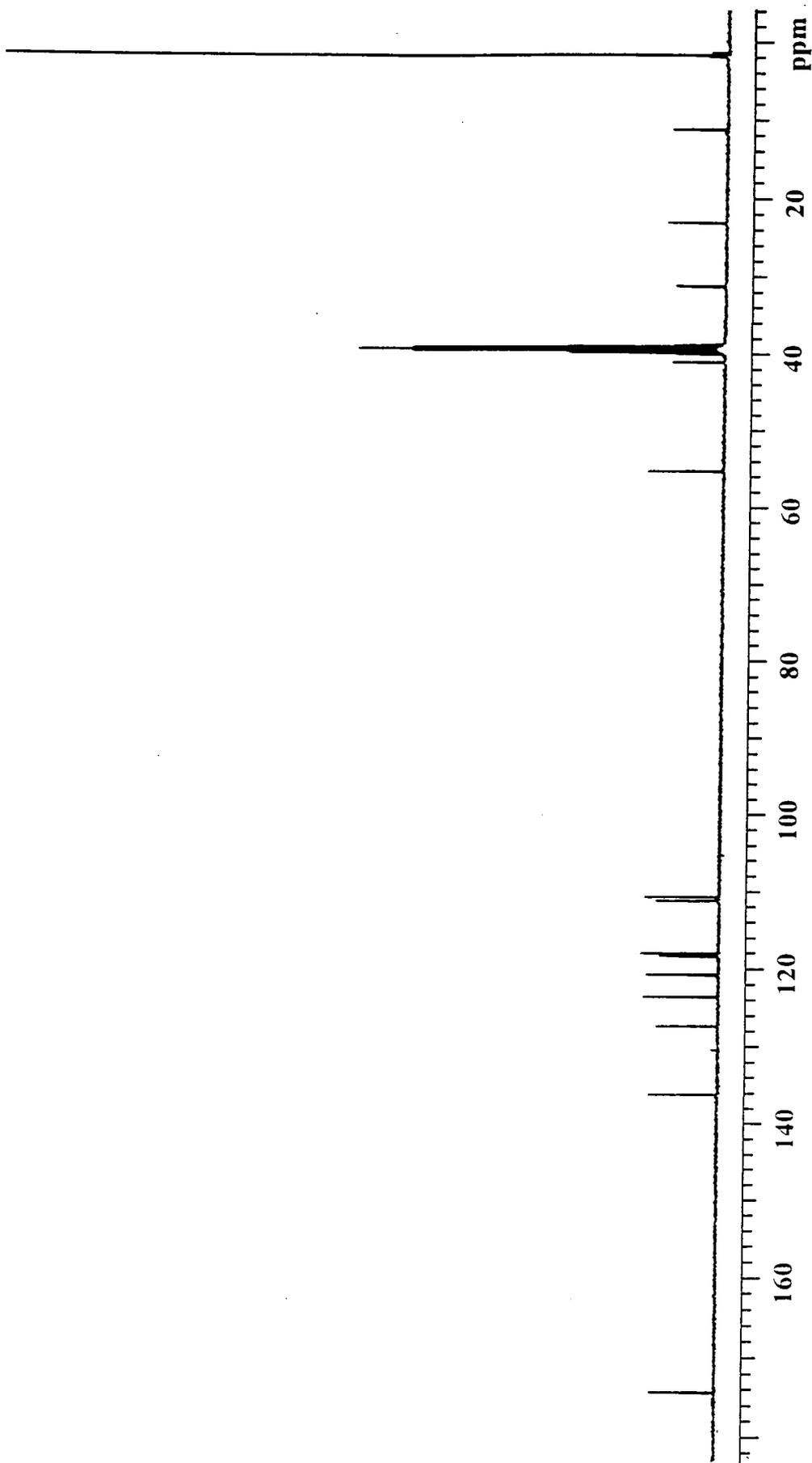
Appendix 2.2.22 ^{13}C nmr spectrum of Si-*wedge*-trp in DMSOd$_6$.
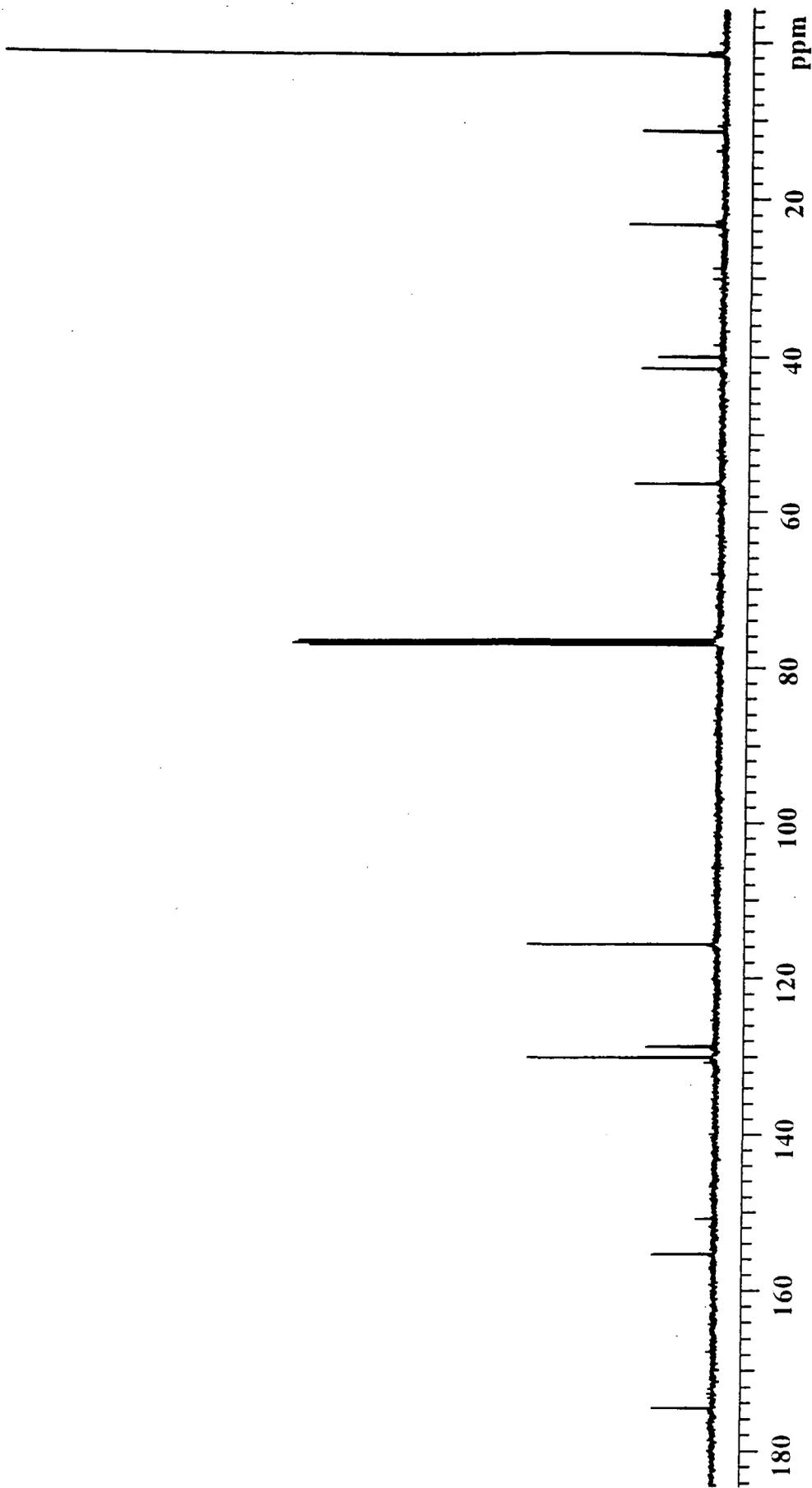
Appendix 2.2.23 ^{13}C nmr spectrum of Si-*wedge*-tyr in CDCl$_3$.
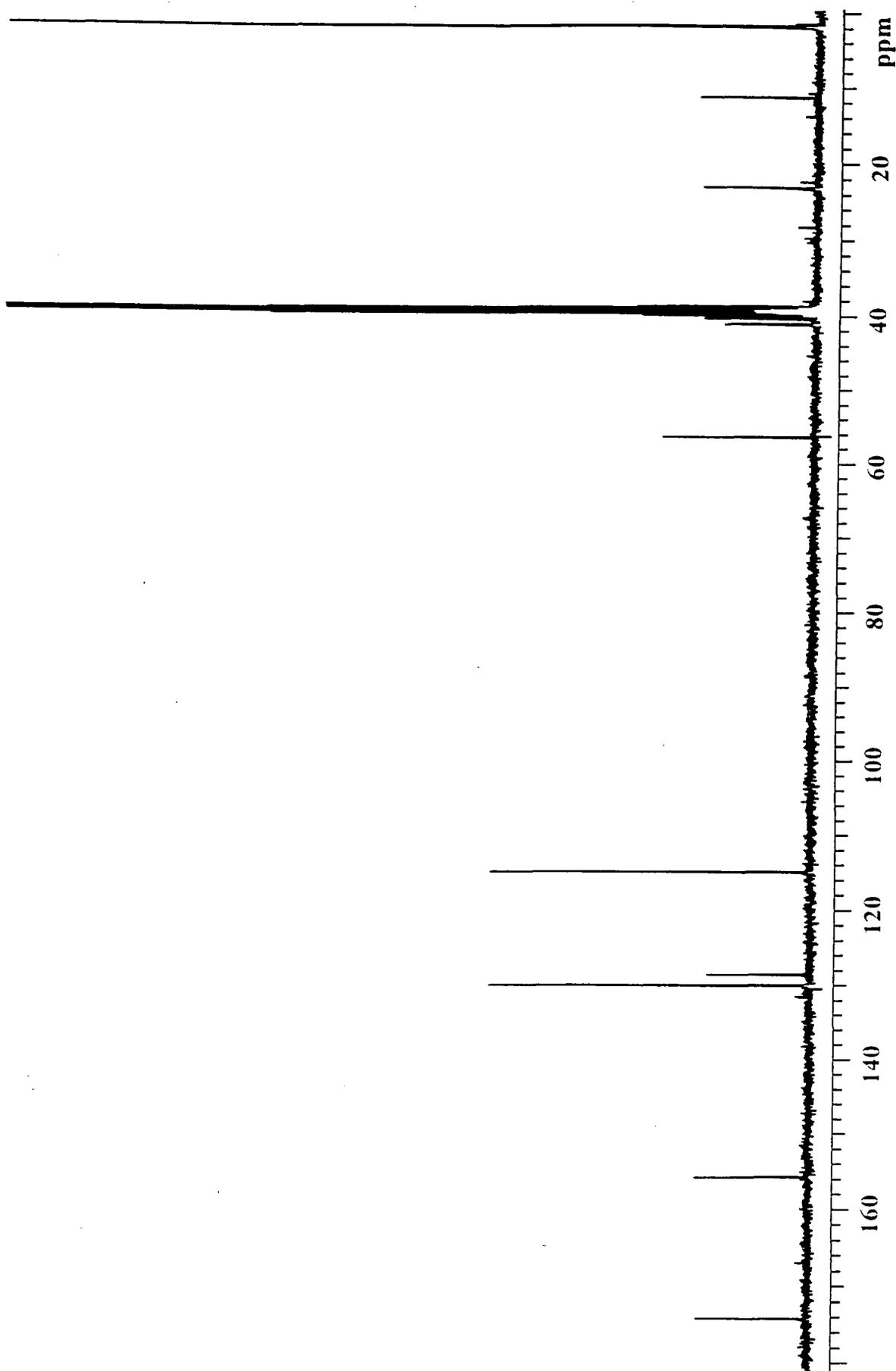
Appendix 2.2.24 13C nmr spectrum of Si-*wedge*-tyr in DMSOd6.

Appendix 2

297
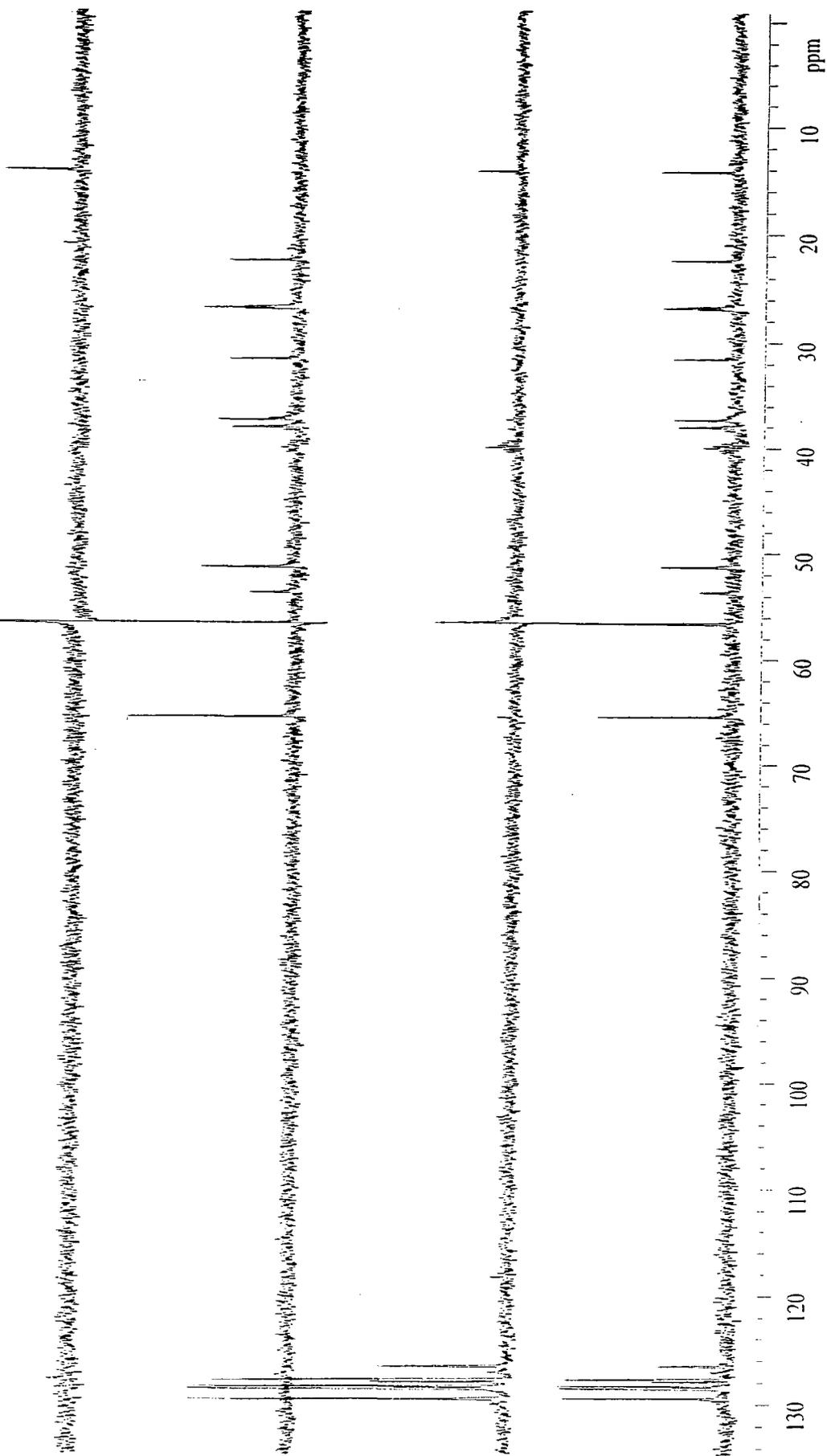
Appendix 2.3.1 DEPT nmr spectrum of Hex-*wedge*-phe$_2$-CBZ$_2$ in DMSOd$_6$.
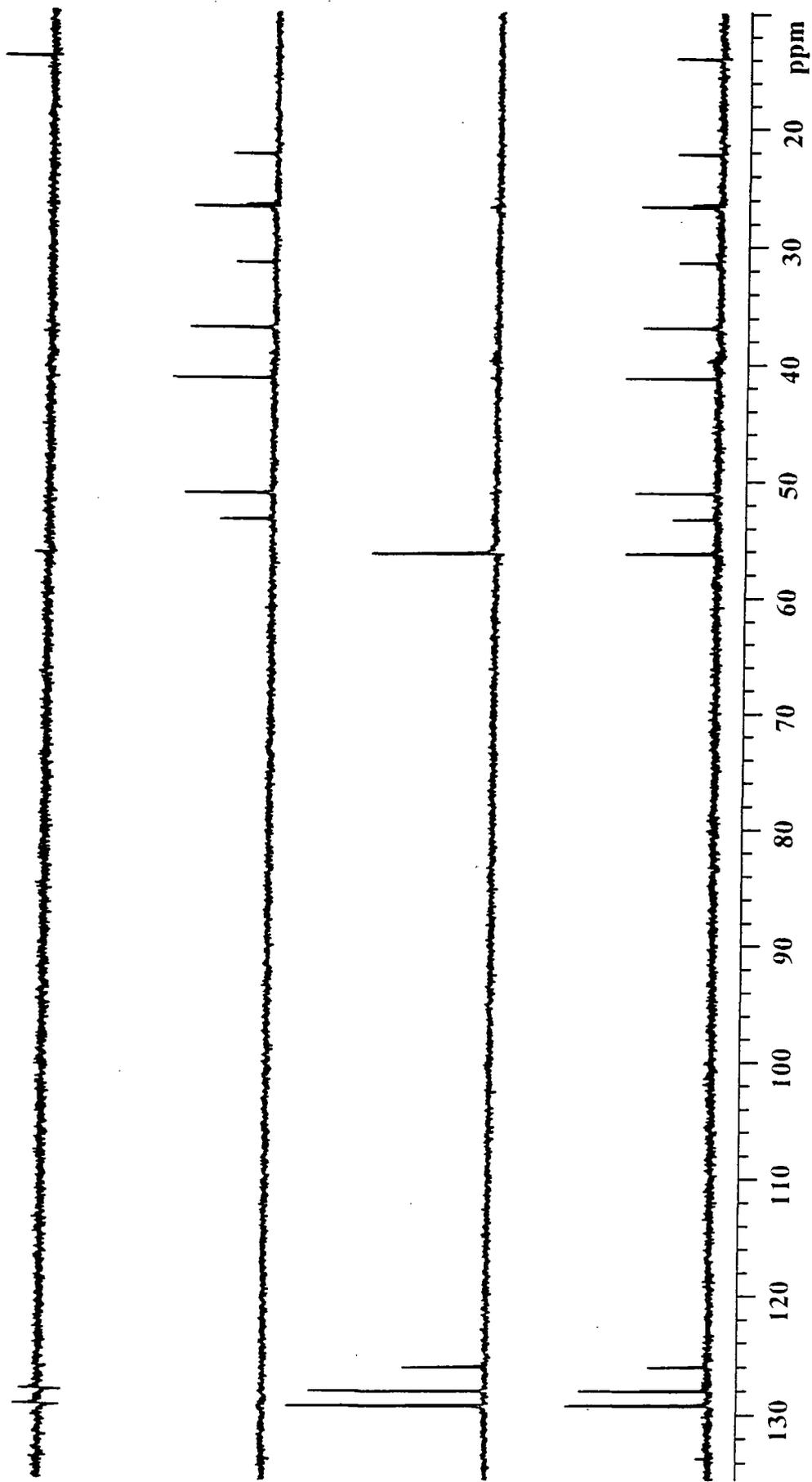
Appendix 2.3.2 DEPT nmr spectrum of Hex-*wedge*-phe$_2$ in DMSOd$_6$.
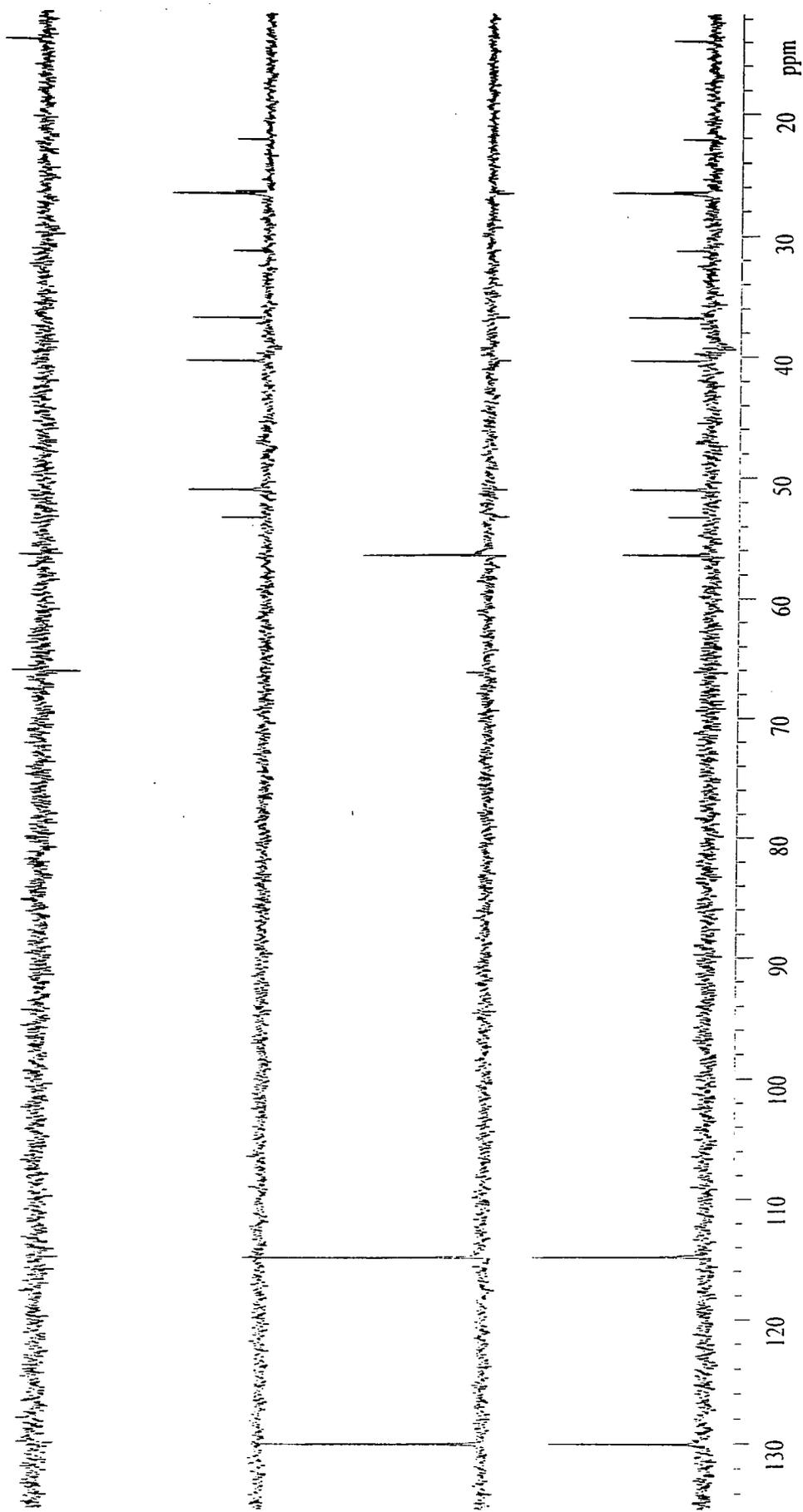
Appendix 2.3.3 DEPT nmr spectrum of Hex-*wedge*-tyr$_2$ in DMSOd$_6$.
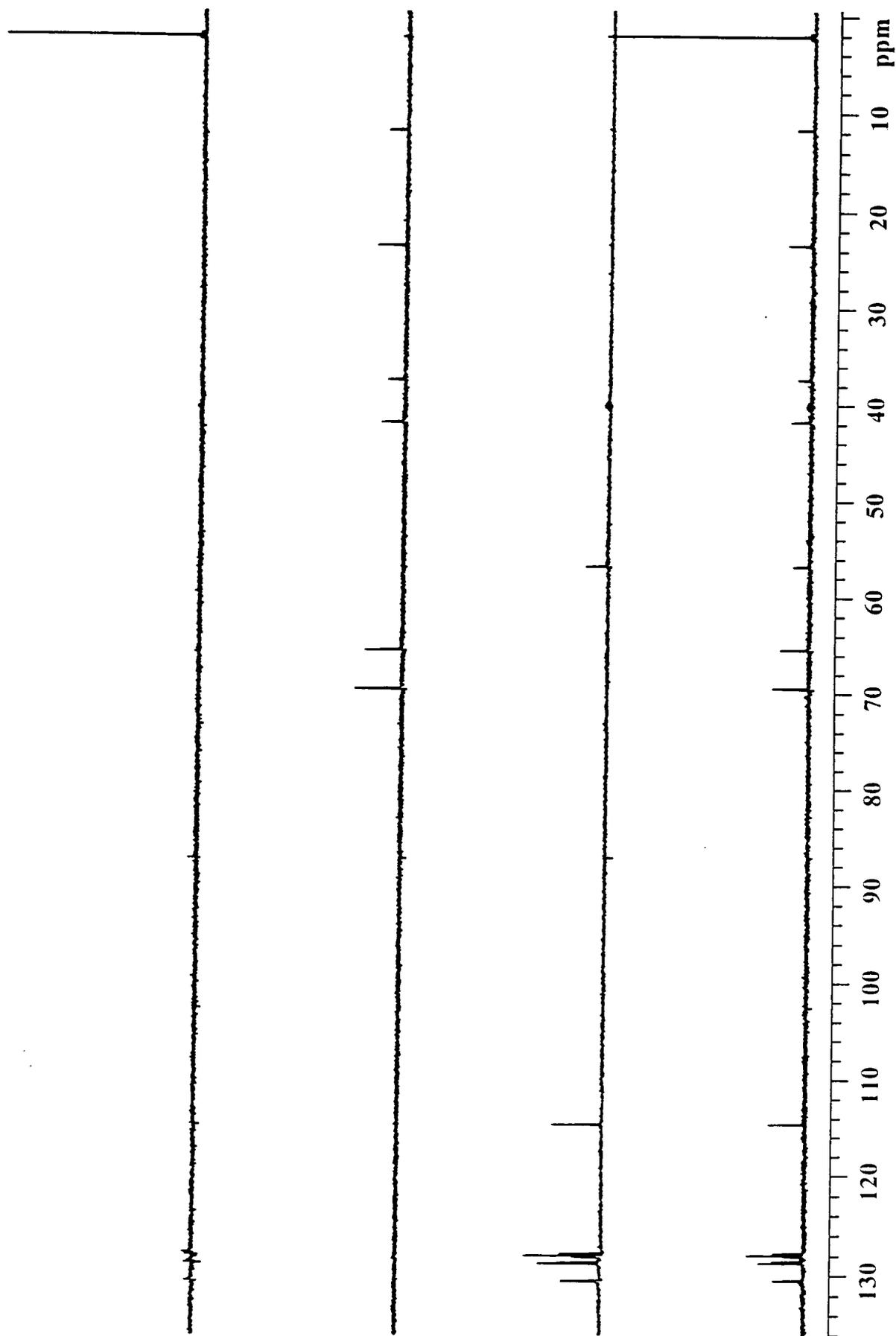
Appendix 2.3.4 DEPT nmr spectrum of Si-*wedge-o-benzyl*-tyr-CBZ in DMSOd$_6$.
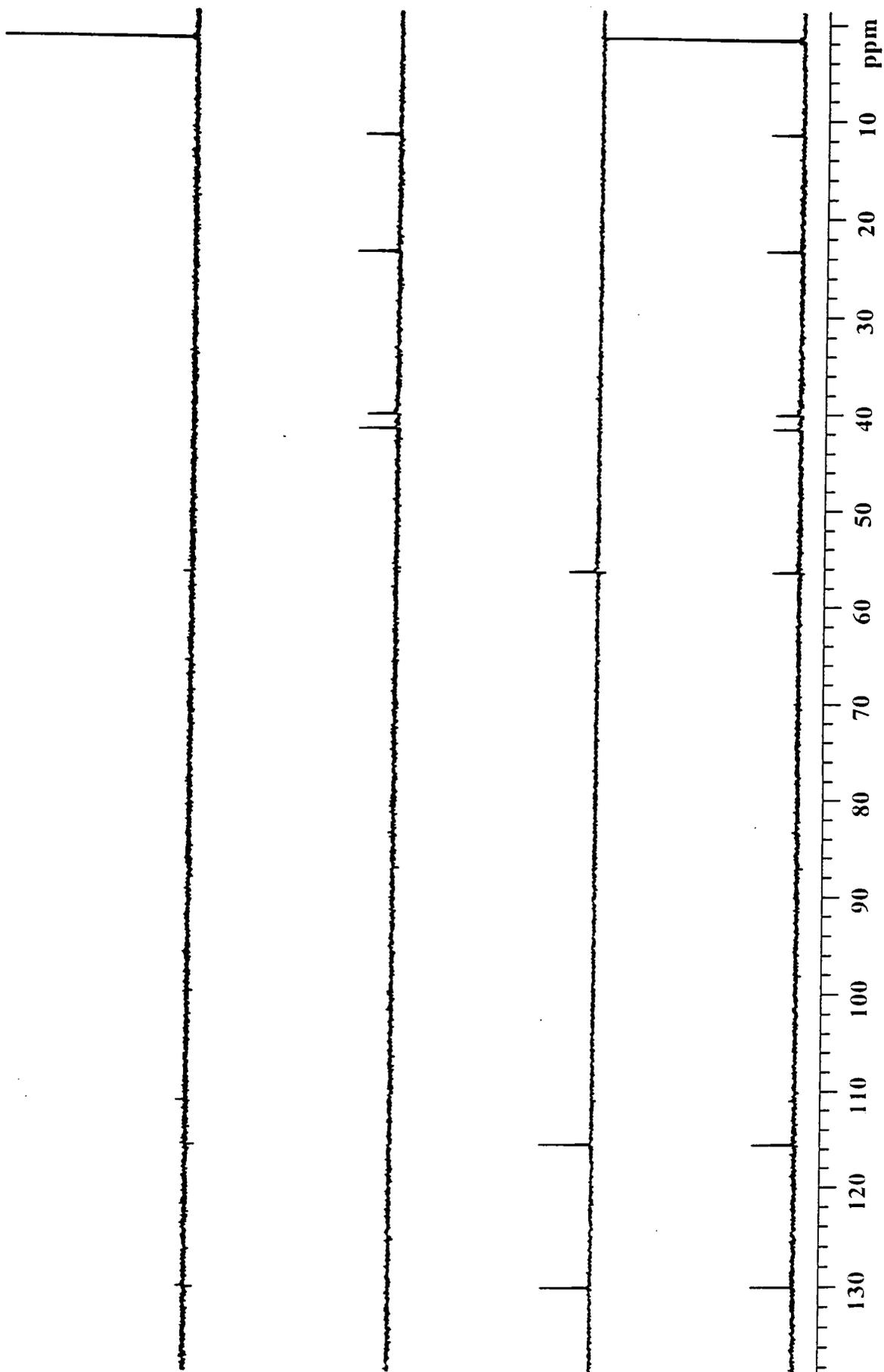
Appendix 2.3.5 DEPT nmr spectrum of Si-*wedge*-tyr in CDCl₃.
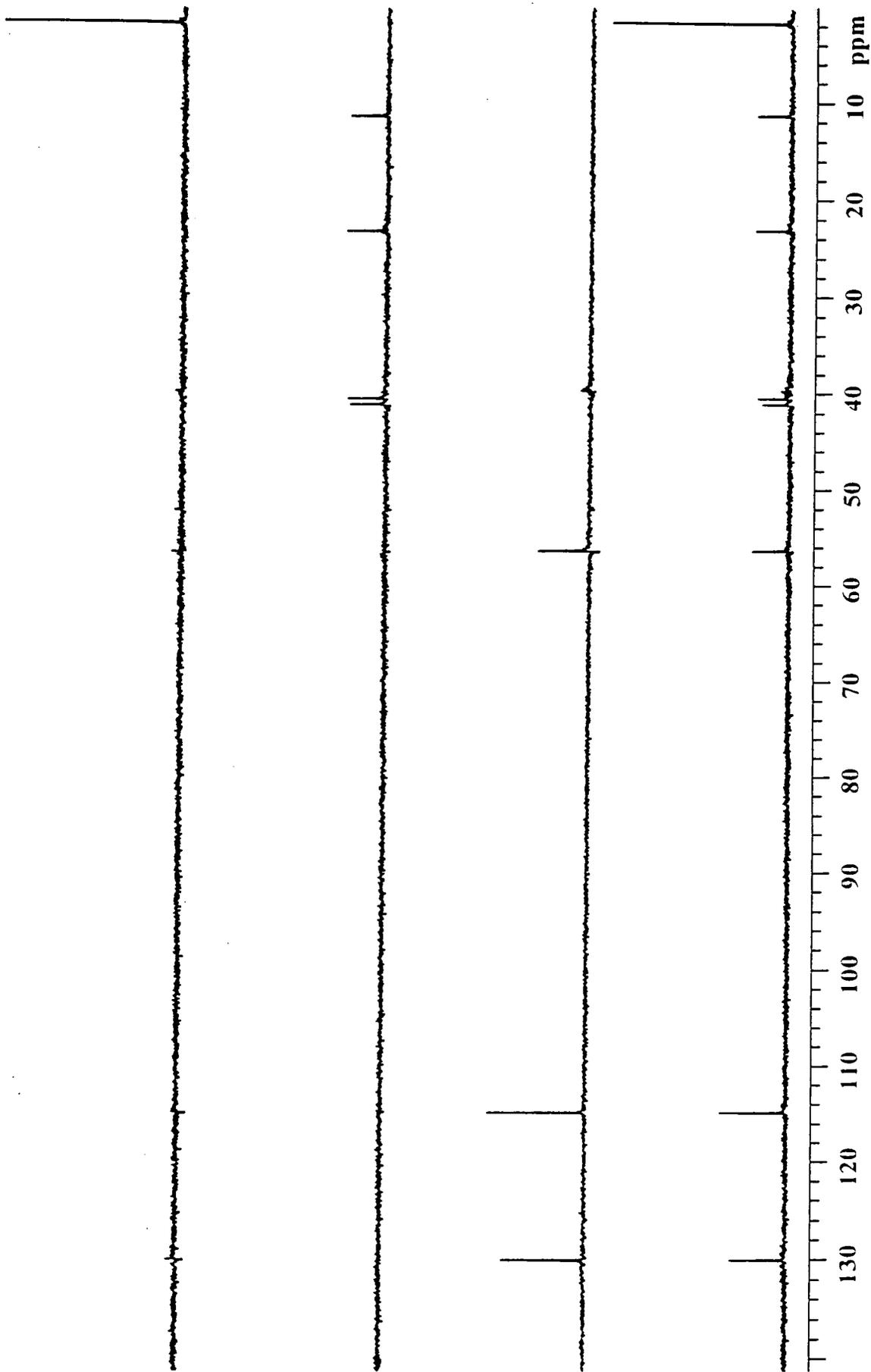
Appendix 2.3.6 DEPT nmr spectrum of Si-*wedge*-tyr in DMSOd$_6$.

CH3 carbons

CH2 carbons
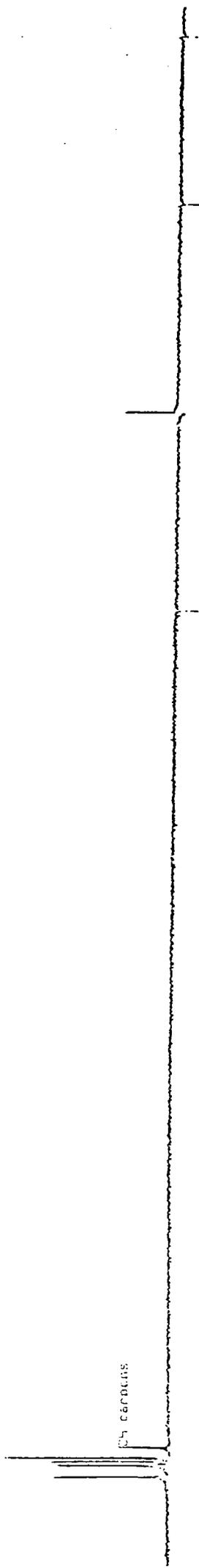
CH carbons

all protonated carbons
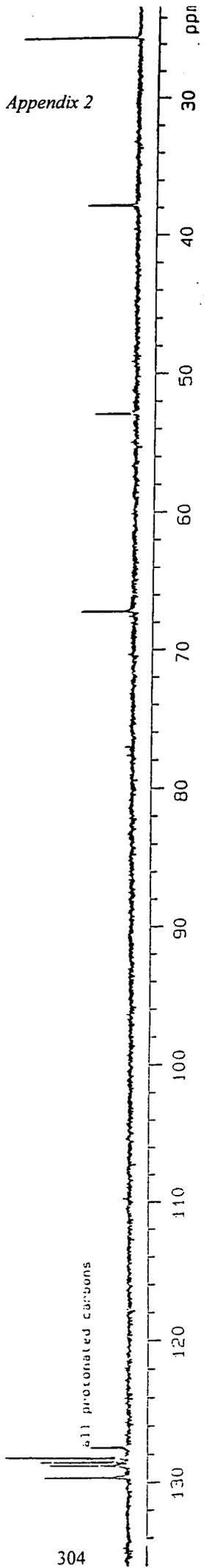
304

Appendix 2.3.7 DEPT spectrum of NCBZ-phe-hydroxysuccinimide ester in CDCl₃.

CH3 carbons

CH2 carbons
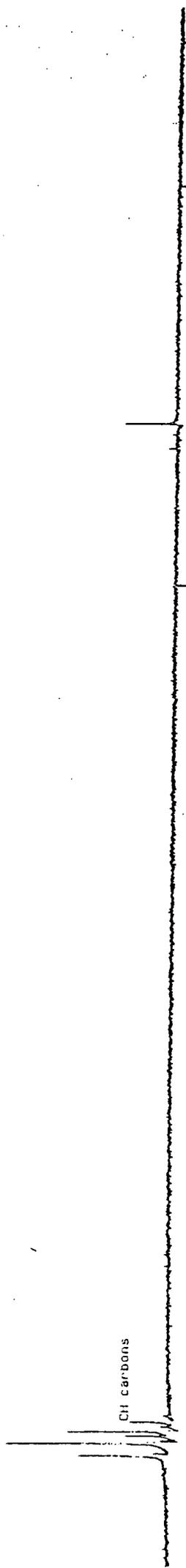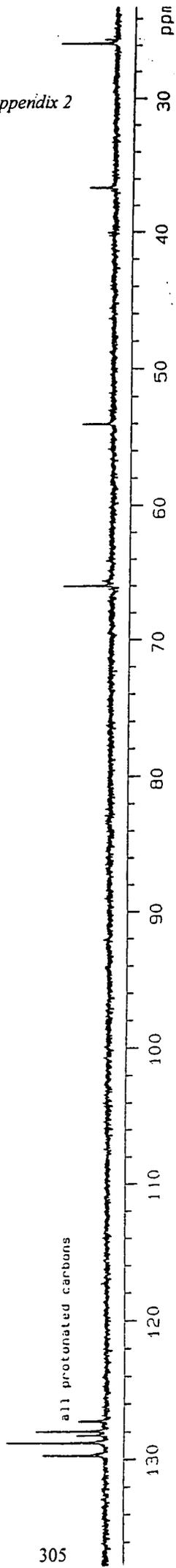
CH carbons

all protonated carbons

Appendix 2.3.8 DEPT spectrum of NCBZ-phe-hydroxysuccinimide ester in DMSOd₆.
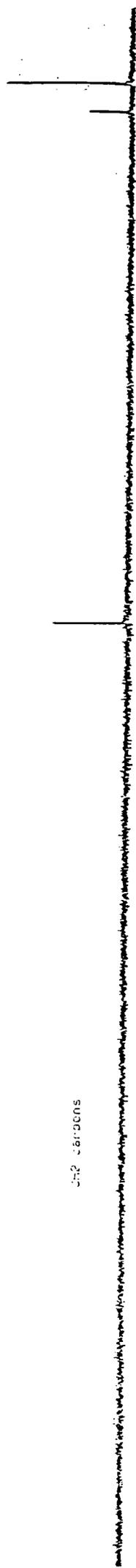
CH3 carbons
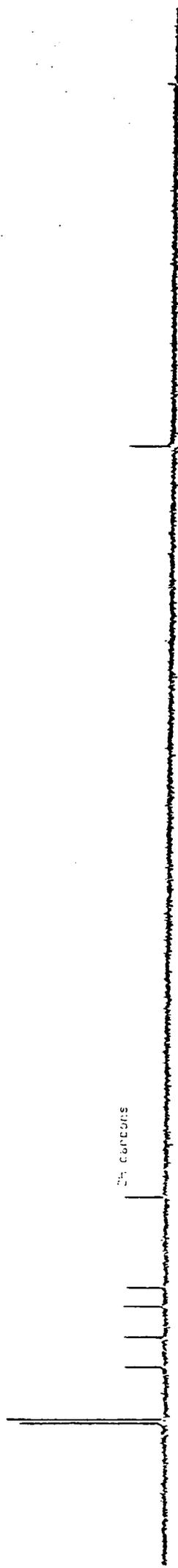
CH2 carbons

CH carbons
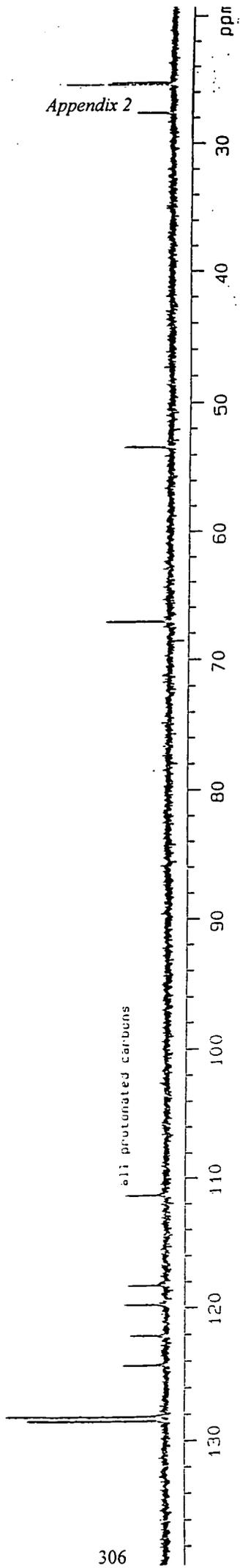
all protonated carbons

Appendix 2.3.9 DEPT spectrum of NCBZ-trp-hydroxysuccinimide ester in CDCl₃.

ppm

30

40

50

60

70

80

90

100

110

120

130
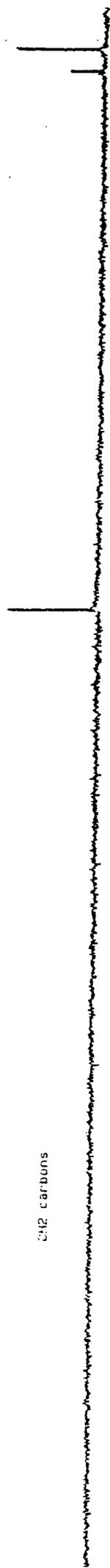
CH3 carbons

CH2 carbons

CH carbons
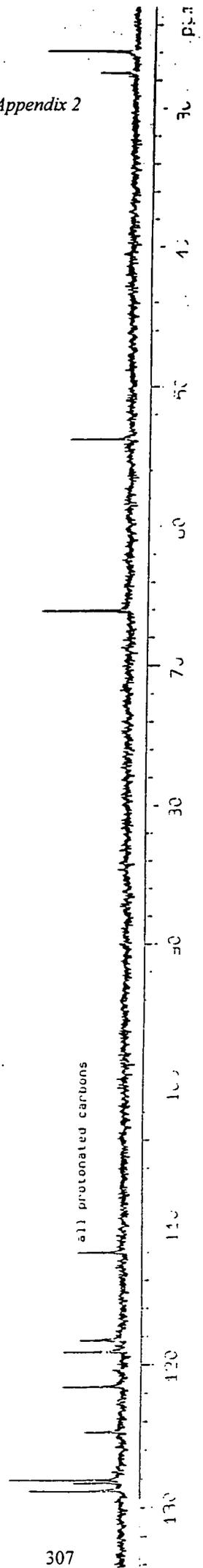
all protonated carbons

Appendix 2.3.10 DEPT spectrum of NCBZ-trp-hydroxysuccinimide ester in DMSOd6.

307

CH3 carbons

CH2 carbons
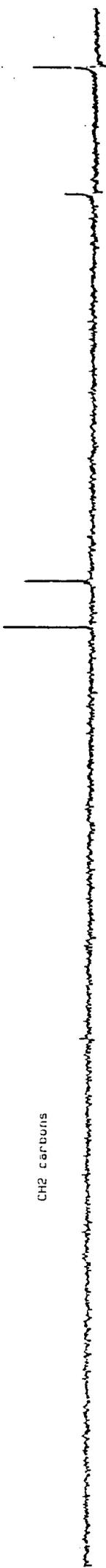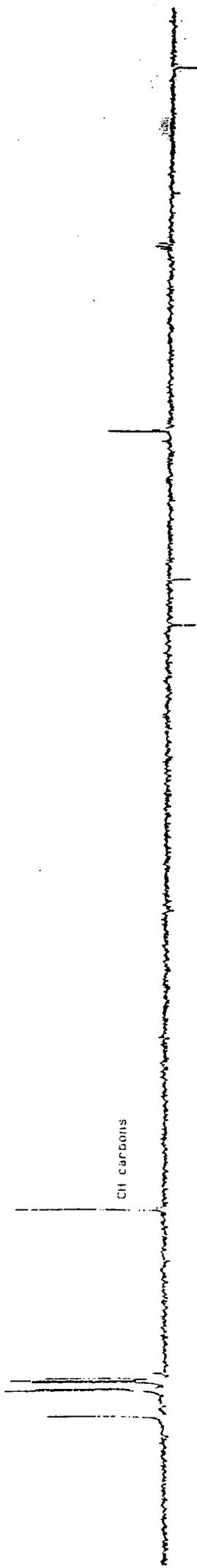
CH carbons

all protonated carbons
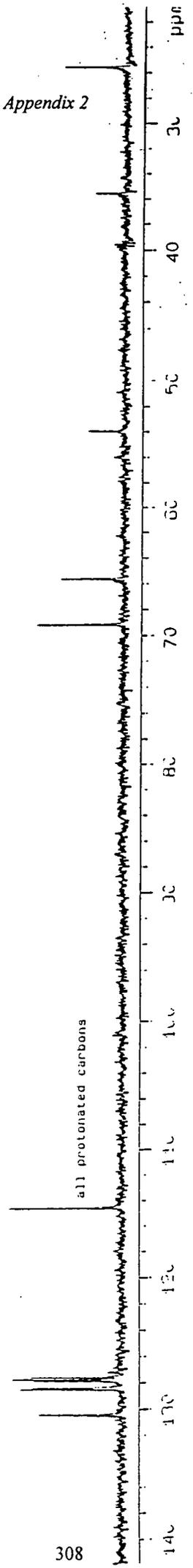
Appendix 2.3.11 DEPT spectrum of NCBZ-tyr-hydroxysuccinimide ester in DMSOd$_6$.
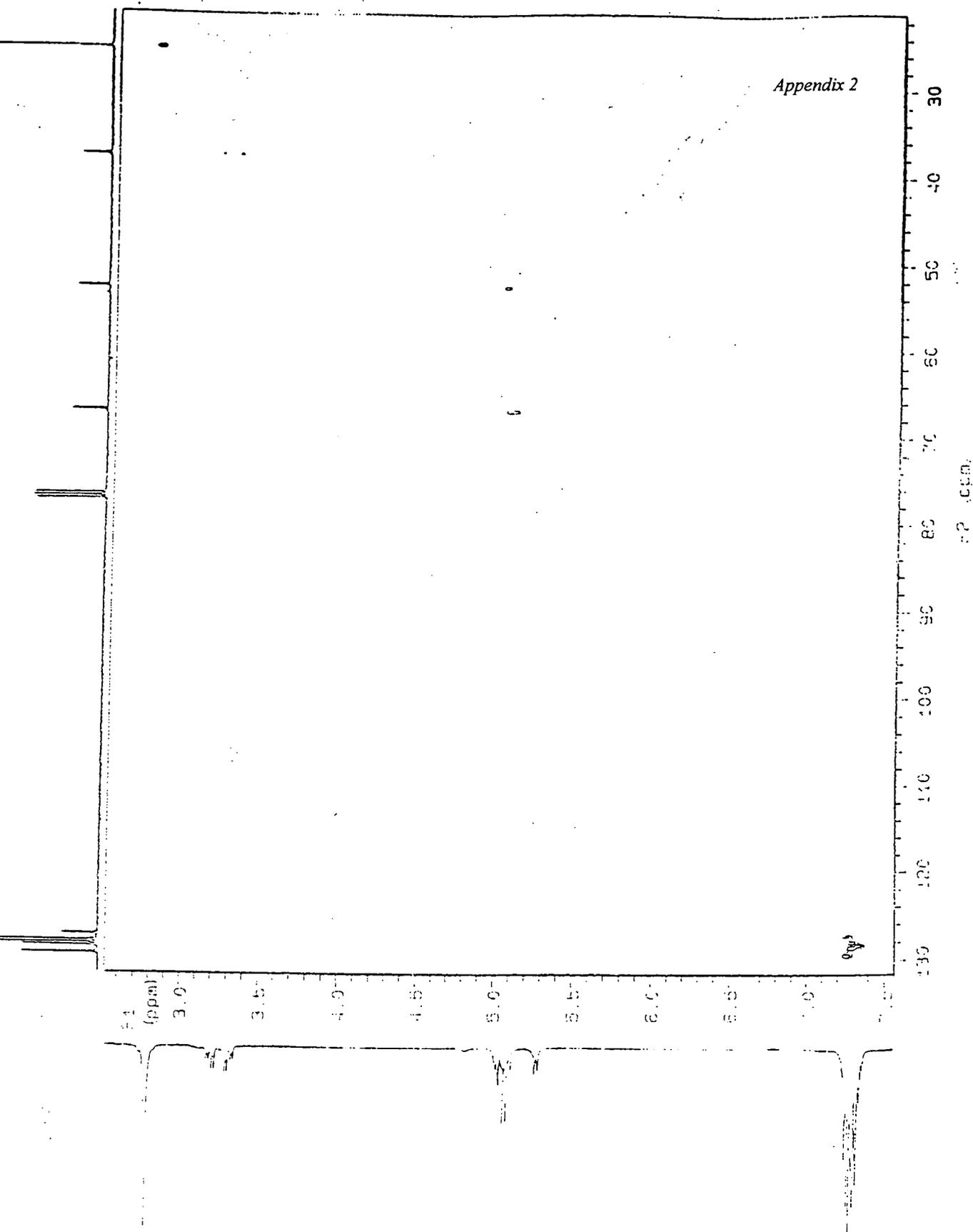
Appendix 2.4.1 HETCOR spectrum of NCBZ-phe-hydroxysuccinimide ester in CDCl₃.

F1
(ppm)

F2 (ppm)
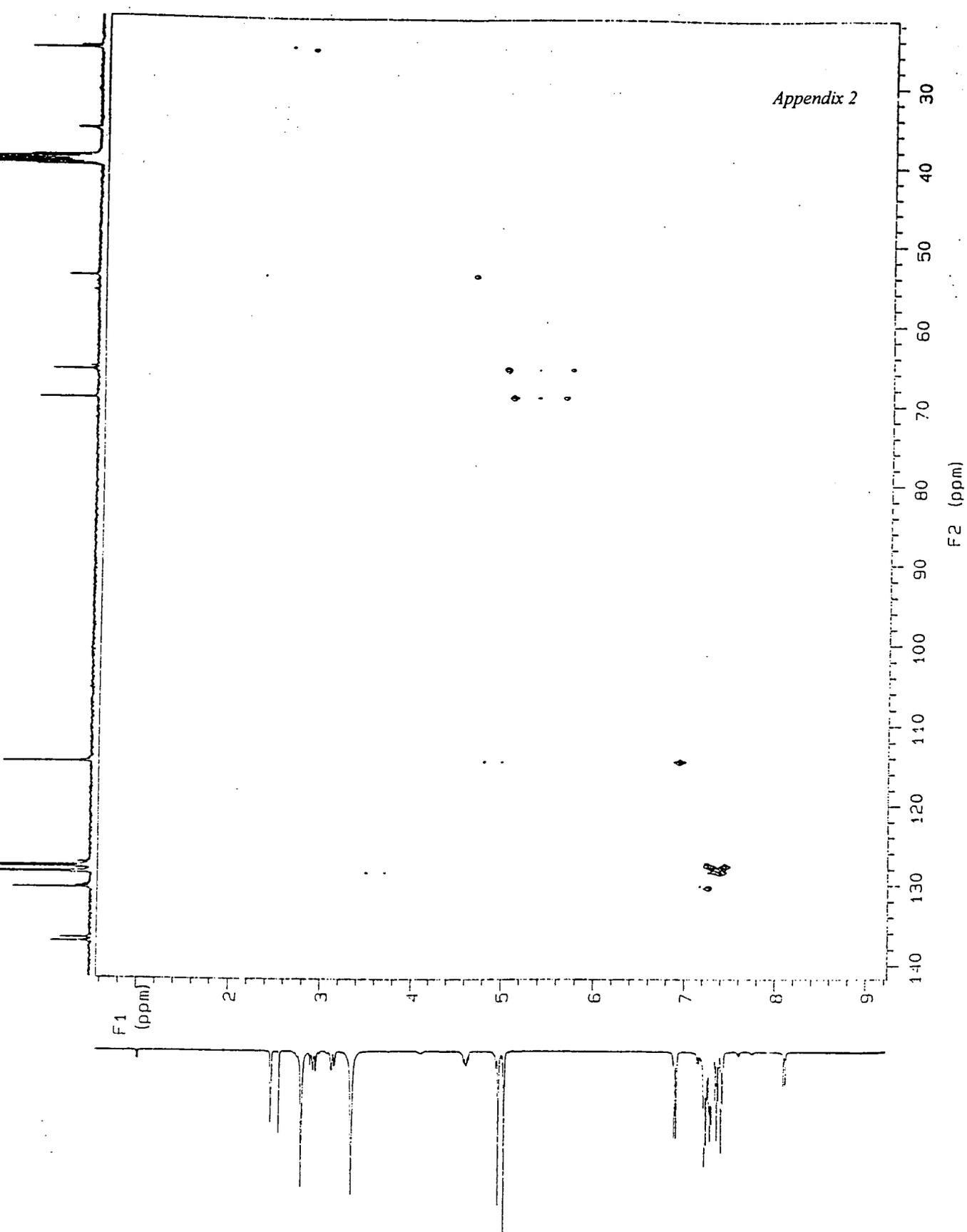
Appendix 2.4.2 HETCOR spectrum of NCBZ-tyr-hydroxysuccinimide ester in DMSOd$_6$.
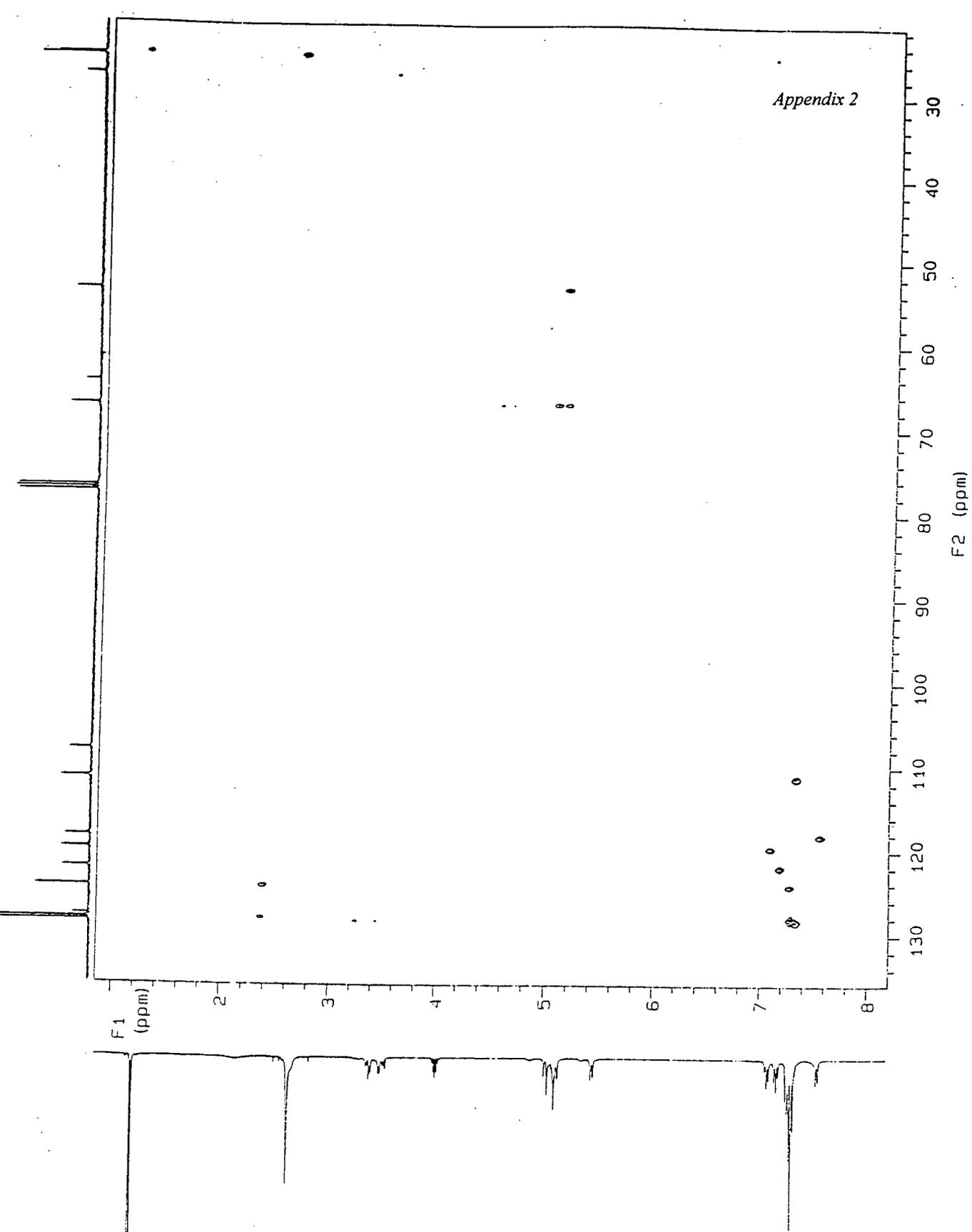
Appendix 2.4.3 HETCOR spectrum of NCBZ-trp-hydroxysuccinimide ester in CDCl₃.
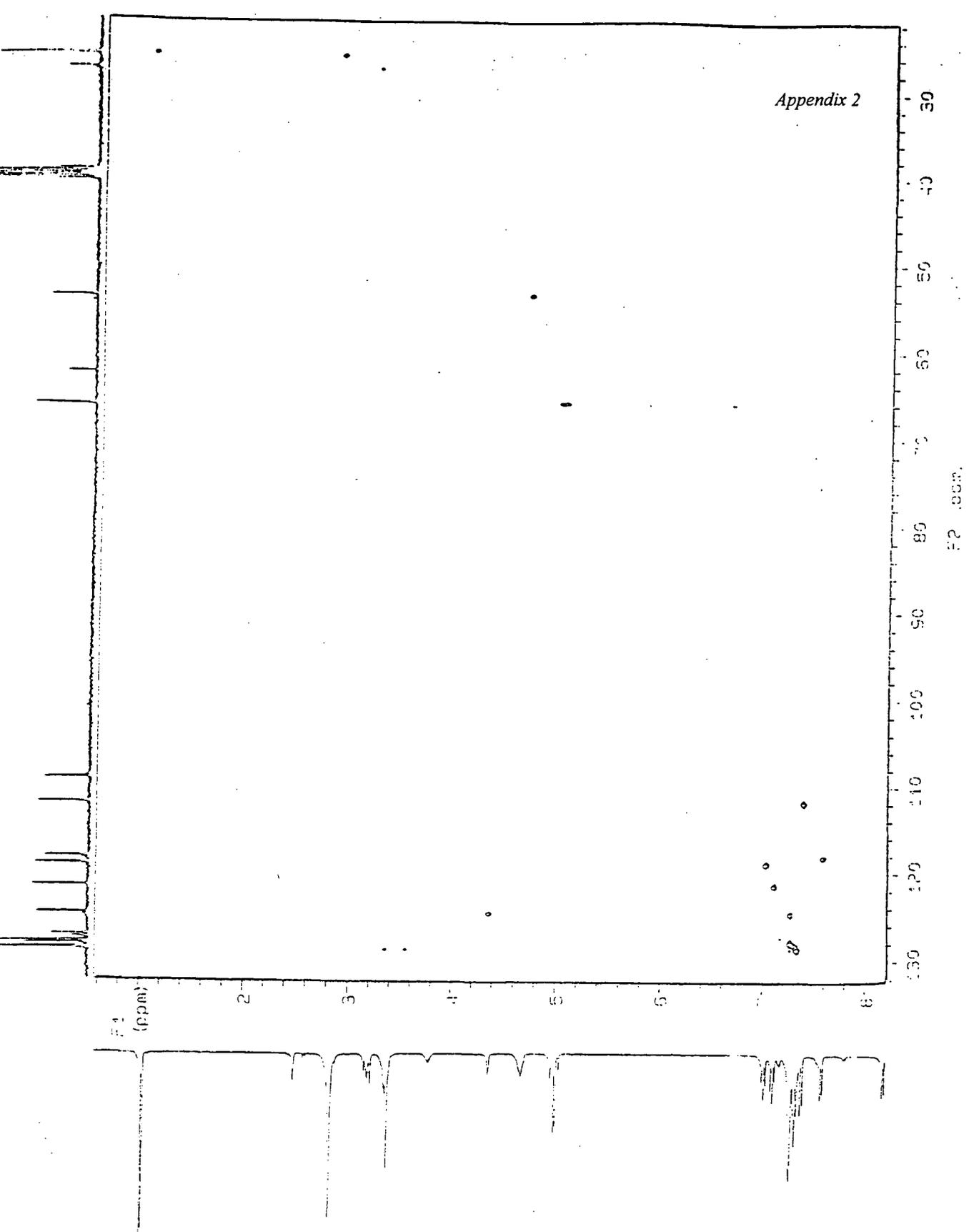
Appendix 2.4.4 HETCOR spectrum of NCBZ-trp-hydroxysuccinimide ester in DMSOd$_6$.
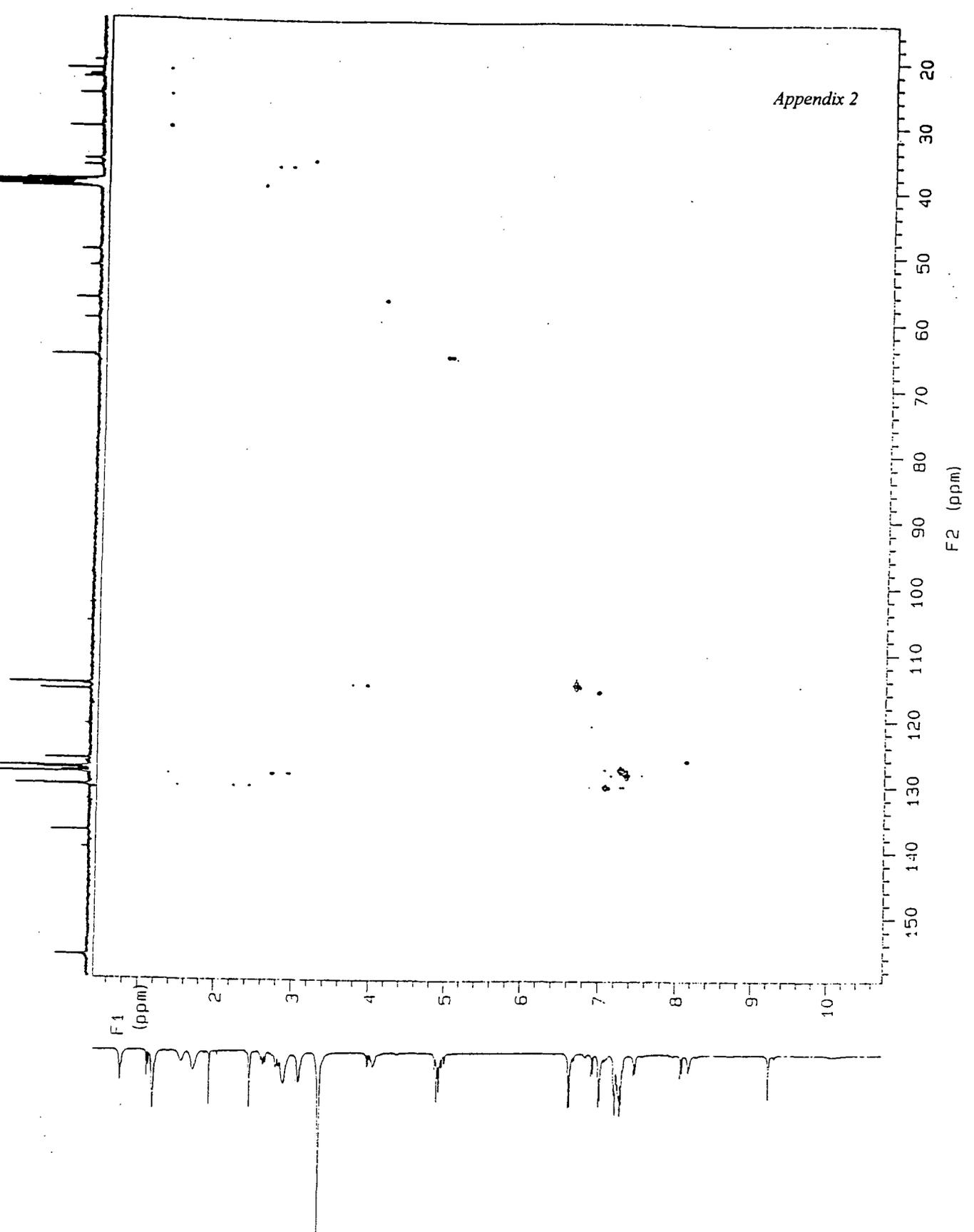
Appendix 2.4.5 HETCOR spectrum of Hex-*wedge*-tyr$_2$-CBZ$_2$ in DMSOd$_6$.
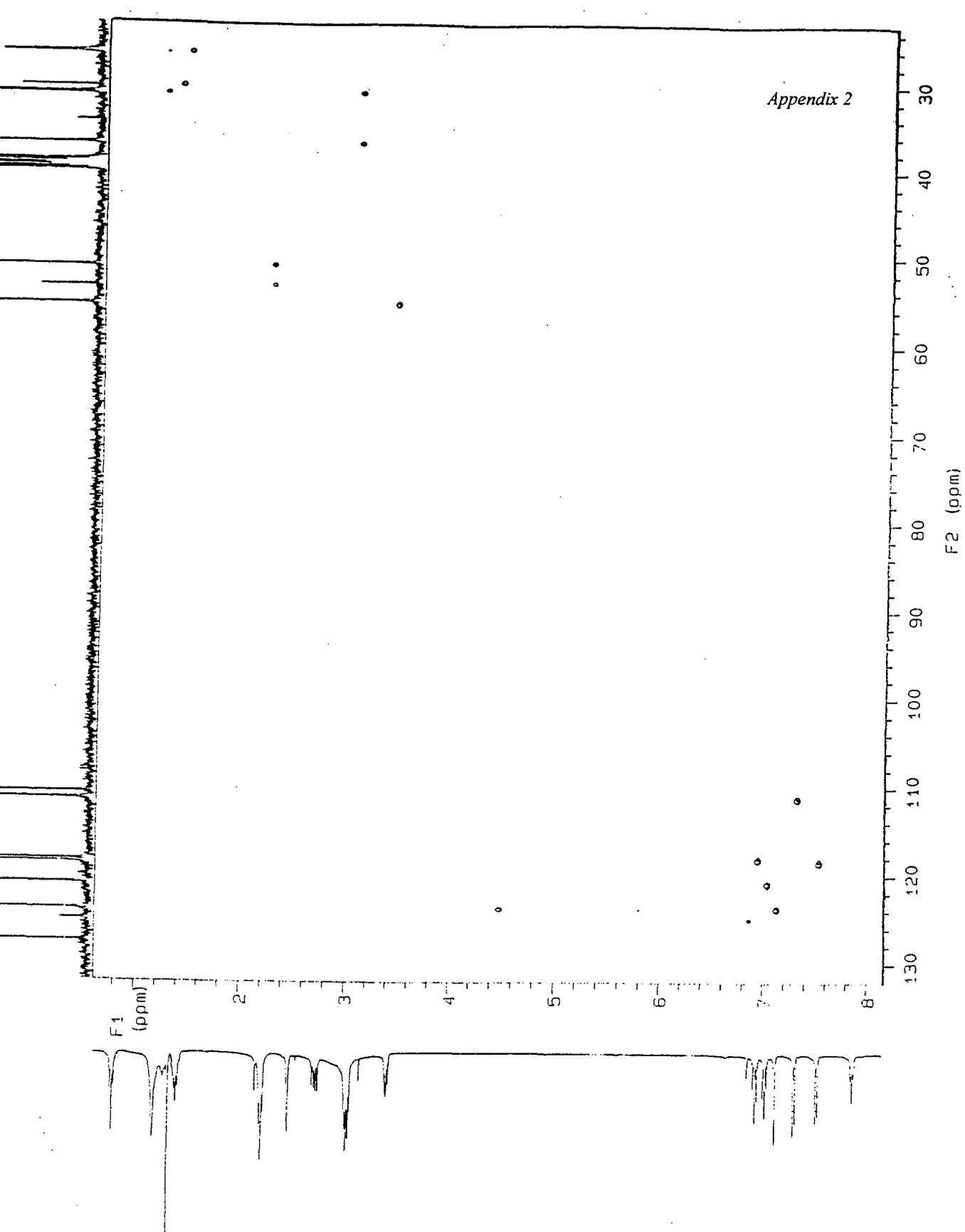
Appendix 2.4.6 HETCOR spectrum of Hex-*wedge*-trp₂ in DMSOd₆.
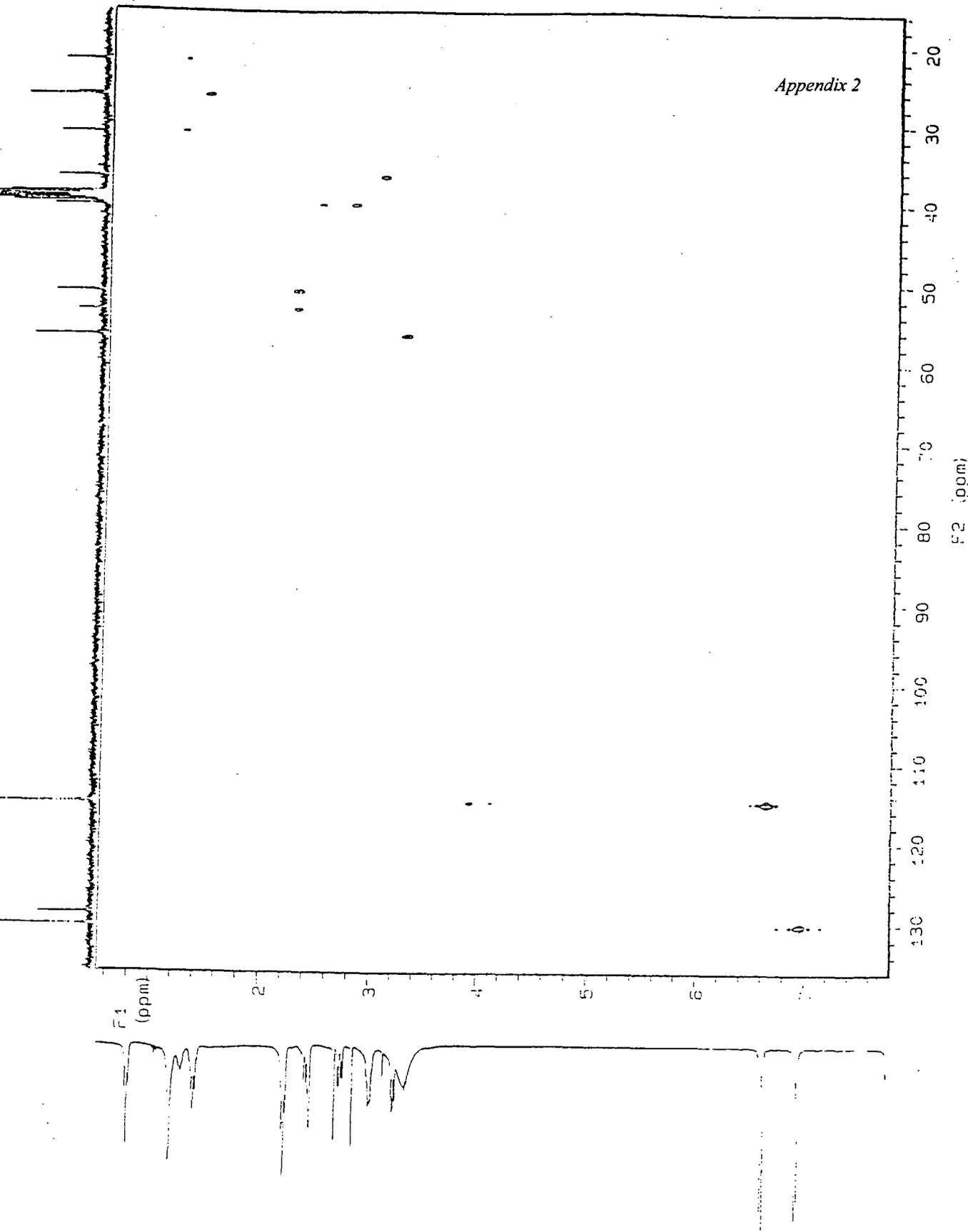
Appendix 2.4.7 HETCOR spectrum of Hex-*wedge*-tyr$_2$ in DMSOd$_6$.
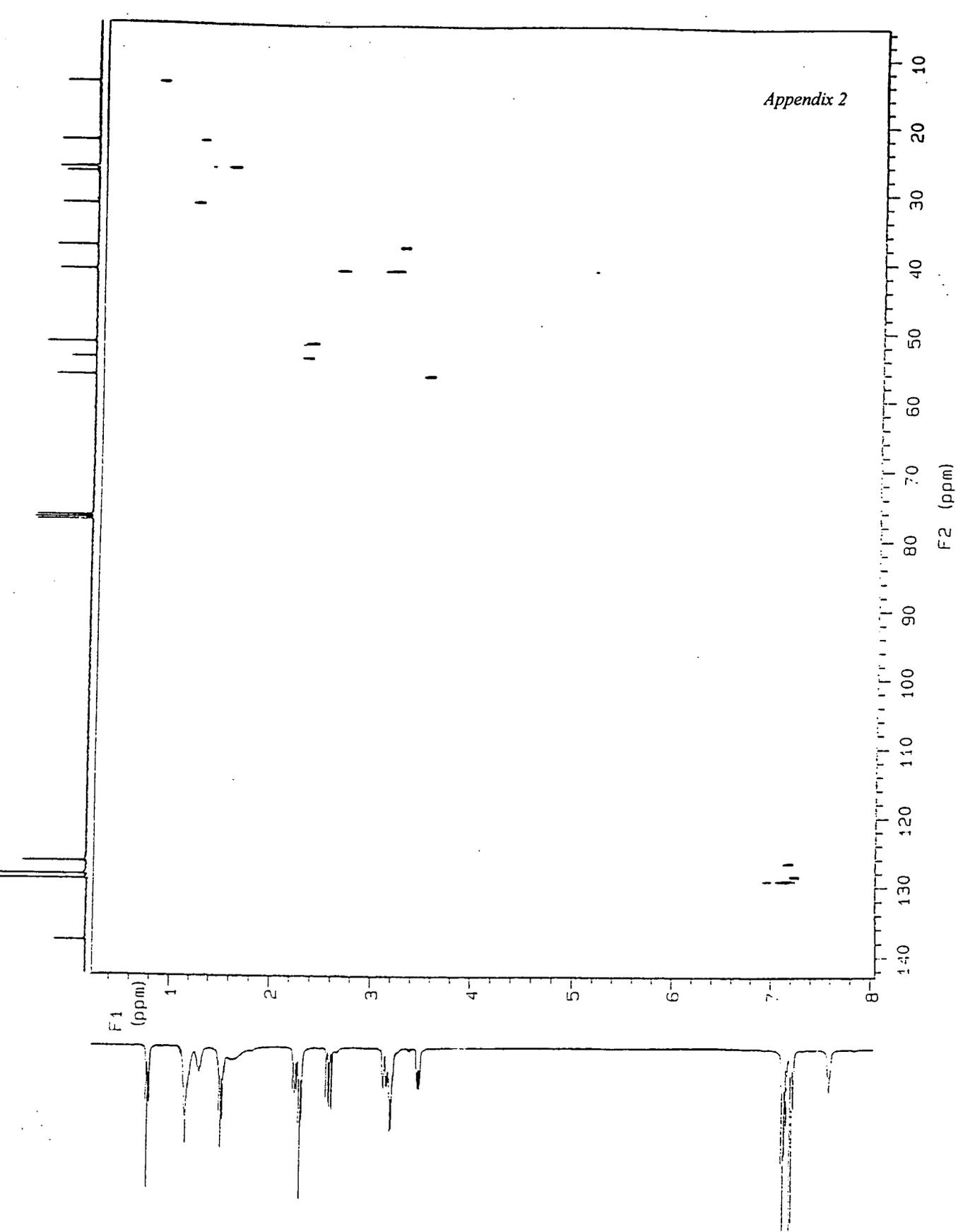
Appendix 2.4.8 HETCOR spectrum of Hex-*wedge*-phe₂ in CDCl₃.
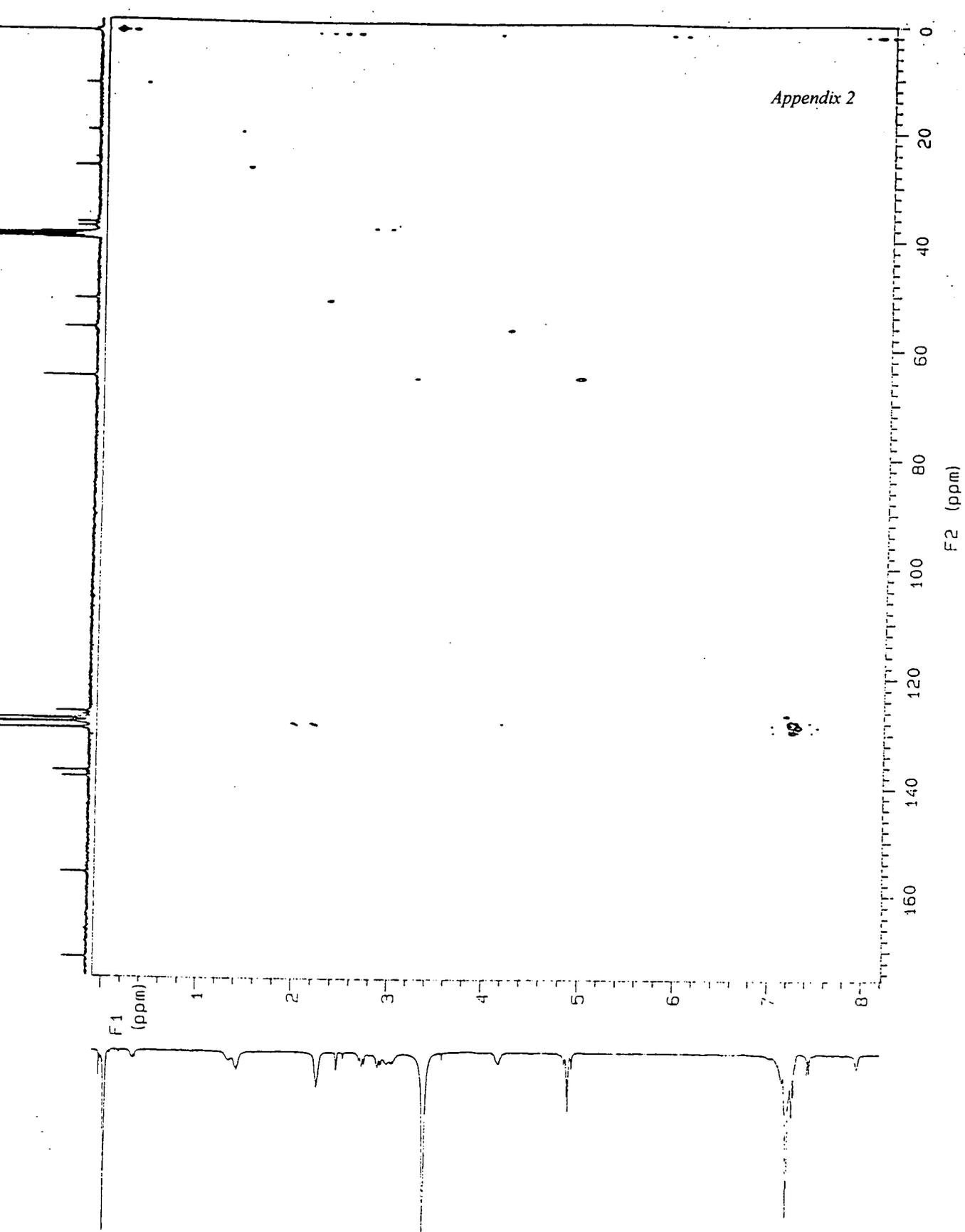
Appendix 2.4.9 HETCOR spectrum of Si-*wedge*-phe$_2$-CBZ$_2$ in DMSOd$_6$.

Appendix 2

F2 (ppm)

F1 (ppm)
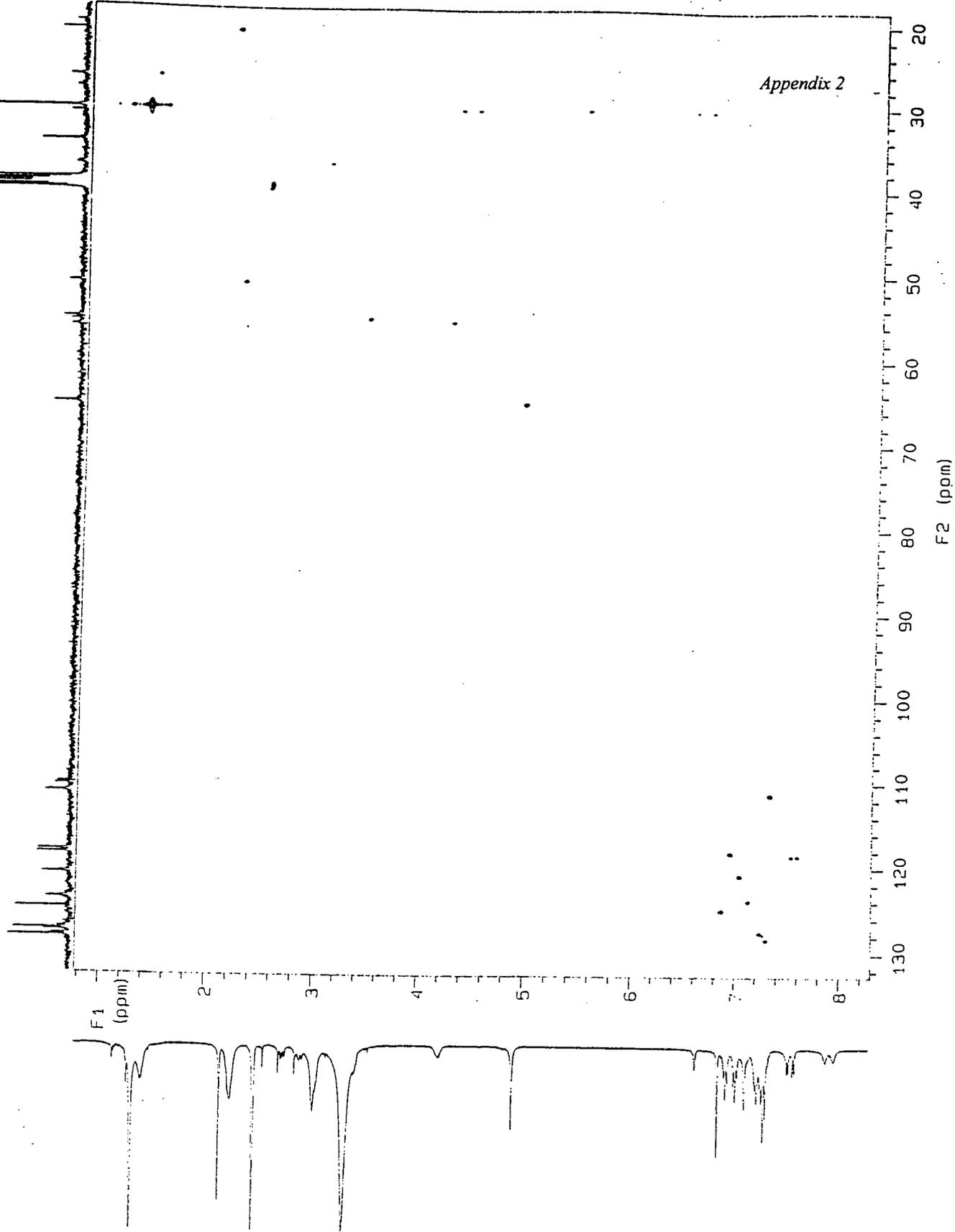
Appendix 2.4.10 HETCOR spectrum of Si-*wedge*-trp$_2$-NH$_2$-CBZ in DMSOd$_6$.

318
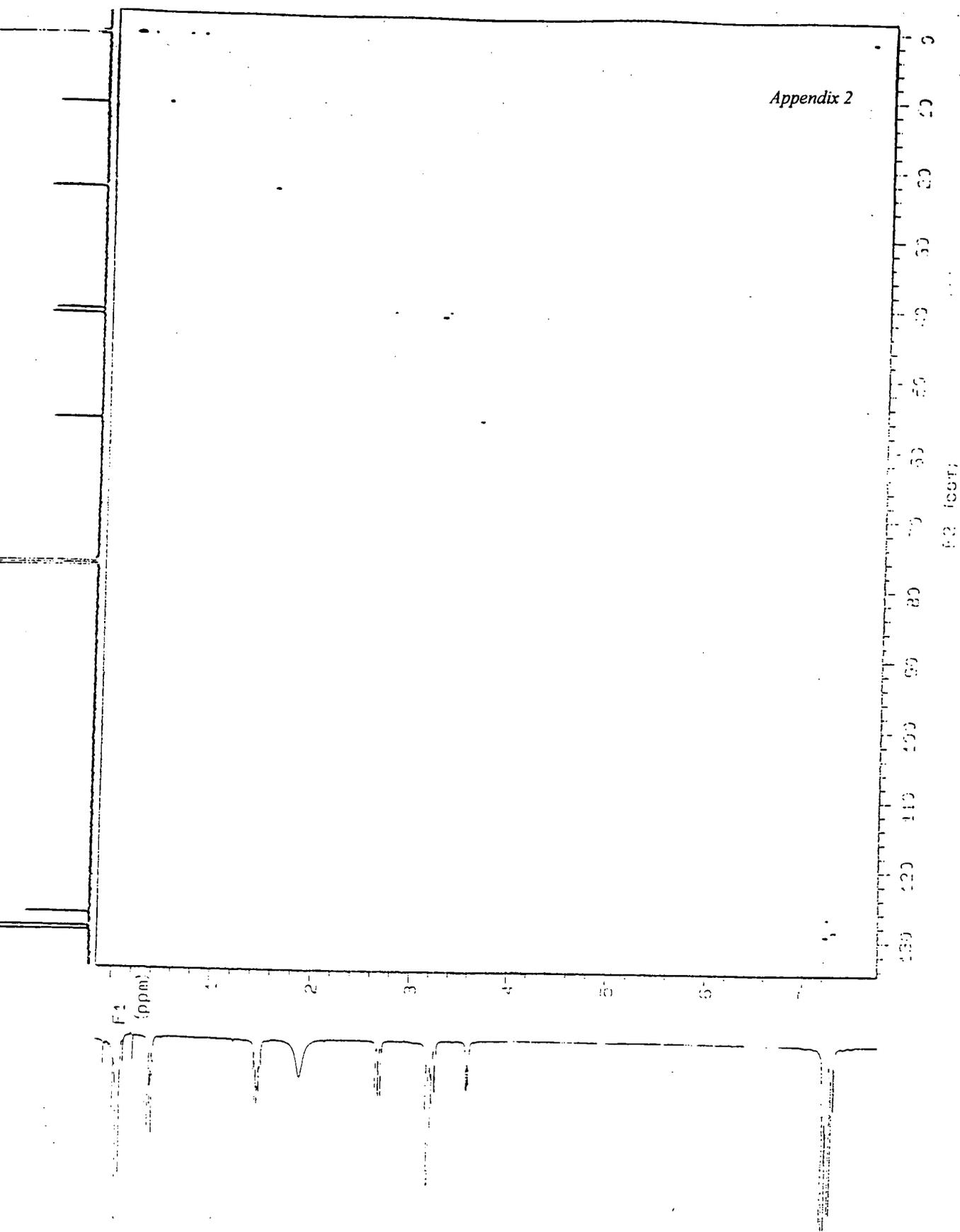
Appendix 2.4.11 HETCOR spectrum of Si-*wedge*-phe in CDCl₃.
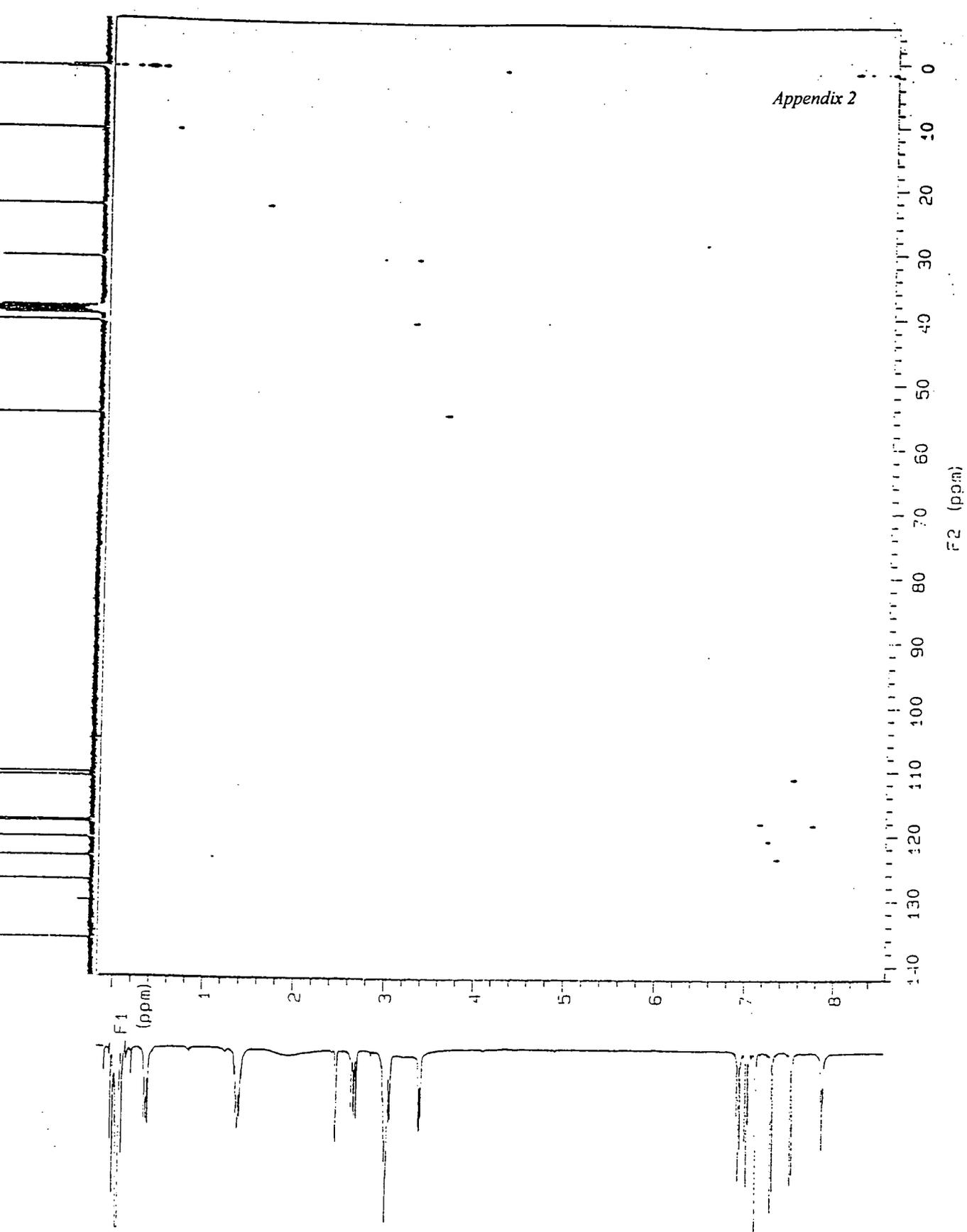
Appendix 2.4.12 HETCOR spectrum of Si-*wedge*-trp in DMSOd$_6$.
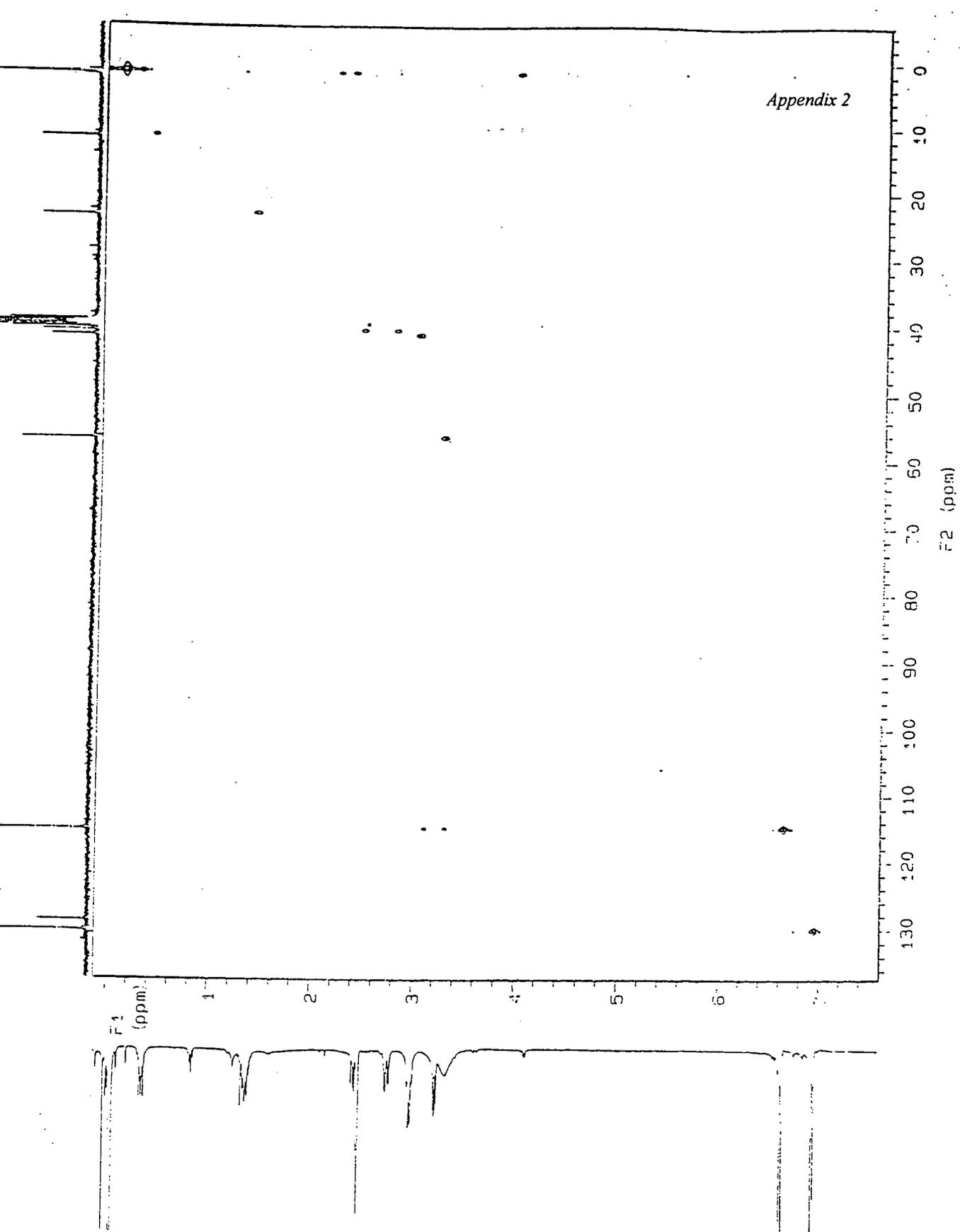
Appendix 2.4.13 HETCOR spectrum of Si-*wedge*-tyr in DMSOd_6.
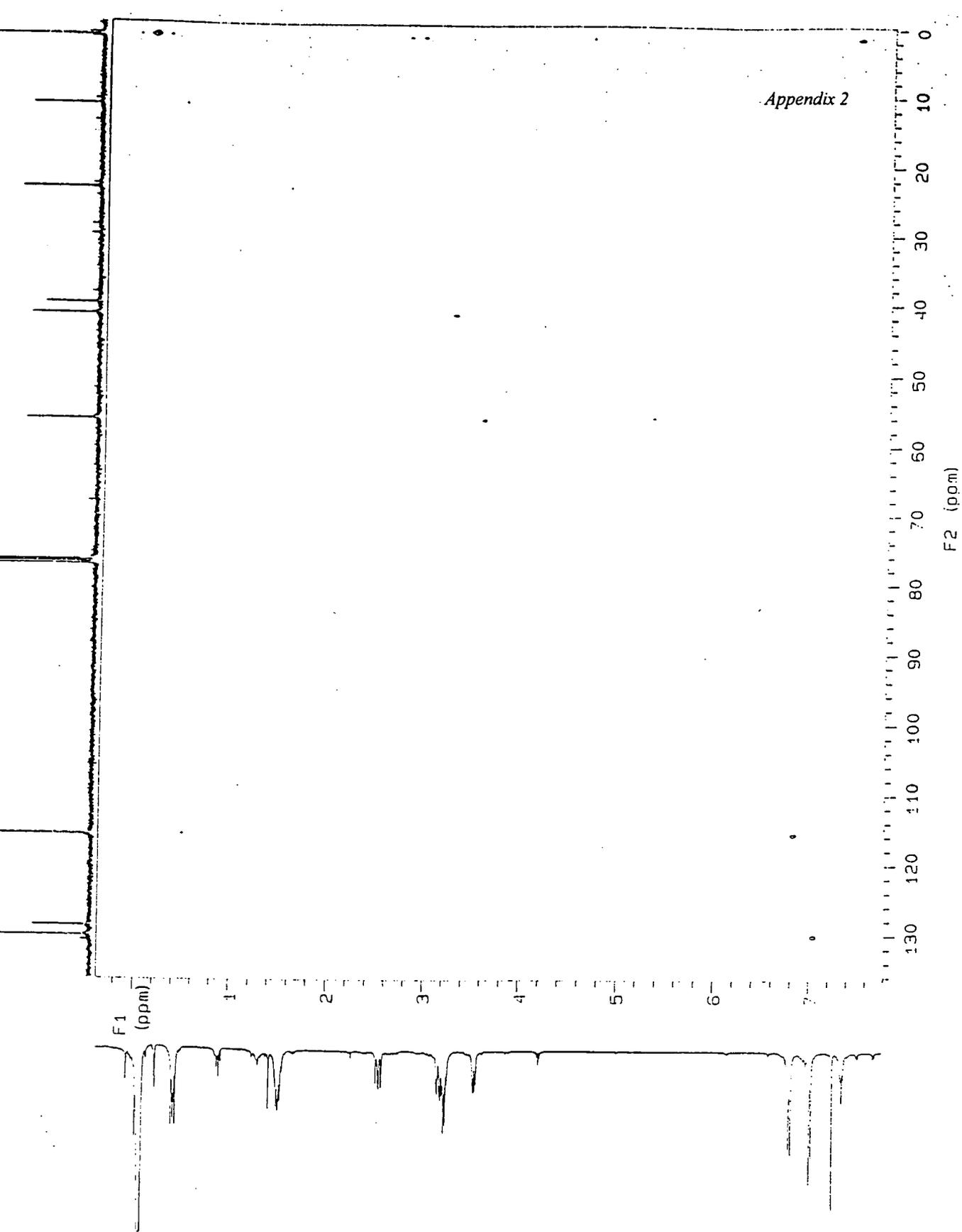
Appendix 2.4.14 HETCOR spectrum of Si-*wedge*-tyr in CDCl₃.

322

Appendix 2.4.15 COSY spectrum of NCBZ-phe-hydroxysuccinimide ester in DMSOd$_6$.
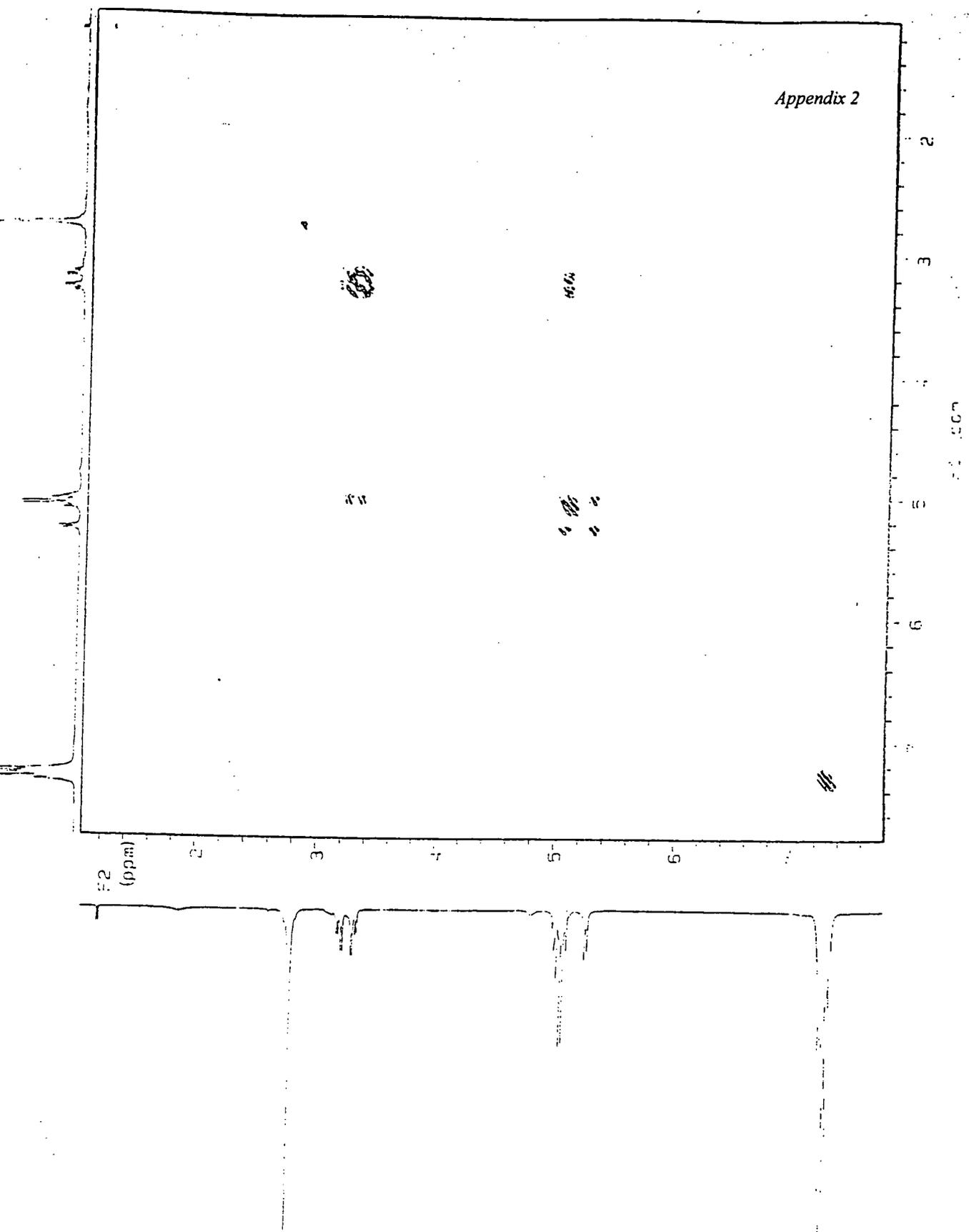
Appendix 2.4.16 COSY spectrum of NCBZ-phe-hydroxysuccinimide ester in CDCl₃.
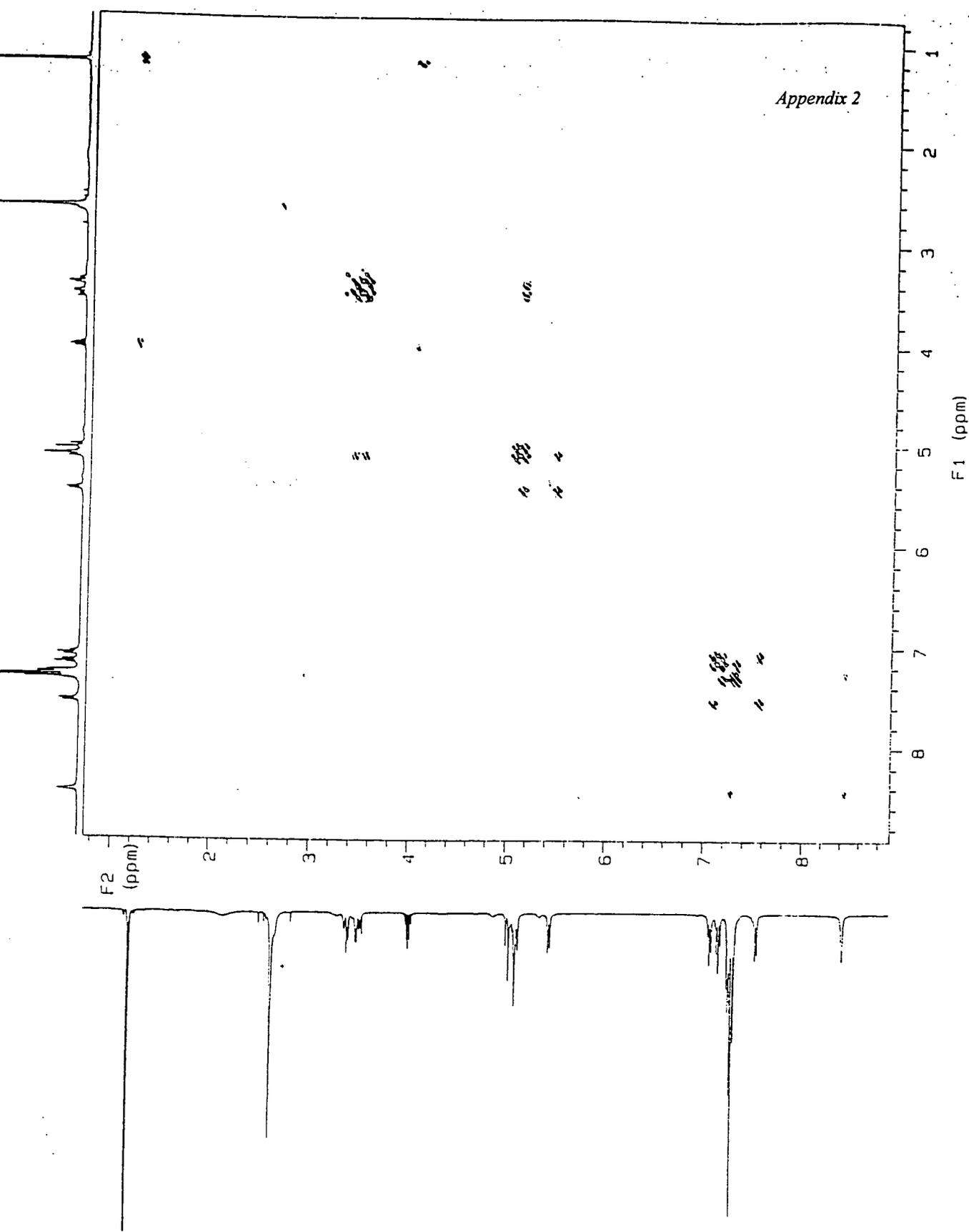
Appendix 2.4.17 COSY spectrum of NCBZ-trp-hydroxysuccinimide ester in CDCl₃.
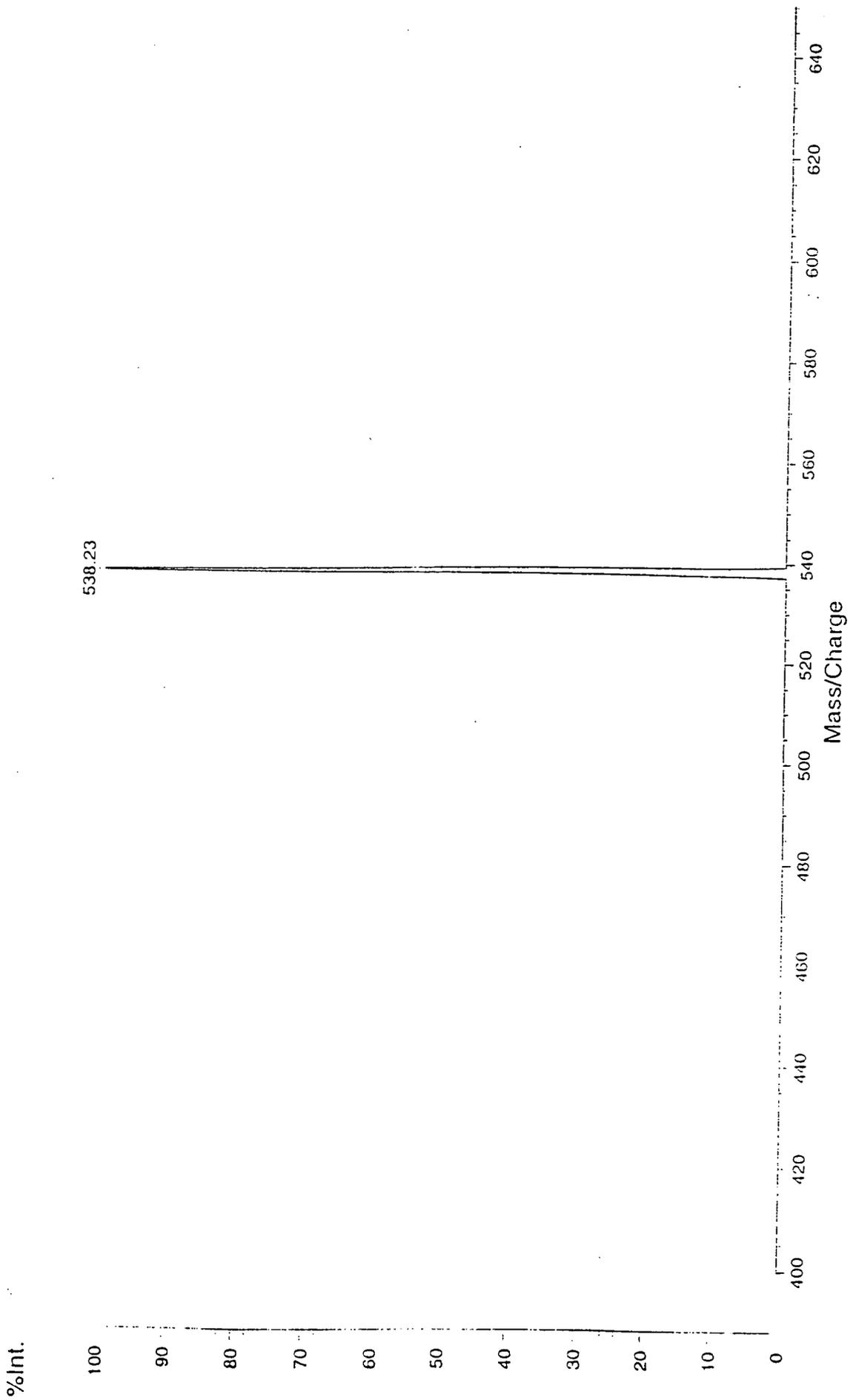
Appendix 2.5.1 MALDI-TOF-MS spectrum of Si-*wedge*-tyr.

538.23

%Int.

Mass/Charge
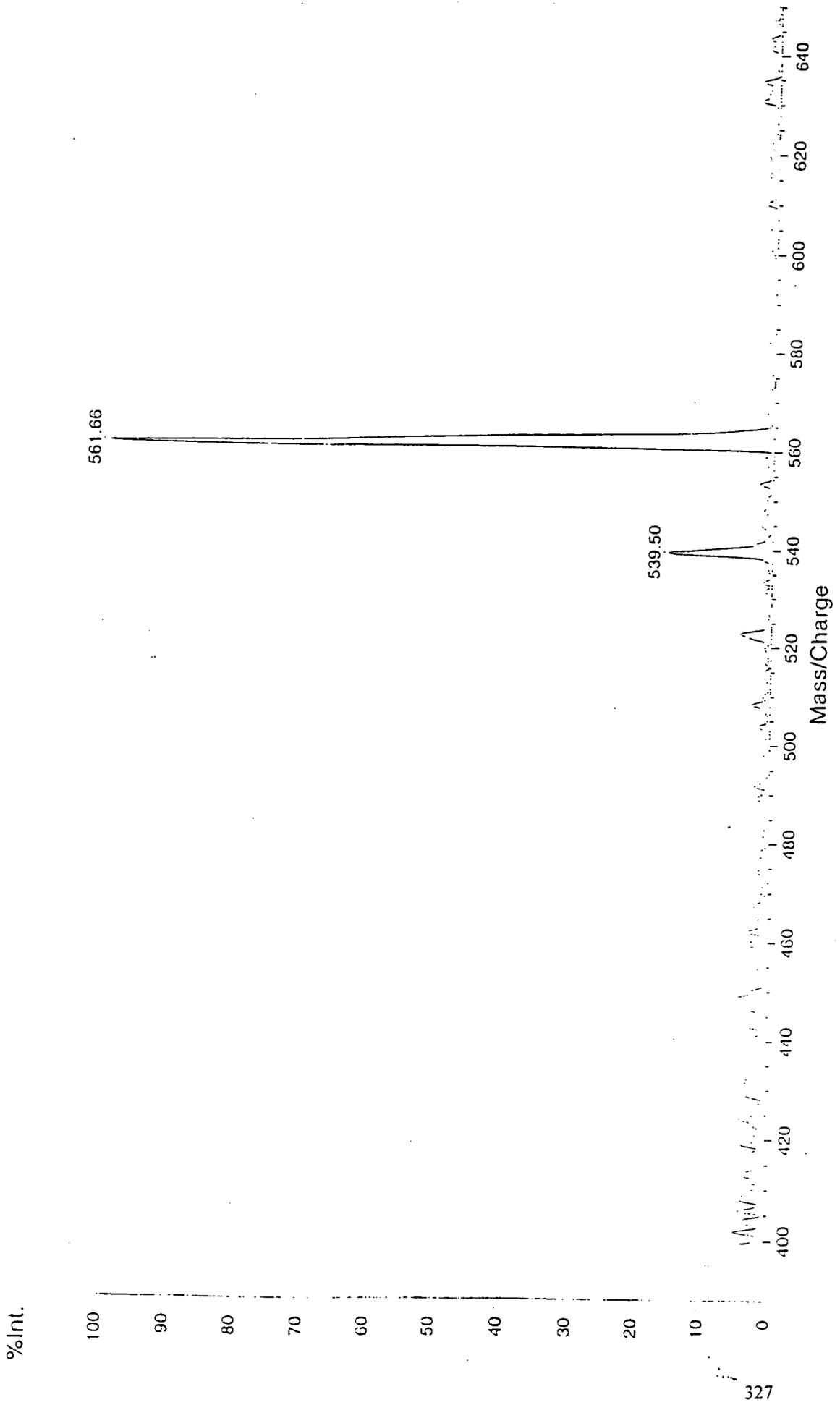
Appendix 2.5.2 MALDI-TOF-MS spectrum of Si-*wedge*-trp.

%Int.

100 —

90 —

80 —

70 —

60 —

50 —

40 —

30 —

20 —

10 —

0 —

153.26

497.59

100   200   300   400   500   600   700

Mass/Charge
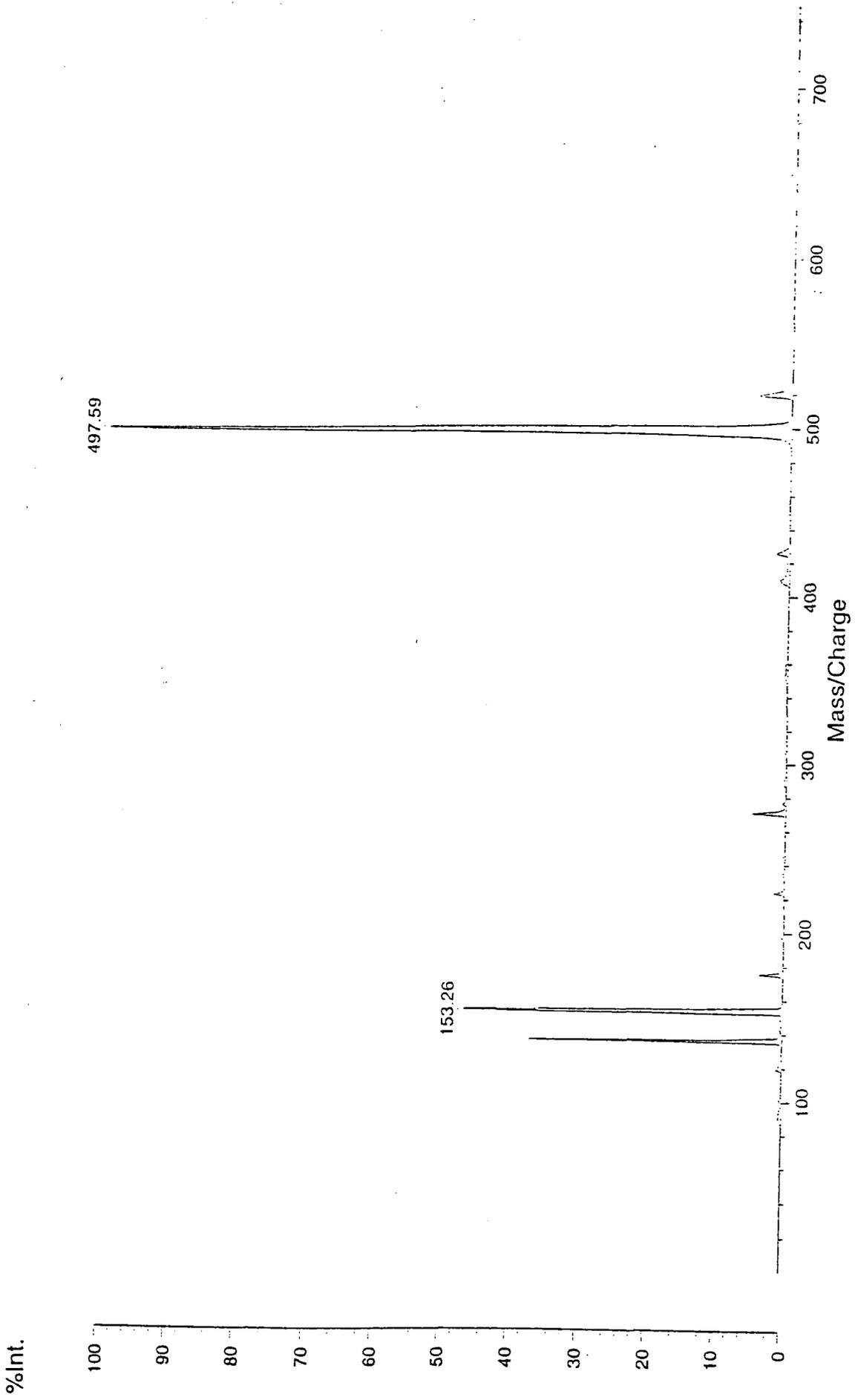
Appendix 2.5.3 MALDI-TOF-MS spectrum of Si-*wedge*-phe.
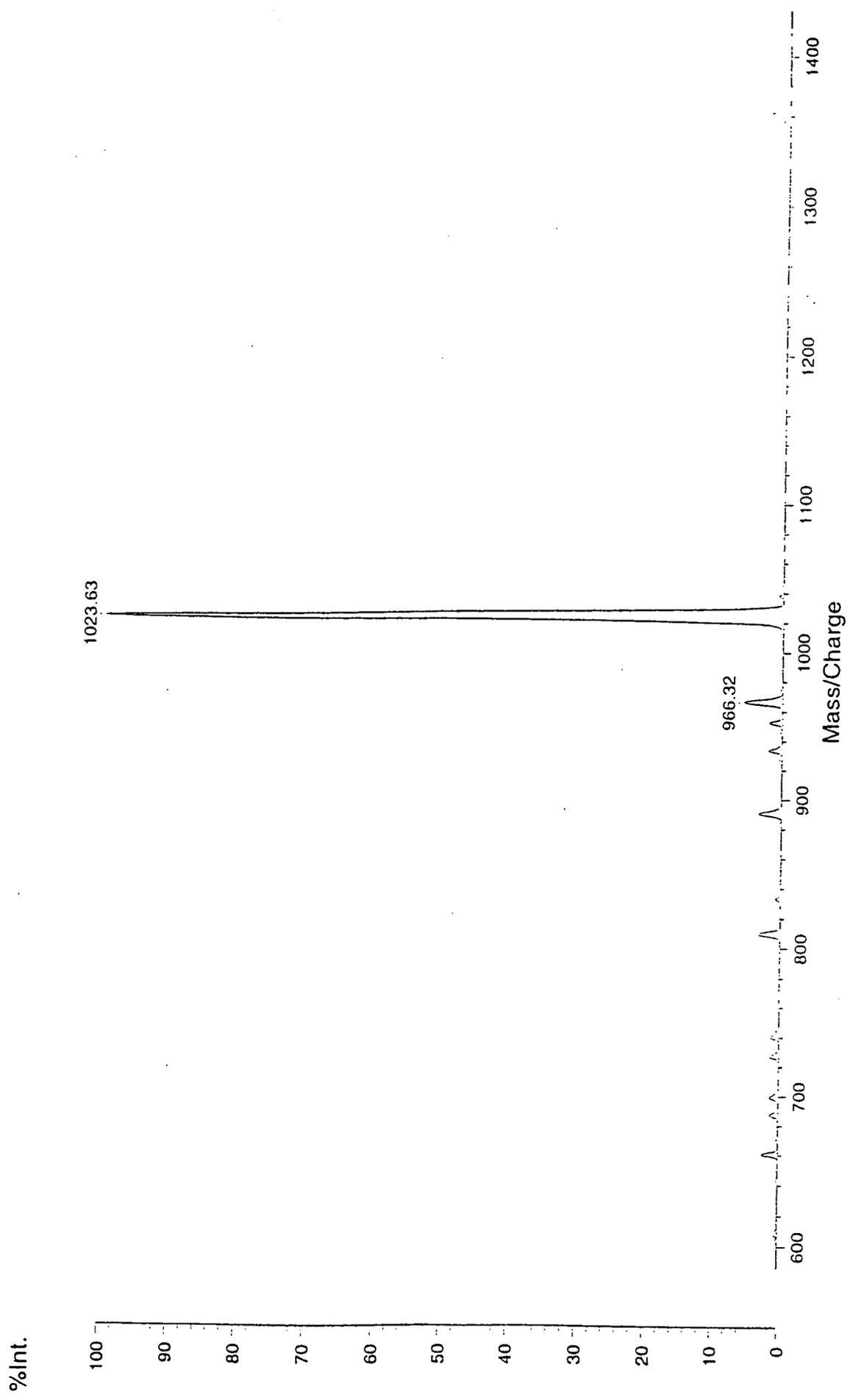
Appendix 2.5.4 MALDI-TOF-MS spectrum of Si-*wedge*-phe₂.
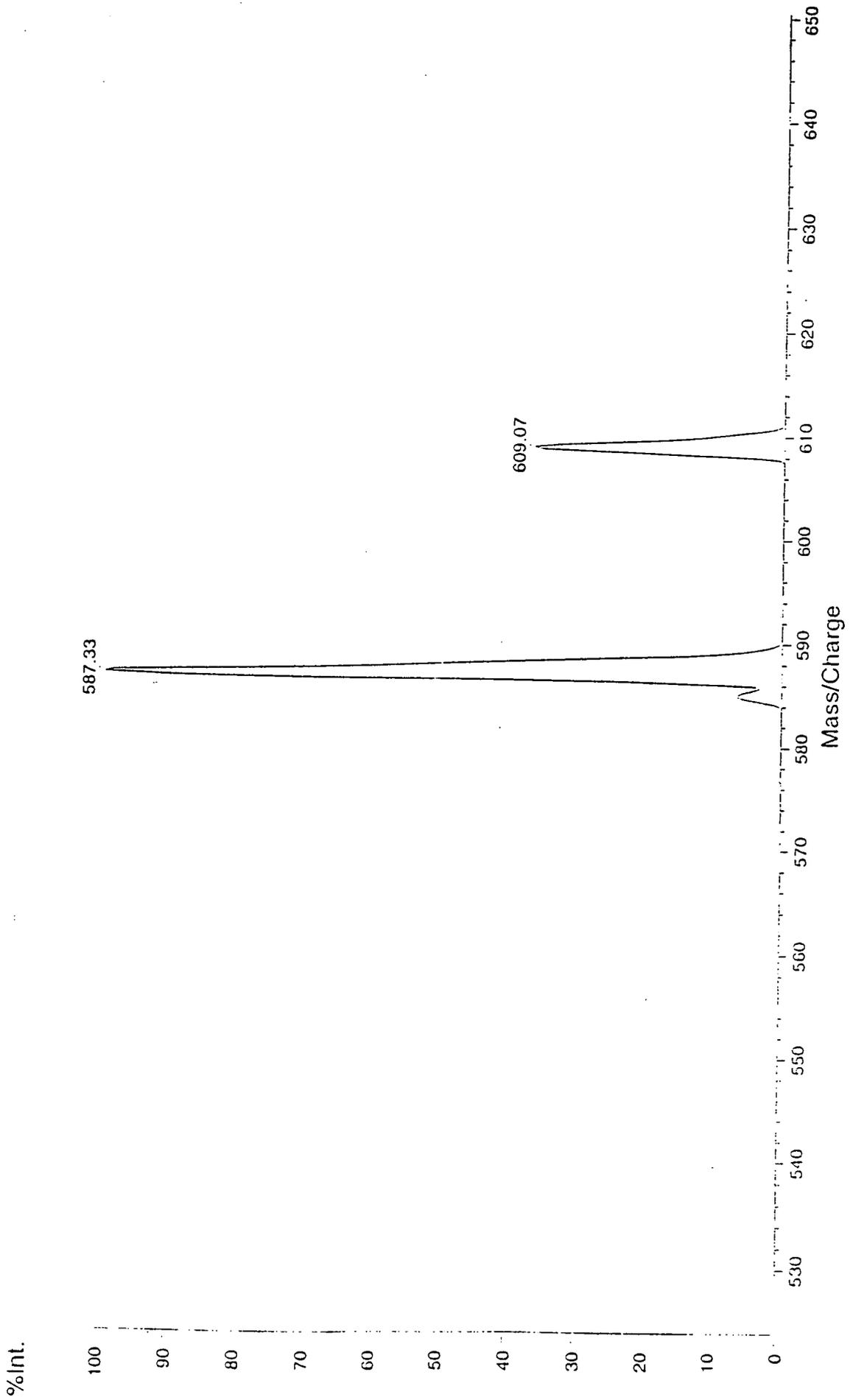
Appendix 2.5.5 MALDI-TOF-MS spectrum of Hex-*wedge*-trp₂.
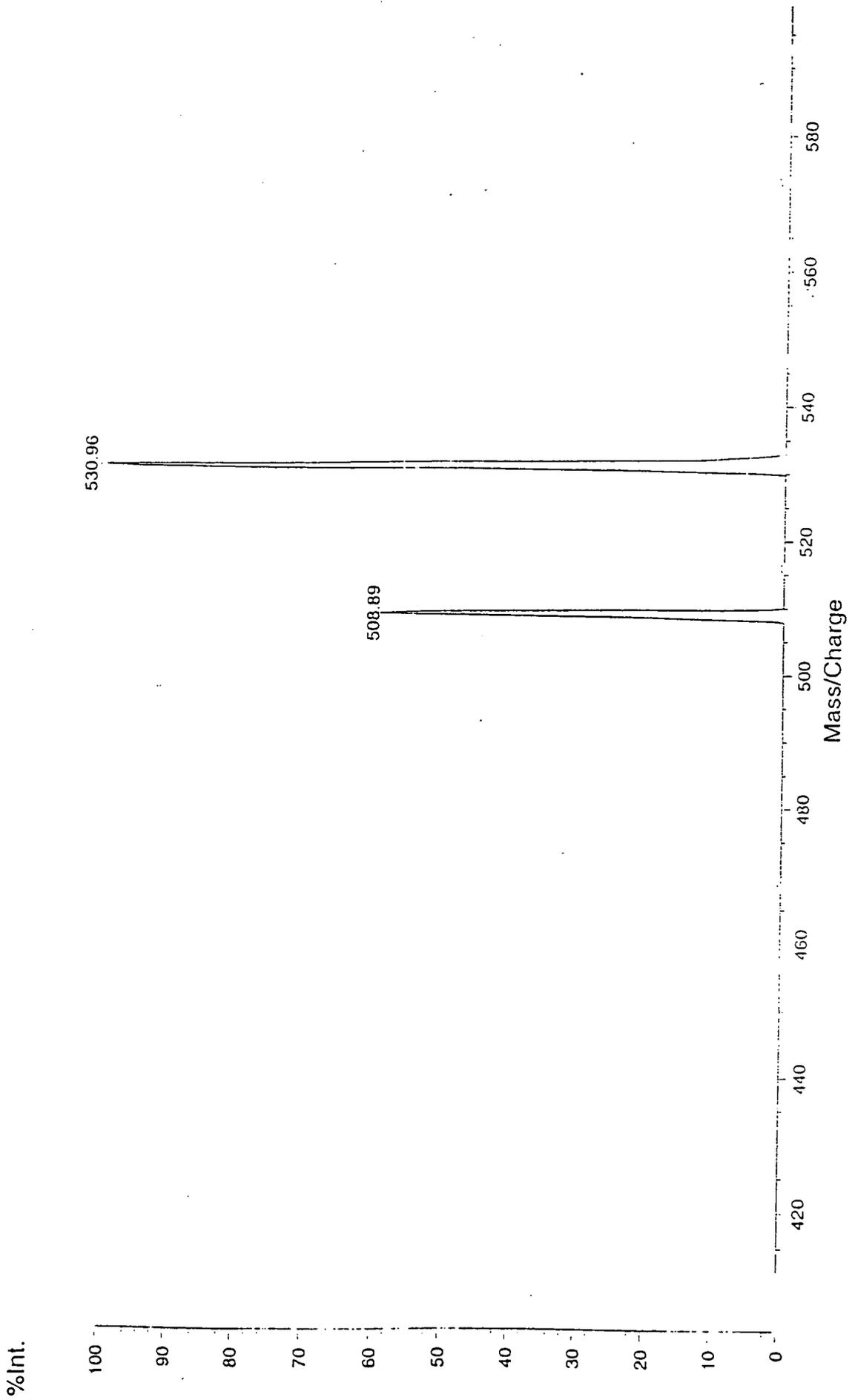
Appendix 2.5.6 MALDI-TOF-MS spectrum of Hex-*wedge*-phe₂.
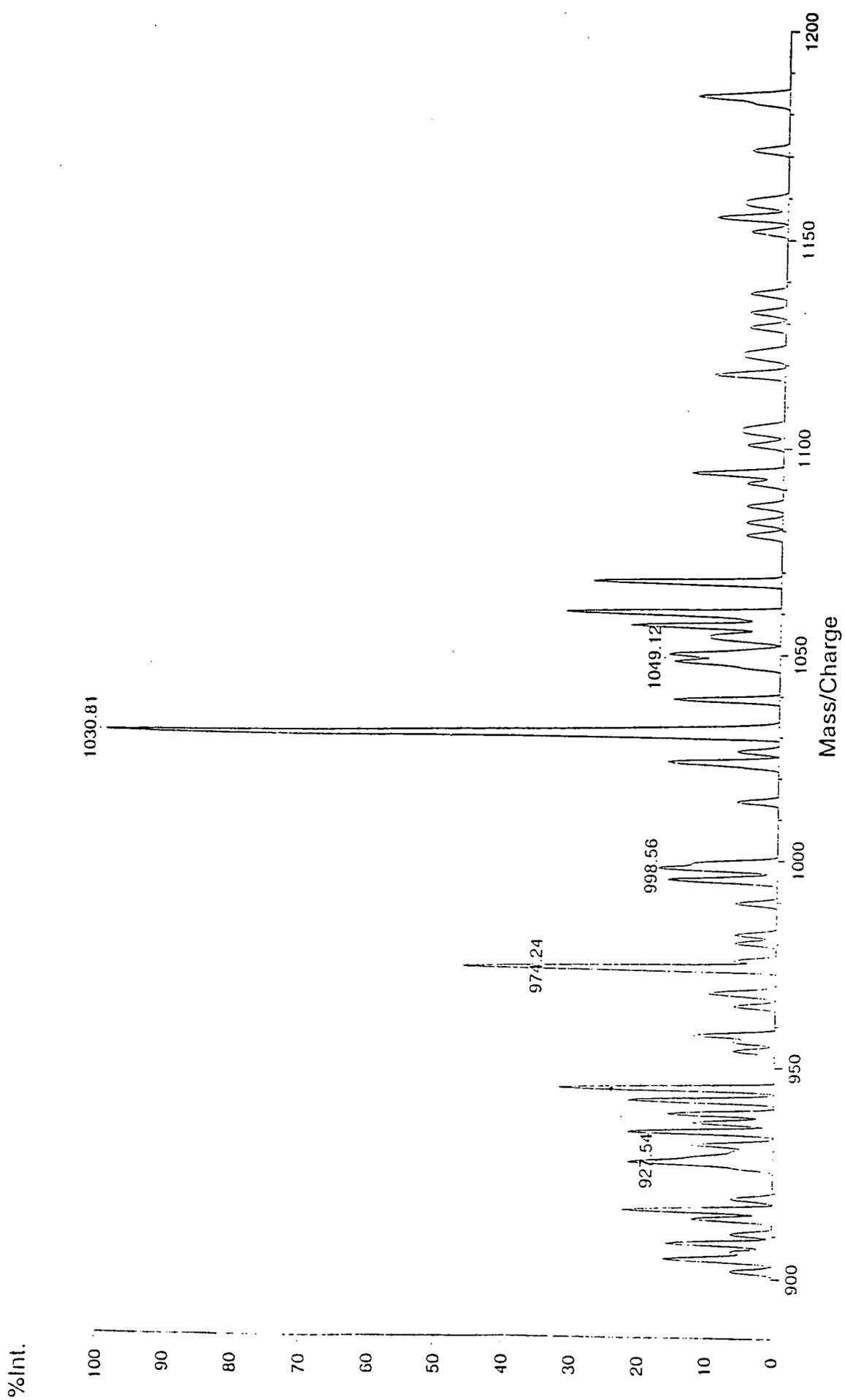
Appendix 2.5.7 MALDI-TOF-MS spectrum of Hex-*wedge*-phe₄.

%Int.

1557.82

1103.17

Mass/Charge
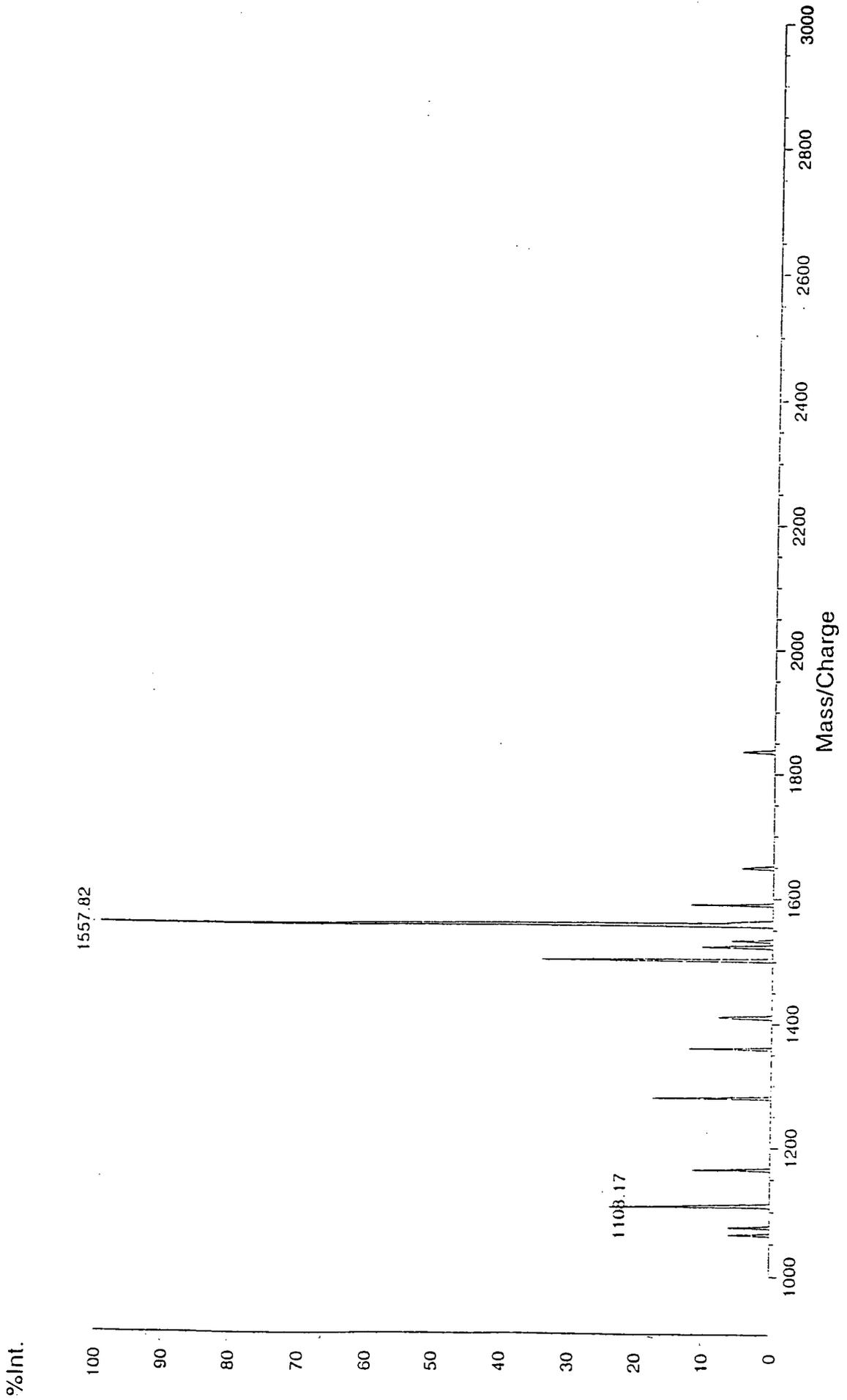
Appendix 2.5.8 MALDI-TOF-MS spectrum of Hex-*wedge*-phe$_4$-CBZ$_4$.

Appendix 3

Analytical Data for Chapter 4

Appendix 3.1 Dental Anti-Stain $\Delta \bar{L}*$ Test Results

Appendix 3.2 UV-visible absorption spectra

3.1 Dental Anti-Stain $\Delta\bar{L}*$ Test Results: second study.

Control discs			APTTMSS			Si-*wedge*-$(NH_2)_2$			Si-*wedge*-$(NH_2)_4$		
$\bar{L}_0*$	a_0*	b_0*	$\bar{L}_0*$	a_0*	b_0*	$\bar{L}_0*$	a_0*	b_0*	$\bar{L}_0*$	a_0*	b_0*
94.79	+0.28	+1.32	94.86	+0.33	+1.00	94.77	+0.32	+1.11	95.31	+0.26	+1.57
95.64	+0.30	+1.07	95.86	+0.31	+1.11	94.39	+0.37	+2.00	95.06	+0.25	+1.70
94.75	+0.32	+0.94	95.44	+0.31	+1.13	95.39	+0.19	+1.44	94.77	+0.26	+1.14
94.67	+0.26	+1.42	95.87	+0.20	+1.17	95.84	+0.30	+0.85	95.34	+0.34	+0.84
94.91	+0.26	+1.74				94.63	+0.30	+0.69	94.73	+0.24	+0.93

Table 1. Initial L*a*b* lightness values (Day 0) for hydroxyapetite discs prior to treatment with dendrimer wedge solution and submersion in synthetic stain solution.

Control discs			APTTMSS			Si-*wedge*-$(NH_2)_2$			Si-*wedge*-$(NH_2)_4$		
$\bar{L}_1*$	a_1*	b_1*	$\bar{L}_1*$	a_1*	b_1*	$\bar{L}_1*$	a_1*	b_1*	$\bar{L}_1*$	a_1*	b_1*
64.62	+1.28	+16.25	19.19	+0.02	+2.23	32.36	+1.14	+10.99	79.47	-0.20	+8.92
67.41	+0.85	+15.46	18.35	+0.39	+3.76	20.04	+0.44	+3.29	68.10	-0.19	+9.49
67.84	+1.34	+15.27	20.73	+0.32	+4.56	21.05	+0.30	+1.94	76.13	-0.35	+8.23
62.25	+1.52	+16.16	20.36	+0.33	+4.95	19.04	+0.57	+2.28	81.28	-0.17	+7.32
66.89	+1.34	+16.10				18.43	+0.40	+1.86	85.88	-0.40	+6.41

Table 2. Day 1. Change in lightness values ($\Delta L*$) for hydroxyapatite discs after 17 hours in synthetic stain solution.

Control discs			APTTMSS			Si-*wedge*-(NH₂)₂			Si-*wedge*-(NH₂)₄		
$\overline{L}_2{}^*$	$a_2{}^*$	$b_2{}^*$	$\overline{L}_2{}^*$	$a_2{}^*$	$b_2{}^*$	$\overline{L}_2{}^*$	$a_2{}^*$	$b_2{}^*$	$\overline{L}_2{}^*$	$a_2{}^*$	$b_2{}^*$
55.70	+2.36	+16.52	40.69	+0.20	+10.46	36.76	+0.44	+8.84	54.56	-0.70	+12.02
59.17	+2.24	+16.32	32.56	-0.20	+8.04	31.51	-0.05	+7.05	56.82	-0.76	+10.57
59.26	+2.16	+15.75	42.58	+0.39	+11.42	36.74	+0.44	+8.56	55.88	-0.61	+10.66
54.61	+2.28	+16.16	44.91	+0.36	+11.89	31.35	-0.11	+6.62	65.29	-0.57	+10.64
58.35	+2.18	+16.18				33.11	-0.03	+7.36	65.25	-0.64	+9.79

Table 3. Day 2. Change in lightness values (Δ**L***) for hydroxyapatite discs after

41 hours in synthetic stain solution.

Control discs			APTTMSS			Si-*wedge*-(NH₂)₂			Si-*wedge*-(NH₂)₄		
$\overline{L}_3{}^*$	$a_3{}^*$	$b_3{}^*$	$\overline{L}_3{}^*$	$a_3{}^*$	$b_3{}^*$	$\overline{L}_3{}^*$	$a_3{}^*$	$b_3{}^*$	$\overline{L}_3{}^*$	$a_3{}^*$	$b_3{}^*$
55.98	+2.25	+16.73	27.66	+0.45	+7.64	32.10	+1.15	+7.86	50.75	-0.45	+11.90
59.57	+2.06	+16.58	39.40	+0.26	+10.44	30.20	+0.92	+6.76	54.83	-0.66	+11.12
59.13	+1.94	+16.07	34.15	-0.38	+8.24	62.50	+0.32	+9.84	53.31	-0.72	+10.41
53.37	+2.02	+16.95	33.48	-0.15	+9.25	28.04	+1.00	+8.14	60.60	-0.55	+11.26
58.53	+2.02	+16.61				34.44	+0.79	+8.57	62.08	-0.34	+10.18

Table 4. Day 3. Change in lightness values (Δ**L***) for hydroxyapatite discs after

65 hours in synthetic stain solution.

Control discs			APTTMSS			Si-*wedge*-$(NH_2)_2$			Si-*wedge*-$(NH_2)_4$		
$\overline{L}_3{}^*$	$a_3{}^*$	$b_3{}^*$	$\overline{L}_3{}^*$	$a_3{}^*$	$b_3{}^*$	$\overline{L}_3{}^*$	$a_3{}^*$	$b_3{}^*$	$\overline{L}_3{}^*$	$a_3{}^*$	$b_3{}^*$
82.35	+0.99	+9.00	83.88	+0.23	+6.80	85.03	+0.24	+5.61	76.66	-0.21	+6.89
78.95	+1.13	+10.31	85.37	+0.27	+6.69	85.25	+0.25	+5.61	68.50	-0.33	+8.08
78.76	+1.12	+9.75	83.57	+0.17	+7.30	86.43	+0.23	+5.40	80.02	+0.04	+5.89
81.92	+0.98	+9.07	85.06	+0.15	+6.75	87.38	+0.33	+5.21	78.28	+0.00	+6.64
79.68	+1.18	+10.25				84.94	+0.17	+5.34	81.80	+0.11	+5.94

Table 5. Day 3; Lightness values for hydroxyapatite discs brushed with Signal

5S toothpaste.

Control discs	APTTMSS	Si-*wedge*-$(NH_2)_2$	Si-*wedge*-$(NH_2)_4$
$\Delta L_1{}^*$	$\Delta L_1{}^*$	$\Delta L_1{}^*$	$\Delta L_1{}^*$
30.17	75.67	62.41	15.84
28.23	77.51	74.35	26.96
26.91	74.71	74.34	18.64
32.42	75.51	76.80	14.06
28.02		76.20	8.85

$\Delta\overline{L}_1{}^*$ 29.15   75.85   75.42[*]   16.87

SD   2.17   1.18   1.27   6.67

Table 6. Change in lightness values (ΔL^*) for hydroxyapatite discs after 17

hours in synthetic stain solution compared to values taken on day 0.

---

[*] The value of 62.41 was omitted from the calculation of the mean as it was considered not a general representation of the other values. If it is included the mean drops to a value of 72.82, with a corresponding standard deviation of 5.92.

Control discs	APTTMSS	Si-*wedge*-(NH$_2$)$_2$	Si-*wedge*-(NH$_2$)$_4$
ΔL_2*	ΔL_2*	ΔL_2*	ΔL_2*
39.09	54.17	58.01	40.75
36.47	63.30	62.88	38.24
35.49	52.86	58.65	38.89
40.06	50.96	64.49	30.05
36.56		61.52	29.48
$\Delta \bar{L}_2$* 37.53	55.32	61.11	35.48
SD 1.94	5.48	2.76	5.30

Table 7. Day 2. Change in lightness values (ΔL*) for hydroxyapatite discs after

41 hours in synthetic stain solution compared to values taken on day 0.

Control discs	APTTMSS	Si-*wedge*-(NH$_2$)$_2$	Si-*wedge*-(NH$_2$)$_4$
ΔL_3*	ΔL_3*	ΔL_3*	ΔL_3*
38.81	67.20	62.67	44.56
36.07	56.46	64.19	40.23
35.62	61.29	32.89	41.46
41.30	62.39	67.80	34.74
36.38		60.19	32.65
$\Delta \bar{L}_3$* 37.64	61.84	63.71*	38.73
SD 2.39	4.41	3.18	4.91

Table 8. Day 3. Change in lightness values (ΔL*) for hydroxyapatite discs after

65 hours in synthetic stain solution compared to values taken on day 0.

Control discs	APTTMSS	Si-*wedge*-(NH$_2$)$_2$	Si-*wedge*-(NH$_2$)$_4$
$\Delta L_{brush}*$	$\Delta L_{brush}*$	$\Delta L_{brush}*$	$\Delta L_{brush}*$
12.44	10.98	9.74	18.65
16.69	10.49	9.14	26.56
15.99	11.87	8.96	14.75
12.75	10.81	8.46	17.06
15.23		9.69	12.93

$\Delta \bar{L}_3*$ 14.62   11.04   9.20   17.99

**SD**   1.92   0.59   0.53   5.26

Table 9. Change in lightness values ($\Delta L*$) for hydroxyapatite discs for day 3 after brushing with Signal 5S toothpaste.

	CONTROL	APTTMSS	Si-*wedge*-(NH$_2$)$_2$	Si-*wedge*-(NH$_2$)$_4$
	$\Delta \bar{L}*$	$\Delta \bar{L}*$	$\Delta \bar{L}*$	$\Delta \bar{L}*$
DAY 1	29.15	75.85	75.42	16.87
DAY 2	37.53	55.32	61.11	35.48
DAY 3	37.64	61.84	63.71	38.73
$\bar{X}$	34.77	64.34	66.75	30.36

Table 10. Mean change in lightness values($\Delta \bar{L}*$) calculated for each day, see Figure 4.22 (page 194) in Chapter 3.

---

* The value of 32.89 was omitted from the calculation of the mean as it was considered not a general representation of the other values. If it is included the mean drops to a value of 57.55, with a corresponding standard deviation of 14.06.

3.2 UV-visible absorption spectra
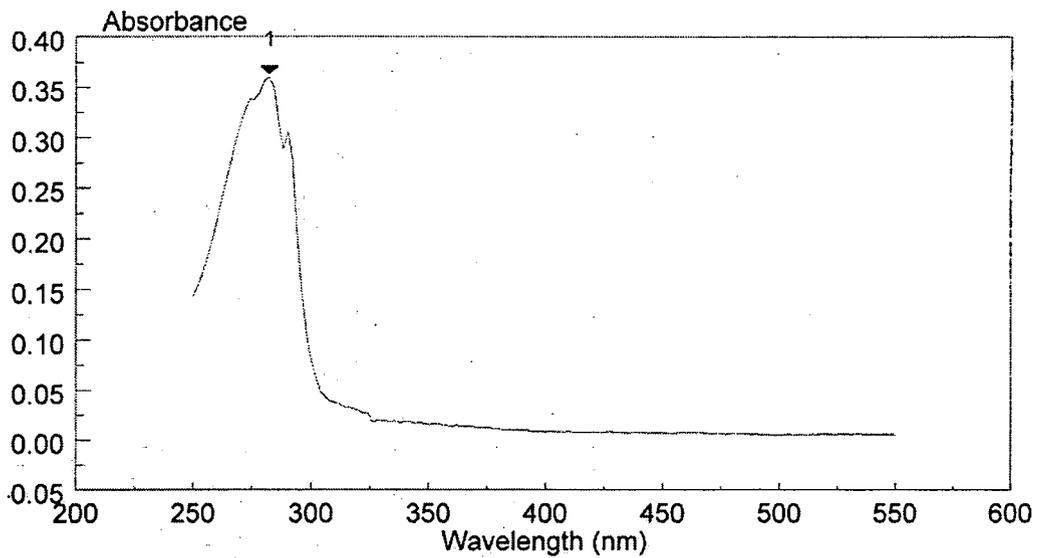
Appendix 3.2.1 UV-visible absorption spectrum of Hex-*wedge*-trp$_2$ in methanol

(30μm) showing a λmax at 282nm.
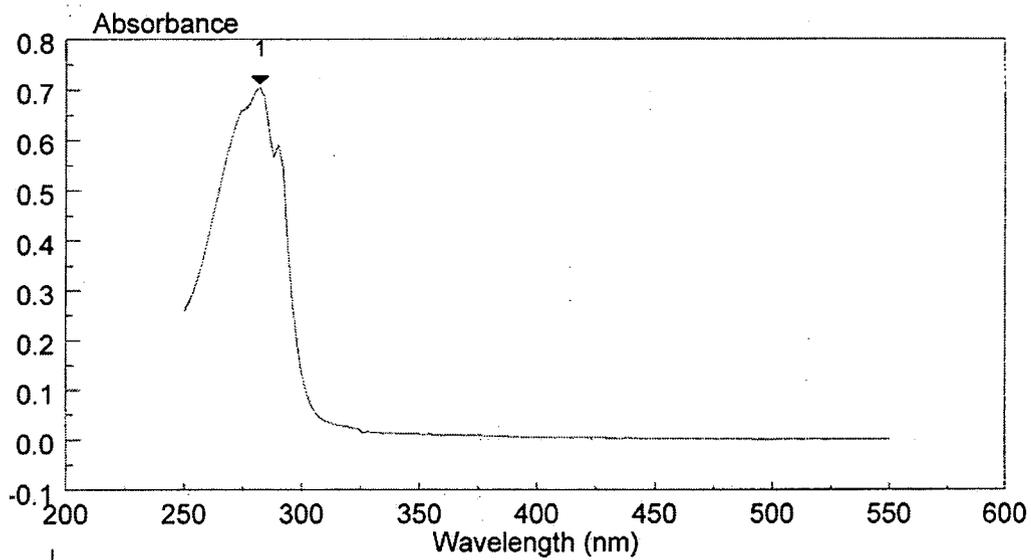
Appendix 3.2.2 UV-visible absorption spectrum of Hex-*wedge*-trp$_4$ in methanol

(30μm) showing a λmax at 282nm.
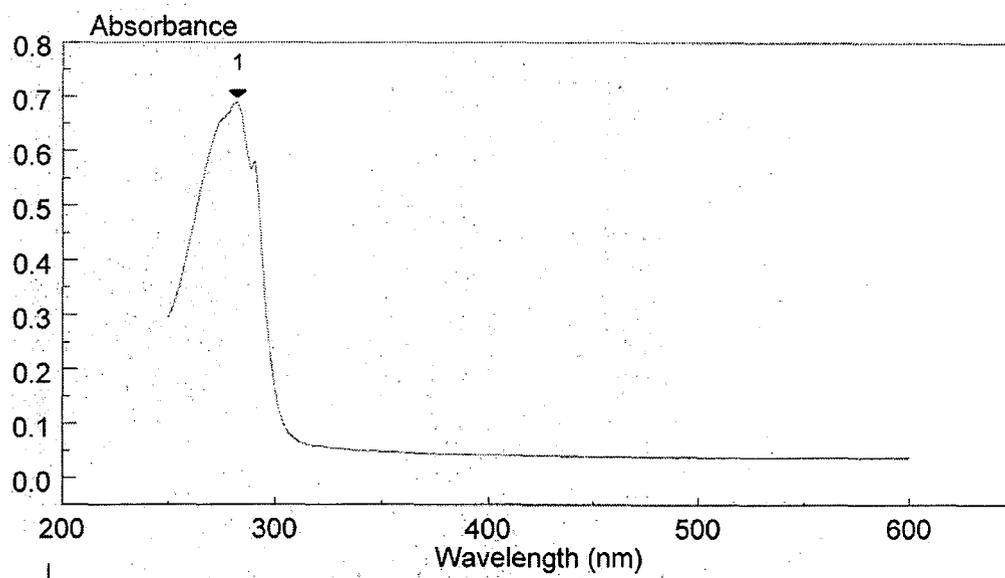
Appendix 3.2.3 UV-visible absorption spectrum of Hex-*wedge*-trp₄ in

methanol/water (30μm) showing a λmax at 282nm.

Appendix 4

Colloquia, Conferences and Courses Attended

UNIVERSITY OF DURHAM

Board of Studies in Chemistry

Colloquia, Lectures and Seminars attended from invited speakers

1994 - 1995 (August 1 - July 31)

1994

October 5   Prof. N. L. Owen, Brigham Young University, Utah, USA

Determining Molecular Structure - the INADEQUATE NMR way

October 19   Prof. N. Bartlett, University of California

Some Aspects of Ag(II) and Ag(III) Chemistry

November 3   Prof. B. F. G. Johnson, Edinburgh University

Arene-metal Clusters

November 10   Dr M. Block, Zeneca Pharmaceuticals, Macclesfield

Large-scale Manufacture of ZD 1542, a Thromboxane Antagonist Synthase Inhibitor

November 16   Prof. M. Page, University of Huddersfield

Four-membered Rings and b-Lactamase

November 23   Dr J. M. J. Williams, University of Loughborough

New Approaches to Asymmetric Catalysis

December 7   Prof. D. Briggs, ICI and University of Durham

Surface Mass Spectrometry

1995

January 11   Prof. P. Parsons, University of Reading

Applications of Tandem Reactions in Organic Synthesis

January 18   Dr G. Rumbles, Imperial College, London

Real or Imaginary Third Order Non-linear Optical Materials

January 25   Dr D. A. Roberts, Zeneca Pharmaceuticals

The Design and Synthesis of Inhibitors of the Renin-angiotensin System

February 1   Dr T. Cosgrove, Bristol University

Polymers do it at Interfaces

February 22   Prof. E. Schaumann, University of Clausthal

Silicon- and Sulphur-mediated Ring-opening Reactions of Epoxide

March 1   Dr M. Rosseinsky, Oxford University

Fullerene Intercalation Chemistry

April 26   Dr M. Schroder, University of Edinburgh

Redox-active Macrocyclic Complexes : Rings, Stacks and Liquid Crystals

April 27   Prof. D.J. Cole-Hamilton, University of St. Andrews

Chemistry on the Nano Scale

May 3   Prof. E.W. Randall, Queen Mary and Westfield Colledge

New Perspectives in NMR Imaging

May 4   Prof. A. J. Kresge, University of Toronto, Canada

             The Ingold Lecture Reactive Intermediates : Carboxylic-acid
             Enols and Other Unstable Species

May 9   Prof. R. Townsend, Unilever Exploratory Research Council

             Polymers for the Year 2000 - The Challenge Ahead

May 30   Prof. P. Calvert, University of Arizona, USA

             Freeforming: Chemical Methods for the Processing of Polymers,
             Ceramics and Composites

1995 - 1996 (August 1 - July 31)

1995

October 11   Prof. P. Lugar, Frei Univ Berlin, FRG
             Low Temperature Crystallography

October 18   Prof. A. Alexakis, Univ. Pierre et Marie Curie, Paris,
             Synthetic and Analytical Uses of Chiral Diamines

October 25   Dr.D.Martin Davies, University of Northumbria
             Chemical reactions in organised systems.

November 1   Prof. W. Motherwell, UCL London
             New Reactions for Organic Synthesis

November 3   Dr B. Langlois, University Claude Bernard-Lyon
             Radical Anionic and Psuedo Cationic Trifluoromethylation

November 15 Dr Andrea Sella, UCL, London

Chemistry of Lanthanides with Polypyrazoylborate Ligands

November 17 Prof. David Bergbreiter, Texas A&M, USA

Design of Smart Catalysts, Substrates and Surfaces from Simple Polymers

November 22 Prof. I Soutar, Lancaster University

A Water of Glass? Luminescence Studies of Water-Soluble Polymers.

November 29 Prof. Dennis Tuck, University of Windsor, Ontario, Canada

New Indium Coordination Chemistry

December 8 Professor M.T. Reetz, Max Planck Institut, Mulheim

Perkin Regional Meeting

1996

January 10 Dr Bill Henderson, Waikato University, NZ

Electrospray Mass Spectrometry - a new sporting technique

January 17 Prof. J. W. Emsley , Southampton University

Liquid Crystals: More than Meets the Eye

January 24 Dr Alan Armstrong, Nottingham Univesity

Alkene Oxidation and Natural Product Synthesis

January 31 Dr J. Penfold, Rutherford Appleton Laboratory,

Soft Soap and Surfaces

February 28   Prof. E. W. Randall, Queen Mary & Westfield College
New Perspectives in NMR Imaging

March 6   Dr Richard Whitby, Univ of Southampton
New approaches to chiral catalysts: Induction of planar and metal
centred asymmetry

March 12   RSC Endowed Lecture - Prof. V. Balzani, Univ of Bologna
Supramolecular Photochemistry

March 13   Prof. Dave Garner, Manchester University
Mushrooming in Chemistry

April 30   Dr L.D.Pettit, Chairman, IUPAC Commission of Equilibrium
Data
pH-metric studies using very small quantities of uncertain purity

1996 - 1997 (August 1 - July 31)

1996

August 15   Prof. K.B. Wagener, University of Florida, USA
Catalyst Selection and Kinetics in ADMET Polymerisation

October 14   Professor A. R. Katritzky, University of Gainesville,University of
Florida, USA
Recent   Advances   in   Benzotriazole   Mediated   Synthetic
Methodology

October 16   Professor Ojima, Guggenheim Fellow, State University of New York at Stony Brook

Silylformylation and Silylcarbocyclisations in Organic Synthesis

October 22   Professor B. J. Tighe, Department of Molecular Sciences and Chemistry, University of Aston

Making Polymers for Biomedical Application - can we meet Nature's Challenge? Joint lecture with the Institute of Materials

October 23   Professor H. Ringsdorf (Perkin Centenary Lecture), Johannes Gutenberg-Universitat, Mainz,Germany

Function Based on Organisation

October 29   Professor D. M. Knight, Department of Philosophy, University of Durham.

The Purpose of Experiment - A Look at Davy and Faraday

November 6   Dr Melinda Duer, Chemistry Department, Cambridge

Solid-state NMR Studies of Organic Solid to Liquid-crystalline Phase Transitions

November 12   Professor R. J. Young, Manchester Materials Centre, UMIST

New Materials - Fact or Fantasy?

Joint Lecture with Zeneca & RSC

November 18   Professor G. A. Olah, University of Southern California, USA

Crossing Conventional Lines in my Chemistry of the Elements

November 20   Professor J. Earnshaw, Deptartment of Physics, Belfast

Surface Light Scattering: Ripples and Relaxation

November 27 Dr Richard Templer, Imperial College, London
> Molecular Tubes and Sponges

December 3 Professor D. Phillips, Imperial College, London
> "A Little Light Relief" -

December 4 Professor K. Muller-Dethlefs, York University
> Chemical Applications of Very High Resolution ZEKE Photoelectron Spectroscopy

1997

January 16 Dr Sally Brooker, University of Otago, NZ
> Macrocycles: Exciting yet Controlled Thiolate Coordination Chemistry

January 21 Mr D. Rudge, Zeneca Pharmaceuticals
> High Speed Automation of Chemical Reactions

January 22 Dr Neil Cooley, BP Chemicals, Sunbury
> Synthesis and Properties of Alternating Polyketones

January 29 Dr Julian Clarke, UMIST
> What can we learn about polymers and biopolymers from computer-generated nanosecond movie-clips?

February 4 Dr A. J. Banister, University of Durham
> From Runways to Non-metallic Metals - A New Chemistry Based on Sulphur

February 5 Dr A. Haynes, University of Sheffield
> Mechanism in Homogeneous Catalytic Carbonylation

February 12   Dr Geert-Jan Boons, University of Birmingham
New Developments in Carbohydrate Chemistry

February 18   Professor Sir James Black, Foundation/King's College London
My Dialogues with Medicinal Chemists

February 25   Professor A. G. Sykes, University of Newcastle
The Synthesis, Structures and Properties of Blue Copper Proteins

February 26   Dr Tony Ryan, UMIST
Making Hairpins from Rings and Chains

March 11   Dr A. D. Taylor, ISIS Facility, Rutherford Appleton Laboratory
Expanding the Frontiers of Neutron Scattering

May 7   Prof. M. Harrington, Caltech, Pasadena, USA
Polymers both Enable and Limit the Discovery of Protein
Alterations in Studies Ranging from Gene Regulation to Mad cow
Disease

May 20   Prof. J. Jin, President, Korean Chemical Society
Poly PPV and its Derivatives - Synthesis, Structure and Properties

June 13   Prof. Dr. S. Kobayashi, Kyoto University, Japan
Synthesis of Polyesters via Enzymatic Polymerisation

Conferences and Courses Attended

1995

January 10   IRC Polymer Physics Introduction Course, University of Leeds

January 12   IRC Polymer Engineering Introduction Course, University of Bradford

July 10-14   International Symposium on Olefin Metathesis (ISOM 11), Durham

Sept. 27-28   IRC Industrial Club Seminar, Durham

1996

April 10-12   Aspects of Contemporary Polymer Science, MACRO Group UK Family Meeting, Manchester

June 3   The Melville Lectureship, Department of Chemistry, University of Cambridge

1997

April 2-4   MACRO Group UK Spring Meeting for Younger Researchers Leeds

Sept 8-11   American Chemical Society, Division of Polymeric Materials: Science and Engineering, 214th National Meeting , Las Vegas, Nevada